



THE UNIVERSITY *of* EDINBURGH

This thesis has been submitted in fulfilment of the requirements for a postgraduate degree (e.g. PhD, MPhil, DClinPsychol) at the University of Edinburgh. Please note the following terms and conditions of use:

This work is protected by copyright and other intellectual property rights, which are retained by the thesis author, unless otherwise stated.

A copy can be downloaded for personal non-commercial research or study, without prior permission or charge.

This thesis cannot be reproduced or quoted extensively from without first obtaining permission in writing from the author.

The content must not be changed in any way or sold commercially in any format or medium without the formal permission of the author.

When referring to this work, full bibliographic details including the author, title, awarding institution and date of the thesis must be given.

Targeting the macrophage in equine post-operative ileus



THE UNIVERSITY
of EDINBURGH



Zofia Maria Lisowski

Doctor of Philosophy

The University of Edinburgh

2018

This page was left intentionally blank

Contents

Summary	v
Abstract	vi
Declaration	viii
Acknowledgements	ix
Contributions of work	xi
List of publications and presentations	xii
Abbreviations	xv
List of figures	xviii
List of tables	xxiii
Chapter 1. General Introduction	1
1.1 Overview	2
1.2 Macrophages and the mononuclear phagocyte system	3
1.2.1 Identification of macrophages	5
1.2.2 Macrophage origins and development	9
1.2.3 Colony Stimulating Factor-1 (CSF-1)	10
1.3 Macrophage activation	12
1.3.1 LPS activation of macrophages	13
1.3.2 Inhibitory Feedback mechanisms in response to LPS	15
1.4 Resident Intestinal Macrophages	16
1.4.1 Ontogeny of resident intestinal macrophages	16
1.4.2 Distribution of resident intestinal macrophages	17
1.4.3 CSF-1 regulates intestinal macrophage homeostasis	19
1.5 Macrophage reporter mice	19
1.6 Response of equine macrophages to LPS	22
1.7 RNA-Seq and microarray analysis	23
1.8 Definitions and clinical features of post-operative ileus	25
1.8.1 General and human	25
1.8.2 Equine	26
1.9 Diagnosis of equine post-operative ileus - mechanical versus functional	27
1.10 Epidemiology and risk factors for equine post-operative ileus	28
1.11 Pathophysiology of post-operative ileus	29
1.11.1 Neurogenic phase	30
1.11.2 Inflammatory phase	37
1.11.3 Pharmacological/therapeutic influences on the development of post-operative ileus	40
1.12 Aims of thesis	41
1.13 Hypotheses	42
Chapter 2. Materials and Methods	43
2.1 Animals	44
2.1.1 Horses	44
2.1.2 Mice	47
2.1.3 Collection of whole blood	48

2.1.4	Collection of samples from the gastrointestinal tract	48
2.2	Isolation and generation of equine bone marrow derived macrophages	49
2.3	Alveolar macrophages	50
2.4	Equine macrophage cell culture conditions (optimised)	50
2.5	Cell viability assay	50
2.6	<i>In vitro</i> stimulation of macrophages	51
2.6.1	Lipopolysaccharide (LPS)	51
2.7	Cryopreservation of cells	51
2.8	Phagocytosis assay	51
2.8.1	Zymosan A <i>S.cerevisiae</i> BioParticles	51
2.8.2	pHrodo red <i>E. coli</i> BioParticles	52
2.9	Nitrite (Griess) assay	52
2.10	Immunohistochemistry	52
2.10.1	Tissue fixation	52
2.10.2	Antigen retrieval	53
2.10.3	Antibody incubation	54
2.11	Cell imaging	55
2.11.1	Light microscopy	55
2.11.2	Confocal microscopy	55
2.12	Mouse intestinal whole mount imaging	55
2.13	Image software	56
2.14	Image analysis pipelines	56
2.15	Quantification of cells in the equine gastrointestinal tract	56
2.16	RNA Extractions	57
2.16.1	Cells	57
2.16.2	Tissues	58
2.17	RNA quantification and quality analysis	59
2.17.1	Nanodrop	59
2.17.2	Qubit	59
2.17.3	TapeStation	59
2.18	cDNA Synthesis from RNA	59
2.19	Primer design	60
2.20	Real – Time quantitative polymerase chain reaction (RT qPCR)	60
2.21	Experimental model of post-operative ileus	61
2.22	Gastrointestinal transit measurement	61
2.23	Treatment of mice with an FC conjugate of CSF-1	62
2.24	Flow cytometry	62
2.25	Microarray analysis	62
2.26	RNASeq analysis	63
2.26.1	Data quality control	63
2.26.2	Differential expression analysis	63
2.26.3	Gene ontology (GO) term enrichment	63
2.27	Statistical analysis	64
Chapter 3. Distribution of macrophages in the equine gastrointestinal tract ..		65

3.1Introduction	66
3.2Results	69
3.2.1Optimisation of immunohistochemistry protocols	69
3.2.2Distribution of macrophages in the equine GIT	74
3.3Discussion	91
Chapter 4. Isolation and generation of Equine Bone Marrow-Derived Macrophages and their response to Lipopolysaccharide.....	95
4.1Introduction	96
4.2Results	98
4.2.1Cell yield from ribs of adult horses	98
4.2.2Optimisation of culture conditions	98
4.2.3Differentiated cells resemble macrophages	103
4.2.4LPS stimulation of eqBMDMs	106
4.2.5RNA-seq analysis of eqBMDMs and their response to LPS	110
4.3Discussion	128
Chapter 5. Inflammatory response in the mucosa and <i>muscularis</i> of horses undergoing gastrointestinal surgery.....	131
5.1Introduction	132
5.2Results	134
5.2.1Animals	134
5.2.2RNA extraction	134
5.2.3Real – Time quantitative polymerase chain reaction of resection margins	135
5.3Discussion	155
Chapter 6. Effect of CSF1-Fc on the murine gastrointestinal tract	161
6.1Introduction	162
6.2Results	164
6.2.1Administration of CSF1-Fc to mice does not affect gastrointestinal transit time	164
6.2.2Administration of CSF1-Fc alters morphology of resident muscularis macrophages	166
6.2.3Administration of CSF1-Fc in a mouse model of POI drives the differentiation of pro resolving macrophages	177
6.2.4Microarray analysis of muscularis externa treated with CSF1-Fc	182
6.3Discussion	184
Chapter 7. General discussion, future directions and conclusion.....	187
7.1General Discussion	188
7.2Limitations of the study	191
7.3Future Directions	192
7.4Conclusion	195
Chapter 8. References.....	197
Chapter 9. Appendices	233
9.1Csf1r-mApple transgene expression and ligand binding in vivo reveal dynamics of CSF1R expression within the mononuclear phagocyte system	234
9.2Species-Specific Transcriptional Regulation of Genes Involved in Nitric Oxide Production and Arginine Metabolism in Macrophages	253

9.3Macrophage colony-stimulating factor (CSF1) controls monocyte production and maturation and the steady-state size of the liver in pigs	267
9.4Activation of macrophages in the mucosa and muscularis of jejunum in horses undergoing abdominal surgery for strangulating small intestinal obstructions	282
9.5Generation and characterisation of equine bone marrow-derived macrophages	283
9.6Transcriptomic response of equine bone marrow-derived macrophages cultured in macrophage colony-stimulating factor (CSF-1) to lipopolysaccharide (LPS)	284
9.7Distribution of Macrophages in the Gastrointestinal Tract of Horses	285
9.8Isolation and characterisation of the equine bone marrow derived macrophage.	286
9.9Distribution of macrophages in the gastrointestinal tract of normal horses	287
9.10Targeting the macrophage in equine post-operative ileus	288
9.11Appendix 8: Table of $2^{-\Delta\Delta C_t}$ values used in analysis of colic cases	289

Summary

Colic, the syndrome of abdominal pain, is a frequent condition in horses. Whilst the majority of horses with colic resolve spontaneously or with medical treatment alone, a proportion require abdominal surgery to address the underlying cause. Any horse undergoing abdominal surgery is at risk of developing post-operative ileus (POI). POI is the functional inhibition of normal intestinal motility. POI affects up to 60% of horses undergoing abdominal surgery and has reported mortality rates as high as 86%. POI also increases the duration of post-operative hospitalisation and increases costs. Most published studies in the field of equine POI report on associated risk factors or have tried to evaluate the efficacy of various treatments. There remains a lack of study of the mechanisms underpinning POI in the horse, with applicable data largely extrapolated from human and rodent studies. The aims of this thesis were to study the mechanisms of POI in the horse, specifically targeting immune cells in the intestine called macrophages. These cells become activated by manipulation of the intestine during surgery, with subsequent initiation of a sequence of events which ultimately results in dysfunction of the intestine.

Firstly, the normal population of macrophages in the equine intestine was determined. Macrophages were present in all tissue layers of the intestine. Next, equine macrophages were grown in culture and their response to the toxin, lipopolysaccharide (LPS) was studied. This toxin has been shown in rodent models to activate intestinal macrophages. Equine macrophages responded to LPS as expected; however, although this response was similar to that reported for rodent macrophages, certain differences were observed between species. Next, intestinal tissue from horses undergoing abdominal surgery was collected and levels of specific genes relating to macrophage activation were measured and compared to normal horses. These results showed activation of macrophages in the intestine of horses undergoing colic surgery. In the final part of the study a therapeutic agent which targets the macrophage population in the intestine was administered to mice. This resulted in an increase in macrophages that help repair tissue.

Abstract

Post-operative ileus (POI) is the functional inhibition of propulsive intestinal motility which is a frequent occurrence following abdominal surgery in the horse and in humans. Rodent and human-derived data have shown that manipulation-induced activation of the resident *muscularis externa* (ME) macrophages in the intestine contributes to the pathophysiology of the disease. Most studies of the disease, specifically in the horse, have focussed on identification of risk factors, descriptive studies of the disease or the assessment of the efficacy of various therapeutic and prophylactic interventions. As a result, the proposed pathogenesis of equine POI is largely reliant on the translation of data from rodent models. The aims of this thesis were to identify macrophage populations in the normal equine gastrointestinal tract (GIT) and to study equine macrophage activation by stimulating equine bone marrow-derived macrophages (eqBMDMs) with lipopolysaccharide (LPS) as a model for intestinal macrophage activation.

Firstly, the normal population of macrophages in the equine GIT was determined. Using CD163 as an immunohistochemical marker for macrophages. CD163^{+ve} cells were present in all tissue layers of the equine intestine: mucosa, submucosa, ME and serosa. CD163^{+ve} cells were regularly distributed within the ME, with accumulations adjacent to the myenteric plexus, and therefore to intestinal motility effector cells such as neurons and the Interstitial Cells of Cajal.

The differentiation and survival of intestinal macrophages depends upon signals from the macrophage colony-stimulating factor (CSF-1) receptor. LPS translocation from the gut lumen is thought to be a key activator of ME macrophages. To provide a model for gut macrophages, a protocol was optimised to produce pure populations of equine bone marrow-derived macrophages (eqBMDMs) by cultivation of equine bone marrow in CSF-1. Macrophage functionality was assessed using microscopy, flow cytometry and phagocytosis assays. EqBMDMs responded to LPS stimulation with increases in expression of positive control genes, tumour necrosis factor alpha (*TNF- α*) and Indoleamine 2,3-dioxygenase (*IDO1*). The same mRNA was subjected to transcriptomic (RNA-Seq) analysis. Differential gene expression and network cluster analysis demonstrated an inflammatory response characterised by the production of pro-inflammatory cytokines such as interleukin 1 beta (IL-1 β) and interleukin 6 (IL-6). However, in contrast to rodent macrophages, eqBMDMs failed to produce nitric oxide in response to LPS, showing species-specific variation in innate immune biology.

Using these data, we compared gene expression in normal equine intestine and in intestine from horses undergoing abdominal surgery for colic (abdominal pain). Horses undergoing abdominal surgery showed evidence of increased expression of *IL-1 β* , *IL-6* and *TNF- α* in the mucosa and ME when compared to control tissue. Horses with post-operative reflux (POR), a clinical sign of POI, had increased gene expression of *IL-1 β* , *IL-6* and *TNF- α* compared to horses that did not develop POR following abdominal surgery. These preliminary data suggest that there is macrophage activation within the ME of the intestine during abdominal surgery in the horse, and that a greater activation state is present in horses that subsequently develop POR.

The final part of this study was to investigate the effect of a long-acting form of CSF-1, an Fc fusion protein (CSF1-Fc), as a potential treatment for POI using a mouse model. This work, performed in collaboration with another research group, found that mice lacking the C-C chemokine receptor type 2 (CCR2) gene, which is required for monocyte recruitment into tissues, had a longer recovery period following intestinal manipulation (IM) than wild type (WT) mice. With the administration of CSF1-Fc, infiltration of neutrophils to the ME was reduced and the number of macrophages in the ME was increased in both WT and CCR2^{-/-} mice following IM. Administration of CSF1-Fc in CCR2^{-/-} mice improved recovery of gastrointestinal transit three days following IM, to the same extent as WT mice. Network cluster analysis and RT-qPCR of the ME revealed clusters of genes induced and downregulated by CSF1-Fc, with increased expression of anti-inflammatory and pro-resolving genes after IM in WT and CCR2^{-/-} mice following treatment with CSF1-Fc.

Declaration

I declare that this thesis has been composed by myself and that the work has not been submitted for any other degree or professional qualification. I confirm that the work submitted is my own, except that included which formed part of jointly-authored publications. My contribution and those of the other authors to this work have been explicitly indicated below and in the relevant sections of the thesis. I confirm that appropriate credit has been given within this thesis where reference has been made to the work of others.

Some parts of the work presented in **Chapter 1** has previously been published in the *Equine Veterinary Journal* as 'An update on equine post-operative ileus: Definitions, pathophysiology and management', Z. M. Lisowski, R. S. Pirie, A. T. Blikslager, D. Lefebvre, D. A. Hume & N. P. H. Hudson, *Equine Veterinary Journal* 50 (3), © 2017 EVJ Ltd. Z.M.L., R.S.P. and N.P.H.H conceptualised the article. Z.M.L wrote the article. The co-authors assisted with the final version of the manuscript.

The work presented in **Chapter 6** was published in *Gut* as 'CCR2-dependent monocyte-derived macrophages resolve inflammation and restore gut motility in post-operative ileus', Farro, G., Stakenborg, M., Gomez-Pinilla, P. J., Labeeuw, E., Goverse, G., Di Giovangiulio, M., Stakenborg, N., Meroni, E., D'Errico, F., Elkrin, Y. Laoui, D., Lisowski, Z. M., Sauter, K. A., Hume, D. A., Van Ginderachter, J. A., Boeckxstaens, G. E., Matteoli, G. 66:20982109, © Article authors 2017 with permission from BMJ Publishing Group Ltd. In this publication, the work on *Ccr2*^{-/-} mice was unrelated to this project. My involvement with the publication relates to the effects of CSF1-Fc. I assisted with the measurement of gastrointestinal transit following intestinal manipulation and treatment with CSF1-Fc and assisted with the preparation and analysis of samples for flow cytometry.

Work presented in **Chapter 7** was previously published in the *Journal of Immunology* as '*Csf1r-1* mApple transgene expression and ligand binding in vivo reveal dynamics of CSF1R expression within the mononuclear phagocyte system' by Catherine A Hawley, Rocio Rojo, Anna Raper, Kristin A Sauter, Zofia M Lisowski, Kathleen Grabert, Calum C Bain, Gemma M Davis, Pieter A Louwe, Michael C Ostrowski, David A Hume, Clare Pridans, and Stephen J Jenkins. I carried out imaging of the *muscularis externa* following treatment with CSF1-Fc.

Zofia Maria Lisowski

June 2018

Acknowledgements

I am grateful to many people who have made this PhD possible. First and foremost, I must thank my supervisors Professor David Hume, Professor Scott Pirie and Dr Neil Hudson, not only for the opportunity to work on this project but for all their support, encouragement and guidance throughout. A special thank-you to Professor Tim Mair; a great mentor, who first inspired me to consider a career in research by answering a question I once asked about immune cells in the equine gastrointestinal tract with 'there's a PhD in that' and thus, planting the seed. I am grateful to the Horserace Betting Levy Board for awarding me the Veterinary Research Training Scholarship which enabled me to leave clinical practice to pursue a PhD. I would also like to thank Professor Gianluca Matteoli for his help with the work on CSF1-Fc on a mouse model of post-operative ileus, which would not have been possible without his contribution.

I would like to thank the many Humies in Maclab that all helped with 'Team Horse'. Firstly, 'Team Bone Marrow' aka Kristin, Rachel, Lindsay and Lucas. Without you guys bone marrow days would not have been possible and certainly not as entertaining. Kristin, no one looks better than you in a blue boiler suit; Rachel and Lindsay - we will never agree on what a swede or a turnip is (it is a swede); Lucas - no one can clean up a rib as well as you do and thank you for devoting so much time carrying out qPCR experiments. I would also like to say a big thank-you to Kristin and Clare, who spent time teaching me how to plan experiments and all the lab techniques I required. Thanks both for all your patience, guidance and time (and thankfully I did finally learn how to use a pipette!). Other members of the lab to thank are; Anna for her help with the flow cytometer, Kathleen, Charity, Sara and Evi for their help on tissue collection days, Steve for all his help with bioinformatics and Emily for all her support throughout, particularly through the writing process. Thanks also to the rest of Maclab (Kim, Ailsa, Mary, Mark, Bala, Rocio, Ivet, Lucy, Carola and Tim) who have no doubt helped me at some point over the past 3 years.

On a personal note, I'd like to thank my parents for all their support and advice. They are such an inspiration for both me and my sister. Without them, none of this would have been possible. I'm sure they will be relieved that after 10 years of study, this is it. Thanks to my sister, her husband and my two nieces for their entertaining Skype chats. A big thank you to Emily, Kathleen, Gurå, Rachel, Lindsay and Lucas for not only keeping me topped up with coffee and providing welcome distractions but also for their encouragement and ensuring I carried on writing!

A mention must also go to Hector and Cassie, who have been very patiently waiting for the thesis to be written, so that they can get back to long walks in the mountains again. Thank you to Jasmin, Konrad, Rowan and Moss for keeping them entertained in the meantime.

And finally, a huge thanks to my wonderful husband Stuart, for being so understanding and supportive, particularly throughout the writing up period. Just like the dogs and myself, I am sure he's looking forward to getting back out in the mountains again.

Contributions of work

Chapter 3:

- Assistance with post mortem tissue collection from horses
 - Craig Pennycook and Chandra Logie from R(D)SVS Pathology

Chapter 4:

- Assistance with post mortem tissue collection from horses
 - Craig Pennycook and Chandra Logie from R(D)SVS Pathology
- Assistance with horse bone marrow harvest (aka Team Bone Marrow)
 - Dr Kristin Sauter, Lindsey Waddell, Dr Rachel Young and Lucas Lefevre, Hume Group, The Roslin Institute
- Assistance with flow cytometry (antibody optimisation, flow cytometry, analysis)
 - Dr Anna Raper, Hume Group, The Roslin Institute
- Generation of RNA-Seq pipelines for data analysis:
 - Dr Stephen Bush, Hume Group, The Roslin Institute

Chapter 5:

- Sample collection from colic cases
 - Prof. Tim Mair, Bell Equine Veterinary Clinic, UK and
 - Clinicians at the R(D)SVS Equine hospital
- Assistance with primer design and performing qPCR
 - Lucas Lefevre, Hume Group, The Roslin Institute

Chapter 6:

- Intestinal manipulations and dissociation of *muscularis* for flow cytometry
 - Dr Giovanna Farro, Translation Research in Gastroenterology Disorders (TARGID), Belgium
- Flow cytometry
 - Dr Giovanni Farro, Michelle Stakenborg and Prof. Gianluca Matteoli, TARGID, Belgium
- Gastrointestinal transit and RNA extractions
 - Michelle Stakenborg, TARGID, Belgium
- Generation of microarray expression files for analysis:
 - Dr Stephen Bush, Hume Group, The Roslin Institute
 -

List of publications and presentations

Publications relevant to thesis

Catherine A Hawley, Rocio Rojo, Anna Raper, Kristin A Sauter, Zofia M. Lisowski, Kathleen Grabert, Calum C Bain, Gemma Davis, Michael C Ostrowski, David A Hume, Clare Pridans, Stephen J Jenkins. (2018) Csf1r-mApple transgene expression and ligand binding in vivo reveal dynamics of CSF1R expression within the mononuclear phagocyte system. *The Journal of Immunology*. 200 (6): 2209-2223 (**Appendix 9.1**)

Rachel Young, Stephen J. Bush, Lucas Lefevre, Mary E.B. McCulloch, Zofia M. Lisowski, Charity Muriuki, Lindsey A. Waddell, Kristin A. Sauter, Clare Pridans, Emily L. Clark and David A. Hume (2018) Species-Specific Transcriptional Regulation of Genes Involved in Nitric Oxide Production and Arginine Metabolism in Macrophages. *ImmunoHorizons*. 2 (1): 27-37 (**Appendix 9.2**)

Z M. Lisowski, R.S. Pirie, A.T. Blikslager, D. Lefebvre, D.A. Hume and N.P.H Hudson (2017) An update on equine post-operative ileus: Definitions, pathophysiology and management. *Equine Veterinary Journal*. 50 (3): 292-303.

Giovanna Farro, Michelle Stakenborg, Pedro J Gomez-Pinilla, Evelien Labeeuw, Gera Goverse, Martina Di Giovangiulio, Nathalie Stakenborg, Elisa Meroni, Francesca D'Errico, Yvon Elkrim, Damya Laoui, Zofia M. Lisowski, Kristin A. Sauter, David A. Hume, Jo A. Van Ginderachter, Guy E. Boeckxstaens & Gianluca Matteoli. (2017) CCR2-dependent moocyte-derived macrophages resolve inflammation and restore gut motility in post-operative ileus. *Gut*. 66 (12): 2098-2109

Publications relevant to, but not part of thesis

Clare Pridans, Anna Raper, Gemma M. Davis, Joana Alves, Kristin A. Sauter, Lucas Lefevre, Tim Regan, Stephen Meek, Linda Sutherland, Alison J. Thomson, Sara Clohisey, Stephen J. Bush, Rocío Rojo, Zofia M. Lisowski, Robert Wallace, Kathleen Grabert, Kyle R. Upton, Yi Ting Tsai, Deborah Brown, Lee B. Smith, Kim M. Summers, Neil A. Mabbott, Pedro Piccardo, Michael T. Cheeseman, Tom Burdon, David A. Hume. (2018) Pleiotropic impacts of macrophage and microglial deficiency on development in rats with targeted mutation of the Csf1r locus. *The Journal of Immunology*. DOI:10.4049/jimmunol.1701783

Lindsey A. Waddell, Lucas Lefevre, Stephen J. Bush, Anna Raper, Rachel Young, Zofia M. Lisowski, Mary E. B. McCulloch, Charity Muriuki, Kristin A. Sauter, Emily L. Clark,

Katharine M. Irvine, Clare Pridans, Jayne Hope & David A. Hume. (2018) The regulated expression of ADGRE1 (EMR1, F4/80) is a rapidly evolving gene expressed in mammalian monocyte-macrophages. *Frontiers in Immunology*. doi:10.3389/fimmu.2018.02246

Cortés-Araya Y, Amilon K, Rink BE, Black G, **Lisowski Z**, Donadeu FX, Esteves CL. (2018) Comparison of antibacterial and immunological properties of Mesenchymal Stem/Stromal cells from equine Bone Marrow, Endometrium and Adipose tissue. *Stem Cells and Development*. doi: 10.1089/scd.2017.0241

Kristin A. Sauter, Lindsey A. Waddell, **Zofia M. Lisowski**, Rachel Young, Lucas LeFevre, Gemma M. Davis, Sara M. Clohisey, Mary McCulloch, Elizabeth Magowan, Neil A. Mabbott, Kim M. Summers, & David A. Hume. (2016) Macrophage colony-stimulating factor (CSF1) controls monocyte production and maturation and the steady-state size of the liver in pigs. *American Journal of Physiology - Gastrointestinal and Liver Physiology*. 311(3): G533-47 (**Appendix 9.3**)

Clare Pridans, Gemma M. Davis, Kristin A. Sauter, **Zofia M. Lisowski**, Anna Raper, Yolanda Corripio-Miyar, Rachel Young, Mary E. McCulloch, Lucas Lefevre, Simon Lillico, Elspeth Milne, Bruce Whitelaw and David A. Hume. (2016). A Csf1r-EGFP transgene provides a novel marker for monocyte subsets in sheep. *The Journal of Immunology*. 197 (6): 2297-305.

Conference abstracts and posters

Lisowski, Z., Mair, T., Lefevre, L., Hudson, N. & Pirie, R. (Sept 2018) Activation of macrophages in the mucosa and muscularis of jejunum in horses undergoing abdominal surgery for strangulating small intestinal obstructions. Proceedings of 6th European Veterinary Immunology Workshop, Utrecht, Netherlands. (Poster Presentation) (**Appendix 9.4**)

Lisowski, Z., Sauter, K., Pridans, C., Young, R., Lefevre, L., Waddell, L., Raper, A., Hume, D., Pirie, R. & Hudson, N. (Sept 2018) Generation and characterisation of equine bone marrow-derived macrophages. Proceedings of 6th European Veterinary Immunology Workshop, Utrecht, Netherlands. (Poster Presentation) (**Appendix 9.5**)

Lisowski, Z., Bush, S., Pirie, R., Hudson, N. & Hume, D. (Sept 2018) Transcriptomic response of equine bone marrow-derived macrophages cultured in macrophage colony-stimulating factor (CSF-1) to lipopolysaccharide (LPS). Proceedings of 6th

European Veterinary Immunology Workshop, Utrecht, Netherlands. (Poster Presentation) (**Appendix 9.6**)

Lisowski Z.M., Mair T.S., Sauter K.A., Waddell L.A., Pirie R.S., Hudson N.P.H. and Hume D.A (2017), Distribution of Macrophages in the Gastrointestinal Tract of Horses. *Equine Vet Educ*, 29: 10. doi:10.1111/eve.13_12792 (**Appendix 9.7**)

(Oral presentation - presented on my behalf by T.S.Mair)

Z.M. Lisowski, C. Pridans, L.A. Waddell, R. Young, K.A. Sauter, L. Lefevre, A. Raper, E.L. Clark, N.P.H. Hudson, S.R. Pirie, D.A. Hume. (Sept 2016). Isolation and characterisation of the equine bone marrow derived macrophage. Proceedings of Cell Symposia: 100 Years of Phagocytes at Giardini Naxos, Italy. (Poster presentation) (**Appendix 9.8**)

Z.M Lisowski, K.A. Sauter, L.A Waddell, T.S Mair, R.S. Pirie, N.P.H Hudson, D.A Hume. April 2016. Distribution of macrophages in the gastrointestinal tract of normal horses. (April 2016). Proceedings of the Research Student Day - Postgraduate Presentations at the Roslin Institute and the Royal (Dick) School of Veterinary Studies (Poster presentation*) (**Appendix 9.9**)

*runner up prize for 2nd year poster award

Z.M Lisowski, R.S. Pirie, N.P.H. Hudson, D.A. Hume. (April 2015). Targeting the macrophage in equine post-operative ileus. Proceedings of the Research Student Day - Postgraduate Presentations at the Roslin Institute and the Royal (Dick) School of Veterinary Studies (Poster presentation) (**Appendix 9.10**)

Abbreviations

BCP	1-Bromo-3-chloropropane
BM	Bone marrow
BMDM	Bone marrow-derived macrophage
BMP	Bone morphogenetic protein
BMP2	Bone morphogenetic protein 2
BSA	Bovine serum albumin
CAT	Cationic arginine transporter
CCL2	Chemokine (C-C motif) ligand 2
CCR2	C-C motif chemokine receptor 2
CD	Cluster of differentiation
CDK	Cyclin-dependent kinase
CI	Confidence intervals
CNS	Central nervous system
CSF-1	Macrophage colony-stimulating factor 1
CSF1-Fc	Fc conjugate of macrophage colony-stimulating factor 1
CSF-1R	Macrophage colony-stimulating factor 1 receptor
CSF-2	Colony stimulating factor 2
DAB	3,3'-diaminobenzidine
DMP	Deep myenteric plexus
DMSO	Dimethyl sulfoxide
e-CAS	Equine macrophage cell line
EDTA	Ethylenediaminetetraacetic acid
EGF	Epidermal growth factor
EGFP	Enhanced green fluorescent protein
ENS	Enteric nervous system
eqBMDMs	Equine bone marrow-derived macrophages
FANTOM	Functional annotation of the mammalian genome
fc	Fold change
FCS	Fetal calf serum
FFPE	Formalin fixed paraffin embedded
FSC	Forward light scatter
GATHER	Gene Annotation Tool to Help Explain Relationships
GC	Geometric centre
G-CFU	Granulocyte colony forming unit
GI	Gastrointestinal
GIT	Gastrointestinal tract
GM-CFU	Granulocyte macrophage colony forming unit

GM-CSF	Granulocyte-macrophage colony-stimulating factor
GO	Gene ontology
GT	Gastrointestinal transit
H&E	Haematoxylin and eosin
HI	Heat inactivated
HS	Horse serum
i.v.	Intravenous
ICC	Interstitial cells of Cajal
IDO	Indoleamine dioxygenase
IFN	Interferon
IFN-γ	Interferon-gamma
IHC	Immunohistochemistry
IKK	I κ B kinase
iNOS	Inducible nitric oxide synthase
IRAK	Interleukin-1 receptor-associated kinase
IRF	Interferon regulatory factor
ITGAM	Integrin subunit alpha M
LBP	Lipopolysaccharide-binding protein
LP	Lamina propria
LpM	Lamina propria macrophages
LPS	Lipopolysaccharide
MAL	MyD88 adapter-like
M-CFU	Macrophage colony forming unit
MCL	Markov clustering algorithm
MCP-1	Monocyte chemoattractant protein -1
M-CSF	Macrophage-colony stimulating factor
MD2	Myeloid Differentiation Protein-2
MDM	Monocyte-derived macrophages
ME	<i>Muscularis externa</i>
MHC	Major histocompatibility complex
MM	Muscularis externa macrophages
MP	Myenteric plexus
MPS	Mononuclear phagocyte system
MTT	3-(4,5-dimethylthiazol-2-yl)-2,5-diphenyltetrazolium bromide
MyD88	Myeloid differentiation primary response 88
NF-κB	nuclear factor kappa-light-chain-enhancer of activated B cells
NGS	Normal goat serum
NK	Neurokinin receptor
NO	Nitric oxide

NOD	Nucleotide-binding oligomerization domain-like receptors
NS	Not significant
PAMP	Pathogen associated molecular pattern
PBMC	Peripheral blood mononuclear cell
PBS	Phosphate buffered saline
PCA	Principal-component analysis
PCA	Principal component analysis
PDGFRα	Platelet derived growth factor α
PFA	Paraformaldehyde
PGP 9.5	Protein gene product 9.5
POI	Post-operative ileus
PRR	Pattern recognition receptor
qRT-PCR	Quantitative reverse transcription polymerase chain reaction
r	Correlation
rcf	Relative centrifugal force
rhCSF-1	Recombinant human macrophage colony-stimulating factor 1
RIN	RNA Integrity number
RMA	Robust Multi-array Average
RNA-Seq	RNA sequencing
rpm	Revolutions per minute
RQ	Relative quantification
RT	Room temperature
SPF	Specific pathogen free
SSC	Side scatter
TANK	TRAF family member-associated NF- κ - β activator
TBS	Tris-buffered saline
TIR	The Toll/interleukin-1 receptor domain
TLR	Toll-like receptor
TNF	Tumour necrosis factor
TPM	Transcripts per million
TRAM	TRIF-related adaptor molecule
TRIF	TIR-domain-containing adapter-inducing interferon- β
WT	Wild type
β-ME	β -mercaptoethanol

List of figures

Figure 1-1 Summary of the main macrophage populations in tissues in the steady state.....	5
Figure 1-2 Expression of mApple and EGFP tagged with the <i>Csf1r</i> in adult mouse tissues ...	6
Figure 1-3 Differentiation of cells from the mononuclear phagocyte system	9
Figure 1-4 Growth factors in the mononuclear phagocyte system.....	11
Figure 1-5 Expression of the MacBlue (ECFP) transgene in the lamina propria of mice injected with CSF1-Fc.....	17
Figure 1-6 EGFP ⁺ macrophages in the intestinal lamina propria	20
Figure 1-7 Oesophagus from MacBlue mice.....	20
Figure 1-8 Comparison of expression of MacBlue and MacGreen transgenes in the small intestine.	21
Figure 2-1 Example of cell quantification method	57
Figure 3-1 Comparison of antigen retrieval techniques for CD163 staining in equine jejunum	71
Figure 3-2 CD117 staining in equine jejunum	72
Figure 3-3 PGP 9.5 staining in equine small colon	73
Figure 3-4 Distribution of CD163 ⁺ macrophages in the equine gastrointestinal tract.....	75
Figure 3-5 Distribution of CD163 ⁺ macrophages in the layers of the equine gastrointestinal tract.....	76
Figure 3-6 Lamina propria macrophages in the equine stomach, jejunum and right ventral colon	78
Figure 3-7 Morphology of lamina propria macrophages in the equine jejunum and right dorsal colon	79
Figure 3-8 Morphology of macrophages in the submucosa of the equine small intestine	80
Figure 3-9 Morphology of macrophages in the submucosa of equine large intestine.....	81
Figure 3-10 Macrophages in gut- associated lymphoid tissues in the equine large intestine	82
Figure 3-11 Macrophages in the equine <i>muscularis externa</i>	83
Figure 3-12 Serosal macrophages in the equine gastrointestinal tract.....	86
Figure 3-13 Ramified macrophages in the serosa of equine left ventral colon	87
Figure 3-14 <i>Muscularis</i> macrophages in the equine ileum.....	87

Figure 3-15 <i>Muscularis</i> macrophages in equine duodenum.....	88
Figure 3-16 Morphology of intermuscular <i>muscularis</i> macrophages in equine ileum.....	89
Figure 3-17 Macrophages associated with the myenteric plexus in the equine gastrointestinal tract	89
Figure 3-18 Morphology of myenteric plexus macrophages in the equine gastrointestinal tract	90
Figure 4-1 Workflow for isolation and characterisation of eqBMDMs	98
Figure 4-2 Effect of the addition of rhCSF-1 on eqBMDMs in culture in various media	100
Figure 4-3 Light microscopy images of eqBMDMs in different culture conditions	101
Figure 4-4 Comparison of cell survival and proliferation in culture media containing either 20% fetal calf (FCS) or 20% horse serum (HS)	102
Figure 4-5 Comparison of cell survival and proliferation in culture media containing either 10% or 20% horse serum.....	103
Figure 4-6 Analysis of cell morphology by light and confocal microscopy.....	104
Figure 4-7 Zymosan phagocytosis assay.	104
Figure 4-8 pHrodo BioParticle phagocytosis assay.	105
Figure 4-9 Gating strategy for eqBMDMs	105
Figure 4-10 Flow cytometry of equine alveolar macrophages and eqBMDMs	107
Figure 4-11 Relative quantification (RQ) of <i>TNF-α</i> , <i>IDO</i> and <i>NOS2</i> in eqBMDMs after being in culture with LPS for 7hrs	109
Figure 4-12 Nitrite production of eqBMDMs following stimulation with LPS (100ng/ml) at 7 and 24 hours	109
Figure 4-13 Principal component analysis (PCA) of LPS treated eqBMDMs and untreated eqBMDMs plotted in two dimensions.....	112
Figure 4-14 Network analysis of differentially expressed transcripts between eqBMDMs stimulated with LPS and control (unstimulated) eqBMDMs.....	113
Figure 4-15 Top 100 genes in eqBMDMs induced by LPS.....	114
Figure 4-16 Top 100 genes suppressed by LPS in eqBMDMs.....	115
Figure 4-17 Main functional groups of induced and repressed genes of eqBMDMs stimulated with LPS	117

Figure 4-18 Venn diagram of genes differentially expressed in eqBMDMs and equine alveolar macrophages stimulated with LPS	121
Figure 4-19 TPM (A) and Log ₂ fc (B) values of transcripts involved in the arginine metabolism pathway in eqBMDMs, with and without exposure to LPS	126
Figure 4-20 TPM (A) and Log ₂ fc (B) values of transcripts involved in the tryptophan metabolism pathway in eqBMDMs, with and without exposure to LPS	127
Figure 5-1 Proposed role of intra-operative factors in the neurogenic and inflammatory phases of POI.....	133
Figure 5-2 Relative gene expression of <i>IL-1B</i> , <i>IL6</i> , <i>PTGS2</i> , <i>TNF-α</i> , <i>CCL2</i> and <i>IDO1</i> in mucosa of horses undergoing intestinal surgery	136
Figure 5-3 Relative gene expression of <i>IL-1B</i> , <i>IL6</i> , <i>PTGS2</i> , <i>TNF-α</i> , <i>CCL2</i> and <i>IDO1</i> in the muscularis of horses undergoing intestinal surgery	137
Figure 5-4 Relative gene expression of <i>IL-1B</i> , <i>IL6</i> , <i>PTGS2</i> , <i>TNF-α</i> , <i>CCL2</i> and <i>IDO1</i> in the mucosa and muscularis of horses undergoing intestinal surgery	139
Figure 5-5 Effect of age on relative gene expression of <i>IL1B</i> , <i>IL6</i> , <i>PTGS2</i> , <i>TNF-α</i> , <i>CCL2</i> and <i>IDO1</i> in the <i>muscularis</i> of horses undergoing intestinal surgery.....	141
Figure 5-6 Effect of age on relative gene expression of <i>IL1B</i> , <i>IL6</i> , <i>PTGS2</i> , <i>TNF-α</i> , <i>CCL2</i> and <i>IDO1</i> in the mucosa of horses undergoing intestinal surgery	142
Figure 5-7 Effect of colic duration on relative gene expression of <i>IL1B</i> , <i>IL6</i> , <i>PTGS2</i> , <i>TNF-α</i> , <i>CCL2</i> and <i>IDO1</i> in the mucosa of horses undergoing intestinal surgery	144
Figure 5-8 Effect of colic duration on relative gene expression of <i>IL1B</i> , <i>IL6</i> , <i>PTGS2</i> , <i>TNF-α</i> , <i>CCL2</i> and <i>IDO1</i> in the muscularis of horses undergoing intestinal surgery	145
Figure 5-9 Relative gene expression of <i>IL1B</i> , <i>IL6</i> , <i>PTGS2</i> , <i>TNF-α</i> , <i>CCL2</i> and <i>IDO1</i> in the mucosa of horses presenting with and without pre-operative reflux.	146
Figure 5-10 Relative gene expression of <i>IL1B</i> , <i>IL6</i> , <i>PTGS2</i> , <i>TNF-α</i> , <i>CCL2</i> and <i>IDO1</i> in the muscularis of horses presenting with and without pre-operative reflux	147
Figure 5-11 Association of resection length and relative gene expression of <i>IL1B</i> , <i>IL6</i> , <i>PTGS2</i> , <i>TNF-α</i> , <i>CCL2</i> and <i>IDO1</i> in the mucosa of horses undergoing intestinal surgery.....	149
Figure 5-12 Association of resection length and relative gene expression of <i>IL1B</i> , <i>IL6</i> , <i>PTGS2</i> , <i>TNF-α</i> , <i>CCL2</i> and <i>IDO1</i> in the <i>muscularis</i> of horses undergoing intestinal surgery	150
Figure 5-13 Relative gene expression of <i>IL1B</i> , <i>IL6</i> , <i>PTGS2</i> , <i>TNF-α</i> , <i>CCL2</i> and <i>IDO1</i> in the mucosa of horses with and without post-operative reflux	151

Figure 5-14 Relative gene expression of <i>IL1B</i> , <i>IL6</i> , <i>PTGS2</i> , <i>TNF-α</i> , <i>CCL2</i> and <i>IDO1</i> in the <i>muscularis</i> of horses with and without post-operative reflux	152
Figure 5-15 Association of relative gene expression of <i>IL1B</i> , <i>IL6</i> , <i>PTGS2</i> , <i>TNF-α</i> , <i>CCL2</i> and <i>IDO1</i> and short-term survival	153
Figure 5-16 Association of relative gene expression of <i>IL1B</i> , <i>IL6</i> , <i>PTGS2</i> , <i>TNF-α</i> , <i>CCL2</i> and <i>IDO1</i> and short-term survival	154
Figure 6-1 Effect of CSF1-Fc on spleen and liver weights in mice	165
Figure 6-2 Effect of 3 and 5 days of CSF1-Fc administration on gastrointestinal transit times in wildtype mice.....	166
Figure 6-3 Gene expression chart for <i>Cx3cr1</i> in mouse	167
Figure 6-4 Intestinal whole mount images of the lamina propria (A) and <i>muscularis</i> (B) of the jejunum and <i>muscularis</i> of the colon (C).....	169
Figure 6-5 Intestinal whole mount imaging of the colon of MacGreen mice.....	170
Figure 6-6 Whole mount fluorescence microscopy of the intestines of mApple mice	171
Figure 6-7 Intestinal whole mount fluorescent imaging of the <i>muscularis externa</i> in MacGreen and mApple mice	172
Figure 6-8 Intestinal whole mount fluorescent imaging of the <i>muscularis externa</i> in MacGreen mouse.....	173
Figure 6-9 Intestinal whole mount fluorescent imaging of the <i>muscularis externa</i> in MacGreen mouse.....	174
Figure 6-10 Effect of CSF1-Fc on <i>muscularis externa</i> macrophages.....	176
Figure 6-11 CSF1-Fc treatment increases spleen and liver weight (Supplementary Figure 10 Farro <i>et al.</i> 2017).....	178
Figure 6-12 Colony-stimulating factor (CSF) 1 drives pro-resolving macrophage differentiation and favours recovery of GI motility (Figure 8 Farro <i>et al.</i> 2017)	179
Figure 6-13 CSF1 reduces influx of neutrophils and drives accumulation of macrophages into the <i>muscularis externa</i> during recovery after IM (Supplementary Figure 11 Farro <i>et al.</i> 2017)	180
Figure 6-14 CSF1-Fc treatment drives expression of anti-inflammatory genes in the <i>muscularis externa</i> during recovery (Supplementary Figure 12 Farro <i>et al.</i> 2017).....	181
Figure 6-15 Top genes induced and suppressed following CSF1-Fc administration in manipulated <i>muscularis externa</i>	183
Figure 9-1 $2^{-\Delta\Delta Ct}$ values of target genes from colic and control cases	289

Figure 9-2 $2^{-\Delta\Delta Ct}$ values of target genes in colic cases and non-colic control horses..... 290

List of tables

Table 1-1 Features shared by mononuclear phagocytes in tissues. Adapted from Hume, 2006	5
Table 1-2 Expression of ADGRE1 as transcripts per million (TPM) in non-human BMDMs and related cell populations. Table from Waddell <i>et al.</i> 2018).....	8
Table 1-3 Comparison of large animal genome assemblies.....	24
Table 1-4 Summary of anatomical locations and functions of ICC in the GI tract (Adapted from Ward and Sanders, 2001).....	34
Table 2-1 Details of non-colic cases used.....	45
Table 2-2 Details of colic cases.....	46
Table 2-3 Details of mouse strains used.....	47
Table 2-4 Description of anatomical locations used for tissue collection of the gastrointestinal tract.....	49
Table 2-5 Programme used for processing tissue for formalin fixed paraffin embedded tissue sections.....	53
Table 2-6 Rehydration steps for formalin fixed paraffin embedded tissue sections.....	53
Table 2-7 List of antibodies used for immunohistochemistry.....	54
Table 2-8 Dehydration program for slides (no counterstain).....	54
Table 2-9 Counterstain and dehydration program for slides.....	55
Table 2-10 Primers used in Real – Time quantitative PCR.....	60
Table 2-11 Antibodies used for flow cytometry.....	62
Table 3-1 Summary of antibodies used to identify macrophages in the GIT of species other than horse.....	67
Table 3-2 Summary of results with various antigen retrieval techniques for CD163 staining in formalin-fixed paraffin embedded equine intestinal tissue.....	70
Table 3-3 Transcripts per million (TPM) of CD163 in equine bone marrow derived macrophages cultured in CSF-1 (Data from Chapter 4).....	92
Table 4-1 Culture conditions tested for differentiation of eqBMDMs.....	99
Table 4-2 Summary of RNA-Seq transcripts.....	111
Table 4-3 TPM values for LPS inducible genes and transcription factors associated with apoptosis in eqBMDMs.....	116

Table 4-4 Effect of LPS stimulation on cyclin-dependent kinases (CDK) involved in the cell cycle in eqBMDMs	118
Table 4-5 TPM values for genes induced or repressed by LPS in eqBMDMs	119
Table 4-6 TPM values of genes involved in the neutrophilic response	121
Table 4-7 TPM values for genes involved in LPS inducible feedback in LPS stimulated eqBMDMs	123
Table 4-8 Genes associated with an increase in LPS sensitivity in mice present in eqBMDMs significantly DE gene list	124
Table 4-9 Genes associated with a decreased sensitivity to LPS in mice present in eqBMDMs significantly DE gene lists	124
Table 4-10 TPM values for genes in eqBMDMs associated with arginine (Young et al., 2018) and tryptophan metabolism	125
Table 5-1 TPM values of IDO and IL1B in eqBMDMs stimulated with LPS (Data from Chapter 4)	158
Table 6-1 Average expression values of monocyte-macrophage markers	182

Chapter 1. General Introduction

1.1 Overview

The gastrointestinal tract (GIT), which goes from the mouth through the oesophagus, stomach, small intestine, caecum, large intestine and rectum to the anus is the largest mucosal surface in the body. Its function, of absorbing nutrients and water, necessitates a simple barrier. Consequently, microbiota, food products and potentially pathogenic organisms with the capability to generate significant pathology are only a few cells away from possible translocation across the epithelial barrier. In part to deal with this threat, the resident gastrointestinal (GI) macrophages are the largest pool of tissue macrophages in the body (Lee et al., 1985). Resident intestinal macrophages are made up of two distinct populations, namely mucosal, or lamina propria macrophages (LpM) and *muscularis externa* (ME) macrophages (MM) (Gabanyi et al., 2016). LpM maintain epithelial barrier integrity and sample luminal content (Muller et al., 2014, Bain and Mowat, 2014). It is crucial to their function that they do not respond excessively to microbial stimuli to generate inflammation. Less is known about the role of MM, which are the major focus of this thesis.

Colic is a term used to describe the 'display of abdominal pain' in the horse. It usually occurs because of disruption to the normal function of the GIT because of obstruction, distention or torsion to part of the GIT, or due to abnormal intestinal motility. It is of great concern to horse owners (Mellor et al., 2001) and is reported by insurance companies and universities as the single most common cause of equine mortality (White, 1990), with a reported incidence of up to 10 cases per 100 horse years (Tinker et al., 1997, Traub-Dargatz et al., 2001). Furthermore, with the estimated cost associated with colic in the USA exceeding \$115 million dollars per annum (Traub-Dargatz et al., 2001) it is also a significant economic issue for horse owners.

Whilst most cases resolve spontaneously, or with medical treatment alone, 1.4% to 10% of horses require surgery (Hillyer et al., 2001, Traub-Dargatz et al., 2001). Any horse undergoing abdominal surgery is at risk of developing post-operative ileus (POI) which is a serious post-operative complication, not only reported in the horse but also in humans (Delaney et al., 2005, Earnshaw et al., 2015, Vather and Bissett, 2013, Vather et al., 2014, Vather et al., 2013). The term POI describes the cessation of, or reduction in, gastrointestinal transit (GT) following surgical stress (Gero et al., 2017). Activation of MM has been shown to contribute to the pathogenesis of POI following abdominal surgery (Wehner et al., 2007, Kalff et al., 2003). However, in keeping with the additional macrophage functions of tissue repair and maintaining tissue homeostasis, infiltrating monocytes (destined to become macrophages) to the

intestine are required for resolution of POI in rodent models (Farro et al., 2017). POI is a condition involving complex interactions between immune cells and motility effector cells. In addition, several pre-, intra- and post-operative factors not only further complicate its pathophysiology but also its diagnosis, treatment and management.

Efforts have been made in human medicine to establish a standardised definition of POI (Vather et al., 2013, Kehlet et al., 2005), an exercise which, based on the variation in POI definitions used amongst equine clinicians (Hunt et al., 1986, Blikslager et al., 1994, Lefebvre et al., 2016a, Merritt and Blikslager, 2008, Roussel et al., 2001, Lefebvre et al., 2016b, Freeman, 2008), also appears warranted in the field of equine veterinary medicine. In the horse, POI is almost exclusively associated with gastrointestinal (GI) surgery. In human medicine, it has also been reported following non-GI surgeries, including orthopaedic and gynaecological procedures. POI has the potential to significantly increase hospitalisation time, treatment costs and post-operative morbidity and mortality and is therefore of significant concern to both the medical and veterinary professions. The estimated financial impact of human POI in North America alone approximates US \$1.46 billion/year as a result of increased hospitalisation and treatment costs (Goldstein et al., 2007). Horses that develop POI are much less likely to survive after surgery (Morton and Blikslager, 2002, Mair and Smith, 2005c). In recent years, equine POI research has largely focused on (a) the provision of descriptive statistics relating to the syndrome (e.g. incidence and survival rates), (b) the identification of associated risk factors, and (c) determining the efficacy of certain therapeutic and prophylactic interventions. There are little research-derived data focused on the pathogenesis of the syndrome in the horse, with reliance placed on the translational application of data derived from other species.¹

1.2 Macrophages and the mononuclear phagocyte system

The mononuclear phagocyte system (MPS) is comprised of cells derived from bone marrow progenitors which differentiate into blood monocytes prior to entering the circulation before ultimately entering tissues to become resident tissue macrophages

¹ Paragraph reproduced from: An update on equine post-operative ileus: Definitions, pathophysiology and management, Z. M. Lisowski, R. S. Pirie, A. T. Blikslager, D. Lefebvre, D. A. Hume & N. P. H. Hudson, *Equine Veterinary Journal* 50 (3), © 2017 EVJ Ltd

(Van Furth, 1992). Since their discovery by Ellie Metchnikoff in the 19th Century, macrophages have been described in most tissues and organs of the body (**Figure 1-1** and **Figure 1-2**) where they may make up to 15% of the total cell population within the tissue. Their roles within the innate immune system include phagocytosis, extracellular killing and induction of inflammation. They also contribute to acquired immunity through presentation of antigen to T lymphocytes. Macrophages are also effector cells for the acquired immune system, utilising antibodies to opsonise pathogens for enhanced uptake and clearance/killing and responding to T cell products such as interferon gamma (Schroder et al., 2004, Gordon, 2003) and interleukin 4 (Gordon, 2003). They are often found in close association with epithelial surfaces, such as blood vessels and the lamina propria of the GIT. They are well adapted to detecting pathogen-associated molecular patterns (PAMP) via pattern recognition receptors (PRR) such as toll-like (TLR) and nod-like (NLR) receptors. In addition to these roles within innate and adaptive immunity, macrophages also have functions in embryonic development, tissue homeostasis and repair (Chazaud, 2014, Davies et al., 2013, Geissmann et al., 2010, Hume et al., 2002)

Macrophages distributed in tissues are referred to as resident tissue macrophages. Tissue macrophages are heterogenous in terms of function and surface marker expression (Hume, 2008a). The development of the monoclonal antibody, F4/80, first permitted the number of macrophages in tissues to be established, as well as identifying specific anatomical niches that they occupy (Hume et al., 1984). Macrophages from different tissues will all differ functionally and phenotypically as a result of their adaptation to specific functions in differing organs (Mass et al., 2016, Gosselin et al., 2014, Ginhoux and Guilliams, 2016, Guilliams and Scott, 2017). Differences in macrophage populations and functions also occur within the same tissue; lamina propria macrophages (LpM) are different to ME macrophages (MM) despite both subpopulations residing in the GIT (Gabanyi et al., 2016, Kalff et al., 1998b, Weigmann et al., 2007, Pohl et al., 2017).

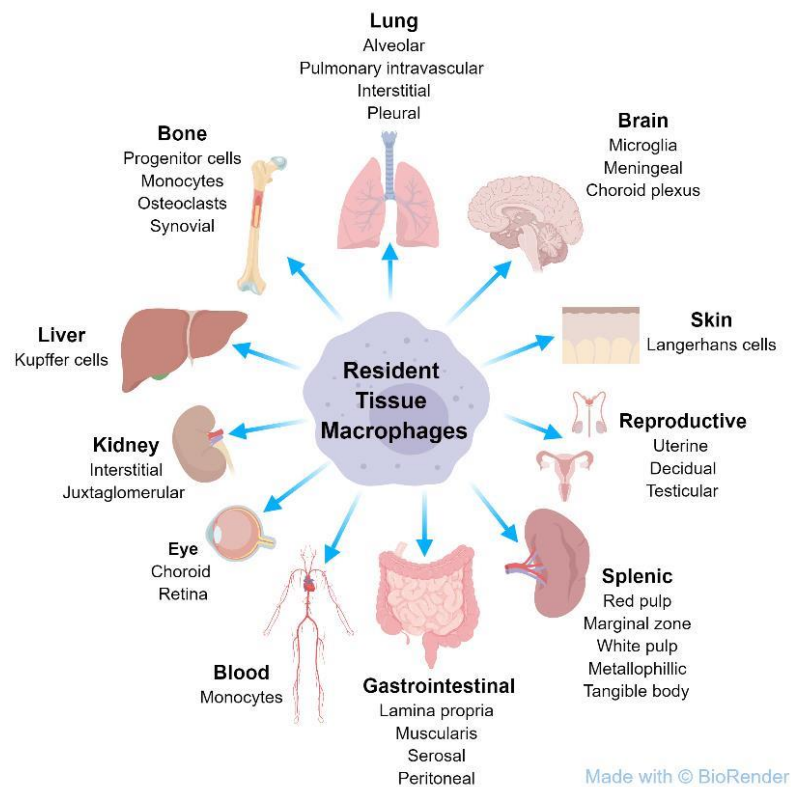


Figure 1-1 Summary of the main macrophage populations in tissues in the steady state

Macrophages are distributed throughout the body. Each tissue macrophage population will have specialised functions.

1.2.1 Identification of macrophages

Mononuclear phagocytes were originally identified by shared characteristics such as their morphology, the expression of enzymes and the non-specific uptake of particles (Table 1-1); however, none of these define a tissue macrophage (Hume, 2006). The development of monoclonal antibodies, permitting the identification of surface cell proteins, has been instrumental, not only in defining mononuclear phagocytes, but also demonstrating the diverse phenotypes attributable to these cells.

Table 1-1 Features shared by mononuclear phagocytes in tissues. Adapted from Hume, 2006

Characteristic	Description
Morphology	Stellate Ultrastructural evidence of endocytic activity
Expression of enzymes	Enzymes identified by histochemical staining: Non-specific esterase Lysosomal hydrolases Ecto-enzymes
Phagocytosis	Non-specific - uptake of latex or colloidal carbon Specific – endocytic receptors especially for the Fc portion of immunoglobulin and complement-coated particles

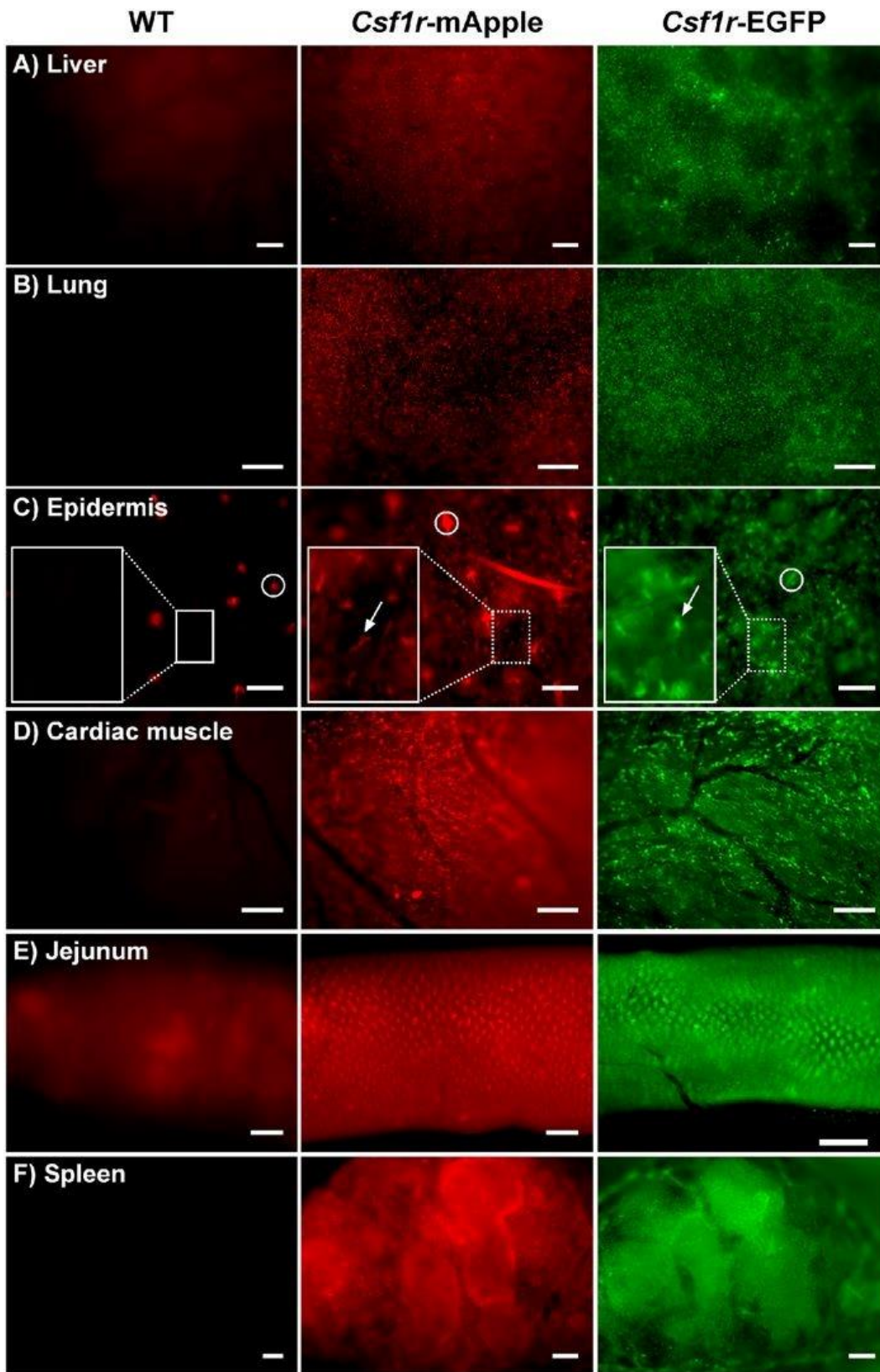


Figure 1-2 Expression of mApple and EGFP tagged with the *Csf1r* in adult mouse tissues

Distribution of *Csf1r*-mApple and *Csf1r*-EGFP transgenes throughout different tissues in the mouse. Figure adapted from Hawley *et al.* 2018. (**Appendix 9.1**)

The most commonly used marker in mice is F4/80 (Austyn and Gordon, 1981). Cloning of the mouse cDNA encoding F4/80 revealed orthology with a previously cloned human cDNA, called *Emr1*. The cDNA encodes seven calcium-binding Epidermal Growth Factor (EGF)-like domains linked to seven transmembrane domains characteristic of a G protein coupled receptor (McKnight et al., 1996). Subsequent studies identified related receptors called EGF-TM7 proteins (McKnight and Gordon, 1998), but more recently, these receptors have been reclassified to a subdivision of adhesion G protein coupled receptors (ADGRE). Therefore, F4/80 is encoded by the *Adgre1* gene (Hamann et al., 2015). Comparative analysis in the Hume laboratory, based upon RNA-Seq data, including data generated as part of this thesis (see **Chapter 4**) indicate that *ADGRE1* is expressed by macrophages in all large animals, including the horse (Waddell et al., 2018). The sequence and number of extracellular EGGF-like domains varies greatly between species ((Waddell et al., 2018). Other commonly used markers include CD68, CD11b and CD115 (Sasmono et al., 2003). In addition, CD14, CD16, CCR1, CCR2 and CX3CR1 have also been used to subgroup monocytes and macrophages in both blood and tissues (Hume, 2006, Gordon and Taylor, 2005). Species differences in marker expression exists as does variation in expression on the same mononuclear phagocyte subsets. For example, in humans, monocytes can be classified as CD14^{hi}CD16^{lo} cells and CD14^{lo}CD16^{hi} monocytes. Human monocytes will express MHC class II whereas mouse monocytes do not (Gordon and Taylor, 2005). CD14, a GPI-anchored protein and LPS co-receptor, and CD16 (Fc γ RIII), are the markers most commonly used to differentiate between monocyte subsets in both humans and mice.

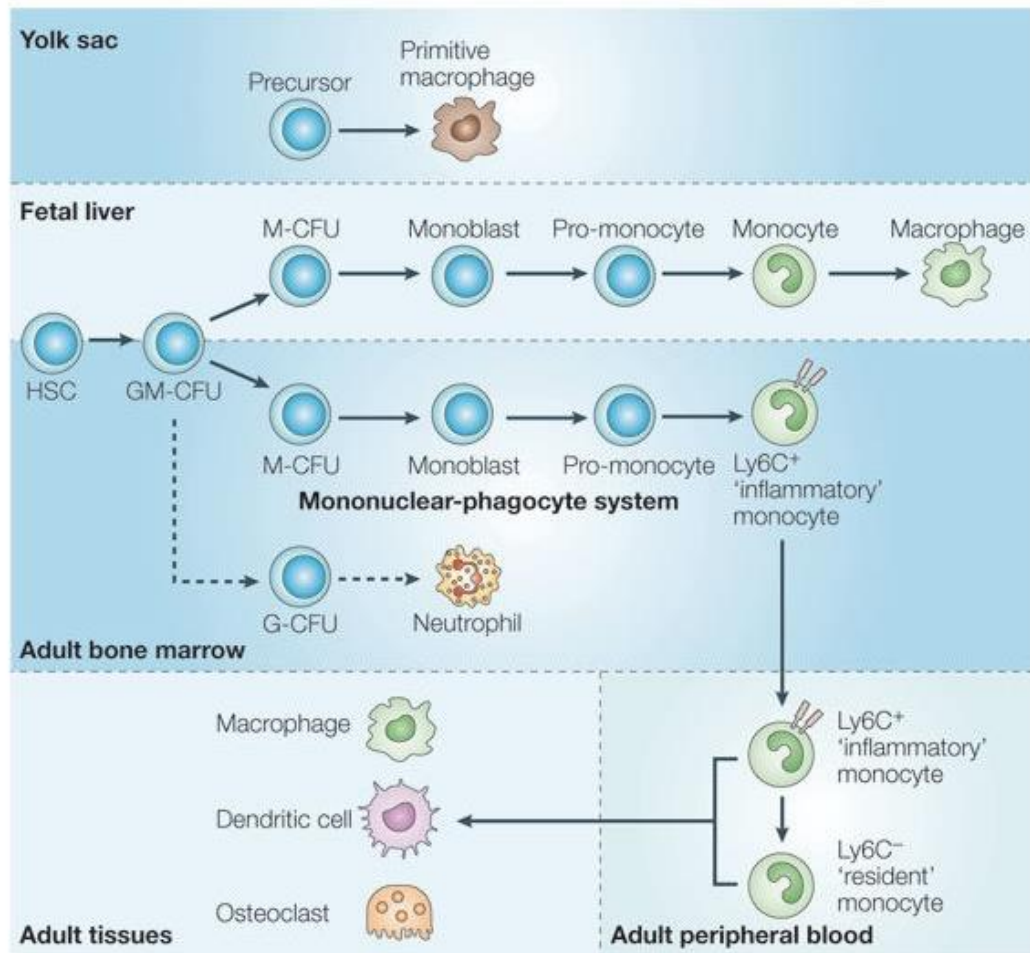
The task of categorising macrophages into ‘populations’ seems almost futile as the number of cell types that we attempt to define is exponentially related to the number of markers that we apply to those cells (Hume, 2006). Each cell has its own transcriptional profile and a cell expressing one gene does not mean another gene will, or will not, be expressed as a result.

Table 1-2 Expression of ADGRE1 as transcripts per million (TPM) in non-human BMDMs and related cell populations. Table from Waddell et al. 2018)

Species	Version	Gene name	Gene ID	BMDM	BMDM + 7 hr LPS	MDM	alveolar macrophages	alveolar macrophages + LPS	microglia	non-classical monocytes	classical (CD14+) monocytes
sheep	Oar v3.1	ADGRE1	ENSOARG00000004807	195.237	342.868	442.71 ⁸	257.591	n/a	n/a	n/a	n/a
		ADGRE4	ENSOARG00000004738	0.317	2.918	0.72	5.195	n/a	n/a	n/a	n/a
goat	ARS1	ADGRE1	rna14114	4.015	9.112	n/a	367.727	n/a	n/a	n/a	n/a
		ADGRE4	rna14115	0.077	0.154	n/a	0.133	n/a	n/a	n/a	n/a
cattle	UMD3.1	ADGRE1	ENSBTAG00000007901	18.433	97.262	n/a	n/a	n/a	n/a	n/a	n/a
		ADGRE4	ENSBTAG00000038981	4.478	2.313	n/a	n/a	n/a	n/a	n/a	n/a
buffalo	UMD_CASPUR_WB_2.0	ADGRE1	gene27167	11.671	27.825	231.65 ⁶	746.56	n/a	n/a	n/a	n/a
		ADGRE4	gene27164	0.01	0.029	0.061	0	n/a	n/a	n/a	n/a
horse	EquCab2	ADGRE1	ENSECAG00000017237	188.437	230.782	n/a	n/a	n/a	n/a	n/a	n/a
		ADGRE4	ENSECAG00000015885	4.651	2.892	n/a	n/a	n/a	n/a	n/a	n/a
pig	Sscrofa11.1	ADGRE1	ENSSCG00000013556	99.69	84.817	n/a	n/a	n/a	n/a	n/a	n/a
		ADGRE4	ENSSCG00000040016	199.336	221.096	n/a	n/a	n/a	n/a	n/a	n/a
rat	Rnor_6.0	ADGRE1	ENSRNOG00000046254	475.376	443.538	n/a	n/a	n/a	n/a	n/a	n/a
		ADGRE4	ENSRNOG00000050325	0.293	0.153	n/a	n/a	n/a	n/a	n/a	n/a
human	GRCh38.p10	ADGRE1	ENSG00000174837	n/a	n/a	n/a	32.94	54.55	6.77	125.32	49.76
		ADGRE4	ENSG00000268758	n/a	n/a	n/a	4.15	1.36	16.54	3.17	21.46

1.2.2 Macrophage origins and development

The differentiation of monocytes from CD34⁺ haematopoietic stem cells (HSCs) requires the cells to go through several distinct intermediate stages (**Figure 1-3**). Studies in mice have identified the yolk sac as the region where developing macrophages are first found (Hume et al., 1995). As the embryo develops, the fetal liver becomes the main site of haematopoiesis, in the mouse by embryonic day 10.5 to 11 (Lichanska and Hume). Once a neonate or adult, the bone marrow becomes the primary site of haematopoiesis.



Copyright © 2005 Nature Publishing Group
Nature Reviews | Immunology

Figure 1-3 Differentiation of cells from the mononuclear phagocyte system

Pluripotent haematopoietic stem cells (HSCs) differentiate into granulocyte monocyte colony forming unit (GM-CFU) before committing to more specific lineages; macrophage colony-forming unit (M-CFU) or granulocyte colony-forming unit (G-CFU). Figure reproduced with permission from Springer Nature: Nature Reviews Immunology. Monocyte and macrophage heterogeneity, Gordon, S., Taylor, P.R., Nat Rev Immunol. 5 (12), © 2005.

All monocytes are derived from the same common progenitor cell, the granulocyte macrophage colony forming unit (GM-CFU), which is also a progenitor cell for granulocytes. The GM-CFU then further commits to specific lineages of either the macrophage colony forming unit (M-CFU) or granulocyte colony forming unit (G-CFU). These committed progenitors further differentiate through monoblastic and pro-monocyte stages before becoming a monocyte/macrophage (Gordon and Taylor, 2005). The differentiation of cells from HSCs to GM-CFU, M-CFU and G-CFU requires a group of cytokines called growth factors (Barreda et al., 2004). Examples of growth factors include macrophage colony-stimulating factor (M-CSF or CSF-1), granulocyte-macrophage colony-stimulating factor (GM-CSF or CSF-2), granulocyte colony-stimulating factor (G-CSF or CSF-3) and multi colony-stimulating factor (multi-CSF or IL-3) (**Figure 1-4**).

The entry of monocytes into the circulation requires chemokine signals generated by ligands of the chemokine receptor, CCR2, which is itself a marker for the 'classical' subset of blood monocytes in both mice and humans. Mice lacking the *Ccr2* gene have reduced circulating monocytes (Serbina and Pamer, 2006). Resident tissue macrophages originate from blood monocytes (van Furth and Cohn, 1968). Cells either remain as monocytes (Ly6C^{hi} or Ly6C^{med}) in the blood or enter tissues (Ly6C^{low}) to differentiate into tissue resident macrophages (**Figure 1-3**) (Gordon and Taylor, 2005). Several papers have questioned this model of monocyte replenishment of resident tissue macrophages, instead suggesting that resident cells are embryonic in origin and maintained by local proliferation (Greter and Merad, 2013, Geissmann et al., 2010, Epelman et al., 2014, Hashimoto et al., 2013, Volkman et al., 1983). Jenkins and Hume have highlighted questions around the interpretation of lineage trace systems used to argue for the embryonic origin of tissue macrophages (Jenkins and Hume, 2014). What is clearly the case is that LpM of the intestine turn over rapidly and are constantly replaced by blood monocytes (Bain et al., 2014).

1.2.3 Colony Stimulating Factor-1 (CSF-1)

CSF-1 is the growth factor required for the differentiation, proliferation and survival of cells in the macrophage lineage (Stanley et al., 1978). Administration of recombinant human CSF-1 (rhCSF-1) to mice first highlighted its role as a circulating regulator of the mononuclear phagocyte system, whereby it resulted in a significant increase in both circulating monocytes and the tissue macrophage population (Hume et al., 1988). Its receptor, CSF-1R (or CD115) is required for definitive macrophage differentiation and is expressed in all progenitors and cells of the myeloid lineage (**Figure 1-2**), mediated by the ligands CSF-1 and IL-34. Administration of an antibody

against the CSF-1R results in depletion of both monocytes and tissue resident macrophages (MacDonald et al., 2010). The function of these ligands in macrophage development was studied in natural mutant mice ($Csf1^{op/op}$), $Csf1r$ knockout mice ($Csf1r^{-/-}/Csf1r^{-/-}$) and IL-34 ligand knockout mice. $Csf1^{op/op}$ or $Csf1r^{-/-}/Csf1r^{-/-}$ rodents highlight the importance of CSF-1 in macrophage development. These animals are deficient in tissue macrophage and osteoclast populations with pleiotropic effects on growth and development (Dai et al., 2002). The more severe $Csf1r^{-/-}/Csf1r^{-/-}$ phenotype revealed the existence of IL-34 as a second ligand of the CSF1-R (Wang et al., 2012b), thus explaining why the $Csf1r^{-/-}/Csf1r^{-/-}$ had a more severe phenotype compared to the $Csf1^{op/op}$ mouse.

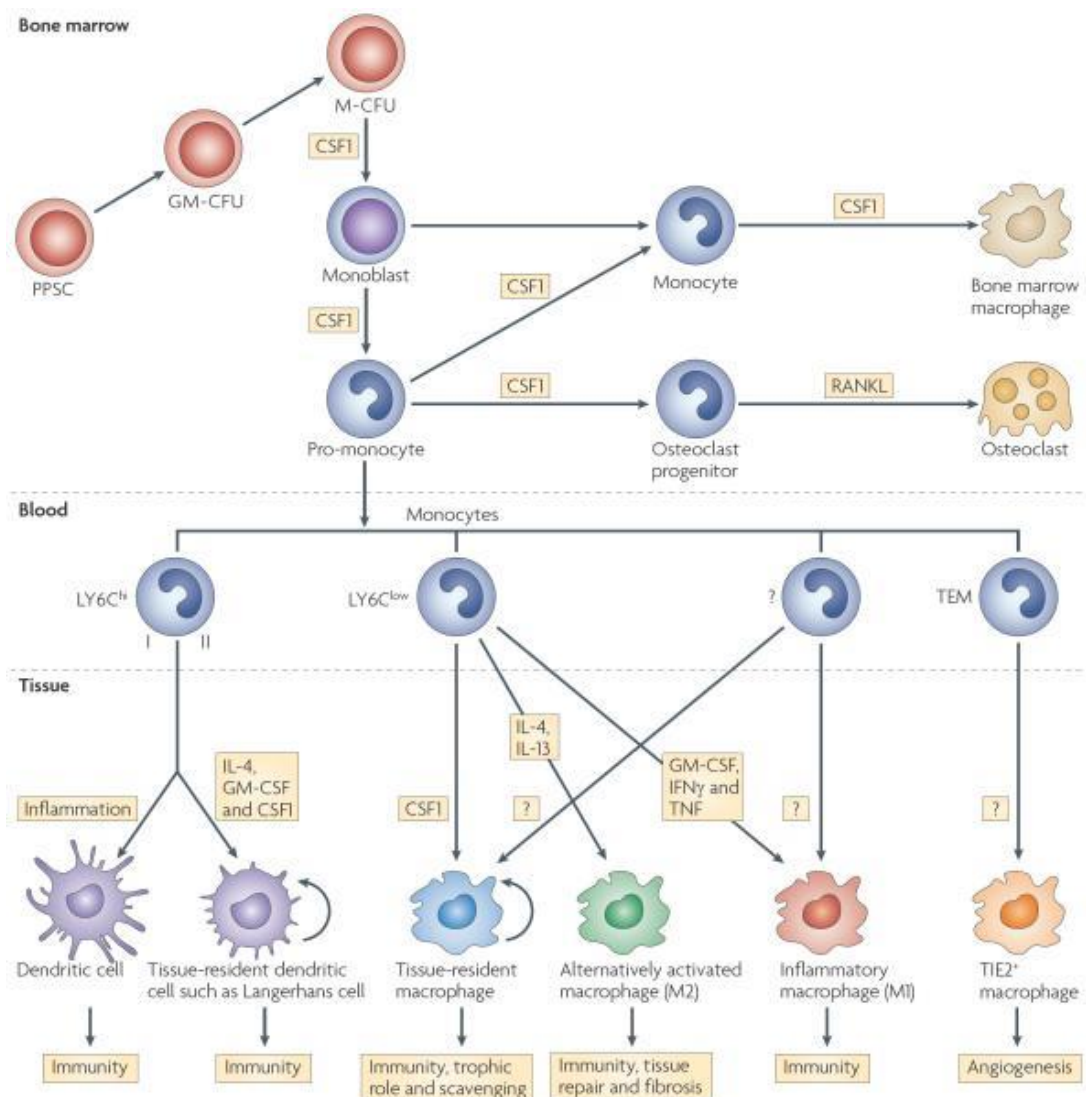


Figure 1-4 Growth factors in the mononuclear phagocyte system

Progenitor cells in the bone marrow differentiate into several lineages, under the control of growth factors. Reproduced with permission from Springer Nature: Nature Reviews Immunology. Trophic macrophages in development and disease, Pollard, J.W., Nat Rev Immunol. 9 (4), © 2009.

Recombinant human CSF-1 (rhCSF-1) has been shown to be active on several species-derived macrophages, including the horse (Kapetanovic et al., 2012, Karagianni et al., 2013, Gow et al., 2013). Cross reactivity between species is constrained in some measure by variation in sequences between species in CSF-1 and IL-34 sequences (Gow et al., 2013), although equine CSF-1 has not been cloned.

Therapeutic applications of Fc conjugate of CSF-1 (CSF1-Fc)

Tissue damage or injury triggers an inflammatory response consisting of several cell types including macrophages, neutrophils, NK Cells, B and T cells, epithelial cells and stem cells that collectively contribute to a well regulated tissue repair response (Wynn, 2008). Macrophages are critical regulators of repair and are required for tissue repair in several organs (Chazaud, 2014). Consequently, macrophages are an obvious choice as therapeutic targets.

CSF-1 is present in the circulation. In patients with liver injury, low circulating CSF-1 was associated with reduced survival (Stutchfield et al., 2015). The addition of CSF-1 to monocytes *in vitro* drives the polarisation of differentiated macrophages towards an immunosuppressive role (Hume, 2008a), and are therefore occasionally referred to in the literature as alternatively-activated (M2-like) (Martinez et al., 2006). Based on *in vitro* data, CSF-1 can be considered as a stimulus for macrophages that promote tissue repair and suppress cell-mediated immunity (Hume and MacDonald, 2012).

Several studies have evaluated the use of CSF-1 as a potential therapeutic tool in various experimental scenarios which might reflect a clinical need; these include liver disease (partial hepatectomy) (Stutchfield et al., 2015), fracture repair (Alexander et al., 2011), ischaemic kidney (Alikhan et al., 2011) and heart (Okazaki et al., 2007) injury, promotion of angiogenesis (Okuno et al., 2011) and amyloid deposition in the brain (Boissonneault et al., 2009). Resolution of POI requires monocyte-derived macrophages (Farro et al., 2017); in this study the administration of CSF1-Fc promoted tissue recovery by reducing tissue neutrophil infiltration and increasing circulating monocytes and tissue macrophages, thus promoting repair.

1.3 Macrophage activation

Disruption to tissue homeostasis by inflammation or trauma causes macrophage activation. The recognition of pathogens by macrophages is dependent on the expression of various surface and intracellular pattern recognition receptors (PRRs) that enable the macrophage to distinguish between self and non-self or

altered/damaged self. PRRs bind specifically to pathogen associated molecular patterns (PAMPs) such as lipopolysaccharide (LPS) (Eskandari et al., 1997) and damage associated molecular patterns (DAMPs) such as adenosine triphosphate (ATP) (Ozaki et al., 2004). The recognition of microorganisms, toxins, cytoplasmic PAMPs and/or endogenous DAMPs by PRR triggers a signalling cascade referred to as the inflammasome (Takeuchi and Akira, 2010). Examples of PRRs include toll-like receptors (TLRs) and nucleotide oligomerisation domain (NOD)-like receptors (Taylor et al., 2005, Zhou et al., 2015). PRRs can be divided into two classes; those that mediate phagocytosis and those that trigger an inflammatory cascade (Aderem and Ulevitch, 2000). Different PRR will recognise different microorganisms self and non-self-molecular patterns (Takeuchi and Akira, 2010). Macrophage activation is defined as the acquisition/induction of effector functions that mediate some components of T cell-mediated immunity. By analogy with the two major classes of CD4-positive helper T lymphocyte, Th1 and Th2, attempts have been made to classify macrophage activation into two polarised 'states' in the literature; classical (M1) or alternative (M2) (Mantovani et al., 2005, Mantovani et al., 2004, Gordon, 2003). Classical activation of macrophages occurs in response to microorganisms. The classical activating factors for macrophages are interferon-gamma (Schroder et al., 2004) and LPS. LPS, a component of gram-negative bacterial cell walls, is also a well characterised PAMP that leads to macrophage activation (Hume et al., 2001). The alternatively-activated macrophage is associated with the cytokines IL-4 and IL-13 (Gordon, 2003) and is associated with wound healing, fibrosis and homeostasis (Mantovani et al., 2004). However, more recently it has been argued that due to the diversity of environmental stimuli and macrophage heterogeneity that it is over simplistic to fit macrophages into either a 'classical' or 'alternative' category (Mosser and Edwards, 2008). A recent review refers to the many alternative faces of macrophage activation (Hume, 2015). An alternative model recognises that individual macrophages may exist in a broad spectrum of activation states, intermediate between or distinct from, the M1/M2 polarisation states. Indeed, intestinal macrophages for example have been characterised as having overlapping states between M1 and M2 (Bain and Mowat, 2011, Mowat and Bain, 2011).

1.3.1 LPS activation of macrophages

Pathogen associated molecular patterns

Pathogens and PAMPs are recognised by PRR, such as TLRs and NLRs. Each PRR detects specific ligands; TLR4 with its co-receptors CD14 and MD2, recognises the Lipid A part of LPS.; TLR2-TLR1 recognise microbial lipoproteins; TLR3 recognises

single or double stranded RNA; TLR5 recognises flagellin; TLR9 recognising unmethylated DNA (Kawai and Akira, 2010, Aderem and Ulevitch, 2000). Recognition of its ligand by a TLR will initiate a signalling cascade which leads to the production of cytokines and chemokines which promotes recruitment of cells to the area of inflammation (Hume, 2008b).

Toll-like receptors

The TLR receptors have been extensively studied. Ten have been identified in human and horse and 13 in mice. TLRs are broadly divided into 2 groups; TLR1,2,4,5,6, and 10 are expressed on the cell surface and predominantly recognise microbial membrane components such as lipid; and TLR3, 7, 8 and 9 are found intracellularly and mainly recognise microbial nucleic acids (Blasius and Beutler, 2010, Kawai and Akira, 2010, Miyake, 2004). Each TLR is a type 1 transmembrane protein with cytoplasmic Toll/IL-1R homology (TIR) domain. The TIR domains have several adaptors (Takeuchi and Akira, 2010):

- Myeloid differentiation primary response 88 (MyD88)
- MyD88 adapter-like (MAL) also called TIRAP
- TIR domain-containing adaptor inducing IFN- β (TRIF)
- TRIF-related adaptor molecule (TRAM)

Each TLR differs in their TIR domain-contain adapter and this results in specific responses by individual TLRs. As an example, TLR4 generates both type 1 IFN and inflammatory cytokine response whereas TLR1 mainly induces inflammatory cytokines (Kawai and Akira, 2010). TLR signalling is divided into two distinct pathways depending on the usage of MyD88 (MyD88-dependent pathway which drives the production of inflammatory cytokines) and TRIF (MyD88-independent pathway which drives the production of type 1 IFN and inflammatory cytokines) (Kawai and Akira, 2010).

MyD88-dependent TLR signalling pathway

In the MyD88-dependent pathway, MyD88 is recruited to the TIR domain, triggering the phosphorylation of IL-1 receptor associated kinases (IRAK) 4. IRAK-4 activates other kinases from the IRAK family, IRAK1 and IRAK2. These bind to TNF receptor activated factor (TRAF) 6. The IRAK-TRAF6 complex separates from the MyD88 adapter and binds to TGF β -activated kinase (TAK). The TAK complex phosphorylates I κ B kinase (IKK)- β , which in turn phosphorylates I κ B-A which is an inhibitory protein

of NF- κ B. This causes the release of NF- κ B, which translocates from the nucleus (Takeuchi and Akira, 2010, Aderem and Ulevitch, 2000).

MyD88- independent TLR signalling pathway

This pathway activates both IFN-regulatory factor (IRF) 3 and NF- κ B. Unlike TLR3, TLR4 requires TRAM to activate TRIF. Following activation of TRIF, TRIF associates with and TRAF3 and TRAF6. TRAF6 activates TAK1 for NF- κ B activation, in a similar way to the MyD88-dependent pathway. TRAF3 with TANK (a TRAF-binding protein) bridge IKK related kinases which mediate phosphorylation of IRF3. Phosphorylated IRF3 translocates to the nucleus, inducing the expression of Type 1 IFN genes (Kawai and Akira, 2010, Mogensen, 2009).

Toll-like receptor 4

The recognition of LPS by its receptor TLR4, is activated in endotoxemia as well as being involved in the activation of intestinal macrophages in POI. Mice lacking *Tlr4* do not respond to pure LPS (Deng et al., 2013, Hoshino et al., 1999). The TLR4 receptor requires its co-receptors CD14 and MD-2 to bind to the Lipid A component of LPS to form an active complex (Shimazu et al., 1999). LPS is removed from circulation in the plasma by the serum protein lipopolysaccharide binding protein (LBP) (Steinemann et al., 1994), after which the Lipid A component of LPS is transferred to the TLR4-MD2 complex via CD14 (Wright et al., 1990, Shimazu et al., 1999). The recognition of the LPS ligand results in a conformational change in the TLR4 receptor, TIR domains and results in recruitment of the adaptors TIRAP, MyD88, TRIF and TRAM (Aderem and Ulevitch, 2000, Takeuchi and Akira, 2010). TLR4 triggers both MyD88-independent and MyD88-dependent signalling.

1.3.2 Inhibitory Feedback mechanisms in response to LPS

As discussed in the section above LPS induces inflammation via the TLR4-CD14-MD2 complex. Prolonged or sustained exposure to LPS can result in tissue injury and sepsis (Bone et al., 1992, Hotchkiss and Karl, 2003). The macrophage response to LPS triggers a sequences of inducible gene expression, which occurs in waves (Baillie et al., 2017). Each wave is likely to include induced genes or transcripts that inhibit genes or transcripts already upregulated in response to LPS. A well-known inhibitory cytokine released in response to LPS is IL-10 (Bogdan et al., 1992). Other inhibitory genes that target the MyD88 signalling pathway that were upregulated in human MDMs in response to LPS include NF- κ B inhibitors (*NFKBIA*, *NFKBIB*, *NFKBIE*, *NFKBIZ*, *BCL3*), multiple members of the TRIM family of E3 ubiquitin ligases which promote

degradation of signalling molecules (*TRIM5*, *TRIM10*, *TRIM25*, *TRIM35*, *TRIM36*, *TRIM38*) and the TRAF inhibitor *TANK* (Baillie et al., 2017).

Macrophages *in vivo* can develop 'endotoxin tolerance', whereby they become refractory to subsequent endotoxin challenges which provides some protection against continued LPS exposure. These macrophages show a down regulation in inflammatory cytokines (e.g. TNF- α , IL-6) and an upregulation in anti-inflammatory cytokines (e.g. IL-10) (Biswas and Lopez-Collazo, 2009).

1.4 Resident Intestinal Macrophages

Intestinal macrophages are tissue resident macrophages i.e. macrophages that occur in specific sites in normal, non-inflamed tissue. They are heterogeneous, as a consequence of tissue and anatomical specific functions that are integral to tissue homeostasis (Davies et al., 2013). The GIT, although an internal organ, has the largest surface area in contact with the external environment of all the body organs. This provides a vast and constant antigenic challenge. It is therefore not surprising that the GIT has the largest number of immune cells and represents the largest reservoir of mononuclear phagocytes in the body (Lee et al., 1985), comprised of two phenotypically-distinct groups: LpM and MM. LpMs have been extensively studied (LeFevre et al., 1979, Hume, 1985, Hume et al., 1987, Pavli et al., 1990, Smith et al., 1997, Smith et al., 2001, Denning et al., 2007, Geem et al., 2012, Bain et al., 2014, Bain and Mowat, 2012). The recent increasing knowledge base regarding MM has clearly demonstrated their significance in inflammation of the GIT, particularly in POI (Behrendt et al., 2004, Cailotto et al., 2014, Eskandari et al., 1997, Farro et al., 2017, Gabanyi et al., 2016, Hoffman and Fleming, 2010, Hori et al., Kalff et al., 1999b, Kalff et al., 1999a, Kalff et al., 1998b, Kalff et al., 2003, Matteoli et al., 2014, Pohl et al., 2017).

1.4.1 Ontogeny of resident intestinal macrophages

In the mouse, Ly6C^{hi} monocytes replenish LpMs in inflamed and steady-state tissue where they differentiate into F4/80^{hi} CXC3CR1^{hi} MHCII^{+ve} macrophages, which show phagocytic activity and are resistant to TLR stimulation (Bain et al., 2014). Upon consideration of the lifespan of embryonic-derived macrophages in the intestine, it became clear that cells of embryonic origin failed to persist in adulthood. Rather these cells were replenished by infiltration of monocyte-derived macrophages, a process that was dependent on the CCR2 receptor and commensal microbiota (Bain et al., 2014). However, there remains two theories regarding the ontogeny of MMs.

Firstly, those that arise from progenitors in the bone marrow, with infiltrating monocytes representing the immediate precursors of tissue macrophages (as in the lamina propria (LP) of the intestine) (Bain et al., 2014). Secondly, those that arise from embryonic precursors during embryonic development with subsequent self-renewal of this tissue population with little or no influx from blood monocytes (Jenkins and Hume, 2014). The relative contribution of either mechanism to the ultimate establishment of the tissue macrophage population remains to be fully determined. Whilst no studies have addressed this question directly, administration of CSF1-Fc in adult mice only resulted in an influx of monocytes into the LP, yet not the ME (Figure 1-5) (Sauter et al., 2014). Whilst not conclusive, it suggests that MM are not renewed by monocytes. Alternatively, there is replacement of the MM; however, due to a lower turnover of cells, this is less apparent than the influx observed with the LpMs.

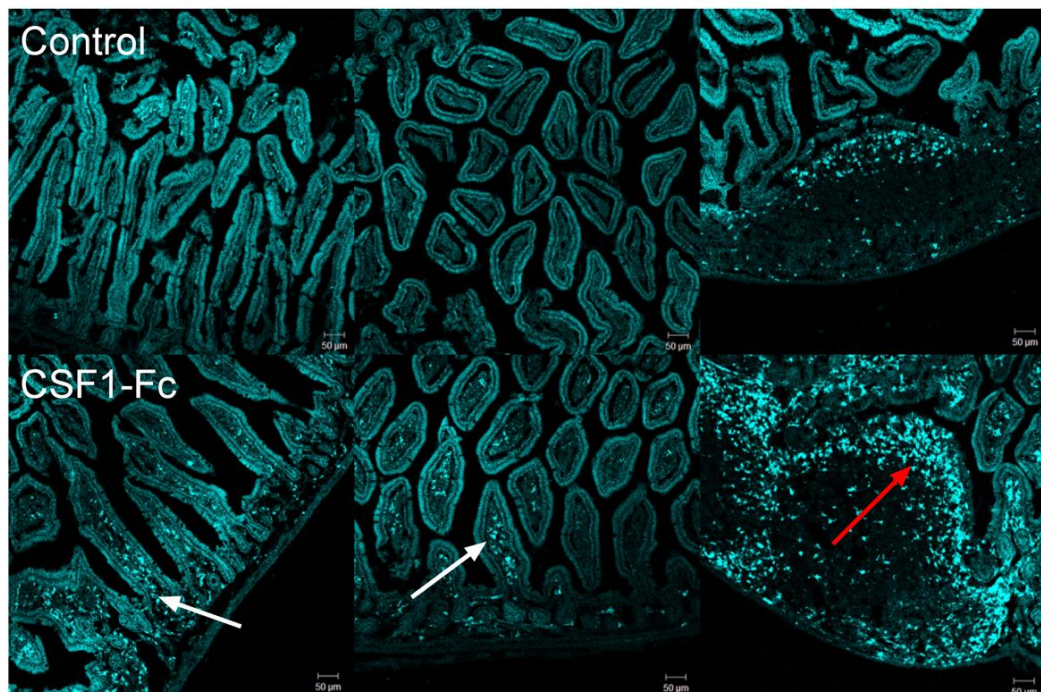


Figure 1-5 Expression of the MacBlue (ECFP) transgene in the lamina propria of mice injected with CSF1-Fc

Mice were injected with CSF1-Fc or PBS for 4 days prior to sacrifice. Tissues were examined via confocal microscopy for expression of ECFP. CSF1-Fc administration increased expression of ECFP in the lamina propria of the intestine. White arrow: villi. Red arrow: sub-epithelial dome. Image adapted from Sauter *et al.* 2014.

1.4.2 Distribution of resident intestinal macrophages

LpM are found in the mucosa of the GI tract, predominantly in the LP (Hume et al., 1984). LpM numbers differ between the small intestine and colon of rodents and humans, with higher numbers of macrophages found in the colon (Bain and Mowat,

2011). Macrophage numbers in the human colon appear to be similar throughout its length, whereas in the mouse there appears to be a continuous increasing density from proximal to distal ends of the entire mouse intestine (Nagashima et al., 1996, Bain et al., 2014).

Several studies investigating the phenotype of LpMs have shown them to differ from other tissue macrophages (Rogler et al., 1998). Unlike other tissue macrophages, they appear to be in a state of 'hypo-responsiveness' (Kristek et al., 2015). Macrophages isolated from the jejunum of both mice and humans express CD163, do not express either CD16 (Mahida et al., 1989) or CD14 (Smith et al., 1997) and low numbers express CD11b (Malizia et al., 1991). As CD14 promotes LPS binding and intestinal luminal fluid can contain large amounts of bacteria, the absence of CD14 prevents the LpMs from being in a constant state of activation. Furthermore, LpMs do not express TLR4 (which also detects LPS) (Schenk and Mueller, 2007) and TLR2 is also down regulated (Abreu et al., 2005). A gene expression study in the pig found that the number of genes for C-type lectins including *CLEC7A* (dectin), *CD68* (macrosialin) and *SIGLEC1* (sialoadhesin) were down regulated in the GIT, compared to alveolar macrophages, again suggesting intestinal macrophages are adapted to be hypo-responsive to intestinal luminal contents (Freeman et al., 2012).

MM in the mouse are located in the serosa, at the level of the myenteric plexus (MP) and in the circular muscle layer. Macrophages are regularly distributed in the serosa and MP and in close association with ICC (Mikkelsen, 1995, Kalff et al., 1998b). In addition, MMs within the smooth muscle were observed to encircle blood vessels penetrating the smooth muscle (Kalff et al., 1998b). In adult mice, multiple markers for identification of MM have been used. In adult mice MM, are constitutively MHCII⁺, F4/80⁺, CD11b⁺ and CD169⁺ (Mikkelsen, 2010) with two different subtypes proposed, depending on the state of activation (Mikkelsen et al., 2008). In the human, CD68⁺ and CD11b⁺ cells have been identified in the serosa, muscle layers, the connective tissue of the serosa and submucosa as well as in the lining of Auerbach's Plexus. MHCII⁺ cells were scarce in the serosa and submucosa (Mikkelsen, 2010). Interestingly, MMs may participate in endotoxin-mediated responses within the *muscularis* as just over half were identified to express the CD14 receptor (Kalff et al., 1998b).

There are little data relating to the distribution of macrophages in the normal horse GIT. Macrophages have been found in the mucosa of the colon (Grosche et al., 2011) and jejunum (Packer et al., 2005). They have been identified in the ME, however, their distribution has not been described in detail (Yamate et al., 2000).

1.4.3 CSF-1 regulates intestinal macrophage homeostasis

An important element in the homeostasis of resident macrophage populations is the regulator CSF-1. As previously mentioned, CSF-1 controls proliferation, differentiation, adaptation and survival of cells in the mononuclear phagocyte system. The majority of cells designated as mononuclear phagocytes express the CSF-1 receptor (CSF-1R). Treatment of mice with an antibody against CSF-1R resulted in an almost complete disappearance of the *Csf1r*-EGFP-positive stellate macrophage population in the small intestine (MacDonald et al., 2010).

1.5 Macrophage reporter mice

The development of Mac-Green (Sasmono et al., 2003), mApple (Hawley et al., 2018) and Mac-Blue (Sauter et al., 2014) transgenic mice has permitted the detection of macrophages in embryos through to adult mice (**Figure 1-2**). In Mac-Green and mApple mice the *Csf-1r* promoter (encoded by the *c-fms* proto-oncogene) directs expression of enhanced green fluorescent protein (EGFP) to cells of the mononuclear phagocyte lineage. The Mac-Blue mice use the Mac-Green transgene to create a binary transgene in which the *Csf-1r* promoter driving the transcription factor, gal4-VP16, is integrated with a Gal4-responsive UAS-CFP (cyan fluorescent protein) cassette.

In Mac-Green and mApple adult mice, EGFP and mApple was detected in all of the major macrophage populations of the body (**Figure 1-2**) (Sasmono et al., 2003, Hawley et al., 2018). Within the intestine, there was a large population of macrophages in the intestinal lamina propria (**Figure 1-6**) (Sasmono et al., 2003). In the adult Mac-Blue mice, CFP was expressed in monocytes (both Ly6C⁺ and Ly6C⁻) and in a large majority of microglia and Langerhans cells (Sauter et al., 2014). However, CFP expression was lost from most tissue macrophages, including those in the intestine (**Figure 1-8**). Those that were positive were identified as classical dendritic cells or blood monocytes. Immunohistochemistry showed large numbers of CFP⁺ cells in the Peyer's patch and isolated lymphoid follicles. CFP⁺ cells were visible in the ME of the oesophagus in adult mice (**Figure 1-7**).

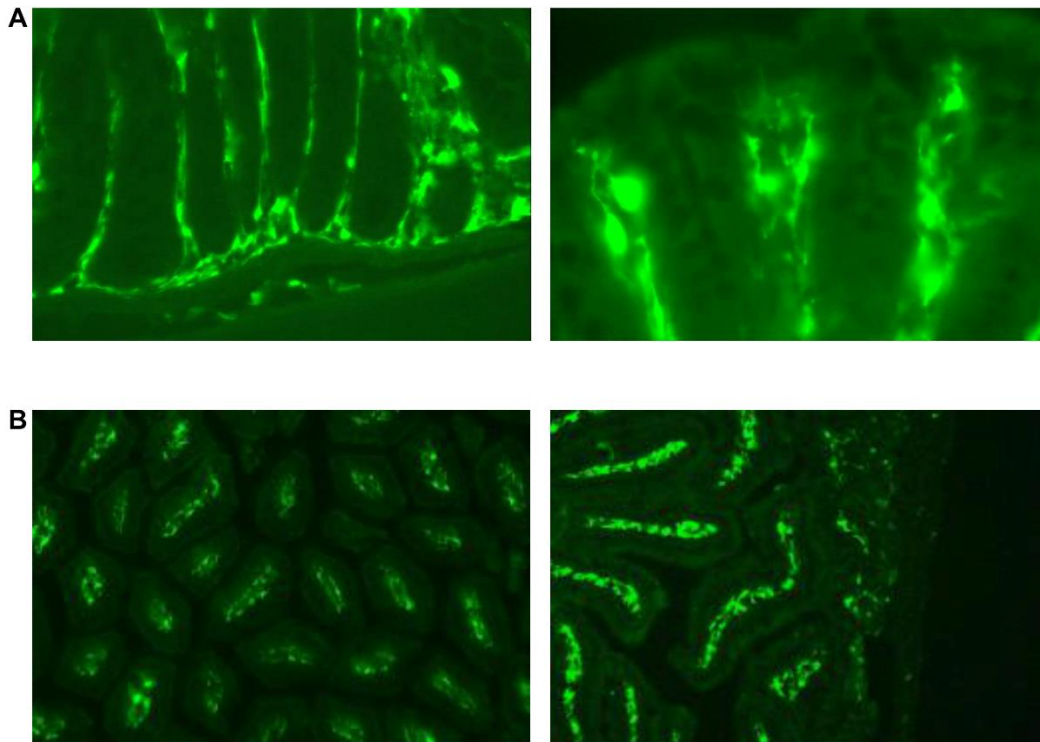


Figure 1-6 EGFP⁺ macrophages in the intestinal lamina propria

EGFP-positive macrophages in the lamina propria of the colon (A) and small intestine (B). Images on the left are low magnification. Images on right are high magnification. Images reproduced from www.macrophages.com (Robert *et al.* 2011).

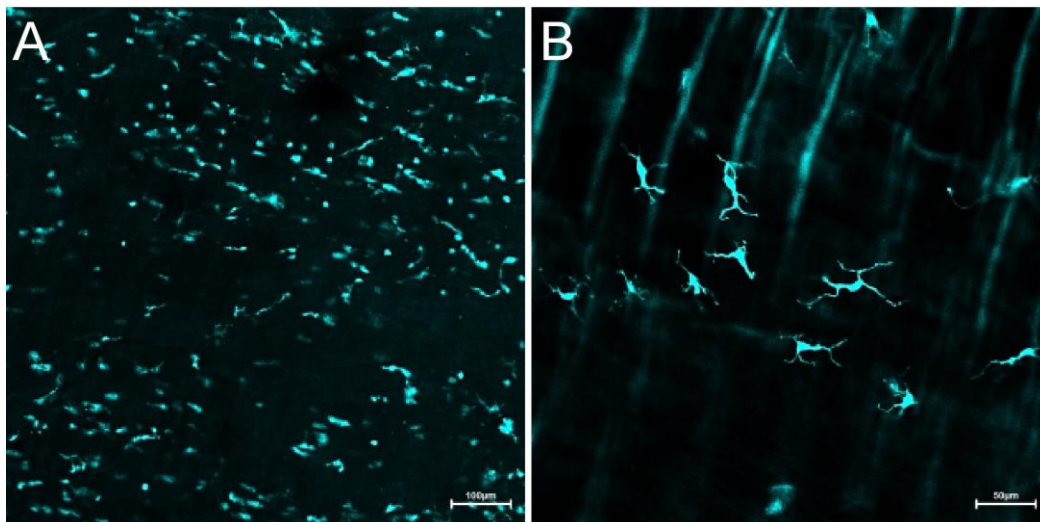


Figure 1-7 Oesophagus from MacBlue mice

ECFP expression examined in the submucosa (A) and *muscularis* (B) of MacBlue mice. Image adapted from Sauter *et al.* 2014.

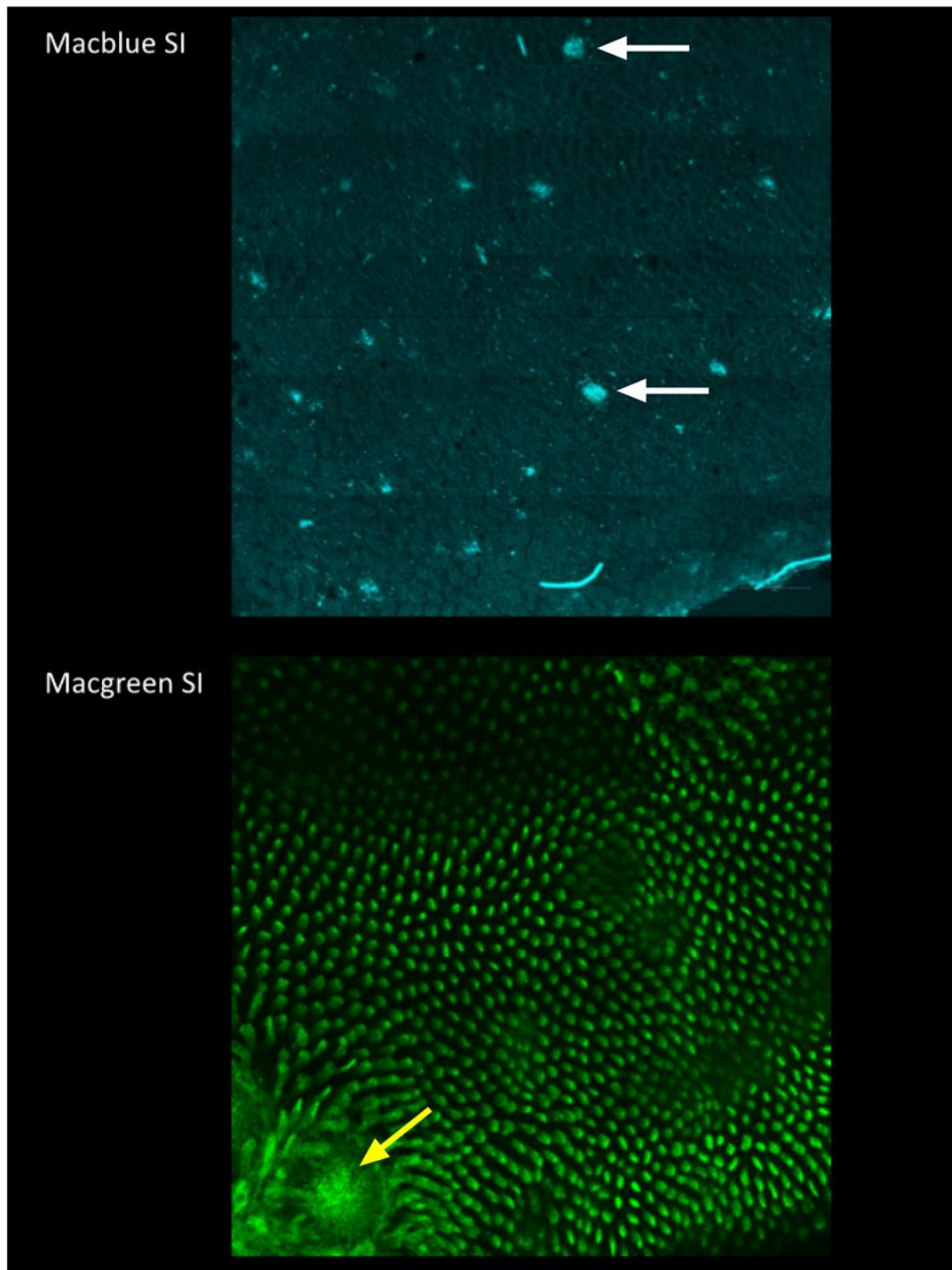


Figure 1-8 Comparison of expression of MacBlue and MacGreen transgenes in the small intestine.

White arrows indicate isolated lymphoid follicles in the MacBlue mouse. Yellow arrow indicates the dome region of a Peyer's patch in the MacGreen. The large numbers of EGFP^{+ve} macrophages in the lamina propria highlight the individual villi in the lower image. Image reproduced from Sauter *et al.* 2014.

1.6 Response of equine macrophages to LPS

Studies of equine macrophages to date have included monocyte-derived macrophages (MDMs) (Watson et al., 1990, Raabe et al., 1998, Moore et al., 2003, May et al., 1990), a macrophage cell line derived from equine bone marrow cells (eCAS) (Werners et al., 2004), alveolar macrophages (Watson et al., 1990, Karagianni et al., 2017) and peritoneal macrophages (Karagianni et al., 2013). In comparison to rodents, humans and horses are sensitive to LPS. The lethal estimated dose of LPS in humans is thought to be 1-2 μ g (Dinges and Schlievert, 2001) and 50-200 μ g/kg in the horse (Burrows, 1981). In contrast, the LD₅₀ dose in the mouse is 25.6mg/kg (Tateda et al., 1996).

The Lipid A component of LPS is detected by macrophages by the PRR TLR4 and the co-receptors, CD14 and MD2. The Lipid A component varies in structure in different bacterial species. This results in varying host responses at the TLR4 (Bryant et al., 2010). These variations in Lipid A structure also results in differences between species in ligand recognition. For example, the Lipid A from *Salmonella enterica* serovar Typhimurium (*S. Typhimurium*) is an agonist in all species. The Lipid IVa structure of *Escherichia coli* is a partial agonist in horses (Walsh et al., 2008) whereas in humans it is a full antagonist (Kovach et al., 1990) and a full agonist in mice (Vogel et al., 1984). Again, differences in *Rhodobacter sphaeroides* Lipid A recognition also exist between mice, humans and the horse (Lohmann et al., 2007) Likewise, there are species differences in the recognition of lipopeptides by the PRRs TLR2 and TLR1 (Irvine et al., 2013). Walsh *et al.* (2008) found sequence differences in the MD2-TLR4 complex between species. A consequence of these differences was variation in the local charge distribution on the MD2-TLR4 complex. This suggests that the ability of Lipid IVa recognition and subsequent signal transduction is governed by electrostatic forces and partial contact of the ligand to the MD2-TLR4 complex interface is the cause of reduced signalling and the reason for differences in response to Lipid IVa between species (Walsh et al., 2008). The full clinical significance of these differences is not yet fully understood. However, variation in innate immunity between species clearly exists and that these differences may affect how equids deal with LPS, or indeed other PAMPs and DAMPs. These differences may necessitate alternative therapeutic targets.

In response to PAMPs such as LPS, TLRs in macrophages initiate a signalling cascade through either MyD88 and TRIF-dependent pathways. These pathways trigger the transcription factor NF- κ B, resulting in proinflammatory cytokine and chemokine release (Mogensen, 2009, Mantovani et al., 2004). MyD88 associated cytokines include

TNF- α , IL-10, IL-1 β and IL-6 whilst TRIF associated genes include IFN- β , IP-10, RANTES and TRAF1 (Figueiredo et al., 2009, Mogensen, 2009). In contrast to monocytes derived from other species, equine monocytes predominantly respond via the MyD88 pathway (Figueiredo et al., 2009).

1.7 RNA-Seq and microarray analysis

In 2006, the first horse to be sequenced was Twilight, a Thoroughbred mare. A second horse, a Quarter Horse, was sequenced in 2015 as part of the Horse Genome Project by the Broad Institute (<https://www.broadinstitute.org/horse/horse-genome-project>). In total, 85% of the horse genome has been sequenced, with the remainder proving difficult to sequence (Ramery et al., 2009). The next challenge is to annotate the sequences, a process which is currently in progress by the Horse Genome Project. In comparison to other species, coverage of the horse genome is poor (6.8x in the horse compared to 166.0x in the sheep [Table 1-3]).

Differences in a cell's state can be correlated to changes in mRNA levels of genes (DeRisi et al., 1997). Microarrays can be used to measure expression changes in genes and preliminary microarray studies in the horse used provisionally annotated genes (Gu and Bertone, 2004). These preliminary findings facilitated further annotation of the genome including a multi-tissue gene expression atlas (Huang et al., 2008). An alternative to equine-specific microarrays is to use human or mouse microarrays (Barrey et al., 2006). Microarray analysis is limited to the identification of sequences that the array is designed to detect, meaning genes not annotated to the genome will not be detected (Bumgarner, 2013). Given the poor annotation of the horse genome, this limits the information microarray analysis can provide. RNA-Seq analysis provides an advantage over microarray analysis in that whole transcriptome analysis can be performed without previous fore-knowledge of the transcriptome, and is therefore useful in species, such as the horse, that have an incomplete annotation (Coleman et al., 2013). Reads from the RNA-Seq analysis can either be mapped to the current genome or a *de novo* assembly can be performed. A recent example is the high-resolution atlas for sheep, which is the largest transcriptomic dataset for any livestock species (Clark et al., 2017). This transcriptomic dataset improved the annotation of the current reference genome for sheep. By improving the transcriptome, it is possible to annotate the functional elements of the genome. Whilst not on the same scale as the sheep atlas, several studies have contributed towards improving the equine transcriptome using single and pooled tissues,

including lamellar tissue, peripheral blood, brainstem, cerebellum, muscle and skin (Mansour et al., 2017).

Table 1-3 Comparison of large animal genome assemblies

	Ovis aries (Sheep)	Sus scrofa (Pig)	Bos Taurus (Cow)	Equus caballus (Horse)
<i>Assembly</i>	Oar_vv4.0	Sscrofa11	Bos_taurus_UM D_3.1.1	EquCab2.0
<i>Coverage</i>	166.0x	65.0x	9x	6.8x
<i>Genome size</i>	3 Gb	2.6 Gb	3 Gb	2.5-2.7 Gb
<i>Total sequence length</i>	2,615,516,299	2,501,912,388	2,615,516,299	2,474,929,062
<i>Total assembly gap length</i>	28,000,626	29,864,641	28,000,626	46,138,889
<i>Gaps between scaffolds</i>	0	93	0	51
<i>Number of scaffolds</i>	5,466	706	5,466	9,688
<i>Scaffold N50</i>	100,009,711	88,231,837	100,009,711	46,749,900
<i>Scaffold L50</i>	8	9	8	19
<i>Number of contigs</i>	48,482	1,118	48,482	55,317
<i>Contig N50</i>	150,472	48,231,277	150,472	112,381
<i>Contig L50</i>	5,008	15	5,008	6,246
<i>Total number of chromosomes and plasmids</i>	28	21	28	33

In the horse, RNA-Seq analysis and Next-Generation sequencing have been used to study the LPS response in equine peripheral blood mononuclear cells (PBMCs) (Parkinson et al., 2017, Pacholewska et al., 2017). Parkinson *et al.* discovered that LPS induced the upregulation of miR-155, a finding consistent with human- and mouse-derived data (Parkinson et al., 2017). Pacholewska *et al.* also reported some similarity to humans with respect to the response of equine PBMCs to LPS (Pacholewska et al., 2017). Whilst mice are commonly used as models of human disease, in light of the similarities between horse and human LPS responses, these data suggest that the horse may be a more appropriate model for human inflammatory disease.

1.8 Definitions and clinical features of post-operative ileus²

1.8.1 General and human

The word ileus derives from the Greek word *εἰλεός* or *eileós* (meaning “twisting” or “rolling”) and was initially defined in human medicine as “severe and prolonged twisting of the intestine”. The term could be applied to several conditions (e.g. intussusception, volvulus) which shared several presenting symptoms. This particular use of the term ceased in the 19th century following the adoption of a classification system of intestinal obstruction based on specific cause (Ballantyne, 1984) and more recently its use was further restricted to a state of reduced or absent peristalsis as a result of a non-mechanical pathological response of the GI tract (Gero et al., 2017, Livingston and Passaro, 1990). Consequently, the majority of references to the term POI in current literature define the syndrome as a delay in the return of normal GI motility following surgery, or ‘a syndrome of functional inhibition of propulsive bowel motility’ (Livingston and Passaro, 1990).

In humans, overall intestinal motility should be normal by 5 days post-operatively. The small intestine (SI) recovers within 5 -10 hours, followed by return of gastric function at 24 - 48 hours, with a more prolonged time for restoration of colonic function (3-5 days) (Nachlas et al., 1972, Waldhausen et al., 1990). Defaecation and tolerance of solid food ingestion are considered to reflect recovery of GIT motility following surgery in humans and are regarded as appropriate primary outcome measures in clinical trials of POI and decision-informing criteria relating to readiness for discharge (van Bree et al., 2014).

In humans, various additional qualifying terms have been applied to POI, such as ‘physiological (or normal) POI’, ‘pathological (or prolonged) POI’ (PPOI) and ‘recurrent PPOI’ (RPPOI). The criteria used for classification vary greatly, which probably contributes to the disparity in certain study-derived data. For example, the reported prevalence of human POI ranges from 2% to 60% depending on the POI or PPOI descriptors applied in the study (Vather and Bissett, 2013, Venara et al., 2016). Efforts

² Reproduced from: An update on equine post-operative ileus: Definitions, pathophysiology and management, Z. M. Lisowski, R. S. Pirie, A. T. Blikslager, D. Lefebvre, D. A. Hume & N. P. H. Hudson, *Equine Veterinary Journal* 50 (3), © 2017 EVJ Ltd

to establish more specific criteria for each of these POI subcategories (Vather et al., 2013) might facilitate comparisons between individual studies.

1.8.2 Equine

Similar differences in diagnostic criteria probably underlie marked variation (0 – 62%) in the reported equine POI prevalence rates following abdominal surgery. The presence of nasogastric reflux on intubation represents a universally-applied diagnostic criterion which, along with ultrasonographic and palpable (via *per rectum* examination) evidence of distended SI are the most commonly applied diagnostic indications (Lefebvre et al., 2016a, Lefebvre et al., 2016b). The ambiguity in POI definition is largely attributable to variations in the volume or rate of reflux as well as the inclusion or omission of associated clinical signs such as tachycardia and abdominal discomfort. There is a wide disparity in the volume of reflux considered to reflect the presence of POI, either on a single intubation and/or over multiple intubations within a 24-hour period. In an effort to standardise the definition of POI across all studies, Merritt and Blikslager (2008) proposed the following clinical criteria: gastric reflux of ≥ 4 l upon any given intubation, or >2 l/h on repeated intubation, of gastric contents of pH >4.0 ; persistent tachycardia (>40 beats/min); mild to severe signs of abdominal discomfort; rectal and/or ultrasonographic evidence of multiple loops of fluid distended small bowel (Merritt and Blikslager, 2008). Recent surveys of European and American equine clinical specialists confirmed the presence of nasogastric reflux as the most important criterion for defining POI but there was no consensus with respect to the rate and volume of reflux adopted as diagnostic markers (Lefebvre et al., 2016a, Lefebvre et al., 2016b). Agreement on, and adherence to, a universal syndrome definition would be a significant advance in equine POI research.

The term post-operative reflux (POR), proposed to describe solely the presence of reflux following surgery without any causal assumptions (Freeman, 2017) includes both mechanical obstructions and functional motility inhibition as potential underlying mechanisms. In the interest of clarity, this thesis will focus on POI; namely, the functional inhibition of motility following abdominal surgery.

As in humans, a transient decrease in intestinal motility likely occurs normally following equine abdominal surgery. Data are available on the influence of anaesthesia (with or without orthopaedic surgery) on the GIT motility. Orally-administered chromium oxide was detected in faeces for 18-90 hours following general anaesthesia alone (Teixeira Neto et al., 2004) and 15-105 hours following

general anaesthesia (isoflurane) and orthopaedic surgery (Durongphongtorn et al., 2006). Following experimental jejunocecostomy, Sasaki *et al.* (2008) demonstrated an immediate reduction in caecal motility which lasted 2 days; this was followed by an unstable period lasting 7 days and then a period of gradual recovery lasting up to 31 days (Sasaki et al., 2008). However, unlike humans, where large intestinal (LI) dysmotility is commonly recognised and reflected in a delay in defaecation (van Bree et al., 2014, Waldhausen et al., 1990), the clinical significance of POI in the horse is predominantly related to the SI. Therefore, data on the time taken for normal restoration of SI motility in a cohort of horses following abdominal surgery would have greater clinical relevance.

The greater clinical significance of SI dysmotility in equine POI may mask LI involvement. Nelson *et al.* (2013) demonstrated a greater delay in post-operative passage of first faeces in horses which had post-operative GI complications, compared with those that did not, following elective non-GI surgery (Nelson et al., 2013). Little *et al.* (2001) independently demonstrated only a 12% prevalence of post-operative colic in horses with reduced faecal output following non-GI surgery (Little et al., 2001). Faecal output measurement might enable the early identification of cases with 'LI POI', thus enabling the implementation of treatment before the development of caecal or large colon impactions.

1.9 Diagnosis of equine post-operative ileus - mechanical versus functional³

As discussed above, equine POI is most frequently diagnosed by the presence of reflux following nasogastric intubation. The ultrasonographic and/or palpable (via *per rectum* examination) detection of distended SI, tachycardia, abdominal discomfort, reduced faecal output and reduced/absent borborygmi are also valuable means of POI diagnosis (Lefebvre et al., 2016a, Lefebvre et al., 2016b). Importantly, the above clinical signs may also be present in other conditions, particularly those associated with a mechanical obstruction to the aboral passage of SI ingesta and fluid. In the immediate post-operative period, most consideration is given to an obstruction at the surgical anastomosis site (Freeman, 2008). Clinical distinction between a

³ Reproduced from: An update on equine post-operative ileus: Definitions, pathophysiology and management, Z. M. Lisowski, R. S. Pirie, A. T. Blikslager, D. Lefebvre, D. A. Hume & N. P. H. Hudson, *Equine Veterinary Journal* 50 (3), © 2017 EVJ Ltd

functional and physical obstruction is challenging. Although mechanical obstructions associated with leakage at the anastomosis site would likely result in worsening pain, increasing rectal temperature and cardiovascular deterioration, those attributable to adhesions or simple intestinal kinking may, like POI, simply result in distended SI and persistent gastric reflux. The absolute distinction between these differing disorders may require a second laparotomy, re-examination of the anastomosis site and confirmation that no physical obstruction is present. In one study of 27 horses that underwent relaparotomy (out of 254 that survived the first surgery) the most common diagnoses were functional ileus (25.9%) and obstruction at the site of anastomosis (22.2%). However, of those that underwent a second laparotomy 62% developed POI (Mair and Smith, 2005a). In a more recent study of 22 horses that underwent relaparotomy, 16 out of 19 horses with precipitating clinical signs (POR and post-operative colic) had these clinical signs eliminated by relaparotomy; furthermore, the authors reported that relaparotomy did not appear to exacerbate the POR (Bauck et al., 2017).

1.10 Epidemiology and risk factors for equine post-operative ileus⁴

Equine surgical cases with SI lesions are consistently associated with an increased risk of POI. Extensive manipulation of the intestines associated with decompression and performing resections and anastomoses of the intestine is likely to induce a greater degree of tissue damage and a more profound inflammatory response in the *muscularis* (Hopster-Iversen et al., 2014). Additionally, studies in mice have demonstrated that even exteriorisation of SI from the abdominal cavity is also likely to contribute to the inflammatory response (van Bree et al., 2012). While some equine studies have reported a greater risk of POI in cases with strangulating, compared with non-strangulating, SI lesions (Freeman et al., 2000, French et al., 2002), others have failed to identify such an association (Mair and Smith, 2005c, Blikslager et al., 1994, Roussel et al., 2001). The onset of pathology is probably attributable to endotoxin release from ischaemic bowel resulting in systemic endotoxemia (King and Gerring, 1988), which, in itself, will result in reduced intestinal motility (King and Gerring, 1991). One study identified the presence of a strangulating pedunculated lipoma as

⁴ Reproduced from: An update on equine post-operative ileus: Definitions, pathophysiology and management, Z. M. Lisowski, R. S. Pirie, A. T. Blikslager, D. Lefebvre, D. A. Hume & N. P. H. Hudson, *Equine Veterinary Journal* 50 (3), © 2017 EVJ Ltd

a specific risk factor for POI, a finding which may reflect a dual association with both intestinal ischaemia and age, the latter also being reported as a significant risk factor for POI (Holcombe et al., 2009).

Other common risk factors relate to cardiovascular and haematological status. High packed cell volume (PCV) at the time of admission (French et al., 2002, Blikslager et al., 1994, Roussel et al., 2001, Cohen et al., 2004, Holcombe et al., 2009), increased serum total protein concentration (Cohen et al., 2004, Roussel et al., 2001) and tachycardia (Blikslager et al., 1994) have all been associated with an increased risk of horses developing POI. These parameters all reflect a degree of dehydration and/or hypovolaemia resulting from both haemodynamic consequences of endotoxemia and fluid sequestration within obstructed bowel and, therefore, may simply reflect the strangulating nature of the underlying intestinal lesion.

Performing a pelvic flexure enterotomy may reduce POI risk (Mair and Smith, 2005c, Roussel et al., 2001); although this may be restricted to cases with LI, but not SI lesions (Cohen et al., 2004). Although the protective influence of this procedure may be attributable to a reduction in the intraluminal source of endotoxin, the potential value of evacuating the colon should be weighed against the increased anaesthesia and surgical time required to perform the surgery, as both of these factors have been associated with an increased risk of POI (Little et al., 2001, Roussel et al., 2001).

1.11 Pathophysiology of post-operative ileus⁵

The development of POI has been attributed to several causes and mechanisms. These include the following: anaesthetic agents, opioids, intravenous fluids, electrolyte imbalances, disruption to GI hormones and neuropeptides, disruption of neural continuity, autonomic dysfunction and inflammatory cell activation (Vather et al., 2014). Such contributory factors may act in isolation or in combination, ultimately resulting in a common endpoint; namely, impaired contractility of the intestinal smooth muscle (SM).

The majority of POI research has been performed on rodent models with only a relatively small number of studies in the horse. The most commonly used rodent POI

⁵ Reproduced from: An update on equine post-operative ileus: Definitions, pathophysiology and management, Z. M. Lisowski, R. S. Pirie, A. T. Blikslager, D. Lefebvre, D. A. Hume & N. P. H. Hudson, *Equine Veterinary Journal* 50 (3), © 2017 EVJ Ltd

model relies on small intestinal manipulation (IM) to induce ileus (Kalff et al., 1998a, van Bree et al., 2012), thus replicating, in part, the processes normally involved in abdominal and GI surgery. This model does not account for the additional processes of intestinal resection, enterotomies and large intestinal manipulation which are regularly undertaken and associated with an increased risk of equine POI. It is currently accepted that the pathogenesis of POI involves two phases: an initial neurogenic phase resulting in immediate post-operative impairment of bowel motility and a subsequent inflammatory phase lasting for several days. Despite representing distinct phases in POI progression, recent findings support a bi-directional interaction between the nervous and immune systems.

1.11.1 Neurogenic phase

The enteric nervous system and normal regulation of gastrointestinal motility

The autonomic nervous system is made up of three components; sympathetic (noradrenergic) and parasympathetic (cholinergic) systems which originate in the central nervous system (CNS) and the enteric nervous system (ENS) which is found in the wall of the GI tract. Unlike other organs in the body, the GI tract has an intrinsic nervous system, the ENS, which can function independently of the CNS, as first demonstrated by Starling and Bayliss in 1899 (Bayliss and Starling, 1899). The ENS is not fully autonomous and it does retain some communications with the CNS via sympathetic and parasympathetic afferent and efferent neurons (Furness and Costa, 1980). The part of the CNS that is connected with the ENS is known as the central autonomic neural network (Goyal and Hirano, 1996). Together, these connections provide neural control of the numerous functions of the GI tract; these include regulation of motility (Kunze and Furness, 1999), control of exocrine and endocrine secretions (Cooke, 1994), circulation of the GI tract (Goyal and Hirano, 1996) and regulation of immune and inflammatory processes (Lundgren et al., 1989, de Jonge, 2013).

The enteric neurons are organised in two interconnected ganglionated plexuses: the myenteric plexus located between the longitudinal and circular muscle layers of the ME, and the submucosal plexus located in the submucosa (Furness, 2012). The myenteric plexus is primarily involved in motor innervation of the two muscle layers and secretomotor innervation to the mucosa and extends the entire length of the intestine. The submucosal plexus functions locally to control intestinal secretion and absorption and contraction of the submucosal muscle and submucosal blood vessels

and is best developed in the small intestine (Goyal and Hirano, 1996, Sharkey et al., 1998).

Both ganglia consist of tightly-packed nerve cell bodies, nerve fibres, glial cells and their processes (Goyal and Hirano, 1996). Although the ENS is responsible for innervation of the intestine, it frequently acts through various intermediary cell types between nerves and the target tissues (Sharkey and Savidge, 2014). For example, motor activity is regulated by interstitial cells of Cajal (ICC), platelet derived growth factor receptor alpha-positive (PDGFR α) cells (Sanders et al., 2006, Sanders et al., 2010) and MM (Muller et al., 2014). Secretion is partly regulated by enteric mast and glial cells (Sharkey and Savidge, 2014).

The ENS is connected to the CNS through both motor and sensory innervation via the sympathetic and parasympathetic nervous systems (Goyal and Hirano, 1996) The parasympathetic nervous system, via the vagal and sacral preganglionic neurons, innervates enteric neurons in the myenteric plexuses of the foregut and distal hind gut respectively (Furness, 2012) and serves the broad function of stimulating an increase in activity of the entire ENS. A small population of myenteric neurons, the intestinofugal neurons, project from the myenteric plexus back to the same prevertebral sympathetic neurons in the abdominal prevertebral ganglia, creating a peripheral sympathetic-enteric neural control circuit that regulates motility (Sharkey and Savidge, 2014, Lomax et al., 2010).

The majority of studies looking at the organisation of the ENS have been predominantly conducted on the small intestine of the guinea pig (Kunze and Furness, 1999, Furness and Costa, 1980, Gunn, 1968, Christensen et al., 1992) and more recently, the colon (Chen et al., 2015, Sharkey et al., 1998). It should not be considered unexpected to find variation in structure of the ENS and the chemical coding of neurons between species, especially as differences in structure and organisation of the ENS of the horse and small mammals have been documented (Pearson, 1994). Studies suggest that primary neurotransmitters are strongly conserved, meaning that the same neurotransmitter will be used in functionally equivalent neurons in differing regions of the GI tract and in different species (Furness et al., 1995, McConalogue and Furness, 1994) although organisational differences between species have been reported.

Our knowledge of the equine ENS is very basic. In small animals, the submucosal plexus forms a single layer (Kunze and Furness, 1999). Studies of the submucosal plexus of the horse in the small intestine have identified two separate networks,

found on the inner and outer laminae of the submucosa respectively (Pearson, 1994). This has also been reported in the pig (Gunn, 1968) and human (Hoyle and Burnstock, 1989). Unlike the pig, no structural differences were observed between the plexus submucosus internus and the plexus submucosus externus of the horse (Timmermans et al., 1990, Pearson, 1994).

As with the submucosal plexus, variations between small mammals and large mammals also occur in relation to the myenteric plexus. Distinctive form variations between the large and small intestinal myenteric plexuses have been reported in the horse, similar to that also been reported in other large mammals, such as sheep and cattle (Freytag et al., 2008). Additionally, further differences between different regions of small intestine have also been reported. The neurons of the myenteric plexus in the ileum extend well into the longitudinal muscle layer, and small numbers of neurons are found to extend to near the serosa. This is in contrast to the myenteric plexus of the jejunum, where neurons appear to be confined to the inter muscular layer (Doxey et al., 1995). The distal ileum represents a highly specialised intestinal region in which the flow of ingesta is dramatically slowed and this organisation of the ENS appears to be a unique feature in the equine GI tract (Doxey et al., 1995).

The term 'motility' is used to describe the contraction of the longitudinal and circular muscle and encompasses two different muscular movements - propulsion via peristaltic contractions and mixing via segmental contractions. Contraction of the circular muscle narrows the intestinal lumen and lengthens the segment, while contraction of the longitudinal muscle is associated with widening of the intestinal lumen and shortening of the segment (Wong et al., 2011a). Control of the muscles varies with the region of the GI tract. For example the CNS has a role in determining the movements of the oesophagus, controlling the volume in the stomach, controlling contractions of the stomach wall, regulating acid secretion and the regulating defecation (Furness, 2012). The ENS regulates motility of the small and large intestines, with some secondary input from the extrinsic nervous system. Components involved in the regulation of motility include smooth muscle cells, ICC, PDGFR α ^{+ve} cells, excitatory and inhibitory enteric motor neurons, afferent neurons and the CNS. Additionally, hormones and immune cells such as mast cells and resident ME macrophages also affect motor output (De Winter et al., 2012, Muller et al., 2014). Peristalsis is closely dependent upon parasympathetic stimulation and is inhibited by sympathetic stimulation.

Neurons and neurotransmitters

Over 30 different types of neurons have been identified in the ENS, which have been classified by their morphology and physiology, with up to 25 chemical mediators, or neurotransmitters, having been identified. The majority of neurons will utilise numerous transmitters, comprising a primary neurotransmitter and subsidiary transmitters (Furness and Costa, 1980, McConalogue and Furness, 1994, Goyal and Hirano, 1996).

The primary neurotransmitter of the sympathetic neurons supplying the intestine is noradrenaline acting on adrenoreceptors, which inhibit motility (Finkleman, 1930, Costa and Furness, 1984) and cause vasoconstriction (Dresel and Wallentin, 1966). Acetylcholine is the predominant neurotransmitter of the parasympathetic nervous system affecting digestive function (McConalogue and Furness, 1994). However, enteric inhibitory motor neurons utilise nitric oxide (NO) as their primary neurotransmitter (Furness, 2012). ATP and vasoactive intestinal peptide (VIP) are thought to be subsidiary transmitters of these neurons, although in some regions they may have a primary transmitter role (McConalogue and Furness, 1994). VIP is the primary transmitter of non-cholinergic secretomotor neurones (Furness, 2012).

Smooth muscle activity is dependent upon excitatory and inhibitory neurotransmitters. Myenteric neurons are either excitatory or inhibitory. Acetylcholine is the main excitatory neurotransmitter (Kunze and Furness, 1999), including in the horse (Malone et al., 1999). Neurokinins (of which substance P has been studied in the horse (Sonea et al.) activate similar pathways to acetylcholine by binding to NK1, NK2 and NK3 receptors. In the horse, these are widely distributed throughout the GIT (Cummings et al., 1985, Belloli et al., 1994, Sonea et al.). Tachykinins are used by sensory neurons, particularly those that detect painful stimuli. They constrict equine enteric smooth muscle (Belloli et al., 1994) and are thought to contribute to acute and chronic inflammation of the GI tract.

Interstitial cells of Cajal

The ICC are commonly referred to as the pacemaker cells of the GI tract. As opposed to pacemaker cells in the heart, the ICC do not occupy a single region, but form a continuous electrically-coupled network of cells that extends from the stomach to the colon. The ICC generate spontaneous electrical slow waves in the GI tract which leads to the depolarisation of the membrane of smooth muscle cells, initiating calcium entry into the smooth muscle cell, resulting in muscle contraction. These

slow waves result in phasic contractions of the GI muscle, resulting in peristalsis and segmentation (Sanders et al., 2006).

Morphologically, the ICC are arranged in close proximity to neurons and smooth muscle cells (Mikkelsen, 2010). The second main motility-associated function of ICC relates to their role as intermediaries of nitrenergic and cholinergic neural inputs to smooth muscle cells (Publicover et al., 1993, Burns et al., 1996, Vannucchi, 1999, Ward et al., 2000). Other receptors related to neurotransmission on the surface of ICC include NK1 (tachykinins), somatostatin receptor and nitric oxide synthase (Vannucchi, 1999).

Several subsets of ICC have been described according to their anatomical location and these differing locations may relate to their various described functions (**Table 1-4**). There are limited studies in the horse, however the distribution of ICC cells in the equine GI tract have been described (Hudson et al., 1999). This revealed no specific accumulation of ICC in the deep myenteric plexus (DMP) of the small intestine or the submucosal surface of the colonic circular muscle layer but did reveal an increase in ICC cells in the inner third of the circular muscle layer. However, the small intestine did have a higher number of ICC in the myenteric plexus region, compared to the large intestine where the majority of ICC were seen throughout the circular muscle layer. This difference is potentially reflective of slow waves in the stomach and small intestine originating in the myenteric region, whilst in the large intestine they originate from the circular muscle layer.

Table 1-4 Summary of anatomical locations and functions of ICC in the GI tract (Adapted from Ward and Sanders, 2001)

Classification	Description of location	Function
ICC – MY	Within the intermuscular space between the circular and longitudinal muscle layers (myenteric region)	Slow wave generation (pacemaker) (Ward and Sanders, 2001)
ICC – SM	Along the submucosal surface of the circular muscle of the colon	Slow wave generation (pacemaker) (Ward and Sanders, 2001)
ICC – DMP	Found within the deep muscularis plexus of the small intestine	Mediators of circular muscle inhibitory innervation (Matini, 1997)
ICC - IM	Intramuscular ICC of the oesophagus, lower oesophageal sphincter, stomach, pylorus, cecum and colon.	Mediators of circular muscle inhibitory innervation (Matini, 1997)

Platelet derived growth factor receptor alpha-positive cells

PDGFR α^{+ve} cells are a more recently documented type of interstitial cell in the gastrointestinal muscles, which have been shown to respond to purines, which are inhibitory neurotransmitters released from enteric motor neurons (Sanders et al., 2012). Limited data are available, but it is thought that PDGFR α^{+ve} cells are more likely to mediate purine (inhibitory) neurotransmission than smooth muscle cells. There are no data to date on these cells in the horse.

Immune cells

Little is known about the role of immune cells in motility in the non-inflammatory state. Macrophages and ICC in the mouse ME are in close spatial contact with each other and have a constant and regularly distributed cell population, strongly suggesting that macrophages and ICC can functionally interact (Mikkelsen, 2010). Muller et al. 2014 demonstrated in mice that resident MM found along nerve fibres regulate motility in the non-inflamed intestine through the production of bone morphogenetic protein-2 (BMP2) (Muller et al., 2014). Enteric neurons were also shown to contribute to the maintenance of ME macrophages through secretion of the macrophage growth factor CSF-1. This study, alongside another demonstrating a vagal anti-inflammatory pathway modulating the MM (Matteoli et al., 2014) show a bidirectional communication between the ENS and MM, maintaining a physiological homeostasis in the resting state. This was highlighted by disrupted contractility in the colon occurring after depletion of the MM (Muller et al., 2014). What these studies have highlighted is the similarity between the neuroimmune crosstalk in the ENS and CNS; namely that the specialised macrophages of the brain (the microglia) and MM are both under the continuous control of neurons and support neuronal homeostasis (Verheijden et al., 2015). Resident MM differ from other tissue-resident macrophages, such as macrophages resident in the lung, spleen, peritoneum and BMDMs, as they share several marker genes with the CNS microglia, notably *Cx3cr1*, *Fcrls*, *P2ry12*, *Olfml3*, *Mertk* and *Gas6*. In addition, they express the transcription factors *Egr1*, *Atf3* and *Junb*, meaning both populations undergo similar transcriptional process in order to establish their phenotype (Verheijden et al., 2015).

Disruption to the enteric nervous system in colic and post-operative ileus

Reduction of neurons and interstitial cells of Cajal in colic cases

A reduction in the number of neurons, in the caecum and large colon, has been reported in horses with colic as a result of chronic obstruction of the colons or

recurrent caecal impactions (Schusser et al., 2000, Schusser and White, 1997). It is unclear if the reduction in neurons was the cause of disease or occurred as a result of disease. Likewise, a reduction in the density of ICC in horses with large intestinal lesions has also been reported (Fintl et al., 2004). However, no studies have shown a relationship between a reduction in neurons and ICC and an increased risk in developing POI.

Activation of neural pathways in abdominal surgery⁶

During abdominal surgery, the surgical incision, peritoneal breach and intestinal manipulation (IM) act as nociceptive stimuli that activate neural pathways. Surgical incision of the abdominal wall of rats creates a somatic wound activating adrenergic pathways (Boeckxstaens et al., 1999, Bueno et al., 1978). This pathway involves a spinal reflex; afferent splanchnic nerves synapse in the dorsal column of the spinal cord, stimulating glutamate release. Both activate spinothalamic projections, causing the perception of pain at the surgical incision and mediate a sympathetic efferent response, resulting in reduced motility (Zittel et al., 1994a, Livingston and Passaro, 1990, Uemura et al., 2004, Fukuda et al., 2007, Bueno et al., 1978). The degree of ileus relates to the length of incision (Uemura et al., 2004) and depletion of adrenergic innervation prevents this from occurring (Plourde et al., 1993, De Winter et al., 1997, Fukuda et al., 2007).

IM and breach of the peritoneum is a more intense stimulus than the skin incision alone, and in turn results in a longer period of inhibition of motility (Boeckxstaens et al., 1999, Bueno et al., 1978), which, in rats, is only partially blocked by adrenergic antagonists (Zittel et al., 1998). As early as 1899, Starling and Bayliss observed a reduction in intestinal motility following intestinal handling in the dog, a phenomenon which was abolished by sectioning the vagus and splanchnic nerves (Bayliss and Starling, 1899). As largely deduced from rodent studies, sensory information from the peritoneum and intestine is conveyed via the vagus nerve which, through the expression of interleukin-1 receptors (IL-1R) (Ek et al., 1998), is also sensitised by inflammatory stimuli. Afferents travel to the *nucleus tractus solitarius* of the brainstem, resulting in corticotrophin-releasing factor-mediated stimulation of neurons in the supraoptic nucleus of the hypothalamus. Hypothalamic neurons then project to sympathetic preganglionic neurons in the spinal cord,

⁶ Reproduced from: An update on equine post-operative ileus: Definitions, pathophysiology and management, Z. M. Lisowski, R. S. Pirie, A. T. Blikslager, D. Lefebvre, D. A. Hume & N. P. H. Hudson, Equine Veterinary Journal 50 (3), © 2017 EVJ Ltd

activation of which inhibits GI motility (Zittel et al., 1993, Zittel et al., 1994b, Barquist et al., 1996). Intense stimulation of splanchnic afferents also triggers an inhibitory non-adrenergic, non-cholinergic vagally-mediated pathway that impairs motility via local release of nitric oxide (NO) and vasoactive intestinal peptide (Boeckxstaens et al., 1999, Lefebvre et al., 1995).

Neuronal inhibition of GI motility is self-limiting, with normalisation of function returning upon cessation of nociceptor and mechanoreceptor stimulation. In comparison, the subsequent inflammatory response, and its effect on motility, results in a significantly more prolonged period of ileus. These two periods, an early neurogenic phase, and a later inflammatory phase have been recognised in humans (Boeckxstaens and de Jonge, 2009) and hypothesised in horses (Doherty, 2009).

1.11.2 Inflammatory phase⁷

Results derived predominantly from rodent studies have attributed the prolonged phase of POI to inflammation within the intestinal *muscularis* (Kalff et al., 1999b, Kalff et al., 1998a, Farro et al., 2017). Accordingly, the experimental induction of POI by IM has been prevented by the inhibition of mast cells (de Jonge et al., 2004), macrophages (Wehner et al., 2007) or more general leukocytic infiltration (The et al., 2005, De Jonge et al., 2003).

The activation of peritoneal mast cells, located within the serosa and mesentery and in close association with afferent nerve fibres (Williams et al., 1997), is an early event during abdominal surgery reported in the mouse (de Jonge et al., 2004) and human (The et al., 2008). Neuropeptides (substance P or calcitonin gene-related peptide) released from afferent nerves have been hypothesised as playing a role (Overman et al., 2012, Suzuki et al., 1999). In addition to the release of histamine, mast cell proteinase-1, tryptase and IL-6 (The et al., 2008), activated mast cells also release IL-8 which, along with intercellular adhesion molecule-1 (ICAM-1), may directly result in neutrophil chemotaxis (Compton et al., 1998). Alternatively, their close association with mesenteric blood vessels may facilitate the diffusion of mediators directly into the mesenteric circulation, resulting in the recognised increase in epithelial permeability following intestinal manipulation. This may in turn permit either the translocation of luminal-derived pathogen-associated molecular patterns (PAMPs)

⁷ Reproduced from: An update on equine post-operative ileus: Definitions, pathophysiology and management, Z. M. Lisowski, R. S. Pirie, A. T. Blikslager, D. Lefebvre, D. A. Hume & N. P. H. Hudson, *Equine Veterinary Journal* 50 (3), © 2017 EVJ Ltd

across the intestinal mucosa and/or stimulate the production of damage-associated molecular patterns (DAMPs), both of which may trigger a subsequent key step in the inflammatory cascade; namely, the activation of resident *muscularis* macrophages (MM) (Kalff et al., 1998a). Notwithstanding these findings, intestinal inflammation and delayed GIT following IM were still present in a mast cell-deficient mouse strain (Gomez-Pinilla et al., 2014).

Activation of MM occurs through DAMPs, such as adenosine triphosphate (ATP) (Ozaki et al., 2004), and PAMPs, such as lipopolysaccharide (LPS) (Eskandari et al., 1997). In mice, the activation of toll-like receptors (TLR) and receptors for advanced glycation end products (RAGE) by PAMPs and DAMPs, results in recruitment of intracellular signalling pathways (p38, JNK/SAP), the activation of which are increased within an hour of IM (Wehner et al., 2009). This subsequently leads to the release of pro-inflammatory cytokines, including tumour necrosis factor- α (TNF- α), IL-1 β and IL-6, and chemokines, including macrophage inflammatory protein -1 α (MIP-1 α) and monocyte chemoattractant protein-1 (MCP-1), with a resultant upregulation of ICAM-1 in the endothelium and the influx of leukocytes (Choi et al., 2013, Hopster-Iversen et al., 2014, Kalff et al., 1998a). The leukocytic infiltrate, which predominantly comprises monocytes, mast cells and neutrophils, is detectable within 3 hours following surgery and continues to increase until it peaks at approximately 24 hours (Kalff et al., 1999a, Farro et al., 2017). Inducible NO synthase (iNOS) and cyclooxygenase-2 (COX-2) (Schwarz et al., 2001) upregulation has been reported in MM in rodents, thus facilitating the production of NO and prostaglandins, both of which impair the contractile activity of SM cells (Schwarz et al., 2001). Prostaglandins also increase the sensitivity of spinal afferent nerves (Ek et al., 1998). Macrophage depletion (with chlodronate liposomes and using a mutant mouse with an inactivated colony stimulating factor-1 gene resulting in absence of *muscularis* macrophages) prevents intestinal inflammation and the development of POI (Wehner et al., 2007), strongly supporting their role in the inflammatory phase of POI.

As mentioned previously, most of the studies of POI are performed on the SI. A recent study by Pohl *et al.* has shown differences in the inflammatory response of resident cells in the SI and colon in a mouse model of POI (Pohl et al., 2017). Whilst activation of resident MM in the SI results from translocation of luminal derived DAMPs or PAMPs, this does not occur with the colonic MM, due to the colonic MM macrophages being less reactive, most likely reflecting the larger microbial load in the colon. In addition, differences in the response of infiltrating monocytes, and evidence that

monocytes in the colon are affected by the microbiota, highlights significant regional differences in the response of the SI and colon to IM (Pohl et al., 2017).

As in every tissue injury, immune cells and their products also contribute to the resolution of inflammation and POI; one key effector is IL-10. IL-10 knockout mice fail to resolve their *muscularis* inflammatory response compared to wild type mice, resulting in high mortality rates (Stoffels et al., 2009). Administration of exogenous IL-10 improved GIT post-operatively and reduced inflammatory cytokines, chemokines and NO. Additionally, whilst the initial leukocytic infiltrate of neutrophils and monocytes to the *muscularis* has been associated with SM dysfunction leading to POI, the role of monocytes/macrophages in resolution of POI has not been studied, until recently. Farro *et al.* (2017) demonstrated that blocking the influx of monocytes to the *muscularis* did not prevent POI but resulted in a prolonged period of smooth muscle dysfunction and an increased neutrophilic inflammatory response (Farro et al., 2017). The administration of macrophage colony stimulating factor-1 fusion protein (CSF1-Fc) (Gow et al., 2014) not only restored monocyte and MM numbers but reduced neutrophil infiltration in the *muscularis*, increased anti-inflammatory gene expression and improved GIT transit time following IM (Farro et al., 2017). Continued work focusing on the recovery process is warranted, with the potential to inform the development of therapeutic interventions which accelerate this process rather than solely targeting the onset of inflammation.

In the horse, post-operative neutrophilic and eosinophilic inflammation of the jejunum has been identified up to 18 hours post-operatively (Little et al., 2005, Hopster-Iversen et al., 2011, Hopster-Iversen et al., 2014). Direct manipulation of the LI in the horse resulted in an inflammatory response; this also occurred following manipulation of the SI alone (Hopster-Iversen et al., 2011). A similar response has been reported in rodents (Schwarz et al., 2004). In addition to this pan-enteric response, an increase in apoptotic cells (neurons, SM and glial cells) has been demonstrated in strangulating lesions of the LI and SI at sites distant to the lesion, most likely reflective of a generalised stress response of the GI tract to ischaemia, reperfusion and inflammation (Rowe et al., 2003). A localised stress response in the SM and neurons has been reported in the borders of healthy resection margins (De Ceulaer et al., 2011). Activation of MM by manipulation-induced translocation of luminal-derived LPS is a recognised phenomenon in humans and rodents leading to loss of SM contractility (Snoek et al., 2012, Eskandari et al., 1997). In light of IM-induced loss of mucosal epithelial cells in the horse it is likely that a similar LPS translocation process also occurs in this species (Hopster-Iversen et al., 2011). IM-

induced inflammation in a TLR-2 and TLR-4 double knockout mouse model was only partially protective against a delay in GIT (Stoffels et al., 2014), demonstrating that alternative TLR-2 and TLR-4 independent pathways of macrophage activation must also exist.

Although the translational application of data derived from rodent models can provide a valuable insight into the basic cellular and molecular responses of the equine GI tract to laparotomy and IM there are significant species-related differences in innate immune biology. For example, handling-induced NO liberation by murine MM contributes towards intestinal SM dysfunction in the mouse GI tract (Kalff et al., 2000); however, as in other large animals (pigs and humans (Kapetanovic et al., 2012)), equine alveolar and peritoneal macrophages do not produce NO. Consequently, this mediator is not likely to be involved in equine inflammation (Karagianni et al., 2013).

Another important factor to consider when extrapolating findings from rodent studies to equine colic cases is the absence of pre-existing conditions, such as ischaemic bowel, peritonitis and endotoxaemia in the rodent models of IM used to study POI. A model of caecal ligation and perforation in rats resulted in reduced GI motility and a leukocytic inflammatory response within the *muscularis* (Overhaus et al., 2004). Whilst not the most commonly adopted rodent model of POI, it does demonstrate the effect of polymicrobial sepsis on GI motility. Horses undergoing abdominal surgery will usually have significant primary disease, such as ischaemic bowel, peritonitis associated with non-viable intestine and intestinal distention secondary to a strangulation/amotility. As previously mentioned, endotoxin release from ischaemic bowel can cause reduced intestinal motility (King and Gerring, 1991, King and Gerring, 1988). Horses with amotile intestine may also have increased bowel oedema because of reduced lymphatic drainage (Drake et al., 1998, Shah et al., 2011). How these pre-surgical factors affect the pathogenesis of equine POI is not completely understood; however, in light of the fact that horses presenting with compromised cardiovascular status/endotoxemia (Blikslager et al., 1994, Roussel et al., 2001) and with pre-operative reflux (Mair and Smith, 2005c) are at increased risk of developing POI (see section above), one could assume that they play a significant role in the pathogenesis of equine POI.

1.11.3 Pharmacological/therapeutic influences on the development of post-operative ileus

In addition to the key neurogenic and inflammatory phases of POI, a variety of pharmacologic agents and therapeutic interventions have also been identified as

either increasing the risk or duration of POI. These include the use of opioids, and anaesthetic agents and a failure to correct any disease-associated fluid and electrolyte imbalances.

1.12 Aims of thesis

Macrophages are important for the initiation and resolution of inflammation, including in POI. Despite all macrophages deriving from the same progenitor cells, different macrophage populations will develop different phenotypes according to their intended function. In addition, species-related differences in phenotype may also result in differing functions between species. Therefore, reliance on rodent- or human-derived data to elucidate the pathophysiology of equine POI may yield inappropriate conclusions as a result of subtle inter-species differences in innate immunity. In humans and mice, the activation of resident MMs initiates an inflammatory response within the ME which ultimately results in smooth muscle dysfunction. Therefore, the overall aim of this thesis was to determine if a similar process of macrophage activation occurs in the horse. The administration of CSF1-Fc, a conjugate protein of the growth factor needed for macrophage development, has been shown to be beneficial in several disease models, such as liver, kidney and bone injury. The secondary aim of this thesis was to evaluate if administration of CSF1-Fc will have a beneficial effect in a mouse model of manipulation-induced POI.

To address this question the aims of the project were subdivided, as follows:

1. Characterise the number, distribution, phenotype and functional status of different macrophage populations (mucosal and ME) within healthy equine intestine.
2. Analyse the effect of LPS stimulation on eqBMDMs.
3.
 - a) Compare healthy intestine and intestine excised from small intestinal surgical resections (the “healthy margin”) by evaluating markers of resident macrophage activation, the choice of markers being informed by Aim 2.
 - b) Determine if there is a correlation between markers of macrophage activation in resected intestine (“healthy margin” of resection) and (i) time from abdominal incision, (ii) type of colic lesion and (iii) presence of clinically-apparent POI.
4. Evaluate the effect of CSF1-Fc, a growth factor for macrophages, on the murine GIT, in the steady state and in a model of POI.

1.13 Hypotheses

The distribution and density of macrophages in the equine intestine is similar to other species

Abdominal surgery will induce a macrophage inflammatory response in the equine gastrointestinal tract

CSF1-Fc will improve recovery in the gastrointestinal tract of mice in a rodent model of POI

Chapter 2. Materials and Methods

2.1 Animals

2.1.1 Horses

Horse details and tissues collected from each horse are summarised in **Table 2-1** and **Table 2-2**.

Non-colic horses

Twenty-two horses (median age 16 years., range 6 - 26 years) of various breeds, were admitted to the Equine Hospital at the Royal (Dick) School of Veterinary Studies for elective euthanasia. Horses were euthanased with secobarbital sodium 400mg/ml and cinchocaine hydrochloride 25mg/ml (Somulose™; Arnolds/Dechra), at a dose of 1ml/10kg bodyweight via a pre-placed intravenous (i.v) catheter in the left jugular vein. All animals were systemically healthy and did not have any recent history of gastrointestinal (GI) disease. Post mortem examination confirmed the absence of gross GI pathology in all animals. One animal did have large volumes of sand in the right ventral colon, but no associated gross pathology of the GI tract was seen. The study was approved by the School of Veterinary Medicine Ethical Review Committee.

Colic cases

Twelve horses (median age 21.5 years, range 14 - 25 years) of various breeds were admitted to the Bell Equine Veterinary Clinic, Kent, or the Dick Vet Equine Hospital, Edinburgh for further investigation of abdominal pain. Tissues were collected at laparotomy from horses that required intestinal resection (from resection margins) because of strangulating lesions of the intestine. Owner permission was granted for the collection of tissues and tissue collection was approved by the School of Veterinary Medicine Ethical Review Committee.

ID	Age	Sex	Breed	Comments	Tissues collected	Comment
H1	12	Mare	Standardbred	Elective euthanasia. Chronic lameness. Had phenylbutazone prior to euthanasia	Gut	
H2	19	Gelding	Thoroughbred cross	Elective euthanasia -blood bank.	Gut	qPCR control
H3	23	Mare	Thoroughbred cross	Elective euthanasia -blood bank. Sand in ingesta predominantly in left ventral colon	Gut	
H4	14	Gelding	Irish Sports Horse	Elective euthanasia -blood bank. Large pituitary gland, fibrotic lesions in the lungs	Gut	
H5	26	Gelding	Thoroughbred cross	Elective euthanasia -blood bank.	Gut	
H6	21	Mare	Thoroughbred cross	Elective euthanasia -blood bank.	Gut	
H8	10	Gelding	Thoroughbred	Elective euthanasia -blood bank. Fat++	Gut, Bone marrow	
H7	9	Gelding	Irish type	Elective euthanasia -blood bank. Fat ++	Gut	
H9	6	Gelding	Thoroughbred	Elective euthanasia -blood bank. Fat ++	Gut, Bone marrow, Blood	
H10	23	Gelding	Highland Pony	Elective euthanasia -blood bank.	Gut, Bone marrow, Blood	
H11	19	Gelding	Thoroughbred	Elective euthanasia -blood bank.	Gut, Bone marrow, Blood	
H12	19	Mare	Thoroughbred cross	Elective euthanasia -blood bank.	Gut, Bone marrow,	
H13	15	Gelding	Thoroughbred cross	Elective euthanasia -blood bank. Lipomas	Gut, Bone marrow	qPCR control
H14	11	Gelding	Shire	Elective euthanasia -blood bank.	Gut	
H15	21	Mare	Sports horse	Elective euthanasia -blood bank.	Gut, Bone marrow	qPCR control
H16	17	Gelding	Thoroughbred cross	Elective euthanasia -blood bank.	Gut	qPCR control
H17a	15	Mare	Thoroughbred cross	Elective euthanasia -blood bank.	Gut, Bone marrow	qPCR control
H17b	19	Gelding	Thoroughbred cross	Elective euthanasia -blood bank.	Gut, Bone marrow	
H18	23	Mare	Thoroughbred cross	Elective euthanasia -blood bank.	Gut, Liver, Blood	qPCR control
H19	16	Gelding	Connemara cross	Elective euthanasia -blood bank.	Gut, Liver, Blood	
H20	7	Mare	Scottish Sports Horse	Elective euthanasia -blood bank.	Gut, Blood	
H21	16	Mare	Unknown	Elective euthanasia -blood bank.	Gut	
H22	15	Gelding	Thoroughbred	Elective euthanasia -blood bank.	Gut	

Table 2-1 Details of non-colic cases used

Table 2-2 Details of colic cases

Case ID	Centre	Age	Sex	Breed	Surgical lesion
Case A	Dick Vet	9	Gelding	Thoroughbred	Strangulation of jejunum by pedunculated lipoma. Uneventful recovery
Case B	Dick Vet	11	Mare	Warmblood	Epiploic foramen entrapment. Uneventful recovery.
Case C	Bell Equine	10	Mare	Warmblood	Strangulation of jejunum in gastrosplenic ligament. Owner elected euthanasia on table. Samples collected from margins of strangulated region.
Case D	Bell Equine	27	Mare	Thoroughbred	Strangulation of jejunum by pedunculated lipoma. Resection and anastomosis. Uneventful recovery.
Case E	Bell Equine	20	Mare	Welsh Cross	Strangulation of jejunum in gastrosplenic ligament. Resection and anastomosis. Uneventful recovery.
Case F	Bell Equine	12	Stallion	Oldenburg	Eosinophilic enteritis. Resection of structured segment of jejunum and anastomosis. Uneventful recovery.
Case G	Bell Equine	25	Mare	Cob	Strangulation of distal jejunum and ileum by pedunculated lipoma. Euthanised on table.
Case H	Bell Equine	22	Gelding	Appaloosa	Epiploic foramen entrapment and strangulation of distal half of jejunum / proximal ileum. Euthanised on table.
Case I	Bell Equine	21	Gelding	Welsh Section D	Strangulation of mid jejunum by pedunculated lipoma resection and anastomosis performed. Uneventful recovery
Case J	Bell Equine	14	Gelding	Cob cross	Strangling lipoma of mid jejunum. Resection and end to end anastomosis. Refluxed for 2 days post op (was refluxing before surgery) then resolved spontaneously.
Case K	Bell Equine	19	Mare	Welsh cross	Strangling lipoma of mid jejunum. Resection and end to end anastomosis. Uneventful recovery.
Case L	Bell Equine	24	Gelding	Irish cob	Gastrosplenic ligament entrapment of jejunum. Resection and end to end anastomosis. No reflux but 3 days later suddenly became toxic, tachypnoea, pulmonary oedema and died. No PME possible.

2.1.2 Mice

Mice were kept under specific pathogen-free (SPF) conditions at the Biomedical Research Facility (BRF), University of Edinburgh, UK and KU Leuven Mouse Facility (KU LMF), University of Leuven, Belgium. Procedures were performed when the mice were aged 8-12 weeks. **Table 2-3** summarises the strains used. Procedures were performed according to UK Home Office regulations and approved by the University of Edinburgh Animal Welfare and Ethical Review Committee. Procedures performed at Leuven (**Chapter 6**) were approved by the Animal Care and Animal Experiments Committee of the University of Leuven (Leuven, Belgium).

Table 2-3 Details of mouse strains used

Strain	Supplier	Description
MacGreen (Csf1r-EGFP) ¹	BRF, University of Edinburgh, UK	Macrophage green fluorescent reporter mouse
MacBlue (Csf1r*-GAL4/VP16,UAS-ECFP) ²	BRF, University of Edinburgh, UK	Macrophage cyan fluorescent protein reporter mouse
MacApple (Csf1r-RFP) ³	BRF, University of Edinburgh, UK	Macrophage red fluorescent reporter mouse
MacApple x MacBlue	BRF, University of Edinburgh, UK	Generated by crossing MacApple with MacBlue
MacGreen x MacBlue	BRF, University of Edinburgh, UK	Generated by crossing MacGreen with MacBlue
C57BL/6	Kindly provided by Prof Gianluca Matteoli (KU Leuven)	Wild type
B6.129S4-Ccr2tm1lfc/J	Kindly provided by Prof Gianluca Matteoli (KU Leuven)	Ccr2 receptor deficient mice

¹ SASMONO, R. T., OCEANDY, D., POLLARD, J. W., TONG, W., PAVLI, P., WAINWRIGHT, B. J., OSTROWSKI, M. C., HIMES, S. R. & HUME, D. A. 2003. A macrophage colony-stimulating factor receptor-green fluorescent protein transgene is expressed throughout the mononuclear phagocyte system of the mouse. *Blood*, 101, 1155-63

² SAUTER, K. A., PRIDANS, C., SEHGAL, A., BAIN, C. C., SCOTT, C., MOFFAT, L., ROJO, R., STUTCHFIELD, B. M., DAVIES, C. L., DONALDSON, D. S., RENAULT, K., MCCOLL, B. W., MOWAT, A. M., SERRELS, A., FRAME, M. C., MABBOTT, N. A. & HUME, D. A. 2014. The MacBlue binary transgene (csf1r-gal4VP16/UAS-ECFP) provides a novel marker for visualisation of subsets of monocytes, macrophages and dendritic cells and responsiveness to CSF1 administration. *PLoS One*, 9, e105429

³ HAWLEY, K.A., ROJO, R., RAPER, A., SAUTER, K. A., LISOWSKI, Z.M, GRABERT, K., BAIN, C.C., DAVIS, G. OSTROWSKI, M.C., HUME, D. A., PRIDANS, C., JENKINS, S.J. (2018) Csf1r-mApple transgene expression and ligand binding in vivo reveal dynamics of CSF1R expression within the mononuclear phagocyte system. *The Journal of Immunology* 200 (6), 2209-2223

2.1.3 Collection of whole blood

Five millilitres of whole blood were collected from the non-colic horses prior to euthanasia via a pre-placed i.v catheter into tubes containing EDTA (BD Vacutainer) as an anticoagulant.

2.1.4 Collection of samples from the gastrointestinal tract

Non-colic Horses

Once euthanased, an incision was made in the ventral midline to expose the abdominal cavity. The GIT was removed from the body by transecting the oesophagus at the level of the diaphragm, removing the mesenteric and body wall attachments and transecting the small colon at the junction with the rectum. The spleen and liver were removed, and the GIT placed on a clean working area. Gross contamination of blood was removed with water.

Tissues were collected as follows:

a) Full thickness 4 cm x 4 cm sections were removed from 14 anatomical locations from the stomach to the small colon (**Table 2-4**). Tissue sections were rinsed in cold phosphate-buffered saline (PBS) (Dulbecco's Phosphate Buffered Saline; Sigma-Aldrich) before being trimmed into smaller segments and placed in 10% neutral buffered formaldehyde (4% formaldehyde in neutral buffered solution) (Sigma-Aldrich).

b) Three 0.5 cm x 0.5 cm full thickness sections were taken from the greater curvature of the stomach, mid jejunum and colonic pelvic flexure. The mucosa and *muscularis* were separated (submucosa remained on the mucosa) and thoroughly rinsed in cold PBS. Tissues were placed in ammonium sulphate (RNAlater Stabilization Solution; Thermo Fisher Scientific) and stored at 4°C for at least 24 hrs. Excess solution was removed by tapping on a sterile surface before being transferred for storage at -80°C.

Colic Cases

Collection from healthy margins (proximal and distal) of surgically-resected tissue was conducted between October 2016 and March 2017. Full thickness sections were placed in 10% formalin for immunohistochemistry (IHC). Mucosa and *muscularis* were separated, each placed in RNAlater (Thermo Fisher Scientific) and stored at 4°C for no more than 30 days, before being stored at -80°C. Case details are summarised in **Table 2-2**.

Liver

A 4 cm x 4 cm section from the right liver lobe was removed. Smaller pieces measuring no more than 0.5 cm in any dimension were then cut and placed in RNAlater (Thermo Fisher Scientific) and stored at 4° C for no more than 30 days, before being removed from RNAlater and stored at -80° C.

Table 2-4 Description of anatomical locations used for tissue collection of the gastrointestinal tract

ID #	Location	Description of location
1	Stomach GC	Greater curvature “at the greatest curve”
2	Stomach LC	Midpoint of lesser curvature on inside of curve
3	Duodenum mid	approx. 50-75cm from pylorus
4	Jejunum ¼	Full circumferential sample and then further samples cut from anti-mesenteric aspect
5	Jejunum mid	
6	Jejunum ¾	
7	Ileum mid	Ileum defined by ileocaecal fold, approx. 1m long. Midpoint ileum is midpoint of ileocaecal fold. Anti-mesenteric border.
8	Caecum mid	Find ileocaecal fold and follow towards apex. Sample taken 2 inches away from end of ileocaecal fold including taenial band
9	Right ventral colon mid	Midpoint over taenial band
10	Left ventral colon mid	Midpoint over taenial band
11	Pelvic flexure	At apex from the anti-mesenteric aspect
12	Left dorsal colon mid	Midpoint on outer edge
13	Right dorsal colon mid	Midpoint on outer edge over taenial band
14	Small colon	Midpoint overlying anti-mesenteric taenial band

GC = greater curvature; LC = lesser curvature

2.2 Isolation and generation of equine bone marrow derived macrophages

The protocol used was adapted from Kapetanovic *et al.* (2012). Following euthanasia, the horse was exsanguinated and suspended by the hind limbs. Two ribs (ranging from T8-T11) were disarticulated and removed, ensuring they did not fracture or expose any bone marrow (BM) cavity upon removal. The ribs were thoroughly cleaned by removing any attached muscle and connective tissues and were stored in PBS on ice until processing.

The ribs were rinsed in ethanol and, under a fume hood, cut into segments 5-8 cm in length. Using a 10 ml syringe and 18 G needle, the ribs were flushed with RPMI 1640 (Sigma-Aldrich) with 5mM EDTA (10 mM KHCO₃, 150 mM NH₄Cl, 0.1 mM EDTA [pH 7.0]) at both cut ends until the media ran clear. The media was collected in a falcon

tube and passed through a 100 µm filter to remove any bone debris and/or fat, prior to being centrifuged at 400 *rcf* for 5 minutes to pellet the cells. Once pelleted, the supernatant was carefully removed, and the pellet re-suspended in 5ml of red blood cell lysis buffer and incubated in the dark at room temperature (RT) for 5 minutes. Forty-five mls of PBS were added to the tube and centrifuged at 400 *g* for 5 minutes. The supernatant was discarded, and the pellet re-suspended in an appropriate volume of PBS with 2% heat-inactivated (HI) horse serum (Sigma Aldrich) and the cells then counted.

2.3 Alveolar macrophages

Cryopreserved alveolar macrophages were obtained from Anna Karagianni (Roslin Institute, University of Edinburgh). Cells were cultured overnight before being harvested for flow cytometry (Karagianni, 2015).

2.4 Equine macrophage cell culture conditions (optimised)

Cryopreserved cells (thawed in a water bath at 37 °C for 5 minutes) or freshly isolated cells were seeded on bacteriological plates in medium containing RPMI 1640 with 20% heat-inactivated (HI) horse serum (Sigma), 1 mmol/l GlutaMAX (Life Technologies), 100 U/ml penicillin, 100 µg/ml (Thermo Fisher Scientific). Cells were cultured at a density of 2.5×10^6 cells/ml and medium was supplemented with 10^4 U/ml (100 ng/ml) recombinant human macrophage colony-stimulating factor 1 (CSF-1) (recombinant human CSF-1 (rhCSF1); a gift from Chiron, USA). Fresh media was added at Day 3. On Day 5, adhered cells were removed with medium using a blunt 18G needle and 10ml syringe. Adhered cells and supernatant were centrifuged at 400 *rcf* for 5 minutes and cells were re-suspended in fresh medium and re-plated on new bacteriological plates. Cells were analysed between Days 7 and 10.

2.5 Cell viability assay

To optimise culture conditions, cells were seeded at varying densities (5×10^4 to 4×10^5 cells/well) in a 96-well plate in 200µl of varying mediums (RPMI 1640 with 1 mmol/l GlutaMAX, 100 U/ml penicillin, 100 µg/ml and either 10% or 20% fetal calf serum (FCS) or 10% or 20% horse serum (HS) and with or without 10^4 U/ml (100 ng/ml) rhCSF-1. On Days 7, 10 and 14 the supernatant was removed from the wells and the

well imaged with brightfield microscopy to visualise the cells. Fifty microlitres of 1mg/ml MTT solution (3-(4,5-Dimethylthiazol-2-yl)-2,5-Diphenyltetrazolium Bromide) were added to each well and incubated for 1 hour at 37 °C. The MTT solution was removed and 100 µl of solubilisation buffer added and incubated at 37°C for 10 minutes. Absorbance was read at 570 nm.

2.6 *In vitro* stimulation of macrophages

2.6.1 Lipopolysaccharide (LPS)

On Day 7, adhered differentiated cells were detached with medium using a blunt 18G needle and 10ml syringe. These were washed and counted and seeded on 6- well tissue culture plates with 2×10^6 cells per well in medium supplemented with rhCSF-1, and incubated for 24 hours at 37 °C. After 24 hours, supernatant was removed from each well and replaced with either fresh medium (control) or medium containing LPS from *Salmonella enterica* serotype Minnesota Re 595 (L9764; Sigma-Aldrich) at a final concentration of 100 ng/ml.

2.7 Cryopreservation of cells

Cells were counted prior to cryopreservation in freezing medium (90% heat-inactivated horse serum and 10% DMSO). Cells were frozen overnight at -80 °C and then transferred to -155 °C for long term storage.

2.8 Phagocytosis assay

Phagocytic activity of cells was assessed using either Zymosan A *S. cerevisiae* BioParticles labelled with Fluorescein or pHrodo Red *E.coli* BioParticles (both Thermo Fisher Scientific).

2.8.1 Zymosan A *S.cerevisiae* BioParticles

Cells were seeded in duplicate at 5×10^4 cells/well in a 4-well plate or placed on glass coverslips in full medium and cultured overnight. The medium was removed and Zymosan A *S. cerevisiae* BioParticles were added at a ratio of 100 particles/cell in fresh medium and cultured for 1 hour at 37°C. A control well had particles added but was kept at 4°C. Ice-cold PBS was added after 1 hour and the cells were washed three times in PBS. The cells were fixed with 4% paraformaldehyde (PFA) for 20 minutes at room temperature (RT) and then washed with PBS twice. Cells on plates were viewed

by fluorescence microscopy at this stage. The number of phagocytic cells was counted and percentage of cells that had phagocytosed was calculated.

Cells on glass coverslips were permeabilised with 0.1% Triton X-100 for 5 minutes then washed three times with PBS. Cells were blocked with 3% bovine serum albumin (BSA) in PBS for 1 hour and then stained for 1 hour with a 1/500 dilution of phalloidin (Texas Red-X Phalloidin, ThermoFisher Scientific) in 3% BSA/PBS. Cells were washed three times with PBS and then stained for 10 minutes with 1:1000 Hoechst stain (Hoechst 33258, Sigma-Aldrich), followed by three washes with PBS. Coverslips were mounted using fluorescence mounting medium (Fluorescence Mounting Medium, DAKO) and analysed by confocal microscopy (Zeiss LSM710).

2.8.2 pHrodo red *E. coli* BioParticles

pHrodo Red *E.coli* BioParticles were added to cells in 100 µl medium and placed in a water bath in the dark at 37°C for 1 hour. A control sample containing BioParticles was kept at 4°C during this period. Samples were analysed by flow cytometry.

2.9 Nitrite (Griess) assay

Nitrite concentration of medium harvested from wells with cells stimulated with LPS was measured by the Griess assay. One hundred microlitres of nitrite standards in triplicate or 100µl medium was added in duplicate in a 96-well plate. To each well 100 µl of Griess reagent (0.1% α-naphthyl ethylene diamine dihydrochloride, 1% sulphanilamide in 2.5% phosphoric acid in dH₂O) were added and incubated for 30 minutes at 37°C. Absorbance was read at 570 nm.

2.10 Immunohistochemistry

2.10.1 Tissue fixation

Formalin fixed tissue paraffin embedding

For tissue histology, tissue samples were fixed in formalin for 24-72 hours then processed (see **Table 2-5** for procedure details) using an Excelsior tissue processor (Thermo Fisher Scientific). Sections were placed in moulds and embedded in paraffin wax and left to cool before storage at RT prior to sectioning.

Table 2-5 Programme used for processing tissue for formalin fixed paraffin embedded tissue sections

Step	Reagent	Time
1	70% ethanol	1 hour
2	90% ethanol	1 hour
3	100% ethanol	1 hour
4	100% ethanol	1 hour
5	Xylene	1 hour
6	Xylene	1 hour
7	Xylene	1 hour
8	Paraffin (60°C)	1 hour
9	Paraffin (60°C)	1 hour
10	Paraffin (60°C)	1 hour

Formalin-fixed paraffin embedded tissue sectioning

Sections 5 µm in thickness were cut on a microtome, placed on a 37°C water bath and collected on slides (Superfrost Plus, Thermo Fisher Scientific). Tissues were cut both in transverse section and also in whole mounts. Sections were air dried for one hour followed by further drying at 55°C for 1 hour. Slides were stored at RT until prior to staining.

Deparaffinising formalin-fixed paraffin embedded tissue sections prior to immunohistochemistry

Prior to IHC or staining, tissue sections were deparaffinised in xylene, rehydrated in a graded ethanol series and washed in tap water (Table 2-6) using an automated processor (Leica Autostainer; Leica Biosystems). Routine haematoxylin and eosin (H&E) staining was performed on all sections to assess for any pre-existing underlying pathology.

Table 2-6 Rehydration steps for formalin fixed paraffin embedded tissue sections

Step	Reagent	Time
1	Xylene	5 mins
2	Xylene	5 mins
3	Xylene	5 mins
4	100% ethanol	2 mins
5	100% ethanol	2 mins
6	95% ethanol	1 min
7	Running water	3 mins

2.10.2 Antigen retrieval

Heat-mediated antigen retrieval was performed for all antibodies by placing slides in 600 ml 0.01M sodium citrate buffer (pH 6.0) in a microwaveable pressure cooker at approximately 110°C for 20 minutes.

2.10.3 Antibody incubation

Prior to staining, endogenous peroxidase activity was inhibited in 3% hydrogen peroxide (Peroxidase-blocking solution; Dako REALTM, Agilent Technologies) in methanol for 30 minutes at RT. Slides were incubated with 100-200 μ l blocking serum (1% normal goat serum [NGS]) and 5% BSA in tris-buffered saline [50 mM Tris-Cl, pH 7.6; 150 mM NaCl; TBS] for 30 minutes at RT in a humidity chamber.

The primary antibody was applied diluted in blocking serum (See **Table 2-7** for details of primary antibodies and dilutions used) in 100-300 μ l aliquots to fully cover tissue sections. Slides were incubated for 2 hours at RT in a humidity chamber. Following incubation, a secondary anti-mouse or anti-rabbit antibody was applied (ImmPRESS HRP Anti-Mouse Ig [peroxidase] Polymer Detection Kit and ImmPRESS HRP Anti-Rabbit Ig [peroxidase] Polymer Detection Kit; Vector Labs) for 15-30 minutes at RT, followed by 3,3'-diaminobenzidine (DAB) (3-solution DAB kit; Vector Labs) for 10 minutes. Slides were then either dehydrated and mounted with no counterstain (**Table 2-8**), or counterstained with haematoxylin (and mounted using a xylene based mountant) (**Table 2-9**). Once dried, slides were scanned using a Nanozoomer (Hamamatsu Photonics) and analysed using NDP.view2 (Hamamatsu Photonics) and ImageJ.

Table 2-7 List of antibodies used for immunohistochemistry

Antibody	Clone	Supplier	Host	Target	Dilution
CD163	AM-3K	TransGenic	Mouse	Human	Did not work (Dilutions from 1:50 to 1:1000)
CD163	EDHu1	Abcam	Mouse	Human	1:200
CD117	-	Dako	Rabbit	Human	1:100 – did not work very well
PGP 9.5	-	Dako	Rabbit	Human	1:400

Table 2-8 Dehydration program for slides (no counterstain)

Step	Reagent	Time
1	Running water	3 mins
2	70% ethanol	20 secs
3	95% ethanol	20 secs
4	95% ethanol	30 secs
5	100% ethanol	30 secs
6	100% ethanol	30 secs
7	Ethanol/xylene	1 min
8	Xylene	1 min
9	Xylene	1 min
10	Xylene	1 min

Table 2-9 Counterstain and dehydration program for slides

Step	Reagent	Time
1	Running water	3 mins
2	Haematoxylin	3 mins
3	Running water	5 mins
4	Scott's tap water	2 mins
5	Running water	5 mins
6	70% ethanol	20 secs
7	95% ethanol	20 secs
8	95% ethanol	30 secs
9	100% ethanol	30 secs
10	100% ethanol	30 secs
11	Ethanol/xylene	1 min
12	Xylene	1 min
13	Xylene	1 min
14	Xylene	1 min

2.11 Cell imaging

2.11.1 *Light microscopy*

Cells in culture dishes were placed under a light microscope for imaging. Prior to imaging, the media was replaced with fresh media to discard any non-adhered cells or debris. Images were obtained and analysed using Zen Blue (Zeiss).

2.11.2 *Confocal microscopy*

Cells were placed on glass coverslips in media and left overnight at 37°C to adhere. The media was removed, and cells were permeabilised with 0.1% Triton X-100 for 5 minutes then washed three times with PBS. Cells were blocked with 3% BSA in PBS for 1 hour and then stained for 1 hour with a 1:500 dilution of phalloidin (Texas Red-X Phalloidin, ThermoFisher Scientific) in 3% BSA in PBS. Cells were washed 3 times with PBS and then stained for 10 minutes with 1:1000 Hoechst stain (Hoechst 33258, Sigma-Aldrich), followed by three washes with PBS. Coverslips were mounted using fluorescence mounting medium (Fluorescence Mounting Medium, DAKO) and analysed by confocal microscopy (Zeiss LSM710). Images were obtained using Zen Black (Zeiss).

2.12 Mouse intestinal whole mount imaging

The whole gastrointestinal tract (GIT) was removed whole from distal oesophagus to rectum. Luminal contents were cleared by gently flushing with ice cold Krebs solution (Sigma-Aldrich). The caecum and stomach were removed and discarded. The small or large intestine were opened on the anti-mesenteric border with scissors and the

mucosal surface was thoroughly washed. For mucosal imaging, the tissue was placed mucosal side up onto a slide (Superfrost Plus, Thermo Fisher Scientific) and mounted using fluorescence mounting medium (Dako). For *muscularis* imaging, segments were pinned out onto a dish and the mucosa and submucosa removed. The remaining *muscularis* was then mounted on to a slide as described above. Images were acquired using Zeiss LSM710 confocal or Zeiss Axio Zoom.V16 Fluorescence Stereo Zoom microscope.

2.13 Image software

All light microscope and confocal images were created using Zen Blue (Light microscopy) or Zen Black (confocal microscopy and multiphoton microscopy) software (Zeiss International). Slides were scanned using a Nanozoomer (Hamamatsu Photonics) which generated images of the slide. These were viewed using NDP.view2 (Hamamatsu Photonics). Images were analysed using ImageJ (Schneider et al., 2012) CellProfiler (Jones et al., 2008) or NDP.view2 (Hamamatsu Photonics).

2.14 Image analysis pipelines

Pipelines for image analysis were developed with the help of Dr Kristin Sauter, Roslin Institute, University of Edinburgh (ImageJ) and Dr Barbara Shih, Roslin Institute, University of Edinburgh (CellProfiler).

2.15 Quantification of cells in the equine gastrointestinal tract

Slides were visualised using NDP.view2 (Hamamatsu Photonics). Three areas within a 2 mm region were selected for counting for each layer; 2 mm from the left side edge of tissue, the mid-point of tissue section and 2 mm from the right-side edge of tissue section. Areas to be analysed were drawn using either the rectangle function, or freehand region function. For the mucosa, submucosa and muscle layers, a 0.5 mm² area was measured. For the myenteric plexus and serosa, a 0.1 mm² area was measured. Values were then either multiplied by 2 or 10 respectively, to give values per mm². Cells were marked manually and counted. The three values for each area were averaged for further analysis. See **Figure 2-1** for a summary of the quantification method.

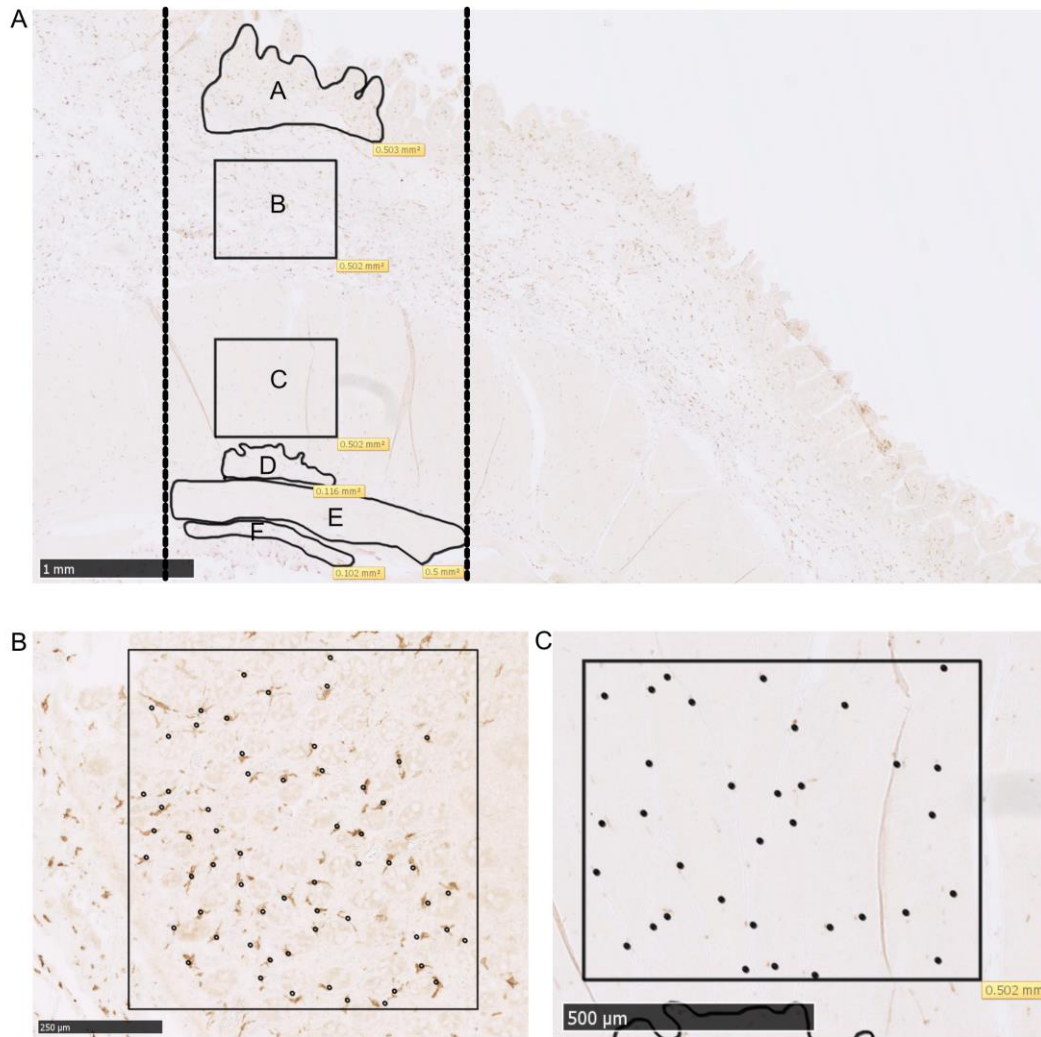


Figure 2-1 Example of cell quantification method

A 2 mm region was identified in the left, middle (A) and right-hand side of the tissue section. Using the rectangle or freehand function in NDP2.view areas measuring either 0.5 mm² (A, B, C, E) or 0.1 mm² (D, F) were drawn within the 2 mm section (region represented by dotted line in A). Positive staining cells were marked to facilitate counting (B and C).

Magnification (A) X2 Bar=1 mm, (B) X5 Bar=250 µm, (C) X10 Bar=500 µm

2.16 RNA Extractions

2.16.1 Cells

For extraction of adhered bone marrow-derived macrophages TRIzol (Ambion, Life Technologies) was added to cell culture wells, after removal of the supernatant, to lyse the adhered cells. After 5 minutes, the TRIzol solution was collected and stored at -80°C.

RNA was extracted using the RNeasy Mini kit (Qiagen), following manufacturer's instructions. The TRIzol and cell solution was thawed and 200 μ L of 1-Bromo-3-chloropropane (BCP) (Sigma-Aldrich) was added. The mixture was shaken vigorously for 15 seconds and incubated at RT for 3 minutes. The solution was centrifuged at 12000 *rcf* for 15 minutes at 4°C. Four hundred microlitres of the upper aqueous phase were transferred to a new tube. To each tube, 400 μ L of 70% ethanol were added and mixed with a pipette. Four hundred microlitres of the ethanol-RNA mix were transferred to a RNeasy Mini spin column (Qiagen) in a collection tube and centrifuged at RT for 10,000 *rcf* for 30 seconds. The flow through was discarded and the remaining ethanol-RNA mix was transferred to the same spin column and centrifuged at 10000 *rcf* for 30 seconds. Again, the flow through was discarded and 700 μ L of Buffer RW1 (Qiagen) was added to the RNeasy column and centrifuged for 30 seconds at 16000 *rcf*. The flow through was discarded and the Buffer RW1 step repeated. Next, 500 μ L Buffer RPE (Qiagen) were added to the RNeasy column and centrifuged for 2 minutes at 16,000 *rcf* and the flow through discarded. This step was repeated but the column centrifuged at 16,000 *rcf* for 30 seconds. To dry the membrane the RNeasy column was placed in a new 2 ml collection tube and centrifuged at full speed for 1 minute. The spin column was transferred into a new 1.5 ml tube and 34 μ L of RNase free water (Qiagen) were added to the spin column to elute the RNA. The column was centrifuged at 10,000 *rcf* for 1 min. RNA was either stored at 4°C for a maximum of 4 hours or at -80°C for long term storage.

2.16.2 Tissues

RNA from tissues was extracted using a RNeasy Plus Mini kit (Qiagen) following manufacturer's instructions. Briefly, 50 μ g of frozen tissue was added to 600 μ L of β -mercaptoethanol (β -ME) in an eppendorf with CK14 beads (Bertin Instruments). Tissues were homogenised (Precellys, Bertin Instruments) using the following settings; horse mucosa and liver 1 x 5800 rpm for 30 seconds and horse *muscularis* 2 x 6500 rpm for 30 seconds with 30 seconds rest. The *muscularis* was added to ProteinaseK (Dako) for 30 minutes at 60°C. The homogenates were centrifuged at 16,000 *rcf* for 3 minutes and the supernatant transferred to a gDNA Eliminator column (Qiagen) and centrifuged for 30 seconds at 10,000 *rcf*. Six hundred microlitres of 70% ethanol were added to the flow through and mixed with a pipette. Six hundred microlitres of the RNA-ethanol mix were transferred to a RNeasy Mini spin column (Qiagen) in a collection tube and centrifuged at RT for 10,000 *rcf* for 30 seconds. The flow through was discarded and the remaining ethanol-RNA mix was

transferred to the same spin column and centrifuged at 10000 *rcf* for 30 seconds. The remainder of the protocol is identical to that described for cells in **Section 2.16.1**.

2.17 RNA quantification and quality analysis

2.17.1 Nanodrop

RNA was quantified by testing 1 μ L of sample using an ND-1000 Nanodrop spectrophotometer (ThermoFisher Scientific, Wilmington, USA). RNA purity was assessed by measuring absorbance at 230 nm, 260 nm and 280 nm. A 260/280 or 260/230 ratio of 2 indicates good purity of RNA (Desjardins and Conklin, 2010).

2.17.2 Qubit

Samples to be sent for microarray analysis and RNA-Sequencing were quantified using the Qubit 3.0 Fluorometer (ThermoFisher Scientific) following manufacturers protocol for the Qubit RNA BR Assay Kit. Briefly 2 μ L of sample was added to the Qubit working solution to a total volume of 200 μ L in thin-walled PCR tubes. After incubation at RT for 2 minutes, RNA concentration was measured using the Qubit 3.0 Fluorometer.

2.17.3 TapeStation

RNA sample integrity was measured using 2200 TapeStation System (Agilent Technologies) using RNA ScreenTape. One microlitre of sample was added to 5 μ L Sample Buffer in PCR tubes. The sample was vortexed at 2000 rpm for 1 minute, heated at 72°C for 3 minutes and cooled for 2 minutes at 4°C before being loaded into the 2200 TapeStation System. An RNA integrity number (RIN) greater than 7 was used for all further work (Schroeder et al., 2006).

2.18 cDNA Synthesis from RNA

cDNA was synthesised from 1 μ g RNA using the SuperScript III First-Strand synthesis system (Invitrogen). One microgramme of RNA was combined with 50 μ M oligo(dT)₂₀, 10 mM dNTP mix and nuclease free water (added to make 10 μ L) in a nuclease-free tube. The solution was incubated at 65°C for 5 minutes followed by rapid cooling at 4°C for 1 minute. Ten microlitres of cDNA synthesis mix (2 μ L 10X RT buffer, 4 μ L 25 mM MgCl₂, 2 μ L 0.1 M DTT, 1 μ L RNaseOUT (40U/ μ L) and 1 μ L SuperScript III RT (200 U/ μ L) per reaction) were added to each RNA mixture and incubated at 50 minutes for 50°C, terminated at 85°C for 5 minutes and then fast cooled to 4°C. Samples were

briefly centrifuged and 1 μ L of RNaseH was added to each tube and incubated for 20 minutes at 37°C. Samples were stored at -20°C.

2.19 Primer design

Primers were designed using Primer3 (Untergasser et al., 2012, Koressaar and Remm, 2007) based on known or predicted equine sequences. Gene sequences were obtained from www.ensembl.org (Ensembl) and the sequence blasted to SeqBuilder13 (DNASar Lasergene 13). The exons were mapped out manually in SeqBuilder13 and suggested primers from Primer3 were mapped out to ensure that they covered more than one exon. Primer sequences used are listed in **Table 2-10**.

Table 2-10 Primers used in Real – Time quantitative PCR

Gene	Forward	Reverse
<i>GAPDH</i>	GGAGTCCACTGGTGTCTTCA	AGCAGAAGGAGCAGAGATGAT
<i>TNF-α</i>	CCTGTAGCCCATGTTGTAGCA	GGACCTGGGAGTAGATGAGGT
<i>IDO1</i>	ACTTCTTGTCTACGCAACGC	CGCCTTCATAGAGCAGACCT
<i>NOS2</i>	CCCAAGCTCTACACCTCAA	TCTGTAGATTCTGCCGCGAT
<i>IL6</i>	CCACTACTCACCCTGCAGA	TTTCATCAGGCAGGTCTCCT
<i>TLR4</i>	GGACCTGAGCTTTAACCCT	CAATTTACACCTGGACAAA
<i>PTGS2</i>	TCACCCAGTTTGTGAATCTTTC	CCTCAATCGACCAGAGCAGA
<i>IL1B</i>	GGGACGAAAGATGGGAAGCC	TCCCATCTTTCGTCCCACAA
<i>CSF1R</i>	TCTGGTCTACGGCATCCTG	CATTTGGTATCCGTCTTGACC
<i>CCL2</i>	AGTACCAGCAGCAAGTGTC	AGCATCCTGGACCCACTTC

2.20 Real – Time quantitative polymerase chain reaction (RT qPCR)

For real-time quantitative PCR (qPCR), cDNA was amplified with Power SYBR Green PCR Master Mix using the 7500 fast Real Time PCR system (ThermoFisher Scientific). Primer efficiency was validated with a standard curve of five serial dilution points (three for *NOS2*) with efficiency ranging between -3.304 and -3.511. Amplification was performed in triplicate and relative gene expression was calculated using the $2^{-\Delta\Delta CT}$ method (Livak and Schmittgen, 2001). Lucas Lefevre assisted with the design and optimisation of primers as well as performing the qPCR for the colic cases.

2.21 Experimental model of post-operative ileus

All work was performed on mice at TARGID, KU Leuven, Leuven, Belgium. A standard model of intestinal manipulation was used (van Bree et al., 2012). Briefly, under general anaesthesia, a midline laparotomy was performed and the small intestine exteriorised, avoiding manipulation of the colon. The small intestine was manipulated three times by the same individual using a purpose designed device with a standardised weight (9g) to allow even and consistent application of pressure (van Bree et al., 2012). The small intestine was placed back in the abdomen and the abdomen closed. Mice were placed on a heat pad until they recovered from the surgery. Naïve mice underwent laparotomy alone, with no manipulation of the intestine. Dr Giovanna Farro (TARGID, KU Leuven) performed all intestinal manipulations.

2.22 Gastrointestinal transit measurement

Gastrointestinal transit was measured as described by Wehner *et al.* 2011. Briefly, mice were administered 10 μ l of a liquid non-absorbable fluorescein isothiocyanate-labelled dextran (FITC-dextran, 70,000 Da; Invitrogen) *per os* after being starved for 90 minutes. After a further 90 minutes, animals were culled by CO₂ overdose followed by cardiac bleeding and/or cervical dislocation. The GIT was removed avoiding excess manipulation thus avoiding disruption of contents. The stomach, small intestine, caecum and large intestine was laid lengthways, avoiding overstretching of the tissue, and the small intestine and colon divided into equal parts (10 for small intestine; 3 for colon). Each segment was placed into an Eppendorf tube with 1 ml of ice-cold Krebs solution (Sigma-Aldrich). Each segment was then minced using scissors and the tube vortexed for 10 seconds. The homogenate was centrifuged at 12,000 *rcf* for 10 minutes and 200 μ l of supernatant in triplicate transferred into a 96-well plate. Fluorescence was read at 488nm using a multi-mode plate reader (BioTek Instruments). By calculating the geometric centre (GC) (Σ (percent of total fluorescent signal in each segment x the segment number)/100), a comparison of the distribution of fluorescent dextran in the GIT was made between groups (van Bree et al., 2012, Wehner et al., 2011).

2.23 Treatment of mice with an FC conjugate of CSF-1

Mice were injected subcutaneously with 0.75 mg/kg of an Fc conjugate of pig CSF-1 (CSF1-Fc) (Zoetis) (Gow et al., 2014) at 24-hour intervals for 3 to 5 days (duration specified for each specific study). The control group were injected with PBS.

2.24 Flow cytometry

Cells were pelleted and re-suspended in blocking solution for 30 minutes in 1% NGS in a 96 well plate on ice. One million (1×10^6) cells per well were used. Following centrifugation for 5 minutes at $400 \times g$, supernatant was removed, and cells were re-suspended in 50 μ l PBS containing either primary or secondary antibody or isotype controls. Samples were incubated in the dark at 4° C for 60 minutes before washing twice with 100 μ l PBS. Cells were resuspended in 500 μ l of PBS with 0.1% Sytox blue (Invitrogen) used as a dead cell marker. Data were acquired using a BD Fortessa LSR (Beckton Dickinson) flow cytometer. Blood was prepared for flow cytometry after staining with the Dako Uti-lyse™ kit (Dako, Denmark).

Primary antibodies used were mouse anti-equine CD14 (Clone 105, 1:100, Wagner Laboratory) or mouse anti human CD163 (Clone EDHu-1, 1:100, Bio-Rad). Secondary antibodies used were rat IgG1-APC (1:100, Bio-Legend). The isotype control used was mouse IgG1 (Bio-Rad). Details of antibodies and concomitant dilutions are shown in Table 2-11.

Data were analysed with FlowJo software (FlowJo, LLC, Ashland, USA). Dr Anna Raper (Roslin Institute, University of Edinburgh) provided assistance with the generation of graphs.

Table 2-11 Antibodies used for flow cytometry

Antibody	Clone	Isotype	Supplier	Host	Target	Dilution
CD163	EDHu-1	IgG1	Bio-Rad	Mouse	Human	1:100
CD14	105	IgG1	Wagner Laboratory	Mouse	Equine	1:100
CSF1R	n/a	n/a	Produced in-house	Pig		1:2000

2.25 Microarray analysis

Total RNA was extracted from jejunal *muscularis* of C57BL/6 mice (n=3) and B6.129S4-Ccr2^{tm1lf}/J mice (n=3) that underwent intestinal manipulation and had been pre-treated with CSF1-Fc for 48 hours prior to surgery. Treatment with CSF1-Fc

continued for three days post-operatively at which point the mice were culled. The control group (n=3 for both genotypes) were treated with PBS. Total RNA was extracted from whole gut (jejunum) from C57BL/6 mice that were treated with CSF1-Fc (n=2) or PBS (n=2) for 5 days but did not undergo intestinal manipulation (See 2.16.2 above for extraction method). *Muscularis* RNA extractions were performed by Michelle Stakenborg (TARGID, KU Leuven, Belgium). Microarrays were processed by Edinburgh Genomics, The University of Edinburgh using the Affymetrix Mouse Gene 1.1 ST Array Strip.

2.26 RNASeq analysis

Total RNA was extracted from eqBMDMs with or without exposure to LPS for 7 hours (n=3 per group) and was used for paired end library preparation and sequenced using HiSeq4000 (Illumina, San Diego, USA) at >100 million paired end reads per sample by Edinburgh Genomics, University of Edinburgh.

2.26.1 Data quality control

Raw data were obtained in the form of fastq. files.

2.26.2 Differential expression analysis

Expression level was quantified, as both transcripts per million (TPM) and estimated read counts, using Kallisto v0.42.4 (Bray et al., 2016). Transcript-level read counts were summarised to the gene level using the R/Bioconductor package tximport v1.0.3 (Soneson et al., 2015), with gene names obtained from the EquCab2.0 annotation (via Ensembl BioMart v90 (Yates et al., 2016, Kinsella et al., 2011)). The tximport package aggregates Kallisto output into a count matrix, useable by the R/Bioconductor package edgeR v3.14.0 (Robinson et al., 2010) for differential expression analysis, as well as calculating an offset that corrects for changes to the average transcript length between samples (which can reflect differential isoform usage). Using edgeR, gene counts were normalised using the ‘trimmed mean of M values’ (TMM) method, with a negative binomial generalized log-linear model fitted, and p-values corrected for multiple testing according to a false discovery rate (FDR) (Benjamini and Hochberg, 1995).

2.26.3 Gene ontology (GO) term enrichment

Clusters were analysed using the Bioconductor package ‘topGO’ to examine if genes within clusters shared similar functions and pathways, based on gene ontology (GO)

(Alexa and Rahnenfuhrer, 2016). GO term enrichments are given for every cluster containing ≥ 10 genes. GO terms are listed only if a) $p < 0.05$ and b) there are ≥ 10 genes across the entire genome annotated with that GO term.

2.27 Statistical analysis

Statistical analysis was performed using GraphPad Prism 7.0 for Windows (GraphPad Software). Significance was assumed at $p < 0.05$. Significance in CD163 staining between regions was determined by paired two-tailed Student's t-test. Significance between colic case relative gene expression and controls was determined with a non-parametric Mann-Whitney U test. All graphs were created using GraphPad Prism 7.0 for Windows (GraphPad Software).

Chapter 3. Distribution of macrophages in the equine gastrointestinal tract

3.1 Introduction

Resident tissue macrophages, such as those found in the gastrointestinal tract (GIT), are specialised cells with tissue-specific roles. They are a heterogeneous population (Gordon and Taylor, 2005), yet are broadly made up of two distinct sub-populations: lamina propria (LpM) or mucosal macrophages and *muscularis* macrophages (MM). LpM are replenished by circulating monocytes, in the presence of the macrophage growth factor CSF-1 (Bain et al., 2014, Baillie et al., 2017). MM have not been studied as extensively as LpM. In comparison to LpM, MM have a slower turnover rate (Mikkelsen et al., 2004) and it is yet to be determined whether this population are monocyte derived or derived from yolk sac progenitors and sustained by self-renewal. Their distribution in mouse embryos is similar to their distribution in adult mice (Mikkelsen et al., 2004), yet low numbers of monocytes have been detected in the normal *muscularis* of rats, which increase in number with intestinal inflammation (Hori et al., 2008). Rodent and human derived data show that, during intestinal surgery, activation of MM plays a role in the pathogenesis of post-operative ileus (Kalff et al., 1998a, Farro et al., 2017, Kalff et al., 2003).

Except one study which quantified the immune cell populations in the lamina propria of the equine jejunum (Packer et al., 2005), there are no studies to date describing or quantifying resident macrophage populations in *muscularis externa* (ME). Yamate *et al.* (2000) demonstrated the presence of CD163⁺ cells, consistent with macrophages, in the mucosa and *muscularis* of the equine GIT (Yamate et al., 2000) but did not investigate their number or distribution.

Immunohistochemistry (IHC) followed by light microscopy allows the identification of positive staining cells (in this case, macrophages). This allows the study of both their location within the tissue and an estimation of their density. By using dual staining techniques, where different chromogens are applied to different antibodies, the relationship of macrophages with other cells, such as the motility effector cells of the GIT (e.g. interstitial cells of Cajal [ICC] and enteric neurons), can be studied. When quantifying cells, it is important to use quantitative methods using a number-weighted, and not size or shape-weighted, method to give accurate results of density within the tissue (Mikkelsen et al., 2011). Other methods of imaging macrophages in mice include the use of transgenic reporters such as those based upon the *Csf1r* promoter (Sauter et al., 2014, Sasmono et al., 2003). The use of these mice is discussed in further detail in **Chapter 1** and **Chapter 6**. Such reporters are clearly not available for the horse.

Markers used to identify macrophages in the GIT of other species are summarised in **Table 3-1**, with most of the studies focusing on LpM, rather than MM, populations. Studies of GIT macrophage populations in various species have adopted the use of antibodies against the following targets: adhesion G-protein coupled receptor F4/80 (Hume et al., 1984, Mikkelsen et al., 1988), macrophage scavenger receptor for the haemoglobin-haptoglobin complex (CD163) (Yamate et al., 2000, Kalff et al., 2003, Dijkstra et al., 1985, Phillips and Powley, 2012), interferon regulatory factor 1 (IRF1) (Hume et al., 1987) major histocompatibility complex (MHC) II (Mikkelsen and Rumessen, 1992), sialoadhesin (Siglec1/CD169) (Dijkstra et al., 1985), class D scavenger receptor (CD68) (Mikkelsen and Rumessen, 1992) and CD11b (*Itgam*) (Mikkelsen and Rumessen, 1992, Mikkelsen et al., 1988). The use of multiple labelled antibodies can also be used to identify different subsets of macrophages and thus potentially provide information on functional differences between different macrophage subsets, based on their regional location within the GIT. Previously used markers for macrophages in the horse include CD163 (clone AM-3K) (Yamate et al., 2000, Grosche et al., 2011) in small and large intestine and MAC387 (MRP-8 and MRP-14) in brain tissue and jejunum (Packer et al., 2005); however both MAC387 and lysozyme are non-specific for macrophages since both are present in granulocytes.

Table 3-1 Summary of antibodies used to identify macrophages in the GIT of species other than horse

Species	Antibody
Mouse	F4/80/EMR1
	CD163
	CD68
	CD169
	M1/70 (CD11b)
Rat	MHCII
	ED1 (CD68)
	ED2 (CD163)
	ED3 (CD169)
Human	MHCII
	CD163
	CD11b
	CD68

Intestinal macrophages are located in all cross-sectional regions of the intestine; the lamina propria, the submucosa, the circular muscle, between the longitudinal and circular muscle (at the level of the myenteric plexus [MP]), the longitudinal muscle and the serosa (Mikkelsen, 1995, Mikkelsen et al., 2004, Kalff et al., 1998b), Their morphology varies depending on their location. In the mouse, serosal macrophages are bipolar, slender, orientated parallel to the longitudinal muscle and occasionally have bifurcated processes (Mikkelsen, 2010). Cells within the circular and

longitudinal muscle layers are found between the muscular bundles and have an elongated thin shape, with those in the longitudinal muscle being less elongated compared with those within the circular muscle (Kalff et al., 1998b). Macrophages between the circular and longitudinal muscle layers, at the level of the MP (also termed Auerbach's Plexus) are stellate with multiple dendrites (Kalff et al., 1998b, Mikkelsen, 2010).

In contrast to serosal and MM associated with the myenteric plexus (MP) which have a regular distribution, those found within the muscle layers have a slightly more heterogeneous distribution, being located lining muscle layers and septa (Mikkelsen, 2010). Compared with mouse serosal macrophages, human serosal macrophages appear rounder and less ramified although the morphology of mouse and human MP macrophages is similar (Mikkelsen and Rumessen, 1992). In horses, humans and mice, LpM are found beneath the epithelium (Nagashima et al., 1996, Mahida et al., 1989, Hume et al., 1987, Packer et al., 2005). In mice, LpM have a ramified structure (Sasmono et al., 2003, Robert et al., 2011), but have reduced dendrite ramifications when compared to MM. Despite shorter ramifications, LpM have increased movement of dendrites (Gabanyi et al., 2016) reflecting their role in luminal sampling across the epithelium. This contrasts with the reported structure of human LpM which were predominantly large and round (Mahida et al., 1989).

The main objective of this chapter was to immunohistochemically identify and plot the distribution of resident macrophages in the normal equine GIT and, using dual staining techniques, study their spatial relationship to motility effector cells such as ICC and enteric neurons. Protein gene product 9.5 (PGP 9.5) was used to detect enteric neurons as described previously (Ramos-Vara et al., 2014, Hudson et al., 2014). ICC identification was attempted using CD117 and the methodology of Hudson et al. (1999), with the exception that formalin-fixed paraffin embedded tissues (FFPE) were used rather than cryosections. For the detection of macrophages, an antibody against CD163 was used. CD163 is a member of the class B scavenger receptor cysteine-rich family and along with M160, is the only one expressed on both monocytes and macrophages (Van den Heuvel et al., 1999). As mentioned above, CD163 has previously been used to identify rat and human intestinal macrophages (Mikkelsen, 2010, Mikkelsen and Rumessen, 1992, Kalff et al., 2003) and has also been used to study equine intestinal (Yamate et al., 2000) and non-intestinal macrophage populations, including the uveal tract and laminae (Faleiros et al., 2011, Sano et al., 2016, Yamate et al., 2000). In the horse, CD163 is highly expressed on alveolar macrophages, but not peritoneal macrophages (Karagianni et al., 2013).

3.2 Results

3.2.1 Optimisation of immunohistochemistry protocols

CD163

The initial aim of this chapter was to optimise and establish a protocol for CD163 staining, to ensure the antibody was targeting the expected antigen (Ramos-Vara et al., 2008). Initially the protocol used by Yamate et al. 2000 was used, which used the AM-3K clone of CD163; however, it was not possible to get this antibody to work for immunohistochemistry of intestinal tissues in this study. The CD163 clone KT-103 was used by our laboratory group in other species (Sauter et al., 2016), so further optimisation was performed with the KT-103 clone of CD163.

Tissue Fixation

Fixation of tissues in 10% neutral-buffered formalin is commonly used as it avoids the use of fresh or snap (fresh) frozen tissues and allows for relatively easy long-term storage of tissue sections. Advantages of formalin fixation include the prevention of tissue necrosis and retention of tissue and cellular architecture (Ramos-Vara, 2005). Conversely, as formalin fixation results in the cross linking of peptides, through the formation of hydroxymethyl groups on certain amino acid chains, it can change the conformation of macromolecules. When affecting specific antigens, this conformational change can interfere with antibody recognition (Ramos-Vara, 2005). In light of the large numbers of tissues collected from each horse in this current study, formalin fixation in 10% neutral-buffered formalin was highly convenient, compared with tissue freezing. To minimise any risk of antigen detection loss resulting from prolonged fixation (Webster et al., 2009), tissues were stored in formalin for no more than 6 weeks.

Antigen retrieval

An antigen retrieval protocol can be adopted prior to antibody labelling to reverse some of the changes associated with cross-linked tissue fixation; such protocols are based on either heat-mediated or enzymatic processes (Ramos-Vara, 2005). Enzymatic protocols, such as ficin, proteinase K, pepsin and trypsin work by the digestion of cross linked proteins formed during fixation (Hecke, 2002). Disadvantages of enzymatic protocols include the low number of epitopes on which the enzymes work, alteration of tissue morphology and alteration or damage to the target epitopes (Ramos-Vara, 2005). Heat-induced retrieval involves breaking the bonds between formalin and the epitope protein by high temperatures and strong

alkaline hydrolysis although the exact mechanism of action is not known (Ramos-Vara, 2005) For this study, protocols were adapted from www.ihcworld.com. Various enzyme and heat-mediated antigen retrieval methods were applied to the equine fixed intestinal tissue samples; results associated with each method are summarised in Table 3-2.

Table 3-2 Summary of results with various antigen retrieval techniques for CD163 staining in formalin-fixed paraffin embedded equine intestinal tissue

Enzymatic antigen retrieval	Enzyme	Result
	Pepsin	No staining
	Trypsin	Some staining (weak)
	Proteinase K	Some staining (weak)
	Ficin	No staining
Heat-mediated antigen retrieval	Buffer	Result
	0.01M sodium citrate buffer (pH 6.0)	Good staining
	0.01M sodium citrate buffer (pH 7.0)	No staining
	0.01M sodium citrate buffer (pH 9.0)	No staining
	1mM EDTA buffer (pH 6.0)	No staining
	1mM EDTA buffer (pH 7.0)	No staining
	1mM EDTA buffer (pH 9.0)	No staining

From Table 3-2, several different sections of jejunum were stained for CD163 (Figure 3-1). The use of trypsin and proteinase K resulted in positive staining in the submucosa and *muscularis*, but no positive staining of LpM in the villi. The use of sodium citrate antigen retrieval resulted in the positive identification of CD163⁺ cells in all layers of this intestine. Therefore, for all subsequent IHC, antigen retrieval using 0.01M sodium citrate buffer (pH 6.0) was adopted.

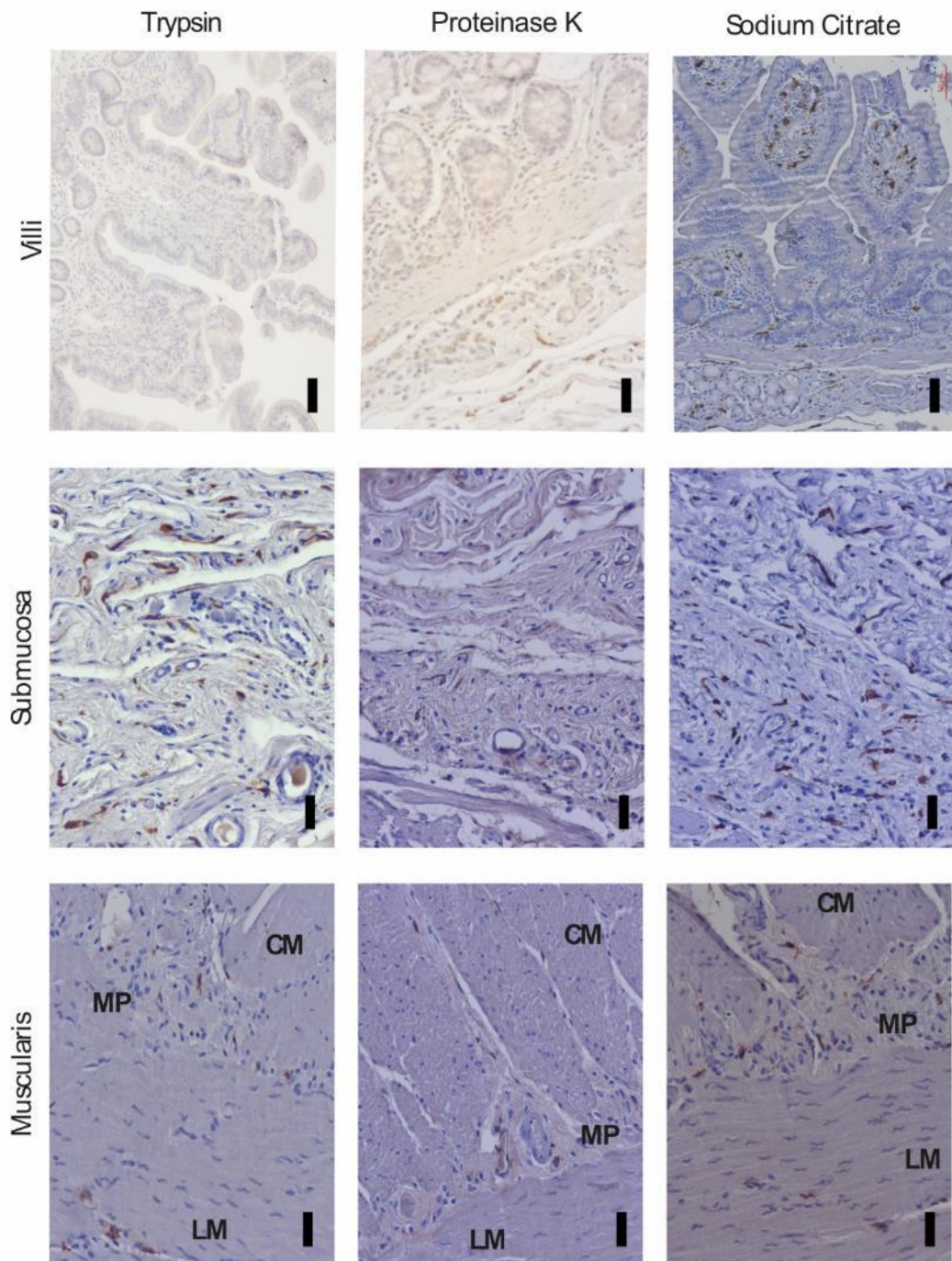


Figure 3-1 Comparison of antigen retrieval techniques for CD163 staining in equine jejunum

Antigen retrieval was performed on formalin-fixed paraffin-embedded jejunum using either trypsin, proteinase K or heat-mediated 0.1mM sodium citrate buffer (pH 6.0). Tissues were then stained for CD163 in a 1:200 dilution and a polymer detection system was used with 3,3'-diaminobenzidine (DAB) to detect positive staining. Images obtained by light microscopy using Zen software at X10 magnification. Image representative of sections of jejunum, right ventral colon and small colon of 3 horses. Bar = 50µm. Images representative of 5 horses. CM, circular muscle; LM, longitudinal muscle; MP, myenteric plexus.

CD117

In contrast to PGP 9.5, there was only weak staining of ICC cells using the optimised protocol with CD117 (**Figure 3-2**). In previous studies, horse ICC immunostaining was achieved on frozen sections (Hudson et al., 1999). It is possible that alternative antigen retrieval protocols would expose the antigenic epitope; however further exploration of this theory was not considered a core objective of the current study.

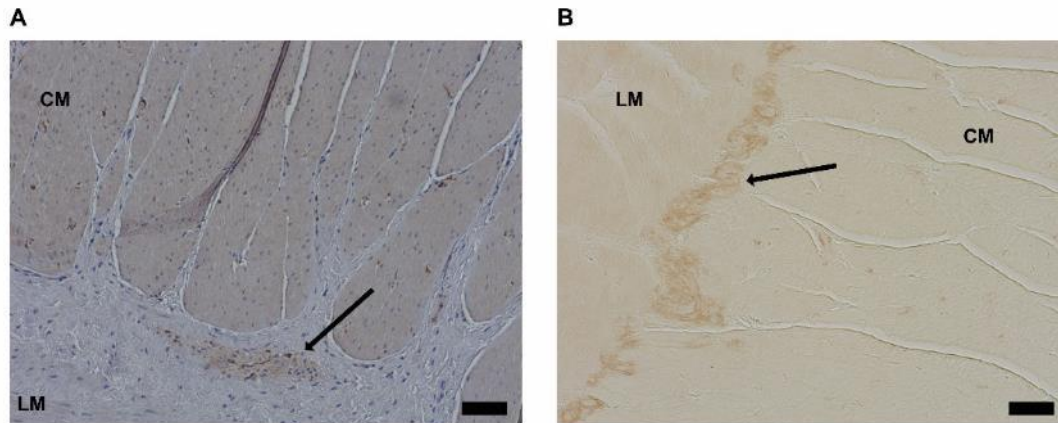


Figure 3-2 CD117 staining in equine jejunum

Staining for CD117 at the level of the myenteric plexus in equine jejunum with (**A**) and without (**B**) haematoxylin counterstain. Staining for interstitial cells of Cajal was present where expected (at the level of the myenteric plexus (black arrows) in between the circular (CM) and longitudinal (LM) muscle layers)

Magnification X20 Bar= 500 μ m. Images representative of 5 horses.

PGP 9.5

As previously reported in the equine GIT (Hudson et al., 2014) expression of PGP 9.5 was detected in all small and large intestinal sections stained in the current study. Expression was also detected in all layers; namely, mucosa, submucosa and ME (**Figure 3-3**). Neuronal axons were visible at the base of the villi, the submucosa, the circular muscle and longitudinal muscle layers. Within the longitudinal muscle layers, the axons were more punctate, as the orientation of the muscle was in transverse section, compared to the circular muscle where neurons were longer, reflecting their parallel orientation to muscle fibres.



Figure 3-3 PGP 9.5 staining in equine small colon

Equine small colon was stained with PGP 9.5, using 3,3'-diaminobenzidine (DAB) as a chromogen with no counterstain. Positive staining was visible in all layers (A X1.25 magnification; Bar=2.5mm). B (X10 magnification; Bar= 250µm) shows immunoreactivity for PGP 9.5 in the mucosa where nerve fibres (black arrows) are seen at the villi base and the submucosal plexus ganglion (asterisk). Nerve fibres can be seen within the *muscularis externa* (C & E X10 magnification; Bar=250µm) and in the myenteric plexus (MP) (D X20 magnification; Bar=500µm). Images representative of samples taken from 5 horses. CM, circular muscle; SM, submucosa, LM, longitudinal muscle; MP, myenteric plexus.

3.2.2 Distribution of macrophages in the equine GIT

Following optimisation of CD163 staining in the equine GIT, sections from 14 regions of equine GIT collected from 10 horses were stained for CD163. CD163⁺ cells were identified in all intestinal layers (mucosa, submucosa, *muscularis* and serosa) in all regions of the GIT (stomach to small colon).

Quantification of macrophages in the equine GIT

Figure 3-4 shows the number of CD163⁺ macrophages per mm² of tissue in all layers and regions of the equine GIT. The distribution of cells across layers was not uniform. The highest densities of cells per mm² of tissue for all regions were found in the mucosa, submucosa, MP and serosa. Both the circular and longitudinal muscle layers had the lowest density of cells in all sections, and the lowest variation in numbers i.e. cell numbers were consistent throughout the muscle layer. With the exception of the submucosa, the number of cells/mm² did not vary significantly throughout the length of the GIT (**Figure 3-5**). In the submucosa, a significant increase in cells/mm² was observed from the distal jejunum and the ileum. This increase in number then remained consistent for the remainder of the GIT. This change in cell numbers was not mirrored in the lamina propria population, where the cell numbers remained relatively consistent from stomach to small colon.

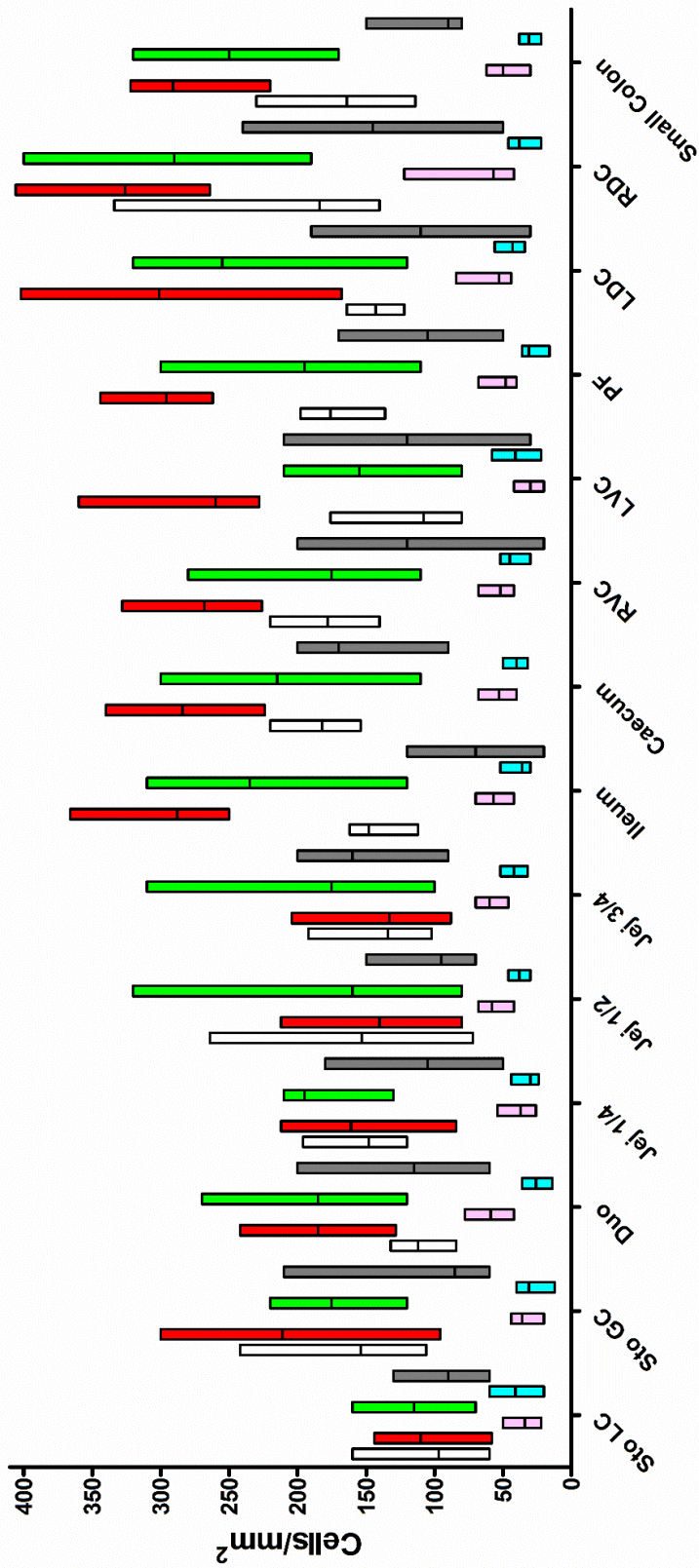


Figure 3-4 Distribution of CD163⁺ve macrophages in the equine gastrointestinal tract

Floating box plots showing maximum, minimum and median cells per mm² for each layer (mucosa, submucosa, muscle, myenteric plexus and serosa) along the length of the equine GI tract from (L-R); stomach lesser curvature (LC), stomach greater curvature(GC), duodenum, jejunum, ileum, caecum, right ventral colon (RVC), left ventral colon (LVC), pelvic flexure (PF), left dorsal colon (LDC), right dorsal colon (RDC) and small colon. n=10

- Mucosa
- Submucosa
- Circular muscle
- Myenteric plexus
- Longitudinal muscle
- Serosa

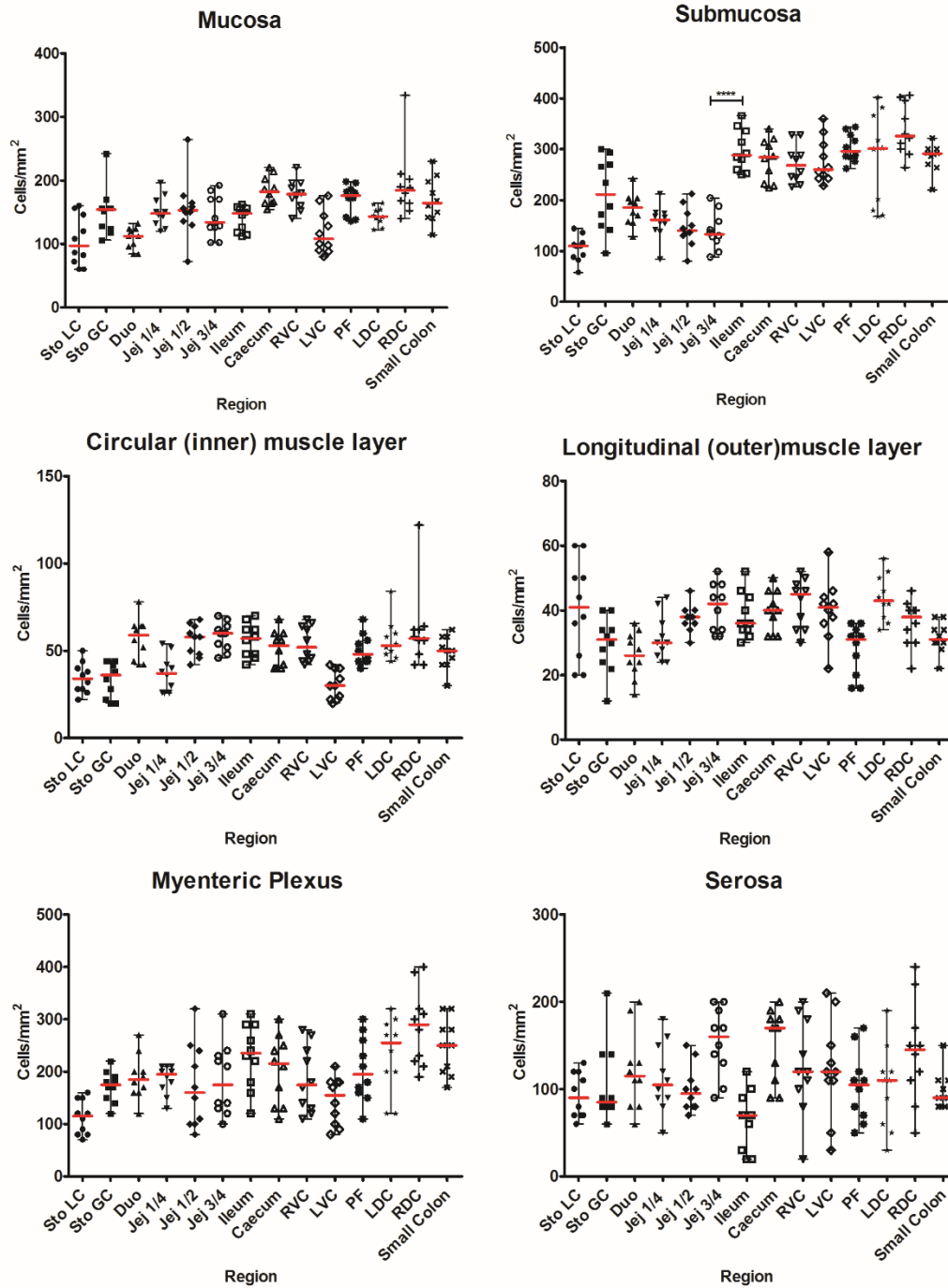


Figure 3-5 Distribution of CD163⁺ve macrophages in the layers of the equine gastrointestinal tract

Scatter plots showing cells/mm² for each layer along the length of the equine gastrointestinal tract from (L-R) stomach (Sto) lesser curvature (LC), stomach greater curvature (GC), duodenum (duo), jejunum (jej), ileum, caecum, right ventral colon (RVC), left ventral colon (LVC), pelvic flexure (PF), left dorsal colon (LDC), right dorsal colon (RDC) and small colon. Red line represents median. Significant difference ($p < 0.0001$) between cells/mm² in submucosa between jejunum (3/4) and ileum as measured by paired t-test. **** $p < 0.0001$. n=10

Morphology of macrophages in the equine GIT

Morphological staining characteristics at each location are detailed below:

Mucosa

As previously reported in humans and rodents, all macrophages within the mucosa were observed in accumulations below the epithelial layer within the lamina propria (Nagashima et al., 1996, Hume et al., 1984). This was evident both in the stomach and the small and large intestines (**Figure 3-6**). In the current study, equine LpMs were predominantly bipolar each with two to three processes (**Figure 3-7**). Other studies in mice have shown LpMs to sample luminal contents via processes extending through the basement membrane, between epithelial cells into the lumen (Muller et al., 2014). In contrast, the current study revealed equine LpMs to be located entirely beneath the basement membrane; no cells or processes were observed crossing the basement membrane and epithelial layer.

Submucosa

CD163⁺ macrophages were present in the submucosa of all tissue sections (**Figure 3-8** and **Figure 3-9**). This region had amongst the greatest density (cells/mm²) of positive staining cells (**Figure 3-4**). In the small intestine, submucosal macrophages were a mix of round and bipolar cells (**Figure 3-8**); whilst in the large intestine, macrophages were predominantly round (**Figure 3-9**). Macrophages were also commonly observed adjacent to gut associated lymphoid tissue (**Figure 3-10**).

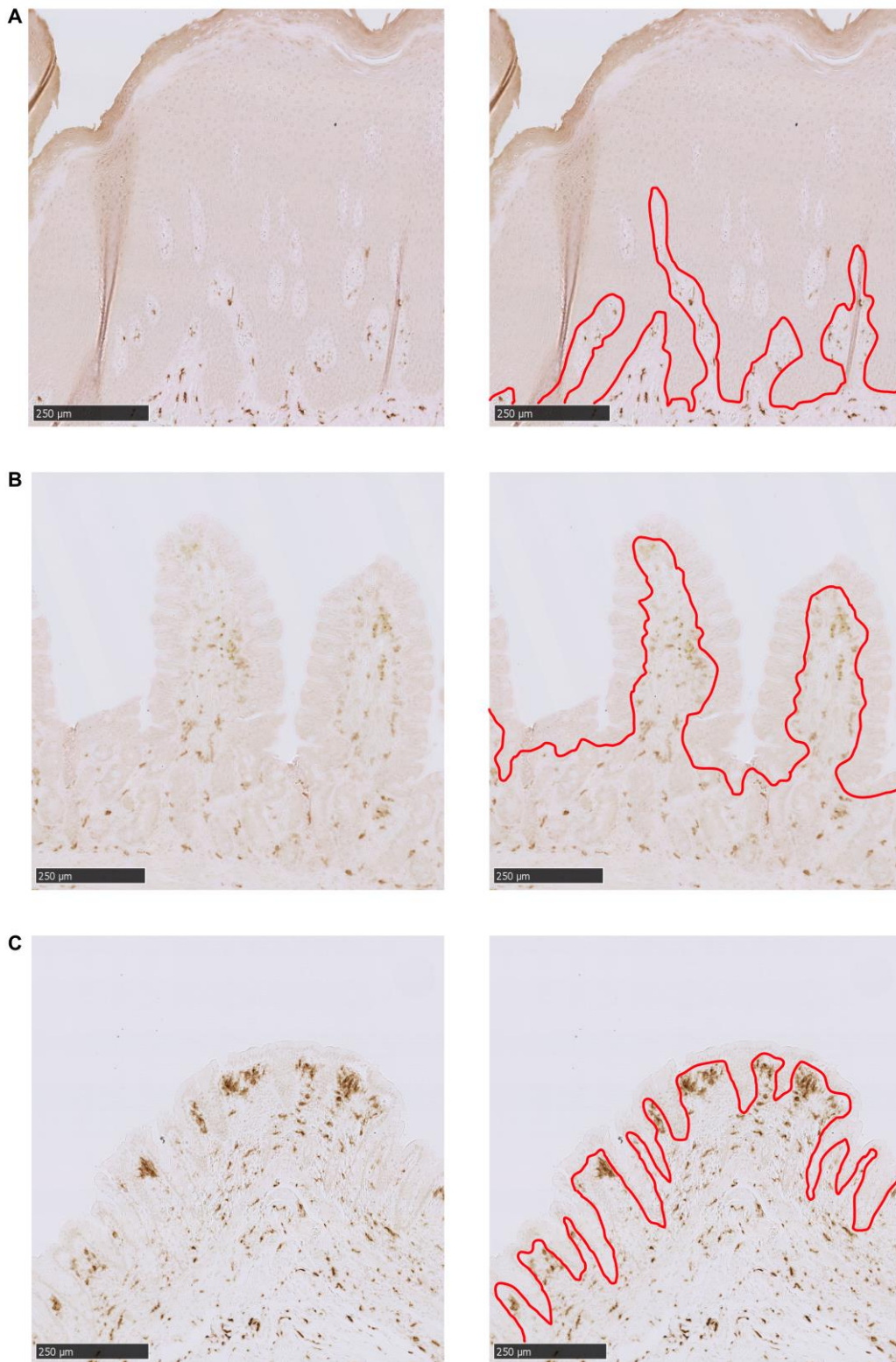


Figure 3-6 Lamina propria macrophages in the equine stomach, jejunum and right ventral colon

Staining for CD163 using 3,3'-diaminobenzidine (DAB) as a chromogen in the mucosa of the equine stomach (A), jejunum (B) and right ventral colon (C). DAB is not visible in the epithelial layer (red line represents basement membrane).

Magnification X10. Bar=250µm. Images representative of samples taken from 10 horses.

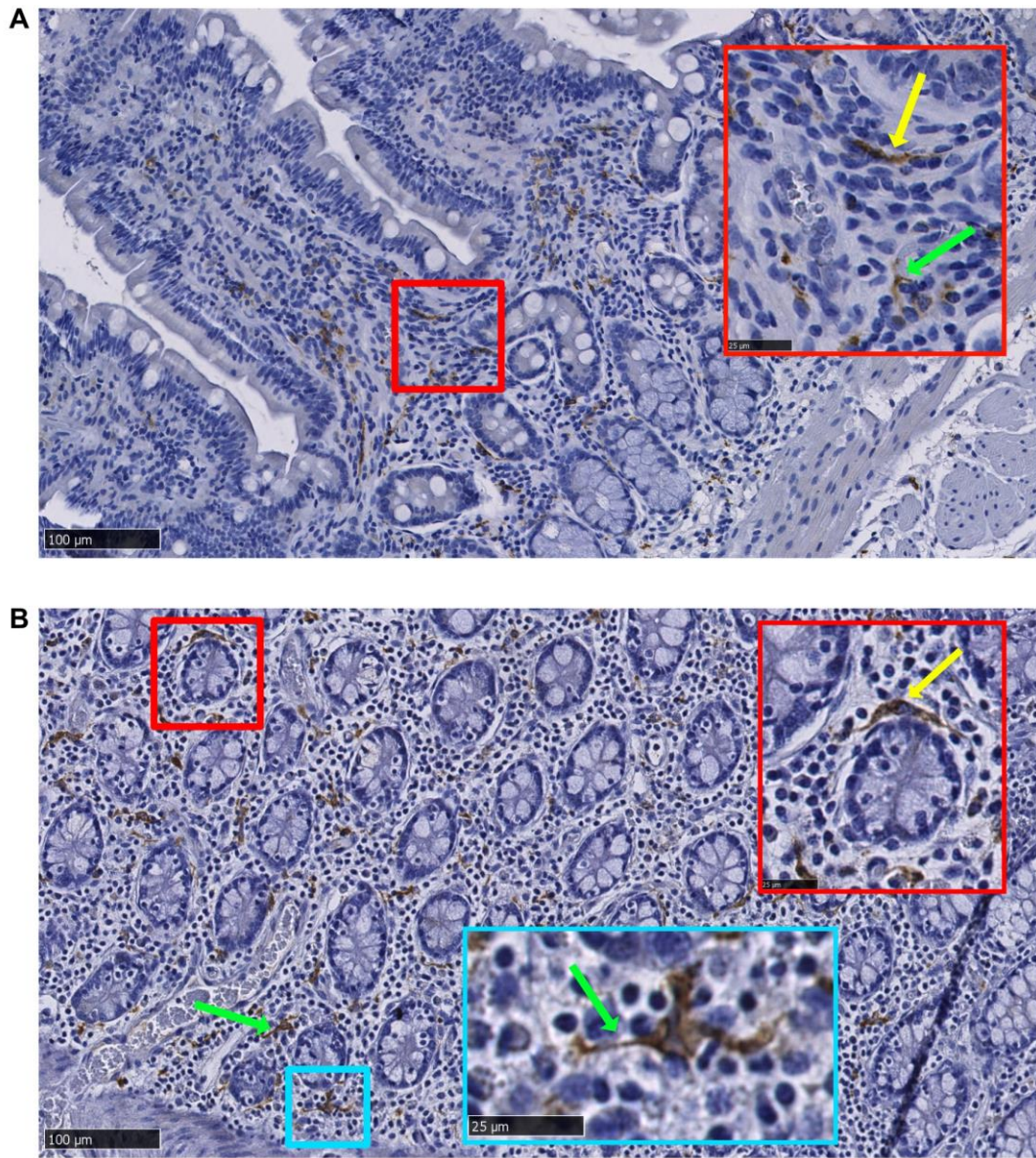


Figure 3-7 Morphology of lamina propria macrophages in the equine jejunum and right dorsal colon

Staining for CD163 in the lamina propria of the equine jejunum (A) and right dorsal colon (B) using 3,3'-diaminobenzidine (DAB) as a chromogen with haematoxylin as a counterstain. (A) is a cross section. (B) is a whole mount. Macrophages in the lamina propria are predominantly bipolar with (yellow arrow) with occasional cells having 3 or more ramifications (green arrow).

(A) and (B) X20 magnification Bar=100µm. Inset X80 Bar=25µm. Images representative of of samples taken from 10 horses.

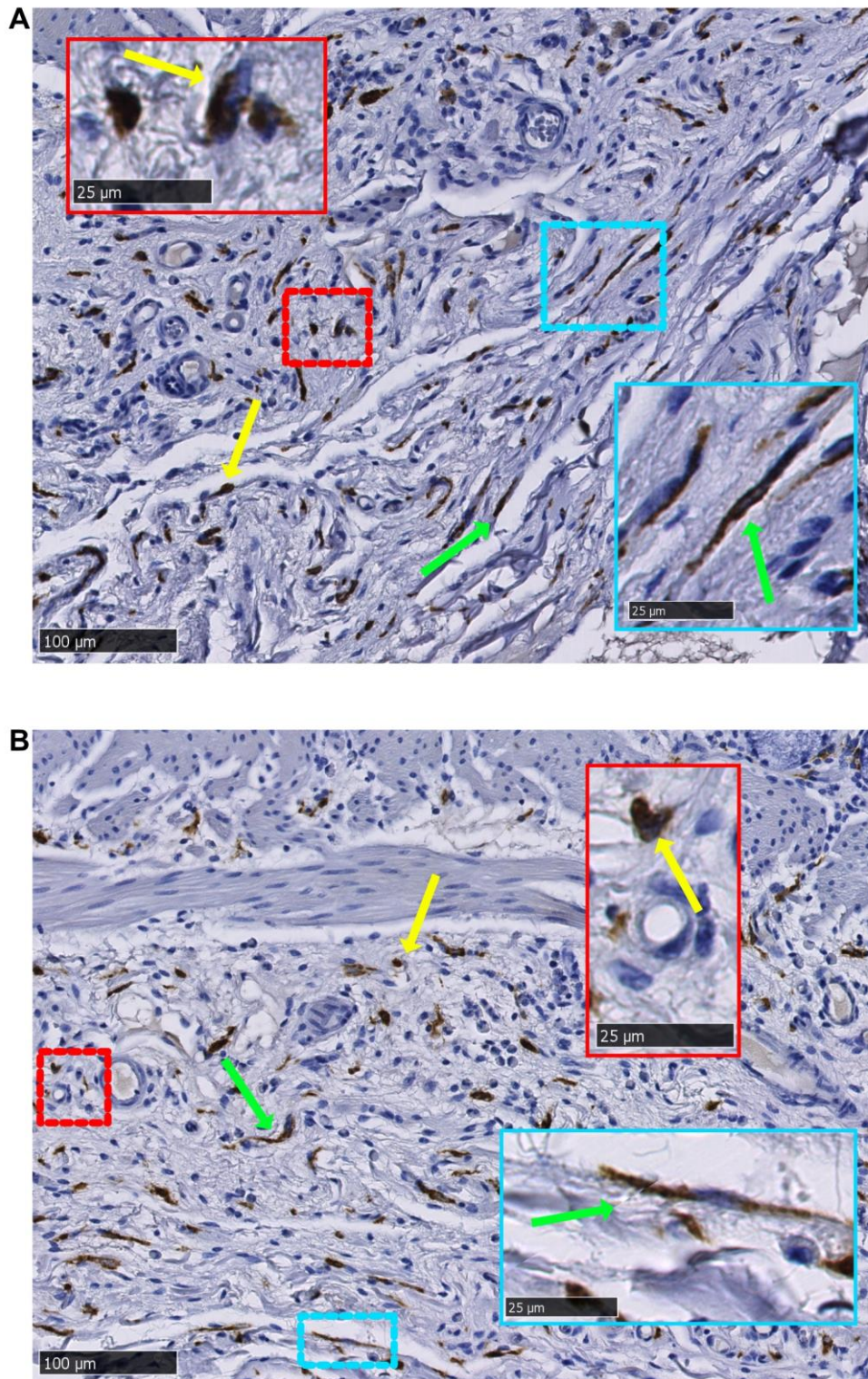


Figure 3-8 Morphology of macrophages in the submucosa of the equine small intestine

Staining for CD163 in the submucosa of the equine jejunum (A) and ileum (B) using 3,3'-diaminobenzidine (DAB) as a chromogen with haematoxylin as a counterstain. Macrophages in the submucosa are either bipolar (green arrow, blue inset) or round (yellow arrow, red inset). (A) and (B) X20 magnification; Bar=100µm. Inset X80 Bar=25µm. Images representative of samples taken from 10 horses.

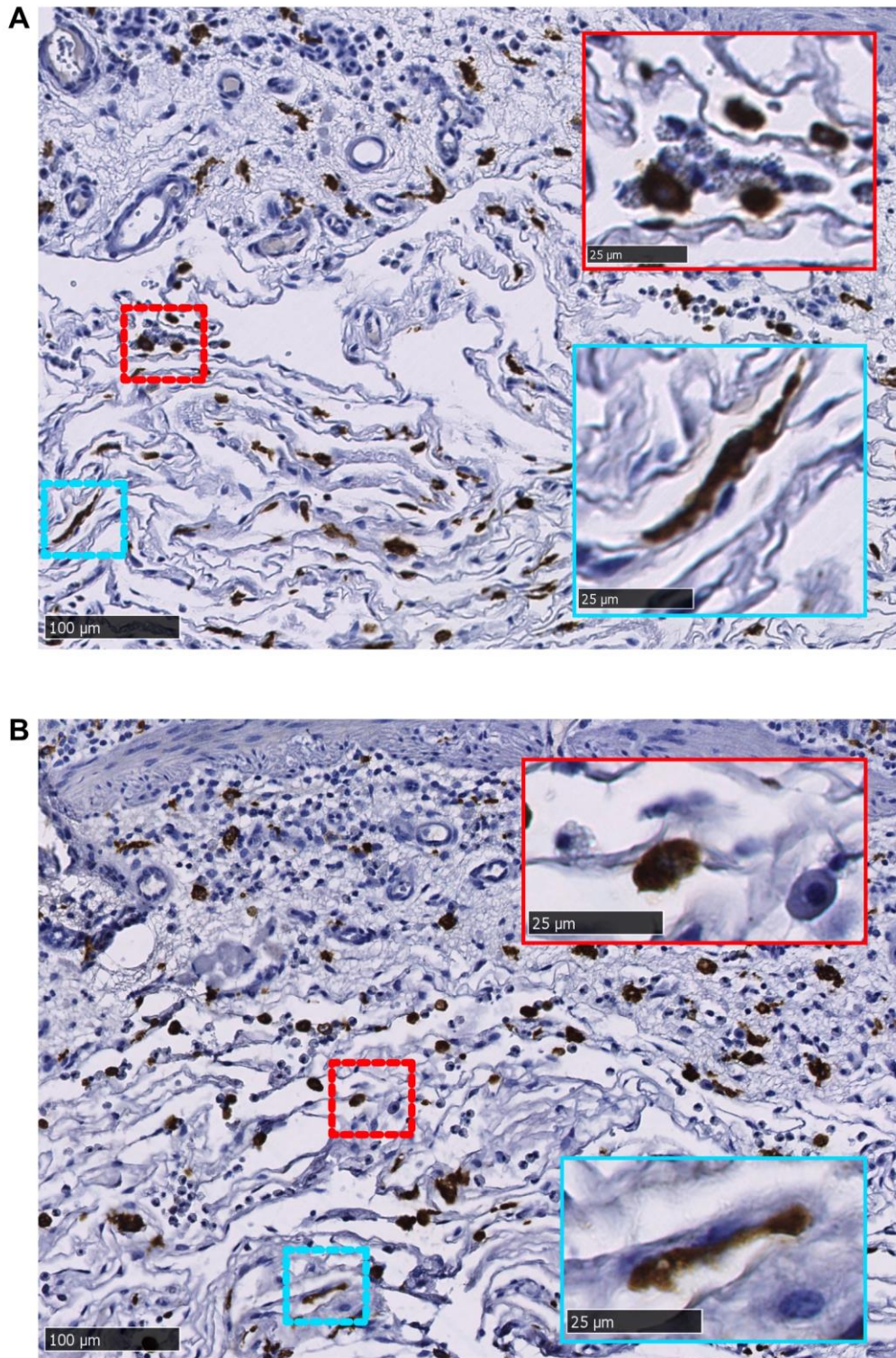


Figure 3-9 Morphology of macrophages in the submucosa of equine large intestine
Staining for CD163 in the submucosa of the equine pelvic flexure (A) and left dorsal colon (B) using 3,3'-diaminobenzidine (DAB) as a chromogen with haematoxylin as a counterstain. Macrophages in the submucosa are predominantly round (red inset) with occasional bipolar cells (blue inset). (A) and (B) X20 magnification Bar=100µm. Inset X80 Bar=25µm. Images representative of samples taken from 10 horses.

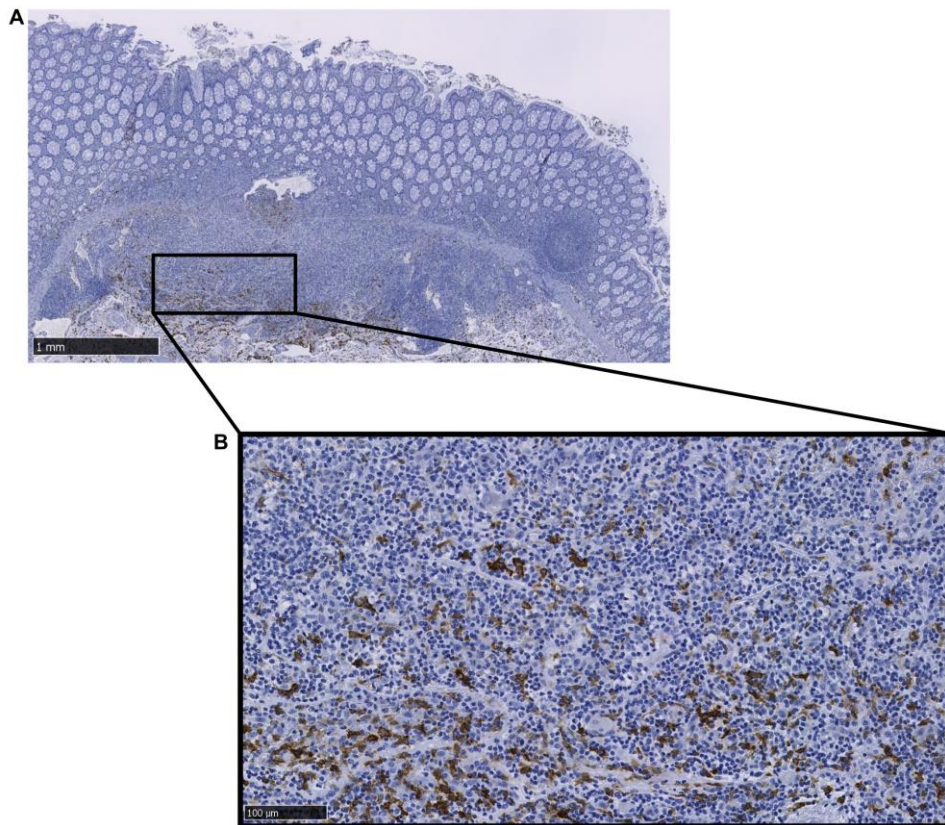


Figure 3-10 Macrophages in gut- associated lymphoid tissues in the equine large intestine

Staining for CD163 in the equine right ventral colon using 3, 3'-diaminobenzidine (DAB) as a chromogen with haematoxylin as a counterstain.

(A) X2.5 magnification; Bar=1mm. Inset (B) X20 Bar=100µm. Images representative of samples taken from 5 horses.

Muscularis externa (comprising serosa, muscularis and myenteric plexus)

In mice, macrophages have been described in three areas of the ME; namely, the serosa, MP and the level of the deep muscular plexus between inner and outer circular muscle (Mikkelsen, 2010). In the rat, ED2⁺/CD163⁺ macrophages were also seen within the longitudinal muscle, between the muscle layers and within the circular muscle itself (Kalff et al., 1998a, Phillips and Powley, 2012). In humans, CD68⁺ cells are also found within the serosa and ME. Within the human ME, CD68⁺ positive staining cells have been shown to be present within intermuscular septa, intralamellar septa between muscle cells and the lining of the MP (Mikkelsen, 2010). In comparison, CD163⁺ macrophages in humans were located between the distinct lamina of the intermuscular bundles of the ME in the jejunum (Kalff et al., 2003). In the current study, CD163⁺ equine macrophages were present in four areas of the ME; the serosa, within the longitudinal (outer) muscle, at the level of the MP and within the circular (inner) muscle (Figure 3-11).

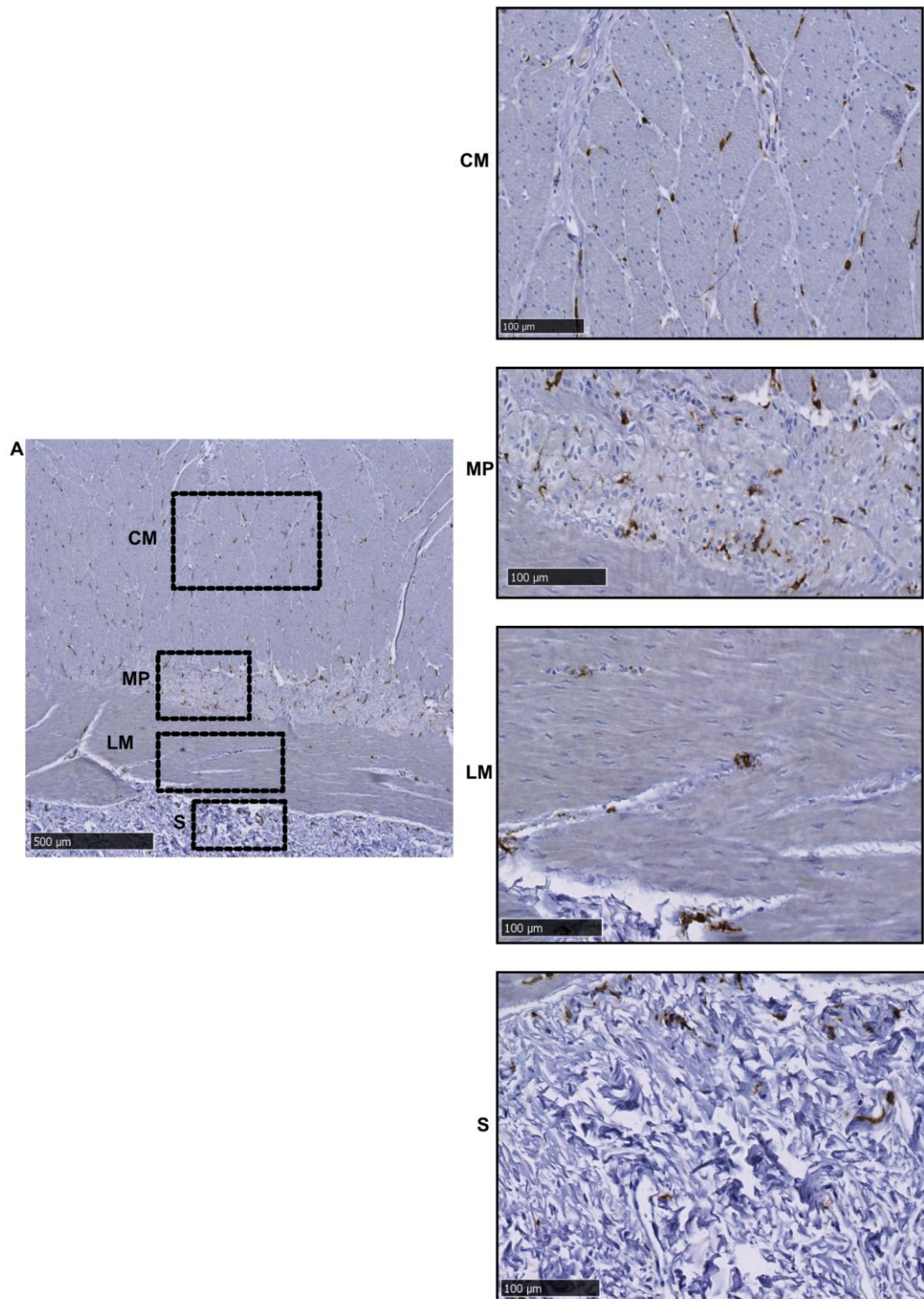


Figure 3-11 Macrophages in the equine *muscularis externa*

Staining for CD163 in the equine duodenum using 3, 3'-diaminobenzidine (DAB) as a chromogen with haematoxylin as a counterstain. (A) shows a low power view X5 magnification of the *muscularis externa* (ME). **CM, MP, LM** and **S** represent high power view X 20 magnification of circular muscle (**CM**), myenteric plexus (**MP**), longitudinal muscle (**LM**) and serosa (**S**).

(A) X5 magnification Bar=500µm. (**CM, MP, LM, S**) X20 magnification Bar=100µm. Images representative of samples taken from 10 horses.

Serosa

Serosal macrophages in rodents are bipolar with several ramifications (Mikkelsen, 2010). In the current study, equine serosal macrophages were relatively regular in their distribution. (Figure 3-12). As sections were examined in cross section only, most macrophages appeared bipolar (Figure 3-12) and it was not possible to visualise whether cells were ramified in this view, although occasional ramified cells were observed (Figure 3-13).

Muscularis

As previously reported in humans (Kalff et al., 2003), equine CD163⁺ macrophages in this study were found within the *muscularis*, predominantly lying between intermuscular bundles (Figure 3-14) (Kalff et al., 2003). These cells were uniformly distributed and orientated with the muscle fibres (Figure 3-15). Most cells appeared bipolar or were identified by single areas of circular positive staining, attributable to the orientation of the cross sections (Figure 3-16).

In order to look at the phenotype of *muscularis* macrophages in more detail, wholemounts of the ME were prepared and stained. In rodent wholemounts, macrophages can be seen regularly and uniformly distributed throughout the muscularis, with no overlap of processes (Phillips and Powley, 2012, Mikkelsen et al., 2011). In equine tissue wholemounts in the current study, the MM were predominantly bipolar but only the occasional CD163⁺ cell was observed within the whole mount preparations, similar to that observed in cross section (Figure 3-14). This apparent interspecies difference may be attributable to the relatively greater thickness of the equine ME and the associated difficulty in visualising the full network of cells within the one 5 µm section. In comparison, it is possible, using light microscopy, to examine the full thickness of the rodent *muscularis* as a whole mount.

Myenteric plexus

Between the two muscle layers (circular and longitudinal) lies the MP, which provides parasympathetic and sympathetic innervation of the GIT. In rodents, the close proximity of macrophages to the MP has been clearly documented (Mikkelsen, 2010, Phillips and Powley, 2012). The functional importance of this co-localisation has been demonstrated in mice. Macrophages regulate GI motility by altering smooth muscle contraction via the secretion of bone morphogenetic protein 2 (BMP2) which activates the BMP receptor on enteric neurons. In return, enteric neurons produce CSF-1 which is necessary for macrophage development (Muller et al., 2014).

In this study, equine CD163⁺ macrophages were observed in close proximity to the MP (**Figure 3-11**). These cells were predominantly on the periphery of the MP, although some were also observed in the centre (**Figure 3-17**). Positive staining cells were bipolar and stellate-shaped in this region (**Figure 3-18**). The macrophage density (cells per mm²) was greater adjacent to the MP compared to observed within the ME (**Figure 3-8**) and similar to that in the mucosa and submucosa. This is consistent with the reported findings in rodents, whereby macrophages are found in close association to neurons and appear to make contact with their axons and dendrites (Phillips and Powley, 2012). As proposed in rodent studies, the reason for this close relationship may reflect either a functional role in motility (Muller et al., 2014) and/or a role in phagocytosis of aged neurons (Phillips and Powley, 2012).

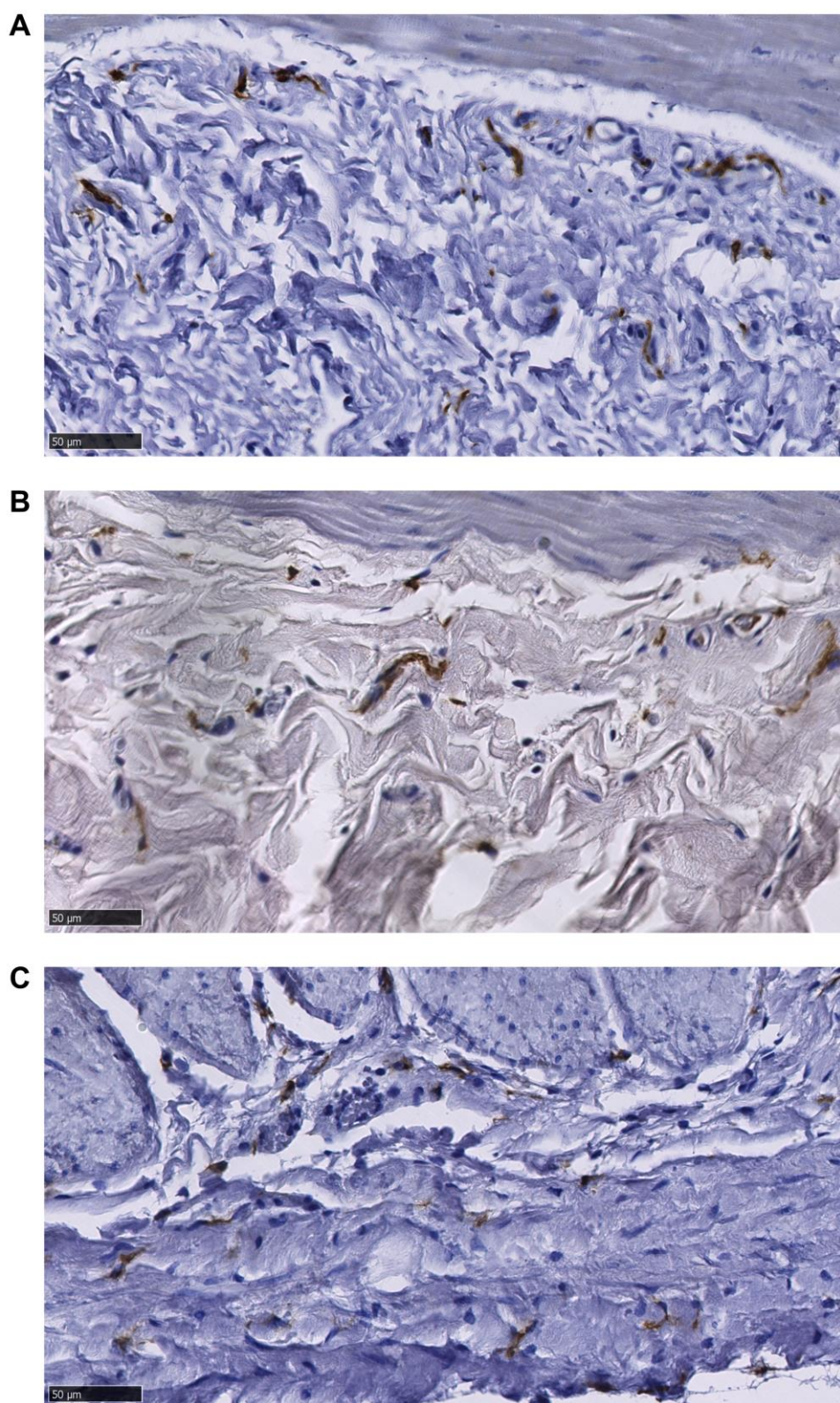


Figure 3-12 Serosal macrophages in the equine gastrointestinal tract
Staining for CD163 in the serosa of the equine duodenum (A), ileum (B) and caecum (C) using 3, 3'-diaminobenzidine (DAB) as a chromogen with haematoxylin as a counterstain. Magnification X40 magnification; Bar=50µm. Images representative of samples taken from 10 horses.

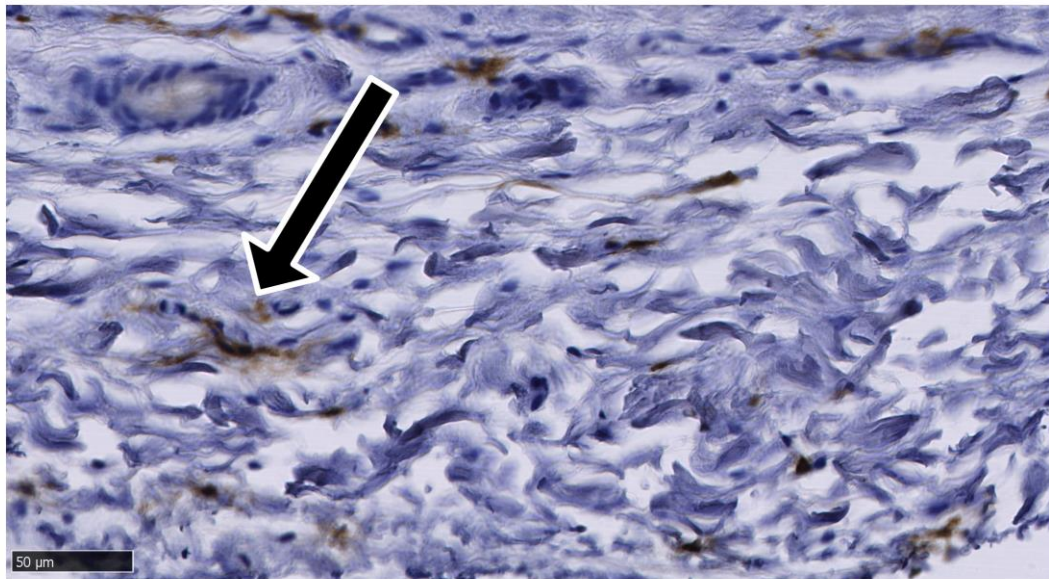


Figure 3-13 Ramified macrophages in the serosa of equine left ventral colon

Staining for CD163 in the serosa of equine left ventral colon using 3, 3'-diaminobenzidine (DAB) as a chromogen with haematoxylin as a counterstain. Black arrow shows macrophage with ramified morphology.

Magnification X40 magnification. Bar=50μm. Image representative of samples taken from 5 horses.

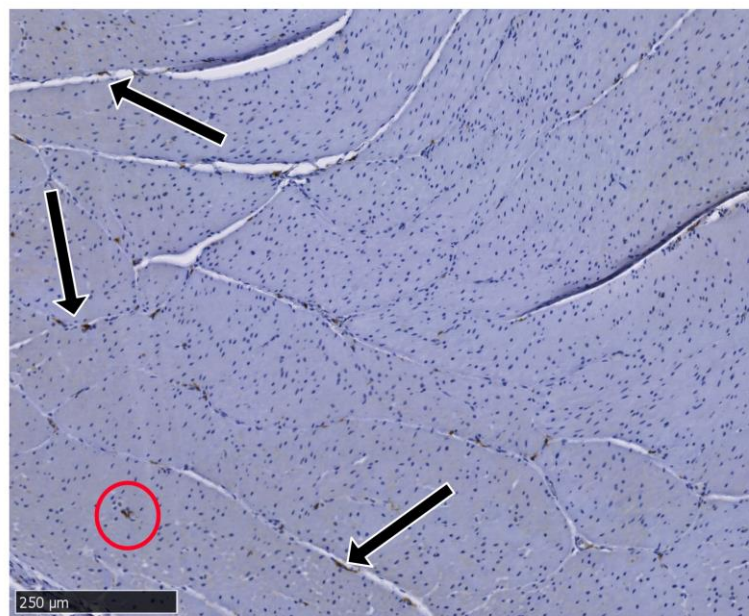


Figure 3-14 Muscularis macrophages in the equine ileum

Staining for CD163 in the muscularis (circular muscle) of the equine ileum colon using 3, 3'-diaminobenzidine (DAB) as a chromogen with haematoxylin as a counterstain. Macrophages were predominantly found between muscle bundles (black arrows) although occasional staining for CD163 was observed within a muscular bundle (red circle).

Magnification X10. Bar=250μm. Image representative of small and large intestinal samples in 10 horses.

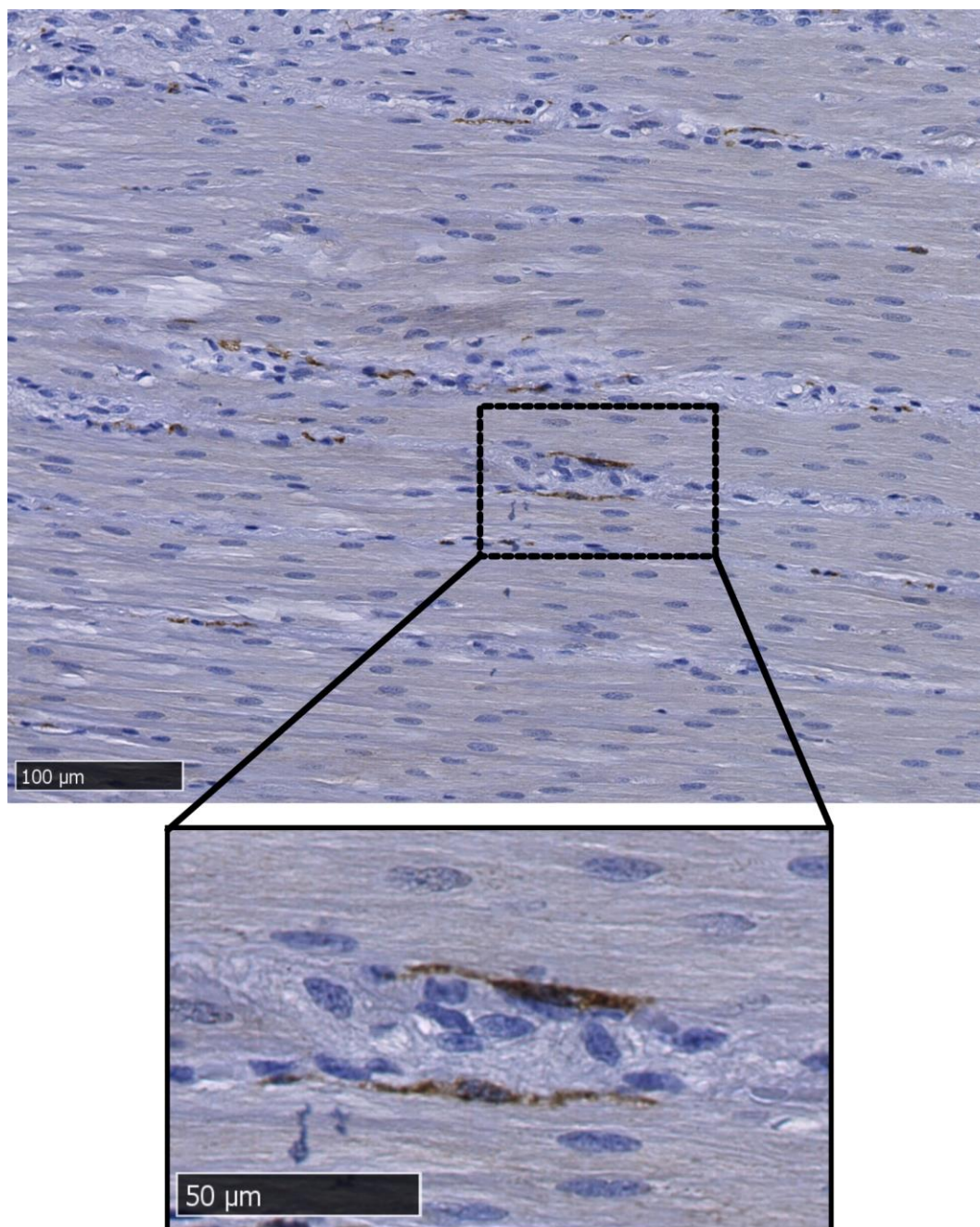


Figure 3-15 Muscularis macrophages in equine duodenum

Staining for CD163 in the muscularis (longitudinal layer) of the equine duodenum using 3, 3'-diaminobenzidine (DAB) as a chromogen with haematoxylin as a counterstain. Macrophages were observed between muscle bundles running longitudinally with the muscle (inset). Magnification X20. Bar=100μm. Inset X40. magnification. Bar=50μm Image representative of small and large intestinal samples in 10 horses.

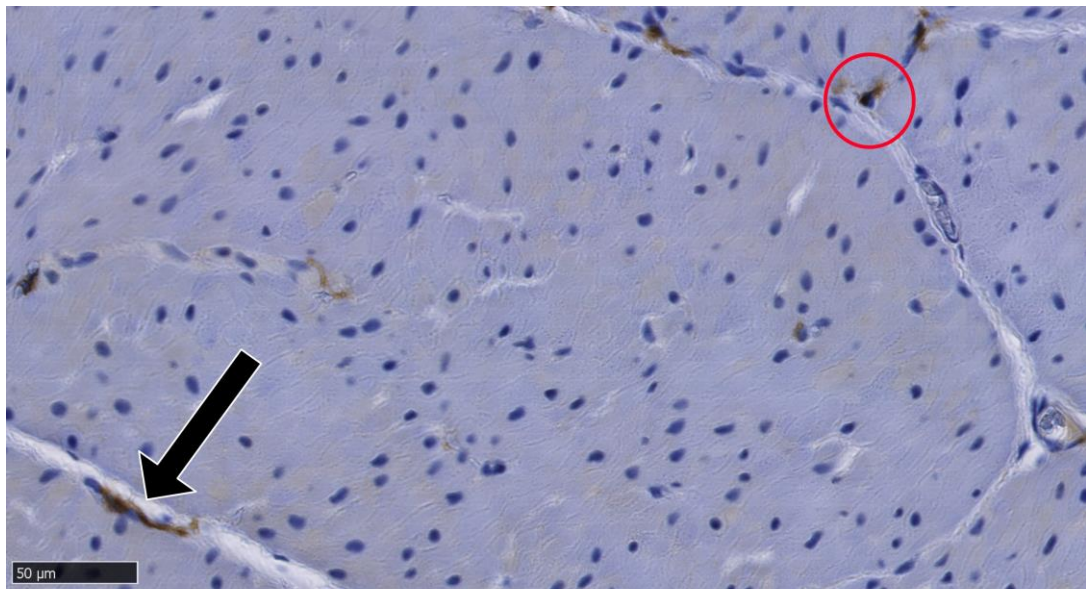


Figure 3-16 Morphology of intermuscular *muscularis* macrophages in equine ileum

Staining for CD163 in the muscularis (circular muscle) of the equine ileum colon using 3, 3'-diaminobenzidine (DAB) as a chromogen with haematoxylin as a counterstain. Macrophages were predominantly bipolar (black arrows) although occasional circular cell bodies were observed (red circle).

Magnification X40. Bar=50µm. Image representative of small and large intestinal samples in 10 horses.

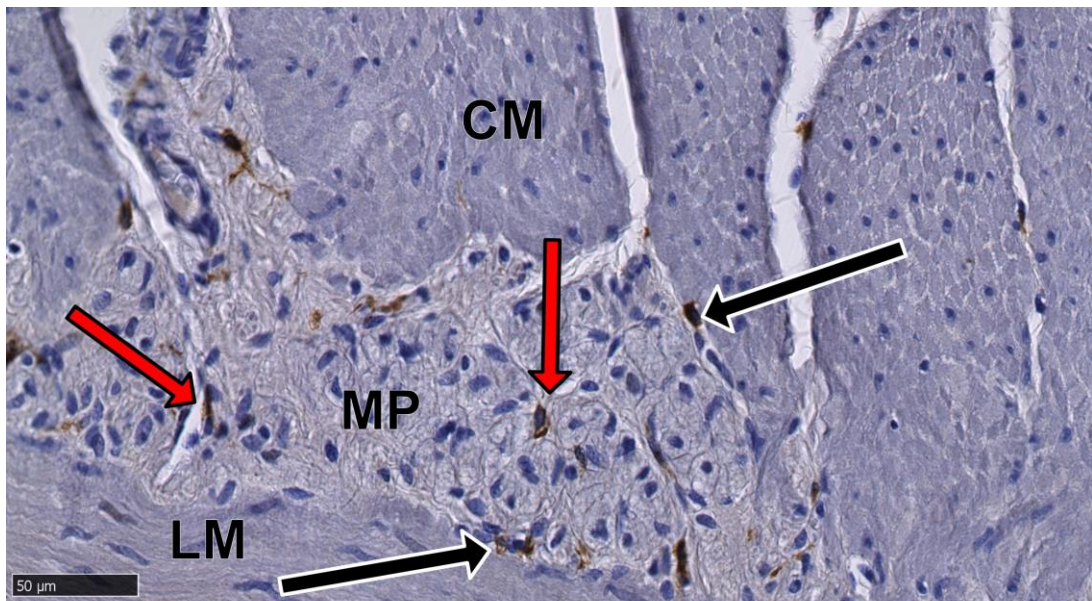


Figure 3-17 Macrophages associated with the myenteric plexus in the equine gastrointestinal tract

Staining for CD163 in the myenteric plexus (MP) of the equine jejunum using 3, 3'-diaminobenzidine (DAB) as a chromogen with haematoxylin as a counterstain. Macrophages were observed both on the edge of the MP (black arrows) and within the MP (red arrows).

Magnification X40. Bar=50µm. CM, circular muscle. LM, longitudinal muscle. Image representative of small and large intestinal samples in 10 horses.

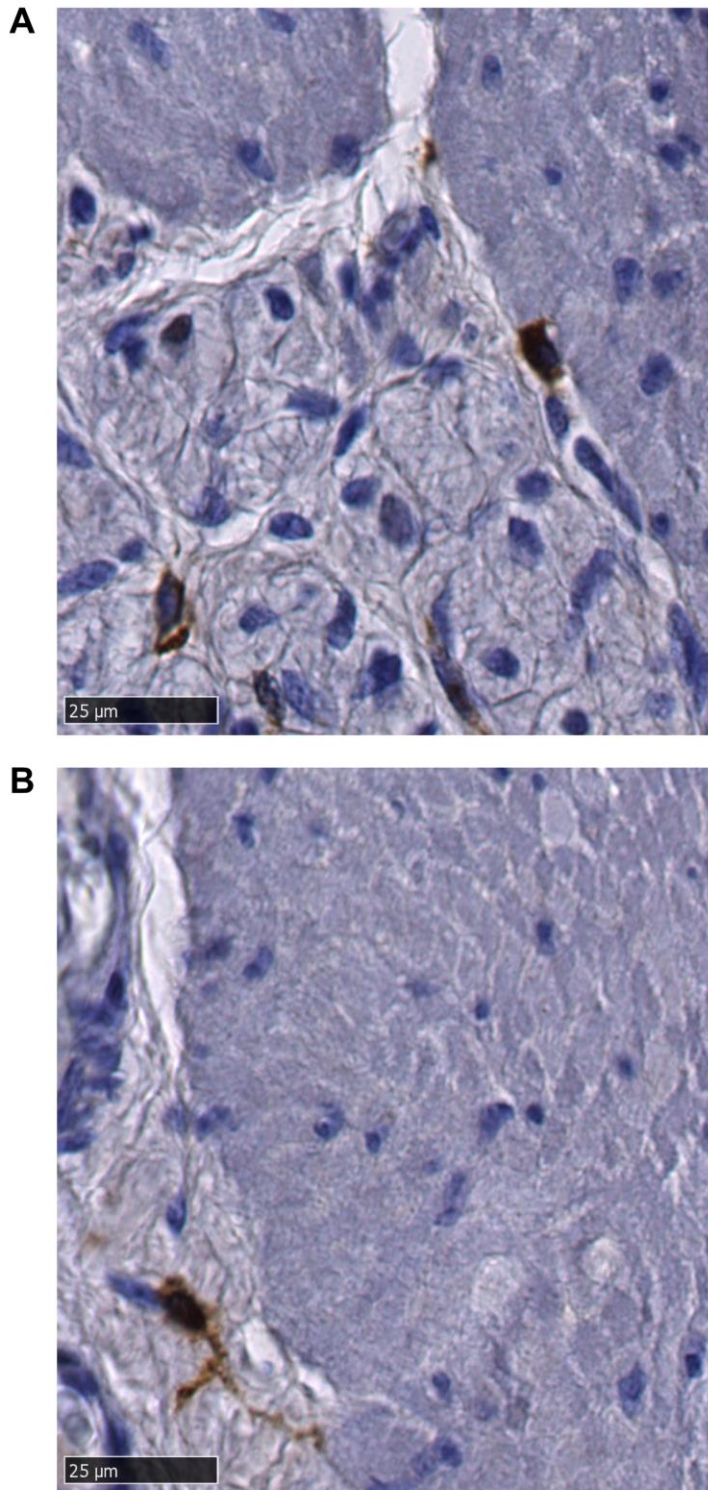


Figure 3-18 Morphology of myenteric plexus macrophages in the equine gastrointestinal tract

Staining for CD163 in the myenteric plexus of the equine jejunum using 3, 3'-diaminobenzidine (DAB) as a chromogen with haematoxylin as a counterstain. The morphology of myenteric plexus macrophages was either round (**A**) or ramified (**B**). Magnification X80. Bar=25µm. Image representative of small and large intestinal samples in 10 horses.

3.3 Discussion

This chapter was designed to provide an overview of the distribution of macrophages in the equine GIT, with a focus on the resident MMs. As previously reported in rodents, macrophages were present in all sections of the equine GIT and occupied all layers of the intestine. Distribution of LpM and serosal macrophages was similar to that reported in other species. The MM distribution in the horse in this study resembled that of rats and humans; namely, cells were present within the muscle layers, between muscular bundles. The identification of macrophages within the longitudinal muscle of the ME was consistent with findings in humans and rats, yet inconsistent with findings in mice, in which macrophages have not been identified at this site (Mikkelsen et al., 1988). The similarity of the distribution of macrophages along the MP suggests that, as in other species, they may play a role in regulation of motility and clearance of apoptotic neurons.

As macrophages are such heterogeneous cells with tissue-specific, and indeed region-specific roles within tissues, it is perhaps not unsurprising that they vary in number in relation to the anatomical region studied and the markers used for their identification. Such variation likely reflects a level of macrophage diversity which is dependent on their location, function and activation status (Gordon et al., 1995). Therefore, by using CD163 as a marker, this current study was limited to the quantification and distribution of a CD163⁺ subgroup of macrophages in the equine GIT. CD163 is a pattern recognition receptor (PRR) belonging to the scavenger receptor cysteine rich (SRCR) domain family and is restricted to cells of monocytic lineage (Hogger et al., 1998, Van den Heuvel et al., 1999) and has been used to identify subpopulations of tissue macrophages in humans (Van den Heuvel et al., 1999), pig (Sauter et al., 2016), rat (ED2) (Dijkstra et al., 1985) and horse (Yamate et al., 2000, Sano et al., 2016). In the colon of mice, once Ly6C⁺ monocytes enter tissues, they undergo a differentiation process which involves the loss of Ly6C expression and upregulation of F4/80, CX3CR1, CD163, CD11c and MHCII expression. Similarly, in humans, the differentiation of CD14⁺ monocytes into intestinal macrophages involves the down regulation of CD14 and upregulation of MHCII and CD163 (Bain et al., 2013). In humans the expression of CD163 on monocytes and macrophages is regulated by both pro- and anti-inflammatory signals. Pro-inflammatory mediators, such as LPS, TNF- α and IFN- γ , suppress CD163 expression; whereas, anti-inflammatory signals, such as IL-10, upregulate CD163 expression (Buechler et al., 2000). The development of monocyte-derived macrophages in CSF-1 also results in the upregulation of CD163 mRNA and protein expression. Consistent with the

response of human monocyte-derived macrophages, LPS stimulation of equine bone marrow-derived macrophages (eqBMDMs) cultured in CSF-1 resulted in a reduced expression of CD163, as determined by RNA-Seq analysis of eqBMDMs performed in **Chapter 4 (Table 3-3)**. However, flow cytometric analysis of the same eqBMDMs cultures in CSF-1 revealed very low expression of CD163 (**Chapter 4**) which is similar to what has been previously reported in pig BMDMs (Kapetanovic et al., 2012). Equine monocytes also express CD163 (Ibrahim et al., 2007, Steinbach et al., 2005), as do equine alveolar and peritoneal macrophages (Karagianni et al., 2013) and prior studies have demonstrated the presence of CD163⁺ macrophages in the equine GIT (Grosche et al., 2011, Yamate et al., 2000). The mechanisms underpinning the absence of cell surface expression in eqBMDMs may be similar to those in the pig, whereby monocytes mature to a more ‘resident’ phenotype in the circulation, and not the bone marrow. Unfortunately, the lack of availability of other macrophage markers in the horse precluded the adoption of an alternative and comparative method of macrophage identification. Such an approach may have shed light on the issue of whether CD163 expression was universal amongst, or limited to a specific sub-set of, equine GIT resident macrophages. Considering the lack of availability of appropriate antibodies in the horse, an alternative approach might have involved the use of *in situ* hybridisation (RNAscope) technology, whereby a labelled cDNA or RNA strand could be labelled with a probe to locate a macrophage-specific sequence within the tissue (Wang et al., 2012a).

Table 3-3 Transcripts per million (TPM) of CD163 in equine bone marrow derived macrophages cultured in CSF-1 (Data from Chapter 4)

Gene	TPM 0 hours (resting)	TPM 7 hours post LPS stimulation
CD163	166.586	91.132

In the horse, CD163⁺ cell density varied across the tissue layers of the GIT (**Figure 3-4**). The *muscularis* had the lowest cell density. Cell density in the ME was consistent along the full length of the GIT. In comparison, the density of ME MHCII⁺ and CD169⁺ cells increased aborally in the mouse small intestine and was lower in the colon (Mikkelsen et al., 2011). Referring to the same study, it would appear that the cell densities in the mouse ME were greater than those in the horse; approximately 200 MHCII⁺ and CD169⁺ cells/mm² in the mouse, compared to < 100 CD163⁺ cells/mm² in the horse. Despite these apparent differences, it is hard to draw any conclusions as the different markers used in the respective studies may have targeted different subpopulations of macrophages. In contrast, Grosche *et al.* (2011) investigated CD163⁺ populations in equine intestinal mucosal tissue, permitting more appropriate comparisons with the current study. Despite this, Grosche *et al.*

(2011) also reported a greater cell density (approx. 300 mucosal CD163⁺ cells/mm²) than the current study (150-250 mucosal CD163⁺ cells/mm²); the reasons for these differences are unclear although Grosche *et al.* used a different CD163 clone (AM-3k). Grosche reported that ischemia reperfusion injury failed to alter the number of CD163⁺ cells, despite the apparent activation of the cells, based on their appearance characterised by large cytoplasmic vacuoles which contained cell debris and apoptotic bodies (Grosche *et al.*, 2011).

A limitation of this current equine study was the use of formalin-fixed tissues. The use of formalin to preserve tissues permitted the prompt collection of large numbers of samples following euthanasia. However, formalin can cause bond formation and conformational changes in the target antigens, compromising their recognition by antibodies. In addition, prolonged fixation can result in false negative results (Ramos-Vara, 2005). Whilst antigen retrieval methods can reverse the formation of bonds, they can also cause further alterations to the target antigen. Therefore, in light of the fixation and antigen retrieval processes employed in the current study, it is possible that the reported CD163⁺ cell densities may have underestimated the *actual* CD163⁺ cell densities. Again, the use of RNAscope technology may have been beneficial whereby a specifically designed probe could have been used to locate a DNA or RNA section of the gene of interest within the tissue (Wang *et al.*, 2012a), thus overcoming some of the issues associated with antibody recognition of altered protein targets. However, it was felt that despite these limitations, useful and novel information regarding the distribution and density of equine GIT macrophages was elicited.

In conclusion, CD163⁺ macrophages were identified and quantified within the equine GIT, and their morphology was analysed. Their distribution was found to be similar to that reported in rodents and humans and their close association with motility effector cells in the MP supports the proposed role of intestinal macrophages in the regulation of intestinal motility. Confirmation of the presence of macrophages in the mucosa and ME in the equine GIT was a necessary pre-requisite to subsequent studies reported in the thesis; most notably, the investigation of macrophage activation in the GIT of horses undergoing abdominal surgery (**Chapter 5**).

This page was left intentionally blank

Chapter 4. Isolation and generation of Equine Bone Marrow-Derived Macrophages and their response to Lipopolysaccharide

4.1 Introduction

The initial aim of this chapter was to develop a protocol to isolate lamina propria macrophages (LpM) and *muscularis* macrophages (MM) from the horse gastrointestinal tract (GIT) and to compare the two populations. Protocols were adapted from Kalff et al., for MM (Kalff et al., 1998a) and Weigmann et al., for LpM (Weigmann et al., 2007). The isolation of viable MM from the intestine of horses proved unachievable due to problems with contamination, low cell yields and the relatively small number of horses from which it was possible to collect tissue to optimise the two techniques. As an alternative, in order to examine the gene expression profile of a relevant macrophage population, a protocol was developed to produce macrophages from bone marrow (BM) using macrophage colony-stimulating factor 1 (CSF-1) to differentiate isolated BM progenitor cells in culture. As discussed in **Chapter 1**, CSF-1 is essential for the proliferation, differentiation and survival of macrophages via signalling through a class III protein kinase receptor (CSF1R or CD115) which is expressed on all myeloid cells. Based upon evidence supporting both a relatively rapid turnover of GI tract macrophages and their CSF-1-dependency (MacDonald et al., 2010, Bain et al., 2014), Baillie *et al.* argued that cultivation of human monocyte-derived macrophages (MDM) in CSF-1 is a de facto model for the differentiation of GI macrophages (Baillie et al., 2017). LpM are replenished by circulating monocytes (Bain et al., 2014) and are a comparatively 'inert' population, being relatively unresponsive to microbial, including LPS, challenge (Mowat and Bain, 2011). Using data from the Functional Annotation of the Mammalian Genome (FANTOM) 5, Baillie *et al.* demonstrated that MDM grown in CSF-1, (conditions which replicate those of intestinal mucosal macrophages) down-regulated the normally high expression of pattern recognition molecules in monocytes and also suppressed CD14 and the associated receptor molecules. Although they still responded to bacterial LPS, in contrast to blood monocytes, they expressed low levels of pro-inflammatory cytokines such as IL-1, and high levels of anti-inflammatory IL-10.

Previous studies from our group, involving the isolation of BM from other large animal species (pig and sheep) with subsequent culture in the presence of recombinant human CSF-1 (rhCSF-1), yielded large numbers of phagocytic cells that expressed macrophage markers (CD14, CD16) and produced tumour necrosis factor (TNF- α) in response to lipopolysaccharide (LPS) (pig) (Kapetanovic et al., 2012, Pridans et al., 2016). In the horse, the generation of macrophages from BM has been described previously (Werners et al., 2004). However, these cells were cultured in granulocyte macrophage colony-stimulating factor (GM-CSF or CSF-2) which, in humans and mice,

generates macrophages with a distinct gene expression profile (Achuthan et al., 2016, Louis et al., 2015, Joshi et al., 2015). Macrophages grown in GM-CSF have been referred to as dendritic cells, but may be more akin to lung macrophages, which depend upon GM-CSF for their development (Guilliams et al., 2013). In addition, these cells were maintained as an equine macrophage cell line (e-CAS). Potential problems associated with cell lines include contamination by other cells or microorganisms (Lorsch et al., 2014) which can result in molecular and cellular changes in the cell line (Oh et al., 2007). These problems have very recently been highlighted by Evans *et al.* who sequenced the eCAS cell line and found the cells to resemble mouse macrophages and not horse macrophages (Evans et al., 2018).

This chapter describes the protocol used for the isolation of equine bone marrow derived macrophages (eqBMDMs) and how the cells were characterised (see **Figure 4-1** for overview). Following this, the response of eqBMDMs to LPS was investigated. In rodents, the translocation of endogenous LPS from the lumen to the *muscularis*, is proposed to activate *muscularis* macrophages in a model of post-operative ileus (Turler et al., 2007, Eskandari et al., 1997). By extension, gene expression data derived from the challenge of eqBMDMs with LPS might facilitate future efforts to identify appropriate markers of macrophage activation in equine intestinal tissue harvested from horses undergoing colic surgery. Other members of our laboratory have conducted parallel studies to optimise BMDM production from sheep, pig, goat, water buffalo and cattle and therefore a secondary objective of the study was to compare the macrophage gene expression profiles of the different species.

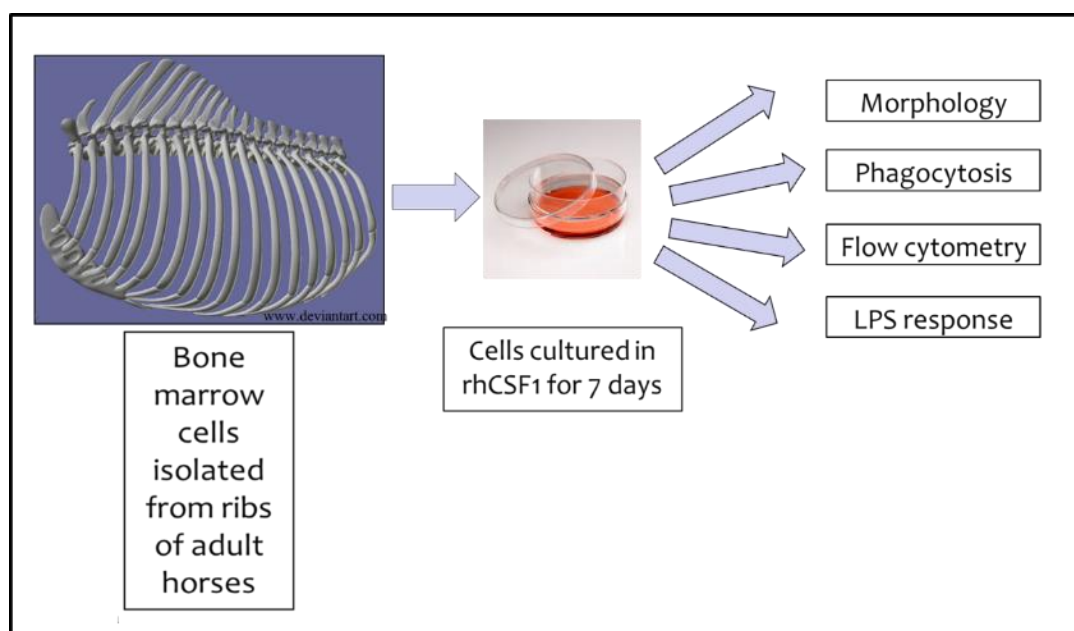


Figure 4-1 Workflow for isolation and characterisation of eqBMDMs

4.2 Results

4.2.1 Cell yield from ribs of adult horses

Cell yield from two ribs varied from 5×10^8 to 1×10^9 cells per adult horse (2.5×10^8 to 5×10^8 per rib). Following cryopreservation in medium containing 10% DMSO in horse serum (Sigma-Aldrich) at -155°C the percentage of viable cells on recovery (from 1 month - to 12 months following cryopreservation), as evaluated by Trypan Blue staining, was between 60-80%.

4.2.2 Optimisation of culture conditions

Optimum culture conditions for eqBMDMs were assessed by performing a cell viability assay (MTT assay). The MTT assay is a quantitative colorimetric assay used for measuring cell survival and proliferation using the dye 3-(4,5-dimethylthiazol-2yl)-2,5-diphenyltetrazolium bromide (MTT) (Mosmann, 1983). NAD(P)H-dependent reductase enzymes in the mitochondria convert soluble tetrazolium into insoluble purple formazan crystals. Signal generated is dependent on viability of cells. The formazan product is solubilised, and absorbance (570 nm) of the coloured solution is measured and quantified using a spectrophotometer. Conditions tested are summarised in **Table 4-1**.

Table 4-1 Culture conditions tested for differentiation of eqBMDMs

Condition	Variables			
Serum	10% horse	20% horse	10% fetal calf	20% fetal calf
rhCSF-1 concentration (U/ml)	No rhCSF1	10 ⁴		
Seeding density (cells)	5 x 10 ⁴	1 x 10 ⁵	2 x 10 ⁵	4 x 10 ⁵

Addition of rhCSF-1 in culture accentuates development of macrophages

Cells cultured at 4 x 10⁵ cells/well in the presence of rhCSF-1 for up to 14 days showed greater metabolic activity, as measured by MTT assay than cells cultured without rhCSF-1. (**Figure 4-2**). In all wells, the presence of rhCSF-1 resulted in greater metabolic activity. The presence of rhCSF-1 in culture media resulted in a significant increase in cell metabolic activity, as measured by absorbance (apart from in 10% FCS) (Two-way ANOVA analysis. 20% HS p=0.001; 10% HS p=0.03; 20% FCS p=0.13 (not significant (ns)); 10%FCS p=0.03).

Analysis by light microscopy (**Figure 4-3**) showed that cells cultured in rhCSF-1 and 20% HS resembled macrophages and, compared with the other conditions, were the most confluent and had low numbers of dead cells. Although culture in 20% FCS generated large numbers of cells, this condition did not appear to generate macrophages; cells were small and round. In the absence of added rhCSF-1 no visible macrophage population was observed by day 14.

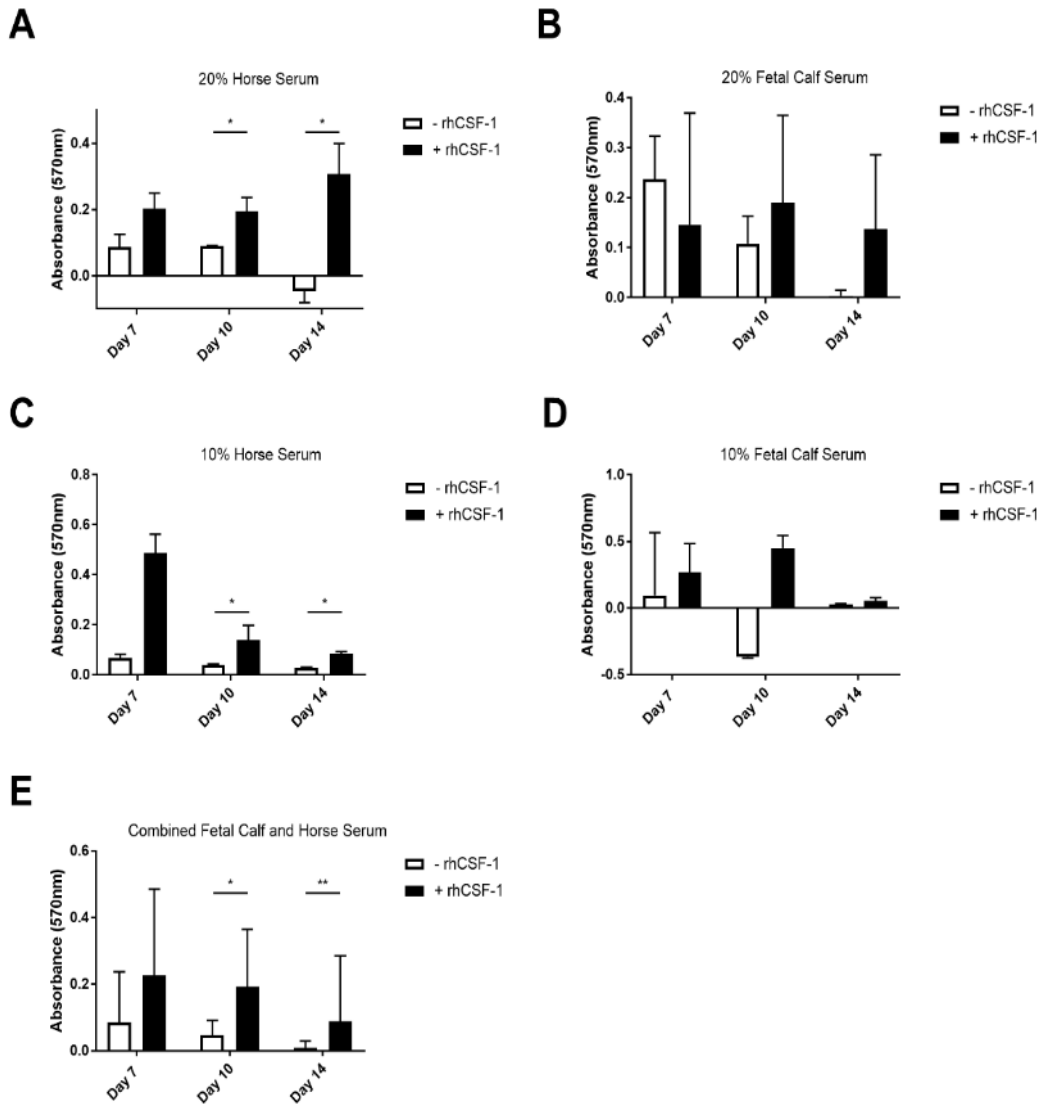


Figure 4-2 Effect of the addition of rhCSF-1 on eqBMDMs in culture in various media eqBMDMs ($n=3$) were cultured in either 10% or 20% horse serum (HS) (A and C) or 10% or 20% fetal calf serum (FCS) (B and D) at 2.5×10^6 cells/ml for up to 14 days with or without rhCSF-1 (+/- rhCSF-1). E is combined data of both HS and FCS. An MTT assay was performed on Days 7, 10 and 14 to assess cell metabolic activity. Results are average of triplicates. Values are median with 95% CI. Significance between +rhCSF-1 and -rhCSF-1 was performed using a paired t-test. * $p<0.05$, ** $p<0.001$

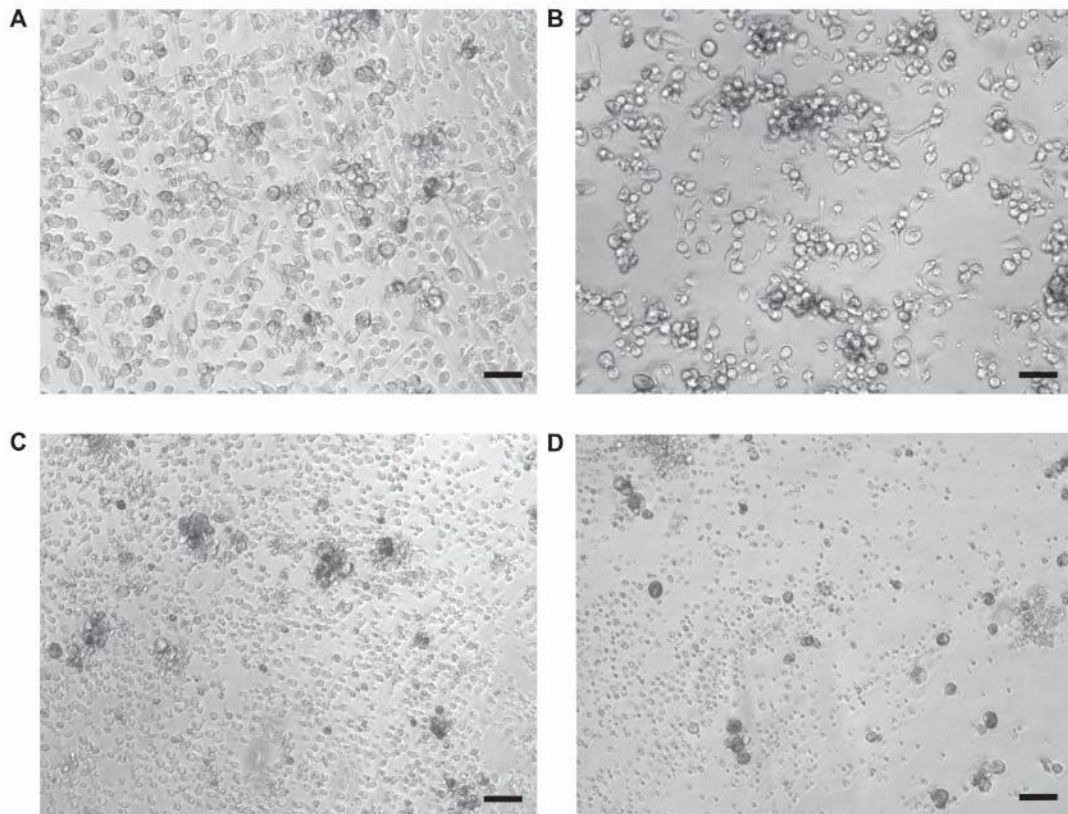


Figure 4-3 Light microscopy images of eqBMDMs in different culture conditions

Cells were imaged on Day 14 by light microscopy to assess morphology in various conditions. Cells in 20% horse serum (HS) and rhCSF-1 at the highest density (4×10^5 /well) (A) were stellate and had good adherence with little evidence of cell death. Cells in 20% HS and rhCSF-1 at a lower density (2×10^5 /well) (B) still adhered and showed the expected stellate morphology; however, there was increased cell death and clumping of cells visible. In addition, some cells were becoming excessively elongated (black arrows). Cells in 20% fetal calf serum (FCS) and rhCSF-1 (C) although mostly viable, did not differentiate into macrophages and were smaller and more circular. The absence of rhCSF-1 in 20% HS resulted in no visible macrophages (D). Bar = 50µm

EqBMDMs differentiation is enhanced in horse serum compared to fetal calf serum

The addition of serum to cell culture media is a critical component providing sources of nutrients, growth factors, hormones and proteins. Serum is usually obtained from either an autologous (e.g. HS for equine studies (Werners et al., 2004, Karagianni et al., 2013, Karagianni et al., 2017)) or a heterologous source (e.g. FCS for equine studies (Okano et al., 2006)) and is usually heat-inactivated (HI) to inactivate serum complement. Two components of serum are particularly relevant to this work, namely CSF-1 and lipopolysaccharide binding protein (LBP). CSF-1 is present in adult serum but not in FCS. LBP transfers LPS to CD14 on macrophages and monocytes, triggering the formation of the TLR4-MD2 complex. This in turn activates the NF-κB pathway

resulting in cytokine production (e.g. IL-6, IL-8) (Miyake, 2004, Steinemann et al., 1994).

In equine monocytes, responses to LPS vary depending on the serum type used in culture. Figueiredo *et al.* (Figueiredo et al., 2008) compared HI FCS, commercial HS, HI commercial HS, autologous HS and HI autologous HS by measuring procoagulant activity of cultured monocytes. They concluded that FCS is not an optimal source of LBP for equine monocytes stimulated with LPS and that FCS resulted in the activation of equine monocytes. Commercial and autologous HS did not directly activate monocytes and gave more consistent results when compared to FCS

In this study, cells in HS and FCS did not show significant differences in the MTT assay (**Figure 4-4**) but did show significant morphological differences when viewed using light microscopy (**Figure 4-3**). Those cultured in HS in the presence of rhCSF-1 differentiated into macrophages, whereas cell populations in FCS did not differentiate and remained small, circular and not very adherent. In contrast, previous work on equine alveolar macrophages by our group found that there were no visible morphological differences between cells cultured in HS and FCS. Alveolar macrophages cultured in HS produced significantly higher levels of TNF- α following stimulation with LPS (Karagianni, 2015). Cells cultured in 20% HS had greater survival and viability compared to cells cultured in 10% HS (**Figure 4-5**).

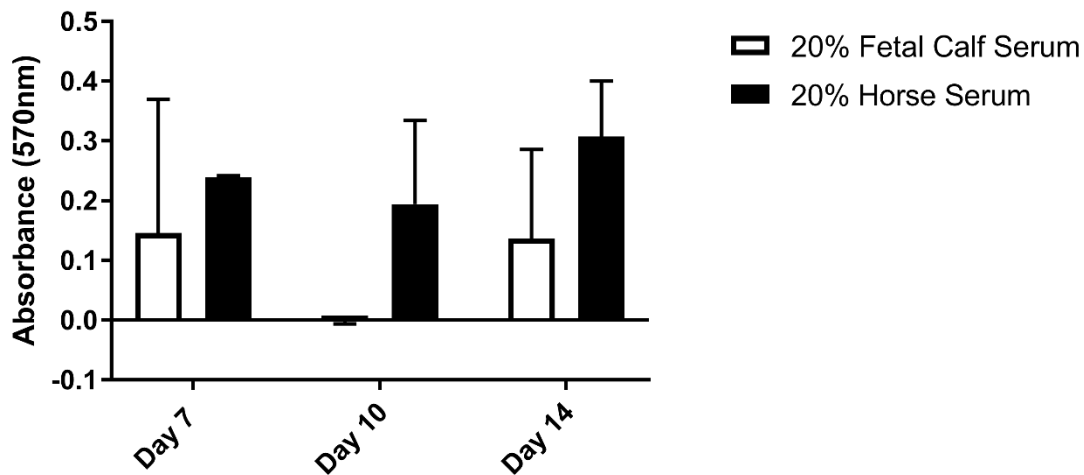


Figure 4-4 Comparison of cell survival and proliferation in culture media containing either 20% fetal calf (FCS) or 20% horse serum (HS)

eqBMDMs (n=3) were cultured in either 20% FCS or HS at 2.5×10^6 cells/ml for up to 14 days with or without rhCSF-1(+/- rhCSF-1). An MTT assay was performed on Days 7, 10 and 14 to assess cell metabolic activity. Results are average of triplicates. Values are median with 95% CI.

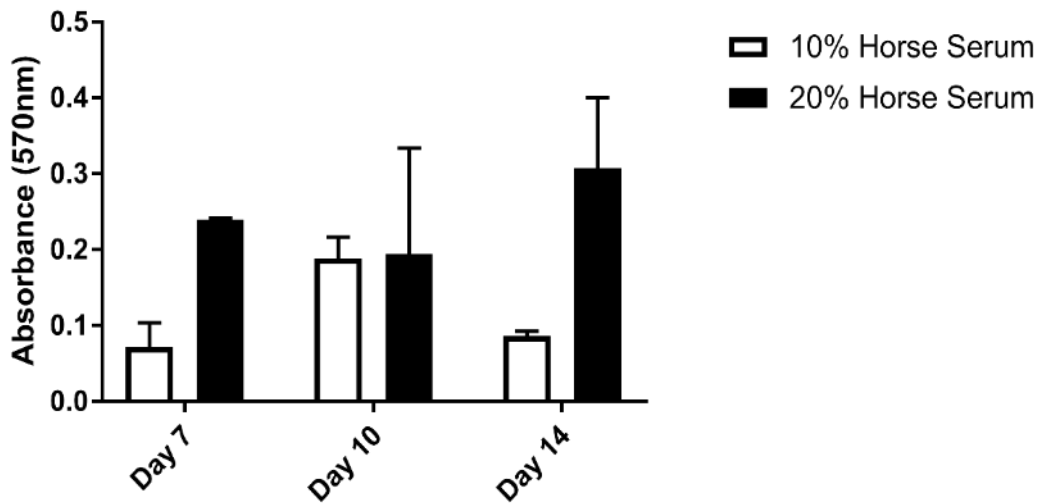


Figure 4-5 Comparison of cell survival and proliferation in culture media containing either 10% or 20% horse serum

eqBMDMs (n=3) were cultured in either 10% or 20% horse serum (HS) at 2.5×10^6 cells/ml for up to 14 days with or without rhCSF-1(+/- rhCSF-1). An MTT assay was performed on Days 7, 10 and 14 to assess cell metabolic activity. Results are average of triplicates. Values are median with 95% CI.

EqBMDMs differentiate better at higher seeding densities

Cells were examined by light microscopy and cells at 4×10^5 /well (2.5×10^6 /ml) were the most confluent and looked the healthiest. At decreasing densities, as cells were sparser, there was increased cell death and areas of clumping (Figure 4-3).

For all further analyses on eqBMDMs, cells were cultured in media containing 20% HS with rhCSF-1 (10^4 U/ml) at an approximate cell density of 2.5×10^6 cells/ml for up to 14 days.

4.2.3 Differentiated cells resemble macrophages

After culture on bacteriological plastic in rhCSF-1 for 10 days, cells had the expected morphology of macrophages; they were stellate and had an increased granularity and were adherent to bacteriological plastic (Figure 4-6).

A key function of macrophages is phagocytosis. Phagocytic activity was evaluated using two methods: (a) Zymosan A *Saccharomyces cerevisiae* BioParticle assay followed by cell fixation, staining with DAPI and phalloidin and confocal microscopy (Figure 4-7); (b) pHrodo Red *Escherichia coli* BioParticle assay followed by flow cytometric analysis (Figure 4-8). Phagocytic activity was seen in 80% of eqBMDMs (median 80%; range 77-84%).

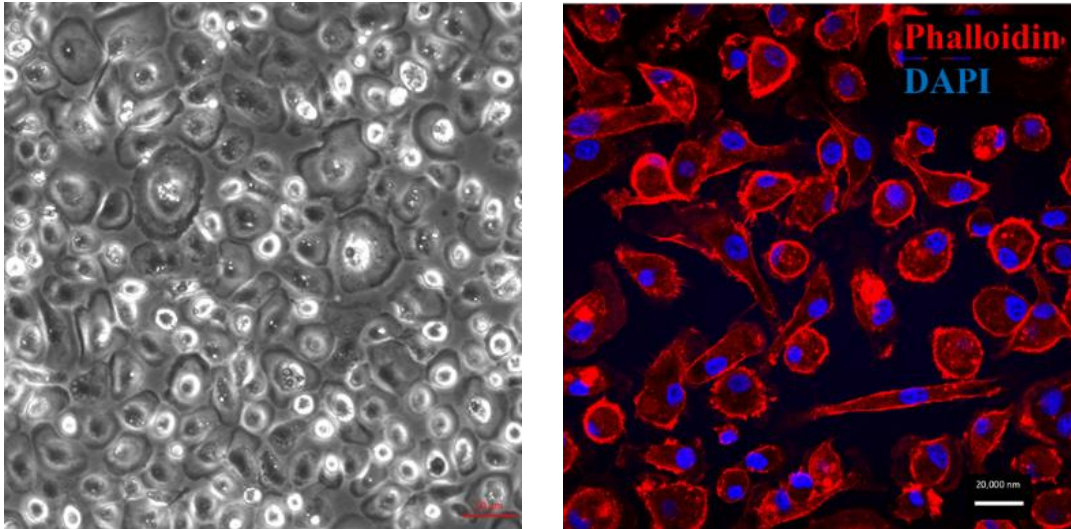


Figure 4-6 Analysis of cell morphology by light and confocal microscopy.

After culture of cryopreserved eqBMDMs in rhCSF-1 for 10 days the supernatant was removed, and cells were examined using light microscopy (A). For confocal microscopy, adhered cells were carefully removed from bacteriological plastic culture dishes and transferred to glass coverslips and cultured for a further 24hrs in rhCSF1, until cells had adhered to the coverslip. Cells were then fixed and stained with DAPI and Phalloidin before being transferred onto microscope slides and examined using a confocal microscope (B). Cell populations showed the expected granular stellate morphology of macrophages and were adherent to bacteriological plastic. Image representative of 3 horses.

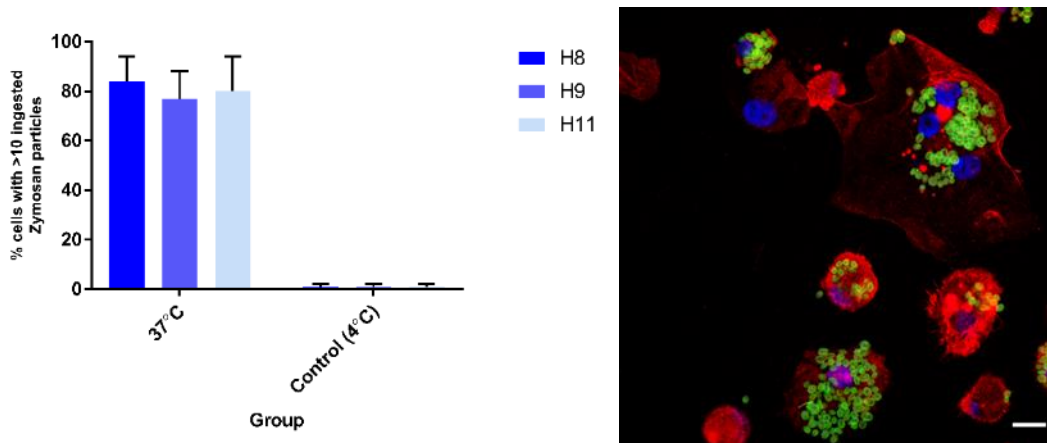


Figure 4-7 Zymosan phagocytosis assay.

Cells from 3 horses were cultured on bacteriological plastic for 10 days in rhCSF-1. On Day 10 media was replaced with media containing Zymosan particles and cells were incubated with the Zymosan particles for 1 hour at 37°C. Control cells had Zymosan particles added but were kept at 4°C. More than 70% of cells had phagocytosed Zymosan bioparticles (A). (B) is a confocal image of macrophages with phagocytosed Zymosan particles. Bar = 20µm

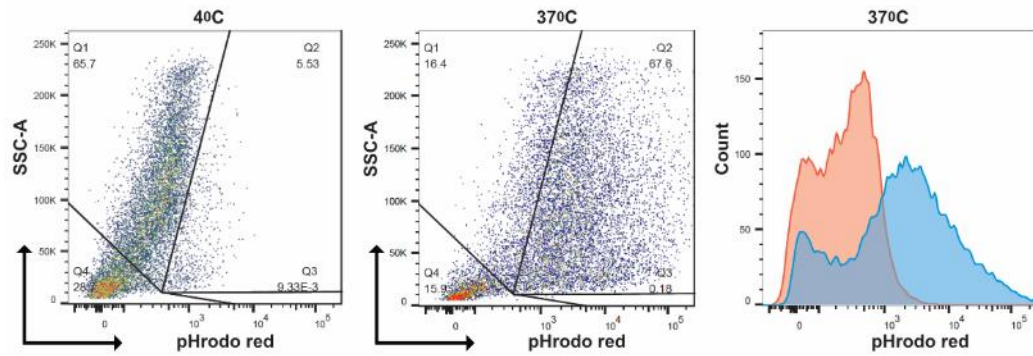


Figure 4-8 pHrodo BioParticle phagocytosis assay.

Cells from 6 horses were cultured with rhCSF-1 on bacteriological plastic for 7 days. On day 10 adhered cells were gently removed and cells combined before adding pHrodo Red *Escherichia coli* BioParticle for 1 hour at 37°C before being analysed by flow cytometry. Control cells were kept at 4°C for 1hr. See **Figure 4-9** for gating strategy.

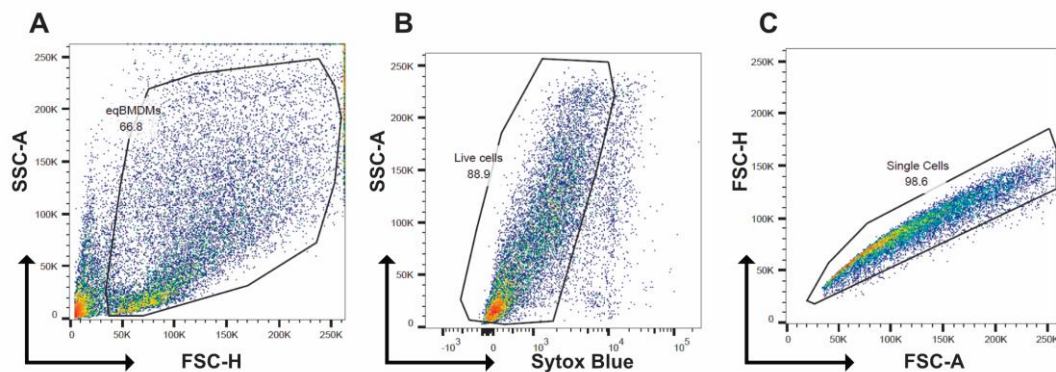


Figure 4-9 Gating strategy for eqBMDMs

Differentiated eqBMDMs were analysed for the expression of CD15 and CD163 by flow cytometry (**Figure 4-10**). SSC-Area (SSC-A) versus FSC-Height (FSC-H) was used to choose largest and most granular cells and excluding debris (A). Sytox blue was used to exclude dead cells (B). (C) identifies single cells and excludes doublets. Results are representative of at least 5 different experiments.

There are a limited number of antibodies against cell surface markers available for the horse. CD14, a co-receptor of the LPS receptor TLR4, is used as a marker for monocyte identification in several species, (Chamorro et al., 2005, Pridans et al., 2016, Wong et al., 2011b) including the horse (Kabithe et al., 2010). CD163, the haemoglobin scavenger receptor used as a marker in the previous chapter, is highly expressed in tissue macrophages in several species, such as pigs, humans and rodents (Van Gorp et al., 2010). It has been detected in some populations of human monocytes (Buechler et al., 2000). In pigs, CD163 is regulated inversely with CD14, defining subpopulations of monocytes (Fairbairn et al., 2011). Equine monocytes also express CD163 (Ibrahim et al., 2007) as do equine alveolar macrophages (Karagianni et al.,

2013) although equine peritoneal macrophages lack this marker (Karagianni et al., 2013).

To test if eqBMDMs expressed the markers CD14 and CD163, adherent differentiated cells were detached and stained for flow cytometry. Forward scatter (FCS) and side scatter (SSC) were used to identify macrophages based on their size (FCS) and granularity (SSC). Dead cells were excluded, and analysis was performed on single cells as described in **Figure 4-9**. The majority (84.2%) of differentiated eqBMDMs expressed CD14 (**Figure 4-10**), as has been previously reported on the eCAS cell line (Werners et al., 2004). By contrast, CD163 was very weakly expressed in eqBMDMs, as previously reported in pig BMDMs (Kapetanovic et al., 2012).

4.2.4 LPS stimulation of eqBMDMs

Lipopolysaccharide (LPS), a structural component of all gram-negative bacterial cell walls, is a pathogen associated molecular pattern (PAMP). TLR4 is the pattern recognition receptor (PRR) for the lipid A component of LPS, and myeloid cells or mice lacking *Tlr4* do not respond to pure LPS (Deng et al., 2013, Hoshino et al., 1999). Humans and horses are sensitive to the actions of LPS, with high mortality and morbidity in both species. In comparison, mice are less sensitive to LPS than humans and horses (Brade, 1999, Dinges and Schlievert, 2001); therefore, the use of rodent models to study sepsis in the horse or human is not optimal and indeed, may not be appropriate (Fink, 2014). A 'humanised' mouse model was considered to be more suitable for studying human sepsis (Warren, 2009, Unsinger et al., 2009) although given potential similarities in the LPS response of horses and humans (Parkinson et al., 2017, Karagianni et al., 2017) it may be more appropriate to use the horse as a model for human sepsis.

Gene expression changes in response to LPS have previously been studied in equine peripheral blood mononuclear cells (PBMCs) (Parkinson et al., 2017, Pacholewska et al., 2017) and alveolar macrophages (Karagianni et al., 2017). To examine the specific macrophage response of eqBMDMs to LPS, adhered differentiated cells were harvested and plated at a concentration of 10^6 cells/ml and left overnight before being stimulated with LPS for 7 and 24 hours. The LPS used was *Salmonella enterica* Serotype Minnesota Re595; a rough mutant which is a pure TLR4 agonist, involving only the TLR4-MD2-CD14 complex, and no other TLRs (Hume et al., 2001). RNA was extracted from control (n=3) and LPS treated (n=3) cells and samples were used for qRT-PCR and total RNA-Sequencing (RNA-Seq).

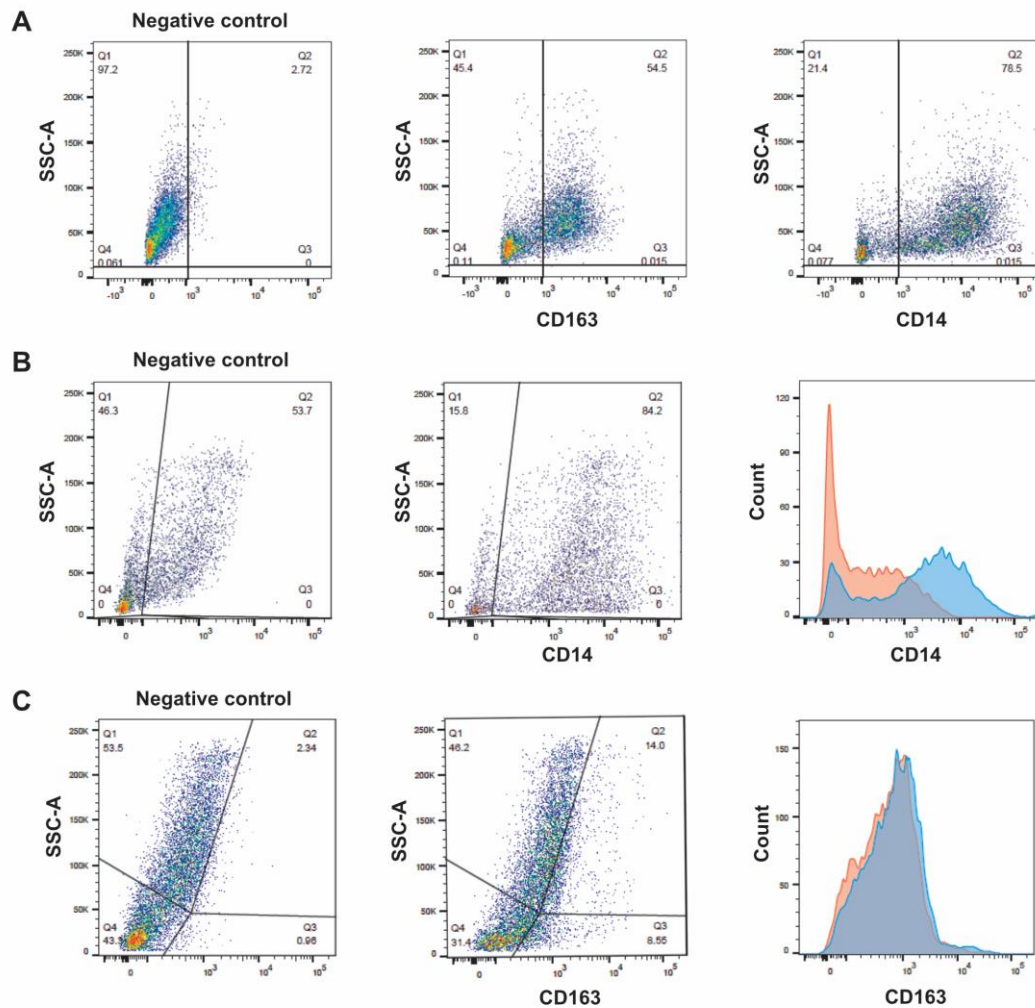


Figure 4-10 Flow cytometry of equine alveolar macrophages and eqBMDMs
EqBMDMs were cultured for 7 – 10 days in rhCSF-1 (n=6). When confluent, adhered cells were stained for flow cytometry. Alveolar macrophages were thawed and cultured overnight in rhCSF-1 and adherent cells harvested for flow cytometry. Size (forward light scatter (FSC)) and granularity (side scatter (SSC)) were used for cell discrimination (data not shown. See **Figure 4-9** for gating strategy). Equine alveolar macrophages were used as a positive control (**A**). eqBMDMs expressed CD14 (**B**) but only a small population of eqBMDMs (12%) expressed CD163 (**C**).

Validating the LPS response with qRT-PCR

Macrophages stimulated with LPS produce the pro-inflammatory cytokine *TNF- α* in response to LPS binding to the CD14-TLR4-MD2 receptor complex (Palsson-McDermott and O'Neill, 2004). *TNF- α* is an early response gene, and in other species, it peaks around 2 hours but is still elevated after 7 hours (Karagianni et al., 2013, Karagianni et al., 2017, Kapetanovic et al., 2012). Here it was used as a positive indicator of eqBMDM LPS-responsiveness. *GAPDH* was used as a reference gene. EqBMDMs showed around 25-fold upregulation of *TNF- α* mRNA after 7 hours in response to LPS (**Figure 4-11**).

LPS induced IDO but not NOS2 expression in eqBMDMs

Nitric oxide (NO) is a product of inducible nitric oxide synthase (*NOS2*) and is synthesized from arginine. It is an important component of the innate immune response of rodent macrophages to various pathogens (MacMicking et al., 1997). As discussed in **Chapter 1**, differences exist between species in the activation of arginine metabolism and release of NO. Mouse macrophages produce NO (Stuehr and Marletta, 1985) but human and porcine macrophages do not (Kapetanovic et al., 2012). There are conflicting data relating to equine macrophages; some studies report NO production from equine alveolar macrophages (Hammond et al., 1999) and the macrophage cell line, e-CAS, (Werners et al., 2004) and *NOS2* induction in response to LPS. However, these studies did not directly compare the magnitude of release with that of rodent-derived macrophages. In contrast, Karagianni et al., (Karagianni et al., 2013). using murine-derived cells as a comparison, found no evidence of *NOS2* induction or NO production by LPS stimulated equine alveolar macrophages. Murine macrophages take up arginine via the cationic arginine transporter (CAT) 2, encoded by the *Cat2/Slc7a2* gene (Kakuda et al., 1999) and metabolise arginine to produce NO, via the induction of *Nos2* (MacMicking et al., 1997). Neither human macrophages (Schroder et al., 2012) nor activated pig macrophages (Kapetanovic et al., 2012) express *CAT2/SLC7A2*. Instead, pig, human and equine alveolar macrophages metabolise tryptophan through the induction of indoleamine dioxygenase (*IDO*) (Karagianni et al., 2013, Kapetanovic et al., 2012, Schneemann et al., 1993). This species-specific regulation was attributed to divergence of the *NOS2* promoter sequences between species, with good conservation between human, pig and horse promoters, but little sequence alignment with mouse promoters (Kapetanovic et al., 2012, Karagianni et al., 2013).

To address this question in eqBMDMs, the production of nitrite by differentiated eqBMDMs was measured following LPS stimulation for 7 and 24 hours. Chicken BMDMs, which produce large amounts of NO in response to LPS, were used as a positive control (Wu et al., 2016). There was no detectable nitrite production in eqBMDMs (**Figure 4-12**). In addition, no increase in *NOS2* expression was detected by qRT-PCR following LPS stimulation. In comparison, and consistent with the findings derived from pig BMDMs and human MDMs (Kapetanovic et al., 2012), *IDO1* mRNA was induced >100-fold at 7 hours (**Figure 4-11**).

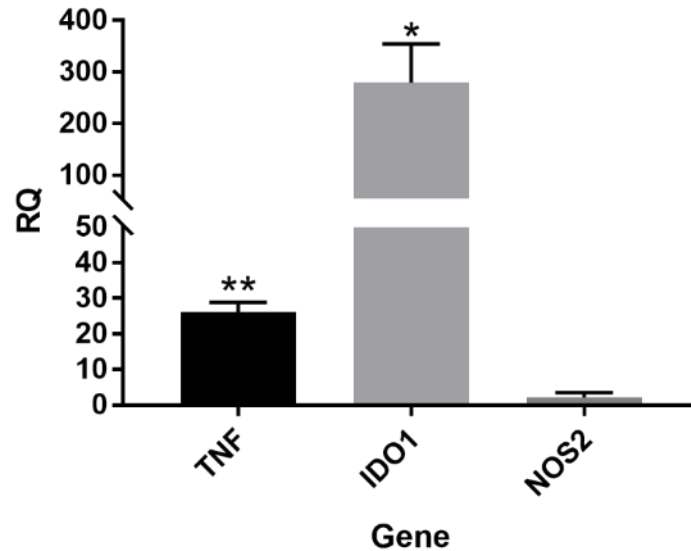


Figure 4-11 Relative quantification (RQ) of *TNF-α*, *IDO* and *NOS2* in eqBMDMs after being in culture with LPS for 7hrs

Cryopreserved eqBMDMs from 3 horses were cultured until confluent and adherent (Day 10). Cells were plated at 2×10^6 cells/well and left to rest overnight, in optimal conditions described in **Section 4.2.2**. The media was replaced and LPS (100ng/ml) added for 7 hours. Control samples had culture media changed only. RNA was extracted and RQ relative to the housekeeping gene *GAPDH* for *TNF-α*, *IDO* and *NOS2* was measured by qPCR. Graphs show median + 95 CI. Significance was determined using a paired t-test. * $p < 0.05$, ** $p < 0.001$.

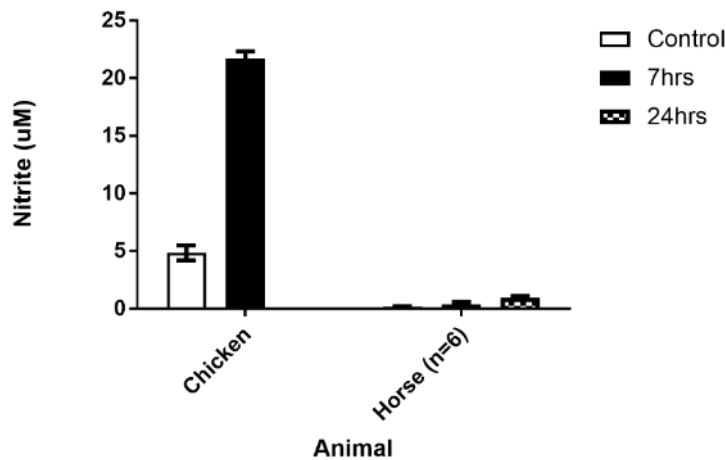


Figure 4-12 Nitrite production of eqBMDMs following stimulation with LPS (100ng/ml) at 7 and 24 hours

Cryopreserved eqBMDMs from horse (n=6) and chicken (n=1) were cultured until confluent and adherent (Day 10). Cells were plated in duplicate at 2×10^6 cells/well and left to rest overnight, in optimal conditions described in **Section 4.2.2**. The media was replaced and LPS (100ng/ml) added for 7 hours. Control samples had culture media changed only. Nitrite ($\mu\text{m}/\text{mL}$) was measured in supernatant. Results shown are median \pm 95% CI.

4.2.5 RNA-seq analysis of eqBMDMs and their response to LPS

Both earlier studies of LPS stimulated equine PBMCs used *E. coli*-derived LPS and analysis was performed at 24 hours. In this study, *Salmonella*-derived LPS was used and analysis performed at 7 hours. As mentioned earlier (**Section 4.2.4**), our group routinely uses *Salmonella enterica* Serotype Minnesota Re595, a pure TLR4 agonist (Hume et al., 2001) and its use in this study permitted direct comparisons with data derived from other species within our group.

Having determined that the eqBMDMs treated for 7 hours with LPS responded with large alterations in expression of positive control genes, *TNF- α* and *IDO1*, the same mRNA was subjected to RNA-Seq analysis to provide a global overview of the LPS response. Parallel studies on the same cellular system (CSF1-stimulated BMDM) in other species (sheep, goat, pig, cattle, water buffalo and rat) provided the opportunity for comparative analysis to identify possible equine-specific responses that could contribute to extreme LPS sensitivity. As discussed in (**Chapter 1**), RNA-Seq has the advantage, compared to microarrays, of permitting the investigation of known and new transcripts; microarrays are limited to existing genomic information. By improving our understanding of the transcriptome, we can improve the functional annotation of the equine (*Equus caballus*) genome (EquCab2.0.). The horse genome is currently a relatively poor assembly. Comparing it to the pig (*Sus scrofa*) genome, Sscrofa11, coverage of the horse is 6.0x compared to 65x in the pig (**Chapter 1**). Contig N50 is also 400x greater in pig compared to horse in part through the use of newer long read technologies such as PacBio (www.pacb.com) in the assembly of the pig genome compared to the shorter read technologies used to assemble the horse genome. There are two studies in horses using RNA-seq to study the response of peripheral blood mononuclear cells (PBMCs) to LPS (Pacholewska et al., 2017, Parkinson et al., 2017). Several equine studies have used human and mouse microarrays (Barrey et al., 2006, Mucher et al., 2006, Smith et al., 2006, Ramery et al., 2008), as well as equine microarrays (Gu and Bertone, 2004, Santangelo et al., 2007, Noschka et al., 2009, Mienaltowski et al., 2008). Studies using equine microarrays were limited by the poor annotation of the arrays, but whilst some probes on mouse and human arrays would fail to hybridise, the overall annotation when using these arrays was superior to the equine microarrays. To date, there are no RNA-Seq studies looking at the specific response of eqBMDMs to LPS in the horse although Werners *et al.* measured *TNF- α* and NO production in e-CAS cells (Werners et al., 2004).

Analysis of differential expression in eqBMDMs stimulated with LPS

Transcripts were quantified, giving expression estimates as transcripts per million (TPM) using Kallisto (Bray et al., 2016) and annotated to the *Equus caballus* reference genome (via Ensembl BioMart v90) (Kinsella et al., 2011). By this method, 21,906 transcripts were found in total. Of these transcripts, 18% (3886) were identified as pseudogenes, 82% (18018) were protein coding and 0.8% (184) were identified as potential novel genes (Table 4-2). A PCA plot (Figure 4-13) showed separation of samples depending on condition (LPS stimulated vs unstimulated).

Table 4-2 Summary of RNA-Seq transcripts

Transcript Description	Number of genes
<i>Protein coding genes</i>	18018
<i>Pseudogenes</i>	3886
<i>Unknown</i>	2
<i>Novel transcripts</i>	184
Total Transcripts	21906

Network cluster analysis was performed using Miru (Kajeka Ltd, Edinburgh, UK) to analyse gene expression in LPS-stimulated eqBMDMs (Freeman et al., 2007, Theocharidis et al., 2009). Using a Pearson correlation threshold (r) of 0.97, a markov clustering algorithm (MCL) inflation value of 2.2 and a minimum cluster size of 8, a network graph was generated that consisted of 11446 nodes connected with 547614 edges within a total of 295 clusters (Figure 4-14-A). Using the animation feature in Miru where closely correlated genes are highlighted, a series of cluster graphs was generated that distinguished two groups of clusters; one group at 0 hours and one group at 7 hours (Figure 4-14-B). Whilst 2 horses had similar graphs, H11 appeared to have a distinct group of co-expressed genes at 7 hours.

Read counts were calculated using Kallisto and summarised to genes using the R/Bioconductor package tximport v1.0.3. This output was used in the R/Bioconductor package, edgeR v3.14.0 (Robinson et al., 2010), to normalise gene counts and to identify genes differentially expressed between control and LPS-treated eqBMDMs (Benjamini and Hochberg, 1995). From this list, using Log₂ fold change (log₂ fc) values of ≥ 1.5 or ≤ -1.5 with $p < 0.02$ a list of upregulated and down regulated genes was generated. Only genes with a minimum read count value of 10 at 7 hours for upregulated genes and a minimum read count of 10 at 0 hours for down regulated genes were included in the analysis. In total, 1070 genes were either induced (733) or repressed (237) by LPS in eqBMDMs. Using this list, the top 100 most differentially expressed genes were identified (Figure 4-15 and Figure 4-16). To compare functional

differences between the groups, gene function analysis was performed using the Gene Ontology (GO) tool in GATHER (Gene Annotation Tool to Help Explain Relationships) (Chang and Nevins, 2006). A total of 182 genes upregulated, and 38 genes downregulated, by LPS in eqBMDMs were not annotated to the horse genome (displayed as Ensembl IDs in **Figure 4-15** and **Figure 4-16**) and did not have any orthologues available in Ensembl. Further analysis of the differential expression would include the identification of these potentially novel genes to further our understanding of the equine specific response to LPS

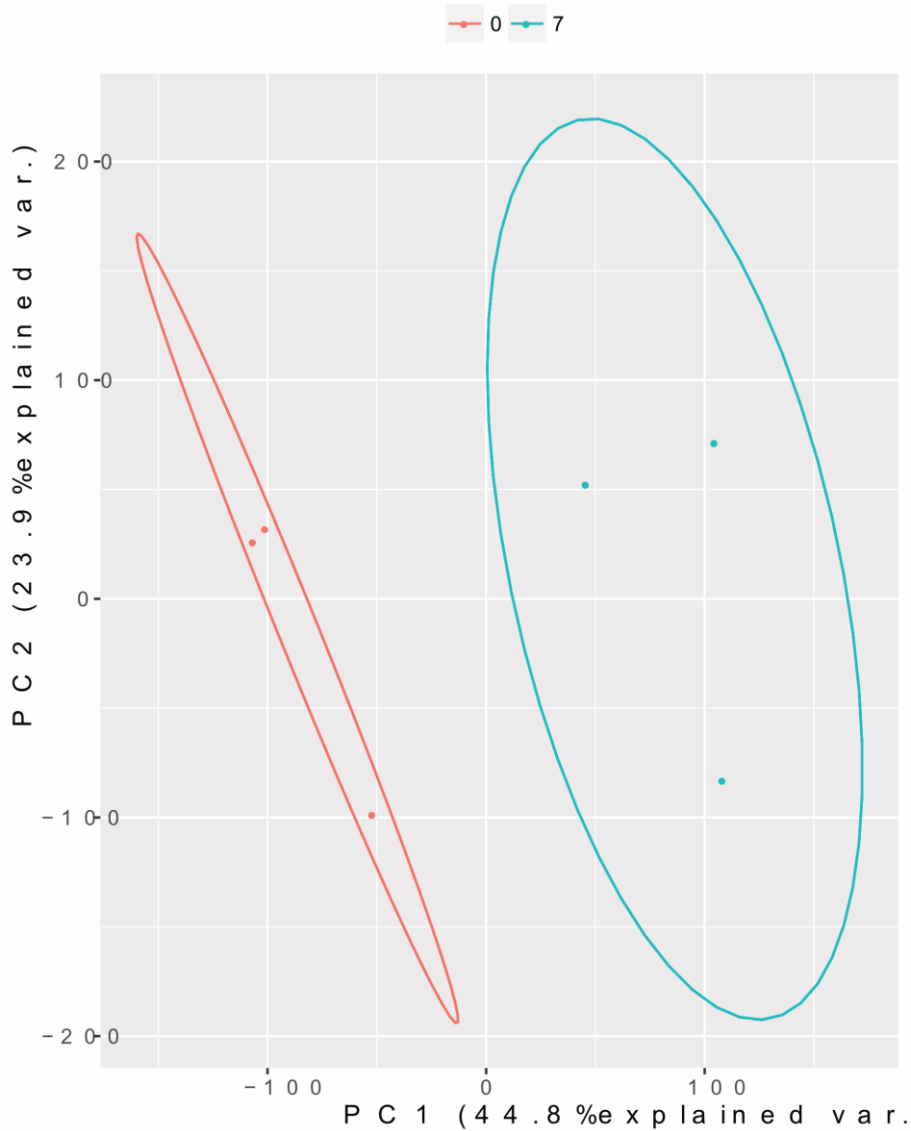


Figure 4-13 Principal component analysis (PCA) of LPS treated eqBMDMs and untreated eqBMDMs plotted in two dimensions

This is a PCA of LPS stimulated (blue) and control (red) eqBMDMs showing a distinct separation between LPS treated and control eqBMDMs. The proportions in each axis represent the percentage variance by each component. The ellipses indicate 95% confidence intervals.

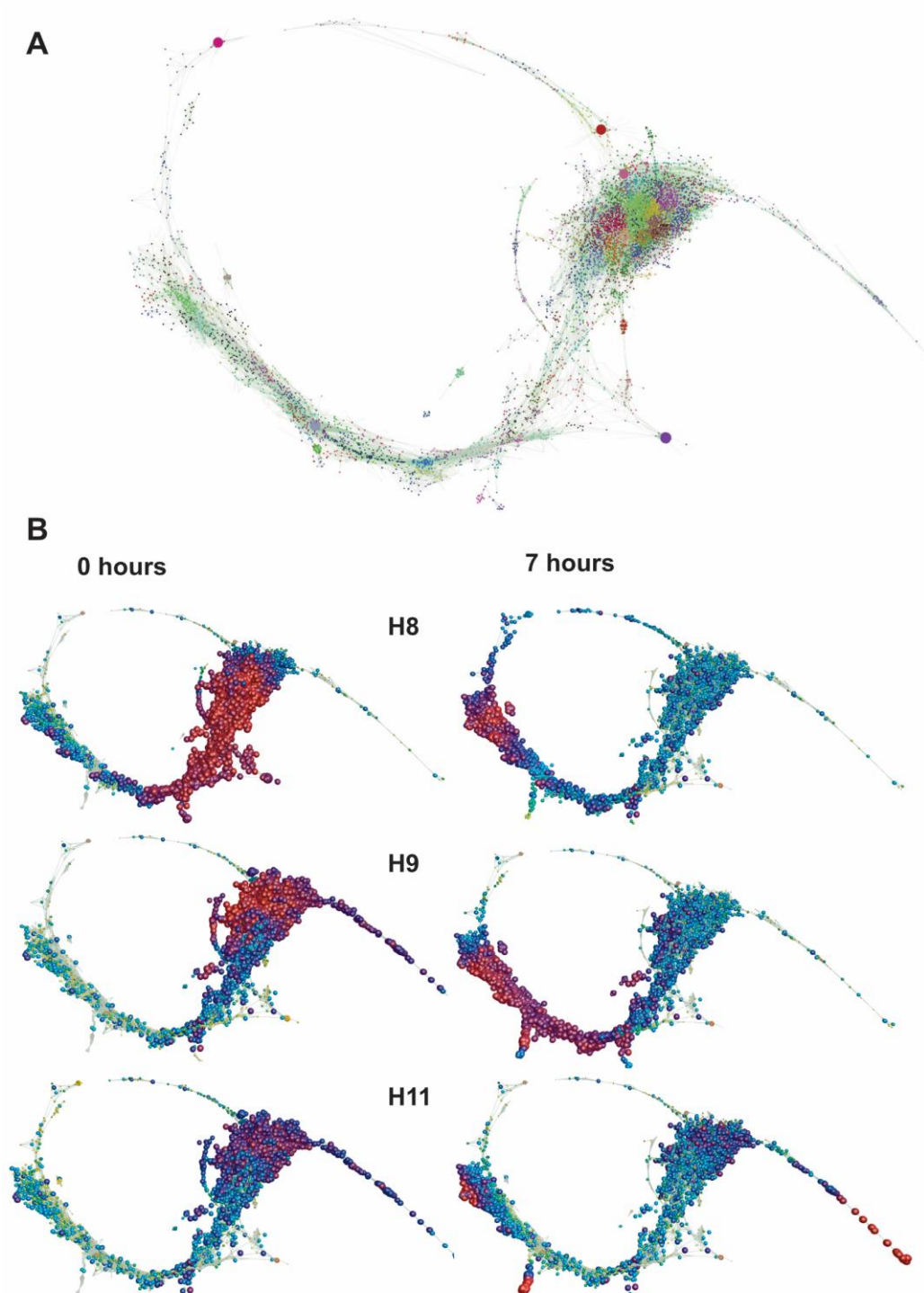


Figure 4-14 Network analysis of differentially expressed transcripts between eqBMDMs stimulated with LPS and control (unstimulated) eqBMDMs

A network analysis graph of all samples (0 and 7 hours) generated in Miru for eqBMDMs (n=3) stimulated with 100ng/ml LPS for 7 hours and for control cells from the same animal (A). Transcript to transcript Pearson correlation was set at $r > 0.99$. The graph contains 11446 nodes (node = transcript) connected by 547614 edges (Pearson correlation relationships). The graph was clustered using MCL algorithm set at an inflation of 2.2 giving 295 clusters. Nodes with clusters of co-expressed transcripts will be closely connected. Using the animation feature, (B) shows nodes that are co-expressed together (expanded red nodes) at 0 and 7 hours for each horse (H8, H9 & H11).

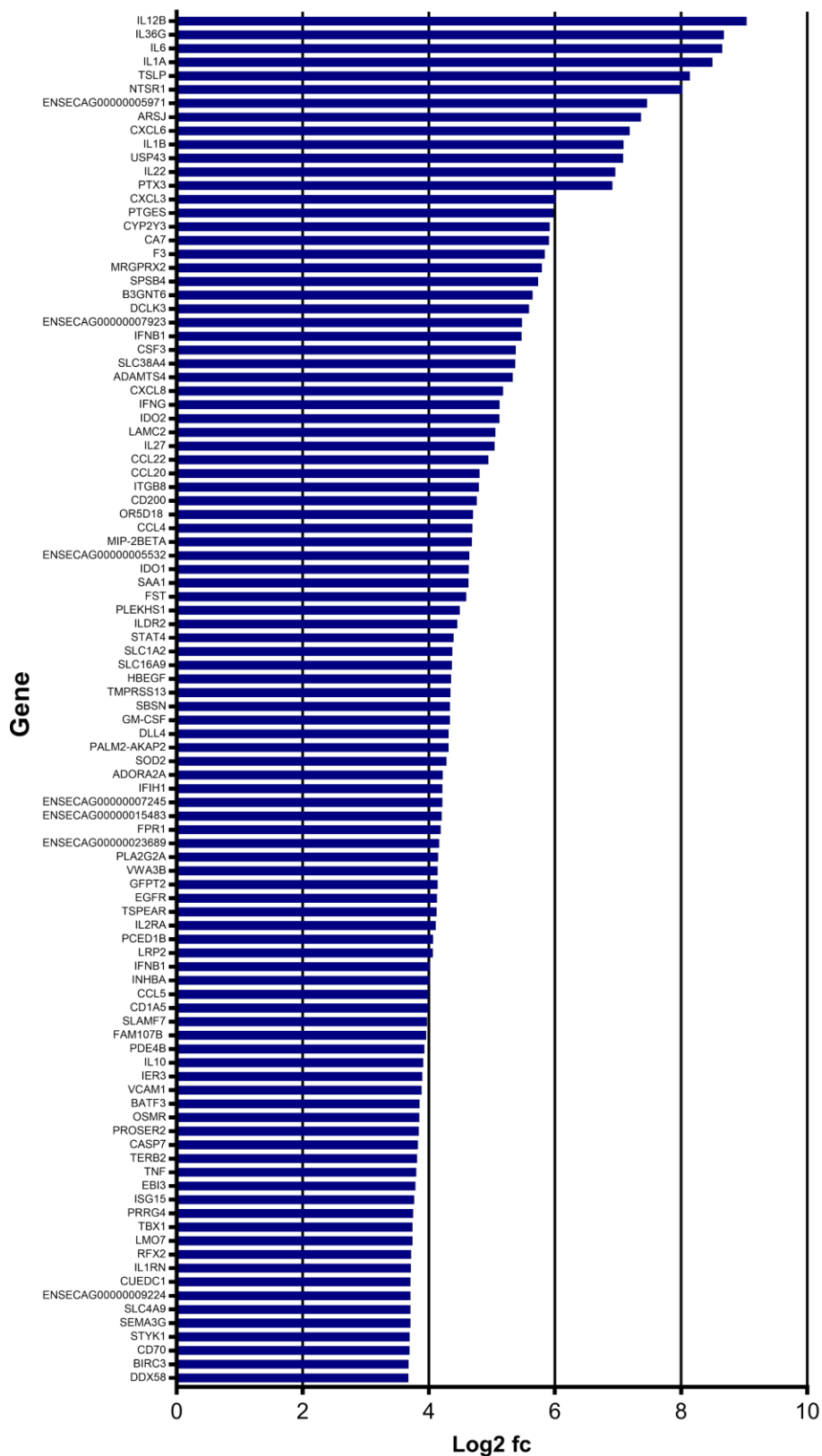


Figure 4-15 Top 100 genes in eqBMDMs induced by LPS

RNA-Seq data of genes induced by LPS in eqBMDMs as identified by Log2 fc and $p < 0.02$. Genes with Ensembl IDs are genes not annotated to the horse genome and with no orthologues.

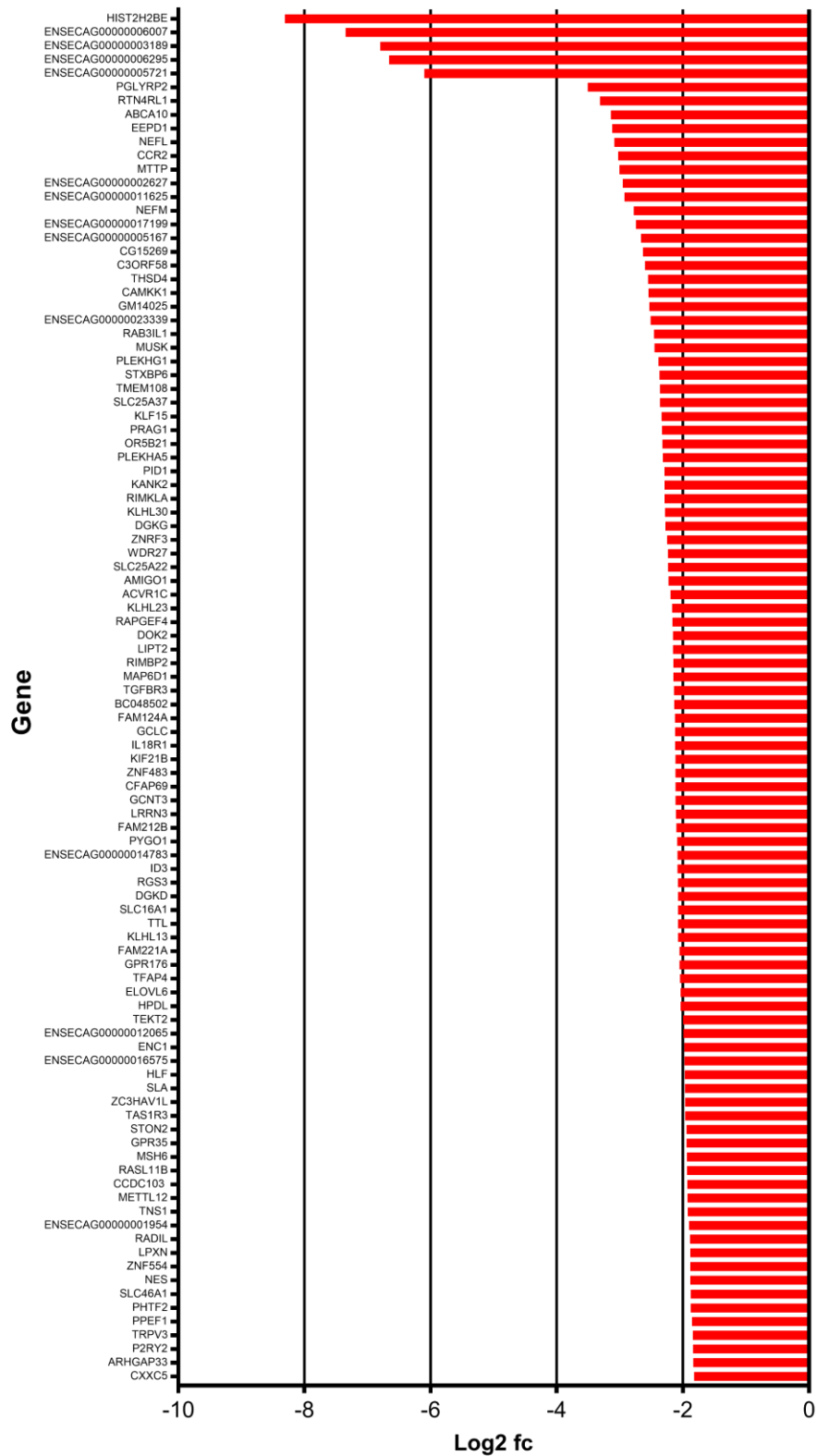


Figure 4-16 Top 100 genes suppressed by LPS in eqBMDMs

RNA-Seq data of genes suppressed by LPS in eqBMDMs as identified by Log2 fc and $p < 0.02$. Genes with Ensembl IDs are genes not annotated to the horse genome and with no identifiable orthologues.

The top 100 (**Figure 4-15**) upregulated genes included genes associated with the initiation and maintenance of inflammation and with LPS stimulation of macrophages (*IL1B*, *IL6*, *TNF- α* , *CXCL8*). GO term analyses using GATHER showed genes associated with *cell communication* and *signal transduction* (e.g. *SOCS1*, *SOCS3*, *MAP2K6*, *STAT1*, *STAT2*, *STAT3* and *STAT4*), *response to stimulus* (e.g. *CXCL2*, *CXCL3*, *CXCL6*, *IL10*, *IL12B* and *TNF- α*) and *immune response* as the main groups of genes upregulated, consistent with LPS stimulation of macrophages (**Figure 4-17-A**). Genes associated with apoptosis (*BCL2*, *CFLAR*, *APAF1*, *CASP3*, *CASP7*, *CASP10*, *NFKB1A*, *TNF- α* , *BIRC3*, *HSPA6*, *TNFSF10*) were also a component of the second main functional pathway identified based upon GO term enrichment. Apoptosis is a feature of septic shock and is reported in models of sepsis (Joshi et al., 2003) and in LPS-induced apoptosis in murine BMDMs (Xaus et al., 2000). An increase in expression of genes involved in apoptosis has been previously detected in equine alveolar macrophages stimulated with LPS (Karagianni et al., 2017). In this dataset, genes associated with cell apoptosis were also LPS inducible (e.g. *PDCD1LG1/CD274*, *PDCD1LG2*, *BCL2*, *CFLAR* and *APAF1*) as were transcription factors (e.g. *STAT4* and *BATF3*) (**Table 4-3**).

Table 4-3 TPM values for LPS inducible genes and transcription factors associated with apoptosis in eqBMDMs

Gene	TPM	TPM
	0 hours	7 hours
<i>PDCD1LG1/CD274</i>	26.217	236.204
<i>PDCD1LG2</i>	4.887	30.256
<i>BCL2</i>	4.718	13.469
<i>CFLAR</i>	81.318	410.644
<i>APAF1</i>	25.176	77.053
<i>STAT4</i>	6.551	106.317
<i>BATF3</i>	13.806	153.497

Downregulated genes (**Figure 4-16**) include *DOK2* a negative regulator of macrophages stimulated with LPS (Shinohara et al., 2005). The largest biological processes involved are *cell communication/signal transduction* e.g. *DOK2*, *TLR1* and *CCR2* and *cell cycle* genes e.g. *FBX043*, *ID3*, *RAPGEF4* and *MYC* (**Figure 4-17-B**). This supports the literature in which it is well documented that LPS inhibits genes associated with proliferation as LPS blocks the action of CSF-1 (Sester et al., 2005, Sweet et al., 2002). Murine BMDMs differentiated in CSF-1 have an elevated response

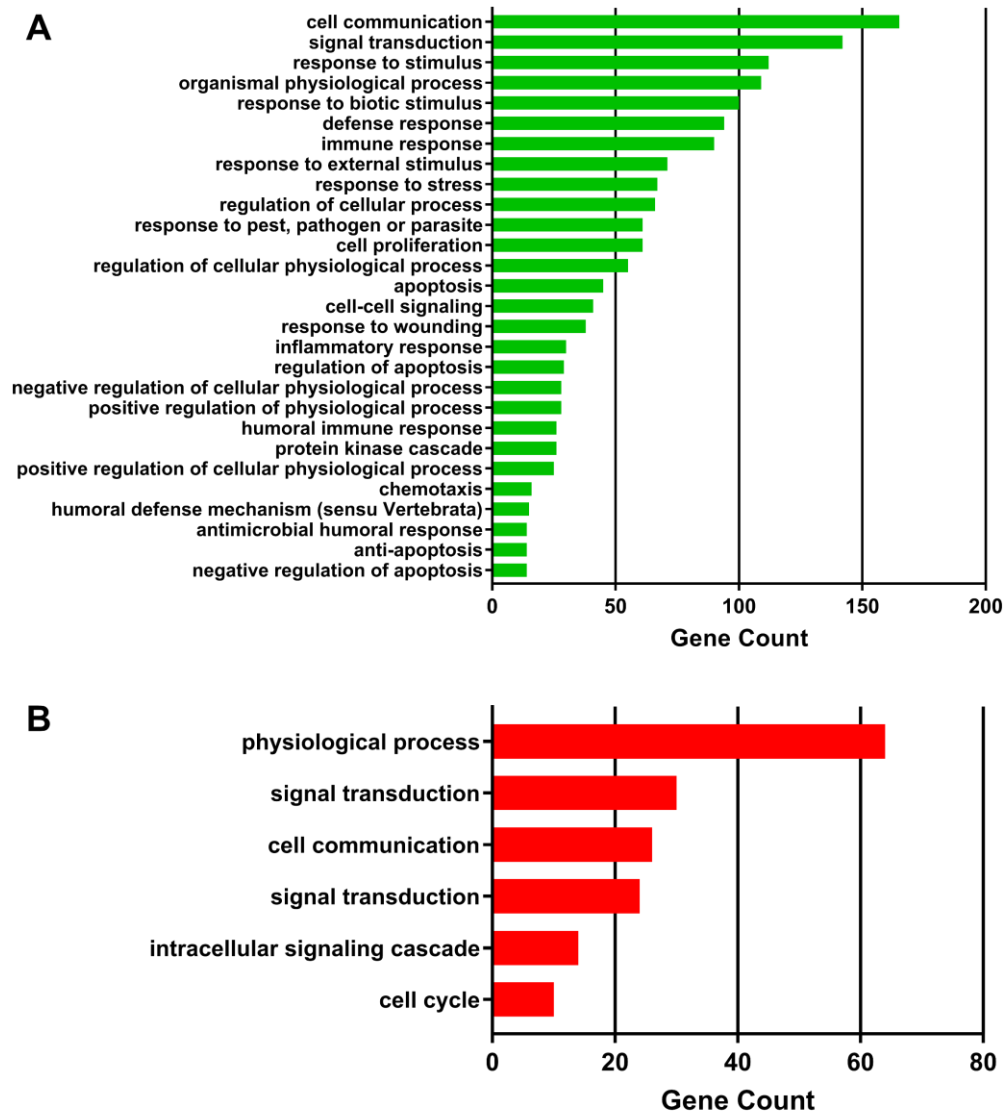


Figure 4-17 Main functional groups of induced and repressed genes of eqBMDMs stimulated with LPS

Histograms show main GO terms either induced (**A**) or suppressed (**B**) by LPS in eqBMDMs. Data was analysed using the GO term analysis tool in GATHER. All genes with Log₂ fc of ≥ 1.5 or ≤ -1.5 with $p < 0.02$ were included. Results are for all GO terms with $p < 0.05$ and Bayes Factor > 6 (Chang and Nevins, 2006).

to LPS, a likely result of its activity as a macrophage growth factor but LPS down-regulates expression of *Csf-1r* in BMDMs (Sweet et al., 2002, Sester et al., 1999). The implication of this is that macrophages at the site of infection have potentially been in contact with LPS and are therefore unlikely to be CSF-1 responsive, but they may be hypersensitive to the effects of bacterial DNA (Sweet et al., 2002). Additionally, the down regulation of the *Csf-1r* is caused by LPS mimicking the action of CSF-1 and resulting in the *Csf-1r* being removed from the cell surface and moved to the perinuclear region (Sester et al., 1999). This results in disruption to the macrophage cell cycle regulation (as CSF-1 can no longer bind to the CSF-1R) by blocking the G1-S phase. An example of genes involved in the cell cycle are cyclin-dependent kinases (CDK) (Morgan, 1997). In the horse *CDK1*, *CDK2*, *CDK3* and *CDK6* were all downregulated by LPS suggesting LPS inhibits the cell cycle as reported in murine BMDMs (Table 4-4).

Table 4-4 Effect of LPS stimulation on cyclin-dependent kinases (CDK) involved in the cell cycle in eqBMDMs

<i>Gene</i>	<i>Phase</i>	TPM 0 hours	TPM 7 hours
<i>CDK1</i>	M, G2	23.305	11.789
<i>CDK2</i>	G1, S	7.185	4.687
<i>CDK3</i>	G0, G1	0.318	0.193
<i>CDK4</i>	G1	62.497	30.474
<i>CDK6</i>	G1	49.128	47.689

Induction of early response genes in eqBMDMs at 7 hours post LPS stimulation

A detailed time-course analysis of the horse response to LPS was beyond the scope of this project – the main function being to study the acute response of eqBMDMs to LPS and to apply this to intestinal surgical colic cases, to identify if macrophage activation occurs within the mucosa and *muscularis* at the time of abdominal surgery. Additionally, the study of the acute inflammatory response will help in the understanding of the innate immune response of the horse, particularly relevant in light of the high sensitivity of the horse to LPS. As well as genes induced by LPS, it is also important to study genes repressed by LPS. Inflammation suppressor genes are also activated by pathogens e.g. LPS and act to provide an ‘off switch’ to inflammatory mechanisms (Wells et al., 2005, Baillie et al., 2017). Without suppressors, there would be no effective resolution of inflammation. Monocytes entering the lamina propria (LP) of the gut must modulate their phenotype, to down regulate their response to bacteria within the intestinal lumen, thus preventing continuous and detrimental inflammation within the intestine (Bain and Mowat, 2014). This phenotypic modulation requires the presence of the macrophage growth factor, CSF-1. The

differentiation of monocytes to macrophages in the presence of CSF-1 therefore provides a good *in vitro* model of the process of differentiation of intestinal macrophages, as suggested by Baillie *et al.* 2017.

LPS stimulation of macrophages triggers a sequence of waves of gene expression extending up to 48 hours, which has been studied in detail in mice (Sweet and Hume, 1996, Takeuchi and Akira, 2010) and in humans (Baillie *et al.*, 2017, Rossol *et al.*, 2011). In humans, early (immediate response genes) induced by LPS included *EGR1*, *EGR2*, *EGR3*, *FOS*, *FOSB* and *NFKBIZ* with their promoters showing an increase in detectable expression as early as 15 minutes post stimulation (Baillie *et al.*, 2017). At 7 hours in eqBMDMs the majority of these genes had the same TPM at 0 and 7 hours (*ERG1*, *ERG2*, *ERG3* and *FOSB*) indicating that by 7 hours this early response “wave” had passed and that these genes had peaked and had returned to normal levels (Table 4-5). *NFKBIZ* was upregulated and *FOS* was downregulated. *NFKBIZ* is a transcriptional regulator of $\text{I}\kappa\text{B}\zeta$ induced in response to IL-1 or LPS (Yamazaki *et al.*, 2001) but not *TNF- α* (Yamamoto *et al.*, 2004). $\text{I}\kappa\text{B}\zeta$, in conjunction with another gene, *AKIRIN2*, is required for IL-6 and IL-12B production. In mouse macrophages, *AKIRIN2* interacts with BAF60 proteins and $\text{I}\kappa\text{B}\zeta$, which as a complex are recruited to the *IL-6* and *IL-12B* promoters to induce chromatin remodelling. These then recruit the SW1/SNF complex to the promoters of the target genes (Tartey *et al.*, 2014). From the eqBMDMs results, both *IL-6* and *IL-12B* are significantly upregulated at 7 hours with Log2 fc of 8.6 and 9 respectively ($p < 0.001$) (Figure 4-15). Table 4-5 shows TPM values for these genes. As with the early response genes, *AKIRIN2* is unchanged between 0 and 7 hours, likely consistent with a return to normal expression following an earlier peak.

Table 4-5 TPM values for genes induced or repressed by LPS in eqBMDMs

Gene	TPM 0 hours	TPM 7 hours
<i>ERG1</i>	3.656	3.294
<i>ERG2</i>	25.784	16.051
<i>ERG3</i>	1.022	0.938
<i>FOS</i>	157.665	57.445
<i>FOSB</i>	0.631	0.746
<i>NFKBIZ</i>	3.198	11.164
<i>IL6</i>	0.370	117.52
<i>IL-12B</i>	0.055	24.49
<i>AKIRIN2</i>	49.259	43.410

Cytokine and chemokine signalling in response to LPS in eqBMDMs

Chemokines are secreted by cells at the site of inflammation to recruit leukocytes to the site of inflammation. Chemokines associated with LPS activation of macrophages

or monocytes in mice include *CXCL1*, *CXCL2*, *CXCL3*, *CXCL5*, *CXCL8*, *CXCL9*, *CCL2*, *CCL3*, *CCL4*, *CCL5*, *CCL11*, *CCL17* and *CCL22* (Mantovani et al., 2004). The expression of genes encoding cytokines and chemokines associated with LPS stimulation of macrophages were all significantly upregulated ($p < 0.02$) and contained within the list of DE genes in eqBMDMs. These included the inflammatory cytokines *TNF- α* , *IL12B*, *IL6*, *IL1B* and *IL10* and chemokines *CXCL2*, *CXCL3*, *CXCL8*, *CCL3*, *CCL4*, *CCL5* and *CCL22*.

In eqBMDMs *CXCL6* is one of the most upregulated genes (**Figure 4-15**), a finding also reported in a study of LPS stimulated equine PBMCs (Pacholewska et al., 2017). In LPS stimulated human PBMCs, *CXCL6* was also upregulated (Pu and Wang, 2014). There is no *Cxcl6* gene in the mouse genome in Ensembl. *CXCL6* is also expressed in alveolar macrophages stimulated with LPS (**Figure 4-18**). *CXCL6*, also known as granulocyte chemotactic protein 2 (GCP-2), signals the recruitment of neutrophils, via their surface expression of CXCR1 and CXCR2 receptors (Wuyts et al., 1997). In humans, pulmonary macrophages from patients undergoing lung resection of carcinoma produced GCP-2, as did human MDMs cultured for 5 days when stimulated with LPS, but not polyIC or IL1B (Wuyts et al., 2003). In the FANTOM5 dataset, *CXCL6* is also upregulated in response to human MDMs in response to LPS (fantom.gsc.riken.jp/zenbu). However, LPS stimulation of freshly isolated PBMCs failed to produce GCP-2, suggesting that differentiation of unstimulated cells (e.g. in culture) influences the capacity for GCP-2 production (Wuyts et al., 2003). Neutrophils have two contrasting roles in sepsis. Impaired neutrophil recruitment and migration results in the inability to successfully fight infection. Conversely the neutrophilic antibacterial inflammatory response is thought to contribute to tissue ischemia, organ damage and even multiple organ dysfunction (Sônego et al., 2016). Other chemokines mediating the recruitment of neutrophils in mice include *CXCL1*, *LFA-1*, *CD11b/Mac-1*, *ICAM-1*, *VCAM-1*, *ICAM-2*, *PECAM-1*, *CXCL2* and (Reichel et al., 2012). In eqBMDMs *CXCL2*, *ICAM-1*, *VCAM-1*, *PECAM-1* and *CCL3* were upregulated (**Table 4-6**), suggesting that the horse may be biased towards a strong neutrophilic response; consequently, it would be interesting to make comparisons with equivalent genes in ruminants.

Table 4-6 TPM values of genes involved in the neutrophilic response

Gene	TPM 0 hours	TPM 7 hours
CXCL6	9.063	978.278
CXCL2	51.594	164.963
ICAM-1	67.395	399.324
ICAM-2	35.219	21.477
VCAM-1	17.361	193.913
PECAM-1	0.295	0.528
CCL3	1394.299	7608.37
LFA-1	7.166	7.314

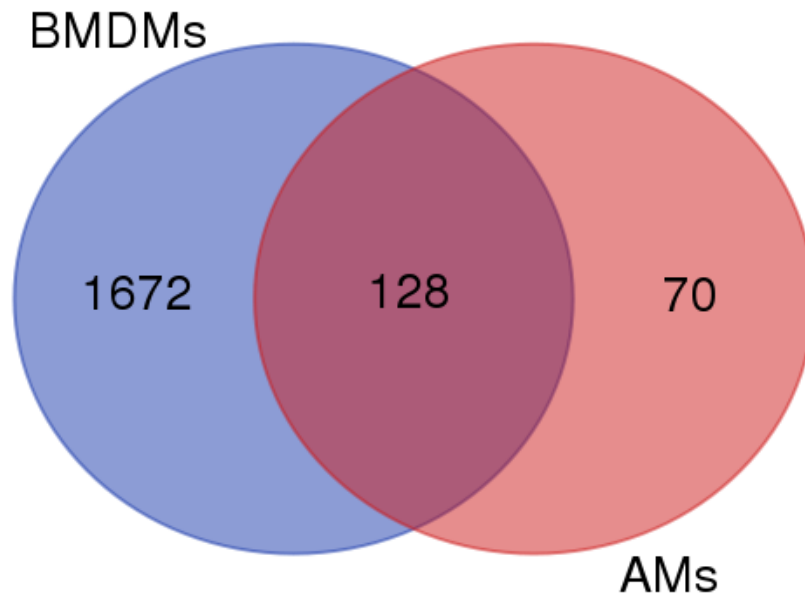


Figure 4-18 Venn diagram of genes differentially expressed in eqBMDMs and equine alveolar macrophages stimulated with LPS

Differentially expressed (DE) genes from eqBMDMs stimulated with LPS for 7 hours and alveolar macrophages (AMs) stimulated with LPS for 6 hours were compared. AMs DE was analysed using microarray and eqBMDMs DE was acquired from RNA-Seq analysis. Diagram showing genes in eqBMDMs and AMs that are significantly ($p < 0.05$) upregulated following LPS stimulation. Genes included are with a fold change > 2 . In total 128 genes were commonly DE between the two datasets.

Common differentially expressed genes: *ADAR AIM2 AKAP7 ALCAM AMPD3 APAF1 ARHGEF3 BATF3 BIRC2 CASP7 CCDC50 CCL22 CCNG2 CD38 CD40 CDS1 CERK CLIC5 CSF3 CXCL6 DDX60L DENND5A DHX58 DTX3L EDN1 EHD4 ENPP4 ETV7 EXT1 FAM129A FAM186B FAM3C FBXO39 FCHSD2 FMNL3 FOXS1 GBP5 GLCCI1 GNB4 GNGT2 GSDMD HELB HERC5 HIVEP2HSPA4L ICAM1 IDO1 IFIH1 IFNB1 IFT74 IL10 IL1A IL1B IL27 IL2RA IL6 ISG15 ISG20 ITGB8 ITPR1 ITSN1 JAK2 KLF12 LIMCH1 MARCKSL1 MASTL MBNL2 MCF2L MIP-2BETA MLKL MOV10 MX2 MYO1G NEK7 NUB1 OAS1 OAS2 OAS3 OASL OBFC1 OTUD4 P2RY10 PARP15 PHF7 PIM1 PLEKHA4 PML PNPT1 PPM1K PRR5L PRRG4 PTGER2 PTGES P XK RAPGEF2 RASGEF1B RFX2 RILPL2 RIN2 SAMD9 SDC4 SERPINB2 SLAMF7 SLC16A9 SLC9A7 SLFN5 SMARCE1 SOCS3 SPRY1 STARD13 STAT4 STRIP2 STX11 TLR3 TMEM47 TNF- α TNFSF13B TNIP3 TRAF3IP2 TREX1 TRIM26 TRPM2 TSG-6 TSPAN33 TTC21A UBE2L6 USP15 ZC3H12A*

LPS-induced feedback

An important feature of the macrophage response to LPS is the mechanisms by which induced transcripts and proteins are 'switched off', such as IL-10 for example. IL-10 is an anti-inflammatory cytokine and the production of IL-10 acts as an inhibitory signalling cascade in macrophages stimulated with LPS (Bogdan et al., 1992). Additionally, IL-10 also forms a group of regulatory cytokines in the gut contributing to intestinal homeostasis and immune function (Manzanillo et al., 2015) EqBMDMs upregulate *IL-10* in response to LPS (**Figure 4-15**). Previous work by our group found that equine alveolar macrophages did not, but monocytes did, produce the protein (as measured by ELISA) in response to LPS. Despite the lack of detectable IL-10 protein secretion, equine alveolar macrophages did upregulate the gene in response to LPS (Karagianni, 2015). It would be beneficial in eqBMDMs to perform an ELISA on eqBMDMs culture supernatant also, to demonstrate protein secretion as well as the increased mRNA expression as reflected in the RNA-Seq data.

IL-10, is just one example of several feedback loops that occur in response to LPS. In human monocytes, repressors of transcription included *PRDM1*, which is an early repressor of cytokine production; *NR4A1* a repressor of NF- κ B and *DUSP1* and *DUSP2* which regulate MAP kinase signalling (Baillie et al., 2017). In eqBMDMs, only *NR4A1* did not have an increase in TPM at 7 hours (**Table 4-7**). This may be due to 7 hours being too late to detect upregulation or may reflect a species difference between mouse and human. In humans, the cluster which *NR4A1* was in, showed most upregulation at 30 minutes to 2 hours post LPS stimulation, with a decrease from baseline from 2 to 20 hours post LPS (Baillie et al., 2017); therefore, it is possible that a similar process occurs in the horse. *NR4A1* is an inhibitor of NF κ B, a protein controlling cytokine production in myeloid cells (McEvoy et al., 2017). Other early inhibitors in humans of NF- κ B include *NFKBIA*, *NFKBIB*, *NFKBIE*, *NFKBIZ* and *BCL3* (Baillie et al., 2017). Apart from *BCL3*, all the other inhibitors of NF κ B were upregulated at 7 hours (**Table 4-7**) demonstrating that eqBMDMs do have an inducible inhibitory feedback pathway acting on NF κ B, activated in response to LPS. In human monocytes, later inhibitors of NF- κ B include *PARP7*, *PARP10* and *PARP12* (Baillie et al., 2017). In eqBMDMs at 7 hours *PARP7* was unchanged, *PARP10* is not annotated and *PARP12* was upregulated in response to LPS (**Table 4-7**).

Table 4-7 TPM values for genes involved in LPS inducible feedback in LPS stimulated eqBMDMs

Gene	TPM 0 hours	TPM 7 hours
<i>PRDM1</i>	32.908	62.634
<i>NR4A1</i>	1.144	1.031
<i>DUSP1</i>	60.55	64.003
<i>DUSP2</i>	0.776	4.409
<i>NFKBIE</i>	51.296	123.129
<i>NFKBIB</i>	19.945	28.167
<i>NFKBIA</i>	150.359	511.619
<i>BCL3</i>	2.464	3.736

Baillie *et al.* (2017) published a table of mouse knockouts (n=188) that influence the LPS response. The resulting mutant phenotype exhibited either a reduced or increased responsiveness to LPS. Using this gene list, genes were segregated into those that suppress the LPS response (n=76) (i.e. where mutant mice showed increased sensitivity to LPS) and those that increased responsiveness to LPS (n=111) (i.e. where mutant mice had a reduced sensitivity to LPS). Using these lists, the DE expressed genes upregulated and downregulated in eqBMDMs in response to LPS were analysed. Amongst genes that suppress the LPS response only 5 (*BIRC3*, *IER3*, *IL27*, *ADORA7A* and *EBI3*) are present in the top 100 genes DE in eqBMDMs. Twenty-two were present out of all the genes (n=808) significantly upregulated in eqBMDMs. Two genes were downregulated (**Table 4-8**). This lack of specific LPS-induced regulators could contribute to the LPS hypersensitivity of the horse (Jackson and Kropp, 1999). Conversely, 13 genes that increase sensitivity to the LPS response were in the most DE genes, with 3 (*STAT4*, *FPR1* and *PDE4B*) being in the top 100 genes (**Table 4-9**)

Table 4-8 Genes associated with an increase in LPS sensitivity in mice present in eqBMDMs significantly DE gene list

Knockout genes present in top 100 DE genes in eqBMDMs stimulated with LPS	Knockout genes present in gene list of all significantly upregulated DE genes in eqBMDMs stimulated with LPS	Knockout genes present in gene list of all significantly DE downregulated genes in eqBMDMs stimulated with LPS
<i>BIRC3</i>	<i>TGM2</i>	<i>APPL2</i>
<i>IER3</i>	<i>TIMP3</i>	<i>CCR2</i>
<i>IL27</i>	<i>NUPR1</i>	
<i>ADORA7A</i>	<i>BIRC3</i>	
<i>EBI3</i>	<i>ZC3H12A</i>	
	<i>ABCA1</i>	
	<i>STEAP4</i>	
	<i>PARP14</i>	
	<i>IER3</i>	
	<i>LYN</i>	
	<i>STAT2</i>	
	<i>SOCS3</i>	
	<i>SOCS1</i>	
	<i>IL27</i>	
	<i>EBI3</i>	
	<i>PDCD1LG2</i>	
	<i>ADORA2A</i>	
	<i>SRC</i>	
	<i>STAT3</i>	
	<i>IL10RA</i>	
	<i>CD83</i>	
	<i>TRPM2</i>	

Table 4-9 Genes associated with a decreased sensitivity to LPS in mice present in eqBMDMs significantly DE gene lists

Knockout genes present in top 100 DE genes in eqBMDMs stimulated with LPS	Knockout genes present in gene list of all significantly upregulated DE genes in eqBMDMs stimulated with LPS	Knockout genes present in gene list of all significantly DE downregulated genes in eqBMDMs stimulated with LPS
<i>STAT4</i>	<i>GPR84</i>	
<i>FPR1</i>	<i>P2RX7</i>	
<i>PDE4B</i>	<i>NFKBIZ</i>	
	<i>IL23A</i>	
	<i>FPR1</i>	
	<i>PDE4B</i>	
	<i>STAT4</i>	
	<i>PELI1</i>	
	<i>NOD2</i>	
	<i>TREM1</i>	
	<i>CASP1</i>	
	<i>ABCA1</i>	
	<i>CFLAR</i>	

RNA-Seq analysis of arginine and tryptophan pathways in eqBMDMs stimulated with LPS

The RNA-Seq dataset enabled analysis of the expression of transcripts associated with the arginine and tryptophan pathways. Expression levels (averaged TPM) of transcripts involved in both pathways are in **Table 4-10**. LPS stimulation of eqBMDMs did not induce any significant expression of transcripts associated with arginine metabolism (**Figure 4-19**). *ARG2*, *OAT*, *ODC1*, *SLC3A2* were all highly expressed (TPM >100) at 0 hours but were downregulated by LPS. Conversely, genes associated with tryptophan metabolism were upregulated with a Log2fc >1; *IDO1*, *KYNU* and *KMO* (**Figure 4-20**). *IDO1* catabolises tryptophan into kynurenine, which is then further catabolised into either anthranilic acid by kynureninase (*KYNU*) or 3-Hydroxykynurenine by kynurenine 3-monooxygenase (*KMO*). These data support the hypothesis that in response to LPS eqBMDMs catabolise tryptophan and not arginine, as do equine alveolar macrophages (Karagianni, 2015), pig BMDMs and human MDMs (Kapetanovic et al., 2012).

Table 4-10 TPM values for genes in eqBMDMs associated with arginine (Young et al., 2018) and tryptophan metabolism

Pathway	Gene	0 hours	7 hours
Arginine metabolism	<i>ARG1</i>	0.098	0.048
	<i>ARG2</i>	119.226	59.716
	<i>ASL</i>	24.06	14.478
	<i>ASS1</i>	25.849	20.336
	<i>GCH1</i>	24.765	31.888
	<i>NOS2</i>	0.002	0.012
	<i>OAT</i>	103.564	68.811
	<i>ODC1</i>	98.475	39.732
	<i>PTS</i>	27.977	16.301
	<i>SLC3A2</i>	168.353	120.178
	<i>SLC7A1</i>	13.267	9.721
	<i>SLC7A2</i>	0.01	0.053
	<i>SLC7A5</i>	8.969	7.278
	<i>SLC7A7</i>	57.119	46.604
	<i>SPR</i>	10.199	3.549
	Tryptophan metabolism	<i>IDO1</i>	0.920
<i>IDO2</i>		0.033	0.972
<i>TDO2</i>		1.255	2.005
<i>KYAT1</i>		25.353	15.300
<i>KYAT3</i>		45.824	35.836
<i>KYNU</i>		25.337	58.783
<i>KMO</i>		37.123	95.635
<i>QPRT</i>		0.004	0.015
<i>AADAT</i>		0.101	0.047
<i>SLC3A2</i>		168.353	120.178
<i>SLC7A8</i>		69.858	31.141
<i>SLC7A5</i>	8.960	7.278	

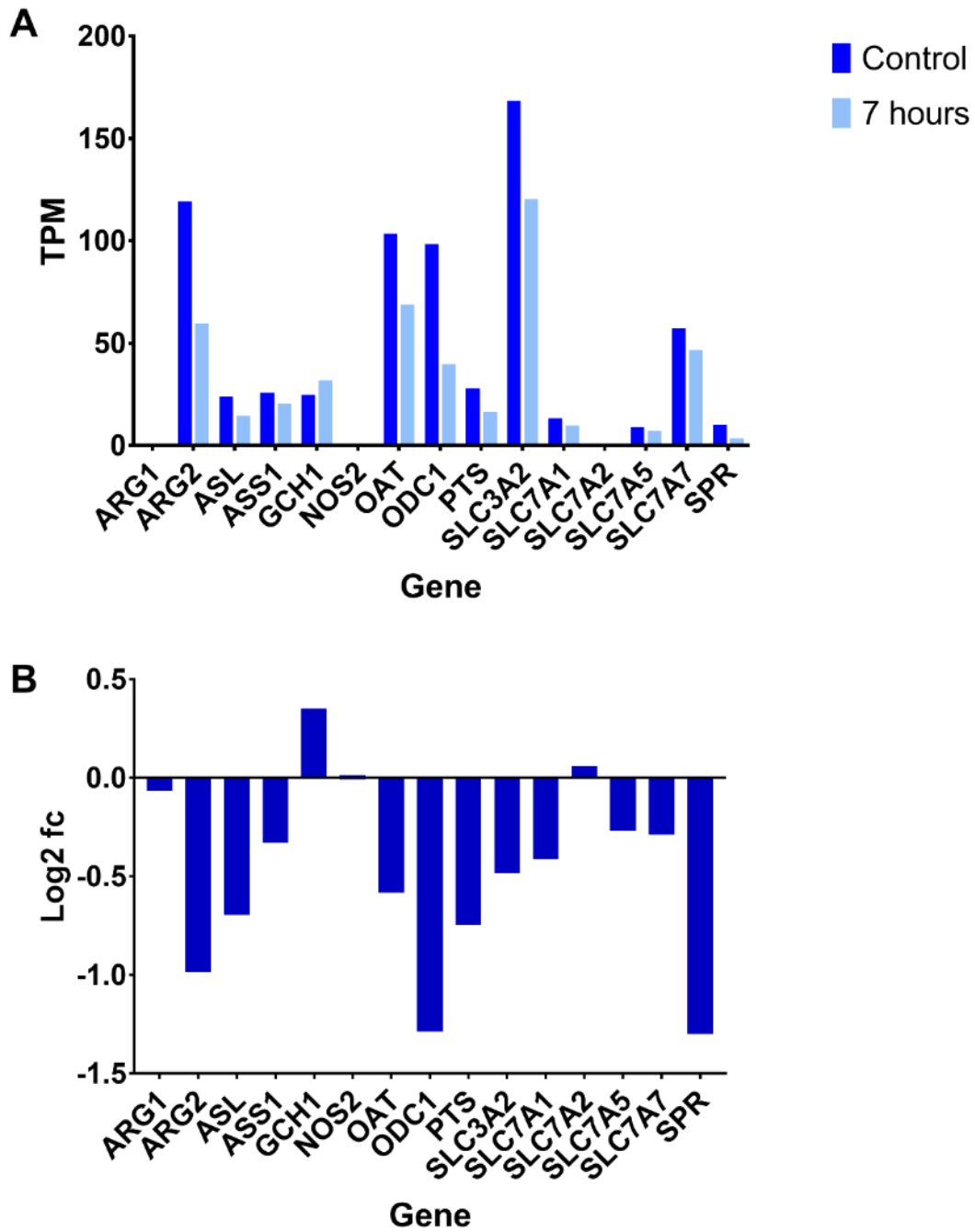


Figure 4-19 TPM (A) and Log2 fc (B) values of transcripts involved in the arginine metabolism pathway in eqBMDMs, with and without exposure to LPS
 Using TPM values generated with Kallisto genes in the arginine/NO pathway were graphed for either TPM values (A) or for Log2 fc. Results shown are the mean for all 3 horses.

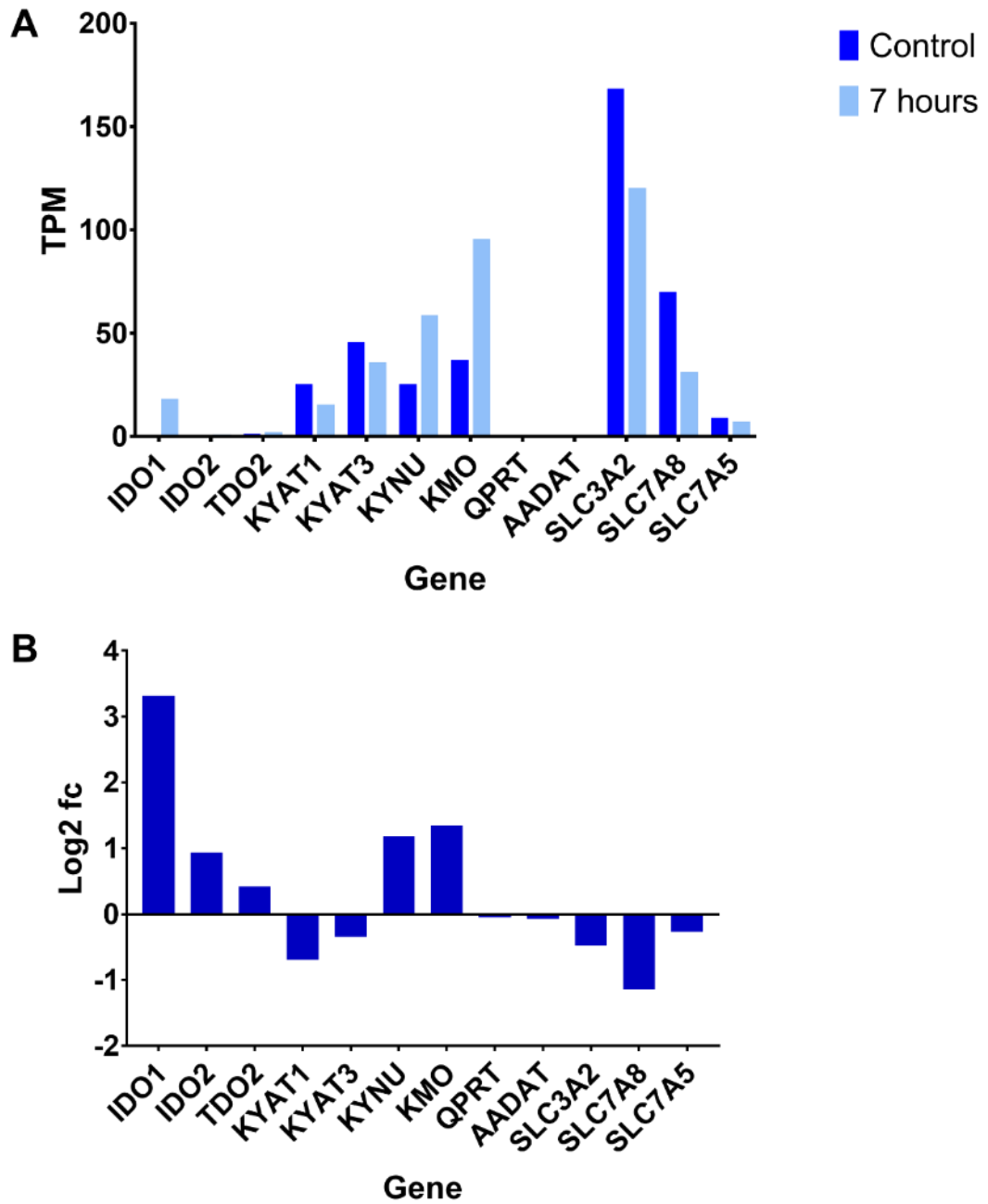


Figure 4-20 TPM (A) and Log₂ fc (B) values of transcripts involved in the tryptophan metabolism pathway in eqBMDMs, with and without exposure to LPS

Using TPM values generated with Kallisto genes in the tryptophan pathway were graphed for either TPM values (A) or for Log₂ fc (B). Results shown are the mean for all 3 horses.

4.3 Discussion

Previous studies on eqBMDMs (eCAS cell line) have harvested cells from sternal biopsies performed on live sedated animals (Werners et al., 2004). Using this method 17×10^6 cells per horse were obtained. In the current study, horses were euthanased prior to collection, and 5×10^8 to 1×10^9 cells were obtained from 2 ribs per adult horse thus resulting in a cell yield considerably greater than the sternal biopsy method. Following cryopreservation in medium containing 10% DMSO in horse serum at -155°C , the percentage of viable cells on recovery, as evaluated by Trypan Blue staining, was between 60-80%. By performing MTT assays the most suitable growing conditions for eqBMDMs were identified; in media supplemented with HS and rhCSF-1 at a density of 2.5×10^6 cells/ml. Differentiated cells had characteristics of typical macrophages including CD14 expression (**Figure 4-10**), characteristically consistent morphology (**Figure 4-6**), phagocytic activity (**Figure 4-8**) and *TNF- α* production in response to LPS (**Figure 4-11**).

With the exception of the anatomical site of BM collection, this study differed from that of Werners *et al.* in relation to the culture conditions under which the cells were differentiated; Werners *et al.* cultured their cells in the presence of GM-CSF, whilst cells were cultured in the present study in the presence of M-CSF (CSF-1). Haemopoietic stem cell (HSC) lineages differ between GM-CSF and CSF-1 induced populations. Culturing of HSCs in GM-CSF promotes proliferation and differentiation into macrophages, dendritic cells (DC) and granulocytes, whereas CSF-1 promotes proliferation and differentiation of monocytes and macrophages (Hamilton, 2008, Hamilton and Achuthan, 2013, Hamilton and Anderson, 2004). In addition, GM-CSF is a pro-inflammatory cytokine whereas CSF-1 is anti-inflammatory (Hamilton, 2008). In humans, morphology of GM-CSF and CSF-1 cultured MDMs was very different with CSF-1- induced macrophages being more spindle like and GM-CSF-induced macrophages more circular (Hashimoto et al., 1999). In contrast, eqBMDMs macrophages cultured in GM-CSF were a combination of rounded and spindle like cells (Werners et al., 2004). In this study, cells cultured in CSF-1 had a stellate morphology (**Figure 4-6**). The most significant difference between eCAS cells and the cells in the present study was the production of NO in response to LPS. The e-CAS equine cells apparently produced NO in response to LPS. As in previous reports on equine alveolar, peritoneal and MDMs, eqBMDMs also did not produce NO in response to LPS (Karagianni, 2015, Karagianni et al., 2013, Karagianni et al., 2017). Rodent macrophages produce NO, but it is not produced by human or pigs (Kapetanovic et al., 2012). This functional difference in NO production between the e-CAS cells and

the eqBMDMs may be attributed to the difference in culture conditions (GM-CSF vs CSF-1) for two reasons; 1) GM-CSF-induced HSC differentiation can also generate DCs and neutrophils in addition to macrophages. Both DCs and neutrophils can produce NO in humans (Wilsmann-Theis et al., 2013, Dinakar et al., 1999) 2) GM-CSF is acting as a proinflammatory cytokine (Hamilton, 2008) resulting in NO production. Alternatively, as noted above, the amounts of NO produced by e-CAS cells were not quantified relative to mice, and Karagianni *et al.* argued that they were likely extremely low by comparison. Recently Evans *et al.* (2018) published sequence data from the eCAS cell line showing that the cells were mouse and not horse (Evans et al., 2018). This result provides an alternative explanation for the difference in NO production between the eCAS cell line and eqBMDMs. The data generated for the horse in this study have been used in a comparative analysis of species-specific regulation of arginine metabolism, alongside sheep, goat, cattle, buffalo, pig, human and rat (Young et al., 2018). The analysis indicated that the pathway is under extensive evolutionary selection associated with sequence variation in promoter regulation. The findings argue that the lack of activity in eqBMDMs, and other macrophage populations, is not simply associated with different culture conditions or cell populations and is actually an evolutionary variation. In POI, NO production by phagocytes in the *muscularis* inhibits gastrointestinal motility following intestinal manipulation in rodents (Kalff et al., 2000, Turler et al., 2006). However, given the inability of eqBMDMs to produce NO in response to LPS (**Figure 4-12**) and with the absence of upregulation of genes involved in arginine metabolism (**Table 4-10**), these data suggest that NO production from macrophages does not contribute to the pathophysiology of equine POI.

The main aim of this chapter was to evaluate the response of eqBMDMs differentiated in CSF-1 to LPS. LPS is an agonist of TLR4, which is expressed by *muscularis* macrophages (MM) but not lamina propria macrophages (LpM) in the intestine (Schenk and Mueller, 2007, Eskandari et al., 1997). This in turn activates MM, resulting in a series of events which ultimately leads to smooth muscle dysfunction. Previous transcriptional studies of the LPS response in horses include microarray analysis of alveolar macrophages cultured in CSF-1 (Karagianni et al., 2017), RNA-Seq analysis of PBMCs (Pacholewska et al., 2017) and next -generation sequencing of PBMCs (Parkinson et al., 2017). Therefore, this study provided the first dataset to analyse the transcriptional profile of eqBMDMs cultured in CSF-1 and stimulated with LPS for 7 hours. This revealed a core group of upregulated genes in response to LPS which form the typical innate immune response to LPS (**Figure 4-15**). Several of these genes (*IL1 β* , *IL-6*, *TNF- α* , *IDO1*) were also upregulated in AMs differentiated in CSF-1 (**Figure 4-18**).

This core set of genes were used in **Chapter 5** to identify if macrophage activation occurs in the mucosa and *muscularis* of the jejunum in horses undergoing abdominal surgery.

CD163 is the macrophage marker used in **Chapter 3** to identify intestinal macrophages in the horse. However, when eqBMDMs were analysed by flow cytometry they expressed very low levels of CD163 (**Figure 4-10**). CD163 is expressed on mature resident tissue macrophages (Van den Heuvel et al., 1999, Fabriek et al., 2005). CD163 is induced by LPS (Gordon, 2003) but in eqBMDMs this also was not observed (TPM in eqBMDMs decreased from 166 at 0 hours to 91 at 7 hours). Expression of receptors on macrophages is dependent on signals from regional tissues such as cytokines, chemokines and growth factors (Gordon et al., 1995) so perhaps in eqBMDMs *in vitro* culture conditions do not replicate the niche of cytokines, chemokines and growth factors that tissues provide for the expression of CD163 in eqBMDMs.

In this chapter a protocol was optimised to produce populations of eqBMDMs by cultivation of bone marrow from the ribs of adult horses in rhCSF1. Morphological features, the ability to phagocytose particles and the ability to produce cytokines in response to LPS confirmed the cells were macrophages. The method described allows generation of a homogenous population of eqBMDMs to further study their role in the equine innate immune system. Transcriptomic analysis of these cells stimulated with LPS identified core genes involved innate immunity of the horse. Additionally, these data show species-specific variation in innate immune biology in the horse. The absence of NO production in response to LPS and the significant upregulation of CXCL6 which signals the recruitment of neutrophils, suggesting the horse may be biased towards a strong neutrophilic response. In the next chapter, intestine from horses undergoing abdominal surgery will be analysed for evidence of macrophage activation.

**Chapter 5. Inflammatory response in the
mucosa and *muscularis* of horses undergoing
gastrointestinal surgery**

5.1 Introduction

Colic, which refers to the syndrome of abdominal pain, is a common health and welfare concern in the horse (Mellor et al., 2001). Whilst the majority of cases will resolve with medical treatment alone, a small percentage (1-10%) will require surgery to correct the underlying cause (Hillyer et al., 2001). Any horse undergoing abdominal surgery is at risk of developing post-operative ileus (POI). The development of POI in horses reduces the likelihood of survival following abdominal surgery (Morton and Blikslager, 2002, Mair and Smith, 2005c). POI can be defined as the functional inhibition of propulsive bowel motility following abdominal surgery (Livingston and Passaro, 1990). As discussed in **Chapter 1**, several causes and mechanisms of POI have been described; these include anaesthetic agents, opioids, levels of intravenous fluid administration, electrolyte imbalances, disruption to gastrointestinal (GI) hormones and neuropeptides, disruption of neural continuity, autonomic dysfunction and inflammatory cell activation (Vather et al., 2014). The proposed neurogenic and inflammatory mechanisms have received most attention in the literature; however, these proposed mechanisms are not mutually exclusive. Different triggers may act independently or collectively to produce a common endpoint, namely, impaired contractility of the intestinal smooth muscle. This impairment results in distention of the intestines and stomach with GI contents, causing abdominal discomfort, post-operative reflux, reduced appetite and reduced faecal output (**Figure 5-1**).

Manipulation of the intestines is generally unavoidable during colic surgery. In rodent models of POI, inflammation of the *muscularis externa* (ME) in response to manipulation is strongly implicated as a significant causative factor in the pathogenesis of POI (Kalff et al., 1998a, Behrendt et al., 2004, Kalff et al., 2000, Kalff et al., 2003, Farro et al., 2017, Kalff et al., 1999a, Kalff et al., 1999b). Activation of *muscularis* macrophages (MM) occurs within hours of surgery (Farro et al., 2017, Kalff et al., 1999b, Kalff et al., 1999a, Kalff et al., 1998a). Macrophage activation following surgical trauma has also been demonstrated in human patients (Kalff et al., 2003). Briefly, the activation of MM by Damage Associated Molecular Patterns (DAMPs) (e.g. ATP (Ozaki et al., 2004)) and/or Pathogen Associated Molecular Patterns (PAMPs) (e.g. LPS (Eskandari et al., 1997)) results in cytokine and chemokine release, followed by infiltration of leukocytes into the *muscularis*. These infiltrating leukocytes inhibit smooth muscle function via the secretion of leukocytic products, such as nitric oxide (NO) and prostaglandins (PG).

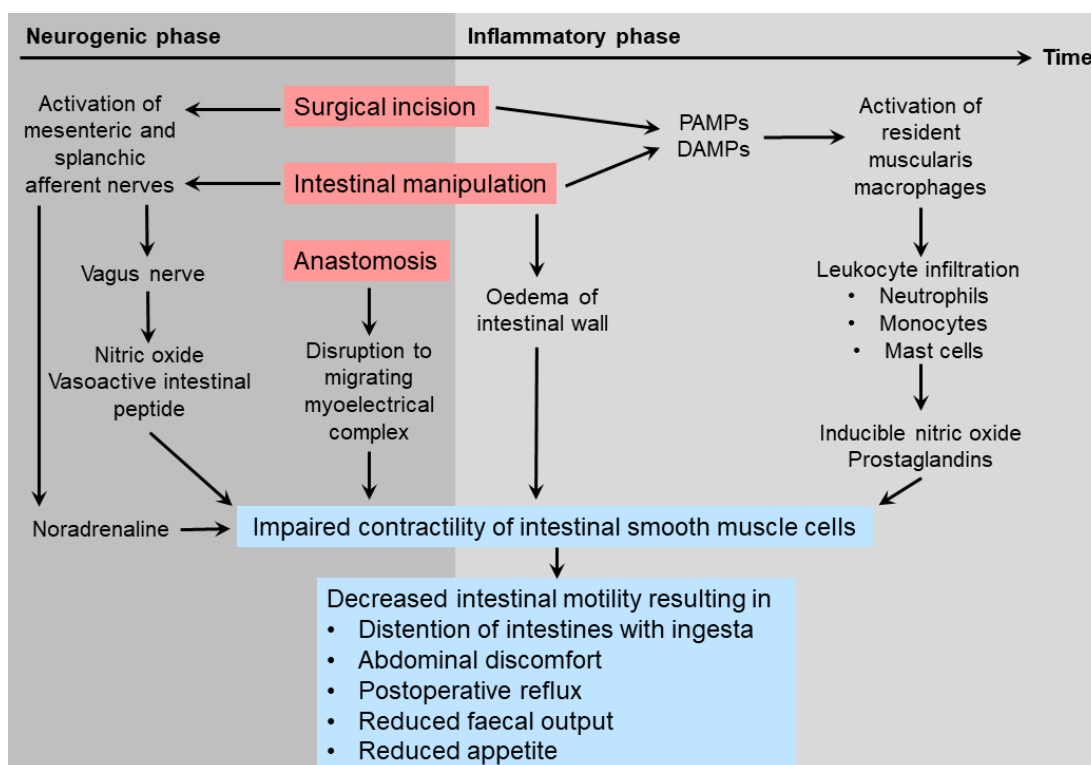


Figure 5-1 Proposed role of intra-operative factors in the neurogenic and inflammatory phases of POI

Reproduced from: An update on equine post-operative ileus: Definitions, pathophysiology and management, Z. M. Lisowski, R. S. Pirie, A. T. Blikslager, D. Lefebvre, D. A. Hume & N. P. H. Hudson, *Equine Veterinary Journal* 50 (3), © 2017 EVJ Ltd

Whilst rodent models offer a convenient way to study the pathogenesis of POI, rodents are evidently not ‘small horses’. One clear species-related difference is the potential role of manipulation-induced nitric oxide (NO) release from infiltrating leukocytes, particularly macrophages. Like macrophages from other large animal species such as pigs and humans (Kapetanovic et al., 2012, Young et al., 2018), horse alveolar and peritoneal macrophages did not produce NO in response to LPS (Karagianni et al., 2013) This difference was further corroborated in **Chapter 4** whereby LPS stimulation also failed to induce neither NO release nor NOS2 mRNA expression in equine bone marrow-derived macrophages (eqBMDMs). In collaboration with other laboratory group members at the University of Edinburgh, the species comparison was further extended to ruminants (Young et al., 2018); LPS stimulation induced NO release in cattle and water buffalo, but not in sheep BMDMs. Such differences have clear implications with regard to translational application of data from one species to another.

Earlier studies on the margins of bowel loops surgically resected from horses have identified a generalised stress response in the smooth muscle, characterised by an increase in apoptotic neurons and smooth muscle and glial cells (Rowe et al., 2003).

Intestinal surgery in the horse has also been shown to induce post-operative neutrophilic and eosinophilic infiltration of the jejunum (Hopster-Iversen et al., 2014, Little et al., 2005, Hopster-Iversen et al., 2011). To date, there have been no studies investigating macrophage activation in horses undergoing abdominal surgery. The work described in this current chapter addresses this issue. Intestinal tissue was harvested from horses undergoing colic surgery. Samples were collected from macroscopically 'healthy' proximal and distal margins of resected intestine. Control tissues were obtained immediately *post mortem* from horses with no recent history of gastrointestinal disease or abdominal surgery. The aim of this chapter was to investigate the intestinal inflammatory response in horses undergoing abdominal surgery by measuring differential gene expression in intestinal tissues harvested from the surgery group and the control group. Selected genes of interest included those identified in **Chapter 4** as being associated with macrophage activation (*IDO1*, the cytokines *IL-6*, *IL-1 β* , *TNF- α* and the chemokine *CCL2/MCP-1*) and those encoding mediators involved in smooth muscle dysfunction (*NOS2* and *COX-2/PTGS2*).

5.2 Results

5.2.1 Animals

Samples of jejunum were collected from 6 control horses. The control animals were selected randomly and consisted of 3 geldings with a median age of 15 years (mean 15.6 years, range 15-17 years) and 3 mares with a median age of 21 years (mean 19.6 years, range 15-23 years).

Samples of jejunum were also collected from the proximal and distal margins of a length of small intestine resected from 12 horses undergoing abdominal surgery for evaluation and treatment of colic. Tissues were collected as described in **Section 2.1**. The cases included 6 males (5 geldings and 1 stallion) and 6 mares with a median age of 20 years (mean 17.8 years, range 9-27 years). Although all cases had ischaemic small intestine that required resection, as the resection was followed by an anastomosis procedure, the margins of the resected intestine was assessed by the surgeon to be healthy and viable. Case details are summarised in **Table 2-2**.

5.2.2 RNA extraction

RNA extraction was performed on separated mucosa and *muscularis* for all colic and control cases. It was not possible to extract RNA of adequate quality (RNA Integrity Number (RIN) >7) from all the surgically acquired and control samples. As a result, a

total of 9 *muscularis* samples (5 proximal and 4 distal) and 24 mucosal samples (12 proximal and 12 distal) from colic cases and 4 *muscularis* and 6 mucosal samples from control horses were used for Real - Time quantitative polymerase chain reaction (RT qPCR) analysis.

5.2.3 Real – Time quantitative polymerase chain reaction of resection margins

No difference in gene expression was observed between proximal and distal samples

When investigating cases of small and large intestinal strangulation, Rowe *et al.* demonstrated an increase in apoptotic neurons, smooth muscle cells and glial cells at locations far from the site of strangulation (Rowe et al., 2003). If such markers of surgical stress are detectable at sites far from the surgical lesion, then inflammatory cell activation may also be evident at such distant locations. The relative expression of target gene mRNA relative to the housekeeping gene, Glyceraldehyde 3-phosphate dehydrogenase (*GAPDH*), in proximal and distal resection margins of tissues from colic cases and control horses for both the mucosa (**Figure 5-2**) and *muscularis* (**Figure 5-3**) was measured. No significant differences were observed between proximal and distal resection margins for both the *muscularis* and mucosa. Consequently, the proximal and distal margins were combined for all further analyses to increase the numbers of *muscularis* samples (n=9). Such further analyses were not applied to proximal and distal margins obtained from the same horse. For the mucosa, distal samples were selected for all cases (n=12) (**Appendix 9.1**). *NOS2* was removed from the set of target genes as no mRNA was detectable in any of the jejunal sections (control and colic cases). This finding was consistent with the lack of *NOS2* expression in stimulated equine BMDMs (**Chapter 4**).

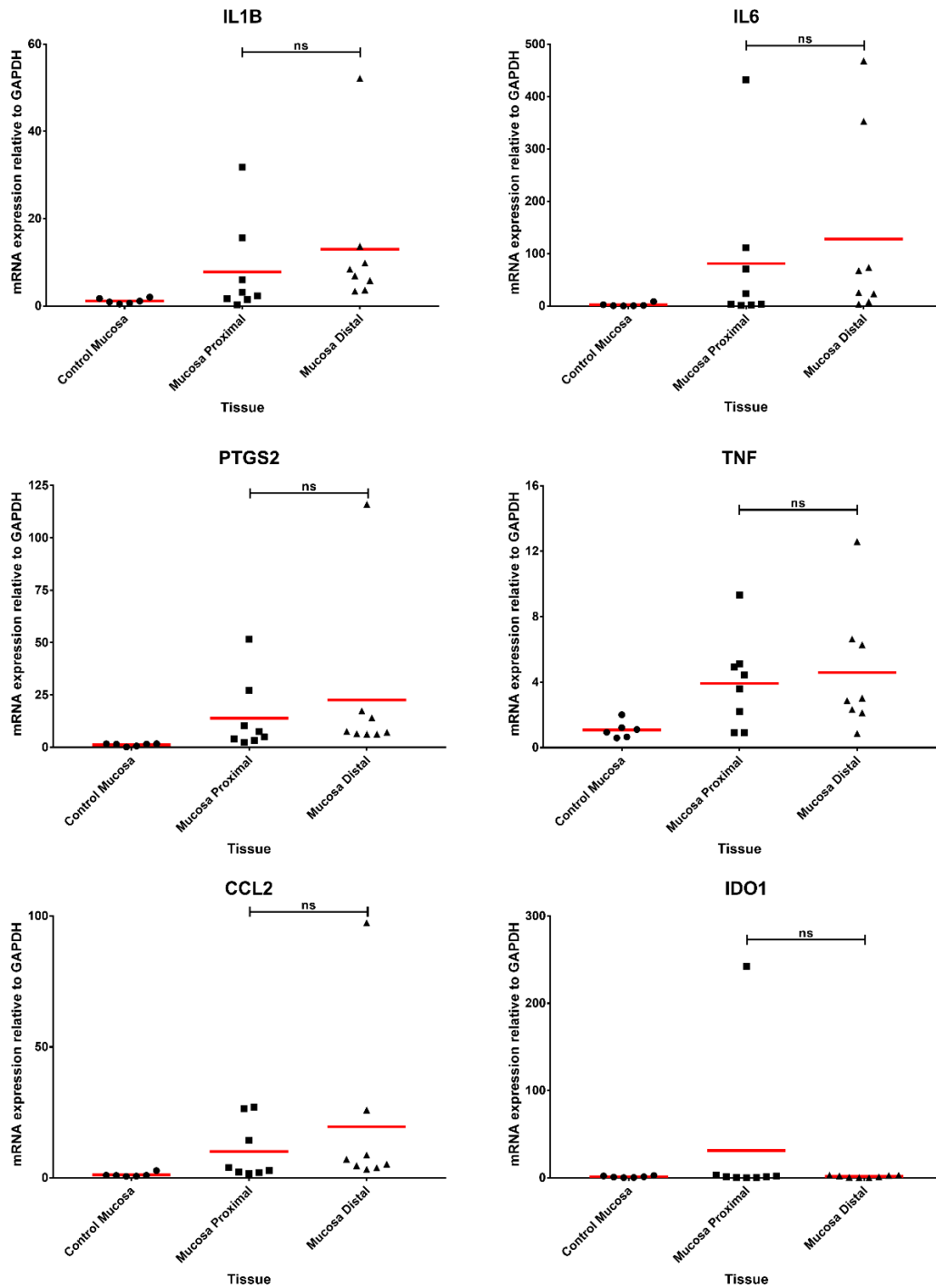


Figure 5-2 Relative gene expression of *IL-1B*, *IL6*, *PTGS2*, *TNF- α* , *CCL2* and *IDO1* in mucosa of horses undergoing intestinal surgery

Scatter plots showing mRNA expression of target genes relative to *GAPDH* in proximal and distal mucosa of resection margins from horses undergoing intestinal surgery (n=12). Control samples were obtained from horses being euthanased for reasons unrelated to the GIT (n=6). Results calculated using $2^{-\Delta\Delta C_t}$ method. Mean value represented by red line. **ns** = not significant ($p > 0.05$) using Mann-Whitney U test.

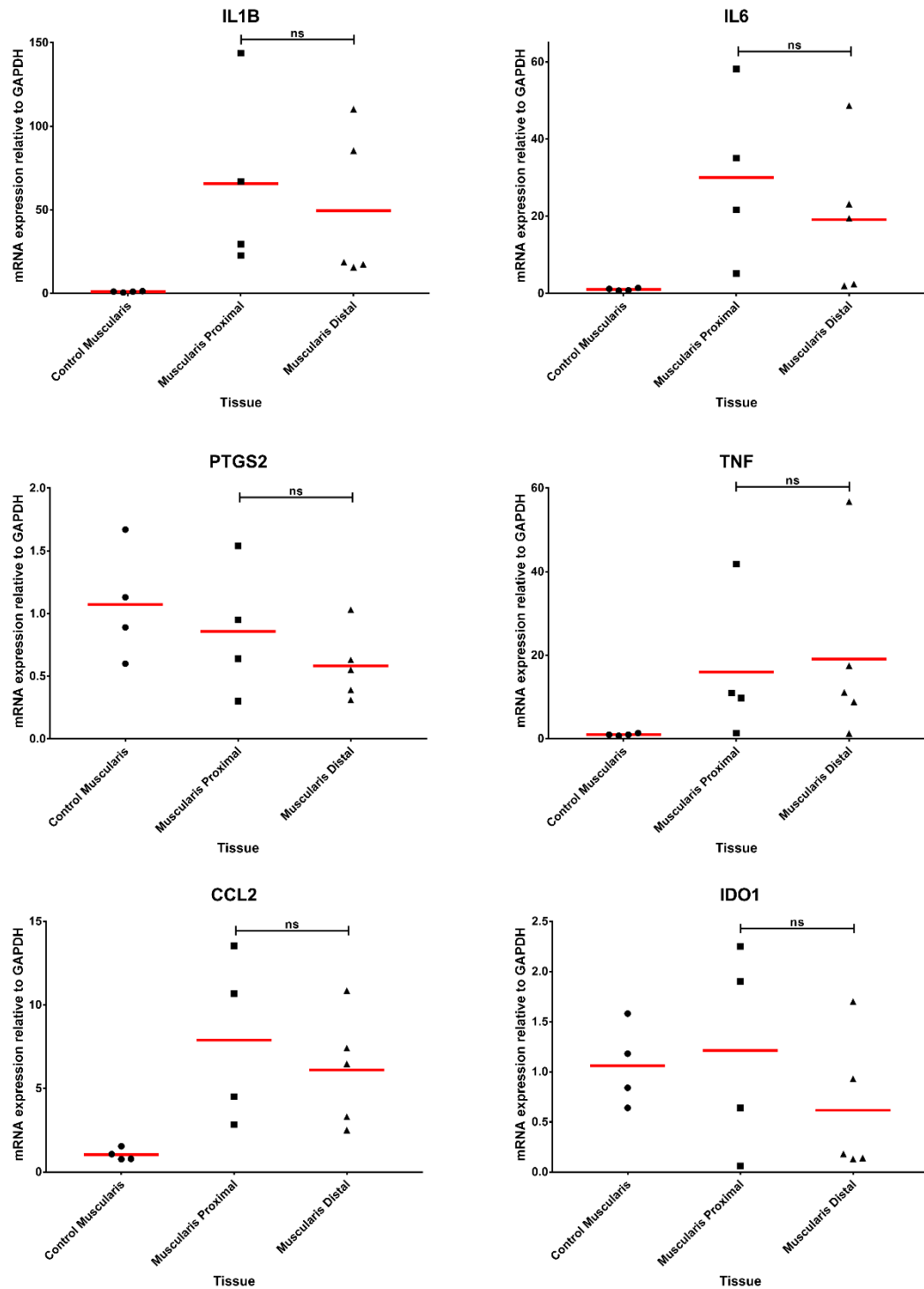


Figure 5-3 Relative gene expression of *IL-1B*, *IL6*, *PTGS2*, *TNF- α* , *CCL2* and *IDO1* in the muscularis of horses undergoing intestinal surgery

Scatter plots showing mRNA expression of target genes relative to *GAPDH* in proximal and distal muscularis of resection margins from horses undergoing intestinal surgery (n=12). Control samples were obtained from horses being euthanased for reasons unrelated to the GIT (n=4). Results calculated using $2^{-\Delta\Delta C_t}$ method. Mean value represented by red line. **ns** = not significant ($p > 0.05$) using Mann-Whitney U test.

Evidence of macrophage activation in the mucosa and muscularis of horses undergoing abdominal surgery

Next, relative expression of the target genes (*IL-6*, *IL-1 β* , *TNF- α* , *CCL2*, *PTGS2* and *IDO1*) was evaluated in the mucosa (n=12) and *muscularis* (n=9) of colic cases and compared to the mucosa and *muscularis* of control cases (mucosa n=6; *muscularis* n=4) (Figure 5-4). In the mucosa, the level of expression of *IL-1 β* , *IL-6*, *PTGS2*, *TNF- α* and *CCL2* was significantly ($p<0.05$) greater in colic cases compared with healthy horses. In the *muscularis*, the level of expression of *IL-1 β* , *IL-6*, *TNF- α* and *CCL2* was significantly ($p<0.05$) greater in colic cases compared with healthy horses. The relative expression of *IL-1 β* was significantly greater in the *muscularis* compared to the mucosa in colic cases. Likewise, the relative expression of *PTGS2* was significantly greater in the mucosa of colic cases, compared to the *muscularis* of colic cases, in which expression was negligible. With the exception of one horse, there was no increase in the relative expression of *IDO1* in colic cases, compared with control horses.

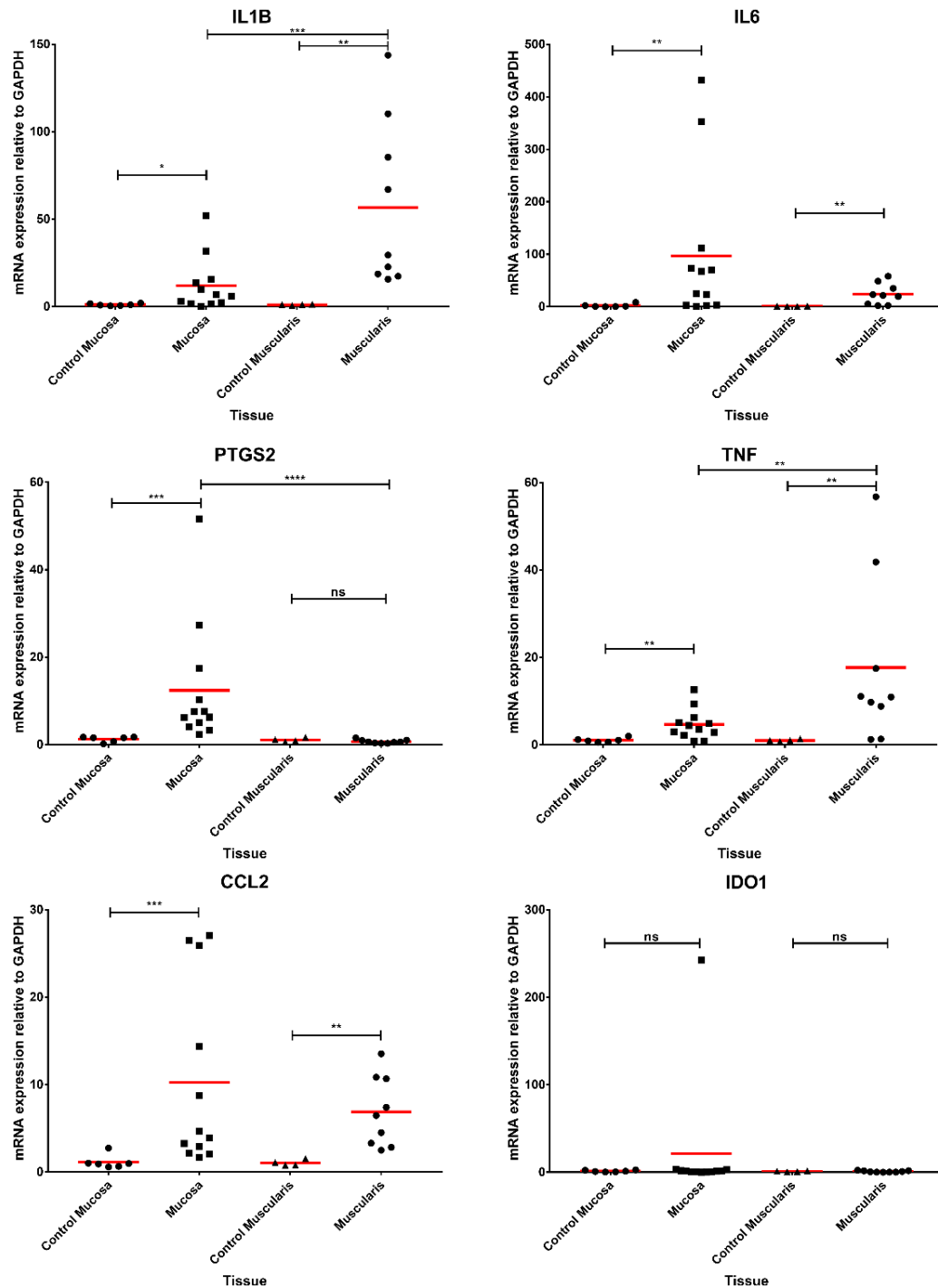


Figure 5-4 Relative gene expression of *IL-1B*, *IL6*, *PTGS2*, *TNF- α* , *CCL2* and *IDO1* in the mucosa and muscularis of horses undergoing intestinal surgery

Scatter plots showing mRNA expression of target genes relative to GAPDH. Proximal and distal mucosa (n=12) and muscularis (n=9) samples were combined. Control samples were obtained from jejunum of horses being euthanased for reasons unrelated to the GIT (mucosa n=6, muscularis n=4). Results calculated using $2^{-\Delta\Delta Ct}$ method. Mean value represented by red line. Significance of relative mRNA expression between control and surgical samples and between mucosa and muscularis surgical samples were performed with a Mann-Whitney U test. ns =not significant, *p<0.05, **p<0.01, ***p<0.001, ****p<0.0001

Analysis of relative expression in relation to pre-, intra- and post-operative factors

The colic cases from which samples were derived differed with respect to several pre-, intra- and post-operative factors. Although the small numbers of horses limits subset analysis, where the possible impact of different variables on the expression of various inflammatory genes is considered below.

Pre-operative factors

The expression of all genes in colic cases (relative to GAPDH) was considered relative to duration of colic prior to surgery, age of the animal and the presence of pre-operative reflux. Duration of colic prior to surgery was evaluated as this was considered to potentially impact on the magnitude of the intestinal inflammatory response. Both increasing age (Roussel et al., 2001) and the presence of pre-operative reflux (Mair and Smith, 2005c, Torfs et al., 2009) have been associated with an increased risk of POI in horses.

Age

Median age of colic horses in the mucosa group (n=12) was 20.5 years (range 10-27 years) and in the *muscularis* group (n=9) was 12 years (range 9-27years). In the *muscularis*, there was no significant relationship between age and relative gene expression, although there was a trend towards an age-related increase in the relative expression of *IL-1 β* , *IL-6*, *TNF- α* and *CCL2* (Figure 5-5). In the mucosa, there was a significant age-associated decrease in the relative expression of *PTGS2* and *CCL2* (Figure 5-6). In contrast to the *muscularis*, there was also a trend towards an age-related decrease in the relative expression of *IL-1 β* and *IL6* consistent with the *muscularis* derived data, there was a trend towards increased relative expression in *TNF- α* in the mucosa.

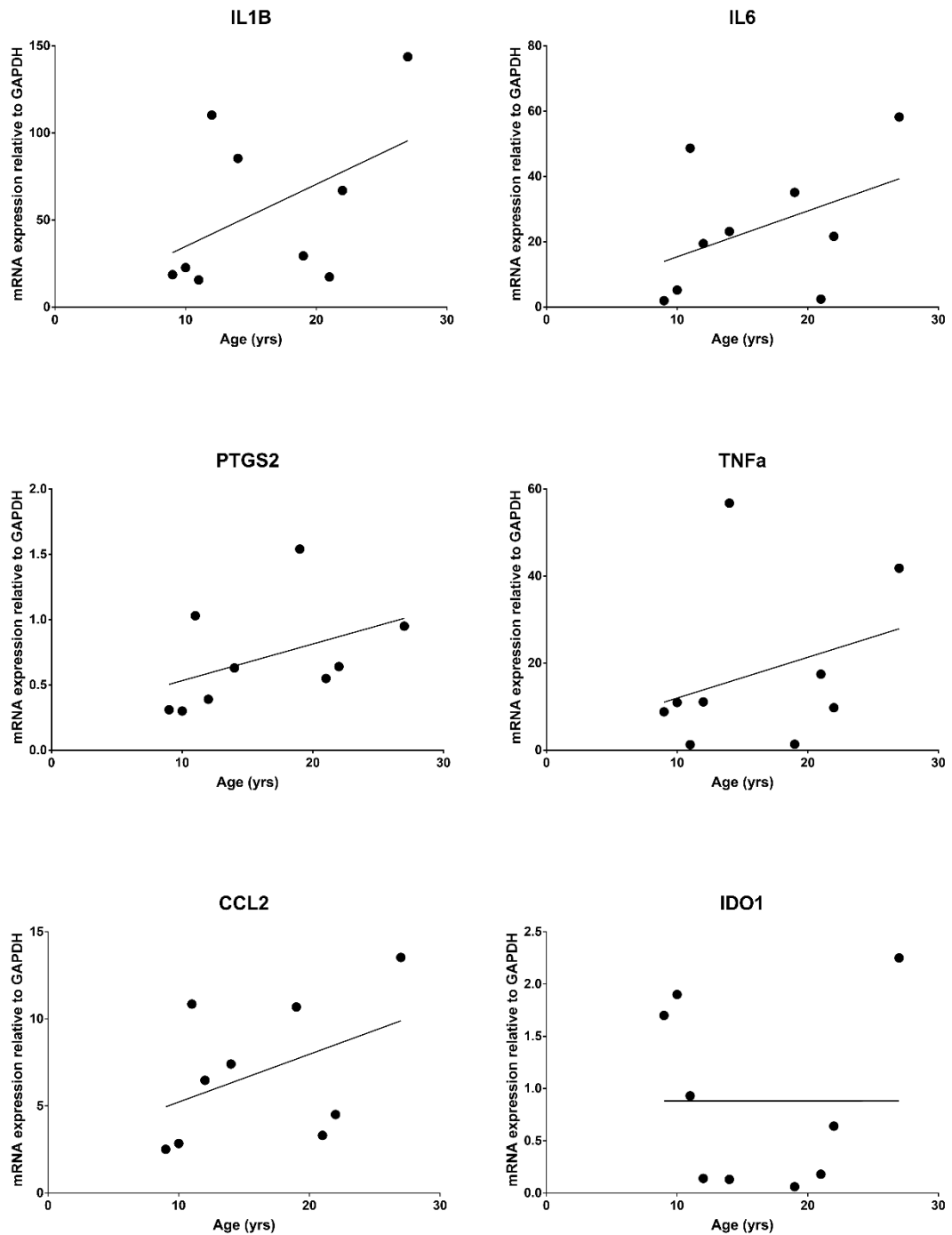


Figure 5-5 Effect of age on relative gene expression of *IL1B*, *IL6*, *PTGS2*, *TNF-α*, *CCL2* and *IDO1* in the *muscularis* of horses undergoing intestinal surgery

Scatter plots showing mRNA expression of target genes relative to *GAPDH* in *muscularis* from resection margins of horses undergoing intestinal surgery (n=9). Results calculated using $2^{-\Delta\Delta Ct}$ method. Significance of age on relative mRNA expression performed by linear regression (represented by black line).

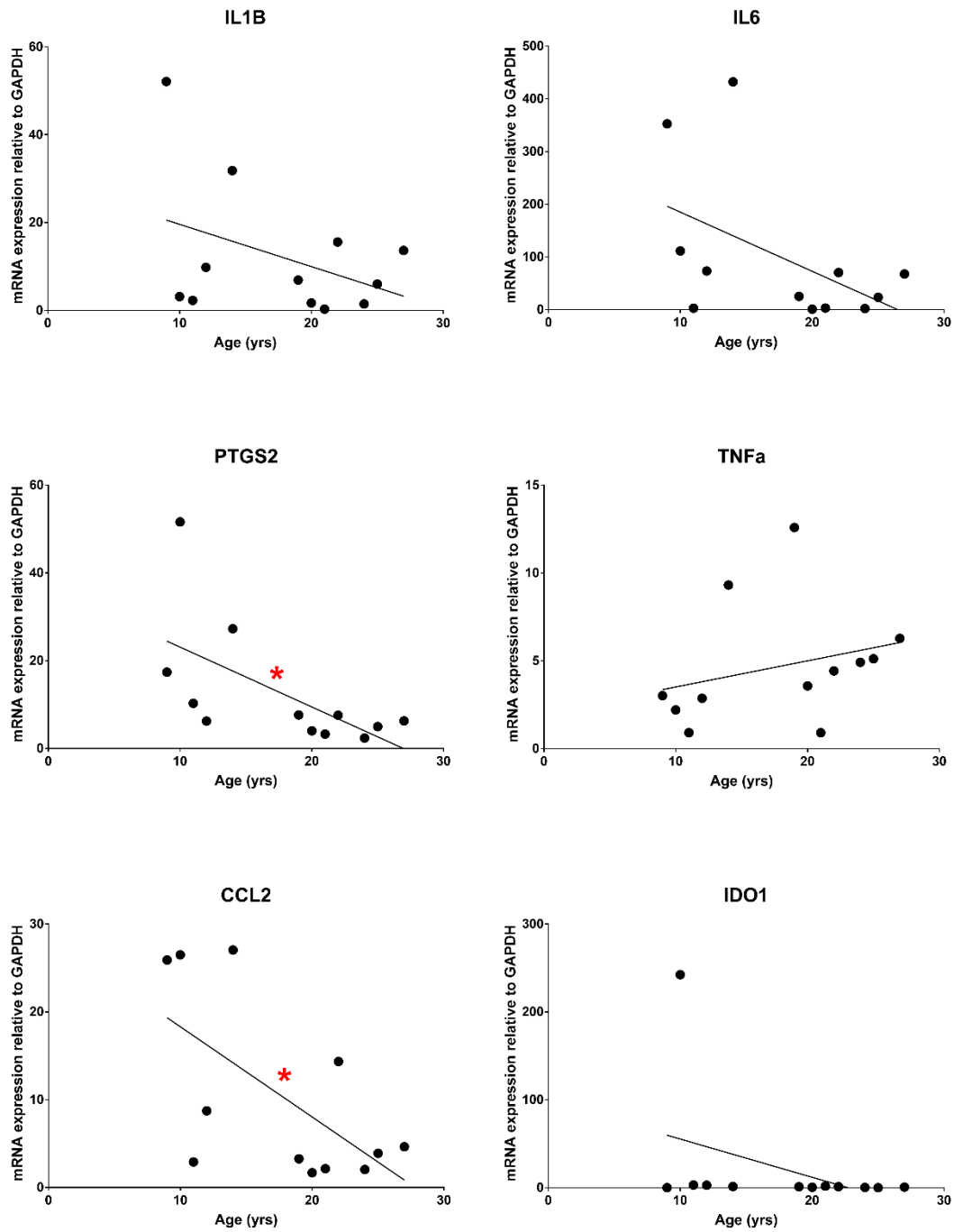


Figure 5-6 Effect of age on relative gene expression of *IL1B*, *IL6*, *PTGS2*, *TNF- α* , *CCL2* and *IDO1* in the mucosa of horses undergoing intestinal surgery
 Scatter plots showing mRNA expression of target genes relative to *GAPDH* in mucosa from resection margins of horses undergoing intestinal surgery (n=12). Results calculated using $2^{-\Delta\Delta Ct}$ method. Significance of age on relative mRNA expression performed by linear regression (represented by black line). * $p < 0.05$.

Duration of colic

Median duration of colic in the mucosa group (n=12) was 6.5 hours (range 2-12 hours) and in the *muscularis* group (n=9) was 4 hours (range 2-5 hours). There were no significant associations between duration of colic and inflammatory gene expression in either the mucosa (**Figure 5-7**) or *muscularis* group (**Figure 5-8**). There was a trend towards a decrease in the relative expression of *IL-1 β* , *IL-6* and *CCL2* in the mucosa and *IL-6*, *CCL2* and *TNF- α* in the *muscularis* with increasing duration of colic prior to surgery.

Presence of pre-operative reflux

Four out of 12 of the mucosa group and 4 out of 9 of the *muscularis* group had pre-operative reflux. The presence of pre-operative reflux was not associated with a greater level of expression of inflammatory genes (**Figure 5-9** and **Figure 5-10**).

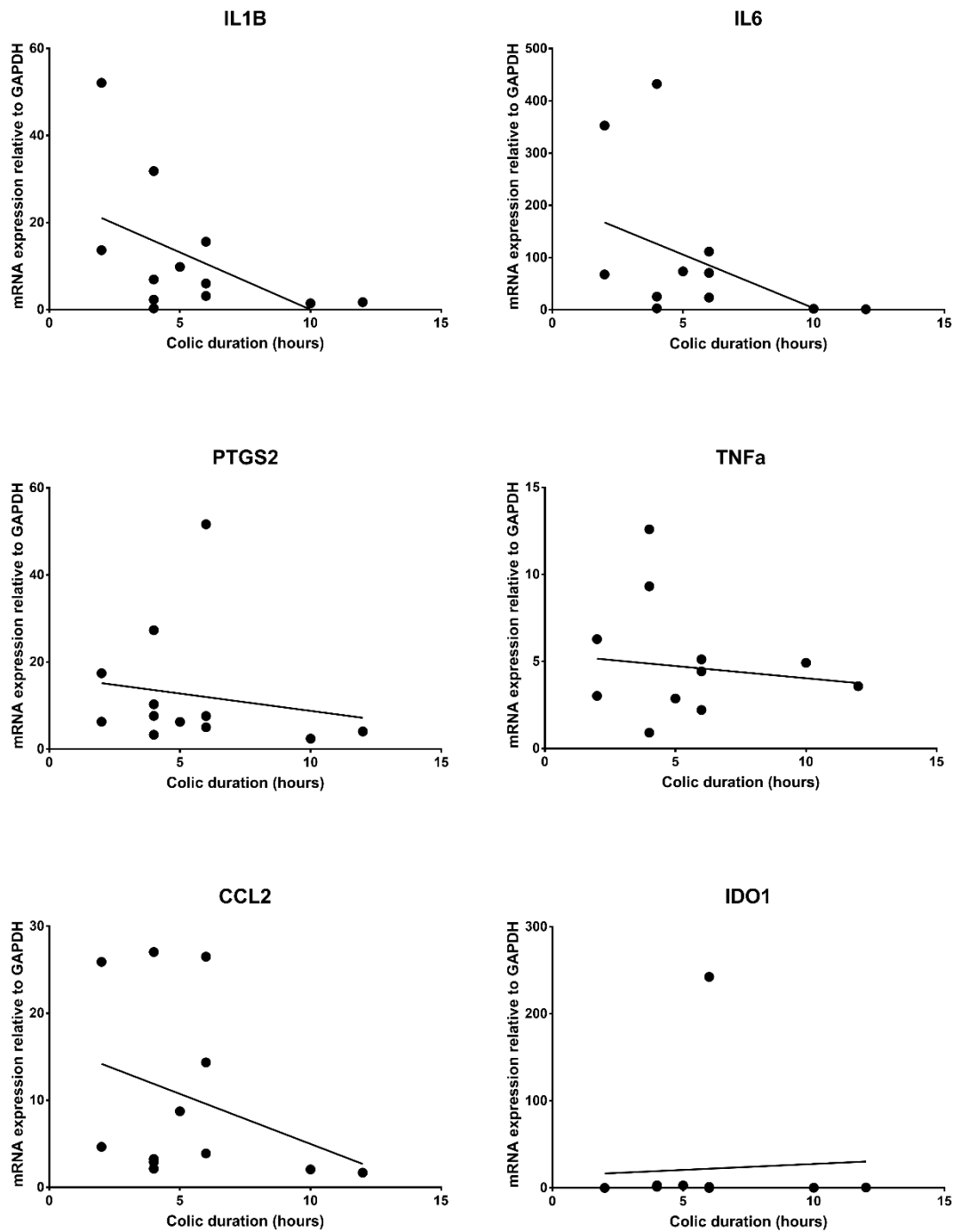


Figure 5-7 Effect of colic duration on relative gene expression of *IL1B*, *IL6*, *PTGS2*, *TNF-α*, *CCL2* and *IDO1* in the mucosa of horses undergoing intestinal surgery
 Scatter plots showing mRNA expression of target genes relative to *GAPDH* in mucosa from resection margins of horses undergoing intestinal surgery (n=12). Results calculated using $2^{-\Delta\Delta Ct}$ method. Significance of colic duration on relative mRNA expression performed by linear regression (represented by black line).

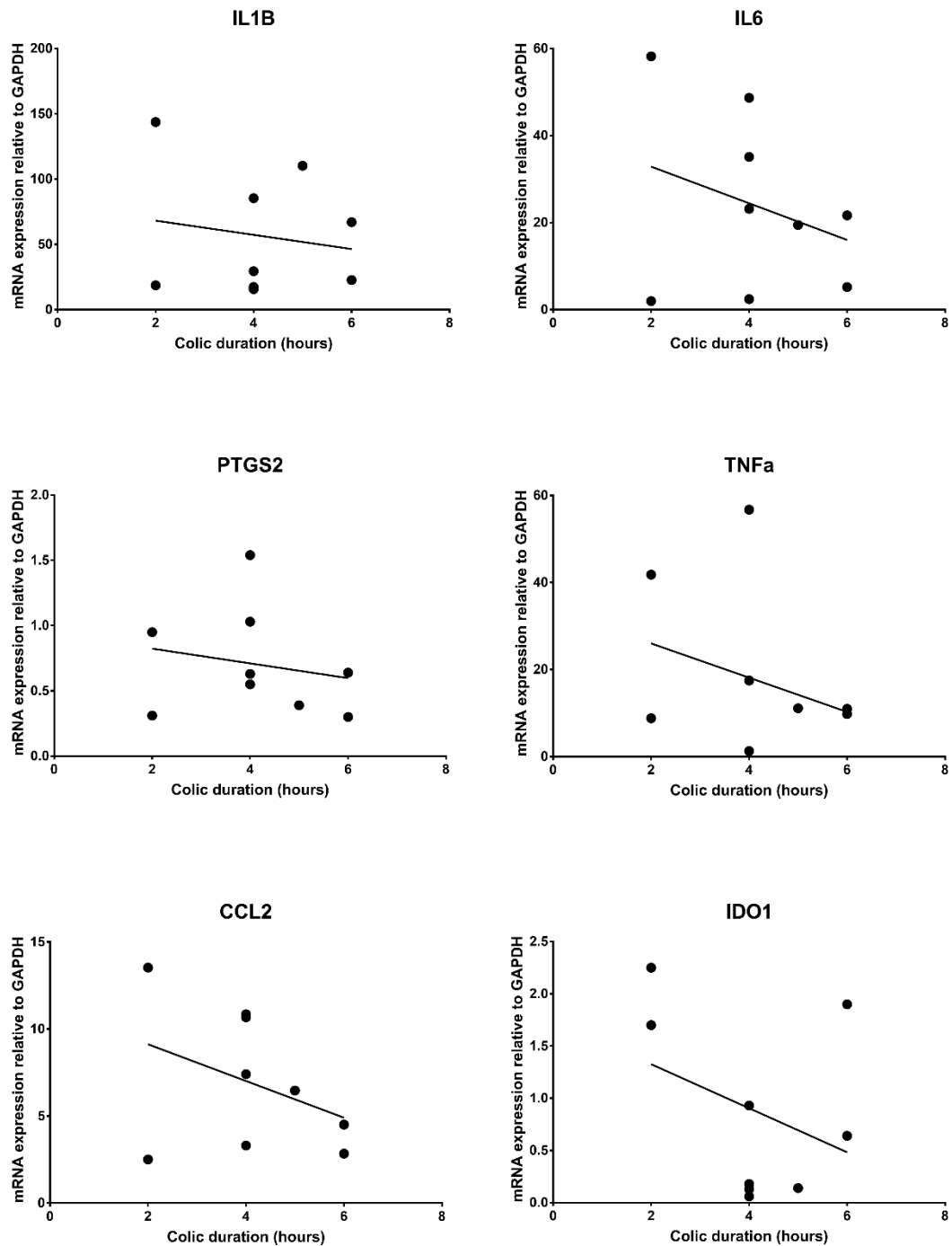


Figure 5-8 Effect of colic duration on relative gene expression of *IL1B*, *IL6*, *PTGS2*, *TNF-α*, *CCL2* and *IDO1* in the muscularis of horses undergoing intestinal surgery

Scatter plots showing mRNA expression of target genes relative to *GAPDH* in *muscularis* from resection margins of horses undergoing intestinal surgery (n=9). Results calculated using $2^{-\Delta\Delta C_t}$ method. Significance of colic duration on relative mRNA expression performed by linear regression (represented by black line).

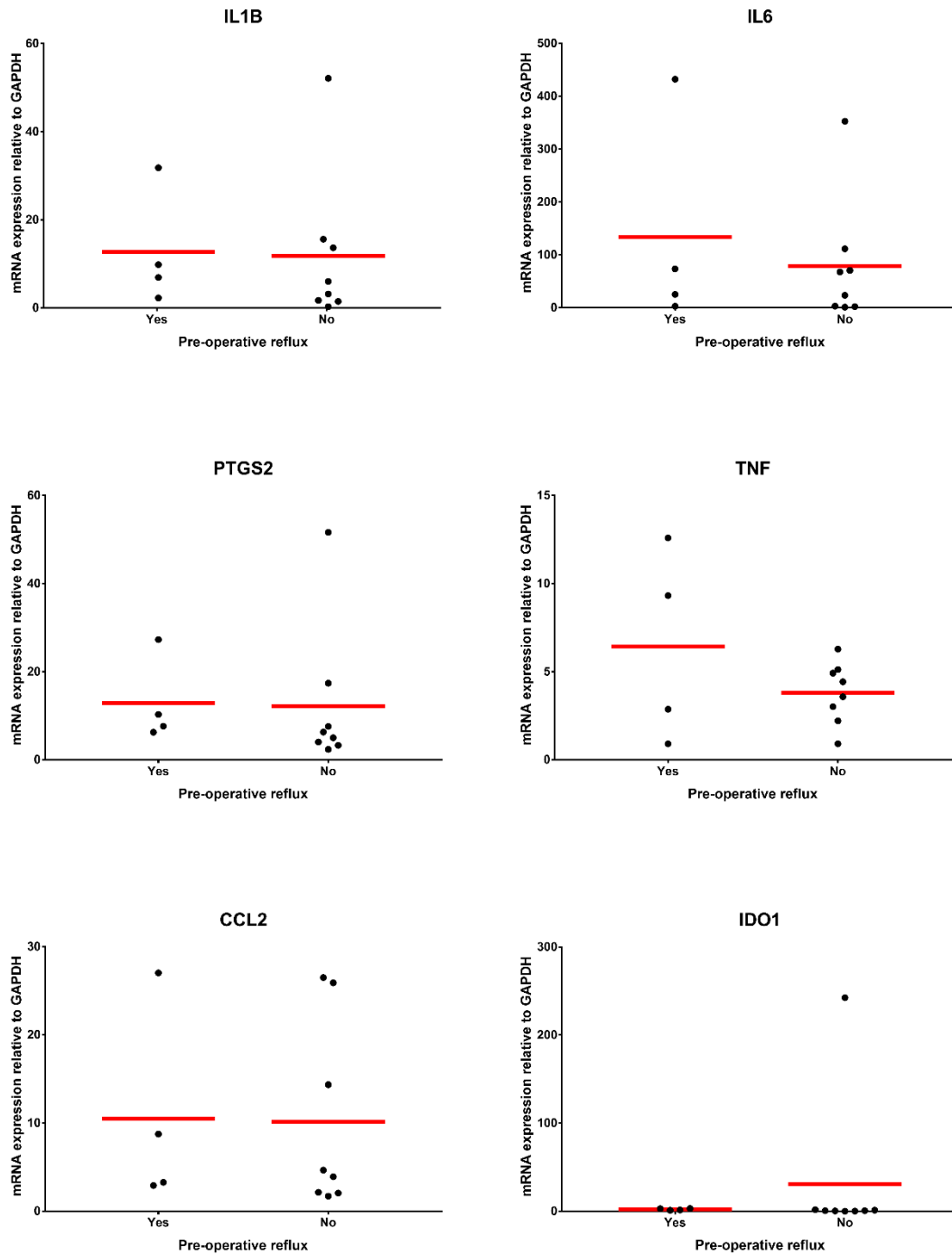


Figure 5-9 Relative gene expression of *IL1B*, *IL6*, *PTGS2*, *TNF- α* , *CCL2* and *IDO1* in the mucosa of horses presenting with and without pre-operative reflux.

Scatter plots showing mRNA expression of target genes relative to *GAPDH* in mucosa from resection margins of horses undergoing intestinal surgery (n=12). Results calculated using $2^{-\Delta\Delta C_t}$ method. Red line represents mean value. Significance of gene expression in horses with pre-operative reflux performed by Mann-Whitney U Test.

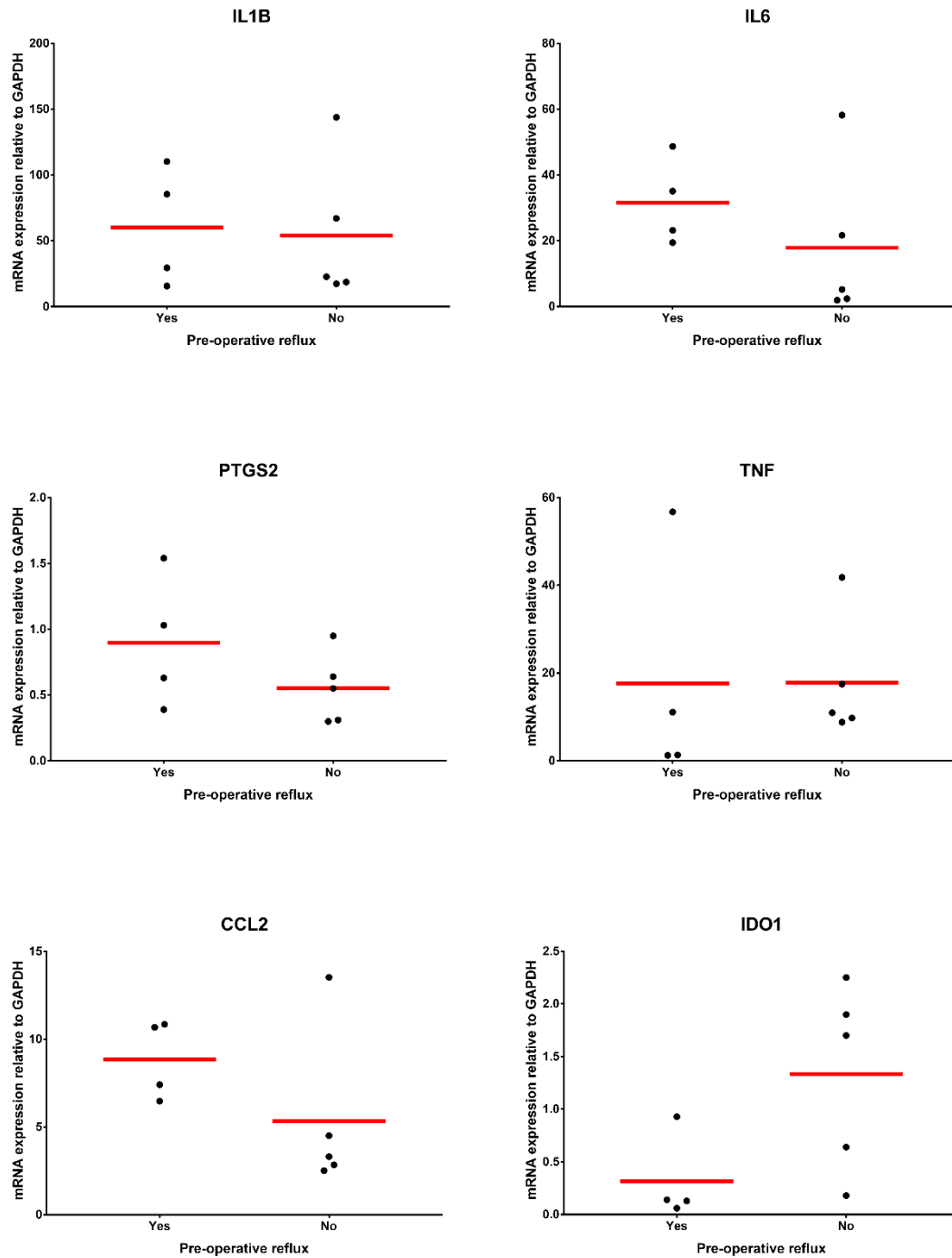


Figure 5-10 Relative gene expression of *IL1B*, *IL6*, *PTGS2*, *TNF- α* , *CCL2* and *IDO1* in the muscularis of horses presenting with and without pre-operative reflux
 Scatter plots showing mRNA expression of target genes relative to *GAPDH* in *muscularis* from resection margins of horses undergoing intestinal surgery (n=9) in horses that presented with (n=4) or without (n=5) pre-operative reflux. Results calculated using $2^{-\Delta\Delta C_t}$ method. Red line represents mean value. Significance of gene expression in horses with pre-operative reflux performed by Mann-Whitney U Test.

Intra-operative factors

Resection length

Resection of intestine has been identified as a risk factor for the development of POI (Roussel et al., 2001). All the horses in this study had resections. Horses in the mucosa group had a median resection length of 1.8 metres (range 0.5-15 metres). Horses in the *muscularis* group had a median resection length of 0.5 metres (range 0.5-1.8 metres). As shown in **Figure 5-11** and **Figure 5-12**, there was no significant association between relative gene expression and length of resected intestine.

Post-operative factors

The development of post-operative reflux (POR) is a consequence of POI; namely that, due to the inhibition of smooth muscle function this results in the accumulation of fluid and ingesta within the GIT resulting in the presence of POR. Horses that develop POI are less likely to survive following surgery (Morton and Blikslager, 2002, Mair and Smith, 2005c). In this current study, short term survival refers to all horses that survived to discharge. In rodent models, a greater inflammatory response is associated with more 'severe' POI (van Bree et al., 2012). Consequently, the horses which did develop POR were compared with those that did not with respect to the relative expression of target genes. Due to the small number of cases, any horse that developed POR of more than 2 litres on more than 2 intubations in the post-operative period was included.

Post-operative reflux

In the mucosa group, there was a significantly greater expression of *TNF- α* in the 3 horses which developed POR, compared with the 9 which did not (**Figure 5-13**). In the *muscularis* group, there was no significant difference in relative gene expression between the 3 horses which developed POR and the 6 which did not. (**Figure 5-14**). In both mucosa and *muscularis* samples, there was a trend towards greater mean expression of *IL-1 β* , *IL-6*, *PTGS2*, *TNF- α* and *CCL2* in horses that did develop POR compared to those that did not.

Short term survival

Within the mucosa group, 4 horses did not survive to discharge. There were no significant differences in expression in horses that did not survive to discharge (**Figure 5-15**). In the *muscularis* group 2 horses did not survive to discharge. As with the mucosa, no differences in relative expression of target genes between horses that did and did not survive to discharge was observed (**Figure 5-16**).

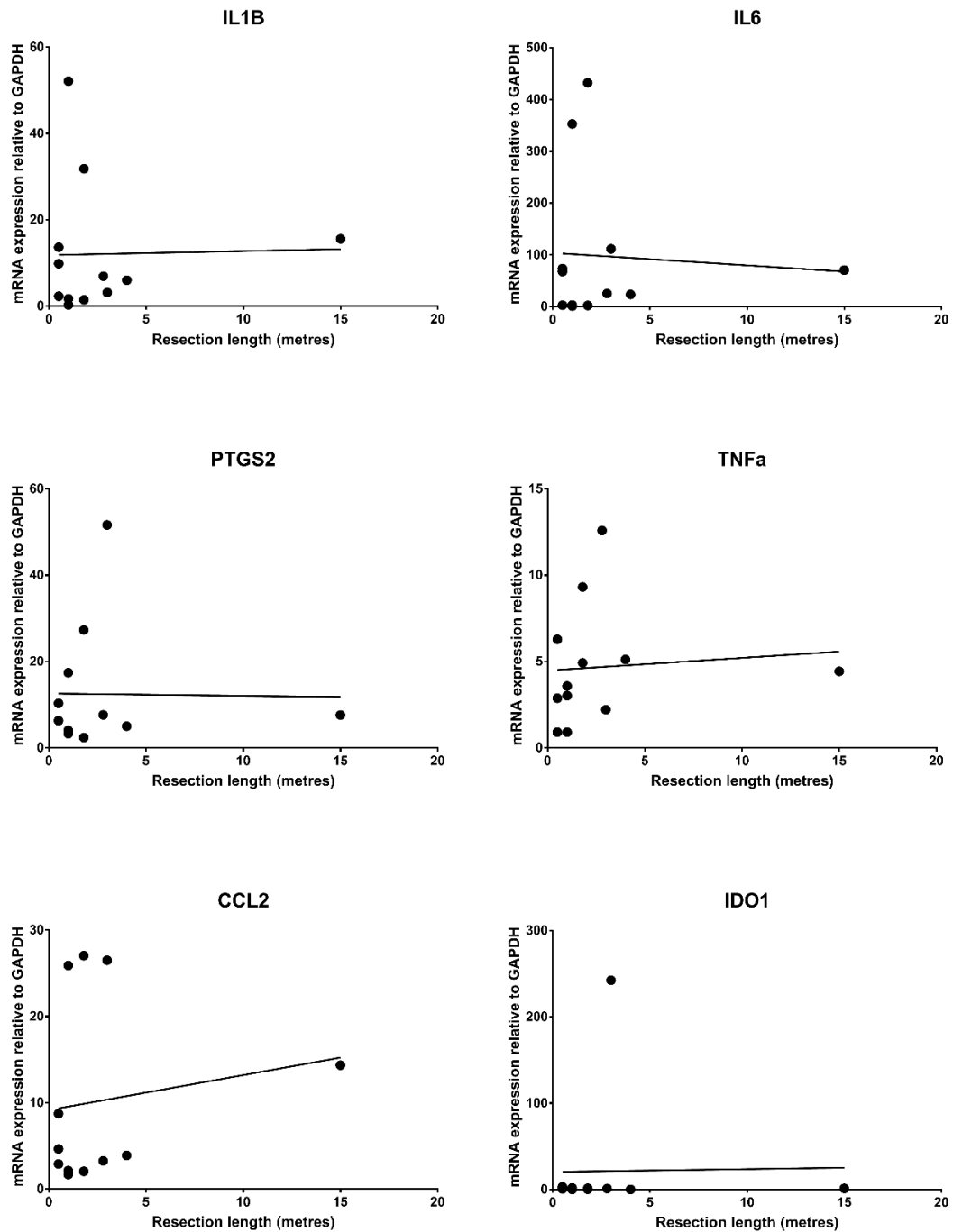


Figure 5-11 Association of resection length and relative gene expression of *IL1B*, *IL6*, *PTGS2*, *TNF- α* , *CCL2* and *IDO1* in the mucosa of horses undergoing intestinal surgery

Scatter plots showing mRNA expression of target genes relative to *GAPDH* in mucosa from resection margins of horses undergoing intestinal surgery (n=12). Results calculated using $2^{-\Delta\Delta C_t}$ method. Significance of resection length on relative mRNA expression performed by linear regression (represented by black line).

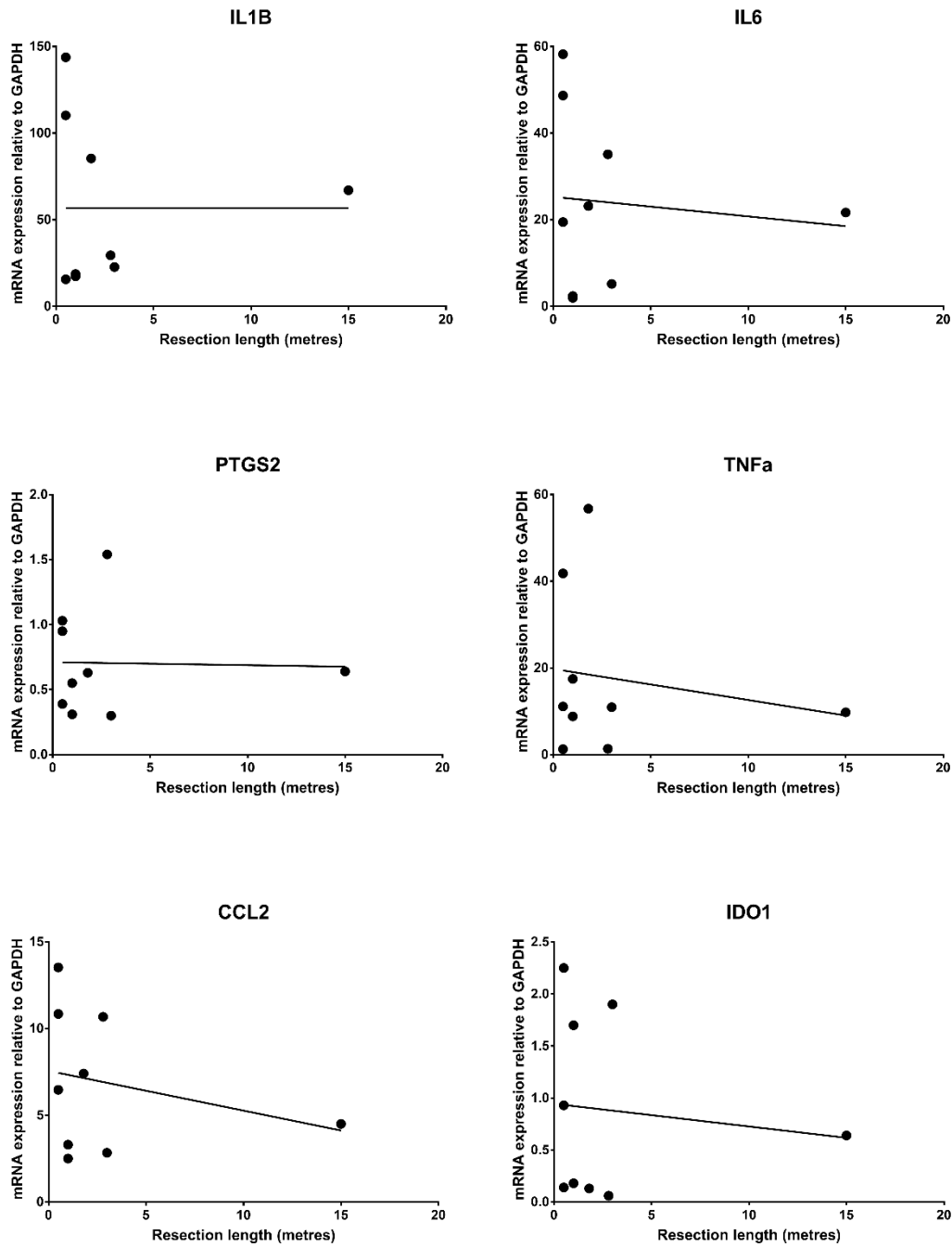


Figure 5-12 Association of resection length and relative gene expression of *IL1B*, *IL6*, *PTGS2*, *TNF- α* , *CCL2* and *IDO1* in the *muscularis* of horses undergoing intestinal surgery

Scatter plots showing mRNA expression of target genes relative to *GAPDH* in *muscularis* from resection margins of horses undergoing intestinal surgery (n=9). Results calculated using $2^{-\Delta\Delta C_t}$ method. Significance of resection length on relative mRNA expression performed by linear regression (represented by black line).

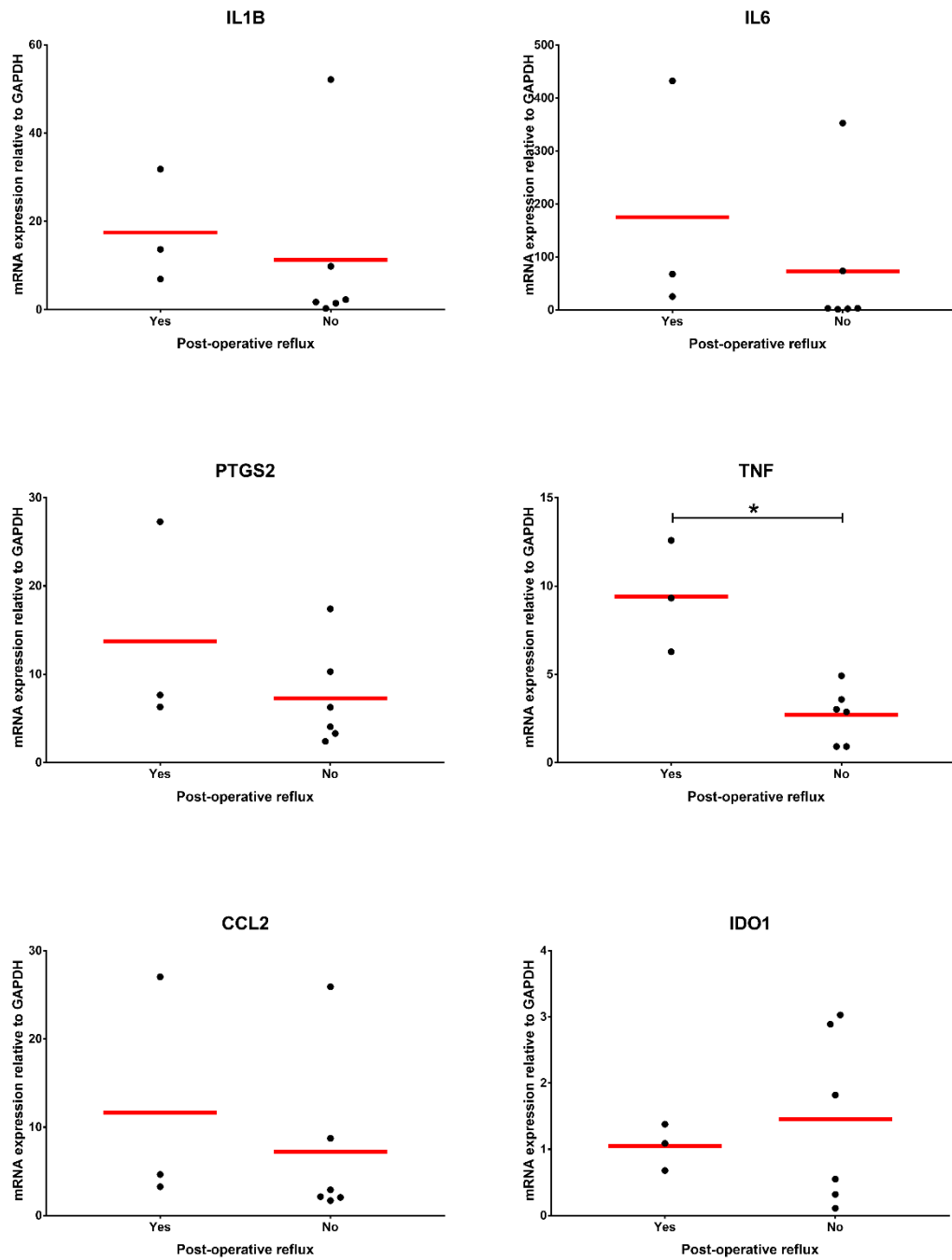


Figure 5-13 Relative gene expression of *IL1B*, *IL6*, *PTGS2*, *TNF- α* , *CCL2* and *IDO1* in the mucosa of horses with and without post-operative reflux

Scatter plots showing mRNA expression of target genes relative to *GAPDH* in mucosa from resection margins of horses undergoing intestinal surgery (n=9) in horses that developed (n=3) post-operative reflux. Results calculated using $2^{-\Delta\Delta C_t}$ method. Red line represents mean value. Significance of gene expression in horses with pre-operative reflux performed by Mann-Whitney U Test. * $p < 0.05$

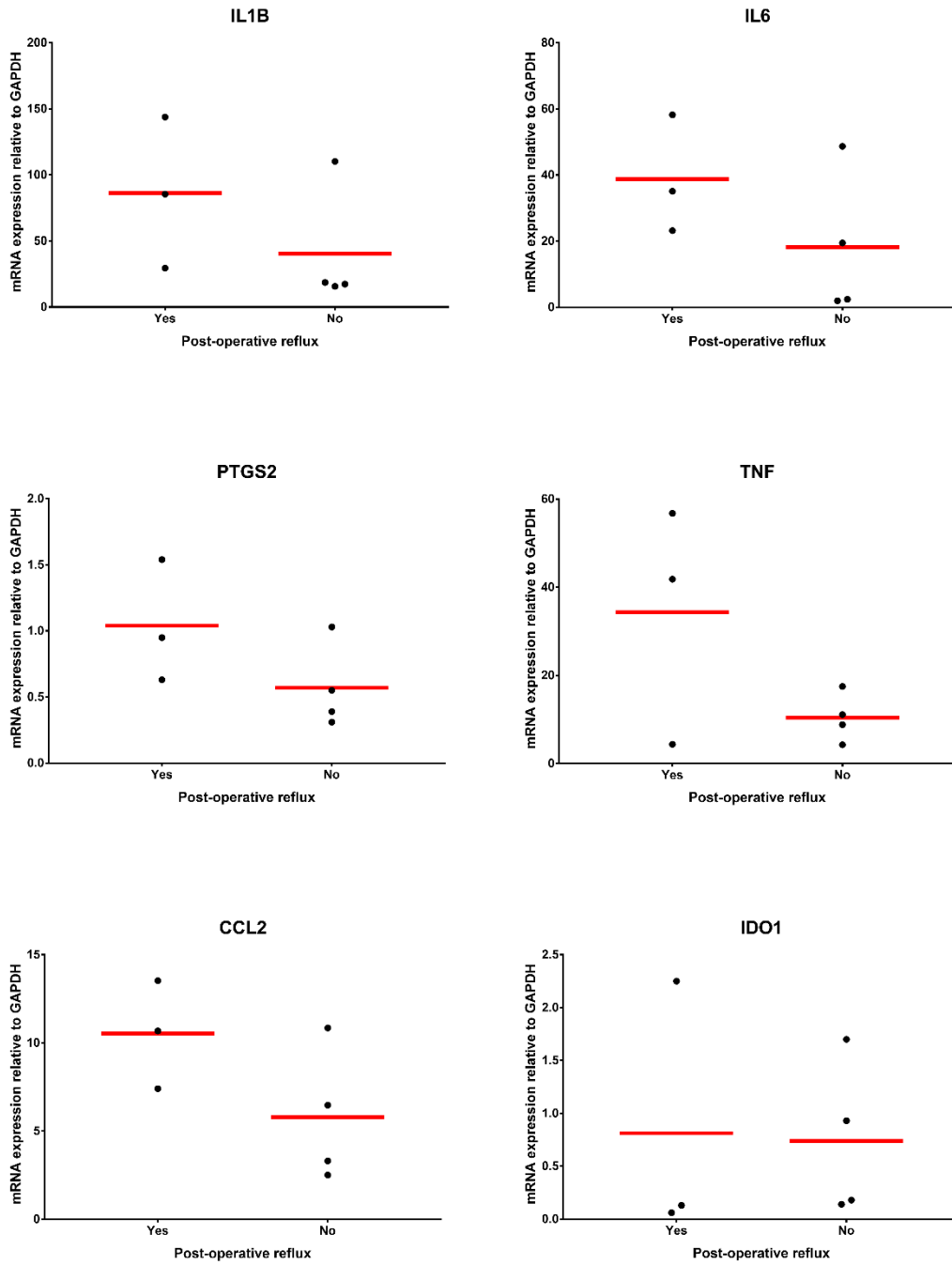


Figure 5-14 Relative gene expression of *IL1B*, *IL6*, *PTGS2*, *TNF- α* , *CCL2* and *IDO1* in the *muscularis* of horses with and without post-operative reflux

Scatter plots showing mRNA expression of target genes relative to *GAPDH* in *muscularis* from resection margins of horses undergoing intestinal surgery (n=7) in horses that developed (n=3) post-operative reflux. Results calculated using $2^{-\Delta\Delta C_t}$ method. Red line represents mean value. Significance of gene expression in horses with pre-operative reflux performed by Mann-Whitney U Test.

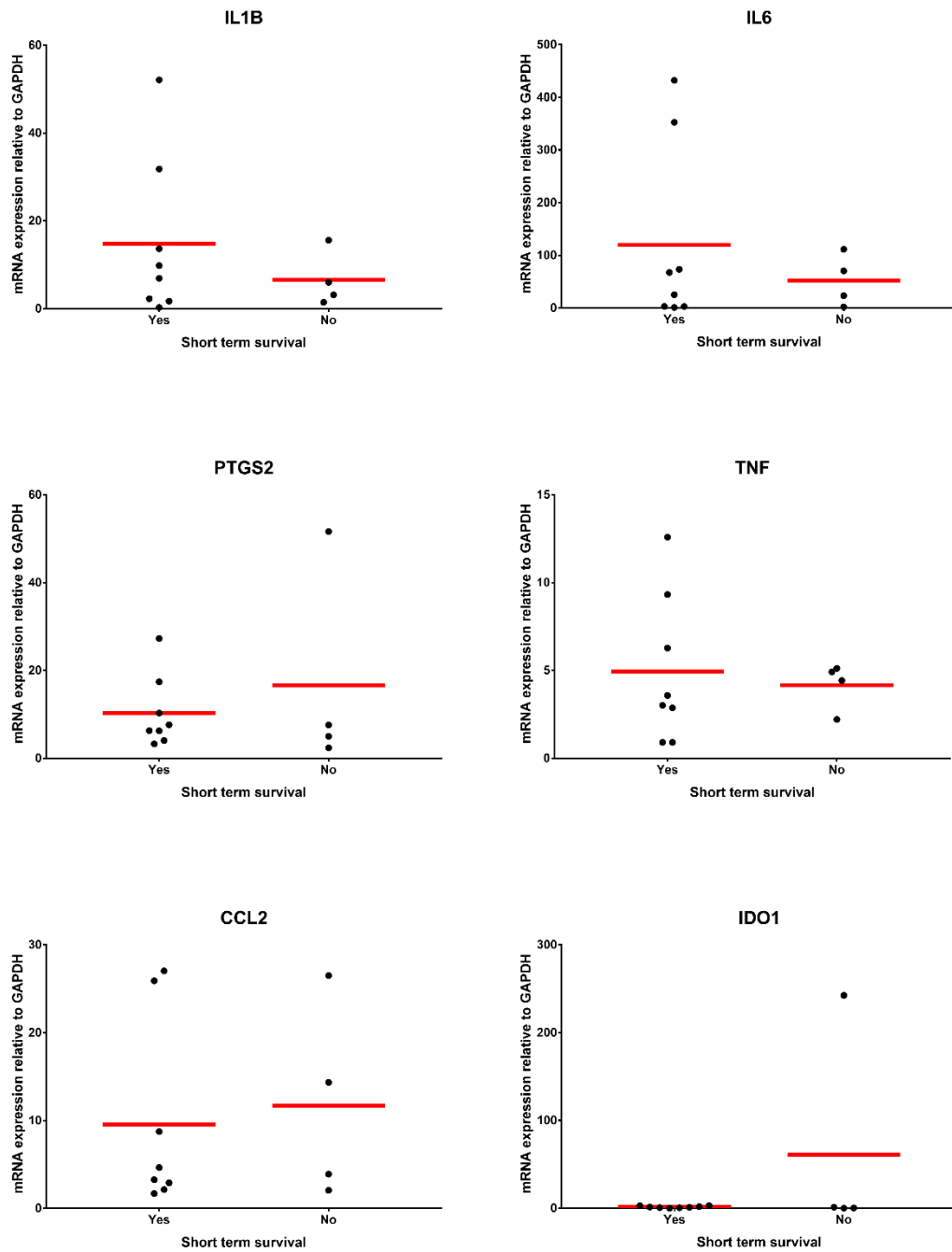


Figure 5-15 Association of relative gene expression of IL1B, IL6, PTGS2, TNF- α , CCL2 and IDO1 and short-term survival

Scatter plots showing mRNA expression of target genes relative to *GAPDH* in mucosa of resection margins (n=12) in horses surviving the immediate post-operative period (n=8) compared to horses requiring euthanasia in the immediate post-operative period (n=4). Results calculated using $2^{-\Delta\Delta C_t}$ method. Red line represents mean value. Significance of gene expression between groups performed by Mann-Whitney U Test.

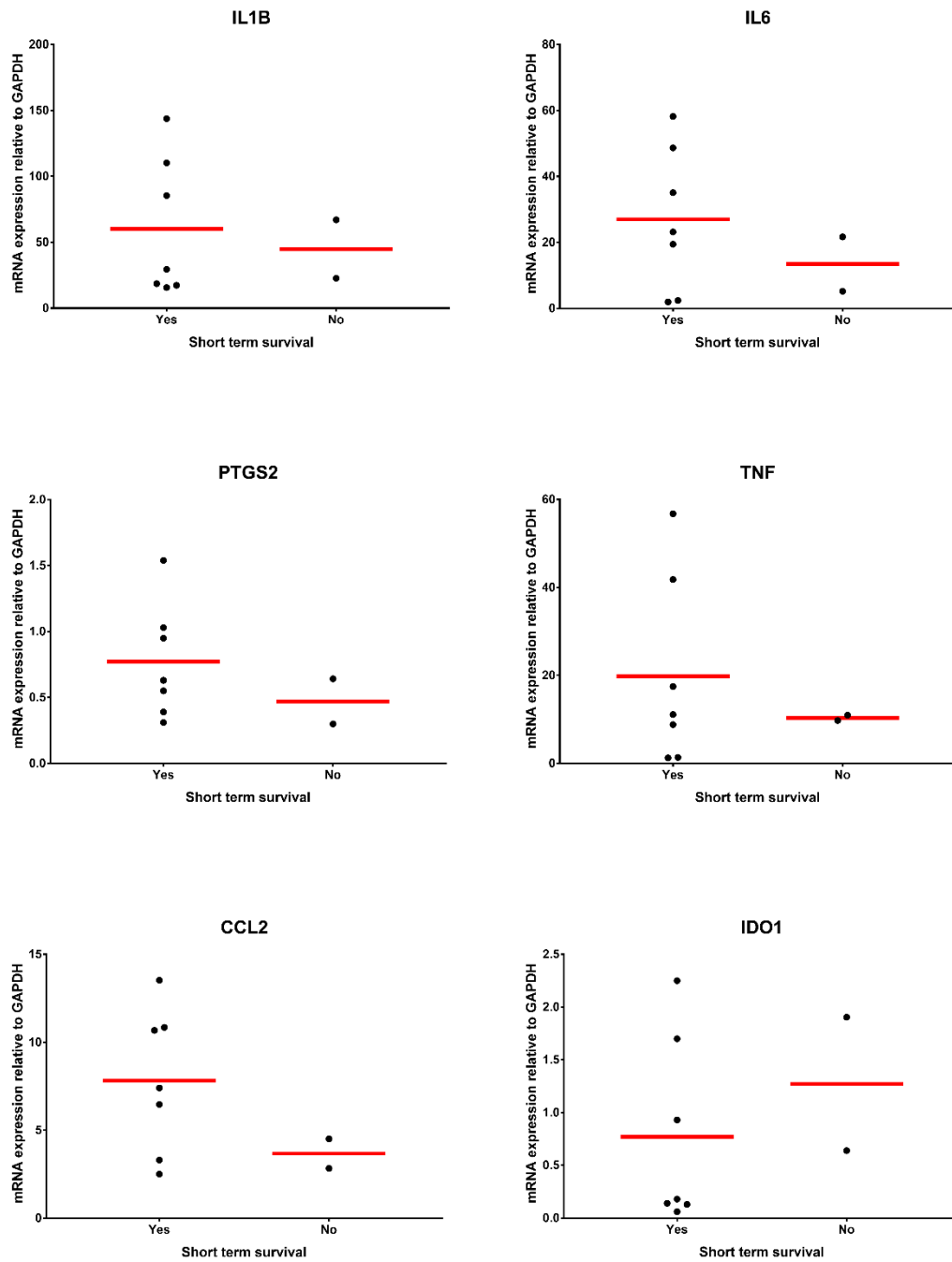


Figure 5-16 Association of relative gene expression of *IL1B*, *IL6*, *PTGS2*, *TNF- α* , *CCL2* and *IDO1* and short-term survival

Scatter plots showing mRNA expression of target genes relative to *GAPDH* in muscularis of resection margins (n=12) in horses surviving the immediate post-operative period (n=7) compared to horses requiring euthanasia in the immediate post-operative period (n=2). Results calculated using $2^{-\Delta\Delta C_t}$ method. Red line represents mean value. Significance of gene expression between groups performed by Mann-Whitney U Test.

5.3 Discussion

The presence of MM in the horse was demonstrated in **Chapter 3**. CD163⁺ macrophages were present within the circular and longitudinal muscle of the equine GIT. The aim of this chapter was to evaluate tissues from horses undergoing abdominal surgery and to investigate whether there was evidence of macrophage activation in these tissues. Whilst neural pathway disruption may result in reduced motility in the immediate post-operative period, rodent models have identified inflammation of the ME as a mechanism for the development of a more prolonged phase of POI (Kalff et al., 1999a, Kalff et al., 1999b, Kalff et al., 1998a, van Bree et al., 2012, Wehner et al., 2007). Activation of resident MM triggers a sequence of events that ultimately ends in smooth muscle dysfunction. Activation of MM triggers the release of cytokines (e.g. IL-1 β , TNF- α) which, along with LPS, induce ICAM-1 and P-selectin expression in the vascular endothelium of the *muscularis*, an effect which can last at least 12 hours following intestinal manipulation. This results in the recruitment of leukocytes into the ME, and the release of leukocyte-derived factors (e.g. nitric oxide, prostaglandins) which cause smooth muscle dysfunction (Kalff et al., 1999a).

In this study, mucosa and ME harvested from horses undergoing intestinal surgery was analysed for a specific group of genes; those encoding the cytokines *IL-6*, *IL-1 β* , *CCL2* and *TNF- α* and the mediators *PTGS2* and *IDO1*. These genes are upregulated in the intestinal ME in mouse models of POI (Farro et al., 2017) and in the ME of humans undergoing laparotomy (Kalff et al., 2003).

Firstly, a comparison of relative gene expression between proximal and distal resection margins of the mucosa and ME was performed (**Figure 5-2** and **Figure 5-3**); no significant differences were identified. This may be considered unsurprising in light of the likely symmetrical relationship between marginally located healthy intestine (proximal and distal) relative to the centrally located devitalised intestine in the resected section. However, it does contrast with the reported increase in apoptotic neurons, smooth muscle cells and glial cells at sites distal to the surgical lesions in resected small and large intestine of horses (Rowe et al., 2003) The failure of the symmetric distribution pattern of inflammation observed in this study to follow the reported asymmetric pattern of apoptosis is perhaps not unsurprising, as apoptosis does not induce an inflammatory reaction, unlike necrotic cell death (Szondy et al., 2017).

IL-6, *IL-1 β* , *CCL2* and *TNF- α* were all upregulated in the mucosa and ME in colic cases when compared to controls (**Figure 5-4**). *PTGS2* was upregulated in the mucosa only. These data demonstrate an inflammatory response within grossly non-devitalised intestine in horses undergoing intestinal resection following small intestinal strangulations. This finding is similar to that reported in the ME of humans undergoing laparotomy (Kalff et al., 2003). In contrast to human derived data, these equine results demonstrate a cytokine and mediator response within the intestinal mucosa as well as the ME; this is not reported in human intestine (Kalff et al., 2003). Similarly, intestinal manipulation failed to induce an increase in mucosal *IL-6* in rats (Wehner et al., 2005). Despite these apparent differences, it remains highly feasible that the increase in relative gene expression in the mucosa of the horses was, at least in part, attributable to the small intestinal strangulation and not solely intestinal manipulation during surgery.

The cytokines *IL-6*, *IL-1 β* and *TNF- α* all affect intestinal motility. *TNF- α* induces motor dysfunction in mice by acting directly on the smooth muscle cells (Lodato et al., 1999) (Kinoshita et al., 2006) and in rats via suppression of noradrenaline release in the myenteric plexus (Hurst and Collins, 1994). *TNF- α* (Ohama et al., 2003) and *IL-1 β* (Ohama et al., 2007) both decrease the activity of CPI-17, whose activation is required for inducing smooth muscle contraction, resulting in decreased smooth muscle contractility in the rat. Additionally, *IL-1 β* suppresses acetylcholine (Main et al., 1993) and noradrenaline (Hurst and Collins, 1993) release in rats and acts synergistically with *IL-6* to further suppress noradrenaline release (Ruhl et al., 1994). *IL-6* also suppresses motility, although the exact mechanism is not currently known (Nullens et al., 2016). Unlike *IL-6*, *IL-1 β* and *TNF- α* , *CCL2* does not seem to directly affect neurotransmission or smooth muscle function. However, its upregulation indirectly affects motility via its role in monocyte and leukocyte recruitment. *CCL2* (also referred to as monocyte chemoattractant protein-1 [*MCP-1*]) regulates the migration and infiltration of leukocytes via the CC chemokine receptor 2 (*CCR2*) and is upregulated in intestinal inflammation in rodents (Turler et al., 2002, Tsou et al., 2007, Hori et al., 2008, Kurihara et al., 1997). When inflamed, both the mucosa (Khan et al., 2006) and ME (Turler et al., 2002) show an increase in *CCL2* and MMs were shown to produce *CCL2* in an endotoxaemic model of ileus in the rat (Turler et al., 2002).

Infiltrating neutrophils and monocytes impair smooth muscle contraction via secreted products such as reactive oxygen intermediates, proteases, NO and prostaglandins (Schwarz et al., 2001, Kalff et al., 2000) (Josephs et al., 1999). Of these,

prostaglandins and NO have a profound effect on intestinal motility. In rodents *PTGS2* inhibits smooth muscle function in both an IM (Schwarz et al., 2001) and sepsis (Hori et al.) model of POI. Consistent with such an inhibitory role inhibition of the *PTGS2* pathway results in increased contractility of jejunal circular muscle in humans (Kalff et al., 2003). This somewhat contrasts with the failure to identify any increase in *PTGS2* mRNA expression in the ME of horses undergoing abdominal surgery, despite a significant increase in the mucosa (**Figure 5-4**). This may be attributable to the time course of gene expression, related to the cell infiltrate at the time of the resection, whereby cells in the mucosa are activated sooner than cells within the ME. Gene expression may also vary with stage of disease at which the resection was performed, given that during intestinal inflammation a biphasic response has been reported (Nullens et al., 2018). The increased mucosal expression of *PTGS2* could reflect stimulation of macrophages by inflammatory cytokines, damage associated molecular patterns (DAMPs) or translocated LPS from the intestinal lumen. Cellular origins of *PTGS2* in the ME include endothelial cells, neurones and vascular smooth muscle cells (Dubois et al., 1998) and intestinal manipulation has been shown to induce *PTGS2* release from both ME inflammatory cells and myenteric neurons (Josephs et al., 1999, Schwarz et al., 2001), both of which potentially contribute towards smooth muscle dysfunction.

This observed collective increase in the relative expression of *IL-6*, *IL-1 β* , *TNF- α* , *PTGS2* and *CCL2* in colic cases could potentially play a role in post-operative smooth muscle dysfunction in the horse and thus contribute to POI. The resultant reduction in smooth muscle contractions leads to reduced or arrested peristalsis and the subsequent build-up of ingesta within the GIT. The inability of the horse to vomit necessitates passage of a nasogastric tube to decompress the stomach of fluid. This procedure is often performed both before and regularly after intestinal surgery. Mechanical, as opposed to functional, obstructions will also result in the same main clinical findings; namely, sign of accumulation of gastric fluid. In this study, relative gene expression was evaluated in horses, some of which had pre-operative nasogastric reflux and some of which had POR. Horses with pre-operative reflux did not have any significant differences in relative gene expression compared to those that did not, with the mean expression in both groups being similar (**Figure 5-9** and **Figure 5-10**). The reflux in horses with pre-operative reflux was most likely attributable to a mechanical obstruction of the small intestine resulting in failure of aboral flow of ingesta. This is in contrast to a functional ileus and may explain why no difference in relative gene expression was seen between those with pre-operative reflux and those without. In contrast, relative gene expression of *TNF- α* was

significantly greater ($p < 0.05$) in the mucosa of horses with POR than those without. Although not statistically significant, the mean relative expression of *IL-6*, *IL-1 β* , *CCL2* and *TNF- α* was greater in horses with POR compared to those without (**Figure 5-13** and **Figure 5-14**).

In contrast to other inflammatory markers (with the exception of one horse) there was no detectable difference in *IDO1* expression between colic cases and healthy horses, in either mucosa or ME (**Figure 5-4**). This was surprising considering the increase in *IDO1* expression observed in eqBMDMs in response to LPS stimulation (**Chapter 4**); although, in comparison to *IL-1 β* , its level of expression was low (**Table 5-1**). IDO is expressed (both mRNA and protein) throughout the whole murine GIT, particularly in the jejunum and ileum, and is largely associated with CD11c⁺ dendritic cells (Matteoli et al., 2010). IDO1 expression also increases in inflammation, via infiltration of CD123⁺ mononuclear cells in human inflammatory bowel disease (Wolf et al., 2004).

Table 5-1 TPM values of IDO and IL1B in eqBMDMs stimulated with LPS (Data from Chapter 4)

Gene	TPM 0 hours (resting)	TPM 7 hours post LPS stimulation
<i>IDO1</i>	0.920	18.103
<i>IL-1β</i>	10.59	1097.029

IDO1 induction can be mediated through IFN- γ dependent and independent pathways and its LPS-mediated induction can be further potentiated via inflammatory cytokines such as TNF- α , IL-6 and IL-1 β (Fujigaki et al., 2006, Fujigaki et al., 2001). However, the most potent inducer of IDO is thought to be IFN- γ , which induces both gene expression and enzyme activity of IDO1 (Dai and Gupta, 1990). The lack of IDO1 induction in the current study may have been attributable to either a failure of abdominal surgery to activate the IFN- γ pathway or insufficient time to have lapsed for the induction of *IDO1* via IFN- γ independent pathways (LPS/TNF- α).

NO is an inhibitor of intestinal motility and is produced by NOS2 derived from infiltrating leukocytes in the ME in rodents; this is reversed by inhibition of NOS2 (Kalff et al., 2000). No *NOS2* mRNA was detectable in any equine jejunal sections (control and colic cases); consequently, *NOS2* was removed from the set of target genes. These findings were consistent with the lack of *NOS2* expression in stimulated equine BMDMs and highlights the interspecies variation in NO production and the importance of studying species specific pathophysiology of POI (Young et al., 2018).

NO may still play a role in POI via NOS1, which relates to the neuronal control of intestinal motility (Stark et al., 1991).

Several factors such as age and the presence of pre-operative nasogastric reflux have been associated with an increased incidence of POI in horses (Mair and Smith, 2005b). Subset analysis was performed to determine if any association with clinical variables was present. In the mucosa, all genes apart from *TNF- α* reduced with age (**Figure 5-6**). In the ME the converse was true (**Figure 5-5**), where all genes showed an increase in relative gene expression with age. A confounding factor in these data is age; 6 out of the 12 colic cases were diagnosed with pedunculated lipomas at surgery (**Table 2-2**). Pedunculated lipomas have a higher incidence in older horses (Edwards and Proudman, 1994). The effect of aging on the intestinal barrier is unknown. In a study of healthy human of varying ages (7-77 years) no changes in *TNF- α* , *IFN- γ* and *IL-1 β* expression occurred in older patients but *IL-6* was significantly increased in the aging group (Man et al., 2015). However, an increase in intestinal permeability as a result of age-associated changes in intestinal epithelial tight junctions has been reported (Tran and Greenwood-Van Meerveld, 2013, Man et al., 2015). The association of an increase in gene expression in the *muscularis* with age in the colic cases may therefore be attributable to an increase in intestinal permeability with age in the colic cases. The increased intestinal permeability could result in a greater translocation of PAMPs and DAMPs from the gut lumen, causing greater activation of the resident *muscularis* macrophages which is reflected by the higher relative changes in gene expression.

Relative gene expression was lower in horses that had a longer duration of colic prior to surgery in both the mucosa (**Figure 5-7**) and ME (**Figure 5-8**). Neither intestinal resection length (**Figure 5-11**) (**Figure 5-12**) nor short-term survival (**Figure 5-16**) showed any association with relative gene expression in both mucosa and ME. The small group sizes constitute a significant limitation of this analysis; therefore, it is difficult to make definitive conclusions from these data. The gene expression data for resection length had 1 outlier (1 horse that required 15m of intestine to be resected). On removing this outlier, no significant difference in relative gene expression was associated with resection length although *PTGS2* and *TNF- α* in the mucosa had an increasing trend with resection length, whilst in the ME *IL-1 β* and *IL-6* decreased with resection length.

In conclusion, these data demonstrate an inflammatory response within the GIT of horses undergoing abdominal surgery. The data suggest an upregulation of genes associated with activation of macrophages (*IL-6*, *TNF- α* , *IL1B*). These, along with *PTGS2* and *CCL2* are all capable of inhibiting smooth muscle contractility, therefore

disrupting normal intestinal motility and resulting in functional POI. The absence of *NOS2* upregulation highlights inter-species variation in this inflammatory pathway, thus emphasising the importance of considering the target species when developing potential therapeutic targets. Further work could include targeted analysis of the resident macrophage population. Furthermore, whilst the intestinal recruitment of neutrophils in equine abdominal surgery has been studied (Little et al., 2005), to date no studies have focused on the infiltration of monocytes/macrophages in the horse.

Chapter 6. Effect of CSF1-Fc on the murine gastrointestinal tract

6.1 Introduction

The gastrointestinal (GI) *muscularis* macrophages (MM), which are distributed throughout the length of the *muscularis externa* (ME), respond to alterations in intestinal luminal contents and regulate gastrointestinal motility by interactions with enteric neurons by secreting bone morphogenetic protein 2 (BMP2) (Muller et al., 2014). In turn, enteric neurons were believed to be a major source of the growth factor CSF-1, required for macrophage proliferation, differentiation and survival.

As discussed in **Chapter 1**, the activation of MM is a component of the inflammatory cascade following abdominal surgery which leads to the development of post-operative ileus (POI). Activation of the MM results in an influx of leukocytes within hours of the commencement of abdominal surgery, ultimately resulting in smooth muscle dysfunction and impaired GI motility (De Jonge et al., 2003).

The majority of POI studies focus on the depletion of MM or blocking the leukocytic infiltrate (Wehner et al., 2007, Kalff et al., 1999b, The et al., 2005). The function of macrophages in the resolution of inflammation and POI has received less interest. With every tissue injury, immune cells and their products will also contribute to the resolution of inflammation. In mouse models of POI, *Il-10* knockout mice are unable to resolve their *muscularis* inflammatory response compared to wild type (WT) mice which results in higher mortality rates (Stoffels et al., 2009). The administration of exogenous IL-10 improved post-operative GI transit and reduced inflammatory cytokines, chemokine and nitric oxide (NO). Until recently, the role of monocytes and macrophages in the resolution of POI had not been studied. In mouse models of other disease such as liver disease, stroke and spinal disease, infiltrating monocyte-derived macrophages (MDM) are needed for recovery (Shechter et al., 2009, Wattananit et al., 2016, Zigmond et al., 2014). Using C-C motif chemokine receptor 2 (CCR2) deficient mice (*Ccr2*^{-/-}), Farro *et al.* (2017) reached a similar conclusion in a model of intestinal manipulation-induced POI (Farro et al., 2017). The receptor encoded by the *Ccr2* gene mediates monocyte chemotaxis in tissues and *Ccr2*^{-/-} mice have defective monocyte recruitment to sites of inflammation (Kurihara et al., 1997). Following intestinal manipulation (IM), *Ccr2*^{-/-} mice still develop POI to the same extent as WT mice 24 hours post-operatively. They also have similar expression of pro-inflammatory cytokines (*tnf*, *il6* and *il1a*) and chemokines (*ccl2*, *cxcl1* and *cxcl2*) as WT mice. This supports previously published data that resident MM are responsible for the initiation of the inflammatory response rather than recruited leukocytes, such as MDMs and neutrophils. However, WT and *Ccr2*^{-/-} mice differ in their recovery from the challenge.

Ccr2^{-/-} mice had a more persistent inflammatory response with higher expression of pro-inflammatory cytokines and chemokines, increased neutrophil-mediated pathology, increased neuronal and smooth muscle dysfunction, increased fibrosis of the *muscularis* and a delay in return of normal GI transit when compared to WT mice. WT mice had higher mRNA levels of pro-resolving genes such as *Arg1*, *Mrc1* and *Yml*, when compared to *Ccr2*^{-/-} mice. The impaired monocyte recruitment in *Ccr2*^{-/-} mice therefore appeared to prevent resolution of the inflammatory process in POI, implying that recruited cells are pro-resolving and therefore required to restore normal intestinal homeostasis (Farro et al., 2017).

The macrophage growth factor, CSF-1, promotes monocyte production, recruitment, maturation and local macrophage proliferation (Hume et al., 1988). Administration of CSF-1 promotes regeneration and repair in several murine disease models such as those involving the kidney (Alikhan et al., 2011), liver (Stutchfield et al., 2015) and brain (Boissonneault et al., 2009). The development of CSF1-Fc, a fusion of pig CSF-1 and the Fc region of pig IgG1a, addressed the initial limitations of CSF-1 therapy by generating a protein with an increased half-life at lower doses than the native protein (Gow et al., 2014). The administration of CSF1-Fc to WT mice and pigs increases circulating monocyte and tissue macrophage numbers (Gow et al., 2014, Sauter et al., 2016, Stutchfield et al., 2015, Sauter et al., 2014). It was previously thought that release of Ly6C^{hi} monocytes from the bone marrow depended upon CCR2 signalling (Shi and Pamer, 2011). but CSF-1-Fc was able to override the CCR2 requirement for the release of monocytes from the bone marrow (Stutchfield et al., 2015).

Muller *et al.* (2014) showed previously that the MM express *Csf1r*, and CSF-1 is required for their development and maintenance. MM were absent from juvenile *Csf1r*^(-/-) or *Csf1*^(op/op) mice, and rapidly became depleted following treatment with anti-CSF-1R antibody, as shown previously by Macdonald *et al.* (2010) using a different antibody. Muller *et al.* favoured a model in which regulated production of CSF-1 by neurons controls the function of MM, which in turn regulated neuronal function through production of BMP2. However, their analysis did not directly demonstrate that increased availability of CSF-1 can regulate MM function or gene expression, nor did they show that CSF-1 can modulate gastrointestinal motility. A more recent study in neonatal mice without enteric neurons and in intestine from humans with Hirschsprung's disease, which also lack enteric neurons, found that normal colonisation by MM occurs (Avetisyan et al., 2018). This suggests that enteric neurons are not required for colonisation by MM, and that neuronal-macrophage interactions develop postnatally. Many aspects of gene expression in MM resemble microglia. In the brain, increased CSF-1 is strongly-associated with microgliosis seen in many

neurodegenerative diseases (Askew et al., 2017) and increased neuronal CSF-1 has also been implicated in neuropathic pain (Tang et al., 2018, Guan et al., 2016).

Most of the work of Muller *et al.* utilised a widely-used *Cx3cr1*-EGFP reporter gene to locate MM. In this chapter, *Csf1r* reporter genes (Hawley et al., 2018, Sasmono et al., 2003) are used to image macrophages in the layers of the ME. In combination with the novel CSF1-Fc agent, the direct impact of CSF-1 in regulating MM numbers and the impact of CSF1-Fc on the phenotype of intestinal macrophages is examined. Based upon these data, in a collaboration with Professor Gianluca Matteoli (Translational Research in Gastrointestinal Disorders [TARGID], KU Leuven, Belgium) who was investigating the role of MDMs in POI, we administered CSF1-Fc to WT and *CCr2*^{-/-} mice in a mouse model of IM-induced POI. Some of the data presented in this chapter were published in collaboration with Professor Gianluca Matteoli (Farro et al., 2017).

6.2 Results

6.2.1 Administration of CSF1-Fc to mice does not affect gastrointestinal transit time

Mice (12-week-old males and females, n=3 per group) were injected daily with 0.75mg/kg of CSF1-Fc for either 3 days or 5 days. The control group received an equal volume of PBS.

As has been reported previously, CSF1-Fc administration resulted in increased spleen weight (Farro et al., 2017, Gow et al., 2014, Stutchfield et al., 2015). No difference was observed in liver weights between the 2 groups following 3 days of treatment but was present after 5 days of treatment with CSF1-Fc (**Figure 6-1**). The removal of MM is thought to result in intestinal dysmotility (Muller et al., 2014). Currently no data exist regarding the effect of increased intestinal macrophage populations on motility. Mice were treated with CSF1-Fc which has previously been shown to increase LpM (Sauter et al., 2014). Alterations in MM populations have not been studied to date. In the present study, there was no difference in GI motility between CSF1-Fc and saline treated mice (**Figure 6-2**). In all but one mouse, fluorescent dextran material had reached the caecum after 90 minutes, which is equivalent to section 11 on the scale used to measure geometric centre (GC). To evaluate if this result was due to a failure of CSF1-Fc to act on MM, imaging was performed on intestinal whole mounts to evaluate the MM.

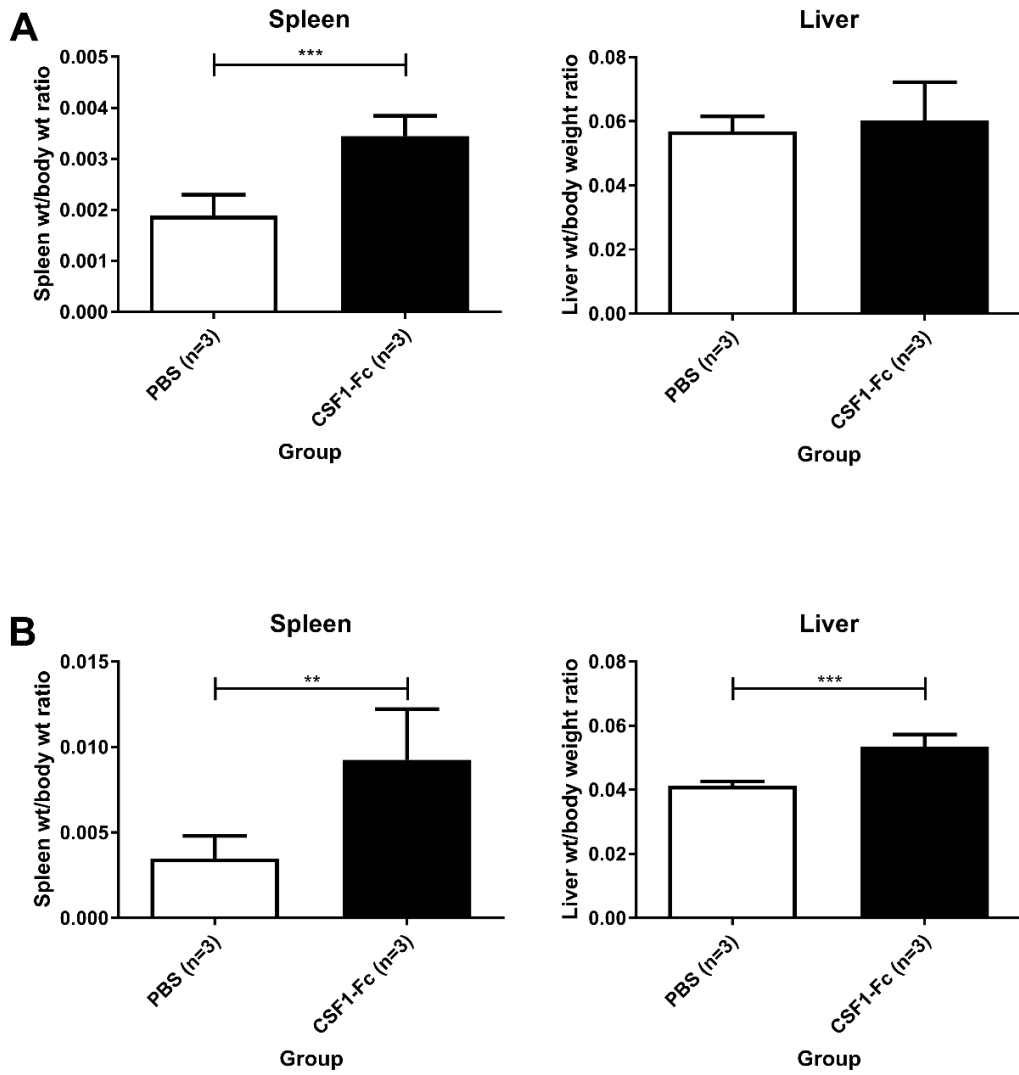


Figure 6-1 Effect of CSF1-Fc on spleen and liver weights in mice

Bar graphs showing spleen and liver weight to bodyweight ratio in mice administered CSF-Fc daily for 3 days (A) and 5 days (B). Graphs show mean \pm 95% CI. ** $p < 0.001$, *** $p < 0.001$, **** $p < 0.001$ by unpaired t-test.

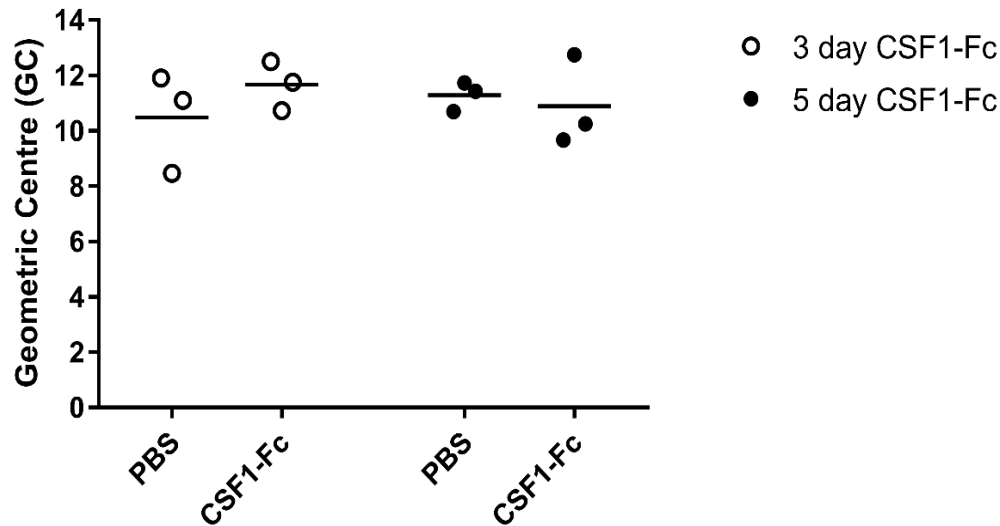


Figure 6-2 Effect of 3 and 5 days of CSF1-Fc administration on gastrointestinal transit times in wildtype mice

Wildtype mice were treated for 3 or 5 days with 0.75mg/kg of CSF1-Fc once daily subcutaneously. Control mice were treated with PBS. Dots represent geometric centre (GC) values from individual mice. Mean is also shown. No significant differences between CSF1-Fc and saline treated data sets as determined via unpaired t-test.

6.2.2 Administration of CSF1-Fc alters morphology of resident muscularis macrophages

Distribution of resident gastrointestinal macrophages is identical in MacGreen and mApple macrophage reporter mice

Prior to analysis of tissues from mice treated with CSF1-Fc, imaging was optimised for a new macrophage reporter mouse; the *Csf1r*-mApple (Hawley et al., 2018). The MacGreen mouse is an EGFP reporter mouse driven by regulatory elements of *Csf1r* (Sasmono et al., 2003) that allows the imaging of *Csf1r*-expressing cells to be visualised *in situ*. The mApple transgenic mouse is also a *Csf1r* fluorescent reporter, using the red reporter gene, mApple (Hawley et al., 2018). Muller *et al.* used the *Cx3cr1* fluorescent reporter mouse, a gene which is highly expressed in microglia and mast cells of mice and expressed at lower levels in BMDMs (Figure 6-3). *Cx3cr1* is commonly used as a microglial marker but is not expressed on all microglia detected with the *Csf1r*-ECFP transgene and is not expressed by all resident macrophage populations, particularly those derived recently from *Cx3cr1*-negative monocytes (D.A. Hume, personal communication).

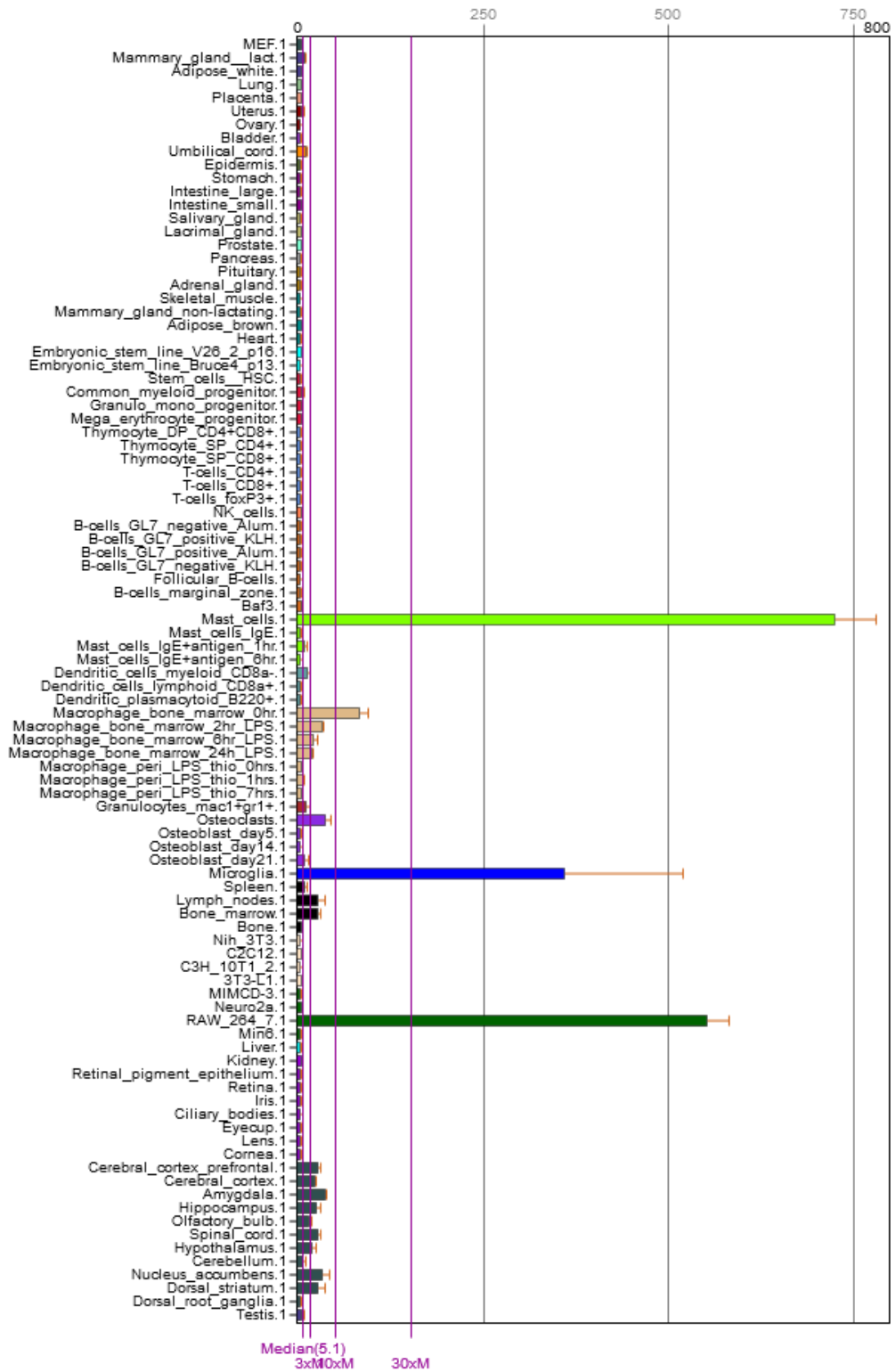


Figure 6-3 Gene expression chart for *Cx3cr1* in mouse

Gene expression chart for *Cx3cr1* gene in mice from a variety of tissues, organs and cell lines. Microglia (Blue); RAW_264 cells (Dark Green); Bone marrow-derived macrophages (ochre); Mast cells (light green); brain regions (Grey). Gene expression data from Mouse MOE430 Gene Atlas (GEO: GSE10246) (Su et al., 2002)

Firstly, confocal images from MacGreen mice were obtained from *ex situ* intestinal whole mounts (**Figure 6-4**). The distribution of the transgene in tissues of the MacGreen mouse has been well documented (Sasmono et al., 2003, Sauter et al., 2014) but no studies have imaged MM. Expression of the transgene was visible in the lamina propria and ME of the small and large intestine (**Figure 6-5**). The transgene emphasised the base of each villus in the lamina propria whilst in the ME of both the small and large intestine, a dense network of microglial-like macrophages was visible. This is consistent with other studies, which have used *Cx3cr1^{GFP/+}* reporter mice to image intestinal macrophages (Gabanyi et al., 2016). As discussed in **Chapter 3**, immunohistochemical studies have demonstrated that MM within the muscle layers are elongated, bipolar with MM between the muscle layers being more stellate with multiple dendrites (Kalff et al., 1998b, Mikkelsen, 2010). In the MacGreen mouse, amongst the MM population within the ME there were two distinct morphological sub populations; bipolar cells within the muscle layer and stellate cells in the intermuscular layer (at the level of the myenteric plexus) (**Figure 6-5**). Imaging of mApple *ex-situ* intestinal whole mounts revealed identical transgene expression in the GIT to the MacGreen (**Figure 6-6** and **Figure 6-7**). Morphology of macrophages in the ME was also alike in mApple and MacGreen mice (**Figure 6-7**). This is consistent with imaging of other mApple tissues, where expression patterns are the same between the two transgenes (Hawley et al., 2018).

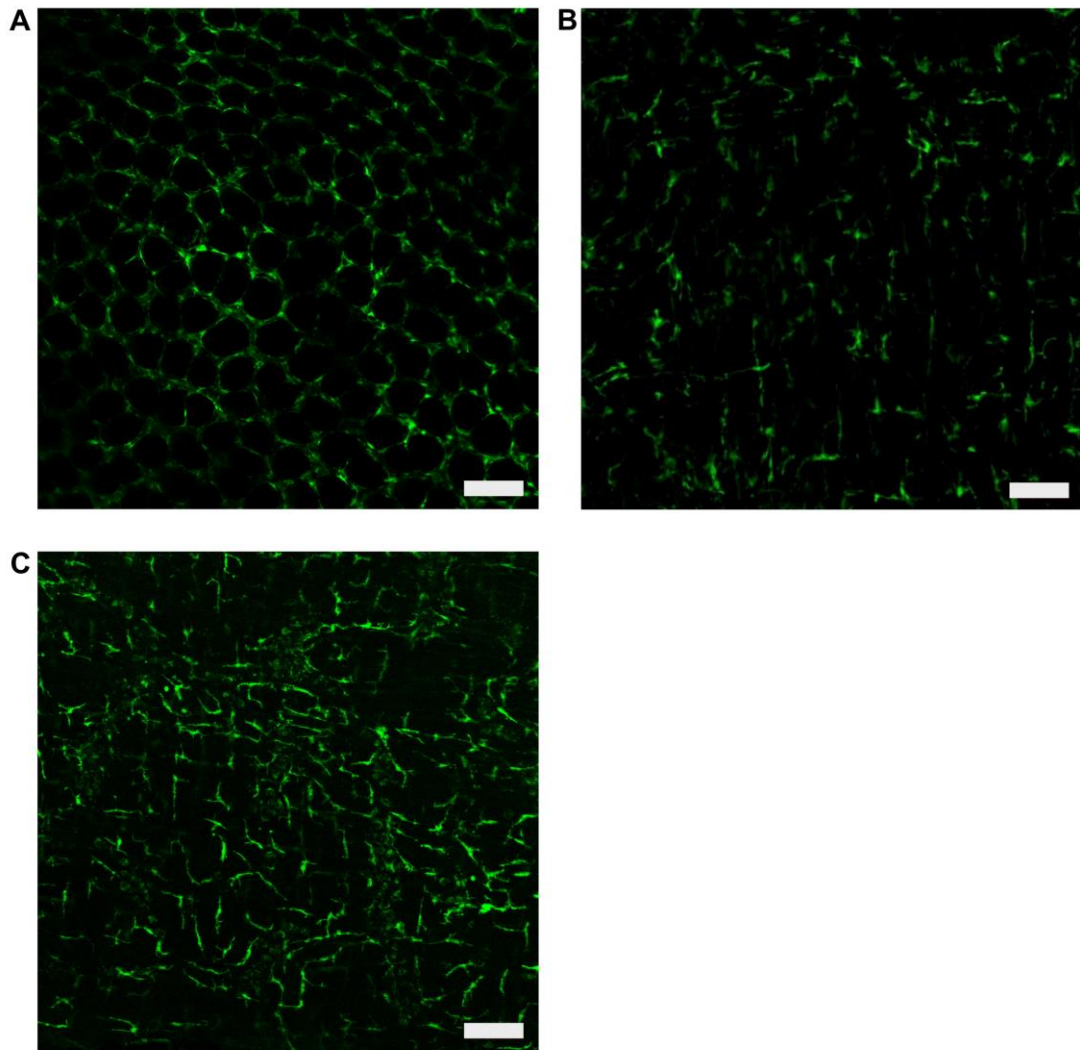


Figure 6-4 Intestinal whole mount images of the lamina propria (A) and muscularis (B) of the jejunum and muscularis of the colon (C)

Confocal microscopy images of intestinal whole mounts of the small (A and B) and large (C) intestine. (A) is a single slice. (B) and (C) are image stacks of whole muscularis. Magnification X10. Bar=100 μ m. Images representative of 3 experiments, n=3 per experiment

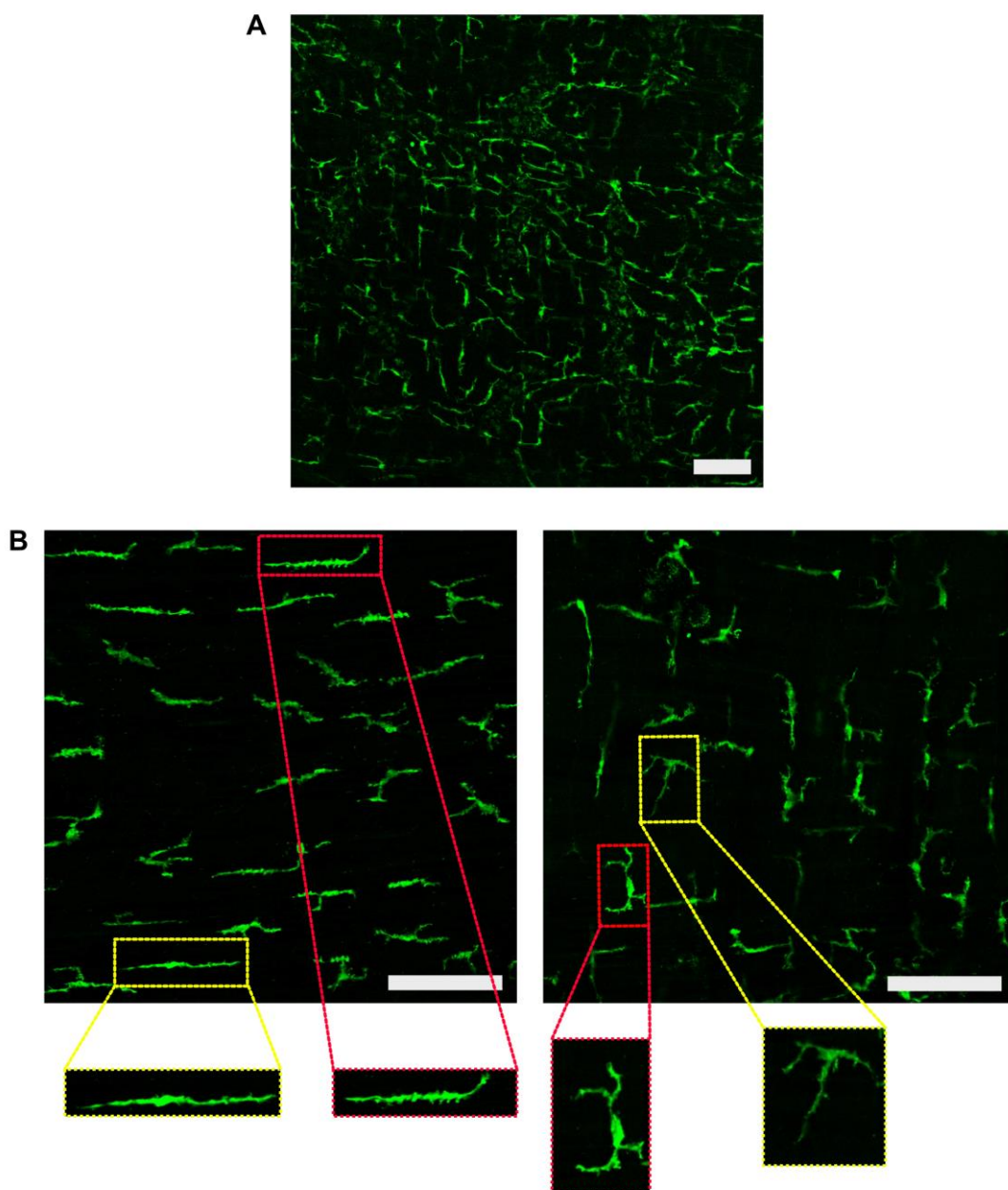


Figure 6-5 Intestinal whole mount imaging of the colon of MacGreen mice
Whole mount images of colon showing image stack of *muscularis externa* (A). (B) represents single slices of the inner (circular) muscle (LEFT) and myenteric plexus and outer muscle region, (RIGHT). Insets show magnified individual macrophage morphology. Magnification (A) X10, (B) X20. Bar =100 μ m. Images representative of 3 experiments, n=3 per experiment

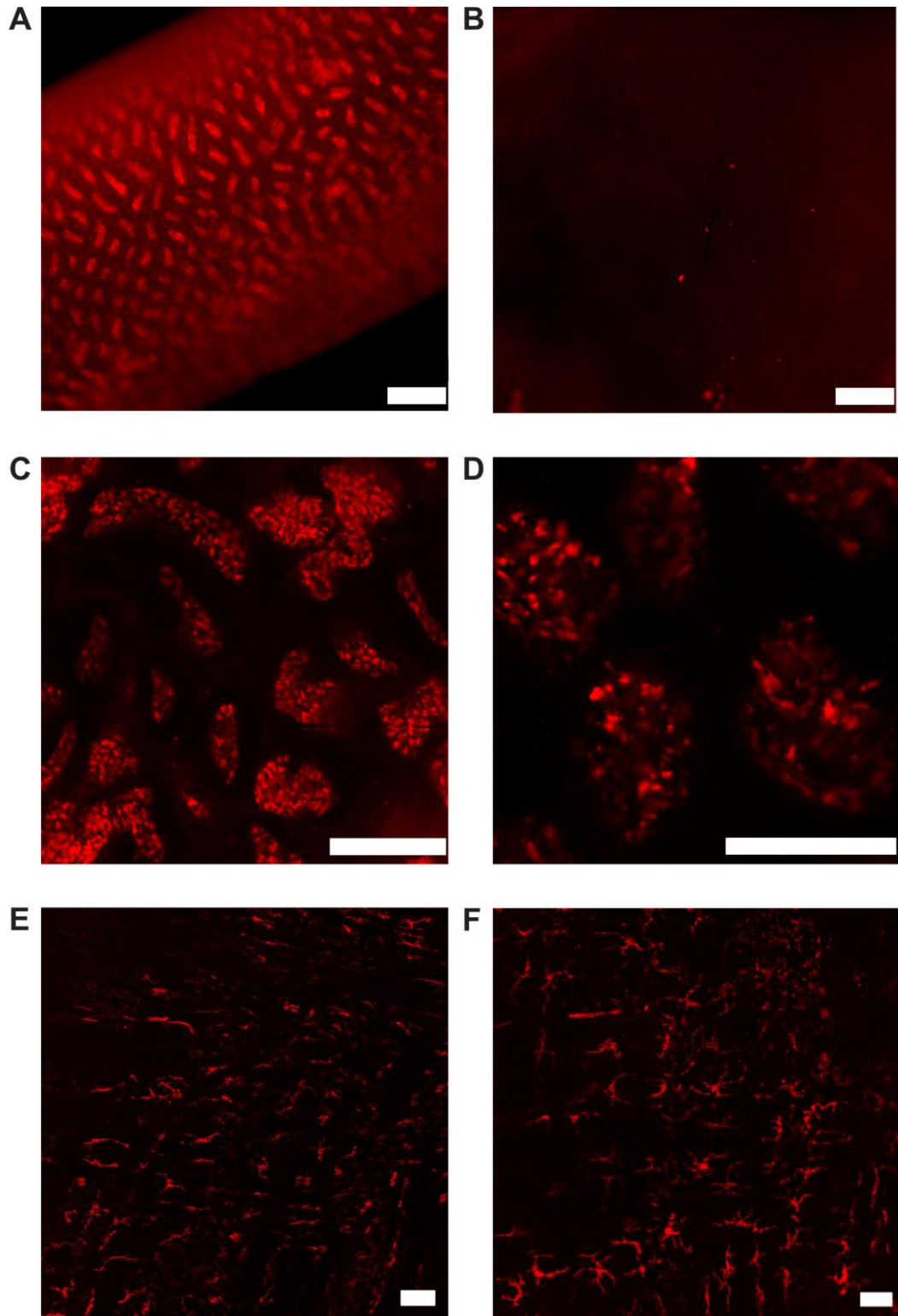


Figure 6-6 Whole mount fluorescence microscopy of the intestines of mApple mice
Ex-situ fresh intestinal whole mounts of mApple mice (A,C,D,E,F) and wild type mice (B) were imaged by fluorescence microscopy. Sections imaged are jejunum (A and B), villi of jejunum (C and D) and muscularis of jejunum (E) and colon (F). Magnification (A) and (B) X5. (C) X10. (D), (E) and (F) X20. A – D Bar=200 μ m. (E) and (F) Bar=50 μ m.

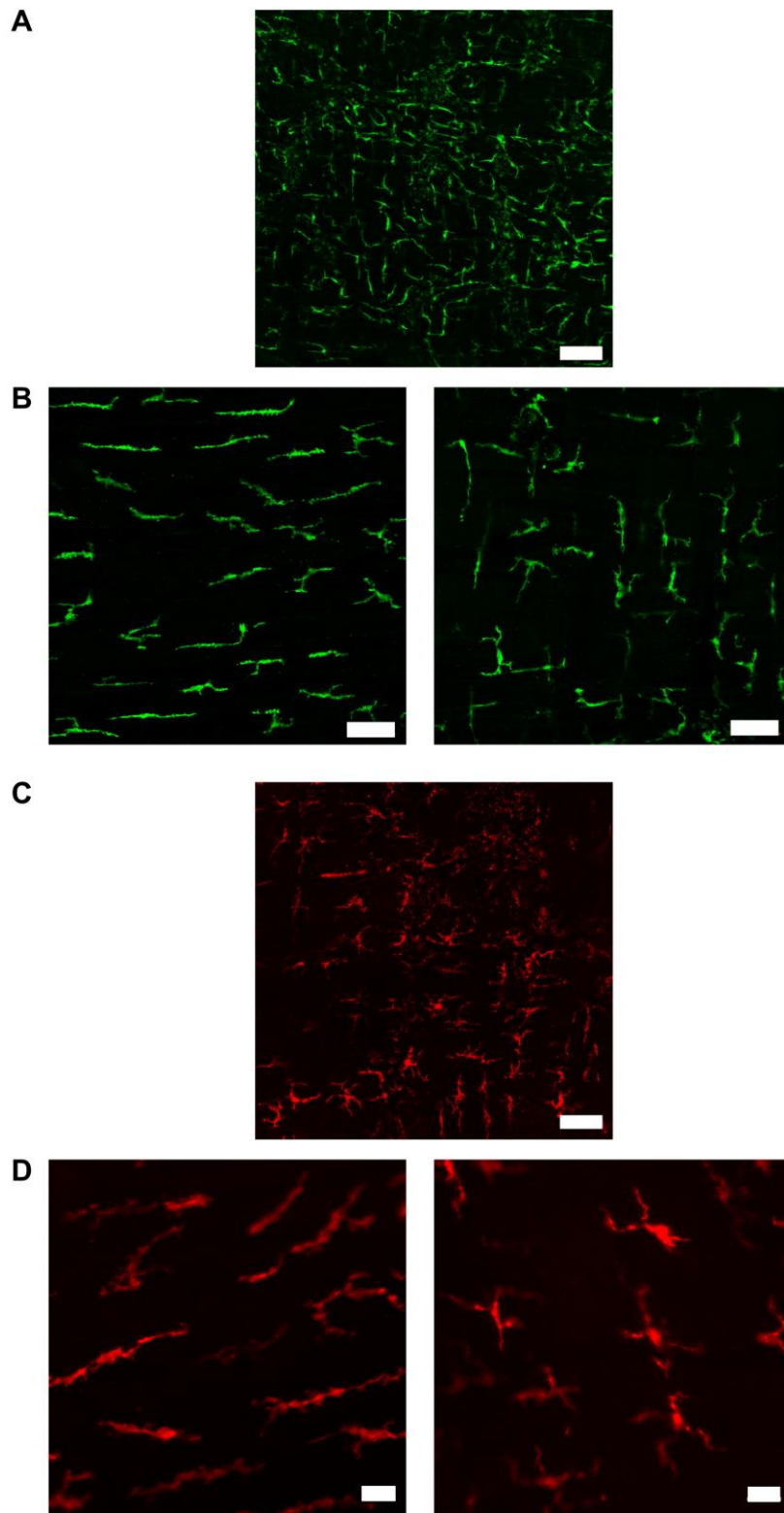


Figure 6-7 Intestinal whole mount fluorescent imaging of the *muscularis externa* in MacGreen and mApple mice

Whole mount images of colon showing image stack of *muscularis externa* in MacGreen (A) and mApple (C) mice. (B) and (D) represent single slices of the inner (circular) muscle (LEFT) and myenteric plexus and outer muscle region, (RIGHT).

Magnification: (A) and (C) X10 Bar=100 μ m, (B) X20. Bar =50 μ m. (D) X40 Bar=10 μ m.

A striking feature observed in the whole mounts is the regularity of the distribution of the MM throughout the GIT (**Figure 6-7**). This distribution and regularity resembles that seen in other resident macrophage populations particularly those in the skin (Langerhans cells) and brain (microglia). A feature of Langerhans cells and microglia is that they occupy an area within the tissue, with no overlapping of dendrites (Tremblay et al., 2011), although contact between microglia cell components has been observed (Hanisch and Kettenmann, 2007). MM also occupy a specific area with no overlapping of dendrites (**Figure 6-8**). Some dendrites were in very close proximity to each other but did not overlap (**Figure 6-9**). This close proximity suggests that, as microglia do, MM dendrites do come into contact with each other, although live imaging of whole mounts would need to be performed to demonstrate this.

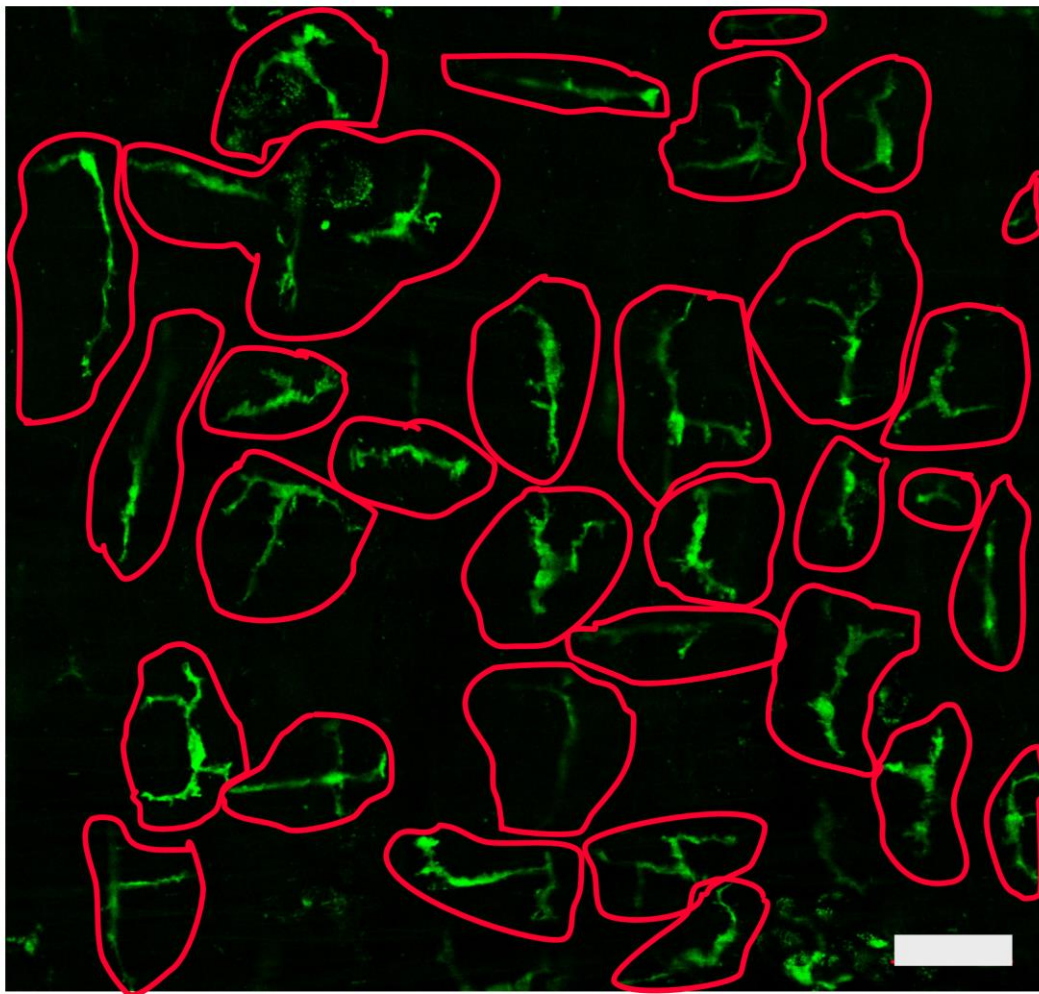


Figure 6-8 Intestinal whole mount fluorescent imaging of the *muscularis externa* in MacGreen mouse

Whole mount image of colon in a MacGreen mouse with the regional space occupied by each muscularis mapped out (red line).
Magnification X20. Bar =50 μ m

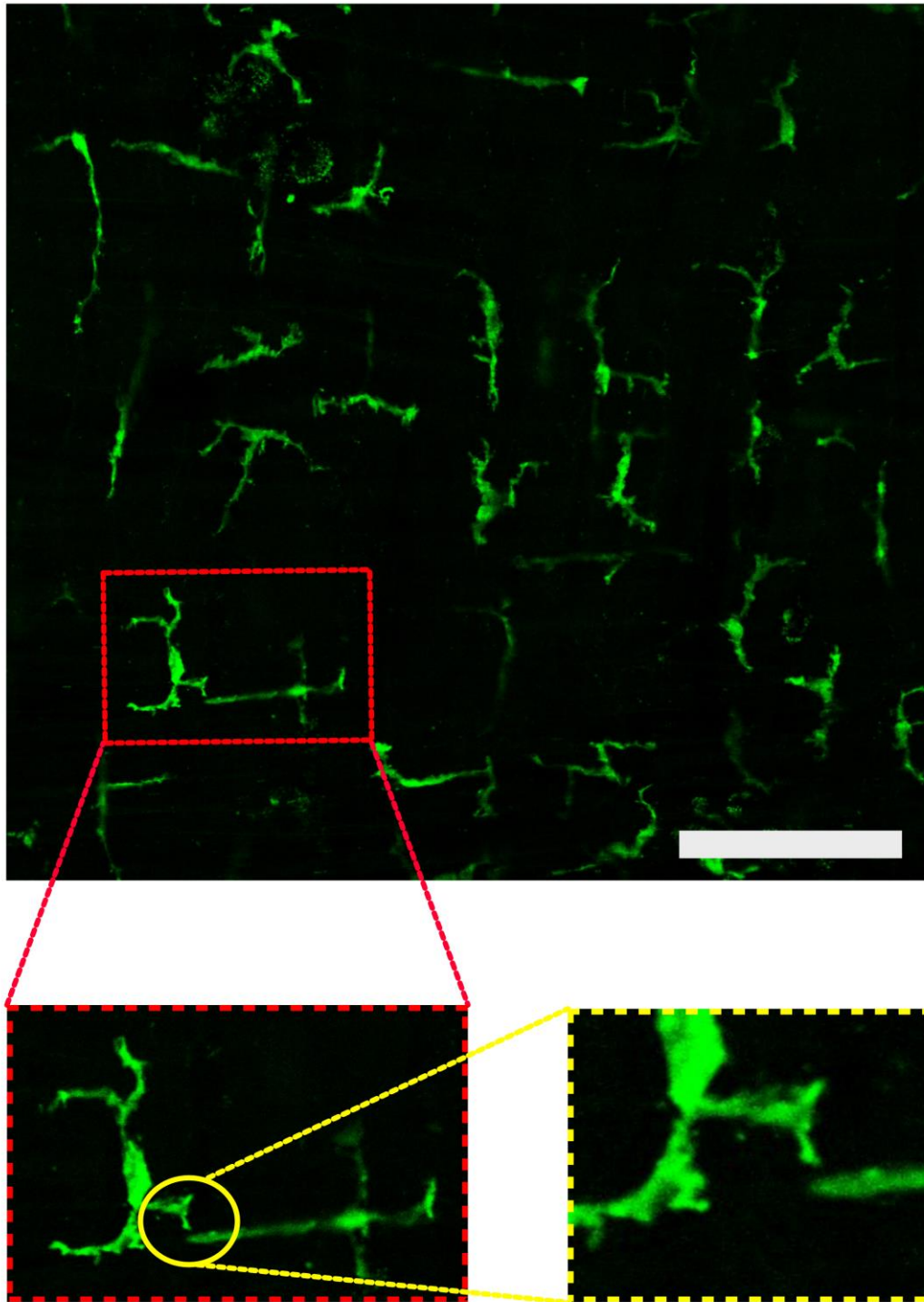


Figure 6-9 Intestinal whole mount fluorescent imaging of the *muscularis externa* in MacGreen mouse

Whole mount image of colon in a MacGreen mouse showing the proximity of dendrites to each other.

Magnification X20. Bar =100 μ m

Administration of CSF1-Fc alters cell size but not number in the muscularis externa

Previous studies, using a *Csf1r*-ECFP reporter that labels monocytes, but only a subset of tissue macrophages and DC, demonstrated that CSF1-Fc elicited an influx of monocyte-derived cells into the lamina propria (Sauter et al., 2014). CSF1-Fc also greatly increased macrophage numbers in the liver, spleen and lung (Gow et al., 2014). This change was due to both monocyte infiltration and proliferation of resident tissue macrophages (Stutchfield et al., 2015). To test the ability of CSF-1 to modulate MM numbers or function, WT mApple mice were administered either CSF1-Fc (n=3) or PBS (n=3) daily for 5 days. Following sacrifice, whole-mount fluorescence microscopy of the intestines was performed. Administration of CSF1-Fc resulted in an increase in cell size (measured as total area of fluorescence) in both the small and large intestine (**Figure 6-10**). The regular distribution of the MM remained unchanged and there was no significant difference in cell numbers, neither from infiltration of monocyte-like cells nor from regional proliferation. This differs from the effect on LpM, whereby administration of CSF1-Fc resulted in an influx of cells into the lamina propria (Sauter et al., 2014). Despite there being no effect on MM in number, there was a dramatic morphological change in response to CSF1-Fc administration, whereby MM in intestine became more amoeboid.

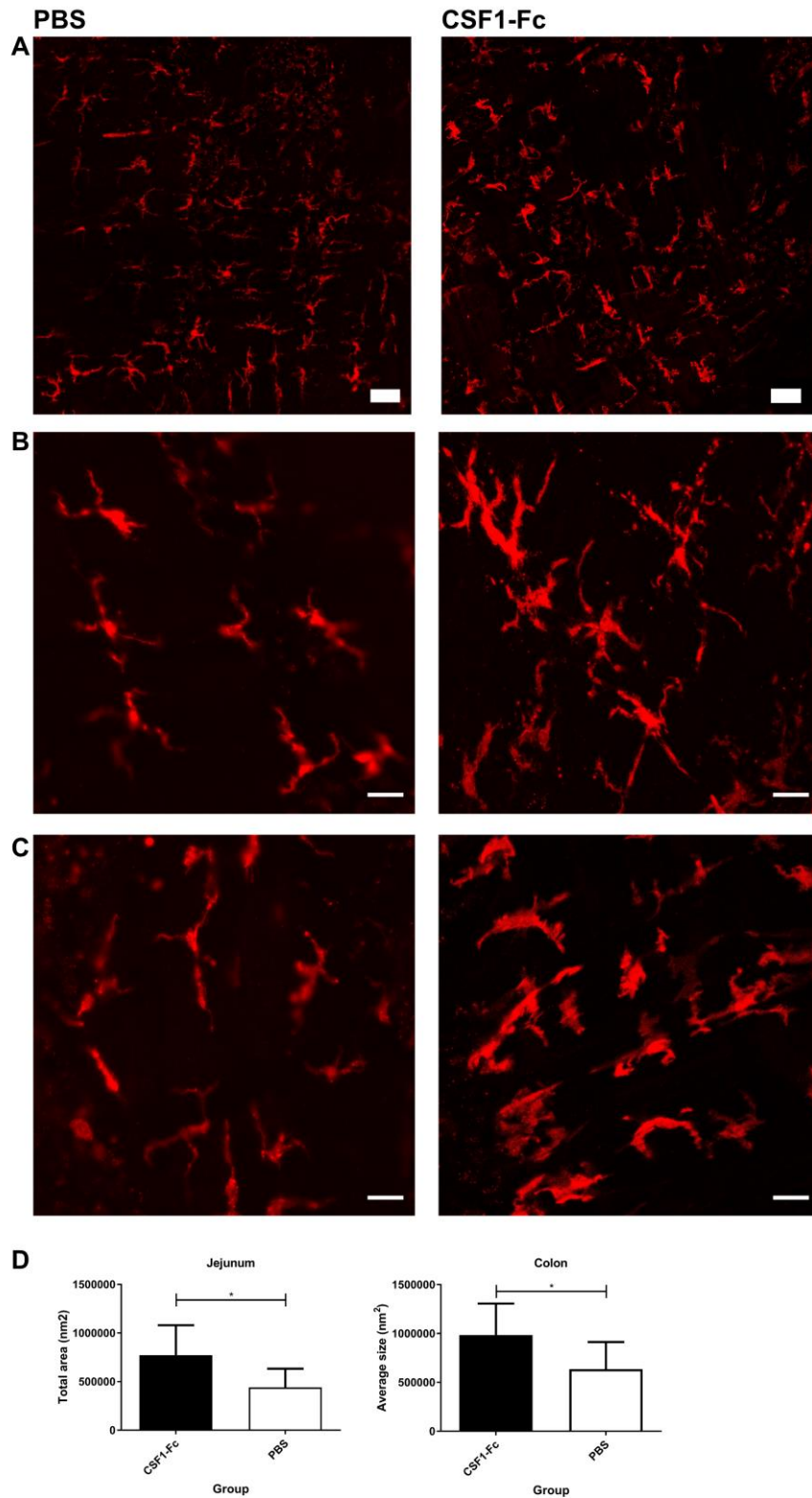


Figure 6-10 Effect of CSF1-Fc on *muscularis externa* macrophages

Whole mount image stack (A) and slices (B and C) of jejunum (B) and colon (C) showing morphology of *muscularis externa* macrophages after 5 days of CSF1-Fc treatment. (D) Bar plot showing area of fluorescence in jejunum and colon. Data shown mean \pm 95% CI. Significance determined via unpaired t-test. * $p < 0.05$ Magnification: (A) X10 Bar=50 μ m. Magnification: (B) and (C) X40 Bar=10 μ m

6.2.3 Administration of CSF1-Fc in a mouse model of POI drives the differentiation of pro resolving macrophages

This section of work has been previously published in Gut entitled 'CCR2-dependent monocyte-derived macrophages resolve inflammation and restore gut motility in postoperative ileus' and was performed in collaboration with Professor Gianluca Matteoli. The aim for this study was to evaluate the effect of CSF1-Fc in a murine model of IM-induced POI in WT mice. Professor Matteoli's group was interested in the effect of CSF1-Fc administration to *CCr2^{-/-}* mice. The work on both WT and *CCr2^{-/-}* mice was performed concurrently at TARGID, Leuven, Belgium. Full results are in published in Farro *et al.* 2017 and are summarised below.

CSF1-Fc was administered to WT mice for 5 days, commencing 24 hours prior to IM and then daily until sacrifice (Day 3 post manipulation). CSF1-Fc treatment increased spleen and liver weight compared to mice receiving saline alone (**Figure 6-11**) as seen in previous studies (Gow *et al.*, 2014, Sauter *et al.*, 2016, Stutchfield *et al.*, 2015). No significant difference in GI motility was observed between the two groups (**Figure 6-12-C**). CSF1-Fc administration increased the number of monocytes in the muscularis 3 days following IM, as well as the number of Ly6C^{hi}MHCII⁺ immature macrophages and Ly6C^{lo}MHCII^{lo} macrophages (**Figure 6-12-A**). CSF1-Fc administration failed to increase cell numbers in WT gut which had not undergone manipulation (see section above). This would imply that manipulation induced infiltration occurred, which was increased with CSF1-Fc treatment. The two data sets are not entirely comparable as, measurement between the two are different; manipulated ME cell numbers were measured by flow cytometry following digestion of the ME whereas non-manipulated WT muscularis was analysed by imaging alone. Nevertheless, the results are consistent with the finding that CSF1-Fc acts on monocyte-derived cell populations and not resident cell populations (Stutchfield *et al.*, 2015). In contrast however, Sauter *et al.* demonstrated local resident cell proliferation (namely, Kupffer cells in the liver) in response to CSF1-Fc by (Sauter *et al.*, 2016).

The main impact of CSF1-Fc treatment on WT mice was to inhibit neutrophil infiltration into the ME (**Figure 6-13**) suggesting monocytes and/or macrophages limit neutrophil migration into the ME. As a result, CSF1-Fc treated mice had significantly lower numbers of reactive oxygen species (ROS)-producing neutrophils (**Figure 6-12-B**). Expression of anti-inflammatory and pro-resolving genes was also increased with CSF1-Fc treatment. Expression of the anti-inflammatory genes *Arg1* and *Il10* were increased (although *Arg1* not significantly) with CSF1-Fc treatment as were pro-resolving genes such as *Stab1*, *Lyve1*, *Mrc1* and *Cd163* (**Figure 6-14**).

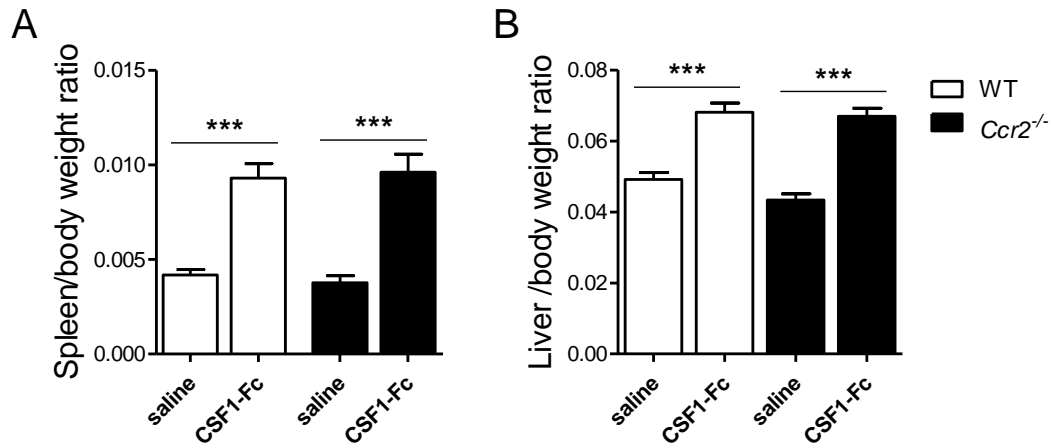


Figure 6-11 CSF1-Fc treatment increases spleen and liver weight (Supplementary Figure 10 Farro *et al.* 2017).

Spleen (A) and liver (B) weight ratio over body weight of WT and *Ccr2*^{-/-} mice treated with (0.75 µg/g) CSF1 Fc or saline for 4 consecutive days. Statistical significance between CSF1-Fc and saline-treated data sets was determined via unpaired t-test (***) P < 0.0001)

Reproduced from: CCR2-dependent monocyte-derived macrophages resolve inflammation and restore gut motility in post-operative ileus, Farro, G., Stakenborg, M., Gomez-Pinilla, P. J., Labeeuw, E., Goverse, G., Di Giovangiulio, M., Stakenborg, N., Meroni, E., D'Errico, F., Elkrim, Y. Laoui, D., Lisowski, Z. M., Sauter, K. A., Hume, D. A., Van Ginderachter, J. A., Boeckxstaens, G. E., Matteoli, G. 66:20982109, © Article authors 2017 with permission from BMJ Publishing Group Ltd.

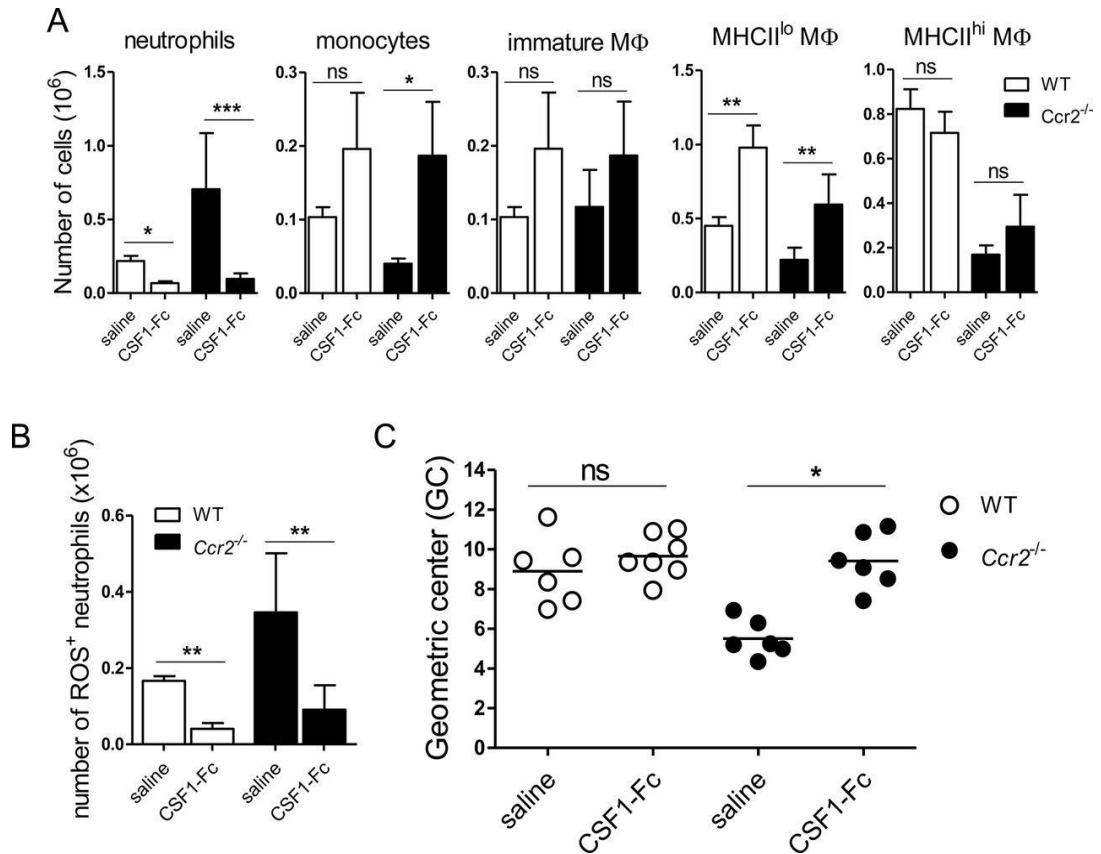


Figure 6-12 Colony-stimulating factor (CSF) 1 drives pro-resolving macrophage differentiation and favours recovery of GI motility (Figure 8 Farro *et al.* 2017)

WT and *Ccr2*^{-/-} mice undergoing intestinal manipulation (IM) were treated with either 0.75 µg/g CSF1-Fc or saline. Functional and inflammatory parameters were assessed 3 days after IM. **(A)** Absolute numbers of Ly6C^{hi}MHCII⁻ monocytes, Ly6C⁺MHCII⁺ immature MΦs, Ly6C⁻MHCII^{lo} and Ly6C⁻MHCII^{hi} MΦs in WT and *Ccr2*^{-/-} mice. Statistical significance between CSF1-Fc and saline-treated data sets was determined via unpaired t-test (*p<0.05, **p<0.001, ***p<0.0001; ns, not significant). **(B)** Absolute numbers of ROS⁺ neutrophils. Statistical significance between CSF1-Fc and saline-treated data sets was determined via unpaired t-test (**p<0.001). **(C)** Dots represent GC values from individual mice; mean is also shown. Statistical significance between CSF1-Fc and saline-treated data sets was determined via unpaired t-test (*p<0.05).

Reproduced from: CCR2-dependent monocyte-derived macrophages resolve inflammation and restore gut motility in post-operative ileus, Farro, G., Stakenborg, M., Gomez-Pinilla, P. J., Labeeuw, E., Goverse, G., Di Giovangiulio, M., Stakenborg, N., Meroni, E., D'Errico, F., Elkrim, Y. Laoui, D., Lisowski, Z. M., Sauter, K. A., Hume, D. A., Van Ginderachter, J. A., Boeckstaens, G. E., Matteoli, G. 66:20982109, © Article authors 2017 with permission from BMJ Publishing Group Ltd.

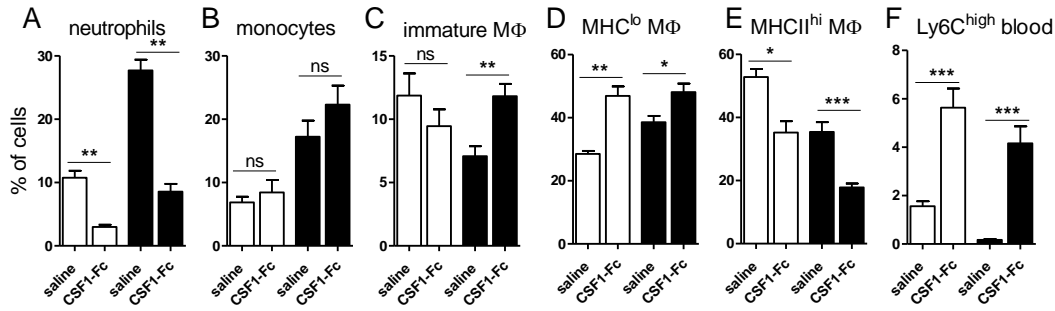


Figure 6-13 CSF1 reduces influx of neutrophils and drives accumulation of macrophages into the muscularis externa during recovery after IM (Supplementary Figure 11 Farro *et al.* 2017)

WT and *Ccr2*^{-/-} mice undergoing IM were treated with either CSF1-Fc or saline. Percentages of CD11b⁺Ly6G⁺ neutrophils (A), Ly6C^{hi}MHCII^{lo} monocytes (B), Ly6C⁺MHCII⁺ immature MΦ (C), Ly6C⁺MHCII^{lo} (D) Ly6C^{hi}MHCII^{hi} MΦ (E) in the ME and Ly6C^{hi}MHCII^{lo} blood monocytes (F) in WT and *Ccr2*^{-/-} mice 3 days after IM. Statistical significance between CSF1-Fc and saline-treated data sets was determined via unpaired t-test (* P < 0.05, ** P < 0.001, *** P < 0.0001 and ns= not significant).

Reproduced from: CCR2-dependent monocyte-derived macrophages resolve inflammation and restore gut motility in post-operative ileus, Farro, G., Stakenborg, M., Gomez-Pinilla, P. J., Labeeuw, E., Goverse, G., Di Giovangiulio, M., Stakenborg, N., Meroni, E., D'Errico, F., Elkrim, Y. Laoui, D., Lisowski, Z. M., Sauter, K. A., Hume, D. A., Van Ginderachter, J. A., Boeckxstaens, G. E., Matteoli, G. 66:20982109, © Article authors 2017 with permission from BMJ Publishing Group Ltd.

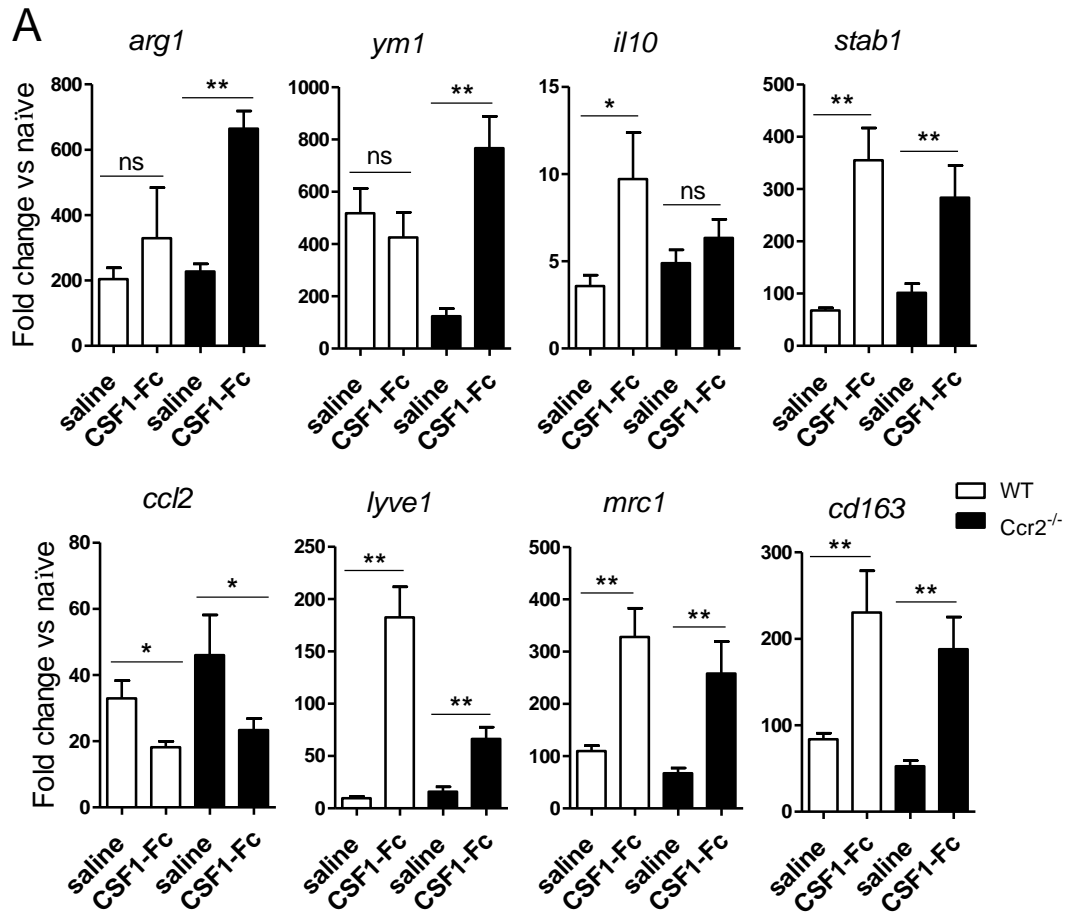


Figure 6-14 CSF1-Fc treatment drives expression of anti-inflammatory genes in the muscularis externa during recovery (Supplementary Figure 12 Farro et al. 2017)

Gene expression levels of anti-inflammatory genes were measured in homogenates of ME from WT and *Ccr2*^{-/-} mice treated with either CSF1-Fc or saline 3 days after IM. (A) mRNA levels are expressed as fold change mean values \pm SEM versus naïve. Statistical significance between CSF1-Fc and saline-treated data sets was determined via unpaired t-test (* $P < 0.05$, ** $P < 0.001$ and ns= not significant).

Reproduced from: CCR2-dependent monocyte-derived macrophages resolve inflammation and restore gut motility in post-operative ileus, Farro, G., Stakenborg, M., Gomez-Pinilla, P. J., Labeeuw, E., Goverse, G., Di Giovangiulio, M., Stakenborg, N., Meroni, E., D'Errico, F., Elkrin, Y., Laoui, D., Lisowski, Z. M., Sauter, K. A., Hume, D. A., Van Ginderachter, J. A., Boeckstaens, G. E., Matteoli, G. 66:20982109, © Article authors 2017 with permission from BMJ Publishing Group Ltd.

6.2.4 Microarray analysis of muscularis externa treated with CSF1-Fc

Based upon the morphological impacts detected with the *Csf1r*-mApple transgene, it appeared that MM were responsive to exogenous CSF-1. To analyse gene expression changes in non-manipulated *muscularis* in response to CSF1-Fc administration, gene expression arrays were performed to further determine the potential pro-resolving benefit of CSF1-Fc. RNA was extracted from the muscularis of PBS-treated (n=3) and CSF1-Fc treated (n=3) mice that had undergone IM. RNA extractions were performed by Michelle Stakenbourg, TARGID, KU Leuven. RNA quality was analysed using TapeStation and samples with a RIN >7 were used. This was performed at The Roslin Institute, University of Edinburgh.

Expression data were Robust Multi-array Average (RMA) normalised prior to analysis. Differential expression analysis was performed to identify genes most differentially expressed between PBS and CSF1-Fc treated ME in WT mice. Of 22,407 genes 716 showed significant differential expression with only 15 upregulated with a log₂ fold change (fc) of >1 and 38 downregulated <-1 log₂ fc (**Figure 6-15**). **Figure 6-15** shows a reduction in the detection of neutrophil markers (*S100a8* and *S100a9*) which agrees with the findings in the previous section showing reduced neutrophil numbers in CSF1-Fc-treated mice in manipulate intestine, and with previous published studies (Stutchfield et al., 2015). There is no evidence of a substantially increased detection of monocyte-macrophage markers such as *Csf1r* and *Cd14*, although *Cx3cr1* expression was increased (**Table 6-1**).

Table 6-1 Average expression values of monocyte-macrophage markers

Gene	Avg expression Saline	Average expression CSF1-Fc	LogFC	p
<i>Cx3cr1</i>	7.39	8.44	1.05	0.01
<i>Csf1r</i>	10.26	10.90	0.64	0.02
<i>CD14</i>	7.90	8.26	0.36	0.35

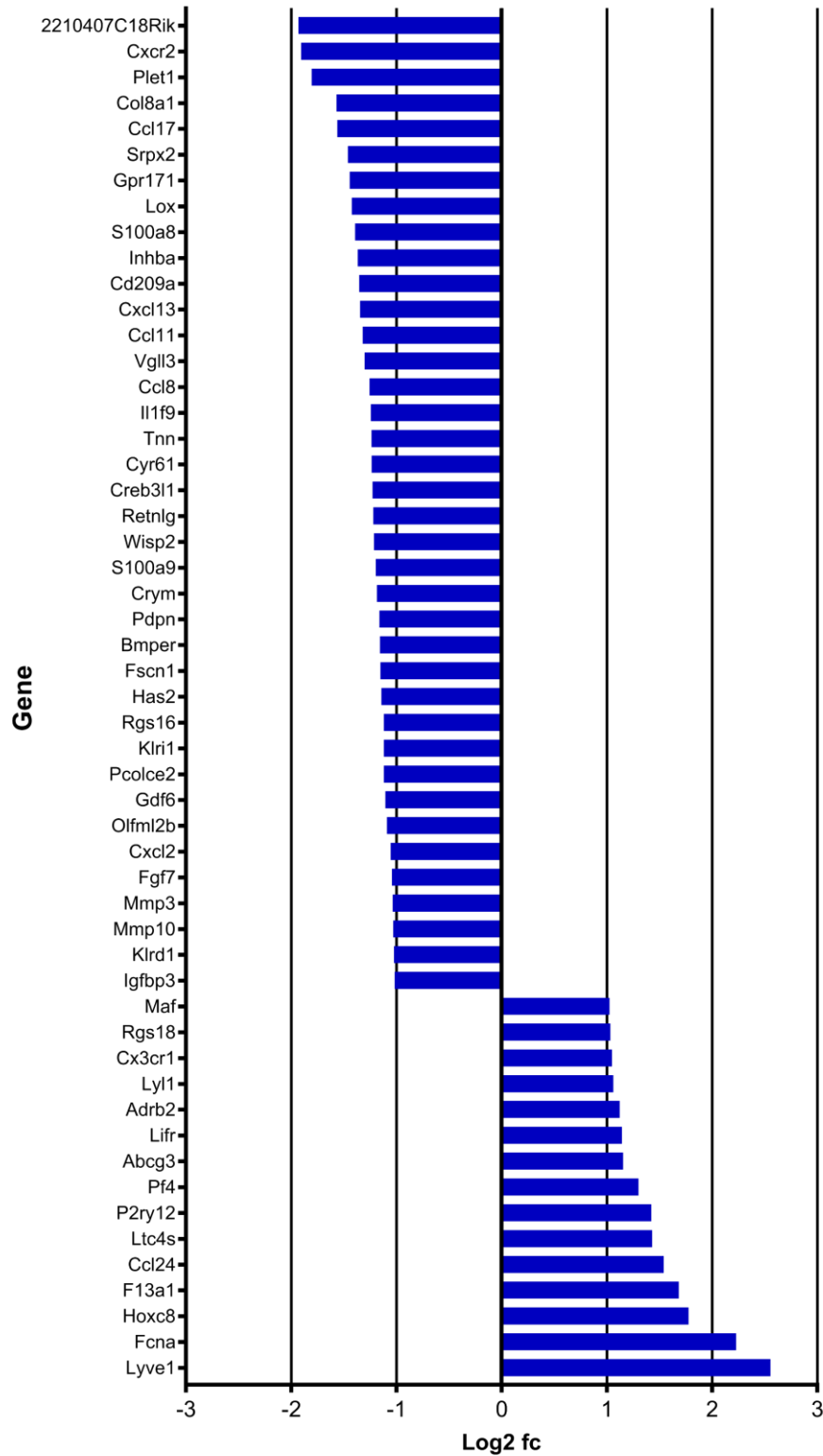


Figure 6-15 Top genes induced and suppressed following CSF1-Fc administration in manipulated muscularis externa
 Microarray data of genes induced ($\text{Log}_2\text{fc} > 1$) or suppressed ($\text{log}_2\text{fc} < -1$) by CSF1-Fc in the muscularis externa of mice following intestinal manipulation.

6.3 Discussion

The aim of this chapter was to evaluate the effect of CSF1-Fc, a novel agent that promotes monocyte production and recruitment and macrophage maturation and local proliferation, as a potential therapeutic approach in a mouse model of POI. POI occurs following abdominal surgery. IM during surgery is thought to trigger DAMPs and PAMPs, triggering an inflammatory reaction of the MMs which results in infiltration of the ME with leukocytes (De Jonge et al., 2003, Kalff et al., 1999b). The administration of CSF-1 has been tested in several diseases with multiple effects (Hume and MacDonald, 2012). In some circumstances, such as in disseminated candidiasis, CSF-1 treatment exacerbated the disease; whereas, pre-treatment with CSF-1 was found to be protective from the disease (Cenci et al., 1991). This is not unsurprising given that some pathologies are macrophage-mediated, but also due to CSF-1 driving a pro-inflammatory macrophage phenotype in some scenarios (Abd et al., 1991). In models of ischaemic kidney disease (Alikhan et al., 2011) and partial hepatectomy (Stutchfield et al., 2015), the increase in pro-resolving macrophages improved recovery. In this preliminary study, it was decided to initially evaluate the effect of CSF1-Fc administration to mice undergoing IM-induced POI model as a pre-treatment.

Prior to use in association with the mouse model of POI, the effect of CSF1-Fc on normal intestine was evaluated using the *Csf1r*-EGFP and *Csf1r*-mApple mouse (Sasmono et al., 2003, Hawley et al., 2018). Firstly, the MM populations were evaluated in both transgenes (**Figure 6-4**, **Figure 6-5**, **Figure 6-6** and **Figure 6-7**). This confirmed that the *Csf1r*-mApple transgene (a newer strain of mouse) had identical expression in the ME in both the small and large intestine. The MM formed a regular network throughout the whole GIT, with either a stellate or bipolar morphology (**Figure 6-5** and **Figure 6-7**). This difference in morphology represents two subsets of MMs with different phenotypes, with stellate macrophages associated with the myenteric plexus and bipolar macrophages associated with the muscle layers (Gabanyi et al., 2016). Other macrophage populations with a stellate morphology are microglia (Tremblay et al., 2011, Nimmerjahn et al., 2005) and Langerhans cells (Mulholland et al., 2006). MM occupy an area in the ME and there is no overlapping of dendrites (**Figure 6-8** and **Figure 6-9**) although some do come into close proximity (**Figure 6-9**) suggesting that, as observed in microglia (Nimmerjahn et al., 2005, Hanisch and Kettenmann, 2007), cell contact and communication does occur. These data suggest that MM occupy a specific niche, a feature also seen with other intestinal

macrophages; for example, LpM are closely associated with the intestinal crypt epithelium (Sehgal et al., 2018).

Intestinal transit time (**Figure 6-2**) and the morphology of the MM population (**Figure 6-10**) was evaluated following administration of CSF1-Fc to normal WT mice. Administration of CSF1-Fc did not alter transit time, and therefore does not appear to regulate intestinal motility. Neurons secrete CSF-1 to maintain MM populations (Muller et al., 2014) although enteric neurons are not required for MM colonisation of the intestine (Avetisyan et al., 2018). In return, MM, via secretion of BMP2, maintain intestinal motility (Muller et al., 2014). The data in the present study suggest that an increase in CSF1-Fc does not result in an alteration of intestinal motility. To determine whether this was due to a failure of CSF1-Fc acting on MM, whole mount imaging of ME was performed. In response to CSF1-Fc, MMs became more amoeboid, with a greater area occupied by each cell, thus demonstrating that MM do indeed respond to CSF1-Fc administration (**Figure 6-10**). Although CSF1-Fc administration results in an increase in monocyte-derived macrophages in the lamina propria (Sauter et al., 2014) and increased local proliferation of macrophages in the liver (Stutchfield et al., 2015, Sauter et al., 2016), there was no evidence of this cellular expansion with respect to the MMs. This may reflect the fact that LpMs and Kupffer cells are replenished by monocytes (Bain et al., 2014, Sauter et al., 2016). To date very few fate mapping data of MMs exist, but some early work does show that MMs expressing MHCII are present in the ME and myenteric plexus in embryos and new-born mice (Mikkelsen et al., 2004).

Next, CSF1-Fc was administered to mice prior to undergoing IM. Again, mice showed the expected increase in liver and spleen weight (**Figure 6-11**) as reported previously (Gow et al., 2014, Sauter et al., 2016). CSF1-Fc treatment increased circulating monocytes and pro-tissue repair macrophages (**Figure 6-12** and **Figure 6-13**). CSF1-Fc drives macrophages towards a pro-tissue repair phenotype (Martinez et al., 2006) and as such has been shown to be beneficial in recovery of kidney and liver disease models. In this model of POI, CSF1-Fc increased macrophages in the ME (**Figure 6-13**) and reduced ROS-producing neutrophils (**Figure 6-12**). Secondly, as reported in other disease models, there was an increase in anti-inflammatory gene expression of *Arg1*, *Ym1*, *Il10*, *Stab1*, *lyve1*, *Mrc1* and *Cd163* (**Figure 6-14**). Preliminary analysis of differential gene expression of manipulated ME corroborates these findings with a reduction in neutrophil (e.g. *S100a8*, *S100a9*) associated genes and an upregulation in anti-inflammatory genes (e.g. *Lyve1*, *Ccl24*).

These data show that CSF1-Fc does act on MM in non-manipulated mouse intestine, although this doesn't result in an alteration of intestinal motility. Furthermore, in a mouse model of IM-induced POI, CSF1-Fc administration reduces neutrophilic infiltration in the ME and promotes tissue recovery by increasing monocytes and macrophages in the *muscularis*. In addition, CSF1-Fc promotes further tissue repair by increasing anti-inflammatory gene expression in the ME. These data suggest that CSF1-Fc may be beneficial in POI to promote tissue repair and recovery. Together with the data by Professor Matteoli's group using *Ccr2*^{-/-} mice demonstrating a requirement for monocytes in tissue repair in POI, these findings support a potential need for future therapeutic discovery initiatives to focus on the promotion of tissue repair by monocytes and macrophages and not solely on anti-inflammatory treatments aimed at blocking these pathways.

Chapter 7. General discussion, future directions and conclusion

7.1 General Discussion

The aims of this thesis were to further our knowledge of equine macrophage biology with a focus on intestinal macrophages and their role in post-operative ileus (POI). Few studies have been conducted on the pathophysiology of POI in the horse. No studies have been conducted on the contributory role of equine resident intestinal macrophages, cells which have been shown to be pivotal in both rodent (Kalff et al., 1998a, Farro et al., 2017) and human (Kalff et al., 2003) POI studies via their role in triggering the inflammatory response that ultimately results in smooth muscle dysfunction.

In **Chapter 3**, the distribution of macrophages in the equine GIT was analysed. The first aim of the chapter was to identify a suitable macrophage marker. A significant limiting factor in the study of equine immunology is the lack of available antibodies. CD163, a macrophage scavenger receptor, is expressed on most macrophage tissue populations (Fabriek et al., 2005) and in rats this marker is present on the most abundant macrophage population in the *muscularis externa* (ME) (Kalff et al., 1998b). CD163 (Clone AM-3K) has previously been used in equine intestinal tissue (Yamate et al., 2000, Grosche et al., 2011). Following antibody optimisation, intestinal tissue from the stomach to the small colon from 10 non-colic horses was stained for CD163 (Clone KT-103 as Clone AM-3K did not work). CD163⁺ cells were present in all tissue layers of the equine intestine: mucosa, submucosa, ME and the serosa. CD163⁺ cells were regularly distributed within the ME, with accumulations adjacent to the myenteric plexus, and therefore to intestinal motility effector cells such as neurons and the Interstitial Cells of Cajal (ICC), supporting a potential influential role of macrophages on intestinal motility, as reported in mice (Muller et al., 2014).

Building upon the work in **Chapter 3**, **Chapter 4** describes the attempt to optimise protocols aimed at isolating intestinal macrophages from the horse GIT to characterise the function and phenotype of the 2 subpopulations (lamina propria and MM). Due to several methodological problems, an alternative project strategy was formulated and equine bone marrow derived macrophages (eqBMDMs) were instead isolated, differentiated with CSF-1 and characterised and stimulated with LPS. Bone marrow-derived macrophages (BMDMs) are primary macrophage cells. They are derived from progenitor cells and in the presence of the macrophage lineage specific growth factor CSF-1 they differentiate and proliferate into macrophages (Hume and Gordon, 1983). This technique has been used extensively in the Hume laboratory in other large animal species such as pig (Kapetanovic et al., 2012), sheep (Clark et al.,

2017, Pridans et al., 2016), goat, cow and buffalo (Young et al., 2018). Previous work in the group demonstrated that equine cells do respond to recombinant human CSF-1 (rhCSF1) (Karagianni et al., 2013, Karagianni, 2015, Karagianni et al., 2017). In this present study, progenitor cells from adult equine bone marrow were successfully differentiated into macrophages in the presence of rhCSF-1. EqBMDMs morphology and functionality was assessed using microscopy, flow cytometry and phagocytosis assays, thus confirming their identity as macrophages.

Flow cytometry analysis of eqBMDMs failed to show expression of CD163 on eqBMDMs, a similar finding to that observed with pig bone-marrow derived macrophages (Kapetanovic et al., 2012). Alveolar macrophages did express CD163 (Karagianni et al., 2013) as did intestinal macrophages in the equine GIT in this present study (**Chapter 3**) and in prior studies (Yamate et al., 2000). CD163 is expressed on mature resident tissue macrophages (Fabriek et al., 2005). Bone marrow-derived macrophages are primary cells, and alveolar macrophages are resident tissue macrophages. Therefore, a possible explanation of the difference in expression could be the lack of regional signals in bone marrow derived macrophages that are needed for the expression of certain receptors such as CD163. Alveolar macrophages may have 'received' these signals from the lung, prior to collection and culture.

LPS translocation from the gut lumen is an activator of ME macrophages in POI (Eskandari et al., 1997). The response of eqBMDMs to LPS stimulation included increased expression of positive control genes, *TNF- α* and *IDO1*. Extracted mRNA was also subjected to transcriptomic (RNA-Seq) analysis. Differential gene expression and network cluster analysis demonstrated an inflammatory response, indicated by the production of pro-inflammatory cytokines such as interleukin 1 beta (IL-1 β) and interleukin 6 (IL-6). However, in contrast to rodent macrophages, eqBMDMs failed to produce nitric oxide in response to LPS, indicating species-specific variation in innate immune biology. This corroborates earlier findings by our group that equine alveolar macrophages do not produce NO in response to LPS (Karagianni et al., 2013, Karagianni et al., 2017). This difference between rodents and horse is not surprising given the species divergence in arginine metabolism demonstrated in a recent study looking at transcriptional regulation of genes associated with the arginine pathway in several species (Young et al., 2018). Rats produce NO in response to LPS, a response shared with mice. Goat macrophages produce detectable NO, but sheep do not although both species showed an induction in *NOS2* mRNA. Horse and pig do not produce NO nor is there an induction in mRNA. Cattle produce NO and induce the mRNA; buffalo produced lower levels of NO production and mRNA induction when

compared to cattle. These differing response to LPS were attributed to divergence in the *iNOS* (*NOS2*) promoter sequences between all the species (Young et al., 2018). The NO pathway is important in innate immune response to pathogens therefore these differences in the metabolism of arginine imply species-specific responses to pathogens.

A feature of the equine LPS response was the number of negative feedback regulators identified in mouse and human macrophage responses that were apparently absent in the equine DE genes. This may explain why the horse is more susceptible to LPS/endotoxaemia compared to other species, such as mouse (Brade, 1999, Dinges and Schlievert, 2001).

Utilising the data generated in **Chapter 4**, **Chapter 5** compared gene expression in intestinal samples from horses undergoing abdominal surgery for colic (abdominal pain) with non-colic control horses. The colic group had evidence of induction *IL-1 β* , *IL-6*, *CCL2* and *TNF- α* mRNA expression in the mucosa and ME when compared to the control group, consistent with activation of the resident macrophages. This corroborates findings in humans undergoing laparotomy (Kalff et al., 2003) and mice undergoing IM (Farro et al., 2017). Whilst some similarities between species exist, the absence of *NOS2* upregulation highlights inter-species variation stressing the importance of considering the target species when using alternative species models to develop potential therapeutic targets. Horses that developed post-operative reflux (POR), a clinical indicator of POI, had increased gene expression of *IL-1 β* , *IL-6* and *TNF- α* compared to horses that did not develop POR. These preliminary data are consistent with activation of macrophages within the ME of horses undergoing abdominal surgery for colic and support a potential association with the subsequent development of POI. *IL-6*, *TNF- α* , *IL1B* and *PTGS2* can all inhibit smooth muscle contractility, which results in a functional inhibition of intestinal motility. These data do not however permit any definitive conclusions regarding the mechanism of macrophage activation; this may be attributable to either intestinal manipulation or the nature of the pre-existing condition which warranted surgical intervention.

The final part of this project investigated the potential value of Fc fusion protein (CSF1-Fc), a long-acting form of CSF-1, as a treatment for POI using a mouse model (**Chapter 6**). Firstly, the effect of CSF1-Fc on the mouse *muscularis* was evaluated by measuring intestinal transit and confocal microscopy of the *muscularis*. Due to the close spatial relationship of resident MM with the myenteric plexus in the intestine, communication between MMs and the motility effector cells within the myenteric plexus has long been hypothesised. This was recently demonstrated in mice, whereby

MM communicate with enteric neurons via signalling with BMP2. In return, enteric neurons produce CSF-1, a factor required for macrophage survival, suggesting a synergistic relationship between the enteric nervous system and MMS. In this study, administration of exogenous CSF-1 did not alter intestinal motility, although morphological changes in the MM were observed. In contrast to LpM, CSF-1 administration failed to result in an influx of macrophages into the ME of the intestine (Bain et al., 2014). In comparison, in a murine manipulation-induced POI model, administration of CSF1-Fc resulted in a reduction in neutrophil infiltration into the ME and an increase in the number of macrophages in the ME. RT-qPCR and network cluster analysis of the ME revealed clusters of genes induced and downregulated in association with CSF1-Fc administration prior to IM in WT mice. This revealed increased expression of both anti-inflammatory and pro-resolving genes. These data, when considered in conjunction with the data confirming the role of monocytes in the resolution of POI, suggest that future efforts to identify potential therapeutic targets should focus on the mechanisms which underpin the resolution of inflammation as well as mechanisms which reduce inflammation.

In this study cohort, mice were pre-treated with CSF1-Fc prior to IM. This differs from the clinical situation with respect to colic surgery in the horse, whereby surgical intervention is generally required immediately upon clinical presentation to a surgical facility. Furthermore, such cases will generally have pre-existing inflammatory/ischaemic intestinal lesions. These factors would require consideration prior to any attempts to evaluate CSF1-Fc as a potential therapeutic approach in equine POI. In the majority of equine colic cases, pre-treatment with CSF1-Fc would not be possible; this would only be applicable in cases undergoing an elective exploratory procedure (e.g. for the investigation of recurrent colic episodes). Furthermore, it should also be considered that CSF-1 administration has resulted in a worsening of clinical signs in relation to certain diseases, such as disseminated candidiasis, (Cenci et al., 1991).

7.2 Limitations of the study

Horses used in this study were of varying ages, breeds and backgrounds. Despite appearing 'clinically normal' the full clinical histories of horses used, either as non-colic or colic cases was unknown. The heterogenous nature of these equine subjects is an unavoidable limitation in these large animal studies involving clinical patients, but should not preclude clinical studies such as this, owing to the species differences observed between the horse and small laboratory mammals.

In **Chapter 3**, CD163 was the sole marker used for the identification of macrophages. The use of only one macrophage marker limits these results to only particular subset of intestinal macrophages in the horse. Given the heterogeneity in macrophage populations, ideally other markers should be used e.g. CD14, CD68, MHCII to further identify and characterise the macrophage populations in the equine GIT. The lack of available reagents (e.g. antibodies) represents a significant limiting factor in studies of the equine innate immune system. Whilst cross reactivity of reagents does occur (as in this study with CD163), the required optimisation exercise for each antibody and/or reagent used can be time consuming, costly and is not always successful. Therefore, the development of reagents specific for horse would be of great benefit.

In **Chapter 4**, due to financial and time constraints only one time point following LPS stimulation was studied (7 hours). The transcriptomic response to LPS is a succession of waves of induction and repression of genes over 48 hours. Therefore, by studying one time point, this limits the evaluation of the horse's full response to LPS. A full-time course analysis (including sequential time points from 0 hours up to 24-48 hours) would greatly expand on our knowledge of regulatory loops in the equine LPS response. Furthermore, the equine genome is poorly annotated meaning some genes may have been annotated incorrectly, or important pieces of information may be missing.

A significant limitation of **Chapter 5** was the small numbers used in the analysis of colic cases. On this basis, the recruitment of more colic cases would improve this preliminary data set. In addition, significant variation existed within the cohort of horses undergoing colic surgery, in relation to the following factors: intestinal lesion, duration of colic prior to surgery, age and breed of the horse. Although unavoidable in such a clinical-based study, this variation may have influenced the relative gene expression data generated and therefore the ability to draw definitive conclusions from the study. This contrasts with the mouse model of POI, where each mouse underwent the same procedure, thus reducing the likelihood of the results being confounded by variability within the model.

7.3 Future Directions

Each of the chapters in this thesis have provided usable preliminary data which can be further developed and researched.

To expand the work in **Chapter 3**, the use of dual labelling techniques could be implemented to label both the enteric nervous system and macrophages and analyse if any close spatial relationships exist, as has been observed in mice. The further development and optimisation of antibodies for use in horses would facilitate this work. Enteric neurons produce CSF-1 which helps maintain the MM population in mouse ME (Muller et al., 2014). Equine dysautonomia (also referred to as equine grass sickness) is a polyneuropathy affecting horses (Pirie et al., 2014). A feature of equine dysautonomia is neuronal degeneration of the neurons in the myenteric plexus which ultimately results in intestinal dysmotility (Cottrell et al., 1999). Therefore, MM in equine dysautonomia cases could be evaluated for evidence of any macrophage population alterations in the absence of CSF-1 signalling from enteric neurons.

The potential for future work with the RNA-Seq dataset generated in this project (**Chapter 4**) is vast. Firstly, expanding the dataset to other time points (0-48 hours) would improve our understanding of the full genetic regulation of the equine macrophage's response to LPS. The approach to quantification used in this study does not use the full information content of the RNA-Seq data, for example to identify examples of alternative splicing. Two emerging interests in the lab relate to the expression by macrophages of the adhesion receptor, *Adgre1*, widely used as a macrophage marker in mice (Austyn and Gordon, 1981, Hume et al., 2002) and of the growth factor CSF-1. Both have alternative splice isoforms and Sashimi plots revealed exon skipping which was highly variable between species (Waddell et al., 2018). The epidermal growth factor (EGF)-like calcium binding domain of ADRGE1 showed sequence variation between species. Pig, human and rat have 7 EGF-like transmembrane domains whereas the ruminants (sheep, goat, cow and buffalo) and the horse had longer sequences, which probably encode 14 EGF-like domains, likely arising from a duplication of the 7-domain structure in rat, pig and human.

RNA-Seq analysis pipelines (such as StringTie (Pertea et al., 2016, Pertea et al., 2015)), used in other projects in our laboratory (Clark et al., 2017)), depend upon the availability of a quality genome to identify splice junctions. In this thesis, many unannotated genes identified by RNA-Seq and expressed or induced in macrophages were not further studied. In many instances, detailed annotation awaits an improved horse genome. However, in many cases the likely identity can be inferred from cross-species mapping, with further confidence derived from the pattern of expression. Consequently, further functional annotation of the horse macrophage transcriptome will help improve our understanding and knowledge of the equine innate immune response to LPS. Furthermore, the data generated can be used to help further

annotate the next release of the equine genome. The availability of new technologies such as long-read sequencing is rapidly expanding the set of high quality contiguous mammalian genomes, with recent release of the goat (Bickhart et al., 2017) and upcoming release of pig and water buffalo (involving members of our laboratory) rivalling human and mouse genomes. Another class of transcripts that remains currently unannotated in the horse is the long non-coding RNAs (LncRNA). These are a significant component of the LPS-inducible transcriptome in mice and human macrophages (Akcora et al., 2013, Ilott et al., 2014, Mao et al., 2015, Pefanis et al., 2015, Mumtaz et al., 2017). Because of their low expression, these are difficult to assemble from short-read RNA-Seq, but additional evidence can be derived from cross-species comparison (Bush et al., 2018)).

The failure of eqBMDMs to induce LPS suppressor genes warrants further investigation. The horse BMDM system optimised here offers the possibility of generating clustered, regularly interspaced, short palindromic repeats (CRISPR)-associated nuclease Cas9 system mediated mutations (Shalem et al., 2014) in horse macrophages. A specific focus could be on the response to LPS. For example, targeting of cellular signalling pathways (Sharma and Petsalaki, 2018) in normal and LPS stimulated macrophages could help identify potential therapeutic targets.

Development of the work in **Chapter 5** in colic cases, could involve evaluation of macrophage populations (and other immune cell populations) by immunohistochemistry. By using monocyte markers this may help identify if monocytes are recruited to the intestine during abdominal surgery as reported in mice. Further study to look at risk factors or associations with the development of POI may then be evaluated. An increase in numbers for further qPCR analysis would also be beneficial.

In **Chapter 6** pre-treatment of mice with CSF1-Fc in a model of POI was beneficial by increasing monocyte-derived macrophages required for tissue repair, reducing neutrophils and inducing anti-inflammatory genes in the *muscularis*. The next stage would be to evaluate the effect of CSF1-Fc when administered at the time of surgery, which would better reflect the clinical scenario of equine abdominal surgery, where pre-treatment is unlikely to be an option, due to the nature of the clinical presentation of colic. Furthermore, further analysis of microarray data of non-manipulated and manipulated *muscularis* treated with CSF1-Fc, and with the blocking antibody to the CSF-1 receptor will help our understanding of the effect of CSF-1 in the intestine.

7.4 Conclusion

This thesis has explored several aspects of macrophage biology in the horse with a focus on the relevance to post-operative ileus. The work has generated a protocol to produce populations of equine primary macrophages (eqBMDMs) by culturing bone marrow in rhCSF-1 and thus providing a tissue macrophage surrogate to study LPS-induced gene expression. RNA-Seq analysis of eqBMDMs stimulated with LPS clearly demonstrated a species-specific variation in innate immune biology and highlighted the potential caveats when translating data derived from other species to the horse (including data relating to the pathophysiology of POI). Macrophages were identified in all layers of the equine gastrointestinal tract of normal horse. Compared to controls, horses undergoing abdominal surgery had increased expression of *IL-1 β* , *IL-6* and *TNF- α* in the mucosa and *muscularis*. These preliminary data support the hypothesis that intestinal surgery in the horse results in the activation of the intestinal macrophage population. Finally, the beneficial effect of CSF1-Fc on resolution of inflammation in a mouse model of POI warrants further investigation and research into its use as a potential therapeutic agent.

This page was left intentionally blank

Chapter 8. References

- ABD, A. H., SAVAGE, N. W., HALLIDAY, W. J. & HUME, D. A. 1991. The role of macrophages in experimental arthritis induced by *Streptococcus agalactiae* sonicate: actions of macrophage colony-stimulating factor (CSF-1) and other macrophage-modulating agents. *Lymphokine Cytokine Res*, 10, 43-50.
- ABREU, M. T., FUKATA, M. & ARDITI, M. 2005. TLR signaling in the gut in health and disease. *J Immunol*, 174, 4453-60.
- ACHUTHAN, A., COOK, A. D., LEE, M. C., SALEH, R., KHIEW, H. W., CHANG, M. W., LOUIS, C., FLEETWOOD, A. J., LACEY, D. C., CHRISTENSEN, A. D., FRYE, A. T., LAM, P. Y., KUSANO, H., NOMURA, K., STEINER, N., FORSTER, I., NUTT, S. L., OLSHANSKY, M., TURNER, S. J. & HAMILTON, J. A. 2016. Granulocyte macrophage colony-stimulating factor induces CCL17 production via IRF4 to mediate inflammation. *J Clin Invest*, 126, 3453-66.
- ADEREM, A. & ULEVITCH, R. J. 2000. Toll-like receptors in the induction of the innate immune response. *Nature*, 406, 782-7.
- AKCORA, D., HUYNH, D., LIGHTOWLER, S., GERMANN, M., ROBINE, S., DE MAY, J. R., POLLARD, J. W., STANLEY, E. R., MALATERRE, J. & RAMSAY, R. G. 2013. The CSF-1 receptor fashions the intestinal stem cell niche. *Stem Cell Res*, 10, 203-12.
- ALEXA, A. & RAHNENFUHRER, J. 2016. topGO: Enrichment analysis for Gene Ontology 2010. Available from: <http://www.bioconductor.org/packages/release/bioc/html/topGO.html>.
- ALEXANDER, K. A., CHANG, M. K., MAYLIN, E. R., KOHLER, T., MULLER, R., WU, A. C., VAN ROOIJEN, N., SWEET, M. J., HUME, D. A., RAGGATT, L. J. & PETTIT, A. R. 2011. Osteal macrophages promote in vivo intramembranous bone healing in a mouse tibial injury model. *J Bone Miner Res*, 26, 1517-32.
- ALIKHAN, M. A., JONES, C. V., WILLIAMS, T. M., BECKHOUSE, A. G., FLETCHER, A. L., KETT, M. M., SAKKAL, S., SAMUEL, C. S., RAMSAY, R. G., DEANE, J. A., WELLS, C. A., LITTLE, M. H., HUME, D. A. & RICARDO, S. D. 2011. Colony-stimulating factor-1 promotes kidney growth and repair via alteration of macrophage responses. *Am J Pathol*, 179, 1243-56.
- ASKEW, K., LI, K., OLMOS-ALONSO, A., GARCIA-MORENO, F., LIANG, Y., RICHARDSON, P., TIPTON, T., CHAPMAN, M. A., RIECKEN, K., BECCARI, S., SIERRA, A., MOLNAR, Z., CRAGG, M. S., GARASCHUK, O., PERRY, V. H. & GOMEZ-NICOLA, D. 2017. Coupled Proliferation and Apoptosis Maintain the Rapid Turnover of Microglia in the Adult Brain. *Cell Rep*, 18, 391-405.
- AUSTYN, J. M. & GORDON, S. 1981. F4/80, a monoclonal antibody directed specifically against the mouse macrophage. *Eur J Immunol*, 11, 805-15.
- AVETISYAN, M., ROOD, J. E., HUERTA LOPEZ, S., SENGUPTA, R., WRIGHT-JIN, E., DOUGHERTY, J. D., BEHRENS, E. M. & HEUCKEROTH, R. O. 2018. Muscularis macrophage development in the absence of an enteric nervous system. *Proceedings of the National Academy of Sciences*.
- BAILLIE, J. K., ARNER, E., DAUB, C., DE HOON, M., ITOH, M., KAWAJI, H., LASSMANN, T., CARNINCI, P., FORREST, A. R., HAYASHIZAKI, Y., CONSORTIUM, F., FAULKNER, G. J., WELLS, C. A., REHLI, M.,

- PAVLI, P., SUMMERS, K. M. & HUME, D. A. 2017. Analysis of the human monocyte-derived macrophage transcriptome and response to lipopolysaccharide provides new insights into genetic aetiology of inflammatory bowel disease. *PLoS Genet*, 13, e1006641.
- BAIN, C. C., BRAVO-BLAS, A., SCOTT, C. L., PERDIGUERO, E. G., GEISSMANN, F., HENRI, S., MALISSEN, B., OSBORNE, L. C., ARTIS, D. & MOWAT, A. M. 2014. Constant replenishment from circulating monocytes maintains the macrophage pool in the intestine of adult mice. *Nat Immunol*, 15, 929-937.
- BAIN, C. C. & MOWAT, A. M. 2011. Intestinal macrophages - specialised adaptation to a unique environment. *Eur J Immunol*, 41, 2494-8.
- BAIN, C. C. & MOWAT, A. M. 2012. CD200 receptor and macrophage function in the intestine. *Immunobiology*, 217, 643-51.
- BAIN, C. C. & MOWAT, A. M. 2014. Macrophages in intestinal homeostasis and inflammation. *Immunol Rev*, 260, 102-17.
- BAIN, C. C., SCOTT, C. L., URONEN-HANSSON, H., GUDJONSSON, S., JANSSON, O., GRIP, O., GUILLIAMS, M., MALISSEN, B., AGACE, W. W. & MOWAT, A. M. 2013. Resident and pro-inflammatory macrophages in the colon represent alternative context-dependent fates of the same Ly6Chi monocyte precursors. *Mucosal Immunol*, 6, 498-510.
- BALLANTYNE, G. H. 1984. The meaning of ileus. Its changing definition over three millennia. *Am J Surg*, 148, 252-6.
- BARQUIST, E., BONAZ, B., MARTINEZ, V., RIVIER, J., ZINNER, M. J. & TACHE, Y. 1996. Neuronal pathways involved in abdominal surgery-induced gastric ileus in rats. *Am J Physiol*, 270, R888-94.
- BARREDA, D. R., HANINGTON, P. C. & BELOSEVIC, M. 2004. Regulation of myeloid development and function by colony stimulating factors. *Dev Comp Immunol*, 28, 509-54.
- BARREY, E., MUCHER, E., ROBERT, C., AMIOT, F. & GIDROL, X. 2006. Gene expression profiling in blood cells of endurance horses completing competition or disqualified due to metabolic disorder. *Equine Vet J Suppl*, 43-9.
- BAUCK, A. G., EASLEY, J. T., CLEARY, O. B., GRAHAM, S., MORTON, A. J., ROTTING, A. K., SCHAEFFER, D. J., SMITH, A. D. & FREEMAN, D. E. 2017. Response to early repeat celiotomy in horses after a surgical treatment of jejunal strangulation. *Vet Surg*, 46, 843-850.
- BAYLISS, W. M. & STARLING, E. H. 1899. The movements and innervation of the small intestine. *J Physiol*, 24, 99-143.
- BEHRENDT, F. F., WEHNER, S., LYSSON, M., BAUER, A. J., HIRNER, A. & KALFF, J. C. 2004. Depletion and inactivation of intestinal muscularis macrophages prevent postoperative ileus. *Journal of the American College of Surgeons*, 199, S22-S23.
- BELLOLI, C., ARIOLI, F., BERETTA, C. & MADONNA, M. 1994. In vitro effects of tachykinins on the smooth musculature of horse gut. *J Vet Pharmacol Ther*, 17, 379-83.
- BENJAMINI, Y. & HOCHBERG, Y. 1995. Controlling the False Discovery Rate - a Practical and Powerful Approach to Multiple Testing. *Journal of the Royal Statistical Society Series B-Methodological*, 57, 289-300.

- BICKHART, D. M., ROSEN, B. D., KOREN, S., SAYRE, B. L., HASTIE, A. R., CHAN, S., LEE, J., LAM, E. T., LIACHKO, I., SULLIVAN, S. T., BURTON, J. N., HUSON, H. J., NYSTROM, J. C., KELLEY, C. M., HUTCHISON, J. L., ZHOU, Y., SUN, J., CRISÀ, A., PONCE DE LEÓN, F. A., SCHWARTZ, J. C., HAMMOND, J. A., WALDBIESER, G. C., SCHROEDER, S. G., LIU, G. E., DUNHAM, M. J., SHENDURE, J., SONSTEGARD, T. S., PHILLIPPY, A. M., VAN TASSELL, C. P. & SMITH, T. P. L. 2017. Single-molecule sequencing and chromatin conformation capture enable de novo reference assembly of the domestic goat genome. *Nature Genetics*, 49, 643.
- BISWAS, S. K. & LOPEZ-COLLAZO, E. 2009. Endotoxin tolerance: new mechanisms, molecules and clinical significance. *Trends Immunol*, 30, 475-87.
- BLASIUS, A. L. & BEUTLER, B. 2010. Intracellular toll-like receptors. *Immunity*, 32, 305-15.
- BLIKSLAGER, A. T., BOWMAN, K. F., LEVINE, J. F., BRISTOL, D. G. & ROBERTS, M. C. 1994. Evaluation of factors associated with postoperative ileus in horses: 31 cases (1990-1992). *J Am Vet Med Assoc*, 205, 1748-52.
- BOECKXSTAENS, G. E. & DE JONGE, W. J. 2009. Neuroimmune mechanisms in postoperative ileus. *Gut*, 58, 1300-11.
- BOECKXSTAENS, G. E., HIRSCH, D. P., KODDE, A., MOOJEN, T. M., BLACKSHAW, A., TYTGAT, G. N. & BLOMMAART, P. J. 1999. Activation of an adrenergic and vagally-mediated NANC pathway in surgery-induced fundic relaxation in the rat. *Neurogastroenterol Motil*, 11, 467-74.
- BOGDAN, C., PAIK, J., VODOVOTZ, Y. & NATHAN, C. 1992. Contrasting mechanisms for suppression of macrophage cytokine release by transforming growth factor-beta and interleukin-10. *J Biol Chem*, 267, 23301-8.
- BOISSONNEAULT, V., FILALI, M., LESSARD, M., RELTON, J., WONG, G. & RIVEST, S. 2009. Powerful beneficial effects of macrophage colony-stimulating factor on beta-amyloid deposition and cognitive impairment in Alzheimer's disease. *Brain*, 132, 1078-92.
- BONE, R. C., BALK, R. A., CERRA, F. B., DELLINGER, R. P., FEIN, A. M., KNAUS, W. A., SCHEIN, R. M. H. & SIBBALD, W. J. 1992. Definitions for Sepsis and Organ Failure and Guidelines for the Use of Innovative Therapies in Sepsis. *Chest*, 101, 1644-1655.
- BRADY, H. 1999. *Endotoxin in health and disease*, Marcel Dekke, New York.
- BRAY, N. L., PIMENTEL, H., MELSTED, P. & PACHTER, L. 2016. Near-optimal probabilistic RNA-seq quantification. *Nat Biotechnol*, 34, 525-7.
- BRYANT, C. E., SPRING, D. R., GANGLOFF, M. & GAY, N. J. 2010. The molecular basis of the host response to lipopolysaccharide. *Nat Rev Microbiol*, 8, 8-14.
- BUECHLER, C., RITTER, M., ORSO, E., LANGMANN, T., KLUCKEN, J. & SCHMITZ, G. 2000. Regulation of scavenger receptor CD163 expression in human monocytes and macrophages by pro- and antiinflammatory stimuli. *J Leukoc Biol*, 67, 97-103.
- BUENO, L., FERRE, J. P. & RUCKEBUSCH, Y. 1978. Effects of anesthesia and surgical procedures on intestinal myoelectric activity in rats. *Am J Dig Dis*, 23, 690-5.

- BUMGARNER, R. 2013. DNA microarrays: Types, Applications and their future. *Current protocols in molecular biology / edited by Frederick M. Ausubel ... [et al.]*, 0 22, Unit-22.1.
- BURNS, A. J., LOMAX, A. E., TORIHASHI, S., SANDERS, K. M. & WARD, S. M. 1996. Interstitial cells of Cajal mediate inhibitory neurotransmission in the stomach. *Proc Natl Acad Sci U S A*, 93, 12008-13.
- BURROWS, G. E. 1981. Dose-response of ponies to parenteral Escherichia coli endotoxin. *Can J Comp Med*, 45, 207-10.
- BUSH, S. J., MURIUKI, C., MCCULLOCH, M. E. B., FARQUHAR, I. L., CLARK, E. L. & HUME, D. A. 2018. Cross-species inference of long non-coding RNAs greatly expands the ruminant transcriptome. *Genet Sel Evol*, 50, 20.
- CAILOTTO, C., GOMEZ-PINILLA, P. J., COSTES, L. M., VAN DER VLIET, J., DI GIOVANGIULIO, M., NEMETHOVA, A., MATTEOLI, G. & BOECKXSTAENS, G. E. 2014. Neuro-anatomical evidence indicating indirect modulation of macrophages by vagal efferents in the intestine but not in the spleen. *PLoS One*, 9, e87785.
- CENCI, E., BARTOCCI, A., PUC CETTI, P., MOCCI, S., STANLEY, E. R. & BISTONI, F. 1991. Macrophage colony-stimulating factor in murine candidiasis: serum and tissue levels during infection and protective effect of exogenous administration. *Infection and Immunity*, 59, 868-872.
- CHAMORRO, S., REVILLA, C., ALVAREZ, B., ALONSO, F., EZQUERRA, A. & DOMINGUEZ, J. 2005. Phenotypic and functional heterogeneity of porcine blood monocytes and its relation with maturation. *Immunology*, 114, 63-71.
- CHANG, J. T. & NEVINS, J. R. 2006. GATHER: a systems approach to interpreting genomic signatures. *Bioinformatics*, 22, 2926-33.
- CHAZAUD, B. 2014. Macrophages: supportive cells for tissue repair and regeneration. *Immunobiology*, 219, 172-8.
- CHEN, B. N., SHARRAD, D. F., HIBBERD, T. J., ZAGORODNYUK, V. P., COSTA, M. & BROOKES, S. J. 2015. Neurochemical characterization of extrinsic nerves in myenteric ganglia of the guinea pig distal colon. *J Comp Neurol*, 523, 742-56.
- CHOI, H. K., LEE, Y. J., LEE, Y. H., PARK, J. P., MIN, K. & PARK, H. 2013. Inflammatory responses in the muscle coat of stomach and small bowel in the postoperative ileus model of guinea pig. *Yonsei Med J*, 54, 1336-41.
- CHRISTENSEN, J., RICK, G. A. & LOWE, L. S. 1992. Distributions of interstitial cells of Cajal in stomach and colon of cat, dog, ferret, opossum, rat, guinea pig and rabbit. *J Auton Nerv Syst*, 37, 47-56.
- CLARK, E. L., BUSH, S. J., MCCULLOCH, M. E. B., FARQUHAR, I. L., YOUNG, R., LEFEVRE, L., PRIDANS, C., TSANG, H. G., WU, C., AFRASIABI, C., WATSON, M., WHITELAW, C. B., FREEMAN, T. C., SUMMERS, K. M., ARCHIBALD, A. L. & HUME, D. A. 2017. A high resolution atlas of gene expression in the domestic sheep (*Ovis aries*). *PLoS Genet*, 13, e1006997.
- COHEN, N. D., LESTER, G. D., SANCHEZ, L. C., MERRITT, A. M. & ROUSSEL, A. J., JR. 2004. Evaluation of risk factors associated with development of postoperative ileus in horses. *J Am Vet Med Assoc*, 225, 1070-8.

- COLEMAN, S. J., ZENG, Z., HESTAND, M. S., LIU, J. & MACLEOD, J. N. 2013. Analysis of unannotated equine transcripts identified by mRNA sequencing. *PLoS One*, 8, e70125.
- COMPTON, S. J., CAIRNS, J. A., HOLGATE, S. T. & WALLS, A. F. 1998. The role of mast cell tryptase in regulating endothelial cell proliferation, cytokine release, and adhesion molecule expression: tryptase induces expression of mRNA for IL-1 beta and IL-8 and stimulates the selective release of IL-8 from human umbilical vein endothelial cells. *J Immunol*, 161, 1939-46.
- COOKE, H. J. 1994. Neuroimmune signaling in regulation of intestinal ion transport. *Am J Physiol*, 266, G167-78.
- COSTA, M. & FURNESS, J. B. 1984. Somatostatin Is Present in a Subpopulation of Noradrenergic Nerve-Fibers Supplying the Intestine. *Neuroscience*, 13, 911-919.
- COTTRELL, D. F., MCGORUM, B. C. & PEARSON, G. T. 1999. The neurology and enterology of equine grass sickness: a review of basic mechanisms. *Neurogastroenterol Motil*, 11, 79-92.
- CUMMINGS, J. F., SELLERS, A. F. & LOWE, J. E. 1985. Distribution of substance P-like immunoreactivity in the enteric neurons of the large colon of normal and amitraz-treated ponies: an immunocytochemical study. *Equine Vet J*, 17, 23-9.
- DAI, W. & GUPTA, S. L. 1990. Regulation of indoleamine 2,3-dioxygenase gene expression in human fibroblasts by interferon-gamma. Upstream control region discriminates between interferon-gamma and interferon-alpha. *J Biol Chem*, 265, 19871-7.
- DAI, X. M., RYAN, G. R., HAPPEL, A. J., DOMINGUEZ, M. G., RUSSELL, R. G., KAPP, S., SYLVESTRE, V. & STANLEY, E. R. 2002. Targeted disruption of the mouse colony-stimulating factor 1 receptor gene results in osteopetrosis, mononuclear phagocyte deficiency, increased primitive progenitor cell frequencies, and reproductive defects. *Blood*, 99, 111-20.
- DAVIES, L. C., JENKINS, S. J., ALLEN, J. E. & TAYLOR, P. R. 2013. Tissue-resident macrophages. *Nat Immunol*, 14, 986-95.
- DE CEULAER, K., DELESALLE, C., VAN ELZEN, R., VAN BRANTEGEM, L., WEYNS, A. & VAN GINNEKEN, C. 2011. Morphological changes in the small intestinal smooth muscle layers of horses suffering from small intestinal strangulation. Is there a basis for predisposition for reduced contractility? *Equine Vet J*, 43, 439-45.
- DE JONGE, W. J. 2013. The Gut's Little Brain in Control of Intestinal Immunity. *ISRN Gastroenterol*, 2013, 630159.
- DE JONGE, W. J., THE, F. O., VAN DER COELEN, D., BENNINK, R. J., REITSMA, P. H., VAN DEVENTER, S. J., VAN DEN WIJNGAARD, R. M. & BOECKXSTAENS, G. E. 2004. Mast cell degranulation during abdominal surgery initiates postoperative ileus in mice. *Gastroenterology*, 127, 535-45.
- DE JONGE, W. J., VAN DEN WIJNGAARD, R. M., THE, F. O., TER BEEK, M.-L., BENNINK, R. J., TYTGAT, G. N. J., BUIJS, R. M., REITSMA, P. H., VAN DEVENTER, S. J. & BOECKXSTAENS, G. E. 2003. Postoperative ileus is maintained by intestinal immune infiltrates that activate inhibitory neural pathways in mice. *Gastroenterology*, 125, 1137-1147.

- DE WINTER, B. Y., BOECKXSTAENS, G. E., DE MAN, J. G., MOREELS, T. G., HERMAN, A. G. & PELCKMANS, P. A. 1997. Effect of adrenergic and nitrenergic blockade on experimental ileus in rats. *Br J Pharmacol*, 120, 464-8.
- DE WINTER, B. Y., VAN DEN WIJNGAARD, R. M. & DE JONGE, W. J. 2012. Intestinal mast cells in gut inflammation and motility disturbances. *Biochim Biophys Acta*, 1822, 66-73.
- DELANEY, C. P., WEESE, J. L., HYMAN, N. H., BAUER, J., TECHNER, L., GABRIEL, K., DU, W., SCHMIDT, W. K., WALLIN, B. A. & ALVIMOPAN POSTOPERATIVE ILEUS STUDY, G. 2005. Phase III trial of alvimopan, a novel, peripherally acting, mu opioid antagonist, for postoperative ileus after major abdominal surgery. *Dis Colon Rectum*, 48, 1114-25; discussion 1125-6; author reply 1127-9.
- DENG, H., MAITRA, U., MORRIS, M. & LI, L. 2013. Molecular mechanism responsible for the priming of macrophage activation. *J Biol Chem*, 288, 3897-906.
- DENNING, T. L., WANG, Y. C., PATEL, S. R., WILLIAMS, I. R. & PULENDRAN, B. 2007. Lamina propria macrophages and dendritic cells differentially induce regulatory and interleukin 17-producing T cell responses. *Nat Immunol*, 8, 1086-94.
- DERISI, J. L., IYER, V. R. & BROWN, P. O. 1997. Exploring the metabolic and genetic control of gene expression on a genomic scale. *Science*, 278, 680-6.
- DESJARDINS, P. & CONKLIN, D. 2010. NanoDrop Microvolume Quantitation of Nucleic Acids. *Journal of Visualized Experiments : JoVE*, 2565.
- DIJKSTRA, C. D., DOPP, E. A., JOLING, P. & KRAAL, G. 1985. The heterogeneity of mononuclear phagocytes in lymphoid organs: distinct macrophage subpopulations in the rat recognized by monoclonal antibodies ED1, ED2 and ED3. *Immunology*, 54, 589-99.
- DINAKAR, C., MALUR, A., RAYCHAUDHURI, B., BUHROW, L. T., MELTON, A. L., KAVURU, M. S. & THOMASSEN, M. J. 1999. Differential regulation of human blood monocyte and alveolar macrophage inflammatory cytokine production by nitric oxide. *Annals of Allergy, Asthma & Immunology*, 82, 217-222.
- DINGES, M. M. & SCHLIEVERT, P. M. 2001. Comparative analysis of lipopolysaccharide-induced tumor necrosis factor alpha activity in serum and lethality in mice and rabbits pretreated with the staphylococcal superantigen toxic shock syndrome toxin 1. *Infect Immun*, 69, 7169-72.
- DOHERTY, T. J. 2009. Postoperative ileus: pathogenesis and treatment. *Vet Clin North Am Equine Pract*, 25, 351-62.
- DOXEY, D. L., PEARSON, G. T., MILNE, E. M., GILMOUR, J. S. & CHISHOLM, H. K. 1995. The equine enteric nervous system — Neuron characterization and distribution in adults and juveniles. *Veterinary Research Communications*, 19, 433-449.
- DRAKE, R. E., TEAGUE, R. A. & GABEL, J. C. 1998. Lymphatic drainage reduces intestinal edema and fluid loss. *Lymphology*, 31, 68-73.
- DRESEL, P. & WALLENTIN, I. 1966. Effects of sympathetic vasoconstrictor fibres, noradrenaline and vasopressin on the intestinal vascular resistance during constant blood flow or blood pressure. *Acta Physiol Scand*, 66, 427-36.

- DUBOIS, R. N., ABRAMSON, S. B., CROFFORD, L., GUPTA, R. A., SIMON, L. S., VAN DE PUTTE, L. B. & LIPSKY, P. E. 1998. Cyclooxygenase in biology and disease. *Faseb j*, 12, 1063-73.
- DURONGPHONGTORN, S., MCDONELL, W. N., KERR, C. L., NETO, F. J. & MIRAKHUR, K. K. 2006. Comparison of hemodynamic, clinicopathologic, and gastrointestinal motility effects and recovery characteristics of anesthesia with isoflurane and halothane in horses undergoing arthroscopic surgery. *Am J Vet Res*, 67, 32-42.
- EARNSHAW, S. R., KAUF, T. L., MCDADE, C., POTASHMAN, M. H., PAUYO, C., REESE, E. S. & SENAGORE, A. 2015. Economic Impact of Alvimopan Considering Varying Definitions of Postoperative Ileus. *J Am Coll Surg*, 221, 941-50.
- EDWARDS, G. B. & PROUDMAN, C. J. 1994. An analysis of 75 cases of intestinal obstruction caused by pedunculated lipomas. *Equine Vet J*, 26, 18-21.
- EK, M., KUROSAWA, M., LUNDEBERG, T. & ERICSSON, A. 1998. Activation of vagal afferents after intravenous injection of interleukin-1beta: role of endogenous prostaglandins. *J Neurosci*, 18, 9471-9.
- ENSEMBL Browser EG: <http://www.ensembl.org>.
- EPELMAN, S., LAVINE, K. J., BEAUDIN, A. E., SOJKA, D. K., CARRERO, J. A., CALDERON, B., BRIJA, T., GAUTIER, E. L., IVANOV, S., SATPATHY, A. T., SCHILLING, J. D., SCHWENDENER, R., SERGIN, I., RAZANI, B., FORSBERG, E. C., YOKOYAMA, W. M., UNANUE, E. R., COLONNA, M., RANDOLPH, G. J. & MANN, D. L. 2014. Embryonic and adult-derived resident cardiac macrophages are maintained through distinct mechanisms at steady state and during inflammation. *Immunity*, 40, 91-104.
- ESKANDARI, M. K., KALFF, J. C., BILLIAR, T. R., LEE, K. K. & BAUER, A. J. 1997. Lipopolysaccharide activates the muscularis macrophage network and suppresses circular smooth muscle activity. *Am J Physiol*, 273, G727-34.
- EVANS, E., PAILLOT, R. & LÓPEZ-ÁLVAREZ, M. R. 2018. A comprehensive analysis of e-CAS cell line reveals they are mouse macrophages. *Scientific Reports*, 8, 8237.
- FABRIEK, B. O., DIJKSTRA, C. D. & VAN DEN BERG, T. K. 2005. The macrophage scavenger receptor CD163. *Immunobiology*, 210, 153-60.
- FAIRBAIRN, L., KAPETANOVIC, R., SESTER, D. P. & HUME, D. A. 2011. The mononuclear phagocyte system of the pig as a model for understanding human innate immunity and disease. *J Leukoc Biol*, 89, 855-71.
- FALEIROS, R. R., JOHNSON, P. J., NUOVO, G. J., MESSER, N. T., BLACK, S. J. & BELKNAP, J. K. 2011. Lamellar leukocyte accumulation in horses with carbohydrate overload-induced laminitis. *J Vet Intern Med*, 25, 107-15.
- FARRO, G., STAKENBORG, M., GOMEZ-PINILLA, P. J., LABEEUW, E., GOVERSE, G., DI GIOVANGIULIO, M., STAKENBORG, N., MERONI, E., D'ERRICO, F., ELKRIM, Y., LAOUI, D., LISOWSKI, Z. M., SAUTER, K. A., HUME, D. A., VAN GINDERACHTER, J. A., BOECKXSTAENS, G. E. & MATTEOLI, G. 2017. CCR2-dependent monocyte-derived macrophages resolve inflammation and restore gut motility in postoperative ileus. *Gut*, 66, 2098-2109.
- FIGUEIREDO, M. D., SALTER, C. E., HURLEY, D. J. & MOORE, J. N. 2008. A comparison of equine and bovine sera as sources of lipopolysaccharide-

- binding protein activity in equine monocytes incubated with lipopolysaccharide. *Vet Immunol Immunopathol*, 121, 275-80.
- FIGUEIREDO, M. D., VANDENPLAS, M. L., HURLEY, D. J. & MOORE, J. N. 2009. Differential induction of MyD88- and TRIF-dependent pathways in equine monocytes by Toll-like receptor agonists. *Vet Immunol Immunopathol*, 127, 125-34.
- FINK, M. P. 2014. Animal models of sepsis. *Virulence*, 5, 143-53.
- FINKLEMAN, B. 1930. On the nature of inhibition in the intestine. *J Physiol*, 70, 145-57.
- FINTL, C., HUDSON, N. P., MAYHEW, I. G., EDWARDS, G. B., PROUDMAN, C. J. & PEARSON, G. T. 2004. Interstitial cells of Cajal (ICC) in equine colic: an immunohistochemical study of horses with obstructive disorders of the small and large intestines. *Equine Vet J*, 36, 474-9.
- FREEMAN, D. 2017. Post-operative reflux - a surgeon's perspective. *Equine Veterinary Education*, n/a-n/a.
- FREEMAN, D. E. 2008. Post operative ileus (POI): another perspective. *Equine Vet J*, 40, 297-8.
- FREEMAN, D. E., HAMMOCK, P., BAKER, G. J., GOETZ, T., FOREMAN, J. H., SCHAEFFER, D. J., RICHTER, R. A., INOUE, O. & MAGID, J. H. 2000. Short- and long-term survival and prevalence of postoperative ileus after small intestinal surgery in the horse. *Equine Vet J Suppl*, 32, 42-51.
- FREEMAN, T. C., GOLDOVSKY, L., BROSCHE, M., VAN DONGEN, S., MAZIERE, P., GROCOCK, R. J., FREILICH, S., THORNTON, J. & ENRIGHT, A. J. 2007. Construction, visualisation, and clustering of transcription networks from microarray expression data. *PLoS Comput Biol*, 3, 2032-42.
- FREEMAN, T. C., IVENS, A., BAILLIE, J. K., BERALDI, D., BARNETT, M. W., DORWARD, D., DOWNING, A., FAIRBAIRN, L., KAPETANOVIC, R., RAZA, S., TOMOIU, A., ALBERIO, R., WU, C., SU, A. I., SUMMERS, K. M., TUGGLE, C. K., ARCHIBALD, A. L. & HUME, D. A. 2012. A gene expression atlas of the domestic pig. *BMC Biol*, 10, 90.
- FRENCH, N. P., SMITH, J., EDWARDS, G. B. & PROUDMAN, C. J. 2002. Equine surgical colic: risk factors for postoperative complications. *Equine Vet J*, 34, 444-9.
- FREYTAG, C., SEEGER, J., SIEGEMUND, T., GROSCHE, J., GROSCHE, A., FREEMAN, D. E., SCHUSSER, G. F. & HARTIG, W. 2008. Immunohistochemical characterization and quantitative analysis of neurons in the myenteric plexus of the equine intestine. *Brain Res*, 1244, 53-64.
- FUJIGAKI, H., SAITO, K., FUJIGAKI, S., TAKEMURA, M., SUDO, K., ISHIGURO, H. & SEISHIMA, M. 2006. The signal transducer and activator of transcription 1alpha and interferon regulatory factor 1 are not essential for the induction of indoleamine 2,3-dioxygenase by lipopolysaccharide: involvement of p38 mitogen-activated protein kinase and nuclear factor-kappaB pathways, and synergistic effect of several proinflammatory cytokines. *J Biochem*, 139, 655-62.
- FUJIGAKI, S., SAITO, K., SEKIKAWA, K., TONE, S., TAKIKAWA, O., FUJII, H., WADA, H., NOMA, A. & SEISHIMA, M. 2001. Lipopolysaccharide induction of indoleamine 2,3-dioxygenase is mediated dominantly by an IFN-

- γ -independent mechanism. *European Journal of Immunology*, 31, 2313-2318.
- FUKUDA, H., TSUCHIDA, D., KODA, K., MIYAZAKI, M., PAPPAS, T. N. & TAKAHASHI, T. 2007. Inhibition of sympathetic pathways restores postoperative ileus in the upper and lower gastrointestinal tract. *J Gastroenterol Hepatol*, 22, 1293-9.
- FURNESS, J. B. 2012. The enteric nervous system and neurogastroenterology. *Nat Rev Gastroenterol Hepatol*, 9, 286-94.
- FURNESS, J. B. & COSTA, M. 1980. Types of nerves in the enteric nervous system. *Neuroscience*, 5, 1-20.
- FURNESS, J. B., YOUNG, H. M., POMPOLO, S., BORNSTEIN, J. C., KUNZE, W. A. & MCCONALOGUE, K. 1995. Plurichemical transmission and chemical coding of neurons in the digestive tract. *Gastroenterology*, 108, 554-63.
- GABANYI, I., MULLER, P. A., FEIGHERY, L., OLIVEIRA, T. Y., COSTA-PINTO, F. A. & MUCIDA, D. 2016. Neuro-immune Interactions Drive Tissue Programming in Intestinal Macrophages. *Cell*, 164, 378-91.
- GEEM, D., MEDINA-CONTRERAS, O., KIM, W., HUANG, C. S. & DENNING, T. L. 2012. Isolation and characterization of dendritic cells and macrophages from the mouse intestine. *J Vis Exp*, e4040.
- GEISSMANN, F., MANZ, M. G., JUNG, S., SIEWEKE, M. H., MERAD, M. & LEY, K. 2010. Development of monocytes, macrophages, and dendritic cells. *Science*, 327, 656-61.
- GERO, D., GIE, O., HUBNER, M., DEMARTINES, N. & HAHNLOSER, D. 2017. Postoperative ileus: in search of an international consensus on definition, diagnosis, and treatment. *Langenbecks Arch Surg*, 402, 149-158.
- GINHOUX, F. & GUILLIAMS, M. 2016. Tissue-Resident Macrophage Ontogeny and Homeostasis. *Immunity*, 44, 439-449.
- GOLDSTEIN, J. L., MATUSZEWSKI, K. A., DELANEY, C. P., SENAGORE, A., CHIAO, E. F., SHAH, M., MEYER, K. & BRAMLEY, T. 2007. Inpatient economic burden of postoperative ileus associated with abdominal surgery in the United States. *P and T*, 32, 82-90.
- GOMEZ-PINILLA, P. J., FARRO, G., DI GIOVANGIULIO, M., STAKENBORG, N., NEMETHOVA, A., DE VRIES, A., LISTON, A., FEYERABEND, T. B., RODEWALD, H. R., BOECKXSTAENS, G. E. & MATTEOLI, G. 2014. Mast cells play no role in the pathogenesis of postoperative ileus induced by intestinal manipulation. *PLoS One*, 9, e85304.
- GORDON, S. 2003. Alternative activation of macrophages. *Nat Rev Immunol*, 3, 23-35.
- GORDON, S., CLARKE, S., GREAVES, D. & DOYLE, A. 1995. Molecular immunobiology of macrophages: recent progress. *Curr Opin Immunol*, 7, 24-33.
- GORDON, S. & TAYLOR, P. R. 2005. Monocyte and macrophage heterogeneity. *Nat Rev Immunol*, 5, 953-64.
- GOSSELIN, D., LINK, V. M., ROMANOSKI, CASEY E., FONSECA, GREGORY J., EICHENFIELD, DAWN Z., SPANN, NATHANAEL J., STENDER, JOSHUA D., CHUN, HYUN B., GARNER, H., GEISSMANN, F. & GLASS, CHRISTOPHER K. 2014. Environment Drives Selection and

- Function of Enhancers Controlling Tissue-Specific Macrophage Identities. *Cell*, 159, 1327-1340.
- GOW, D. J., GARCEAU, V., PRIDANS, C., GOW, A. G., SIMPSON, K. E., GUNN-MOORE, D. & HUME, D. A. 2013. Cloning and expression of feline colony stimulating factor receptor (CSF-1R) and analysis of the species specificity of stimulation by colony stimulating factor-1 (CSF-1) and interleukin-34 (IL-34). *Cytokine*, 61, 630-8.
- GOW, D. J., SAUTER, K. A., PRIDANS, C., MOFFAT, L., SEHGAL, A., STUTCHFIELD, B. M., RAZA, S., BEARD, P. M., TSAI, Y. T., BAINBRIDGE, G., BONER, P. L., FICI, G., GARCIA-TAPIA, D., MARTIN, R. A., OLIPHANT, T., SHELLY, J. A., TIWARI, R., WILSON, T. L., SMITH, L. B., MABBOTT, N. A. & HUME, D. A. 2014. Characterisation of a novel Fc conjugate of macrophage colony-stimulating factor. *Mol Ther*, 22, 1580-92.
- GOYAL, R. K. & HIRANO, I. 1996. The enteric nervous system. *N Engl J Med*, 334, 1106-15.
- GRETER, M. & MERAD, M. 2013. Regulation of microglia development and homeostasis. *Glia*, 61, 121-7.
- GROSCHKE, A., MORTON, A. J., GRAHAM, A. S., VALENTINE, J. F., ABBOTT, J. R., POLYAK, M. M. & FREEMAN, D. E. 2011. Mucosal injury and inflammatory cells in response to brief ischaemia and reperfusion in the equine large colon. *Equine Vet J Suppl*, 43, 16-25.
- GU, W. & BERTONE, A. L. 2004. Generation and performance of an equine-specific large-scale gene expression microarray. *Am J Vet Res*, 65, 1664-73.
- GUAN, Z., KUHN, J. A., WANG, X., COLQUITT, B., SOLORZANO, C., VAMAN, S., GUAN, A. K., EVANS-REINSCH, Z., BRAZ, J., DEVOR, M., ABOUD-WERNER, S. L., LANIER, L. L., LOMVARDAS, S. & BASBAUM, A. I. 2016. Injured sensory neuron-derived CSF1 induces microglial proliferation and DAP12-dependent pain. *Nat Neurosci*, 19, 94-101.
- GUILLIAMS, M., DE KLEER, I., HENRI, S., POST, S., VANHOUTTE, L., DE PRIJCK, S., DESWARTE, K., MALISSEN, B., HAMMAD, H. & LAMBRECHT, B. N. 2013. Alveolar macrophages develop from fetal monocytes that differentiate into long-lived cells in the first week of life via GM-CSF. *J Exp Med*, 210, 1977-92.
- GUILLIAMS, M. & SCOTT, C. L. 2017. Does niche competition determine the origin of tissue-resident macrophages? *Nat Rev Immunol*, 17, 451-460.
- GUNN, M. 1968. Histological and histochemical observations on the myenteric and submucous plexuses of mammals. *J Anat*, 102, 223-39.
- HAMANN, J., AUST, G., ARAC, D., ENGEL, F. B., FORMSTONE, C., FREDRIKSSON, R., HALL, R. A., HARTY, B. L., KIRCHHOFF, C., KNAPP, B., KRISHNAN, A., LIEBSCHER, I., LIN, H. H., MARTINELLI, D. C., MONK, K. R., PEETERS, M. C., PIAO, X., PROMEL, S., SCHONEBERG, T., SCHWARTZ, T. W., SINGER, K., STACEY, M., USHKARYOV, Y. A., VALLON, M., WOLFRUM, U., WRIGHT, M. W., XU, L., LANGENHAN, T. & SCHIOTH, H. B. 2015. International Union of Basic and Clinical Pharmacology. XCIV. Adhesion G protein-coupled receptors. *Pharmacol Rev*, 67, 338-67.

- HAMILTON, J. A. 2008. Colony-stimulating factors in inflammation and autoimmunity. *Nat Rev Immunol*, 8, 533-44.
- HAMILTON, J. A. & ACHUTHAN, A. 2013. Colony stimulating factors and myeloid cell biology in health and disease. *Trends Immunol*, 34, 81-9.
- HAMILTON, J. A. & ANDERSON, G. P. 2004. GM-CSF Biology. *Growth Factors*, 22, 225-31.
- HAMMOND, R. A., HANNON, R., FREAN, S. P., ARMSTRONG, S. J., FLOWER, R. J. & BRYANT, C. E. 1999. Endotoxin induction of nitric oxide synthase and cyclooxygenase-2 in equine alveolar macrophages. *Am J Vet Res*, 60, 426-31.
- HANISCH, U. K. & KETTENMANN, H. 2007. Microglia: active sensor and versatile effector cells in the normal and pathologic brain. *Nat Neurosci*, 10, 1387-94.
- HASHIMOTO, D., CHOW, A., NOIZAT, C., TEO, P., BEASLEY, M. B., LEBOEUF, M., BECKER, C. D., SEE, P., PRICE, J., LUCAS, D., GRETER, M., MORTHA, A., BOYER, S. W., FORSBERG, E. C., TANAKA, M., VAN ROOIJEN, N., GARCIA-SASTRE, A., STANLEY, E. R., GINHOUX, F., FRENETTE, P. S. & MERAD, M. 2013. Tissue-resident macrophages self-maintain locally throughout adult life with minimal contribution from circulating monocytes. *Immunity*, 38, 792-804.
- HASHIMOTO, S.-I., SUZUKI, T., DONG, H.-Y., YAMAZAKI, N. & MATSUSHIMA, K. 1999. Serial Analysis of Gene Expression in Human Monocytes and Macrophages. *Blood*, 94, 837-844.
- HAWLEY, C. A., ROJO, R., RAPER, A., SAUTER, K. A., LISOWSKI, Z. M., GRABERT, K., BAIN, C. C., DAVIS, G. M., LOUWE, P. A., OSTROWSKI, M. C., HUME, D. A., PRIDANS, C. & JENKINS, S. J. 2018. Csf1r-mApple Transgene Expression and Ligand Binding In Vivo Reveal Dynamics of CSF1R Expression within the Mononuclear Phagocyte System. *J Immunol*, 200, 2209-2223.
- HECKE, D. V. 2002. Routine Immunohistochemical Staining Today: Choices to Make, Challenges to Take. *Journal of Histotechnology*, 25, 45-54.
- HILLYER, M. H., TAYLOR, F. G. & FRENCH, N. P. 2001. A cross-sectional study of colic in horses on thoroughbred training premises in the British Isles in 1997. *Equine Vet J*, 33, 380-5.
- HOFFMAN, S. M. & FLEMING, S. D. 2010. Natural Helicobacter infection modulates mouse intestinal muscularis macrophage responses. *Cell Biochem Funct*, 28, 686-94.
- HOGGER, P., DREIER, J., DROSTE, A., BUCK, F. & SORG, C. 1998. Identification of the integral membrane protein RM3/1 on human monocytes as a glucocorticoid-inducible member of the scavenger receptor cysteine-rich family (CD163). *J Immunol*, 161, 1883-90.
- HOLCOMBE, S. J., RODRIGUEZ, K. M., HAUPT, J. L., CAMPBELL, J. O., CHANEY, K. P., SPARKS, H. D. & HAUPTMAN, J. G. 2009. Prevalence of and risk factors for postoperative ileus after small intestinal surgery in two hundred and thirty-three horses. *Vet Surg*, 38, 368-72.
- HOPSTER-IVERSEN, C., HOPSTER, K., STASZYK, C., ROHN, K., FREEMAN, D. & ROTTING, A. K. 2011. Influence of mechanical manipulations on the local inflammatory reaction in the equine colon. *Equine Vet J Suppl*, 43, 1-7.

- HOPSTER-IVERSEN, C. C., HOPSTER, K., STASZYK, C., ROHN, K., FREEMAN, D. E. & ROTTING, A. K. 2014. Effects of experimental mechanical manipulations on local inflammation in the jejunum of horses. *Am J Vet Res*, 75, 385-91.
- HORI, M., KITA, M., TORIHASHI, S., MIYAMOTO, S., WON, K. J., SATO, K., OZAKI, H. & KARAKI, H. *Upregulation of iNOS by COX-2 in muscularis resident macrophage of rat intestine stimulated with LPS.*
- HORI, M., NOBE, H., HORIGUCHI, K. & OZAKI, H. 2008. *MCP-1 targeting inhibits muscularis macrophage recruitment and intestinal smooth muscle dysfunction in colonic inflammation.*
- HOSHINO, K., TAKEUCHI, O., KAWAI, T., SANJO, H., OGAWA, T., TAKEDA, Y., TAKEDA, K. & AKIRA, S. 1999. Cutting edge: Toll-like receptor 4 (TLR4)-deficient mice are hyporesponsive to lipopolysaccharide: evidence for TLR4 as the Lps gene product. *J Immunol*, 162, 3749-52.
- HOTCHKISS, R. S. & KARL, I. E. 2003. The pathophysiology and treatment of sepsis. *N Engl J Med*, 348, 138-50.
- HOYLE, C. H. & BURNSTOCK, G. 1989. Neuronal populations in the submucous plexus of the human colon. *J Anat*, 166, 7-22.
- HUANG, L., ZHU, W., SAUNDERS, C. P., MACLEOD, J. N., ZHOU, M., STROMBERG, A. J. & BATHKE, A. C. 2008. A novel application of quantile regression for identification of biomarkers exemplified by equine cartilage microarray data. *BMC Bioinformatics*, 9, 300.
- HUDSON, N. P., PEARSON, G. T., KITAMURA, N. & MAYHEW, I. G. 1999. An immunohistochemical study of interstitial cells of Cajal (ICC) in the equine gastrointestinal tract. *Res Vet Sci*, 66, 265-71.
- HUDSON, N. P., PEARSON, G. T., MAYHEW, I. G., PROUDMAN, C. J., BURDEN, F. A. & FINTL, C. 2014. Expression of PGP 9.5 by enteric neurons in horses and donkeys with and without intestinal disease. *J Comp Pathol*, 150, 225-33.
- HUME, D. A. 1985. Immunohistochemical Analysis of Murine Mononuclear Phagocytes That Express Class-II Major Histocompatibility Antigens. *Immunobiology*, 170, 381-389.
- HUME, D. A. 2006. The mononuclear phagocyte system. *Curr Opin Immunol*, 18, 49-53.
- HUME, D. A. 2008a. Differentiation and heterogeneity in the mononuclear phagocyte system. *Mucosal Immunol*, 1, 432-41.
- HUME, D. A. 2008b. Macrophages as APC and the dendritic cell myth. *J Immunol*, 181, 5829-35.
- HUME, D. A. 2015. The Many Alternative Faces of Macrophage Activation. *Front Immunol*, 6, 370.
- HUME, D. A., ALLAN, W., HOGAN, P. G. & DOE, W. F. 1987. Immunohistochemical characterisation of macrophages in human liver and gastrointestinal tract: expression of CD4, HLA-DR, OKM1, and the mature macrophage marker 25F9 in normal and diseased tissue. *J Leukoc Biol*, 42, 474-84.
- HUME, D. A. & GORDON, S. 1983. Optimal conditions for proliferation of bone marrow-derived mouse macrophages in culture: the roles of CSF-1, serum, Ca²⁺, and adherence. *J Cell Physiol*, 117, 189-94.

- HUME, D. A., LOUITT, J. F., GORDON, S., HUME, D. A., LOUITT, J. F. & GORDON, S. 1984. The mononuclear phagocyte system of the mouse defined by immunohistochemical localization of antigen F4/80. *macrophages of bone and associated connective tissue*, 66, 189-194.
- HUME, D. A. & MACDONALD, K. P. 2012. Therapeutic applications of macrophage colony-stimulating factor-1 (CSF-1) and antagonists of CSF-1 receptor (CSF-1R) signaling. *Blood*, 119, 1810-20.
- HUME, D. A., MONKLEY, S. J. & WAINWRIGHT, B. J. 1995. Detection of c-fms protooncogene in early mouse embryos by whole mount in situ hybridization indicates roles for macrophages in tissue remodelling. *Br J Haematol*, 90, 939-42.
- HUME, D. A., PAVLI, P., DONAHUE, R. E. & FIDLER, I. J. 1988. The effect of human recombinant macrophage colony-stimulating factor (CSF-1) on the murine mononuclear phagocyte system in vivo. *J Immunol*, 141, 3405-9.
- HUME, D. A., ROSS, I. L., HIMES, S. R., SASMONO, R. T., WELLS, C. A. & RAVASI, T. 2002. The mononuclear phagocyte system revisited. *J Leukoc Biol*, 72, 621-7.
- HUME, D. A., UNDERHILL, D. M., SWEET, M. J., OZINSKY, A. O., LIEW, F. Y. & ADEREM, A. 2001. Macrophages exposed continuously to lipopolysaccharide and other agonists that act via toll-like receptors exhibit a sustained and additive activation state. *BMC Immunol*, 2, 11.
- HUNT, J. M., EDWARDS, G. B. & CLARKE, K. W. 1986. Incidence, diagnosis and treatment of postoperative complications in colic cases. *Equine Vet J*, 18, 264-70.
- HURST, S. & COLLINS, S. M. 1993. Interleukin-1 beta modulation of norepinephrine release from rat myenteric nerves. *Am J Physiol*, 264, G30-5.
- HURST, S. M. & COLLINS, S. M. 1994. Mechanism underlying tumor necrosis factor-alpha suppression of norepinephrine release from rat myenteric plexus. *Am J Physiol*, 266, G1123-9.
- IBRAHIM, S., SAUNDERS, K., KYDD, J. H., LUNN, D. P. & STEINBACH, F. 2007. Screening of anti-human leukocyte monoclonal antibodies for reactivity with equine leukocytes. *Vet Immunol Immunopathol*, 119, 63-80.
- ILOTT, N. E., HEWARD, J. A., ROUX, B., TSITSIOU, E., FENWICK, P. S., LENZI, L., GOODHEAD, I., HERTZ-FOWLER, C., HEGER, A., HALL, N., DONNELLY, L. E., SIMS, D. & LINDSAY, M. A. 2014. Long non-coding RNAs and enhancer RNAs regulate the lipopolysaccharide-induced inflammatory response in human monocytes. *Nature Communications*, 5, 3979.
- IRVINE, K. L., HOPKINS, L. J., GANGLOFF, M. & BRYANT, C. E. 2013. The molecular basis for recognition of bacterial ligands at equine TLR2, TLR1 and TLR6. *Vet Res*, 44, 50.
- JACKSON, J. J. & KROPP, H. 1999. *Endotoxin in Health and Disease*.
- JENKINS, S. J. & HUME, D. A. 2014. Homeostasis in the mononuclear phagocyte system. *Trends Immunol*, 35, 358-67.
- JONES, T. R., KANG, I. H., WHEELER, D. B., LINDQUIST, R. A., PAPALLO, A., SABATINI, D. M., GOLLAND, P. & CARPENTER, A. E. 2008. CellProfiler Analyst: data exploration and analysis software for complex image-based screens. *BMC Bioinformatics*, 9, 482.

- JOSEPHS, M. D., CHENG, G., KSONTINI, R., MOLDAWER, L. L. & HOCKING, M. P. 1999. Products of cyclooxygenase-2 catalysis regulate postoperative bowel motility. *J Surg Res*, 86, 50-4.
- JOSHI, A., POOLEY, C., FREEMAN, T. C., LENNARTSSON, A., BABINA, M., SCHMIDL, C., GEIJTENBEEK, T., CONSORTIUM, F., MICHOEL, T., SEVERIN, J., ITOH, M., LASSMANN, T., KAWAJI, H., HAYASHIZAKI, Y., CARNINCI, P., FORREST, A. R., REHLI, M. & HUME, D. A. 2015. Technical Advance: Transcription factor, promoter, and enhancer utilization in human myeloid cells. *J Leukoc Biol*, 97, 985-995.
- JOSHI, V. D., KALVAKOLANU, D. V. & CROSS, A. S. 2003. Simultaneous activation of apoptosis and inflammation in pathogenesis of septic shock: a hypothesis1. *FEBS Letters*, 555, 180-184.
- KABITHE, E., HILLEGAS, J., STOKOL, T., MOORE, J. & WAGNER, B. 2010. Monoclonal antibodies to equine CD14. *Vet Immunol Immunopathol*, 138, 149-53.
- KAKUDA, D. K., SWEET, M. J., MAC LEOD, C. L., HUME, D. A. & MARKOVICH, D. 1999. CAT2-mediated L-arginine transport and nitric oxide production in activated macrophages. *Biochem J*, 340 (Pt 2), 549-53.
- KALFF, J. C., BUCHHOLZ, B. M., ESKANDARI, M. K., HIERHOLZER, C., SCHRAUT, W. H., SIMMONS, R. L. & BAUER, A. J. 1999a. Biphasic response to gut manipulation and temporal correlation of cellular infiltrates and muscle dysfunction in rat. *Surgery*, 126, 498-509.
- KALFF, J. C., CARLOS, T. M., SCHRAUT, W. H., BILLIAR, T. R., SIMMONS, R. L. & BAUER, A. J. 1999b. Surgically induced leukocytic infiltrates within the rat intestinal muscularis mediate postoperative ileus. *Gastroenterology*, 117, 378-387.
- KALFF, J. C., SCHRAUT, W. H., BILLIAR, T. R., SIMMONS, R. L. & BAUER, A. J. 2000. Role of inducible nitric oxide synthase in postoperative intestinal smooth muscle dysfunction in rodents. *Gastroenterology*, 118, 316-27.
- KALFF, J. C., SCHRAUT, W. H., SIMMONS, R. L. & BAUER, A. J. 1998a. Surgical manipulation of the gut elicits an intestinal muscularis inflammatory response resulting in postsurgical ileus. *Ann Surg*, 228, 652-63.
- KALFF, J. C., SCHWARZ, N. T., WALGENBACH, K. J., SCHRAUT, W. H. & BAUER, A. J. 1998b. Leukocytes of the intestinal muscularis: their phenotype and isolation. *J Leukoc Biol*, 63, 683-91.
- KALFF, J. C., TURLER, A., SCHWARZ, N. T., SCHRAUT, W. H., LEE, K. K., TWEARDY, D. J., BILLIAR, T. R., SIMMONS, R. L. & BAUER, A. J. 2003. Intra-abdominal activation of a local inflammatory response within the human muscularis externa during laparotomy. *Ann Surg*, 237, 301-15.
- KAPETANOVIC, R., FAIRBAIRN, L., BERALDI, D., SESTER, D. P., ARCHIBALD, A. L., TUGGLE, C. K. & HUME, D. A. 2012. Pig bone marrow-derived macrophages resemble human macrophages in their response to bacterial lipopolysaccharide. *J Immunol*, 188, 3382-94.
- KARAGIANNI, A. E. 2015. Characterisation of the equine macrophage / monocyte. The University of Edinburgh.
- KARAGIANNI, A. E., KAPETANOVIC, R., MCGORUM, B. C., HUME, D. A. & PIRIE, S. R. 2013. The equine alveolar macrophage: functional and

- phenotypic comparisons with peritoneal macrophages. *Vet Immunol Immunopathol*, 155, 219-28.
- KARAGIANNI, A. E., KAPETANOVIC, R., SUMMERS, K. M., MCGORUM, B. C., HUME, D. A. & PIRIE, R. S. 2017. Comparative transcriptome analysis of equine alveolar macrophages. *Equine Vet J*, 49, 375-382.
- KAWAI, T. & AKIRA, S. 2010. The role of pattern-recognition receptors in innate immunity: update on Toll-like receptors. *Nat Immunol*, 11, 373-84.
- KEHLET, H., WILLIAMSON, R., BUCHLER, M. W. & BEART, R. W. 2005. A survey of perceptions and attitudes among European surgeons towards the clinical impact and management of postoperative ileus. *Colorectal Dis*, 7, 245-50.
- KHAN, W. I., MOTOMURA, Y., WANG, H., EL-SHARKAWY, R. T., VERDU, E. F., VERMA-GANDHU, M., ROLLINS, B. J. & COLLINS, S. M. 2006. Critical role of MCP-1 in the pathogenesis of experimental colitis in the context of immune and enterochromaffin cells. *Am J Physiol Gastrointest Liver Physiol*, 291, G803-11.
- KING, J. N. & GERRING, E. L. 1988. Detection of endotoxin in cases of equine colic. *Vet Rec*, 123, 269-71.
- KING, J. N. & GERRING, E. L. 1991. The action of low dose endotoxin on equine bowel motility. *Equine Vet J*, 23, 11-7.
- KINOSHITA, K., HORI, M., FUJISAWA, M., SATO, K., OHAMA, T., MOMOTANI, E. & OZAKI, H. 2006. Role of TNF-alpha in muscularis inflammation and motility disorder in a TNBS-induced colitis model: clues from TNF-alpha-deficient mice. *Neurogastroenterol Motil*, 18, 578-88.
- KINSELLA, R. J., KAHARI, A., HAIDER, S., ZAMORA, J., PROCTOR, G., SPUDICH, G., ALMEIDA-KING, J., STAINES, D., DERWENT, P., KERHORNOU, A., KERSEY, P. & FLICEK, P. 2011. Ensembl BioMarts: a hub for data retrieval across taxonomic space. *Database (Oxford)*, 2011, bar030.
- KORESSAAR, T. & REMM, M. 2007. Enhancements and modifications of primer design program Primer3. *Bioinformatics*, 23, 1289-91.
- KOVACH, N. L., YEE, E., MUNFORD, R. S., RAETZ, C. R. & HARLAN, J. M. 1990. Lipid IVA inhibits synthesis and release of tumor necrosis factor induced by lipopolysaccharide in human whole blood ex vivo. *J Exp Med*, 172, 77-84.
- KRISTEK, M., COLLINS, L. E., DECOURCEY, J., MCEVOY, F. A. & LOSCHER, C. E. 2015. Soluble factors from colonic epithelial cells contribute to gut homeostasis by modulating macrophage phenotype. *Innate Immun*, 21, 358-69.
- KUNZE, W. A. & FURNESS, J. B. 1999. The enteric nervous system and regulation of intestinal motility. *Annu Rev Physiol*, 61, 117-42.
- KURIHARA, T., WARR, G., LOY, J. & BRAVO, R. 1997. Defects in macrophage recruitment and host defense in mice lacking the CCR2 chemokine receptor. *J Exp Med*, 186, 1757-62.
- LEE, S. H., STARKEY, P. M. & GORDON, S. 1985. Quantitative analysis of total macrophage content in adult mouse tissues. Immunochemical studies with monoclonal antibody F4/80. *J Exp Med*, 161, 475-89.

- LEFEBVRE, D., HUDSON, N. P., ELCE, Y. A., BLIKSLAGER, A., DIVERS, T. J., HANDEL, I. G., TREMAINE, W. H. & PIRIE, R. S. 2016a. Clinical features and management of equine post operative ileus (POI): Survey of Diplomates of the American Colleges of Veterinary Internal Medicine (ACVIM), Veterinary Surgeons (ACVS) and Veterinary Emergency and Critical Care (ACVECC). *Equine Vet J*, 48, 714-719.
- LEFEBVRE, D., PIRIE, R. S., HANDEL, I. G., TREMAINE, W. H. & HUDSON, N. P. 2016b. Clinical features and management of equine post operative ileus: Survey of diplomates of the European Colleges of Equine Internal Medicine (ECEIM) and Veterinary Surgeons (ECVS). *Equine Vet J*, 48, 182-7.
- LEFEBVRE, R. A., SMITS, G. J. & TIMMERMANS, J. P. 1995. Study of NO and VIP as non-adrenergic non-cholinergic neurotransmitters in the pig gastric fundus. *Br J Pharmacol*, 116, 2017-26.
- LEFEVRE, M. E., HAMMER, R. & JOEL, D. D. 1979. Macrophages of the mammalian small intestine: a review. *J Reticuloendothel Soc*, 26, 553-73.
- LICHANSKA, A. M. & HUME, D. A. 2000. Origins and functions of phagocytes in the embryo. *Exp Hematol*, 28, 601-11.
- LITTLE, D., REDDING, W. R. & BLIKSLAGER, A. T. 2001. Risk factors for reduced postoperative fecal output in horses: 37 cases (1997-1998). *J Am Vet Med Assoc*, 218, 414-20.
- LITTLE, D., TOMLINSON, J. E. & BLIKSLAGER, A. T. 2005. Post operative neutrophilic inflammation in equine small intestine after manipulation and ischaemia. *Equine Vet J*, 37, 329-35.
- LIVAK, K. J. & SCHMITTGEN, T. D. 2001. Analysis of relative gene expression data using real-time quantitative PCR and the 2(-Delta Delta C(T)) Method. *Methods*, 25, 402-8.
- LIVINGSTON, E. H. & PASSARO, E. P., JR. 1990. Postoperative ileus. *Dig Dis Sci*, 35, 121-32.
- LODATO, R. F., KHAN, A. R., ZEMBOWICZ, M. J., WEISBRODT, N. W., PRESSLEY, T. A., LI, Y. F., LODATO, J. A., ZEMBOWICZ, A. & MOODY, F. G. 1999. Roles of IL-1 and TNF in the decreased ileal muscle contractility induced by lipopolysaccharide. *Am J Physiol*, 276, G1356-62.
- LOHMANN, K. L., VANDENPLAS, M. L., BARTON, M. H., BRYANT, C. E. & MOORE, J. N. 2007. The equine TLR4/MD-2 complex mediates recognition of lipopolysaccharide from *Rhodobacter sphaeroides* as an agonist. *J Endotoxin Res*, 13, 235-42.
- LOMAX, A. E., SHARKEY, K. A. & FURNESS, J. B. 2010. The participation of the sympathetic innervation of the gastrointestinal tract in disease states. *Neurogastroenterol Motil*, 22, 7-18.
- LORSCH, J. R., COLLINS, F. S. & LIPPINCOTT-SCHWARTZ, J. 2014. Cell Biology. Fixing problems with cell lines. *Science*, 346, 1452-3.
- LOUIS, C., COOK, A. D., LACEY, D., FLEETWOOD, A. J., VLAHOS, R., ANDERSON, G. P. & HAMILTON, J. A. 2015. Specific Contributions of CSF-1 and GM-CSF to the Dynamics of the Mononuclear Phagocyte System. *J Immunol*, 195, 134-44.
- LUNDGREN, O., SVANVIK, J. & JIVEGÅRD, L. 1989. Enteric nervous system. *Digestive diseases and sciences*, 34, 264-283.

- MACDONALD, K. P. A., PALMER, J. S., CRONAU, S., SEPPANEN, E., OLVER, S., RAFFELT, N. C., KUNS, R., PETTIT, A. R., CLOUSTON, A., WAINWRIGHT, B., BRANSTETTER, D., SMITH, J., PAXTON, R. J., CERRETTI, D. P., BONHAM, L., HILL, G. R. & HUME, D. A. 2010. *An antibody against the colony-stimulating factor 1 receptor depletes the resident subset of monocytes and tissue- and tumor-associated macrophages but does not inhibit inflammation.*
- MACMICKING, J., XIE, Q. W. & NATHAN, C. 1997. Nitric oxide and macrophage function. *Annu Rev Immunol*, 15, 323-50.
- MAHIDA, Y. R., PATEL, S., GIONCHETTI, P., VAUX, D. & JEWELL, D. P. 1989. Macrophage subpopulations in lamina propria of normal and inflamed colon and terminal ileum. *Gut*, 30, 826-34.
- MAIN, C., BLENNERHASSETT, P. & COLLINS, S. M. 1993. Human recombinant interleukin 1 beta suppresses acetylcholine release from rat myenteric plexus. *Gastroenterology*, 104, 1648-54.
- MAIR, T. S. & SMITH, L. J. 2005a. Survival and complication rates in 300 horses undergoing surgical treatment of colic. Part 1: Short-term survival following a single laparotomy. *Equine Vet J*, 37, 296-302.
- MAIR, T. S. & SMITH, L. J. 2005b. Survival and complication rates in 300 horses undergoing surgical treatment of colic. Part 2: Short-term complications. *Equine Vet J*, 37, 303-9.
- MAIR, T. S. & SMITH, L. J. 2005c. Survival and complication rates in 300 horses undergoing surgical treatment of colic. Part 3: Long-term complications and survival. *Equine Vet J*, 37, 310-4.
- MALIZIA, G., CALABRESE, A., COTTONE, M., RAIMONDO, M., TREJDOSIEWICZ, L. K., SMART, C. J., OLIVA, L. & PAGLIARO, L. 1991. Expression of leukocyte adhesion molecules by mucosal mononuclear phagocytes in inflammatory bowel disease. *Gastroenterology*, 100, 150-9.
- MALONE, E. D., KANNAN, M. S., BROWN, D. R., TURNER, T. A. & TRENT, A. M. 1999. Adrenergic, cholinergic, and nonadrenergic-noncholinergic intrinsic innervation of the jejunum in horses. *Am J Vet Res*, 60, 898-904.
- MAN, A. L., BERTELLI, E., RENTINI, S., REGOLI, M., BRIARS, G., MARINI, M., WATSON, A. J. & NICOLETTI, C. 2015. Age-associated modifications of intestinal permeability and innate immunity in human small intestine. *Clin Sci (Lond)*, 129, 515-27.
- MANSOUR, T. A., SCOTT, E. Y., FINNO, C. J., BELLONE, R. R., MIENALTOWSKI, M. J., PENEDO, M. C., ROSS, P. J., VALBERG, S. J., MURRAY, J. D. & BROWN, C. T. 2017. Tissue resolved, gene structure refined equine transcriptome. *BMC Genomics*, 18, 103.
- MANTOVANI, A., SICA, A. & LOCATI, M. 2005. Macrophage polarization comes of age. *Immunity*, 23, 344-6.
- MANTOVANI, A., SICA, A., SOZZANI, S., ALLAVENA, P., VECCHI, A. & LOCATI, M. 2004. The chemokine system in diverse forms of macrophage activation and polarization. *Trends Immunol*, 25, 677-86.
- MANZANILLO, P., EIDENSCHENK, C. & OUYANG, W. 2015. Deciphering the crosstalk among IL-1 and IL-10 family cytokines in intestinal immunity. *Trends in Immunology*, 36, 471-478.

- MAO, A. P., SHEN, J. & ZUO, Z. 2015. Expression and regulation of long noncoding RNAs in TLR4 signaling in mouse macrophages. *BMC Genomics*, 16, 45.
- MARTINEZ, F. O., GORDON, S., LOCATI, M. & MANTOVANI, A. 2006. Transcriptional Profiling of the Human Monocyte-to-Macrophage Differentiation and Polarization: New Molecules and Patterns of Gene Expression. *The Journal of Immunology*, 177, 7303-7311.
- MASS, E., BALLESTEROS, I., FARLIK, M., HALBRITTER, F., GUNTHER, P., CROZET, L., JACOME-GALARZA, C. E., HANDLER, K., KLUGHAMMER, J., KOBAYASHI, Y., GOMEZ-PERDIGUERO, E., SCHULTZE, J. L., BEYER, M., BOCK, C. & GEISSMANN, F. 2016. Specification of tissue-resident macrophages during organogenesis. *Science*, 353.
- MATINI, P. A. F.-P., M.S. 1997. *Ultrastructural localization of neuronal nitric oxide synthase-immunoreactivity in the rat ileum*, Amsterdam : Elsevier.
- MATTEOLI, G., GOMEZ-PINILLA, P. J., NEMETHOVA, A., DI GIOVANGIULIO, M., CAILOTTO, C., VAN BREE, S. H., MICHEL, K., TRACEY, K. J., SCHEMANN, M., BOESMANS, W., VANDEN BERGHE, P. & BOECKXSTAENS, G. E. 2014. A distinct vagal anti-inflammatory pathway modulates intestinal muscularis resident macrophages independent of the spleen. *Gut*, 63, 938-48.
- MATTEOLI, G., MAZZINI, E., ILIEV, I. D., MILETI, E., FALLARINO, F., PUCCHETTI, P., CHIEPPA, M. & RESCIGNO, M. 2010. Gut CD103+ dendritic cells express indoleamine 2,3-dioxygenase which influences T regulatory/T effector cell balance and oral tolerance induction. *Gut*, 59, 595-604.
- MAY, S. A., HOOKE, R. E. & LEES, P. 1990. The characterisation of equine interleukin-1. *Veterinary Immunology and Immunopathology*, 24, 169-175.
- MCCONALOGUE, K. & FURNESS, J. B. 1994. Gastrointestinal neurotransmitters. *Baillieres Clin Endocrinol Metab*, 8, 51-76.
- MCEVOY, C., DE GAETANO, M., GIFFNEY, H. E., BAHAR, B., CUMMINS, E. P., BRENNAN, E. P., BARRY, M., BELTON, O., GODSON, C. G., MURPHY, E. P. & CREAN, D. 2017. NR4A Receptors Differentially Regulate NF- κ B Signaling in Myeloid Cells. *Frontiers in Immunology*, 8.
- MCKNIGHT, A. J. & GORDON, S. 1998. The EGF-TM7 family: unusual structures at the leukocyte surface. *J Leukoc Biol*, 63, 271-80.
- MCKNIGHT, A. J., MACFARLANE, A. J., DRI, P., TURLEY, L., WILLIS, A. C. & GORDON, S. 1996. Molecular cloning of F4/80, a murine macrophage-restricted cell surface glycoprotein with homology to the G-protein-linked transmembrane 7 hormone receptor family. *J Biol Chem*, 271, 486-9.
- MELLOR, D. J., LOVE, S., WALKER, R., GETTINBY, G. & REID, S. W. 2001. Sentinel practice-based survey of the management and health of horses in northern Britain. *Vet Rec*, 149, 417-23.
- MERRITT, A. M. & BLIKSLAGER, A. T. 2008. Post operative ileus: to be or not to be? *Equine Vet J*, 40, 295-6.
- MIENALTOWSKI, M. J., HUANG, L., STROMBERG, A. J. & MACLEOD, J. N. 2008. Differential gene expression associated with postnatal equine articular cartilage maturation. *BMC Musculoskelet Disord*, 9, 149.

- MIKKELSEN, H. B. 1995. Macrophages in the external muscle layers of mammalian intestines. *Histol Histopathol*, 10, 719-36.
- MIKKELSEN, H. B. 2010. Interstitial cells of Cajal, macrophages and mast cells in the gut musculature: morphology, distribution, spatial and possible functional interactions. *J Cell Mol Med*, 14, 818-32.
- MIKKELSEN, H. B., GARBARSCHE, C., TRANUM-JENSEN, J. & THUNEBERG, L. 2004. Macrophages in the small intestinal muscularis externa of embryos, newborn and adult germ-free mice. *J Mol Histol*, 35, 377-87.
- MIKKELSEN, H. B., LARSEN, J. O., FROH, P. & NGUYEN, T. H. 2011. Quantitative assessment of macrophages in the muscularis externa of mouse intestines. *Anat Rec (Hoboken)*, 294, 1557-65.
- MIKKELSEN, H. B., LARSEN, J. O. & HADBERG, H. 2008. The macrophage system in the intestinal muscularis externa during inflammation: an immunohistochemical and quantitative study of osteopetrotic mice. *Histochem Cell Biol*, 130, 363-73.
- MIKKELSEN, H. B., MIRSKY, R., JESSEN, K. R. & THUNEBERG, L. 1988. Macrophage-like cells in muscularis externa of mouse small intestine: immunohistochemical localization of F4/80, M1/70, and Ia-antigen. *Cell Tissue Res*, 252, 301-6.
- MIKKELSEN, H. B. & RUMESSEN, J. J. 1992. Characterization of macrophage-like cells in the external layers of human small and large intestine. *Cell Tissue Res*, 270, 273-9.
- MILLER, G. E. 1990. The assessment of clinical skills/competence/performance. *Acad Med*, 65, S63-7.
- MIYAKE, K. 2004. Innate recognition of lipopolysaccharide by Toll-like receptor 4-MD-2. *Trends Microbiol*, 12, 186-92.
- MOGENSEN, T. H. 2009. Pathogen recognition and inflammatory signaling in innate immune defenses. *Clin Microbiol Rev*, 22, 240-73, Table of Contents.
- MOORE, B. D., BALASURIYA, U. B., WATSON, J. L., BOSIO, C. M., MACKAY, R. J. & MACLACHLAN, N. J. 2003. Virulent and avirulent strains of equine arteritis virus induce different quantities of TNF-alpha and other proinflammatory cytokines in alveolar and blood-derived equine macrophages. *Virology*, 314, 662-70.
- MORGAN, D. O. 1997. Cyclin-dependent kinases: engines, clocks, and microprocessors. *Annu Rev Cell Dev Biol*, 13, 261-91.
- MORTON, A. J. & BLIKSLAGER, A. T. 2002. Surgical and postoperative factors influencing short-term survival of horses following small intestinal resection: 92 cases (1994-2001). *Equine Vet J*, 34, 450-4.
- MOSMANN, T. 1983. Rapid colorimetric assay for cellular growth and survival: application to proliferation and cytotoxicity assays. *J Immunol Methods*, 65, 55-63.
- MOSSER, D. M. & EDWARDS, J. P. 2008. Exploring the full spectrum of macrophage activation. *Nat Rev Immunol*, 8, 958-69.
- MOWAT, A. M. & BAIN, C. C. 2011. Mucosal macrophages in intestinal homeostasis and inflammation. *J Innate Immun*, 3, 550-64.
- MUCHER, E., JAYR, L., ROSSIGNOL, F., AMIOT, F., GIDROL, X. & BARREY, E. 2006. Gene expression profiling in equine muscle tissues using mouse cDNA microarrays. *Equine Vet J Suppl*, 359-64.

- MULHOLLAND, W. J., ARBUTHNOTT, E. A. H., BELLHOUSE, B. J., FREDERICK CORNHILL, J., AUSTYN, J. M., KENDALL, M. A. F., CUI, Z. & TIRLAPUR, U. K. 2006. Multiphoton High-Resolution 3D Imaging of Langerhans Cells and Keratinocytes in the Mouse Skin Model Adopted for Epidermal Powdered Immunization. *Journal of Investigative Dermatology*, 126, 1541-1548.
- MULLER, P. A., KOSCSO, B., RAJANI, G. M., STEVANOVIC, K., BERRES, M. L., HASHIMOTO, D., MORTHA, A., LEBOEUF, M., LI, X. M., MUCIDA, D., STANLEY, E. R., DAHAN, S., MARGOLIS, K. G., GERSHON, M. D., MERAD, M. & BOGUNOVIC, M. 2014. Crosstalk between muscularis macrophages and enteric neurons regulates gastrointestinal motility. *Cell*, 158, 300-313.
- MUMTAZ, P. T., BHAT, S. A., AHMAD, S. M., DAR, M. A., AHMED, R., URWAT, U., AYAZ, A., SHRIVASTAVA, D., SHAH, R. A. & GANAI, N. A. 2017. LncRNAs and immunity: watchdogs for host pathogen interactions. *Biol Proced Online*, 19, 3.
- NACHLAS, M. M., YOUNIS, M. T., RODA, C. P. & WITYK, J. J. 1972. Gastrointestinal motility studies as a guide to postoperative management. *Annals of Surgery*, 175, 510-522.
- NAGASHIMA, R., MAEDA, K., IMAI, Y. & TAKAHASHI, T. 1996. Lamina propria macrophages in the human gastrointestinal mucosa: their distribution, immunohistological phenotype, and function. *J Histochem Cytochem*, 44, 721-31.
- NELSON, B. B., LORDAN, E. E. & HASSEL, D. M. 2013. Risk factors associated with gastrointestinal dysfunction in horses undergoing elective procedures under general anaesthesia. *Equine Vet J Suppl*, 45, 8-14.
- NIMMERJAHN, A., KIRCHHOFF, F. & HELMCHEN, F. 2005. Resting microglial cells are highly dynamic surveillants of brain parenchyma in vivo. *Science*, 308, 1314-8.
- NOSCHKA, E., VANDENPLAS, M. L., HURLEY, D. J. & MOORE, J. N. 2009. Temporal aspects of laminar gene expression during the developmental stages of equine laminitis. *Vet Immunol Immunopathol*, 129, 242-53.
- NULLENS, S., DE MAN, J., BRIDTS, C., EBO, D., FRANQUE, S. & DE WINTER, B. 2018. Identifying Therapeutic Targets for Sepsis Research: A Characterization Study of the Inflammatory Players in the Cecal Ligation and Puncture Model. *Mediators of Inflammation*, 2018, 17.
- NULLENS, S., STAESSENS, M., PELEMAN, C., PLAEKE, P., MALHOTRA-KUMAR, S., FRANQUE, S., DE MAN, J. G. & DE WINTER, B. Y. 2016. Beneficial Effects of Anti-Interleukin-6 Antibodies on Impaired Gastrointestinal Motility, Inflammation and Increased Colonic Permeability in a Murine Model of Sepsis Are Most Pronounced When Administered in a Preventive Setup. *PLoS ONE*, 11, e0152914.
- OH, H. Y., JIN, X., KIM, J. G., OH, M. J., PIAN, X., KIM, J. M., YOON, M. S., SON, C. I., LEE, Y. S., HONG, K. C., KIM, H., CHOI, Y. J. & WHANG, K. Y. 2007. Characteristics of primary and immortalized fibroblast cells derived from the miniature and domestic pigs. *BMC Cell Biol*, 8, 20.
- OHAMA, T., HORI, M., MOMOTANI, E., IWAKURA, Y., GUO, F., KISHI, H., KOBAYASHI, S. & OZAKI, H. 2007. Intestinal inflammation downregulates

- smooth muscle CPI-17 through induction of TNF-alpha and causes motility disorders. *Am J Physiol Gastrointest Liver Physiol*, 292, G1429-38.
- OHAMA, T., HORI, M., SATO, K., OZAKI, H. & KARAKI, H. 2003. Chronic treatment with interleukin-1beta attenuates contractions by decreasing the activities of CPI-17 and MYPT-1 in intestinal smooth muscle. *J Biol Chem*, 278, 48794-804.
- OKANO, S., HURLEY, D. J., VANDENPLAS, M. L. & MOORE, J. N. 2006. Effect of fetal bovine serum and heat-inactivated fetal bovine serum on microbial cell wall-induced expression of procoagulant activity by equine and canine mononuclear cells in vitro. *Am J Vet Res*, 67, 1020-4.
- OKAZAKI, T., EBIHARA, S., ASADA, M., YAMANDA, S., SAIJO, Y., SHIRAISHI, Y., EBIHARA, T., NIU, K., MEI, H., ARAI, H. & YAMBE, T. 2007. Macrophage colony-stimulating factor improves cardiac function after ischemic injury by inducing vascular endothelial growth factor production and survival of cardiomyocytes. *Am J Pathol*, 171, 1093-103.
- OKUNO, Y., NAKAMURA-ISHIZU, A., KISHI, K., SUDA, T. & KUBOTA, Y. 2011. Bone marrow-derived cells serve as proangiogenic macrophages but not endothelial cells in wound healing. *Blood*, 117, 5264-5272.
- OVERHAUS, M., TOGEL, S., PEZZONE, M. A. & BAUER, A. J. 2004. Mechanisms of polymicrobial sepsis-induced ileus. *Am J Physiol Gastrointest Liver Physiol*, 287, G685-94.
- OVERMAN, E. L., RIVIER, J. E. & MOESER, A. J. 2012. CRF induces intestinal epithelial barrier injury via the release of mast cell proteases and TNF-alpha. *PLoS One*, 7, e39935.
- OZAKI, H., KAWAI, T., SHUTTLEWORTH, C. W., WON, K. J., SUZUKI, T., SATO, K., Horiguchi, H., HORI, M., KARAKI, H., TORIHASHI, S., WARD, S. M. & SANDERS, K. M. 2004. Isolation and characterization of resident macrophages from the smooth muscle layers of murine small intestine. *Neurogastroenterol Motil*, 16, 39-51.
- PACHOLEWSKA, A., MARTI, E., LEEB, T., JAGANNATHAN, V. & GERBER, V. 2017. LPS-induced modules of co-expressed genes in equine peripheral blood mononuclear cells. *BMC Genomics*, 18, 34.
- PACKER, M., PATTERSON-KANE, J. C., SMITH, K. C. & DURHAM, A. E. 2005. Quantification of immune cell populations in the lamina propria of equine jejunal biopsy specimens. *J Comp Pathol*, 132, 90-5.
- PALSSON-MCDERMOTT, E. M. & O'NEILL, L. A. 2004. Signal transduction by the lipopolysaccharide receptor, Toll-like receptor-4. *Immunology*, 113, 153-62.
- PARKINSON, N. J., BUECHNER-MAXWELL, V. A., WITONSKY, S. G., PLEASANT, R. S., WERRE, S. R. & AHMED, S. A. 2017. Characterization of basal and lipopolysaccharide-induced microRNA expression in equine peripheral blood mononuclear cells using Next-Generation Sequencing. *PLoS One*, 12, e0177664.
- PAVLI, P., WOODHAMS, C. E., DOE, W. F. & HUME, D. A. 1990. Isolation and characterization of antigen-presenting dendritic cells from the mouse intestinal lamina propria. *Immunology*, 70, 40-7.

- PEARSON, G. T. 1994. Structural organization and neuropeptide distributions in the equine enteric nervous system: an immunohistochemical study using whole-mount preparations from the small intestine. *Cell Tissue Res*, 276, 523-34.
- PEFANIS, E., WANG, J., ROTHSCCHILD, G., LIM, J., KAZADI, D., SUN, J., FEDERATION, A., CHAO, J., ELLIOTT, O., LIU, Z.-P., ECONOMIDES, ARIS N., BRADNER, JAMES E., RABADAN, R. & BASU, U. 2015. RNA Exosome-Regulated Long Non-Coding RNA Transcription Controls Super-Enhancer Activity. *Cell*, 161, 774-789.
- PERTEA, M., KIM, D., PERTEA, G. M., LEEK, J. T. & SALZBERG, S. L. 2016. Transcript-level expression analysis of RNA-seq experiments with HISAT, StringTie and Ballgown. *Nature Protocols*, 11, 1650.
- PERTEA, M., PERTEA, G. M., ANTONESCU, C. M., CHANG, T.-C., MENDELL, J. T. & SALZBERG, S. L. 2015. StringTie enables improved reconstruction of a transcriptome from RNA-seq reads. *Nature Biotechnology*, 33, 290.
- PHILLIPS, R. J. & POWLEY, T. L. 2012. Macrophages associated with the intrinsic and extrinsic autonomic innervation of the rat gastrointestinal tract. *Auton Neurosci*, 169, 12-27.
- PIRIE, R. S., JAGO, R. C. & HUDSON, N. P. 2014. Equine grass sickness. *Equine Vet J*, 46, 545-53.
- PLOURDE, V., WONG, H. C., WALSH, J. H., RAYBOULD, H. E. & TACHE, Y. 1993. CGRP antagonists and capsaicin on celiac ganglia partly prevent postoperative gastric ileus. *Peptides*, 14, 1225-9.
- POHL, J. M., GUTWEILER, S., THIEBES, S., VOLKE, J. K., KLEIN-HITPASS, L., ZWANZIGER, D., GUNZER, M., JUNG, S., AGACE, W. W., KURTS, C. & ENGEL, D. R. 2017. Irf4-dependent CD103(+)CD11b(+) dendritic cells and the intestinal microbiome regulate monocyte and macrophage activation and intestinal peristalsis in postoperative ileus. *Gut*, 66, 2110-2120.
- PRIDANS, C., DAVIS, G. M., SAUTER, K. A., LISOWSKI, Z. M., CORRIPIO-MIYAR, Y., RAPER, A., LEFEVRE, L., YOUNG, R., MCCULLOCH, M. E., LILLICO, S., MILNE, E., WHITELAW, B. & HUME, D. A. 2016. A Csf1r-EGFP Transgene Provides a Novel Marker for Monocyte Subsets in Sheep. *J Immunol*, 197, 2297-305.
- PU, D. & WANG, W. 2014. Toll-like receptor 4 agonist, lipopolysaccharide, increases the expression levels of cytokines and chemokines in human peripheral blood mononuclear cells. *Exp Ther Med*, 8, 1914-1918.
- PUBLICOVER, N. G., HAMMOND, E. M. & SANDERS, K. M. 1993. Amplification of nitric oxide signaling by interstitial cells isolated from canine colon. *Proc Natl Acad Sci U S A*, 90, 2087-91.
- RAABE, M. R., ISSEL, C. J. & MONTELARO, R. C. 1998. Equine monocyte-derived macrophage cultures and their applications for infectivity and neutralization studies of equine infectious anemia virus. *J Virol Methods*, 71, 87-104.
- RAMERY, E., CLOSSET, R., ART, T., BUREAU, F. & LEKEUX, P. 2009. Expression microarrays in equine sciences. *Vet Immunol Immunopathol*, 127, 197-202.
- RAMERY, E., CLOSSET, R., BUREAU, F., ART, T. & LEKEUX, P. 2008. Relevance of using a human microarray to study gene expression in heaves-affected horses. *The Veterinary Journal*, 177, 216-221.

- RAMOS-VARA, J. A. 2005. Technical aspects of immunohistochemistry. *Vet Pathol*, 42, 405-26.
- RAMOS-VARA, J. A., FRANK, C. B., DUSOLD, D. & MILLER, M. A. 2014. Immunohistochemical expression of melanocytic antigen PNL2, Melan A, S100, and PGP 9.5 in equine melanocytic neoplasms. *Vet Pathol*, 51, 161-6.
- RAMOS-VARA, J. A., KIUPEL, M., BASZLER, T., BLIVEN, L., BRODERSEN, B., CHELACK, B., CZUB, S., DEL PIERO, F., DIAL, S., EHRHART, E. J., GRAHAM, T., MANNING, L., PAULSEN, D., VALLI, V. E., WEST, K. & AMERICAN ASSOCIATION OF VETERINARY LABORATORY DIAGNOSTICIANS SUBCOMMITTEE ON STANDARDIZATION OF, I. 2008. Suggested guidelines for immunohistochemical techniques in veterinary diagnostic laboratories. *J Vet Diagn Invest*, 20, 393-413.
- REICHEL, C. A., PUHR-WESTERHEIDE, D., ZUCHTRIEGEL, G., UHL, B., BERBERICH, N., ZAHLER, S., WYMAN, M. P., LUCKOW, B. & KROMBACH, F. 2012. C-C motif chemokine CCL3 and canonical neutrophil attractants promote neutrophil extravasation through common and distinct mechanisms. *Blood*, 120, 880-90.
- ROBERT, C., LU, X., LAW, A., FREEMAN, T. C. & HUME, D. A. 2011. Macrophages.com: an on-line community resource for innate immunity research. *Immunobiology*, 216, 1203-11.
- ROBINSON, M. D., MCCARTHY, D. J. & SMYTH, G. K. 2010. edgeR: a Bioconductor package for differential expression analysis of digital gene expression data. *Bioinformatics*, 26, 139-40.
- ROGLER, HAUSMANN, VOGL, ASCHENBRENNER, ANDUS, FALK, ANDREESSEN, SCHÖLMERICH, GROSS & ROGLER, G. 1998. Isolation and phenotypic characterization of colonic macrophages. *Clinical & Experimental Immunology*, 112, 205-215.
- ROSSOL, M., HEINE, H., MEUSCH, U., QUANDT, D., KLEIN, C., SWEET, M. J. & HAUSCHILDT, S. 2011. LPS-induced cytokine production in human monocytes and macrophages. *Crit Rev Immunol*, 31, 379-446.
- ROUSSEL, A. J., JR., COHEN, N. D., HOOPER, R. N. & RAKESTRAW, P. C. 2001. Risk factors associated with development of postoperative ileus in horses. *J Am Vet Med Assoc*, 219, 72-8.
- ROWE, E. L., WHITE, N. A., BUECHNER-MAXWELL, V., ROBERTSON, J. L. & WARD, D. L. 2003. Detection of apoptotic cells in intestines from horses with and without gastrointestinal tract disease. *Am J Vet Res*, 64, 982-8.
- RUHL, A., HURST, S. & COLLINS, S. M. 1994. Synergism between interleukins 1 beta and 6 on noradrenergic nerves in rat myenteric plexus. *Gastroenterology*, 107, 993-1001.
- SANDERS, K. M., HWANG, S. J. & WARD, S. M. 2010. Neuroeffector apparatus in gastrointestinal smooth muscle organs. *J Physiol*, 588, 4621-39.
- SANDERS, K. M., KOH, S. D., RO, S. & WARD, S. M. 2012. Regulation of gastrointestinal motility--insights from smooth muscle biology. *Nat Rev Gastroenterol Hepatol*, 9, 633-45.
- SANDERS, K. M., KOH, S. D. & WARD, S. M. 2006. Interstitial cells of Cajal as pacemakers in the gastrointestinal tract. *Annu. Rev. Physiol.*, 68, 307-343.
- SANO, Y., MATSUDA, K., OKAMOTO, M., TAKEHANA, K., HIRAYAMA, K. & TANIYAMA, H. 2016. Distribution of CD163-positive cell and MHC

- class II-positive cell in the normal equine uveal tract. *J Vet Med Sci*, 78, 287-91.
- SANTANGELO, K. S., JOHNSON, A. L., RUPPERT, A. S. & BERTONE, A. L. 2007. Effects of hyaluronan treatment on lipopolysaccharide-challenged fibroblast-like synovial cells. *Arthritis Res Ther*, 9, R1.
- SASAKI, N., MURATA, A., LEE, I. & YAMADA, H. 2008. Evaluation of equine cecal motility by auscultation, ultrasonography and electrointestinography after jejunocostomy. *Res Vet Sci*, 84, 305-10.
- SASMONO, R. T., OCEANDY, D., POLLARD, J. W., TONG, W., PAVLI, P., WAINWRIGHT, B. J., OSTROWSKI, M. C., HIMES, S. R. & HUME, D. A. 2003. A macrophage colony-stimulating factor receptor-green fluorescent protein transgene is expressed throughout the mononuclear phagocyte system of the mouse. *Blood*, 101, 1155-63.
- SAUTER, K. A., PRIDANS, C., SEHGAL, A., BAIN, C. C., SCOTT, C., MOFFAT, L., ROJO, R., STUTCHFIELD, B. M., DAVIES, C. L., DONALDSON, D. S., RENAULT, K., MCCOLL, B. W., MOWAT, A. M., SERRELS, A., FRAME, M. C., MABBOTT, N. A. & HUME, D. A. 2014. The MacBlue binary transgene (csf1r-gal4VP16/UAS-ECFP) provides a novel marker for visualisation of subsets of monocytes, macrophages and dendritic cells and responsiveness to CSF1 administration. *PLoS One*, 9, e105429.
- SAUTER, K. A., WADDELL, L. A., LISOWSKI, Z. M., YOUNG, R., LEFEVRE, L., DAVIS, G. M., CLOHISEY, S. M., MCCULLOCH, M., MAGOWAN, E., MABBOTT, N. A., SUMMERS, K. M. & HUME, D. A. 2016. Macrophage colony-stimulating factor (CSF1) controls monocyte production and maturation and the steady-state size of the liver in pigs. *Am J Physiol Gastrointest Liver Physiol*, 311, G533-47.
- SCHENK, M. & MUELLER, C. 2007. Adaptations of intestinal macrophages to an antigen-rich environment. *Semin Immunol*, 19, 84-93.
- SCHNEEMANN, M., SCHOEDON, G., HOFER, S., BLAU, N., GUERRERO, L. & SCHAFFNER, A. 1993. Nitric oxide synthase is not a constituent of the antimicrobial armature of human mononuclear phagocytes. *J Infect Dis*, 167, 1358-63.
- SCHNEIDER, C. A., RASBAND, W. S. & ELICEIRI, K. W. 2012. NIH Image to ImageJ: 25 years of image analysis. *Nat Methods*, 9, 671-5.
- SCHRODER, K., HERTZOG, P. J., RAVASI, T. & HUME, D. A. 2004. Interferon-gamma: an overview of signals, mechanisms and functions. *J Leukoc Biol*, 75, 163-89.
- SCHRODER, K., IRVINE, K. M., TAYLOR, M. S., BOKIL, N. J., LE CAO, K. A., MASTERMAN, K. A., LABZIN, L. I., SEMPLE, C. A., KAPETANOVIC, R., FAIRBAIRN, L., AKALIN, A., FAULKNER, G. J., BAILLIE, J. K., GONGORA, M., DAUB, C. O., KAWAJI, H., MCLACHLAN, G. J., GOLDMAN, N., GRIMMOND, S. M., CARNINCI, P., SUZUKI, H., HAYASHIZAKI, Y., LENHARD, B., HUME, D. A. & SWEET, M. J. 2012. Conservation and divergence in Toll-like receptor 4-regulated gene expression in primary human versus mouse macrophages. *Proc Natl Acad Sci U S A*, 109, E944-53.
- SCHROEDER, A., MUELLER, O., STOCKER, S., SALOWSKY, R., LEIBER, M., GASSMANN, M., LIGHTFOOT, S., MENZEL, W., GRANZOW, M. &

- RAGG, T. 2006. The RIN: an RNA integrity number for assigning integrity values to RNA measurements. *BMC Mol Biol*, 7, 3.
- SCHUSSER, G. E. & WHITE, N. A. 1997. Morphologic and quantitative evaluation of the myenteric plexuses and neurons in the large colon of horses. *J Am Vet Med Assoc*, 210, 928-34.
- SCHUSSER, G. F., SCHEIDEMANN, W. & HUSKAMP, B. 2000. Muscle thickness and neuron density in the caecum of horses with chronic recurrent caecal impaction. *Equine Vet J Suppl*, 32, 69-73.
- SCHWARZ, N. T., KALFF, J. C., TURLER, A., ENGEL, B. M., WATKINS, S. C., BILLIAR, T. R. & BAUER, A. J. 2001. Prostanoid production via COX-2 as a causative mechanism of rodent postoperative ileus. *Gastroenterology*, 121, 1354-71.
- SCHWARZ, N. T., KALFF, J. C., TURLER, A., SPEIDEL, N., GRANDIS, J. R., BILLIAR, T. R. & BAUER, A. J. 2004. Selective jejunal manipulation causes postoperative pan-enteric inflammation and dysmotility. *Gastroenterology*, 126, 159-69.
- SEHGAL, A., DONALDSON, D. S., PRIDANS, C., SAUTER, K. A., HUME, D. A. & MABBOTT, N. A. 2018. The role of CSF1R-dependent macrophages in control of the intestinal stem-cell niche. *Nature Communications*, 9, 1272.
- SERBINA, N. V. & PAMER, E. G. 2006. Monocyte emigration from bone marrow during bacterial infection requires signals mediated by chemokine receptor CCR2. *Nat Immunol*, 7, 311-7.
- SESTER, D. P., BEASLEY, S. J., SWEET, M. J., FOWLES, L. F., CRONAU, S. L., STACEY, K. J. & HUME, D. A. 1999. Bacterial/CpG DNA down-modulates colony stimulating factor-1 receptor surface expression on murine bone marrow-derived macrophages with concomitant growth arrest and factor-independent survival. *J Immunol*, 163, 6541-50.
- SESTER, D. P., TRIEU, A., BRION, K., SCHRODER, K., RAVASI, T., ROBINSON, J. A., MCDONALD, R. C., RIPOLL, V., WELLS, C. A., SUZUKI, H., HAYASHIZAKI, Y., STACEY, K. J., HUME, D. A. & SWEET, M. J. 2005. LPS regulates a set of genes in primary murine macrophages by antagonising CSF-1 action. *Immunobiology*, 210, 97-107.
- SHAH, S. K., URAY, K. S., STEWART, R. H., LAINE, G. A. & COX, C. S., JR. 2011. Resuscitation-induced intestinal edema and related dysfunction: state of the science. *J Surg Res*, 166, 120-30.
- SHALEM, O., SANJANA, N. E., HARTENIAN, E., SHI, X., SCOTT, D. A., MIKKELSON, T., HECKL, D., EBERT, B. L., ROOT, D. E., DOENCH, J. G. & ZHANG, F. 2014. Genome-scale CRISPR-Cas9 knockout screening in human cells. *Science*, 343, 84-87.
- SHARKEY, K. A., LOMAX, A. E. G., BERTRAND, P. P. & FURNESS, J. B. 1998. Electrophysiology, shape, and chemistry of neurons that project from guinea pig colon to inferior mesenteric ganglia. *Gastroenterology*, 115, 909-918.
- SHARKEY, K. A. & SAVIDGE, T. C. 2014. Role of enteric neurotransmission in host defense and protection of the gastrointestinal tract. *Auton Neurosci*, 181, 94-106.
- SHARMA, S. & PETSALAKI, E. 2018. Application of CRISPR-Cas9 Based Genome-Wide Screening Approaches to Study Cellular Signalling Mechanisms. *International Journal of Molecular Sciences*, 19, 933.

- SHECHTER, R., LONDON, A., VAROL, C., RAPOSO, C., CUSIMANO, M., YOVEL, G., ROLLS, A., MACK, M., PLUCHINO, S., MARTINO, G., JUNG, S. & SCHWARTZ, M. 2009. Infiltrating blood-derived macrophages are vital cells playing an anti-inflammatory role in recovery from spinal cord injury in mice. *PLoS Med*, 6, e1000113.
- SHI, C. & PAMER, E. G. 2011. Monocyte recruitment during infection and inflammation. *Nat Rev Immunol*, 11, 762-74.
- SHIMAZU, R., AKASHI, S., OGATA, H., NAGAI, Y., FUKUDOME, K., MIYAKE, K. & KIMOTO, M. 1999. MD-2, a Molecule that Confers Lipopolysaccharide Responsiveness on Toll-like Receptor 4. *The Journal of Experimental Medicine*, 189, 1777-1782.
- SHINOHARA, H., INOUE, A., TOYAMA-SORIMACHI, N., NAGAI, Y., YASUDA, T., SUZUKI, H., HORAI, R., IWAKURA, Y., YAMAMOTO, T., KARASUYAMA, H., MIYAKE, K. & YAMANASHI, Y. 2005. Dok-1 and Dok-2 are negative regulators of lipopolysaccharide-induced signaling. *J Exp Med*, 201, 333-9.
- SMITH, K. J., BERTONE, A. L., WEISBRODE, S. E. & RADMACHER, M. 2006. Gross, histologic, and gene expression characteristics of osteoarthritic articular cartilage of the metacarpal condyle of horses. *Am J Vet Res*, 67, 1299-306.
- SMITH, P. D., JANOFF, E. N., MOSTELLER-BARNUM, M., MERGER, M., ORENSTEIN, J. M., KEARNEY, J. F. & GRAHAM, M. F. 1997. Isolation and purification of CD14-negative mucosal macrophages from normal human small intestine. *J Immunol Methods*, 202, 1-11.
- SMITH, P. D., SMYTHIES, L. E., MOSTELLER-BARNUM, M., SIBLEY, D. A., RUSSELL, M. W., MERGER, M., SELLERS, M. T., ORENSTEIN, J. M., SHIMADA, T., GRAHAM, M. F. & KUBAGAWA, H. 2001. Intestinal macrophages lack CD14 and CD89 and consequently are down-regulated for LPS- and IgA-mediated activities. *J Immunol*, 167, 2651-6.
- SNOEK, S. A., DHAWAN, S., VAN BREE, S. H., CAILOTTO, C., VAN DIEST, S. A., DUARTE, J. M., STANISOR, O. I., HILBERS, F. W., NIJHUIS, L., KOEMAN, A., VAN DEN WIJNGAARD, R. M., ZUURBIER, C. J., BOECKXSTAENS, G. E. & DE JONGE, W. J. 2012. Mast cells trigger epithelial barrier dysfunction, bacterial translocation and postoperative ileus in a mouse model. *Neurogastroenterol Motil*, 24, 172-84, e91.
- SONEA, I. M., WILSON, D. V., BOWKER, R. M. & ROBINSON, N. E. 1997. *Tachykinin receptors in the equine pelvic flexure*.
- SÔNIGO, F., CASTANHEIRA, F. V. E. S., FERREIRA, R. G., KANASHIRO, A., LEITE, C. A. V. G., NASCIMENTO, D. C., COLÓN, D. F., BORGES, V. D. F., ALVES-FILHO, J. C. & CUNHA, F. Q. 2016. Paradoxical Roles of the Neutrophil in Sepsis: Protective and Deleterious. *Frontiers in Immunology*, 7, 155.
- SONESON, C., LOVE, M. I. & ROBINSON, M. D. 2015. Differential analyses for RNA-seq: transcript-level estimates improve gene-level inferences. *F1000Res*, 4, 1521.
- STANLEY, E. R., CHEN, D. M. & LIN, H. S. 1978. Induction of macrophage production and proliferation by a purified colony stimulating factor. *Nature*, 274, 168-70.

- STARK, M. E., BAUER, A. J. & SZURSZEWski, J. H. 1991. Effect of nitric oxide on circular muscle of the canine small intestine. *J Physiol*, 444, 743-61.
- STEINBACH, F., STARK, R., IBRAHIM, S., GAWAD, E. A.-E., LUDWIG, H., WALTER, J., COMMANDEUR, U. & MAUEL, S. 2005. Molecular cloning and characterization of markers and cytokines for equid myeloid cells. *Veterinary Immunology and Immunopathology*, 108, 227-236.
- STEINEMANN, S., ULEVITCH, R. J. & MACKMAN, N. 1994. Role of the lipopolysaccharide (LPS)-binding protein/CD14 pathway in LPS induction of tissue factor expression in monocytic cells. *Arterioscler Thromb*, 14, 1202-9.
- STOFFELS, B., HUPA, K. J., SNOEK, S. A., VAN BREE, S., STEIN, K., SCHWANDT, T., VILZ, T. O., LYSSON, M., VEER, C. V., KUMMER, M. P., HORNING, V., KALFF, J. C., DE JONGE, W. J. & WEHNER, S. 2014. Postoperative ileus involves interleukin-1 receptor signaling in enteric glia. *Gastroenterology*, 146, 176-87 e1.
- STOFFELS, B., SCHMIDT, J., NAKAO, A., NAZIR, A., CHANTHAPHAVONG, R. S. & BAUER, A. J. 2009. Role of interleukin 10 in murine postoperative ileus. *Gut*, 58, 648-60.
- STUEHR, D. J. & MARLETTA, M. A. 1985. Mammalian nitrate biosynthesis: mouse macrophages produce nitrite and nitrate in response to Escherichia coli lipopolysaccharide. *Proc Natl Acad Sci U S A*, 82, 7738-42.
- STUTCHFIELD, B. M., ANTOINE, D. J., MACKINNON, A. C., GOW, D. J., BAIN, C. C., HAWLEY, C. A., HUGHES, M. J., FRANCIS, B., WOJTACHA, D., MAN, T. Y., DEAR, J. W., DEVEY, L. R., MOWAT, A. M., POLLARD, J. W., PARK, B. K., JENKINS, S. J., SIMPSON, K. J., HUME, D. A., WIGMORE, S. J. & FORBES, S. J. 2015. CSF1 Restores Innate Immunity After Liver Injury in Mice and Serum Levels Indicate Outcomes of Patients With Acute Liver Failure. *Gastroenterology*, 149, 1896-1909 e14.
- SU, A. I., COOKE, M. P., CHING, K. A., HAKAK, Y., WALKER, J. R., WILTSHIRE, T., ORTH, A. P., VEGA, R. G., SAPINOSO, L. M., MOQRICH, A., PATAPOUTIAN, A., HAMPTON, G. M., SCHULTZ, P. G. & HOGENESCH, J. B. 2002. Large-scale analysis of the human and mouse transcriptomes. *Proc Natl Acad Sci U S A*, 99, 4465-70.
- SUZUKI, R., FURUNO, T., MCKAY, D. M., WOLVERS, D., TESHIMA, R., NAKANISHI, M. & BIENENSTOCK, J. 1999. Direct neurite-mast cell communication in vitro occurs via the neuropeptide substance P. *J Immunol*, 163, 2410-5.
- SWEET, M. J., CAMPBELL, C. C., SESTER, D. P., XU, D., MCDONALD, R. C., STACEY, K. J., HUME, D. A. & LIEW, F. Y. 2002. Colony-stimulating factor-1 suppresses responses to CpG DNA and expression of toll-like receptor 9 but enhances responses to lipopolysaccharide in murine macrophages. *J Immunol*, 168, 392-9.
- SWEET, M. J. & HUME, D. A. 1996. Endotoxin signal transduction in macrophages. *J Leukoc Biol*, 60, 8-26.
- SZONDY, Z., SARANG, Z., KISS, B., GARABUCZI, É. & KÖRÖSKÉNYI, K. 2017. Anti-inflammatory Mechanisms Triggered by Apoptotic Cells during Their Clearance. *Frontiers in Immunology*, 8, 909.

- TAKEUCHI, O. & AKIRA, S. 2010. Pattern recognition receptors and inflammation. *Cell*, 140, 805-20.
- TANG, Y., LIU, L., XU, D., ZHANG, W., ZHANG, Y., ZHOU, J. & HUANG, W. 2018. Interaction between astrocytic colony stimulating factor and its receptor on microglia mediates central sensitization and behavioral hypersensitivity in chronic post ischemic pain model. *Brain Behav Immun*, 68, 248-260.
- TARTEY, S., MATSUSHITA, K., VANDENBON, A., ORI, D., IMAMURA, T., MINO, T., STANDLEY, D. M., HOFFMANN, J. A., REICHHART, J.-M., AKIRA, S. & TAKEUCHI, O. 2014. Akirin2 is critical for inducing inflammatory genes by bridging I κ B- ζ and the SWI/SNF complex. *The EMBO Journal*, 33, 2332-2348.
- TATEDA, K., MATSUMOTO, T., MIYAZAKI, S. & YAMAGUCHI, K. 1996. Lipopolysaccharide-induced lethality and cytokine production in aged mice. *Infect Immun*, 64, 769-74.
- TAYLOR, P. R., MARTINEZ-POMARES, L., STACEY, M., LIN, H. H., BROWN, G. D. & GORDON, S. 2005. Macrophage receptors and immune recognition. *Annu Rev Immunol*, 23, 901-44.
- TEIXEIRA NETO, F. J., MCDONELL, W. N., BLACK, W. D., MORAES, A. N. & DURONGHPHONGTORN, S. 2004. Effects of a muscarinic type-2 antagonist on cardiorespiratory function and intestinal transit in horses anesthetized with halothane and xylazine. *Am J Vet Res*, 65, 464-72.
- THE, F. O., BENNINK, R. J., ANKUM, W. M., BUIST, M. R., BUSCH, O. R., GOUMA, D. J., VAN DER HEIDE, S., VAN DEN WIJNGAARD, R. M., DE JONGE, W. J. & BOECKXSTAENS, G. E. 2008. Intestinal handling-induced mast cell activation and inflammation in human postoperative ileus. *Gut*, 57, 33-40.
- THE, F. O., DE JONGE, W. J., BENNINK, R. J., VAN DEN WIJNGAARD, R. M. & BOECKXSTAENS, G. E. 2005. The ICAM-1 antisense oligonucleotide ISIS-3082 prevents the development of postoperative ileus in mice. *Br J Pharmacol*, 146, 252-8.
- THEOCHARIDIS, A., VAN DONGEN, S., ENRIGHT, A. J. & FREEMAN, T. C. 2009. Network visualization and analysis of gene expression data using BioLayout Express(3D). *Nat Protoc*, 4, 1535-50.
- TIMMERMANS, J. P., SCHEUERMANN, D. W., STACH, W., ADRIAENSEN, D. & DE GROODT-LASSEEL, M. H. 1990. Distinct distribution of CGRP-, enkephalin-, galanin-, neuromedin U-, neuropeptide Y-, somatostatin-, substance P-, VIP- and serotonin-containing neurons in the two submucosal ganglionic neural networks of the porcine small intestine. *Cell Tissue Res*, 260, 367-79.
- TINKER, M. K., WHITE, N. A., LESSARD, P., THATCHER, C. D., PELZER, K. D., DAVIS, B. & CARMEL, D. K. 1997. Prospective study of equine colic incidence and mortality. *Equine Vet J*, 29, 448-53.
- TORFS, S., DELESALLE, C., DEWULF, J., DEVISSCHER, L. & DEPREZ, P. 2009. Risk factors for equine postoperative ileus and effectiveness of prophylactic lidocaine. *J Vet Intern Med*, 23, 606-11.

- TRAN, L. & GREENWOOD-VAN MEERVELD, B. 2013. Age-associated remodeling of the intestinal epithelial barrier. *J Gerontol A Biol Sci Med Sci*, 68, 1045-56.
- TRAUB-DARGATZ, J. L., KOPRAL, C. A., SEITZINGER, A. H., GARBER, L. P., FORDE, K. & WHITE, N. A. 2001. Estimate of the national incidence of and operation-level risk factors for colic among horses in the United States, spring 1998 to spring 1999. *J Am Vet Med Assoc*, 219, 67-71.
- TREMBLAY, M. E., STEVENS, B., SIERRA, A., WAKE, H., BESSIS, A. & NIMMERJAHN, A. 2011. The role of microglia in the healthy brain. *J Neurosci*, 31, 16064-9.
- TSOU, C. L., PETERS, W., SI, Y., SLAYMAKER, S., ASLANIAN, A. M., WEISBERG, S. P., MACK, M. & CHARO, I. F. 2007. Critical roles for CCR2 and MCP-3 in monocyte mobilization from bone marrow and recruitment to inflammatory sites. *J Clin Invest*, 117, 902-9.
- TURLER, A., KALFF, J. C., MOORE, B. A., HOFFMAN, R. A., BILLIAR, T. R., SIMMONS, R. L. & BAUER, A. J. 2006. Leukocyte-derived inducible nitric oxide synthase mediates murine postoperative ileus. *Ann Surg*, 244, 220-9.
- TURLER, A., SCHNURR, C., NAKAO, A., TOGEL, S., MOORE, B. A., MURASE, N., KALFF, J. C. & BAUER, A. J. 2007. Endogenous endotoxin participates in causing a panenteric inflammatory ileus after colonic surgery. *Ann Surg*, 245, 734-44.
- TURLER, A., SCHWARZ, N. T., TURLER, E., KALFF, J. C. & BAUER, A. J. 2002. MCP-1 causes leukocyte recruitment and subsequently endotoxemic ileus in rat. *Am J Physiol Gastrointest Liver Physiol*, 282, G145-55.
- UEMURA, K., TATEWAKI, M., HARRIS, M. B., UENO, T., MANTYH, C. R., PAPPAS, T. N. & TAKAHASHI, T. 2004. Magnitude of abdominal incision affects the duration of postoperative ileus in rats. *Surg Endosc*, 18, 606-10.
- UNSINGER, J., MCDONOUGH, J. S., SHULTZ, L. D., FERGUSON, T. A. & HOTCHKISS, R. S. 2009. Sepsis-induced human lymphocyte apoptosis and cytokine production in "humanized" mice. *J Leukoc Biol*, 86, 219-27.
- UNTERGASSER, A., CUTCUTACHE, I., KORESSAAR, T., YE, J., FAIRCLOTH, B. C., REMM, M. & ROZEN, S. G. 2012. Primer3--new capabilities and interfaces. *Nucleic Acids Res*, 40, e115.
- VAN BREE, S. H., BEMELMAN, W. A., HOLLMANN, M. W., ZWINDERMAN, A. H., MATTEOLI, G., EL TEMNA, S., THE, F. O., VLUG, M. S., BENNINK, R. J. & BOECKXSTAENS, G. E. 2014. Identification of clinical outcome measures for recovery of gastrointestinal motility in postoperative ileus. *Ann Surg*, 259, 708-14.
- VAN BREE, S. H., NEMETHOVA, A., VAN BOVENKAMP, F. S., GOMEZ-PINILLA, P., ELBERS, L., DI GIOVANGIULIO, M., MATTEOLI, G., VAN VLIET, J., CAILOTTO, C., TANCK, M. W. & BOECKXSTAENS, G. E. 2012. Novel method for studying postoperative ileus in mice. *Int J Physiol Pathophysiol Pharmacol*, 4, 219-27.
- VAN DEN HEUVEL, M. M., TENSEN, C. P., VAN AS, J. H., VAN DEN BERG, T. K., FLUITSMA, D. M., DIJKSTRA, C. D., DOPP, E. A., DROSTE, A., VAN GAALLEN, F. A., SORG, C., HOGGER, P. & BEELEN, R. H. 1999. Regulation of CD 163 on human macrophages: cross-linking of CD163 induces signaling and activation. *J Leukoc Biol*, 66, 858-66.

- VAN FURTH, R. 1992. Production and migration of monocytes and kinetics of macrophages. *Mononuclear phagocytes*. Springer.
- VAN FURTH, R. & COHN, Z. A. 1968. The origin and kinetics of mononuclear phagocytes. *J Exp Med*, 128, 415-35.
- VAN GORP, H., DELPUTTE, P. L. & NAUWYNCK, H. J. 2010. Scavenger receptor CD163, a Jack-of-all-trades and potential target for cell-directed therapy. *Molecular Immunology*, 47, 1650-1660.
- VANNUCCHI, M. G. 1999. Receptors in interstitial cells of Cajal: identification and possible physiological roles. *Microsc Res Tech*, 47, 325-35.
- VATHER, R. & BISSETT, I. P. 2013. Risk factors for the development of prolonged post-operative ileus following elective colorectal surgery. *Int J Colorectal Dis*, 28, 1385-91.
- VATHER, R., O'GRADY, G., BISSETT, I. P. & DINNING, P. G. 2014. Postoperative ileus: mechanisms and future directions for research. *Clin Exp Pharmacol Physiol*, 41, 358-70.
- VATHER, R., TRIVEDI, S. & BISSETT, I. 2013. Defining postoperative ileus: results of a systematic review and global survey. *J Gastrointest Surg*, 17, 962-72.
- VENARA, A., NEUNLIST, M., SLIM, K., BARBIEUX, J., COLAS, P. A., HAMY, A. & MEURETTE, G. 2016. Postoperative ileus: Pathophysiology, incidence, and prevention. *J Visc Surg*, 153, 439-446.
- VERHEIJDEN, S., DE SCHEPPER, S. & BOECKXSTAENS, G. E. 2015. Neuron-macrophage crosstalk in the intestine: a "microglia" perspective. *Front Cell Neurosci*, 9, 403.
- VOGEL, S. N., MADONNA, G. S., WAHL, L. M. & RICK, P. D. 1984. In vitro stimulation of C3H/HeJ spleen cells and macrophages by a lipid A precursor molecule derived from Salmonella typhimurium. *J Immunol*, 132, 347-53.
- VOLKMAN, A., CHANG, N. C., STRAUSBAUCH, P. H. & MORAHAN, P. S. 1983. Differential effects of chronic monocyte depletion on macrophage populations. *Lab Invest*, 49, 291-8.
- WADDELL, L. A., LEFEVRE, L., BUSH, S. J., RAPER, A., YOUNG, R., LISOWSKI, Z. M., MCCULLOCH, M., MURIUKI, C., SAUTER, K. A., CLARK, E. L., IRVINE, K., PRIDANS, C., HOPE, J. C. & HUME, D. A. 2018. ADGRE1 (EMR1, 1 F4/80) is a rapidly-evolving gene expressed in mammalian monocyte macrophages. *Frontiers in Immunology*.
- WALDHAUSEN, J. H., SHAFFREY, M. E., SKENDERIS, B. S., 2ND, JONES, R. S. & SCHIRMER, B. D. 1990. Gastrointestinal myoelectric and clinical patterns of recovery after laparotomy. *Ann Surg*, 211, 777-84; discussion 785.
- WALSH, C., GANGLOFF, M., MONIE, T., SMYTH, T., WEI, B., MCKINLEY, T. J., MASKELL, D., GAY, N. & BRYANT, C. 2008. Elucidation of the MD-2/TLR4 interface required for signaling by lipid IVa. *J Immunol*, 181, 1245-54.
- WANG, F., FLANAGAN, J., SU, N., WANG, L.-C., BUI, S., NIELSON, A., WU, X., VO, H.-T., MA, X.-J. & LUO, Y. 2012a. RNAscope: A Novel in Situ RNA Analysis Platform for Formalin-Fixed, Paraffin-Embedded Tissues. *The Journal of Molecular Diagnostics : JMD*, 14, 22-29.
- WANG, Y., SZRETTTER, K. J., VERMI, W., GILFILLAN, S., ROSSINI, C., CELLA, M., BARROW, A. D., DIAMOND, M. S. & COLONNA, M.

- 2012b. IL-34 is a tissue-restricted ligand of CSF1R required for the development of Langerhans cells and microglia. *Nat Immunol*, 13, 753-60.
- WARD, S. M., BECKETT, E. A., WANG, X., BAKER, F., KHOYI, M. & SANDERS, K. M. 2000. Interstitial cells of Cajal mediate cholinergic neurotransmission from enteric motor neurons. *J Neurosci*, 20, 1393-403.
- WARD, S. M. & SANDERS, K. M. 2001. Interstitial cells of Cajal: primary targets of enteric motor innervation. *Anat Rec*, 262, 125-35.
- WARREN, H. S. 2009. Editorial: Mouse models to study sepsis syndrome in humans. *J Leukoc Biol*, 86, 199-201.
- WATSON, E. D., MAIR, T. S. & SWEENEY, C. R. 1990. Immunoreactive prostaglandin production by equine monocytes and alveolar macrophages and concentrations of PGE2 and PGF in bronchoalveolar lavage fluid. *Res Vet Sci*, 49, 88-91.
- WATTANANIT, S., TORNERO, D., GRAUBARDT, N., MEMANISHVILI, T., MONNI, E., TATARISHVILI, J., MISKINYTE, G., GE, R., AHLENIUS, H., LINDVALL, O., SCHWARTZ, M. & KOKAIA, Z. 2016. Monocyte-Derived Macrophages Contribute to Spontaneous Long-Term Functional Recovery after Stroke in Mice. *J Neurosci*, 36, 4182-95.
- WEBSTER, J. D., MILLER, M. A., DUSOLD, D. & RAMOS-VARA, J. 2009. Effects of prolonged formalin fixation on diagnostic immunohistochemistry in domestic animals. *J Histochem Cytochem*, 57, 753-61.
- WEHNER, S., BEHRENDT, F. F., LYUTENSKI, B. N., LYSSON, M., BAUER, A. J., HIRNER, A. & KALFF, J. C. 2007. Inhibition of macrophage function prevents intestinal inflammation and postoperative ileus in rodents. *Gut*, 56, 176-85.
- WEHNER, S., KOSCIELNY, A., VILZ, T. O., STOFFELS, B., ENGEL, D. R., KURTS, C. & KALFF, J. 2011. Measurement of gastrointestinal and colonic transit in mice.
- WEHNER, S., SCHWARZ, N. T., HUNSDOERFER, R., HIERHOLZER, C., TWEARDY, D. J., BILLIAR, T. R., BAUER, A. J. & KALFF, J. C. 2005. Induction of IL-6 within the rodent intestinal muscularis after intestinal surgical stress. *Surgery*, 137, 436-446.
- WEHNER, S., STRAESSER, S., VILZ, T. O., PANTELIS, D., SIELECKI, T., DE LA CRUZ, V. F., HIRNER, A. & KALFF, J. C. 2009. Inhibition of p38 mitogen-activated protein kinase pathway as prophylaxis of postoperative ileus in mice. *Gastroenterology*, 136, 619-29.
- WEIGMANN, B., TUBBE, I., SEIDEL, D., NICOLAEV, A., BECKER, C. & NEURATH, M. F. 2007. Isolation and subsequent analysis of murine lamina propria mononuclear cells from colonic tissue. *Nat Protoc*, 2, 2307-11.
- WELLS, C. A., RAVASI, T. & HUME, D. A. 2005. Inflammation suppressor genes: please switch out all the lights. *J Leukoc Biol*, 78, 9-13.
- WERNERS, A. H., BULL, S., FINK-GREMMELS, J. & BRYANT, C. E. 2004. Generation and characterisation of an equine macrophage cell line (e-CAS cells) derived from equine bone marrow cells. *Vet Immunol Immunopathol*, 97, 65-76.
- WHITE, N. A. 1990. *Epidemiology and aetiology of colic*, Philadelphia, Lea and Febiger.

- WILLIAMS, R. M., BERTHOUD, H. R. & STEAD, R. H. 1997. Vagal afferent nerve fibres contact mast cells in rat small intestinal mucosa. *Neuroimmunomodulation*, 4, 266-70.
- WILSMANN-THEIS, D., KOCH, S., MINDNICH, C., BONNESS, S., SCHNAUTZ, S., VON BUBNOFF, D. & BIEBER, T. 2013. Generation and functional analysis of human TNF-alpha/iNOS-producing dendritic cells (Tip-DC). *Allergy*, 68, 890-8.
- WOLF, A. M., WOLF, D., RUMPOLD, H., MOSCHEN, A. R., KASER, A., OBRIST, P., FUCHS, D., BRANDACHER, G., WINKLER, C., GEBOES, K., RUTGEERTS, P. & TILG, H. 2004. Overexpression of indoleamine 2,3-dioxygenase in human inflammatory bowel disease. *Clin Immunol*, 113, 47-55.
- WONG, D. M., DAVIS, J. L. & WHITE, N. A. 2011a. Motility of the equine gastrointestinal tract: Physiology and pharmacotherapy. *Equine Veterinary Education*, 23, 88-100.
- WONG, K. L., TAI, J. J., WONG, W. C., HAN, H., SEM, X., YEAP, W. H., KOURILSKY, P. & WONG, S. C. 2011b. Gene expression profiling reveals the defining features of the classical, intermediate, and nonclassical human monocyte subsets. *Blood*, 118, e16-31.
- WRIGHT, S. D., RAMOS, R. A., TOBIAS, P. S., ULEVITCH, R. J. & MATHISON, J. C. 1990. CD14, a receptor for complexes of lipopolysaccharide (LPS) and LPS binding protein. *Science*, 249, 1431-3.
- WU, Z., HU, T., ROTHWELL, L., VERVELDE, L., KAISER, P., BOULTON, K., NOLAN, M. J., TOMLEY, F. M., BLAKE, D. P. & HUME, D. A. 2016. Analysis of the function of IL-10 in chickens using specific neutralising antibodies and a sensitive capture ELISA. *Dev Comp Immunol*, 63, 206-12.
- WUYTS, A., STRUYF, S., GIJSBERS, K., SCHUTYSER, E., PUT, W., CONINGS, R., LENAERTS, J.-P., GEBOES, K., OPDENAKKER, G., MENTEN, P., PROOST, P. & VAN DAMME, J. 2003. The CXC Chemokine GCP-2/CXCL6 Is Predominantly Induced in Mesenchymal Cells by Interleukin-1 β and Is Down-Regulated by Interferon- γ : Comparison with Interleukin-8/CXCL8. *Laboratory Investigation*, 83, 23-34.
- WUYTS, A., VAN OSSELAER, N., HAELENS, A., SAMSON, I., HERDEWIJN, P., BEN-BARUCH, A., OPPENHEIM, J. J., PROOST, P. & VAN DAMME, J. 1997. Characterization of synthetic human granulocyte chemotactic protein 2: usage of chemokine receptors CXCR1 and CXCR2 and in vivo inflammatory properties. *Biochemistry*, 36, 2716-23.
- WYNN, T. A. 2008. Cellular and molecular mechanisms of fibrosis. *J Pathol*, 214, 199-210.
- XAUS, J., COMALADA, M., VALLEDOR, A. F., LLOBERAS, J., LOPEZ-SORIANO, F., ARGILES, J. M., BOGDAN, C. & CELADA, A. 2000. LPS induces apoptosis in macrophages mostly through the autocrine production of TNF-alpha. *Blood*, 95, 3823-31.
- YAMAMOTO, M., YAMAZAKI, S., UEMATSU, S., SATO, S., HEMMI, H., HOSHINO, K., KAISHO, T., KUWATA, H., TAKEUCHI, O., TAKESHIGE, K., SAITOH, T., YAMAOKA, S., YAMAMOTO, N., YAMAMOTO, S., MUTA, T., TAKEDA, K. & AKIRA, S. 2004. Regulation

- of Toll/IL-1-receptor-mediated gene expression by the inducible nuclear protein I κ B ζ . *Nature*, 430, 218.
- YAMATE, J., YOSHIDA, H., TSUKAMOTO, Y., IDE, M., KUWAMURA, M., OHASHI, F., MIYAMOTO, T., KOTANI, T., SAKUMA, S. & TAKEYA, M. 2000. Distribution of cells immunopositive for AM-3K, a novel monoclonal antibody recognizing human macrophages, in normal and diseased tissues of dogs, cats, horses, cattle, pigs, and rabbits. *Vet Pathol*, 37, 168-76.
- YAMAZAKI, S., MUTA, T. & TAKESHIGE, K. 2001. A novel IkappaB protein, IkappaB-zeta, induced by proinflammatory stimuli, negatively regulates nuclear factor-kappaB in the nuclei. *J Biol Chem*, 276, 27657-62.
- YATES, A., AKANNI, W., AMODE, M. R., BARRELL, D., BILLIS, K., CARVALHO-SILVA, D., CUMMINS, C., CLAPHAM, P., FITZGERALD, S., GIL, L., GIRÓN, C. G., GORDON, L., HOURLIER, T., HUNT, S. E., JANACEK, S. H., JOHNSON, N., JUETTEMANN, T., KEENAN, S., LAVIDAS, I., MARTIN, F. J., MAUREL, T., MCLAREN, W., MURPHY, D. N., NAG, R., NUHN, M., PARKER, A., PATRICIO, M., PIGNATELLI, M., RAHTZ, M., RIAT, H. S., SHEPPARD, D., TAYLOR, K., THORMANN, A., VULLO, A., WILDER, S. P., ZADISSA, A., BIRNEY, E., HARROW, J., MUFFATO, M., PERRY, E., RUFFIER, M., SPUDICH, G., TREVANION, S. J., CUNNINGHAM, F., AKEN, B. L., ZERBINO, D. R. & FLICEK, P. 2016. Ensembl 2016. *Nucleic Acids Research*, 44, D710-D716.
- YOUNG, R., BUSH, S. J., LEFEVRE, L., MCCULLOCH, M. E. B., LISOWSKI, Z. M., MURIUKI, C., WADDELL, L. A., SAUTER, K. A., PRIDANS, C., CLARK, E. L. & HUME, D. A. 2018. Species-Specific Transcriptional Regulation of Genes Involved in Nitric Oxide Production and Arginine Metabolism in Macrophages. *ImmunoHorizons*, 2, 27-37.
- ZHOU, L., CAO, X., FANG, J., LI, Y. & FAN, M. 2015. Macrophages polarization is mediated by the combination of PRR ligands and distinct inflammatory cytokines. *International Journal of Clinical and Experimental Pathology*, 8, 10964-10974.
- ZIGMOND, E., SAMIA-GRINBERG, S., PASMANIK-CHOR, M., BRAZOWSKI, E., SHIBOLET, O., HALPERN, Z. & VAROL, C. 2014. Infiltrating monocyte-derived macrophages and resident kupffer cells display different ontogeny and functions in acute liver injury. *J Immunol*, 193, 344-53.
- ZITTEL, T. T., DE GIORGIO, R., BRECHA, N. C., STERNINI, C. & RAYBOULD, H. E. 1993. Abdominal surgery induces c-fos expression in the nucleus of the solitary tract in the rat. *Neurosci Lett*, 159, 79-82.
- ZITTEL, T. T., LLOYD, K. C., ROTHENHOFER, I., WONG, H., WALSH, J. H. & RAYBOULD, H. E. 1998. Calcitonin gene-related peptide and spinal afferents partly mediate postoperative colonic ileus in the rat. *Surgery*, 123, 518-27.
- ZITTEL, T. T., REDDY, S. N., PLOURDE, V. & RAYBOULD, H. E. 1994a. Role of spinal afferents and calcitonin gene-related peptide in the postoperative gastric ileus in anesthetized rats. *Ann Surg*, 219, 79-87.

- ZITTEL, T. T., ROTHENHOFER, I., MEYER, J. H. & RAYBOULD, H. E. 1994b. Small intestinal capsaicin-sensitive afferents mediate feedback inhibition of gastric emptying in rats. *Am J Physiol*, 267, G1142-5.

This page was left intentionally blank

Chapter 9. Appendices

9.1 Csf1r-mApple transgene expression and ligand binding in vivo reveal dynamics of CSF1R expression within the mononuclear phagocyte system

Csf1r-mApple Transgene Expression and Ligand Binding In Vivo Reveal Dynamics of CSF1R Expression within the Mononuclear Phagocyte System

Catherine A. Hawley,^{*,1} Rocio Rojo,^{†,1} Anna Raper,^{†,1} Kristin A. Sauter,[†] Zofia M. Lisowski,[†] Kathleen Grabert,[†] Calum C. Bain,^{*} Gemma M. Davis,^{†,‡} Pieter A. Louwe,^{*} Michael C. Ostrowski,[§] David A. Hume,^{*,†,¶} Clare Pridans,^{*,†} and Stephen J. Jenkins^{*}

CSF1 is the primary growth factor controlling macrophage numbers, but whether expression of the CSF1 receptor differs between discrete populations of mononuclear phagocytes remains unclear. We have generated a *Csf1r*-mApple transgenic fluorescent reporter mouse that, in combination with lineage tracing, Alexa Fluor 647-labeled CSF1-Fc and CSF1, and a modified Δ *Csf1*-enhanced cyan fluorescent protein (ECFP) transgene that lacks a 150 bp segment of the distal promoter, we have used to dissect the differentiation and CSF1 responsiveness of mononuclear phagocyte populations in situ. Consistent with previous *Csf1r*-driven reporter lines, *Csf1r*-mApple was expressed in blood monocytes and at higher levels in tissue macrophages, and was readily detectable in whole mounts or with multiphoton microscopy. In the liver and peritoneal cavity, uptake of labeled CSF1 largely reflected transgene expression, with greater receptor activity in mature macrophages than monocytes and tissue-specific expression in conventional dendritic cells. However, CSF1 uptake also differed between subsets of monocytes and discrete populations of tissue macrophages, which in macrophages correlated with their level of dependence on CSF1 receptor signaling for survival rather than degree of transgene expression. A double Δ *Csf1r*-ECFP-*Csf1r*-mApple transgenic mouse distinguished subpopulations of microglia in the brain, and permitted imaging of interstitial macrophages distinct from alveolar macrophages, and pulmonary monocytes and conventional dendritic cells. The *Csf1r*-mApple mice and fluorescently labeled CSF1 will be valuable resources for the study of macrophage and CSF1 biology, which are compatible with existing EGFP-based reporter lines. *The Journal of Immunology*, 2018, 200: 000–000.

The mononuclear phagocyte system (MPS) is a family of functionally related myeloid cells comprising progenitor cells, monocytes, macrophages, and conventional dendritic cells (cDC) (1–5). Macrophages resident in tissues may be

derived from definitive hematopoiesis via circulating monocytes or by self-renewal from cells seeded during embryonic or early postnatal life (1, 2, 4, 5). cDCs have been classified as those cells deriving from common dendritic cell (DC) progenitors via circulating pre-DC (1, 6, 7). Regardless of their developmental origin, macrophages and their precursors express the M-CSF receptor CSF1R, and depend upon signals from two ligands, CSF1 or IL34, for proliferation, differentiation, and survival (2, 3). Receptor-mediated internalization and destruction of CSF1 controls its availability (8) and provides a homeostatic control on macrophage numbers (3). Accordingly, administration of recombinant CSF1 (9) or a more stable CSF1-Fc fusion protein (10–12) to mice produces expansion of blood monocyte and tissue macrophage populations, yet the degree to which CSF1R expression and activity differ between populations of mononuclear phagocytes is unclear.

cDC express high levels of a related tyrosine kinase receptor, Fms-like tyrosine kinase 3 (Flt3). Their numbers are greatly increased following treatment of mice with Flt3 ligand (Flt3L), and depleted in Flt3L-deficient animals (7, 13–17). Two subsets of cDC, cDC1 and cDC2, appear to differ in their expression of *Csf1r*. cDC1 are not generally dependent upon CSF1 and lack *Csf1r* mRNA (14). cDC2 have been more difficult to define because of major overlaps in cellular phenotype with other CD11b⁺ CD11c⁺MHC class II (MHCIId)⁺ monocyte-derived APCs (18–20). Genuine Flt3-dependent cDC2 of common DC progenitor origin have been defined based upon migratory behavior and the lack of the macrophage markers CD64 and F4/80 (6, 15, 21, 22). With this definition, cDC2 in various tissues expressed lower levels of

^{*}Medical Research Council Centre for Inflammation Research, University of Edinburgh, Edinburgh EH16 4TJ, United Kingdom; [†]The Roslin Institute, University of Edinburgh, Midlothian EH25 9RG, United Kingdom; [‡]Faculty of Life Sciences, The University of Manchester, Manchester M13 9PL, United Kingdom; [§]Hollings Cancer Center, Medical University of South Carolina, Charleston, SC 29425; and [¶]Mater Research—University of Queensland, Translational Research Institute, Woolloongabba, Queensland 4104, Australia

¹C.A.H., R.R., and A.R. contributed equally to this work.

ORCID: 0000-0001-9686-3377 (R.R.); 0000-0003-0949-9963 (A.R.); 0000-0002-1323-9593 (Z.M.L.); 0000-0001-8884-327X (C.C.B.); 0000-0001-8323-5013 (G.M.D.); 0000-0001-9423-557X (C.P.); 0000-0002-0233-5424 (S.J.J.).

Received for publication October 30, 2017. Accepted for publication January 17, 2018.

This work was supported by Medical Research Council Grant MR/L008076/1. P.A.L. was supported by a Wellcome Trust Ph.D. studentship.

Address correspondence and reprint requests to Dr. Stephen J. Jenkins, University of Edinburgh, Queens Medical Research Centre, 47 Little France Crescent, Edinburgh EH16 4TJ, U.K. E-mail address: stephen.jenkins@ed.ac.uk

The online version of this article contains supplemental material.

Abbreviations used in this article: AF647, Alexa Fluor 647; BM, bone marrow; cDC, conventional dendritic cell; DC, dendritic cell; ECFP, enhanced cyan fluorescent protein; Flt3, Fms-like tyrosine kinase 3; Flt3L, Flt3 ligand; KC, Kupffer cell; MFI, median fluorescence intensity; MHCIId, MHC class II; MPS, mononuclear phagocyte system; pDC, plasmacytoid DC; WT, wild type.

This article is distributed under the terms of the [CC BY 4.0 Unported license](https://creativecommons.org/licenses/by/4.0/).

Copyright © 2018 The Authors 0022-1767/18/5355.00

www.jimmunol.org/doi/10.4049/jimmunol.1701488

Csf1r mRNA than monocyte-derived APC (15, 22) and have been considered CSF1R independent (1). The levels of surface CSF1R largely distinguish Flt3L-dependent cDC2 from short-lived monocyte-derived CD11c⁺ MHCII⁺ cells in the serous cavities (23, 24). However, cDC2 isolated from spleen express high levels of both *Csf1r* and *Flt3* mRNA (www.biogps.org) and their numbers are controlled by CSF1 *in vivo* (25). Therefore, it remains unclear whether there is a genuine dichotomy between Csf1r and Flt3-dependent myeloid APC.

CSF1R on macrophages is continuously removed from the cell surface by endocytosis and degraded following ligand binding. For that reason, the detection of CSF1R protein by immunohistochemistry or flow cytometry does not provide a clear indication of functional expression. To identify Csf1r-expressing cells *in situ*, regulatory elements of the murine *Csf1r* locus, including a 150 bp segment of the distal promoter, were used to produce *Csf1r*-EGFP reporter mice (26). The same promoter construct was used to drive constitutive (27) and inducible cre-recombinase to support macrophage-specific conditional mutations (28) as well as lineage tracing (29), and these tools have been widely distributed among the research community. However, new resources are required to verify with single-cell resolution the extent to which *Csf1r* transgene expression reflects that of functional CSF1R protein.

In addition to aiding our understanding of the regulation of myeloid cells, visualization of *Csf1r* gene and protein expression may also be useful to study cell interactions *in vivo* due to the lack of tools to identify discrete MPS populations during multicolor imaging. A binary enhanced cyan fluorescent protein (ECFP) reporter (Δ *Csf1r*-Gal4VP16/UAS-ECFP) transgene with a 150 bp segment of the distal Csf1r promoter deleted, termed Δ *Csf1r*-ECFP, has provided a novel tool to support *in vivo* imaging of monocyte trafficking (30, 31), because expression was lost from the large majority of tissue macrophages but remained in blood monocytes, microglia, Langerhans cells, and cDC2 (32). In particular, dual reporter mice, such as those generated by crossing the *Cx3cr1*-EGFP and *Ccr2*-RFP mice, have been valuable tools for visualizing monocyte subsets and their differentiation in the brain and liver (33), findings that would not have been obtainable using single reporter mice. However, many other macrophage and nonmacrophage reporter genes use EGFP, rendering the original *Csf1r*-EGFP transgene of limited use for this purpose. Thus, additional monocyte/macrophage reporter mice that are compatible with existing EGFP-based reporters are needed.

Hence, we have created new tools and assays to image and assess *Csf1r* gene and protein expression that can be combined conveniently with common fluorophores, EGFP transgenes, and the Δ *Csf1r*-ECFP transgene for use in imaging and flow cytometry. In particular, we characterize a new *Csf1r*-mApple line expressing the red reporter gene *mApple* under the same promoter used in the *Csf1r*-EGFP reporter, and apply this in combination with the Δ *Csf1r*-ECFP transgene, lineage tracing, and labeled CSF1-Fc and CSF1 proteins to distinguish different cellular compartments within the MPS, and to dissect the homeostatic roles of CSF1.

Materials and Methods

Plasmid constructs

The 7.2 kb *Csf1r* reporter construct previously used to generate the *Csf1r*-EGFP mice (26) was digested with ApaI and Sall (NEB) to remove EGFP before gel purification using the QIAquick gel extraction kit (Qiagen). Overhangs were removed with Mungbean nuclease (NEB) and DNA was purified using QIAGEN MinElute columns (Qiagen), then dephosphorylated using thermostable alkaline phosphatase (Promega). A construct encoding the fluorescent protein *Csf1r*-mApple (34) was digested with SmaI and AflII, similarly purified, and overhangs removed before both constructs were precipitated with EtOH/NaOAc and then ligated with T4

ligase (NEB) at 16°C overnight. The resulting *Csf1r*-mApple construct was transformed into DH5 α competent cells. The *Csf1r*-rTA-M2 construct utilizing the same 7.2 kb mouse *Csf1r* promoter region was used previously to generate *Csf1r*-rTA transgenic mice (35). For generation of transgenic mice, plasmid backbones were removed by digestion with DrrI/PvuI (*Csf1r*-mApple, NEB) and Sall/MluI (*Csf1r*-rTA, Promega/NEB) and then gel-purified using a QIAquick gel extraction kit. DNA was then further purified using AMPure XP beads (Agencourt) according to the instructions.

Generation of transgenic mice and animal maintenance

Animal experiments were permitted under license by the U.K. Home Office, and were approved by the University of Edinburgh Animal Welfare and Ethical Review Body. All mice including wild-type (WT) C57BL/6J OlaHsd CD45.2⁺, congenic CD45.1⁺CD45.2⁺, *Csf1r*-EGFP (26), Δ *Csf1r*-Gal4VP16/UAS-ECFP (36), and *Ccr2*^{-/-} (37) lines were bred and housed in specific-pathogen free facilities at the University of Edinburgh. *Csf1r*-mApple/*Csf1r*-rTA transgenic mice were generated at the University of Edinburgh's Central Biological Services Transgenic Core facility by microinjection of transgenes into the pronuclei of fertilized oocytes from C57BL/6J OlaHsd mice. The integration of the transgenes was determined by PCR analysis of genomic DNA isolated from ear biopsy using primers that amplified a 565 bp product between the c-fms promoter and rTA gene, and a 507 bp product between the c-fms promoter and *Csf1r*-mApple gene, using primers 5'-TTC CAG AAC CAG AGC CAG AG-3' (forward) and 5'-CTG TTC CTC CAA TAC GCA GC-3' (reverse), and 5'-CCT ACA TGT GTG GCT AAG GA-3' (forward) and 5'-CTT GAA GTA GTC GGG GAT GT-3' (reverse), respectively, and amplification temperatures of 35 cycles of 30 s at 94, 55, and 72°C, after an initial denaturing step of 94°C for 5 min. Expression of *Csf1r*-mApple was verified by screening 10 μ l blood for the presence of *Csf1r*-mApple fluorescence by flow cytometry. One founder positive for both transgenes transmitted the transgenes to progeny and established the *Csf1r*-mApple/*Csf1r*-rTA line (referred to as *Csf1r*-mApple). The *Csf1r*-mApple line was maintained by breeding to C57BL/6J OlaHsd mice, or where specified, bred to the Δ *Csf1r*-ECFP line, for which subsequent analysis was performed on F1 progeny. For maintenance of the *Csf1r*-mApple line, transgenic progeny were initially identified by PCR analysis of genomic DNA and flow-cytometric assessment of the presence of *Csf1r*-mApple in blood cells, and subsequently by flow cytometry alone. For identification of myeloid populations replenished by CCR2-dependent bone marrow (BM) precursors, tissue-protected BM chimeric mice were generated as previously described (23). Briefly, anesthetized C57BL/6 CD45.1⁺CD45.2⁺ congenic mice were exposed to a single dose of 9.5 Gy γ -irradiation, while all but the hind legs and lower abdomen were protected by a 2 inch lead shield. Animals were subsequently given 2–5 \times 10⁶ BM cells from CD45.2⁺ C57BL/6J mice or *Ccr2*^{-/-} animals by *i.v.* injection before being left for 8 wk prior to analysis of chimerism in the tissue compartments. All experiments were performed with age- and sex-matched littermate control mice and approved by the University of Edinburgh Animal Welfare and Ethical Review Body under license granted by the U.K. Home Office.

Tissue digestion and FACS analysis

Unless otherwise stated, mice were culled by a rising concentration of CO₂. Then 100 μ l of blood was collected by cardiac puncture into EDTA tubes. The peritoneal cavity was lavaged with RPMI 1640 containing 2 mM EDTA and 10 mM HEPES (Invitrogen). Cadavers were subsequently perfused and lung and liver removed and chopped finely, and digested in prewarmed collagenase mixture [0.625 mg ml⁻¹ collagenase D (Roche), 0.85 mg ml⁻¹ collagenase V (Sigma-Aldrich), 1 mg ml⁻¹ dispase (Life Technologies, Invitrogen), and 30 U ml⁻¹ DNase (Roche Diagnostics) in RPMI 1640] for 22 and 45 min respectively in a shaking incubator at 37°C before being passed through a 100 μ m filter. Lung preparations were washed in PBS containing 2 mM EDTA (Life Technologies, Invitrogen) and 0.5% BSA (Sigma-Aldrich), termed FACS buffer, followed by centrifugation at 300 g for 5 min, whereas liver preparations were washed in 50 ml then 30 ml of ice-cold RPMI 1640 followed by centrifugation at 300 g for 5 min. Erythrocytes in tissues and blood were lysed using RBC lysis buffer from Sigma-Aldrich or BioLegend, respectively. All cells were maintained on ice until further use. Cellular content of the preparations was assessed by cell counting using a CASY TT counter (Roche). Equal numbers of cells or equivalent volumes of blood were stained with Zombie Aqua viability dye (Invitrogen) blocked with 0.025 μ g anti-CD16/32 (2.4G2; BioLegend) and 1:10 heat-inactivated mouse serum (Invitrogen), and then surface stained with a combination of Abs in FACS buffer. The following Abs were used: F4/80 (BM8), Siglec-F (E50-2440), Siglec-F (E522-10D8), Ly6C (HK1.4), CD11b (M1/70), CD11c (N418), MHCII

(M5/114.15.2), CD19 (6D5), CD3 (17A2), CD3 (17A2), CSF1R (AFS98), CD45.1 (A20), CD45.2 (104), CD226 (10E5), CD64 (X57-5/7), Ly6G (1A8), CD26 (H194-112), and PDCA-1 (927) (eBioscience, Miltenyi Biotec, or BD Europe). Where applicable, cells were subsequently stained with streptavidin-conjugated fluorochromes. Fluorescence minus one controls confirmed gating strategies, whereas discrete populations within lineage-negative cells were confirmed by omission of the corresponding population-specific Ab. Samples were acquired on an LSRFortessa flow cytometer (Becton Dickinson) at the Queens Medical Research Institute Flow Cytometry and Cell Sorting Facility and resulting data were analyzed using FlowJo V9 software. CD45⁺ cells were identified as live single cells by excluding 7AAD⁺ or Zombie Aqua⁺ cells and using forward scatter area versus forward scatter height characteristics. Cells positive for CD19, CD3, Ly6G, and SiglecF, or CD19, CD3, and Ly6G were referred to as Lineage⁻ and were excluded prior to analysis of liver, blood and cavity cells, or lung cells, respectively, as shown in the respective figures.

For the processing of brain tissue, double transgenic mice were perfused transcardially with physiological saline and brains were removed for regional dissection into cerebellum, cortex, hippocampus, and striatum. Mixed brain cell homogenates were prepared as described (32). The single-cell suspension of each region was incubated with 1 $\mu\text{g ml}^{-1}$ anti-CD11b/32 and subsequently stained with rat anti-mouse/human CD11b (M1/70) and rat anti-mouse CD45 (BioLegend). Flow cytometry was acquired using the Fortessa $\times 20$ (Becton Dickinson) and resulting data were analyzed using FlowJo V10 software.

Inhibition of CSF1R signaling

The CSF1R kinase inhibitor GW2580 (LC Laboratories) was suspended in 0.5% hydroxypropylmethylcellulose and 0.1% Tween 20 using a Teflon glass homogenizer. Diluent control or 160 mg/kg GW2580 was administered daily for 4 d by oral gavage before mice were killed on day 5.

Alexa Fluor 647–labeled CSF1 and anti-CSF1R mAb

Preservative-free sterile anti-CSF1R mAb (clone AFS98) was purchased from Bioserv (Sheffield, U.K.). Porcine CSF1 and CSF1-Fc was prepared as described previously (12). CSF1 and CSF1-Fc were conjugated to Alexa Fluor 647 (AF647) using the AF647 Microscale Protein labeling kit from Thermo Fisher Scientific according to manufacturer's instructions, and sodium azide subsequently removed using 7k MWCO Pierce polyacrylamide spin desalting columns (Thermo Fisher Scientific). Mice were injected i.v. with 0.5 mg anti-CSF1R mAb or PBS vehicle control, followed by 5 μg CSF1-Fc^{AF647} or PBS vehicle i.v. 10 min later. After a further 10 min, 60 μl of blood was removed by tail venipuncture, with the animals then immediately culled by cervical dislocation, and tissues perfused with PBS through the inferior vena cava. For study of CSF1 uptake in the peritoneal cavity, mice were injected i.p. with or without 0.5 mg AFS98 followed by 0.5 μg CSF1^{AF647} or PBS vehicle 2 min later, and then culled 10 min later by exposure to increasing levels of CO₂. The degree of CSF1R-dependent uptake of CSF1^{AF647} or CSF1-Fc^{AF647} is presented as the Δ median fluorescence intensity (MFI) calculated as the MFI for individual samples from mice given labeled CSF1 minus the average MFI from all samples pretreated with AFS98.

Imaging of tissues and cells

Whole-mount imaging of freshly isolated tissues from transgenic and WT littermate control mice aged 12–15 wk was performed using a Zeiss AxioZoom.V16 fluorescence microscope. Immediately after excision, tissues were kept at 4°C and protected from light. The fluorescent signal was acquired at 500–550 and 590–650 nm for EGFP and *Csf1r*-mApple, respectively. Acquisition of tissue background signal was performed by imaging WT tissue with the filter used for detection of the *Csf1r*-mApple protein.

Ex vivo confocal imaging of tissues

Male transgenic or WT male littermates were anesthetized, as per regulations, and intravenously injected in the tail vein with 5 $\mu\text{g/g}$ of weight of Lectin-I [from *Griffonia (Bandieraia) simplicifolia*] tagged with FITC (Vector Labs). After 10 min, mice were perfused transcardially with HBSS (Thermo Fisher Scientific), at a rate of 10 ml per min, and the left lobe of the liver was excised. Lungs were inflated with a solution containing 1% low melting-point agarose (Sigma-Aldrich) and, upon agarose solidification, the left lung was excised. Detection of functional CSF1R in lung myeloid subsets was performed by administering 5 μg CSF1-Fc^{AF647} and 5 $\mu\text{g/g}$ of weight of Lectin-I via i.v. injection. Mice were perfused with HBSS, previous to lung excision and inflation with agarose, as described. After dissection, liver and lung were placed on coverslip-bottom chambers

and covered with a sufficient volume of HBSS to prevent the surface of tissues from drying. Chambers were kept on ice and protected from light until tissues were imaged on a Zeiss LSM 710 microscope. Laser wavelengths for ECFP, FITC, and mApple were 405, 488, and 543 nm, respectively. Fluorescence acquisition for ECFP, FITC, and mApple signals in liver and lung was 400–480, 525–600, and 602–758 nm, respectively. Acquisition settings for lung tissue treated with CSF1-Fc^{AF647} were 400–479, 525–583, 593–651, and 651–755 nm for ECFP, FITC, mApple, and AF647, respectively. Postprocessing of images was performed by adjusting the black/white thresholds in the software ZEN 2012 (blue edition) developed by Carl Zeiss as follows: ECFP: 0–175, FITC: 0–100, mApple: 0–75, AF647: 0–200.

Statistics

Statistical tests detailed in the figure legends were performed using GraphPad Prism 6. Where necessary, data were log-transformed to achieve equal variance.

Results

Generation of *Csf1r*-mApple mice

C57BL/6 mouse embryos were comicro-injected with a construct containing the 7.2 kb *Csf1r* promoter region used to create the *Csf1r*-EGFP mice (26) upstream of *mApple*, along with a construct encoding the reverse tetracycline inducible transactivator *rtTA*-m2 under control of the same promoter (*Csf1r*-rtTA), previously used to generate a *Csf1r*-driven Tet-on system (35). mApple was used because it is brighter than its parent mCherry, refractory to photobleaching (38), suffers little from background autofluorescence, and previously enabled whole-mount imaging of the avian response to CSF1 in *Csf1r*-mApple reporter chickens (39). A single founder positive by PCR for both transgenes and for mApple protein in blood cells by flow cytometry was mated with a WT C57BL/6 mouse to establish the *Csf1r*-mApple line. PCR analysis across 77 mice revealed that *Csf1r*-mApple and *Csf1r*-rtTA transgenes were exclusively co-inherited, suggesting coinTEGRATION (data not shown). PCR and flow cytometry analysis of blood demonstrated the *Csf1r*-mApple transgene to be inherited at a frequency of 44.0% ($n = 207$). The utility of the coinTEGRATED Tet-on cassette is under investigation and is not considered further in this study but preliminary data demonstrate *rtTA*-m2 mRNA is expressed in peritoneal cells (data not shown).

Comparison of *Csf1r*-EGFP and *Csf1r*-mApple expression across tissue

In whole-mount fluorescence microscopy of live organs from *Csf1r*-mApple mice expression patterns of mApple recapitulated EGFP in *Csf1r*-EGFP transgenic mice (Fig. 1A–F). Large stellate mApple⁺ cells were observed throughout the liver, lung, epidermis, and cardiac muscle. Both transgenic strains highlighted the abundant macrophage populations of the intestinal lamina propria (Fig. 1E), and the red pulp of spleen (Fig. 1F) (26). Background fluorescence in littermate control mice was negligible (Fig. 1A–F, left panel). The *Csf1r*-EGFP and Δ *Csf1r*-ECFP transgenes have been used extensively for in vivo imaging with multiphoton and spinning disc microscopes (e.g., Refs. 20, 30, 31, 40–43), providing high-resolution analysis of macrophage motility and the extent of their ramified processes. Multiphoton imaging of whole mounts of the muscularis externa of the intestine demonstrated the high signal-to-noise ratio obtainable with the *Csf1r*-mApple reporter (Fig. 1G), enabling visualization of the regular network of microglial-like macrophages in this site (44, 45). Furthermore, the impact of exogenous CSF1-Fc, which regulates the function of these cells (44), could be directly visualized as an increase in cell size.

Csf1r-mApple expression by blood myeloid cells

To determine efficiency, reliability, and specificity of transgene expression, flow cytometry was performed on the blood of a

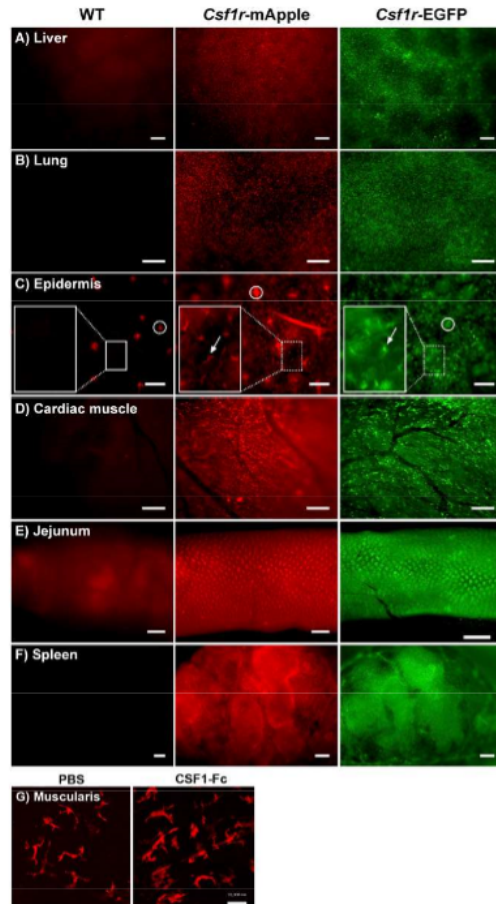


FIGURE 1. Distribution of the *Csf1r*-mApple and *Csf1r*-EGFP transgenes is similar throughout tissues. Whole-mount imaging of freshly isolated liver (A), lung (B), skin epidermis (C), cardiac muscle (D), jejunum (E), and cross-section of spleen (F) from WT (left panel), *Csf1r*-mApple (central), and *Csf1r*-EGFP (right panel) mice, or from muscularis (G) of *Csf1r*-mApple mice treated with PBS (left panel) or CSF1-Fc (right panel). In (C), a region of interest has been further magnified to better show Langerhans cells (white arrows), and hair follicles can be detected as highly autofluorescent structures (white circles). Scale bars in skin represent 100 μm ; 200 μm in liver, spleen, and cardiac muscle; 500 μm in lung and jejunum; and 10 μm in the muscularis.

cohort of *Csf1r*-mApple mice and littermate controls. Circulating CSF1R⁺CD11b⁺ monocytes (Fig. 2A) were uniformly *Csf1r*-mApple⁺ in both Ly6C⁺ and Ly6C⁻ subsets (Fig. 2B, 2C). As reported for the expression of EGFP in *Csf1r*-EGFP mice, neutrophils and eosinophils, which express *Csf1r* mRNA but not protein (46), were also *Csf1r*-mApple positive (Fig. 2B, 2C). The *Csf1r* promoter is active in B cells, which like macrophages, express the key transcription factor, PU.1, albeit at lower levels (47). Accordingly, ~70% of B cells had very low, but detectable, *Csf1r*-mApple (Fig. 2B, 2C). Similar expression of EGFP in *Csf1r*-EGFP mice is not detectable by confocal microscopy on spleen sections (46). The intensity of *Csf1r*-mApple expression was consistent between animals, with

equivalent levels expressed by monocytes and neutrophils and lower levels in eosinophils and B cells (Fig. 2D). Hence, the pattern of *Csf1r*-mApple expression reproduced that reported for EGFP in *Csf1r*-EGFP mice.

The level of Csf1r-mApple expression distinguishes monocytes, macrophages, and cDC in different tissues

To determine if transgene expression distinguished cDC and macrophages across multiple tissues, we first confirmed the identity of marker-defined MPS populations before surveying transgene expression in *Csf1r*-mApple mice. In the peritoneal cavity, we have demonstrated that recruited monocytes continuously replenish rare short-lived F4/80^{lo} MHCII⁺ macrophages that include both CD11c⁺ and CD11c⁻ cells (23), although only slowly replacing the more abundant F4/80^{hi} resident macrophages of embryonic origin (23). Both CD11c⁺ and CD11c⁻ short-lived and F4/80^{hi} peritoneal macrophage populations express detectable surface CSF1R. In contrast, Flt3-dependent cavity cDC of non-macrophage BM origin also express CD11c⁺ and MHCII⁺ and can be found among F4/80^{lo/-} cells, but can be distinguished as CSF1R⁻ (23, 24, 48, 49). Based upon this published gating strategy and previously assigned ontogenies (Fig. 3A) (23), *Csf1r*-mApple was detected in Ly6C⁺ monocytes, all macrophage populations, and in CD11b⁻ cDC1 and CD11b⁺ cDC2 (Fig. 3B, 3C) (24). There was a progressive increase in *Csf1r*-mApple intensity between Ly6C⁺ monocytes, CD11c-defined subsets of short-lived F4/80^{lo}MHCII⁺ macrophages, and long-lived F4/80^{hi} macrophages (Fig. 3D), consistent with the linear developmental relationship between these populations and monocytes in adult mice (23, 48, 50). *Csf1r*-mApple fluorescence in both CD11b⁻ cDC1 and CD11b⁺ cDC2 was lower than in monocytes (Fig. 3D), consistent with the lack of surface CSF1R (Fig. 3A). EGFP expression in *Csf1r*-EGFP mice replicated this pattern (Fig. 3E, 3F).

In the lung, alveolar macrophages are readily identified based upon high levels of CD11c and SiglecF (Fig. 4A) (51, 52). Interstitial cells are more heterogeneous. Some MHCII⁺ cells with varying levels of CD11c have been defined as macrophages based upon their expression of the Fc receptor CD64 and CSF1R dependence (51, 53), which contrasts the Flt3 dependence of CD64⁻ interstitial cDC2 (15). To verify that CD64 expression distinguishes pulmonary interstitial macrophages from CD11b⁺ cDC2, we assessed the turnover kinetics of CD64-defined MHCII⁺ cells and their dependence on CCR2, an established method for determining the likely monocyte dependence of tissue MPS cells (23, 54). We used a BM chimeric system in which WT mice were irradiated with organs of interest shielded to prevent irradiation-induced injury and reconstituted with congenic WT or *Ccr2*^{-/-} BM. This approach results in stable nonhost chimerism in blood leukocytes of ~30% in recipients of WT BM (23, 55) (Fig. 4B, short-dashed line) and allows the turnover kinetics of tissue populations to be assessed. Importantly, in recipients of *Ccr2*^{-/-} BM chimerism in monocytes (Fig. 4B, long-dashed line) but not other circulating leukocytes is largely abolished (23). Notably, putative CD64⁻CD11b⁺MHCII⁺ cDC2 were completely replaced within 8 wk, consistent with the short half-life of DCs (14). This occurred in a completely CCR2-independent manner, with identical chimerism in recipients of WT and *Ccr2*^{-/-} BM (Fig. 4B). In contrast, relatively few CD64⁺MHCII⁺ cells were replaced over 8 wk, although this was completely dependent on CCR2, suggesting slow replenishment from monocytes. Thus, consistent with previous work (15), CD64 accurately defines distinct CD11b⁺ MPS populations. Alveolar macrophages showed no evidence of chimerism (Fig. 4B), consistent with self-maintenance (52, 56, 57). Surprisingly, replenishment of cells

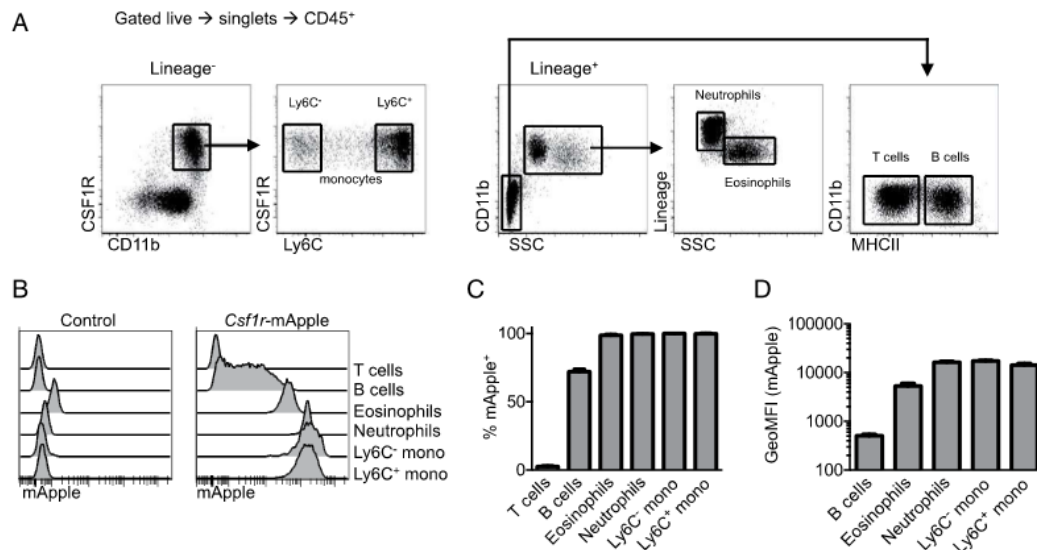


FIGURE 2. *Csf1r*-mApple transgene expression in blood leukocytes. **(A)** Flow cytometric strategy to identify blood leukocytes. **(B)** Expression of *Csf1r*-mApple in venous blood leukocytes from a representative *Csf1r*-mApple (right) and WT littermate control (left) mouse. **(C)** Frequency of cells positive for *Csf1r*-mApple and **(D)** geometric mean fluorescence intensity (GeoMFI) of *Csf1r*-mApple gated on *Csf1r*-mApple⁺ cells for different blood leukocytes. **(B–D)** Representative data from one of three experiments. Data are presented as mean ± SD of four mice (C and D).

defined as cDC1 was also dependent upon CCR2. However, these cells express CCR2 within the lung environment (58) and thus may require this receptor for tissue retention. Based upon the verified ontogenies, Ly6C⁺ monocytes, CD64⁺ interstitial macrophages, and alveolar macrophages in the lungs were all *Csf1r*-mApple⁺ (Fig. 4C, 4D), but expression increased progressively between monocytes and mature macrophages (Fig. 4C, 4E). Both cDC populations also expressed *Csf1r*-mApple, but at lower levels than monocytes (Fig. 4C–E).

In the liver, the largest phagocyte population is the Kupffer cells (KC), but a minority CD11b⁺F4/80^{lo} BM-derived population may include monocytes, cDC2, and possibly F4/80^{lo} BM-derived macrophages (14, 29, 57). KCs [F4/80^{hi}CD11b^{lo} (29, 59, 60)] (Fig. 5A) exhibited uniformly high expression of *Csf1r*-mApple (Fig. 5B–D). The minority CD11b⁺F4/80^{lo} compartment was subdivided based upon Ly6C and MHCII (Fig. 5A). The Ly6C⁺ cells and Ly6C⁻MHCII⁻ cells resembled Ly6C⁺ and Ly6C⁻ blood monocytes in size and marker expression (Fig. 5F). Unlike blood monocytes, MHCII⁺ cells among CD11b⁺F4/80^{lo} cells were larger, exhibited high levels of CD11c, and must include the Flt3-dependent CSF1R-independent CD11b⁺ cDC2 described previously (14); hence, we provisionally assigned these cDC2 (Fig. 5F). All CD11b⁺ populations expressed high levels of *Csf1r*-mApple (Fig. 5B, 5C). In the same CCR2-dependent tissue-protected BM chimera system used for the lung, the putative CD11b⁺ cDC2 population was replenished almost entirely by CCR2-independent BM precursors (Fig. 5E). They also expressed the highest levels of CD26, a marker of cDC conserved across species (61), and were negative for CD64 (Fig. 5F), confirming them as cDC2. CD11b^{-/lo} F4/80⁻ cells were also positive for *Csf1r*-mApple, but expressed markers of cDC1 (Ly6C⁻MHCII⁺CD11c⁺CD26⁺) and plasmacytoid DC (pDC) (Ly6C⁻MHCII⁺PDCA-1⁺) (Fig. 5A, 5F), and were replenished by CCR2-independent precursors (Fig. 5E). Hence, in liver the *Csf1r* transgene did not distinguish cDC from monocytes, but was highest in mature macrophages.

Detection of functional CSF1R using fluorescent CSF1-Fc

Csf1r mRNA may be posttranscriptionally regulated (62) and the protein may be cleaved from the cell surface in response to TLR signals (63). To assess functional CSF1R expression, we investigated the ability of MPS cells to take up labeled pig CSF1-Fc fusion protein, which produces a large increase in tissue macrophage populations when injected into mice (12) or pigs (64). CSF1-Fc conjugated with AF647 (CSF1-Fc^{AF647}) was found to bind specifically to monocytes in vitro (65). CSF1-Fc^{AF647} was injected intravenously 10 min before mice were sacrificed. In the liver, the uptake of CSF1-Fc^{AF647} was detected in KC, monocytes, and cDC2, but not in cDC1, pDC (Fig. 6A, 6B), or neutrophils (data not shown). Within cDC2, CSF1-Fc^{AF647} binding was prevalent in CD11c^{hi} cells (Fig. 6C) precluding any possible confusion with the CD11c^{dim} MHCII⁺ subcapsular macrophages described recently (42). In the lung, the majority of Ly6C⁺ monocytes and interstitial macrophages bound CSF1-Fc^{AF647}, whereas both cDC populations were negative (Fig. 6A, 6B). Uptake of labeled CSF1-Fc by myeloid populations was reduced or abolished by the anti-CSF1R Ab, AFS98 (Fig. 6A, 6B), a weak inhibitor of receptor-ligand binding (66), and an identical labeling profile was observed following injection of a non-Fc-fused AF647-labeled porcine CSF1 (CSF1^{AF647}) (data not shown). No detectable CSF1-Fc^{AF647} was bound by alveolar macrophages (Fig. 6A, 6B) and these cells also failed to bind appreciable levels in vitro (data not shown). Labeled anti-CD45 Ab was able to access all other myeloid populations in lung (data not shown) (67) and liver (Fig. 6D), suggesting a lack of CSF1-Fc^{AF647} or CSF1^{AF647} uptake by certain cDC reflects an absence of surface CSF1R expression rather than the inaccessibility of the sites they may occupy (31, 53).

Consistent with previous population-level data on CSF1 clearance (68), KC bound the highest level of labeled CSF1 per cell in a receptor-dependent manner (Fig. 6B), and considerably more per

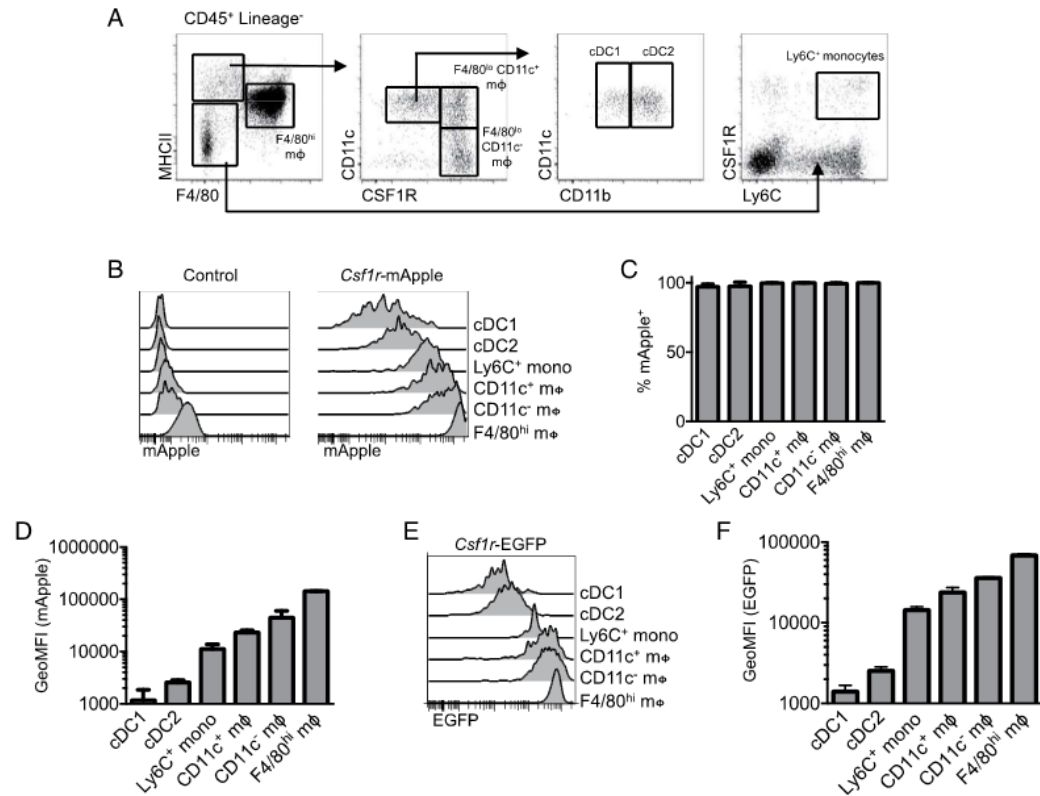


FIGURE 3. *Csf1r* transgene and CSF1R protein expression in the peritoneal cavity. **(A)** Flow cytometric strategy to identify peritoneal cavity myeloid cells as recently described (23). **(B–D)** Expression of *Csf1r*-mApple in peritoneal cavity myeloid populations determined by flow cytometry, showing a representative WT littermate control (left) and *Csf1r*-mApple (right) mouse (B), and graphs depicting the mean frequency of *Csf1r*-mApple⁺ cells in each population (C) and geometric mean fluorescence intensity (GeoMFI) of *Csf1r*-mApple for different peritoneal leukocytes gated on *Csf1r*-mApple⁺ cells (D). **(E and F)** Expression of *Csf1r*-EGFP in peritoneal cavity myeloid populations from *Csf1r*-EGFP mice, showing a representative flow cytometric overlay (E) and graphs depicting the frequency and GeoMFI of *Csf1r*-EGFP⁺ cells in each population (F) across multiple mice. Representative data from one of three experiments (B–D) or a single experiment (E and F). Data are presented as mean \pm SD of four mice (C, D, and F).

cell than blood monocytes (Fig. 6E). In turn, Ly6C⁺ monocytes in lung and liver were more intensely labeled than interstitial lung macrophages or liver CD11b⁺ cDC2 and liver Ly6C⁻ monocytes (Fig. 6B), although distinct intravascular versus parenchymal locations of these cells (31, 53) means exposure to circulating CSF1 cannot be controlled in this comparison. Of note, Ly6C⁺ blood monocytes, identified independently of CSF1R expression (Supplemental Fig. 1A), were more intensely labeled than the Ly6C⁻ subset (Fig. 6E), despite equivalent surface expression of CSF1R (Fig. 6F) (69, 70). Thus, novel differences in capacity to bind CSF1 were revealed using this ligand-binding approach.

The relationship between *Csf1r*-mApple activity and CSF1R-mediated ligand uptake was also examined in the peritoneal cavity following i.p. injection. Monocytes and CD11c⁺ and CD11c⁻F4/80^{lo}CD226⁺ macrophages (49, 50) were identified as described in Supplemental Fig. 1B, avoiding the use of Abs to CSF1R. Neither *Csf1r*-mApple^{lo} cDC population bound appreciable levels of CSF1^{AF647}, whereas all three macrophage populations had higher levels of receptor-dependent uptake of CSF1^{AF647} than Ly6C⁺ cavity monocytes (Fig. 7A). Surprisingly, the CD11c⁻F4/80^{lo} macrophages exhibited the greatest uptake. These differences

were not explained by differential levels of receptor-independent macropinocytosis as uptake of injected OVA–Texas Red was largely equivalent between populations (Fig. 7B). Anti-CSF1R mAb inhibited CSF1 uptake to a similar degree in each population, with a reduction between 63 and 75%. The difference in receptor activity appeared to have functional significance, as treatment of mice daily for 4 d with a CSF1R kinase inhibitor, GW2580 (71), which has been shown to inhibit proliferation of microglia (41) and pleural macrophages (11), partly depleted the CD11c⁻ subset of F4/80^{lo}MHCII⁺ peritoneal macrophages alone (Fig. 7C, left graph), despite inhibiting proliferation (as evidenced by Ki67 staining) of all macrophage populations (Fig. 7C, right graph).

Csf1r-mApple:Δ*Csf1r*-ECFP mice allow in situ imaging of distinct mononuclear phagocytes

The Δ*Csf1r*-ECFP transgene was crossed previously to the *Cx3cr1*^{+/GFP} or *Iigax* (CD11c)-EYFP mouse to distinguish pulmonary monocytes from other myeloid lung populations (31). To determine the utility of the *Csf1r*-mApple mouse to facilitate in vivo imaging of different myeloid populations, we crossed it to

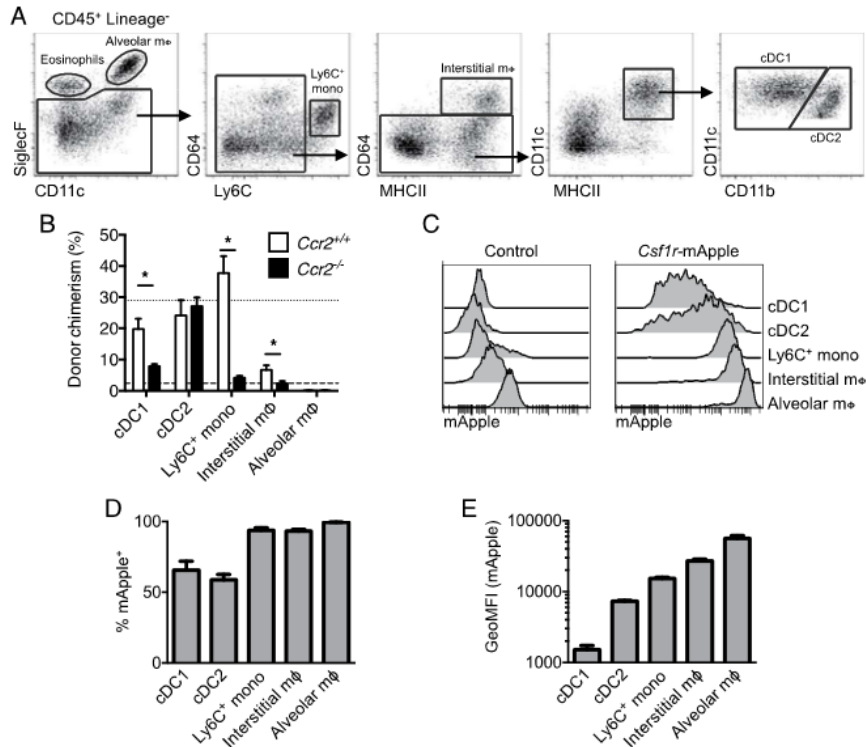


FIGURE 4. Lineage-restricted *Csf1r*-mApple transgene expression in the lung. **(A)** Flow cytometric strategy to identify lung leukocytes. **(B)** Frequency of donor cells within each lung population from tissue protected BM chimeric mice 8 wk after receiving BM from WT (white) or *Ccr2*^{-/-} (black) mice. Mean donor chimerism for circulating Ly6C⁺ monocytes is presented as short- or long-dashed lines for recipients of WT or *Ccr2*^{-/-} BM, respectively. **(C)** Expression of *Csf1r*-mApple in lung leukocytes from a representative WT littermate control (left) and *Csf1r*-mApple (right) mouse. **(D)** Frequency of cells expressing *Csf1r*-mApple and **(E)** geometric mean fluorescence intensity (GeoMFI) of *Csf1r*-mApple gated on *Csf1r*-mApple⁺ cells for different lung leukocytes. Data are from one of two independent experiments. Data presented as mean \pm SD of four mice (D and E) or mean \pm SEM of five mice (B). The asterisk (*) indicates significant differences using multiple *t* tests corrected for multiple comparisons using the Holm-Sidak method.

the $\Delta Csf1r$ -ECFP line (32, 36). As in the intestine (32), the majority of cDC1, cDC2, and Ly6C⁺ and Ly6C⁻ monocytes in the liver expressed high levels of ECFP, whereas pDC expressed intermediate levels. Neutrophils, eosinophils, and lymphocytes were negative (data not shown) as were F4/80^{hi} KC (Supplemental Fig. 2A). All ECFP⁺ cells expressed intermediate levels of mApple (Supplemental Fig. 2B, cyan gate), whereas all mApple^{hi} cells were ECFP⁻ and represent KC (Supplemental Fig. 2B, red gate). We combined the two *Csf1r* reporters with detection of endothelial cells by injection of FITC-labeled Lectin I. In confocal images the mApple⁺ cells were almost completely restricted to the liver sinusoids (e.g., pink boxes), consistent with KC (Fig. 8). In contrast, ECFP⁺mApple⁺ double-positive cells were rarely detected (e.g., white box), despite the presence of numerous ECFP⁺mApple⁻ cells (e.g., yellow box) (Fig. 8). These data suggest the intermediate levels of *Csf1r*-mApple expressed in ECFP⁺ cDC and monocytes (Fig. 5B, Supplemental Fig. 2A) are apparently below the threshold of detection of confocal imaging. This conclusion was supported by only weak detection of mApple expression when peripheral blood was imaged using identical microscope settings (Supplemental Fig. 3A). The *Csf1r*-ECFP⁺ cells in the liver (e.g., yellow box) were mainly detected outside the sinusoids

and likely include the subcapsular liver macrophages that also express the $\Delta Csf1r$ -ECFP transgene (42). The high level of mApple expression in KC therefore allows imaging of these cells without detection of monocytes and other mApple⁺ cells in the liver.

In the lung, interstitial macrophages and DC were ECFP negative (Supplemental Fig. 2C) whereas the majority of alveolar macrophages and Ly6C⁺ monocytes expressed ECFP, as reported previously (31, 32). Combined, all ECFP⁺ cells were mApple⁺ (Supplemental Fig. 2D, cyan gate) and encompassed alveolar macrophages and Ly6C⁺ and Ly6C⁻ monocytes, whereas ECFP⁻mApple^{hi} cells (Supplemental Fig. 2D, red gate) comprised CD64⁺ interstitial macrophages and a minor fraction of ECFP⁻ alveolar macrophages. In confocal images of transverse lung sections, parenchymal populations broadly divided into rounded ECFP⁺mApple⁺ cells (Fig. 9, yellow box) consistent with alveolar macrophages or interstitial migratory monocytes (31, 67) and elongated stellar-shaped ECFP⁻mApple⁺ cells (Fig. 9, white box). Injection of CSF1-Fc^{AF647} into the double transgenic mice selectively labeled the extravascular interstitial ECFP⁻mApple⁺ cells (Supplemental Fig. 4, white box), visible as punctate staining indicative of internalization of labeled ligand,

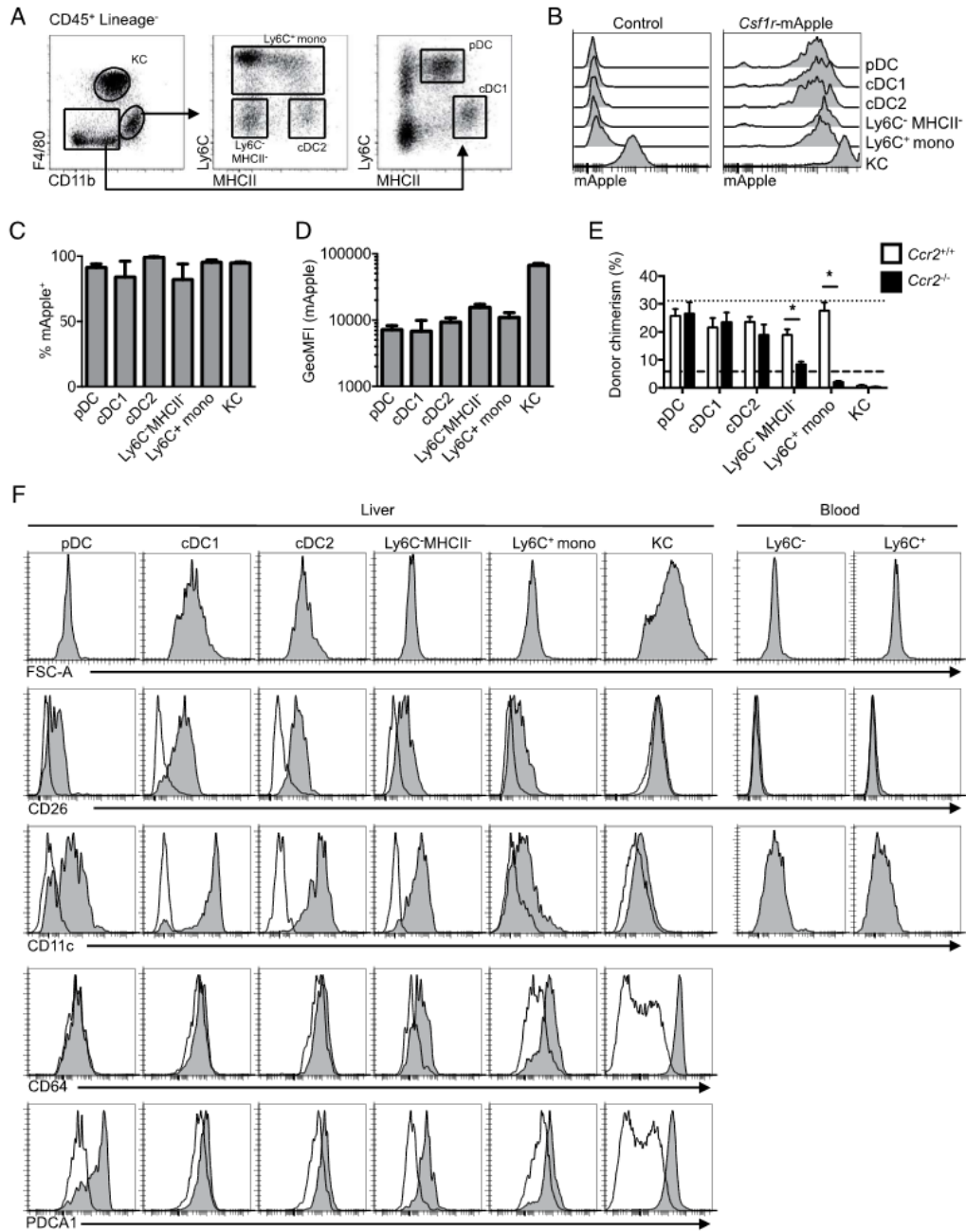
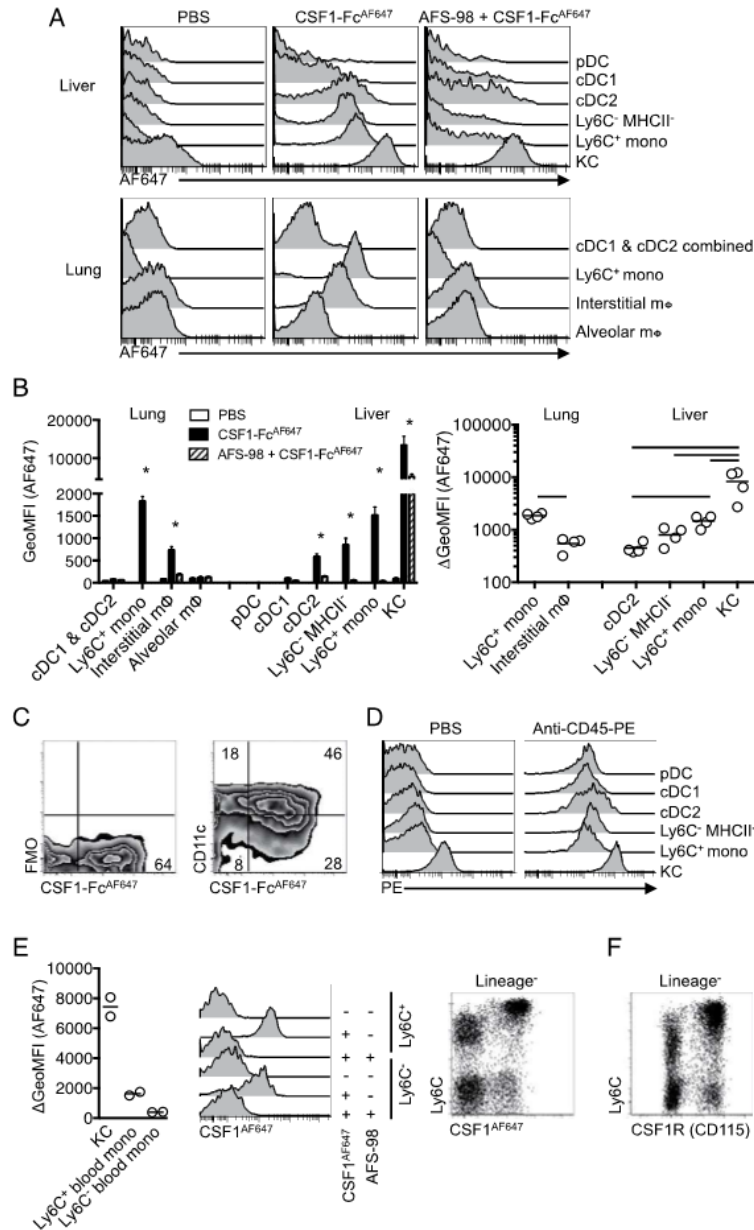


FIGURE 5. *Csflr*-mApple transgene expression in the liver. **(A)** Flow cytometric strategy to identify liver leukocytes. **(B)** Expression of *Csflr*-mApple in liver leukocytes with histograms from a representative *Csflr*-mApple (right) and WT littermate control (left) mouse. **(C)** Frequency of cells expressing *Csflr*-mApple and **(D)** geometric mean fluorescence intensity (GeoMFI) of *Csflr*-mApple gated on *Csflr*-mApple⁺ cells for different liver leukocytes. **(E)** Frequency of donor cells within each hepatic population from tissue protected BM chimeric mice 8 wk after receiving BM from WT (white) or *Ccr2*^{-/-} (black) mice. Mean donor chimerism for blood Ly6C⁺ monocytes is presented as short- or long-dashed lines for recipients of WT or *Ccr2*^{-/-} BM, respectively. **(F)** Representative histograms showing forward scatter area (FSC-A) characteristics and CD26, CD11c, CD64, and PDCA1 expression (tinted) overlaid with FMO controls (open) for liver leukocytes and blood monocytes. **(B–D)** Representative data from one of three or **(E)** two experiments, with data presented as mean ± SD of four mice (C and D) or mean ± SEM of five (E) mice. The asterisk (*) indicates significant differences using multiple *t* tests corrected for multiple comparisons using the Holm–Sidak method.

FIGURE 6. Tissue-specific consumption of CSF1 by cDC2 by *cDC2* in vivo. **(A)** Histograms of AF647 fluorescence of leukocyte populations from lung and liver following i.v. injection of anti-CSF1R mAb AF-S98 or PBS vehicle before subsequent i.v. delivery of CSF1-Fc^{AF647} or PBS vehicle. **(B)** Geometric mean fluorescence intensity (GeoMFI) of AF647 of cells from mice in (A) (left graph) and change in MFI between mice given CSF1-Fc^{AF647} alone or after AFS-98 pretreatment (right graph), with data presented as mean \pm SEM of four mice per group (left), or with data points for individual mice shown (right). Data are from one of two repeat independent experiments. **(C)** Representative plots showing CSF1-Fc^{AF647} uptake versus CD11c expression or FMO control on hepatic cDC2 from mice in (A). **(D)** PE fluorescence of liver leukocytes from C57BL/6 mice injected i.v. with anti-CD45-PE mAb or PBS vehicle 2 min prior to necropsy, showing data from one representative mouse of two per group. **(E)** Histograms of AF647 fluorescence of Ly6C⁺ and Ly6C⁻ blood monocytes from mice treated as in (A) but given CSF1-Fc^{AF647}, and a graph showing change in GeoMFI of blood monocytes and liver KC between mice given CSF1-Fc^{AF647} alone or after pretreatment with AFS98, and a dot plot showing Ly6C versus AF647 uptake on all CD3⁻CD19⁻Ly6G⁻ blood cells with data points representing individual mice. **(F)** Conventional surface CSF1R (CD115) and Ly6C staining on CD3⁻CD19⁻Ly6G⁻ blood cells from naive mice. Data are from one representative experiment of two (B–D and F) or three (E) independent repeats. The asterisk (*) indicates significant differences between CSF1-Fc^{AF647} alone and AFS98 + CSF1-Fc^{AF647} using *t* tests corrected for multiple comparisons with the Holm–Sidak method (B, left graph), whereas lines indicate significant differences using one-way ANOVA (B, right graph).



and confirmed them to be interstitial macrophages rather than ECFP⁻mApple^{lo} pulmonary DC. Many extravascular ECFP⁺mApple⁺ cells also took up CSF1-Fc^{AF647} (Supplemental Fig. 4), most likely migratory monocytes identified previously by live imaging (30, 31). In contrast, the most frequent cells observed within the pulmonary capillaries were ECFP⁻mApple⁺ (Fig. 9D, cyan box) and failed to label with injected CSF1-Fc^{AF647} (Supplemental Fig. 4), consistent with pulmonary neutrophils (72). Consistent with this, imaging of blood cells at

identical power settings confirmed strong detection of mApple in ECFP⁺ monocytes and ECFP⁻ neutrophils (Supplemental Fig. 3B).

Heterogeneous expression of *Csf1r* reporter genes in the brain

Macrophages in the mouse embryo are ECFP positive in the $\Delta Csf1r$ -ECFP line from their earliest appearance in the yolk sac (32). In addition to alveolar macrophages, one of the few locations in adults in which transgene expression is retained is in microglia.

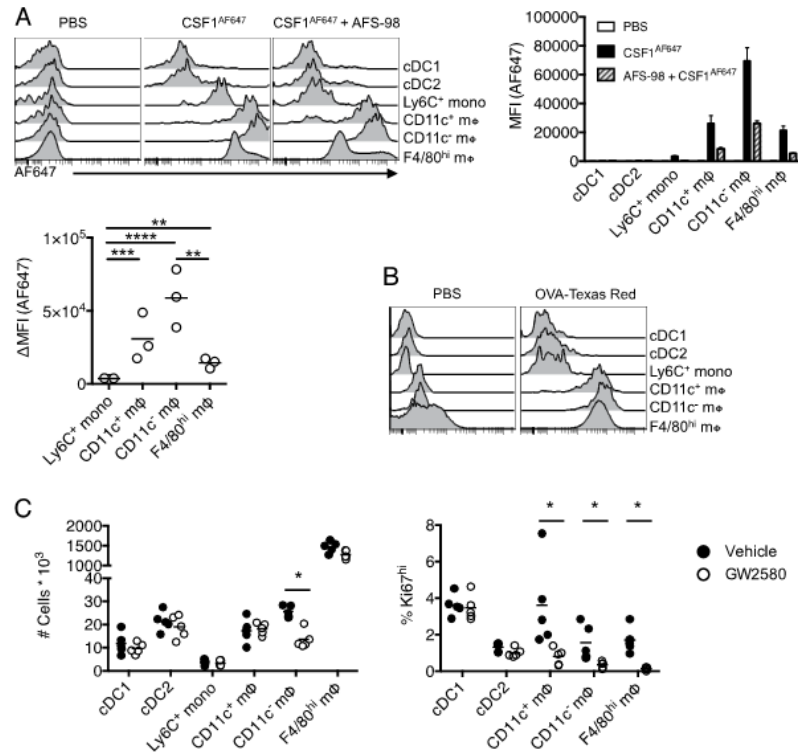


FIGURE 7. Consumption of CSF1 differs between monocytes and resident peritoneal macrophage populations. **(A)** Representative histograms of AF647 fluorescence in cavity leukocytes 10 min after i.p. injection of CSF1^{AF647} or PBS vehicle alone or in combination with pretreatment with AFS98, and graphs showing MFI of AF647 (right of histogram) and change in MFI between mice given CSF1^{AF647} alone or after AFS98 pretreatment (below histogram), with data presented as mean ± SEM of three to four mice per group. Data are from one of three independent repeat experiments. **(B)** Representative histograms of Texas Red fluorescence in cavity leukocytes 10 min after i.p. injection of OVA-Texas Red conjugate from a single experiment. **(C)** Total number of cavity leukocytes and proportion expressing high levels of Ki67 from mice treated for 4 d with GW2580 (open) or vehicle control (closed), with data points depicting individual mice. Data representative of two independent experiments. The asterisk (*) indicates significant differences using multiple *t* tests corrected for multiple comparisons using the Holm-Sidak method.

Grabert et al. (73) reported differences in microglia numbers and gene expression profiles in different mouse brain regions, and changes in gene expression with age. We used the *Csf1r*-mApple: Δ *Csf1r*-ECFP cross to further dissect microglial heterogeneity in different brain regions. CD45^{lo}CD11b⁺ classical microglia were uniformly strongly positive for mApple (Fig. 10A). Like blood monocytes and alveolar macrophages, microglia in cortex, hippocampus, and striatum were largely positive for ECFP, but in the cerebellum the percentage was much lower (37.4%, Fig. 10B). The level of ECFP in these cells was also lower, and lacked a clear peak, reminiscent of the ECFP profiles of macrophages and DC in the gut (32). The brain also contains a separable CD11b⁺, CD45^{hi} macrophage-like microglial population, a subset of which occupies perivascular locations and expresses higher levels of *Csf1r* than monocytes (74). By contrast to the classical microglia and blood monocytes, the CD11b⁺CD45^{hi} cells were >50% ECFP negative in all brain regions (Fig. 10B).

Discussion

We have developed a novel *Csf1r*-mApple reporter line. The *Csf1r* promoter construct used has been remarkably consistent

in generating location and copy-number-independent expression of transgenes (75), further confirmed by the comparable pattern of *Csf1r*-mApple and *Csf1r*-EGFP transgene expression. Expression of *Csf1r*-mApple had no impact on numbers of tissue macrophages or circulating blood leukocytes (data not shown). With optimal microscope settings, the distinct profile of transgene expression across subsets of MPS cells allowed exclusive detection of mApple^{hi} cells. When combined with the Δ *Csf1r*-ECFP reporter gene, which selectively labels subsets of *Csf1r*-positive cells, CSF1-Fc labeled with AF647, and FITC-labeled Lectin, we could identify and image lung interstitial macrophages and liver KC, and distinguish them from other myeloid cells. Despite high levels of *Csf1r*-mApple and *Csf1r*-EGFP (46) transgene expression, neutrophils are identifiable by injection of labeled Abs to Ly6G, a molecule with a negligible role in neutrophil trafficking or function (76, 77). Thus, there are numerous possibilities to produce live images of macrophage behavior and heterogeneity, particularly by combining with other established EGFP-based reporter mice.

In common with the *Csf1r*-EGFP reporter (78), *Csf1r*-mApple expression was uniformly higher in resident macrophages compared with monocytes, a difference reflected in the ability of at

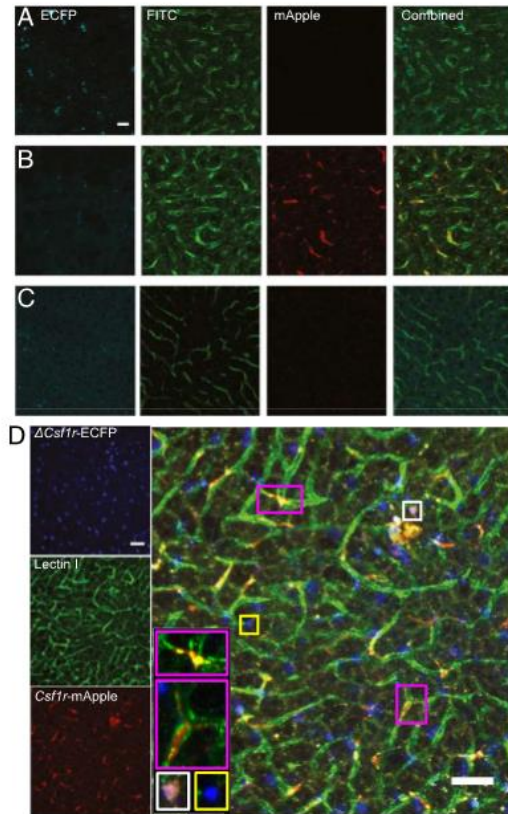


FIGURE 8. *Csf1r*-mApple and Δ *Csf1r*-ECFP transgenes allow imaging of distinct lineages of hepatic myeloid cells. Confocal image of the surface of the left lobe of the liver of a Δ *Csf1r*-ECFP (A), *Csf1r*-mApple (B), WT (C), and *Csf1r*-mApple/ Δ *Csf1r*-ECFP (D) mouse imaged ex vivo. FITC-Lectin I was injected i.v. to reveal liver sinusoidal endothelium. Scale bars represent 20 μ m (A–C) or 50 μ m (D).

least liver and cavity macrophages to capture more CSF1 on a per-cell basis than monocytes in vivo. Consistently, peritoneal macrophages compete effectively for available CSF1 in mixed culture with proliferating BM-derived macrophages (79). The rapid uptake of CSF1^{AF647} by KC is consistent with their role in regulating the circulating CSF1 concentration (68). Hence, upregulation of CSF1R expression may be a general feature of macrophage differentiation that allows them to compete for or control bioavailable CSF1. The apparent inability of alveolar macrophages to capture CSF1 is a notable departure from this tenet. However, alveolar macrophages are unaffected in adult CSF1-deficient op/op mice (80) and their replenishment from BM following irradiation is largely independent of CSF1R (81). Thus, our data are consistent with a lack of role for CSF1 in maintenance of the alveolar macrophage niche. However, it remains unclear why both alveolar macrophages and granulocytes express high levels of *Csf1r* transgene despite lacking a surface receptor. In the blood, Ly6C⁺ monocytes more readily took up CSF1 than their Ly6C⁻ progeny, a feature consistent with the suggestion that Ly6C⁺ monocytes regulate the availability of CSF1, thereby controlling

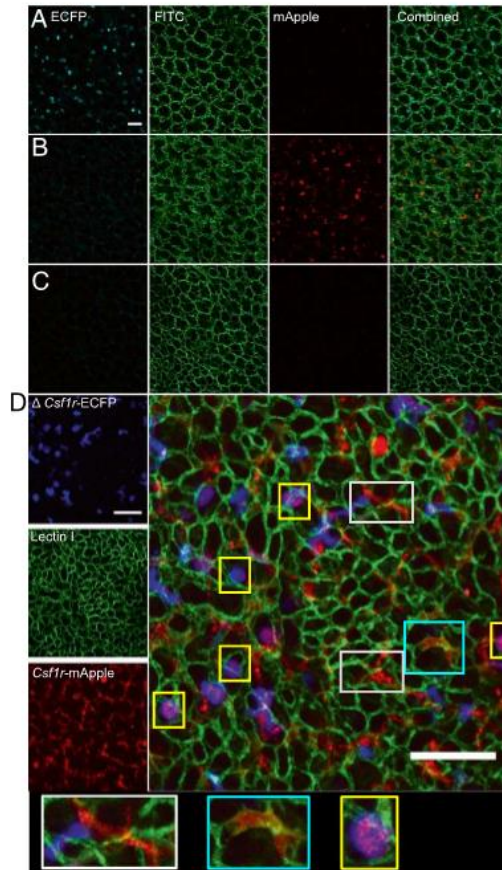


FIGURE 9. *Csf1r*-mApple and Δ *Csf1r*-ECFP transgenes allow imaging of distinct lineages of pulmonary myeloid cells. Confocal image of a transverse section of lung from a Δ *Csf1r*-ECFP (A), *Csf1r*-mApple (B), WT (C), and *Csf1r*-mApple/ Δ *Csf1r*-ECFP (D) mouse imaged ex vivo. FITC-Lectin I was injected i.v. to reveal pulmonary vasculature. Scale bars in all panels represent 50 μ m.

the lifespan of the Ly6C⁻ population (57). Interestingly, higher consumption of CSF1 by classical monocytes is also evident in PBMCs from *Csf1r*-EGFP transgenic sheep (65), suggesting this feature is conserved across species.

Intensity of fluorescence in *Csf1r*-mApple mice also largely distinguished long-lived tissue-resident macrophages (KC, alveolar macrophages, and F4/80^{hi} peritoneal macrophages) from those of more recent monocyte-origin (F4/80^{lo} resident peritoneal and lung interstitial macrophages) but was not correlated with the ability to take up labeled CSF1. In the peritoneal cavity, the receptor activity was greatest in F4/80^{lo}CD11c⁻ cells. Notably, these cells were selectively depleted following treatment with the CSF1R kinase inhibitor GW2580. Dynamics of loss of labeled histone 2B-GFP from peritoneal F4/80^{lo} macrophages places the half-life for replenishment of both CD11c⁺ and CD11c⁻ subsets from monocytes at around 2 wk (23), much longer than the 4 d treatment regimen in this study. Hence, selective loss of F4/80^{lo} CD11c⁻ cells likely results from reduced survival or retention in

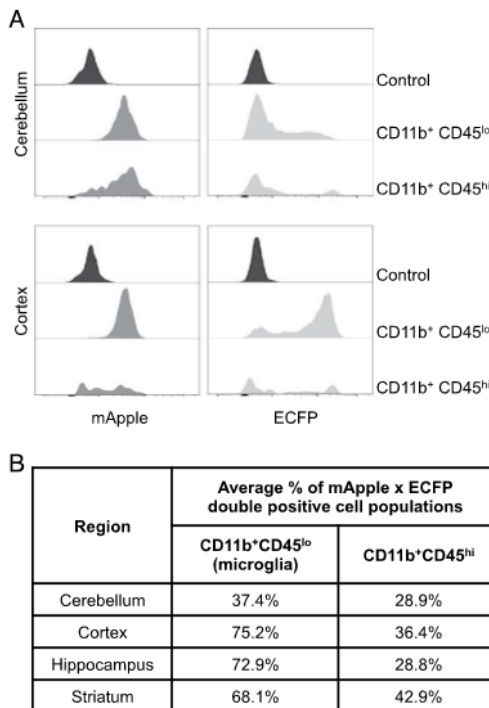


FIGURE 10. The expression of *Csflr*-mApple and Δ *Csflr*-ECFP transgenes in regional brain homogenates. Cerebellum, cortex, hippocampus, and striatum were processed to generate a single-cell suspension. **(A)** Compared are CD11b⁺CD45^{lo} microglia and CD11b⁺CD45^{hi} cells of the cerebellum and cortex regarding their expression of *Csflr*-mApple and ECFP. **(B)** Percentage of double transgene positive CD11b⁺CD45^{lo} and CD11b⁺CD45^{hi} cell populations across all selected regions.

the cavity rather than a failure of monocytes to differentiate and replenish these cells. Both F4/80^{hi} and F4/80^{lo} populations of peritoneal macrophages are rapidly lost upon Ab-mediated neutralization of CSF1 (24), suggesting only partial blockade of CSF1R signaling occurred with the oral inhibitor used in this study. Higher levels of CSF1R signaling are generally required for proliferation than survival of macrophages (8) and hence the uniform inhibition of Ki67 expression observed across the peritoneal macrophage compartment is consistent with a reduction of high-level CSF1R-signaling by GW2580 treatment. In light of this, our data suggest the F4/80^{lo}CD11c⁻ subset require a higher threshold of CSF1R signaling for survival and consequently exhibit greater CSF1R activity. Thus, different populations of peritoneal macrophages would appear to pursue distinct survival strategies. Short-lived cells are more reliant on high levels of CSF1 signaling, whereas long-lived cells are better adapted to efficiently use CSF1, possibly explaining the predominance of the latter under homeostatic CSF1-limited conditions (82). Either way, our data reveal fine-tuning of CSF1R activity but not necessarily *Csflr* transgene or gene expression between distinct macrophage populations.

Relatively low, or absent, expression of the *Csflr*-mApple reporter also provided a useful marker delineating peritoneal and pulmonary CCR2-independent cDC from CCR2-dependent

CD11c⁺-MHCII⁺ APC, likely of monocyte origin. Monocyte-derived CD11c⁺ APC have also been described within the dermis, kidney, and gut (6, 21, 54, 83), in which tissue cDC also expressed lower levels of *Csflr* (22). In the liver, MHCII⁺ CD11c⁺ cells were largely replenished by CCR2-independent BM precursors, uniformly expressed the candidate cDC marker CD26, and lacked the candidate macrophage marker CD64. Consistent with a cDC nature, these cells also uniformly express the transcription factor Zbtb46 (84). Nevertheless, these cells showed similar levels of *Csflr*-mApple transgene expression to monocytes, and the CD11b⁺ cDC2 fraction bound labeled CSF1-Fc. Although juvenile *Csflr*^{-/-} mice have normal numbers of hepatic cDC2 (14), unlike in other tissues, these cells also do not require CSF2 for survival (85), indicating possible redundancy between these growth factors. In adult mice the impact of *Csfl* and *Csflr* mutations are more apparent (86) and anti-CSF1R treatment produced an almost complete depletion of liver cells expressing a *Csflr*-EGFP transgene (87). Hence, in general, our data do not support an absolute division between Csflr and Flt3-dependent APC populations. By analogy with the functional diversity of classical macrophages in different organs (51, 88–90), APC differentiation is likely also organ specific. Because CSF1 drives a largely immunoregulatory program (91), the responsiveness of cDC2 to CSF1 may underlie the relatively weak APC activity in liver (92) and contribute to a tolerogenic environment in the liver (93). Similarly, competition of CSF1R⁺ cDC2 together with KC and classical patrolling monocytes (94) for available CSF1 could provide an explanation for the relative absence of hepatic monocyte-derived MHCII⁺ APC.

In adult mice, labeling of cDC and macrophages in the Δ *Csflr*-ECFP reporter is tissue specific (32). Using the Δ *Csflr*-ECFP transgene, we highlighted the utility of the *Csflr*-mApple strain to be crossed to existing reporter lines, visualizing distinct MPS populations in the lung and liver. Moreover, combined analysis of the *Csflr*-mApple and Δ *Csflr*-ECFP transgenes highlighted heterogeneity among microglia. Intriguingly, the percentages of Δ *Csflr*-ECFP negative microglia correlated with the retention of microglia in the IL-34-knockout mouse in the same brain regions (95). Similarly, in other tissues, ECFP expression occurs predominantly in locations where macrophages are more reliant on IL-34 (for example, Langerhans cells) or CSF2 (alveolar macrophages). Hence, the graded expression of the Δ *Csflr*-ECFP transgene in microglia may reflect its induction during differentiation or the proximity of individual cells to the tissue-specific factors that control its expression.

In overview, the *Csflr*-mApple mouse recapitulates the expression profile of the widely used *Csflr*-EGFP reporter. In combination with other reporters, and labeled CSF1, the *Csflr*-mApple mouse provides a new tool to dissect the differentiation and function of the heterogeneous populations of mouse tissue mononuclear phagocytes and the homeostatic roles of CSF1. How different mononuclear phagocytes regulate CSF1R activity remains an important question given the continued interest in macrophages as possible vehicles for delivery of gene therapies and as targets of therapeutics.

Acknowledgments

We thank Miriam Abraham for help with genotyping the *Csflr*-mApple mice, Judith Allen for critical review of the manuscript, and Marc Vendrell for advice on labeling of CSF1.

Disclosures

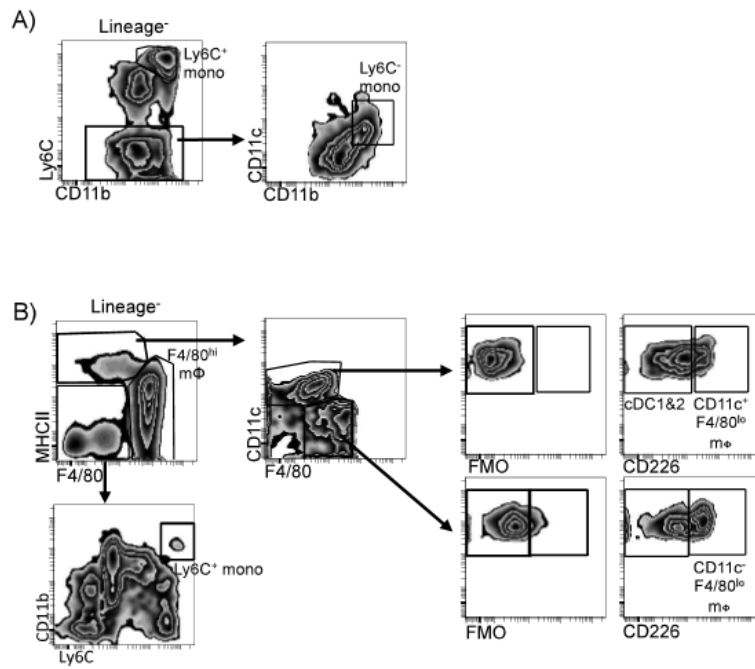
The authors have no financial conflicts of interest.

References

- Guilliams, M., F. Ginhoux, C. Jakubczak, S. H. Naik, N. Onai, B. U. Schraml, E. Segura, R. Tussiwand, and S. Yona. 2014. Dendritic cells, monocytes and macrophages: a unified nomenclature based on ontogeny. *Nat. Rev. Immunol.* 14: 571–578.
- Hume, D. A. 2006. The mononuclear phagocyte system. *Curr. Opin. Immunol.* 18: 49–53.
- Jenkins, S. J., and D. A. Hume. 2014. Homeostasis in the mononuclear phagocyte system. *Trends Immunol.* 35: 358–367.
- Lavin, Y., A. Mortha, A. Rahman, and M. Merad. 2015. Regulation of macrophage development and function in peripheral tissues. *Nat. Rev. Immunol.* 15: 731–744.
- Okabe, Y., and R. Medzhitov. 2016. Tissue biology perspective on macrophages. *Nat. Immunol.* 17: 9–17.
- Schraml, B. U., J. van Blijswijk, S. Zelenay, P. G. Whitney, A. Filby, S. E. Acton, N. C. Rogers, N. Moncaut, J. J. Carvajal, and C. Reis e Sousa. 2013. Genetic tracing via DNGR-1 expression history defines dendritic cells as a hematopoietic lineage. *Cell* 154: 843–858.
- Liu, K., G. D. Victora, T. A. Schwickert, P. Guernonprez, M. M. Mercedith, K. Yao, F. F. Chu, G. J. Randolph, A. Y. Rudensky, and M. Nussenzweig. 2009. In vivo analysis of dendritic cell development and homeostasis. *Science* 324: 392–397.
- Tushinski, R. J., I. T. Oliver, L. J. Guilbert, P. W. Tynan, J. R. Warner, and E. R. Stanley. 1982. Survival of mononuclear phagocytes depends on a lineage-specific growth factor that the differentiated cells selectively destroy. *Cell* 28: 71–81.
- Hume, D. A., P. Pavli, R. E. Donahue, and I. J. Fidler. 1988. The effect of human recombinant macrophage colony-stimulating factor (CSF-1) on the murine mononuclear phagocyte system in vivo. *J. Immunol.* 141: 3405–3409.
- Stutcheff, B. M., D. J. Antoine, A. C. Mackinnon, D. J. Gow, C. C. Bain, C. A. Hawley, M. J. Hughes, B. Francis, D. Wojtacha, T. Y. Man, et al. 2015. CSF1 restores innate immunity after liver injury in mice and serum levels indicate outcomes of patients with acute liver failure. *Gastroenterology* 149: 1896–1909.e14.
- Jenkins, S. J., D. Ruckerl, G. D. Thomas, J. P. Hewitson, S. Duncan, F. Brombacher, R. M. Maizels, D. A. Hume, and J. E. Allen. 2013. IL-4 directly signals tissue-resident macrophages to proliferate beyond homeostatic levels controlled by CSF-1. *J. Exp. Med.* 210: 2477–2491.
- Gow, D. J., K. A. Sauter, C. Pridans, L. Moffat, A. Sehgal, B. M. Stutcheff, S. Raza, P. M. Beard, Y. T. Tsai, G. Bainbridge, et al. 2014. Characterisation of a novel Fc conjugate of macrophage colony-stimulating factor. *Mol. Ther.* 22: 1580–1592.
- Waskow, C., K. Liu, G. Darrasse-Jéze, P. Guernonprez, F. Ginhoux, M. Merad, T. Shengelia, K. Yao, and M. Nussenzweig. 2008. The receptor tyrosine kinase Flt3 is required for dendritic cell development in peripheral lymphoid tissues. *Nat. Immunol.* 9: 676–683.
- Ginhoux, F., K. Liu, J. Helft, M. Bogunovic, M. Greter, D. Hashimoto, J. Price, N. Yin, J. Bromberg, S. A. Lira, et al. 2009. The origin and development of nonlymphoid tissue CD103+ DCs. *J. Exp. Med.* 206: 3115–3130.
- Schlitzer, A., N. McGovern, P. Teo, T. Zelante, K. Atarashi, D. Low, A. W. Ho, P. See, A. Shin, P. S. Wasan, et al. 2013. IRF4 transcription factor-dependent CD11b+ dendritic cells in human and mouse control mucosal IL-17 cytokine responses. *Immunity* 38: 970–983.
- Onai, N., A. Obata-Onai, M. A. Schmid, T. Ohteki, D. Jarrossay, and M. G. Manz. 2007. Identification of clonogenic common Flt3+M-CSFR+ plasmacytoid and conventional dendritic cell progenitors in mouse bone marrow. *Nat. Immunol.* 8: 1207–1216.
- Naik, S. H., P. Sathe, H. Y. Park, D. Metcalf, A. I. Proietto, A. Dakic, S. Carotta, M. O'Keefe, M. Bahlo, A. Papenfuss, et al. 2007. Development of plasmacytoid and conventional dendritic cell subtypes from single precursor cells derived in vitro and in vivo. *Nat. Immunol.* 8: 1217–1226.
- Mabbott, N. A., J. Kenneth Baillie, D. A. Hume, and T. C. Freeman. 2010. Meta-analysis of lineage-specific gene expression signatures in mouse leukocyte populations. *Immunobiology* 215: 724–736.
- Hume, D. A. 2008. Differentiation and heterogeneity in the mononuclear phagocyte system. *Mucosal Immunol.* 1: 432–441.
- Lohela, M., A. J. Casbon, A. Olow, L. Bonham, D. Branstetter, N. Weng, J. Smith, and Z. Werb. 2014. Intravital imaging reveals distinct responses of depleting dynamic tumor-associated macrophage and dendritic cell subpopulations. *Proc. Natl. Acad. Sci. USA* 111: E5086–E5095.
- Tamoutounour, S., M. Guilliams, F. Montanana Sanchis, H. Liu, D. Terhorst, C. Malosse, E. Pollet, L. Ardouin, H. Luche, C. Sanchez, et al. 2013. Origins and functional specialization of macrophages and of conventional and monocyte-derived dendritic cells in mouse skin. *Immunity* 39: 925–938.
- Cerovic, V., S. A. Houston, C. L. Scott, A. Aumeunier, U. Yrlid, A. M. Mowat, and S. W. Milling. 2013. Intestinal CD103(–) dendritic cells migrate to lymph and prime effector T cells. *Mucosal Immunol.* 6: 104–113.
- Bain, C. C., C. A. Hawley, H. Garner, C. L. Scott, A. Schridde, N. J. Steers, M. Mack, A. Joshi, M. Guilliams, A. M. Mowat, et al. 2016. Long-lived self-renewing bone marrow-derived macrophages displace embryo-derived cells to inhabit adult serous cavities. *Nat. Commun.* 7: ncomms11852.
- Louis, C., A. D. Cook, D. Lacey, A. J. Fleetwood, R. Vlahos, G. P. Anderson, and J. A. Hamilton. 2015. Specific contributions of CSF-1 and GM-CSF to the dynamics of the mononuclear phagocyte system. *J. Immunol.* 195: 134–144.
- MacDonald, K. P., V. Rowe, H. M. Bofinger, R. Thomas, T. Sasmono, D. A. Hume, and G. R. Hill. 2005. The colony-stimulating factor 1 receptor is expressed on dendritic cells during differentiation and regulates their expansion. *J. Immunol.* 175: 1399–1405.
- Sasmono, R. T., D. O'ceandy, J. W. Pollard, W. Tong, P. Pavli, B. J. Wainwright, M. C. Ostrowski, S. R. Himes, and D. A. Hume. 2003. A macrophage colony-stimulating factor receptor-green fluorescent protein transgene is expressed throughout the mononuclear phagocyte system of the mouse. *Blood* 101: 1155–1163.
- Deng, L., J. F. Zhou, R. S. Sellers, J. F. Li, A. V. Nguyen, Y. Wang, A. Orloffsky, Q. Liu, D. A. Hume, J. W. Pollard, et al. 2010. A novel mouse model of inflammatory bowel disease links mammalian target of rapamycin-dependent hyperproliferation of colonic epithelium to inflammation-associated tumorigenesis. *Am. J. Pathol.* 176: 952–967.
- Qian, B. Z., J. Li, H. Zhang, T. Kitamura, J. Zhang, L. R. Campion, E. A. Kaiser, L. A. Snyder, and J. W. Pollard. 2011. CCL2 recruits inflammatory monocytes to facilitate breast-tumour metastasis. *Nature* 475: 222–225.
- Schulz, C., E. Gomez Perdiguero, L. Chorro, H. Szabo-Rogers, N. Cagnard, K. Kierdorf, M. Prinz, B. Wu, S. E. Jacobsen, J. W. Pollard, et al. 2012. A lineage of myeloid cells independent of Myb and hematopoietic stem cells. *Science* 336: 86–90.
- Jacquelin, S., F. Licata, K. Dorgham, P. Hermand, L. Poupel, E. Guyon, P. Deterre, D. A. Hume, C. Combadière, and A. Boissonnas. 2013. CX3CR1 reduces Ly6Chigh-monocyte motility within and release from the bone marrow after chemotherapy in mice. *Blood* 122: 674–683.
- Rodero, M. P., L. Poupel, P. L. Loyher, P. Hamon, F. Licata, C. Pessel, D. A. Hume, C. Combadière, and A. Boissonnas. 2015. Immune surveillance of the lung by migrating tissue monocytes. *Elife* 4: e07847.
- Sauter, K. A., C. Pridans, A. Sehgal, C. C. Bain, C. Scott, L. Moffat, R. Rojo, B. M. Stutcheff, C. L. Davies, D. S. Donaldson, et al. 2014. The MacBlue binary transgene (csf1r-gal4VP16/UAS-EYFP) provides a novel marker for visualisation of subsets of monocytes, macrophages and dendritic cells and responsiveness to CSF1 administration. *PLoS One* 9: e105429.
- Saederup, N., A. E. Cardona, K. Croft, M. Mizutani, A. C. Cotleur, C. L. Tsou, R. M. Ransohoff, and I. F. Charo. 2010. Selective chemokine receptor usage by central nervous system myeloid cells in CCR2-red fluorescent protein knock-in mice. [Published erratum appears in 2017 *PLoS One* 12: e0176931.] *PLoS One* 5: e13693.
- Balic, A., C. Garcia-Morales, L. Vervelde, H. Gilhooley, A. Sherman, V. Garceau, M. W. Gutowska, D. W. Burt, P. Kaiser, D. A. Hume, and H. M. Sang. 2014. Visualisation of chicken macrophages using transgenic reporter genes: insights into the development of the avian macrophage lineage. *Development* 141: 3255–3265.
- Connelly, L., W. Barham, H. M. Onishko, L. Chen, T. P. Sherrill, T. Zabauwala, M. C. Ostrowski, T. S. Blackwell, and F. E. Yull. 2011. NF-kappaB activation within macrophages leads to an anti-tumor phenotype in a mammary tumor lung metastasis model. *Breast Cancer Res.* 13: R83.
- Ovchinnikov, D. A., C. E. DeBats, D. P. Sester, M. J. Sweet, and D. A. Hume. 2010. A conserved distal segment of the mouse CSF-1 receptor promoter is required for maximal expression of a reporter gene in macrophages and osteoclasts of transgenic mice. *J. Leukoc. Biol.* 87: 815–822.
- Boring, L., J. Gosling, S. W. Chensue, S. L. Kunkel, R. V. Farese, Jr., H. E. Broxmeyer, and I. F. Charo. 1997. Impaired monocyte migration and reduced type 1 (Th1) cytokine responses in C-C chemokine receptor 2 knockout mice. *J. Clin. Invest.* 100: 2552–2561.
- Shaner, N. C., M. Z. Lin, M. R. McKeown, P. A. Steinbach, K. L. Hazelwood, M. W. Davidson, and R. Y. Tsien. 2008. Improving the photostability of bright monomeric orange and red fluorescent proteins. *Nat. Methods* 5: 545–551.
- Garceau, V., A. Balic, C. Garcia-Morales, K. A. Sauter, M. J. McGrew, J. Smith, L. Vervelde, A. Sherman, T. E. Fuller, T. Oliphant, et al. 2015. The development and maintenance of the mononuclear phagocyte system of the chick is controlled by signals from the macrophage colony-stimulating factor receptor. *BMC Biol.* 13: 12.
- Wyckoff, J. B., Y. Wang, E. Y. Lin, J. F. Li, S. Goswami, E. R. Stanley, J. E. Segall, J. W. Pollard, and J. Condeelis. 2007. Direct visualization of macrophage-assisted tumor cell intravasation in mammary tumors. *Cancer Res.* 67: 2649–2656.
- Askew, K., K. Li, A. Olmos-Alonso, F. Garcia-Moreno, Y. Liang, P. Richardson, T. Tipton, M. A. Chapman, K. Riecken, S. Beccari, et al. 2017. Coupled proliferation and apoptosis maintain the rapid turnover of microglia in the adult brain. *Cell Rep.* 18: 391–405.
- Sierro, F., M. Evrard, S. Rizzetto, M. Melino, A. J. Mitchell, M. Florido, L. Beattie, S. B. Walters, S. S. Tay, B. Lu, et al. 2017. A liver capsular network of monocyte-derived macrophages restricts hepatic dissemination of intraperitoneal bacteria by neutrophil recruitment. *Immunity* 47: 374–388.e6.
- Poché, R. A., C. W. Hsu, M. L. McElwee, A. R. Burns, and M. E. Dickinson. 2015. Macrophages engulf endothelial cell membrane particles preceding pupillary membrane capillary regression. *Dev. Biol.* 403: 30–42.
- Muller, P. A., B. Koscsó, G. M. Rajani, K. Stevanovic, M. L. Berres, D. Hashimoto, A. Mortha, M. Leboeuf, X. M. Li, D. Mucida, et al. 2014. Crosstalk between muscularis macrophages and enteric neurons regulates gastrointestinal motility. [Published erratum appears in 2014 *Cell* 158: 1210.] *Cell* 158: 300–313.
- Farro, G., M. Stakenborg, P. J. Gomez-Pinilla, E. Labeeuw, G. Goveerse, M. D. Giovangiulio, N. Stakenborg, E. Meroni, F. D'Errico, Y. Elkrim, et al. 2017. CCR2-dependent monocyte-derived macrophages resolve inflammation and restore gut motility in postoperative ileus. *Gut* 66: 2098–2109.
- Sasmono, R. T., A. Ehrnsperger, S. L. Cronau, T. Ravasi, R. Kandane, M. J. Hickey, A. D. Cook, S. R. Himes, J. A. Hamilton, and D. A. Hume. 2007. Mouse neutrophilic granulocytes express mRNA encoding the macrophage colony-stimulating factor receptor (CSF-1R) as well as many other macrophage-specific transcripts and can transdifferentiate into macrophages in vitro in response to CSF-1. *J. Leukoc. Biol.* 82: 111–123.
- Ross, I. L., T. L. Dunn, X. Yue, S. Roy, C. J. Barnett, and D. A. Hume. 1994. Comparison of the expression and function of the transcription factor PU.1 (Spi-1

- proto-oncogene) between murine macrophages and B lymphocytes. *Oncogene* 9: 121–132.
48. Cain, D. W., E. G. O'Koren, M. J. Kan, M. Wombie, G. D. Sempowski, K. Hopper, M. D. Gunn, and G. Kelsoc. 2013. Identification of a tissue-specific, C/EBP β -dependent pathway of differentiation for murine peritoneal macrophages. *J. Immunol.* 191: 4665–4675.
 49. Liao, C. T., M. Rosas, L. C. Davies, P. J. Giles, V. J. Tyrrell, V. B. O'Donnell, N. Topley, L. R. Humphreys, D. J. Fraser, S. A. Jones, and P. R. Taylor. 2016. IL-10 differentially controls the infiltration of inflammatory macrophages and antigen-presenting cells during inflammation. *Eur. J. Immunol.* 46: 2222–2232.
 50. Kim, K. W., J. W. Williams, Y. T. Wang, S. Ivanov, S. Gilfillan, M. Colonna, H. W. Virgin, E. L. Gautier, and G. J. Randolph. 2016. MHC II⁺ resident peritoneal and pleural macrophages rely on IRF4 for development from circulating monocytes. *J. Exp. Med.* 213: 1951–1959.
 51. Immunological Genome Consortium. 2012. Gene-expression profiles and transcriptional regulatory pathways that underlie the identity and diversity of mouse tissue macrophages. *Nat. Immunol.* 13: 1118–1128.
 52. Guilliams, M., I. De Kleer, S. Henri, S. Post, L. Vanhouste, S. De Prijck, K. Deswarte, B. Malissen, H. Hammad, and B. N. Lambrecht. 2013. Alveolar macrophages develop from fetal monocytes that differentiate into long-lived cells in the first week of life via GM-CSF. *J. Exp. Med.* 210: 1977–1992.
 53. Gibbins, S. L., S. M. Thomas, S. M. Atif, A. L. McCubrey, A. N. Desch, T. Danhorn, S. M. Leach, D. L. Bratton, P. M. Henson, W. J. Janssen, and C. V. Jakubczik. 2017. Three unique interstitial macrophages in the murine lung at steady state. *Am. J. Respir. Cell Mol. Biol.* 57: 66–76.
 54. Tamoutounour, S., S. Henri, H. Lelouard, B. de Bovis, C. de Haar, C. J. van der Woude, A. M. Woltman, Y. Reyat, D. Bonnet, D. Sichien, et al. 2012. CD64 distinguishes macrophages from dendritic cells in the gut and reveals the Th1-inducing role of mesenteric lymph node macrophages during colitis. *Eur. J. Immunol.* 42: 3150–3166.
 55. Jenkins, S. J., D. Ruckerl, P. C. Cook, L. H. Jones, F. D. Finkelman, N. van Rooijen, A. S. MacDonald, and J. E. Allen. 2011. Local macrophage proliferation, rather than recruitment from the blood, is a signature of TH2 inflammation. *Science* 332: 1284–1288.
 56. Murphy, J., R. Sumner, A. A. Wilson, D. N. Kotton, and A. Fine. 2008. The prolonged life-span of alveolar macrophages. *Am. J. Respir. Cell Mol. Biol.* 38: 380–385.
 57. Yona, S., K. W. Kim, Y. Wolf, A. Mildner, D. Varol, M. Breker, D. Strauss-Ayali, S. Viukov, M. Guilliams, A. Misharin, et al. 2013. Fate mapping reveals origins and dynamics of monocytes and tissue macrophages under homeostasis. [Published erratum appears in 2013 *Immunity* 38: 1073–1079.] *Immunity* 38: 79–91.
 58. Jakubczik, C., F. Tacke, F. Ginhoux, A. J. Wagers, N. van Rooijen, M. Mack, M. Merad, and G. J. Randolph. 2008. Blood monocyte subsets differentially give rise to CD103⁺ and CD103⁻ pulmonary dendritic cell populations. *J. Immunol.* 180: 3109–3027.
 59. Perdiguer, E. G., and F. Geissmann. 2016. The development and maintenance of resident macrophages. *Nat. Immunol.* 17: 2–8.
 60. Scott, C. L., F. Zheng, P. De Baetselier, L. Martens, Y. Saeys, S. De Prijck, S. Lippens, C. Abels, S. Schoonooghe, G. Raes, et al. 2016. Bone marrow-derived monocytes give rise to self-renewing and fully differentiated Kupffer cells. *Nat. Commun.* 7: 10321.
 61. Guilliams, M., C. A. Dutertre, C. L. Scott, N. McGovern, D. Sichien, S. Chakarov, S. Van Gassen, J. Chen, M. Poidinger, S. De Prijck, et al. 2016. Unsupervised high-dimensional analysis aligns dendritic cells across tissues and species. *Immunity* 45: 669–684.
 62. Hiasa, M., M. Abe, A. Nakano, A. Oda, H. Amou, S. Kido, K. Takeuchi, K. Kagawa, K. Yata, T. Hashimoto, et al. 2009. GM-CSF and IL-4 induce dendritic cell differentiation and disrupt osteoclastogenesis through M-CSF receptor shedding by up-regulation of TNF- α converting enzyme (TACE). *Blood* 114: 4517–4526.
 63. Sester, D. P., S. J. Beasley, M. J. Sweet, L. F. Fowles, S. L. Cronau, K. J. Stacey, and D. A. Hume. 1999. Bacterial/CpG DNA down-modulates colony stimulating factor-1 receptor surface expression on murine bone marrow-derived macrophages with concomitant growth arrest and factor-independent survival. *J. Immunol.* 163: 6541–6550.
 64. Sauter, K. A., L. A. Waddell, Z. M. Lisowski, R. Young, L. Lefevre, G. M. Davis, S. M. Clohisey, M. McCulloch, E. Magowan, N. A. Mabbott, et al. 2016. Macrophage colony-stimulating factor (CSF1) controls monocyte production and maturation and the steady-state size of the liver in pigs. *Am. J. Physiol. Gastrointest. Liver Physiol.* 311: G533–G547.
 65. Pridans, C., G. M. Davis, K. A. Sauter, Z. M. Lisowski, Y. Corripio-Miyar, A. Raper, L. Lefevre, R. Young, M. E. McCulloch, S. Lillico, et al. 2016. A Cs1r-EGFP transgene provides a novel marker for monocyte subsets in sheep. *J. Immunol.* 197: 2297–2305.
 66. Fend, L., N. Accart, J. Kintz, S. Cochlin, C. Reymann, F. Le Pogam, J. B. Marchand, T. Menguy, P. Slos, R. Rooke, et al. 2013. Therapeutic effects of anti-CD115 monoclonal antibody in mouse cancer models through dual inhibition of tumor-associated macrophages and osteoclasts. *PLoS One* 8: e73310.
 67. Jakubczik, C., E. L. Gautier, S. L. Gibbins, D. K. Sojka, A. Schlitzer, T. E. Johnson, S. Ivanov, Q. Duan, S. Bala, T. Condon, et al. 2013. Minimal differentiation of classical monocytes as they survey steady-state tissues and transport antigen to lymph nodes. *Immunity* 39: 599–610.
 68. Bartocci, A., D. S. Mastrogrianni, G. Migliorati, R. J. Stockert, A. W. Wolkoff, and E. R. Stanley. 1987. Macrophages specifically regulate the concentration of their own growth factor in the circulation. *Proc. Natl. Acad. Sci. USA* 84: 6179–6183.
 69. Lenzo, J. C., A. L. Turner, A. D. Cook, R. Vlahos, G. P. Anderson, E. C. Reynolds, and J. A. Hamilton. 2012. Control of macrophage lineage populations by CSF-1 receptor and GM-CSF in homeostasis and inflammation. *Immunol. Cell Biol.* 90: 429–440.
 70. Swirski, F. K., M. Nahrendorf, M. Etzrodt, M. Wildgruber, V. Cortez-Retamozo, P. Panizzi, J. L. Figueredo, R. H. Kohler, A. Chudnovsky, P. Waterman, et al. 2009. Identification of splenic reservoir monocytes and their deployment to inflammatory sites. *Science* 325: 612–616.
 71. Conway, J. G., B. McDonald, J. Parham, B. Keith, D. W. Rusnak, E. Shaw, M. Jansen, P. Lin, A. Payne, R. M. Crosby, et al. 2005. Inhibition of colony-stimulating-factor-1 signaling in vivo with the orally bioavailable cFMS kinase inhibitor GW2580. *Proc. Natl. Acad. Sci. USA* 102: 16078–16083.
 72. Yipp, B. G., J. H. Kim, R. Lima, L. D. Zhytniuk, B. Petri, N. Swanlund, M. Ho, V. G. Szeto, T. Tak, L. Koenderman, et al. 2017. The lung is a host defense niche for immediate neutrophil-mediated vascular protection. *Sci. Immunol.* 2: eaam8929.
 73. Grabert, K., T. Michoel, M. H. Karavolos, S. Clohisey, J. K. Baillie, M. P. Stevens, T. C. Freeman, K. M. Summers, and B. W. McColl. 2016. Microglial brain region-dependent diversity and selective regional sensitivities to aging. *Nat. Neurosci.* 19: 504–516.
 74. Goldmann, T., P. Wieghofer, M. J. Jordão, F. Prutek, N. Hagemeyer, K. Frenzel, L. Amann, O. Staszewski, K. Kierdorf, M. Krueger, et al. 2016. Origin, fate and dynamics of macrophages at central nervous system interfaces. *Nat. Immunol.* 17: 797–805.
 75. Hume, D. A. 2011. Applications of myeloid-specific promoters in transgenic mice support in vivo imaging and functional genomics but do not support the concept of distinct macrophage and dendritic cell lineages or roles in immunity. *J. Leukoc. Biol.* 89: 525–538.
 76. Yipp, B. G., and P. Kubers. 2013. Antibodies against neutrophil LY6G do not inhibit leukocyte recruitment in mice in vivo. *Blood* 121: 241–242.
 77. Hasenberg, A., M. Hasenberg, L. Männ, F. Neumann, L. Borckenstein, M. Stecher, A. Kraus, D. R. Engel, A. Klingberg, P. Seddigh, et al. 2015. Catchup: a mouse model for imaging-based tracking and modulation of neutrophil granulocytes. *Nat. Methods* 12: 445–452.
 78. Mooney, J. E., B. E. Rolfe, G. W. Osborne, D. P. Sester, N. van Rooijen, G. R. Campbell, D. A. Hume, and J. H. Campbell. 2010. Cellular plasticity of inflammatory myeloid cells in the peritoneal foreign body response. *Am. J. Pathol.* 176: 369–380.
 79. Hume, D. A., and S. Gordon. 1984. The correlation between plasminogen activator activity and thymidine incorporation in mouse bone marrow-derived macrophages. Opposing actions of colony-stimulating factor, phorbol myristate acetate, dexamethasone and prostaglandin E. *Exp. Cell Res.* 150: 347–355.
 80. Shibata, Y., Z. Zsengeller, K. Otake, N. Palaniyar, and B. C. Trapnell. 2001. Alveolar macrophage deficiency in osteopetrotic mice deficient in macrophage colony-stimulating factor is spontaneously corrected with age and associated with matrix metalloproteinase expression and emphysema. *Blood* 98: 2845–2852.
 81. Hashimoto, D., A. Chow, C. Noizat, P. Teo, M. B. Beasley, M. Leboeuf, C. D. Becker, P. See, J. Price, D. Lucas, et al. 2013. Tissue-resident macrophages self-maintain locally throughout adult life with minimal contribution from circulating monocytes. *Immunity* 38: 792–804.
 82. Ghosn, E. E., A. A. Cassado, G. R. Govoni, T. Fukuhara, Y. Yang, D. M. Monack, K. R. Bortoluci, S. R. Almeida, L. A. Herzenberg, and L. A. Herzenberg. 2010. Two physically, functionally, and developmentally distinct peritoneal macrophage subsets. *Proc. Natl. Acad. Sci. USA* 107: 2568–2573.
 83. Bain, C. C., A. Bravo-Blas, C. L. Scott, E. G. Perdiguer, F. Geissmann, S. Henri, B. Malissen, L. C. Osborne, D. Artis, and A. M. Mowat. 2014. Constant replenishment from circulating monocytes maintains the macrophage pool in the intestine of adult mice. *Nat. Immunol.* 15: 929–937.
 84. Meredith, M. M., K. Liu, G. Darrasse-Jeze, A. O. Kamphorst, H. A. Schreiber, P. Guernonprez, J. Idoyaga, C. Cheong, K. H. Yao, R. E. Niec, and M. C. Nussenzweig. 2012. Expression of the zinc finger transcription factor Zfp644 (Zbtb46, Btb4d) defines the classical dendritic cell lineage. *J. Exp. Med.* 209: 1153–1165.
 85. Greter, M., J. Helft, A. Chow, D. Hashimoto, A. Mortha, J. Agudo-Cantero, M. Bogunovic, E. L. Gautier, J. Miller, M. Leboeuf, et al. 2012. GM-CSF controls nonlymphoid tissue dendritic cell homeostasis but is dispensable for the differentiation of inflammatory dendritic cells. *Immunity* 36: 1031–1046.
 86. Dai, X. M., G. R. Ryan, A. J. Hapel, M. G. Dominguez, R. G. Russell, S. Kapp, V. Sylvestre, and E. R. Stanley. 2002. Targeted disruption of the mouse colony-stimulating factor 1 receptor gene results in osteopetrosis, mononuclear phagocyte deficiency, increased primitive progenitor cell frequencies, and reproductive defects. *Blood* 99: 111–120.
 87. MacDonald, K. P., J. S. Palmer, S. Cronau, E. Seppanen, S. Olver, N. C. Raffelt, R. Kuns, A. R. Pettit, A. Clouston, B. Wainwright, et al. 2010. An antibody against the colony-stimulating factor 1 receptor depletes the resident subset of monocytes and tissue- and tumor-associated macrophages but does not inhibit inflammation. *Blood* 116: 3955–3963.
 88. Mass, E., I. Ballesteros, M. Farlik, F. Halbritter, P. Günther, L. Crozet, C. E. Jacome-Galarza, K. Händler, J. Klughammer, Y. Kobayashi, et al. 2016. Specification of tissue-resident macrophages during organogenesis. *Science* 353: aaf4238.
 89. Lavin, Y., D. Winter, R. Blecher-Gonen, E. David, H. Keren-Shaul, M. Merad, S. Jung, and I. Amit. 2014. Tissue-resident macrophage enhancer landscapes are shaped by the local microenvironment. *Cell* 159: 1312–1326.
 90. Gosselet, D., V. M. Link, C. E. Romanoski, G. J. Fonseca, D. Z. Eichenfield, N. J. Spann, J. D. Stender, H. B. Chun, H. Garner, F. Geissmann, and

- C. K. Glass. 2014. Environment drives selection and function of enhancers controlling tissue-specific macrophage identities. *Cell* 159: 1327–1340.
91. Verreck, F. A., T. de Boer, D. M. Langenberg, M. A. Hoeve, M. Kramer, E. Vaisberg, R. Kastelein, A. Kulk, R. de Waal-Malefyt, and T. H. Ottenhoff. 2004. Human IL-23-producing type 1 macrophages promote but IL-10-producing type 2 macrophages subvert immunity to (myco)bacteria. *Proc. Natl. Acad. Sci. USA* 101: 4560–4565.
92. Pillarisetty, V. G., A. B. Shah, G. Miller, J. I. Bleier, and R. P. DeMatteo. 2004. Liver dendritic cells are less immunogenic than spleen dendritic cells because of differences in subtype composition. *J. Immunol.* 172: 1009–1017.
93. Ju, C., and F. Tacke. 2016. Hepatic macrophages in homeostasis and liver diseases: from pathogenesis to novel therapeutic strategies. *Cell. Mol. Immunol.* 13: 316–327.
94. Dal-Secco, D., J. Wang, Z. Zeng, E. Kolaczowska, C. H. Wong, B. Petri, R. M. Ransohoff, I. F. Charo, C. N. Jenne, and P. Kubers. 2015. A dynamic spectrum of monocytes arising from the in situ reprogramming of CCR2+ monocytes at a site of sterile injury. *J. Exp. Med.* 212: 447–456.
95. Wang, Y., K. J. Szretter, W. Vermi, S. Gilfillan, C. Rossini, M. Cella, A. D. Barrow, M. S. Diamond, and M. Colonna. 2012. IL-34 is a tissue-restricted ligand of CSF1R required for the development of Langerhans cells and microglia. *Nat. Immunol.* 13: 753–760.



SFigure 1: Alternative gating strategies to identify blood monocytes and peritoneal myeloid populations without CSF1R expression. (A) Ly6C⁺ and Ly6C⁻ blood monocytes were identified by high levels of Ly6C and CD11b (left plot), or CD11c and CD11b (right plot), respectively. **(B)** Ly6C⁺ cavity monocytes were identified as MHCII⁺CD11b^{hi}Ly6C^{hi}, while CD226 was used to identify mature CD11c⁺MHCII⁺F4/80^{lo} macrophages and distinguish CD11c⁺MHCII⁺F4/80^{lo} macrophages from CD11c⁺F4/80^{lo} cDC. cDC were further split into CD11b⁻cDC1 and CD11b⁺cDC2 (not shown).

SFig. 2

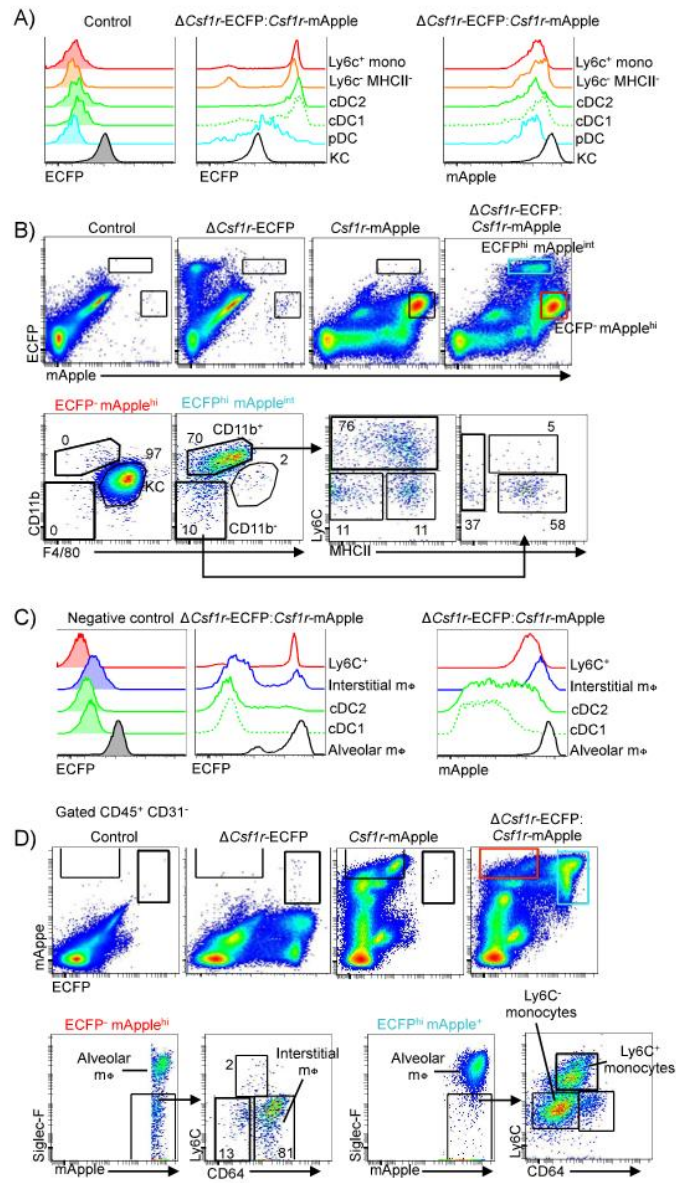
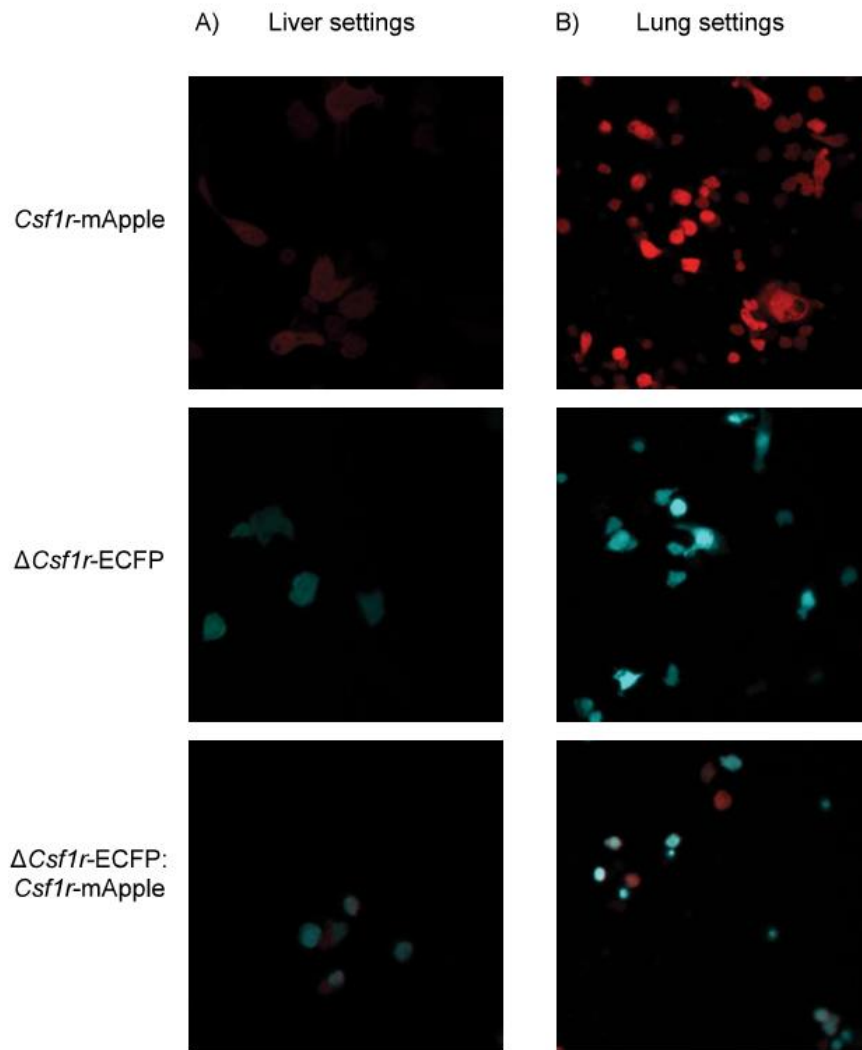


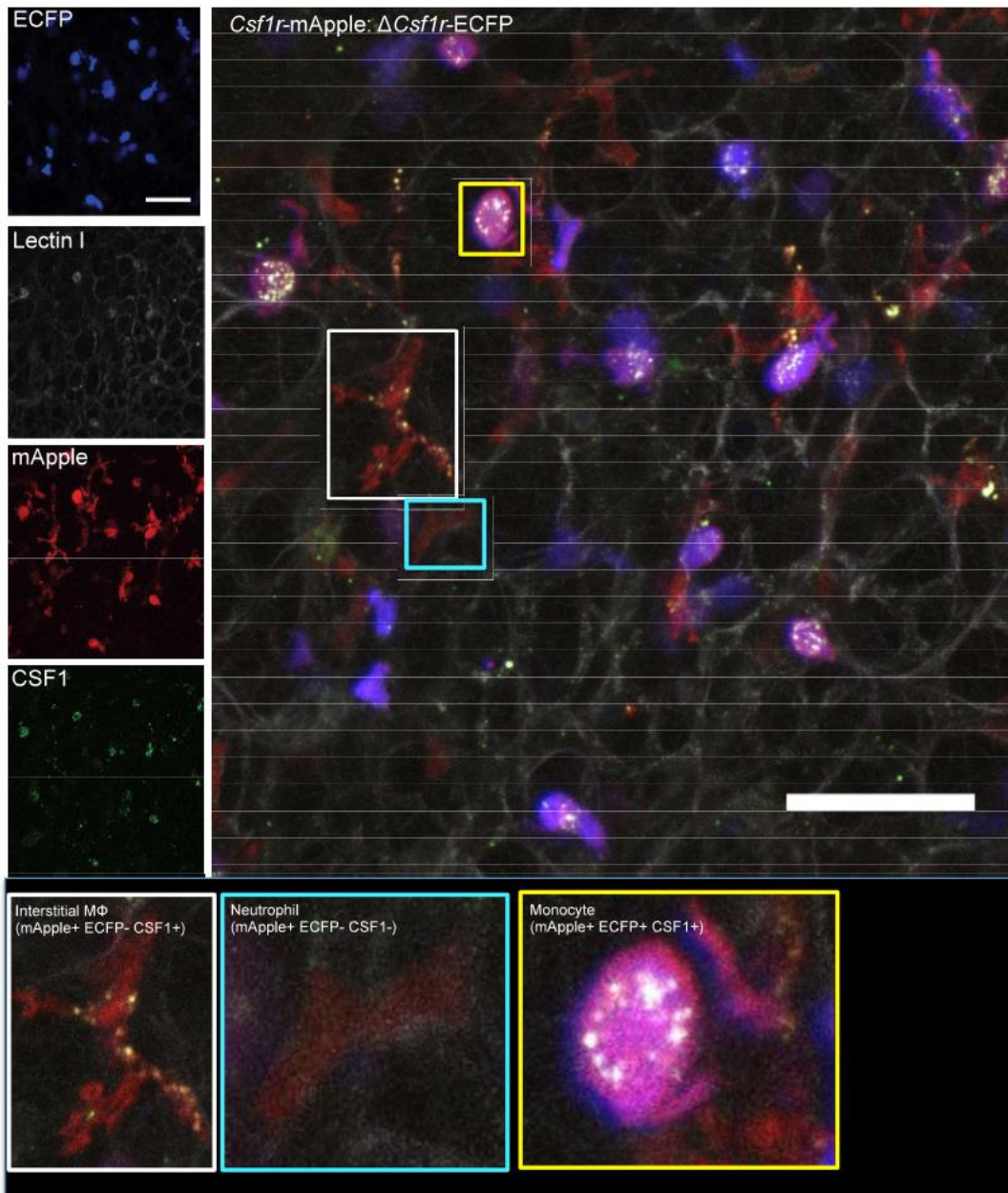
Figure 2: (A) Representative ECFP and mApple expression by hepatic myeloid subsets from *Csf1r*-mApple: Δ *Csf1r*-ECFP double transgenic and control mouse. (B) Gates depicting all ECFP⁺ mApple⁺ cells (green) and mApple^{hi} ECFP⁻ cells (red) within CD45⁺ hepatic cells from a *Csf1r*-mApple: Δ *Csf1r*-ECFP mouse and single *Csf1r*-mApple or Δ *Csf1r*-ECFP or negative controls, and surface marker expression and frequencies of cells falling within these gates. Data is representative of 1-2 mice per group and from 1 representative experiment of 2. (C) As A but for pulmonary myeloid subsets (D) Gates depicting all ECFP⁺ mApple⁺ cells (blue) and mApple^{hi} ECFP⁻ cells (red) within CD45⁺ pulmonary cells from a *Csf1r*-mApple: Δ *Csf1r*-ECFP mouse and single *Csf1r*-mApple, Δ *Csf1r*-ECFP, or negative controls, and surface marker expression and frequencies of Ly6C⁺ CD64^{dim} monocytes, CD64⁺ Ly6C⁻ interstitial macrophages and Ly6C⁻ CD64⁺ monocytes falling within these gates after Siglec-F⁺ alveolar macrophages were first excluded. Data is representative of 1-2 mice per group and from 1 representative experiment of 2.

SFig. 3



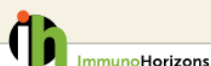
SFigure 3: Combined confocal images of mApple and ECFP in blood cells from *Csf1r*-mApple, Δ *Csf1r*-ECFP or *Csf1r*-mApple: Δ *Csf1r*-ECFP double transgenic mice using microscope settings used to image the liver (A) and lung (B) in Fig. 8 and Fig. 9 respectively.

SFig. 4



SFigure 4: CSF1^{AF647} labelling in *Csf1r*-mApple:Δ*Csf1r*-ECFP double transgenic mice confirms interstitial macrophage identity. Confocal image of a transverse section of lung from a *Csf1r*-mApple:Δ*Csf1r*-ECFP double transgenic mouse injected with FITC-Lectin I and CSF1^{AF647} i.v. to reveal pulmonary vasculature and CSF1R expression. Microscope acquisition settings match those from Fig. 9 using 8% laser power. Autofluorescence was detected using non-fluorescent tissue, and false-positive signal was discarded by using tissues that were single-positive for ECFP, mApple, FITC or AF647.

9.2 Species-Specific Transcriptional Regulation of Genes Involved in Nitric Oxide Production and Arginine Metabolism in Macrophages



RESEARCH ARTICLE

Innate Immunity

Species-Specific Transcriptional Regulation of Genes Involved in Nitric Oxide Production and Arginine Metabolism in Macrophages

Rachel Young,* Stephen J. Bush,* Lucas Lefevre,* Mary E. B. McCulloch,* Zofia M. Lisowski,* Charity Muriuki,* Lindsey A. Waddell,* Kristin A. Sauter,* Clare Pridans,* Emily L. Clark,* and David A. Hume*[†]

*The Roslin Institute and Royal (Dick) School of Veterinary Studies, University of Edinburgh, Easter Bush, Midlothian EH25 9RG, United Kingdom; and [†]Mater Research—University of Queensland, Translational Research Institute, Woolloongabba, Brisbane, Queensland 4102, Australia

ABSTRACT

Activated mouse macrophages metabolize arginine via NO synthase (NOS2) to produce NO as an antimicrobial effector. Published gene expression datasets provide little support for the activation of this pathway in human macrophages. Generation of NO requires the coordinated regulation of multiple genes. We have generated RNA-sequencing data from bone marrow–derived macrophages from representative rodent (rat), monogastric (pig and horse), and ruminant (sheep, goat, cattle, and water buffalo) species, and analyzed the expression of genes involved in arginine metabolism in response to stimulation with LPS. In rats, as in mice, LPS strongly induced *Nos2*, the arginine transporter *Slc7a2*, arginase 1 (*Arg1*), GTP cyclohydrolase (*Gch1*), and argininosuccinate synthase (*Ass1*). None of these responses was conserved across species. Only cattle and water buffalo showed substantial *NOS2* induction. The species studied also differed in expression and regulation of arginase (*ARG2*, rather than *ARG1*), and amino acid transporters. Variation between species was associated with rapid promoter evolution. Differential induction of *NOS2* and *ARG2* between the ruminant species was associated with insertions of the Bov-A2 retrotransposon in the promoter region. Bov-A2 was shown to possess LPS-inducible enhancer activity in transfected RAW264.7 macrophages. Consistent with a function in innate immunity, NO production and arginine metabolism vary greatly between species and differences may contribute to pathogen host restriction.

ImmunoHorizons, 2018, 2: 27–37.

Received for publication December 9, 2017. Accepted for publication December 24, 2017.

Address correspondence and reprint requests to: Prof. David A. Hume, Mater Research—University of Queensland, Translational Research Institute, Woolloongabba, Brisbane, QLD 4102, Australia. E-mail address: David.Hume@uq.edu.au

ORCID: 0000-0002-7904-7260 (R.Y.); 0000-0001-9341-2562 (S.J.B.); 0000-0003-0925-7411 (L.L.); 0000-0002-1323-9593 (Z.M.L.); 0000-0002-6414-6661 (C.M.); 0000-0002-2483-1760 (L.A.W.); 0000-0001-9423-557X (C.P.); 0000-0002-9550-7407 (E.L.C.).

The raw read data presented in this article have been submitted to the European Nucleotide Archive (<https://www.ebi.ac.uk/ena>) under accession numbers PRJEB21180, PRJEB22535, PRJEB22536, PRJEB22537, PRJEB22553, and PRJEB23196.

This work was supported in part by grants from the Biotechnology and Biological Sciences Research Council (www.bbsrc.ac.uk) (Functional Annotation of the Sheep Genome – BB/L001209/1 and Transcriptome Analysis in Indian Buffalo and the Genetics of Innate Immunity – BB/L004623/1), as well as grants from the Institute Strategic Programme (Farm Animal Genomics – BBS/E/D/20211550, Transcriptomes, Networks and Systems – BBS/E/D/20211552, and Blueprints for Healthy Animals – BB/P013732/1). C.M. received Ph.D. scholarship support from the Newton Fund. Z.M.L. received a Ph.D. studentship from the Horserace Betting Levy Board. S.J.B. was supported by the Roslin Foundation. Edinburgh Genomics is supported in part by core grants from the Biotechnology and Biological Sciences Research Council (BB/J004243/1), the Natural Environment Research Council (<http://www.nerc.ac.uk>) (R8/H10/56), and the Medical Research Council (<https://www.mrc.ac.uk>) (MR/K001744/1).

Abbreviations used in this article: ARG1, arginase 1; ASL, argininosuccinate lyase 1; ASS1, argininosuccinate synthase 1; BM, bone marrow; BMDM, BM-derived macrophage; GCH1, GTP cyclohydrolase 1; PTS, 6-pyruvoyl tetrahydrobiopterin synthase; RNA-seq, RNA sequencing; THB4, tetrahydrobiopterin; TPM, transcript per million.

The online version of this article contains supplemental material.

This article is distributed under the terms of the [CC BY 4.0 Unported license](https://creativecommons.org/licenses/by/4.0/).

Copyright © 2018 The Authors

<https://doi.org/10.4049/immunohorizons.1700073>

27

ImmunoHorizons is published by The American Association of Immunologists, Inc.

INTRODUCTION

The ability of rodent macrophages to produce NO through the metabolism of arginine was described in the late 1980s (1) and the cDNA encoding the calcium-dependent, inducible enzyme required for this activity, now known as NO synthase (NOS2), was isolated soon afterward (2, 3). Subsequently, the *Nos2* gene was deleted in the mouse germ line, and shown to be required for optimal host defense against mycobacteria (4) and for numerous other intracellular pathogens and pathogenic processes. A current search of PubMed for “NO AND macrophage” produces ~18,000 hits. Throughout that vast literature, the species being examined is commonly omitted from the title of the work. Yet, almost from the outset, it was clear that there are major species differences in macrophage arginine metabolism and the production of NO. In a recent review, Bogdan (5) stated that “there is no doubt that human cells are able to express NOS2 protein and activity in vitro and in vivo.” However, the data supporting human macrophage NOS2 protein expression in vivo rely heavily upon detection with commercial polyclonal antisera (e.g., Ref. 6). The large majority of published studies where there has been direct comparison with mouse have found little or no detectable NOS2 mRNA or NO production in human monocytes or macrophages stimulated in vitro (e.g., Ref. 7). Gross et al. (8) found that the NOS2 promoter region is methylated and contained in inactive chromatin in human alveolar macrophages. Inactive chromatin status at NOS2 is also evident in freshly isolated human blood monocytes (9). In the large FANTOM5 dataset, based upon deep sequencing of CAGE libraries, NOS2 mRNA was not detectable in human monocyte-derived macrophages stimulated with LPS, or in fresh monocytes stimulated with a wide range of stimuli. In fact, the most abundant site of expression was adipocytes (10). Vitek et al. (11) created a human NOS2 transgene on a mouse *Nos2*-deficient background, and reported that both NOS2 expression and inducible NO production in macrophages were considerably lower than in *Nos2*^{+/+} mice. Substantial differences in the set of LPS-inducible genes between humans and mice can be associated with major differences in promoter architecture; regulatory elements identified in mice are not conserved in humans (7). The regulatory differences between mouse and human macrophages are not restricted to NOS2, and are shared with other species. Pig macrophages also failed to induce NOS2 mRNA in response to activation (12), but share with humans the induction of a substantial set of genes that are not induced in mouse. *Nos2* induction is not even uniform among rodent species. Isolated macrophages from guinea pigs and hamsters produce substantially less NO than mice, and this has been associated with *Nos2* mRNA and promoter variation (13–15). Other species in stimulated macrophages appear to produce little or no detectable NOS2 activity include rabbits, sheep, goats, monkeys, horses, and badgers (15–18).

Mice, humans, and other species also differ in other aspects of arginine metabolism. The production of NO in mouse macrophages depends upon induction of the cationic amino acid transporter encoded by *Slc7a2* (19), which is not detectably expressed in human myeloid cells (7, 10), or in activated pig

macrophages (12). Degradation of arginine by arginase enzymes potentially competes for intracellular arginine to compromise NO production. Thomas and Mattila (20) reviewed the literature on arginine metabolism in human macrophages. In mice, arginase 1 (*Arg1*) has come to be regarded as a marker for M2/IL-4-mediated macrophage polarization, but it is not shared with human macrophages (21). Indeed, in the FANTOM5 CAGE data, *ARG1* mRNA in humans is very strongly expressed by neutrophils, as well as hepatocytes and the liver, but is entirely absent from monocytes and macrophages in any state of activation (10). Finally, the key cofactor for NOS2, tetrahydrobiopterin (THB4), is regulated differently between the species. In both mouse and human, the limiting enzyme GTP cyclohydrolase 1 (GCHI) is strongly inducible in macrophages. However, in human monocytes the downstream enzyme, 6-pyruvoyl THB4 synthase (PTS), was expressed at very low levels, and the major outcome of GCHI induction was the production and secretion of neopterin (22, 23). In this study we take advantage of large RNA sequencing (RNA-seq) datasets from multiple species to reexamine the species specificity of genes involved in arginine metabolism, and analyze the promoters of differentially regulated transcripts to highlight possible mechanisms underlying the gain and loss of gene expression.

MATERIALS AND METHODS

Animals

Approval was obtained from the Protocols and Ethics Committees of The Roslin Institute, The University of Edinburgh, and the Royal (Dick) School of Veterinary Medicine. In accordance with the United Kingdom Animal (Scientific Procedures) Act 1986, this study did not require a Home Office project license as no regulated procedures were carried out. Cattle, water buffalo, and pigs were euthanized by captive bolt, sheep were euthanized by electrocution and exsanguination, and rats were euthanized by CO₂ asphyxiation. Goat samples were collected from the slaughterhouse. Horses were admitted to the Equine Hospital at the Royal (Dick) School of Veterinary Studies for elective euthanasia. Horses were euthanized with i.v. secobarbital sodium 400 mg/ml and cinchocaine hydrochloride 25 mg/ml (Somulose; Arnolds/Dechra).

Generation of bone marrow-derived macrophages

Ribs were collected postmortem from cattle, goats, horses, sheep, pigs, and water buffalo, and femurs were collected postmortem from rats. Bone marrow (BM) cells were isolated using the methods described by Schroder et al. (7) and Kapetanovic et al. (12). BM-derived macrophages (BMDM) were cultured from cryopreserved BM cells for each species. Briefly, BM cells isolated from rats were cultured in DMEM (Sigma-Aldrich), heat-inactivated 10% FBS (GE Healthcare), penicillin/streptomycin (Thermo Fisher Scientific), and GlutaMAX (Thermo Fisher Scientific). BM cells from pigs were cultured as described by Kapetanovic et al. (12), sheep cells were cultured as described by

<https://doi.org/10.4049/immunohorizons.1700073>

Bush et al. (24), and cells from all other animals were cultured in RPMI 1640 (Sigma-Aldrich), heat-inactivated 20% FBS (GE Healthcare) (cattle and water buffalo) or autologous serum (Sigma-Aldrich) (goat and horse), penicillin/streptomycin (Thermo Fisher Scientific), and GlutaMAX (Thermo Fisher Scientific). BMDM were obtained by culturing BM cells for 7–10 d in the presence of recombinant human CSF1 (10^4 U/ml; a gift from Chiron, Emeryville, CA) on bacteriological plates, as described in mouse, pig, and sheep (7, 12, 24); goat BMDMs were differentiated on tissue culture plastic. Differentiated macrophages were detached from plates by either vigorous washing using a syringe and blunt 18 g needle, or using a cell scraper, then washed, counted, and reseeded at 10^6 cells per ml. Cells were treated with LPS from *Salmonella enterica* serotype Minnesota Re 595 (Sigma-Aldrich) for 7 and 24 h at a final concentration of 100 ng/ml for large animals and 10 ng/ml for rats.

RNA isolation

RNA was isolated from control and LPS-stimulated cells using the TRIzol method (Thermo Fisher Scientific) followed by a clean-up step from the RNeasy Mini Kit (Qiagen). Cells were lysed in six-well plates at 0, 7, and 24 h post-LPS stimulation with 1 ml TRIzol, then frozen until RNA extraction was performed. Tissue culture replicates were included. Lysates were thawed and brought to room temperature. Chloroform (200 μ l) was added and samples incubated for 2–3 min at room temperature. The samples were centrifuged at $12,000 \times g$ at 4°C for 15 min to separate the phases. The aqueous phase was collected then precipitated in 1 volume of 70% ethanol. Samples were then transferred immediately to an RNeasy Mini Kit spin column and clean-up performed as specified by the manufacturer. RNA was quantified by Qubit BR dsDNA assay (Thermo Fisher Scientific) and RNA integrity number equivalent was calculated using RNA ScreenTape on the Agilent 2200 TapeStation. All samples had RNA integrity number equivalent values >7 .

Library preparation and sequencing

RNA-seq libraries were generated and sequenced by Edinburgh Genomics. All libraries were prepared using the Illumina TruSeq Stranded library protocol for total RNA libraries (Part: 15031048, Revision E) with the exception of rat and goat where stranded mRNA libraries were prepared (Part: 15031047, Revision E). TruSeq Stranded total RNA libraries were sequenced at a depth of >100 million paired-end reads per sample for cattle, buffalo, horse, and pig using the Illumina HiSeq 2500 platform. Similarly, TruSeq Stranded mRNA libraries were sequenced at a depth of >25 million paired-end reads for rat on the Illumina HiSeq 2500 platform. The sheep RNA-seq dataset is a component of a high resolution atlas of gene expression for sheep, which we have described previously (25). Goat mRNA libraries were sequenced at a depth of >50 million paired-end reads per sample using the Illumina HiSeq 4000 platform. Raw read data for all libraries has been submitted to the European Nucleotide Archive (<https://www.ebi.ac.uk/ena>) under accession numbers PRJEB19199 (sheep), PRJEB21180 (water buffalo), PRJEB22535 (cattle), PRJEB22536

(pig), PRJEB22537 (horse), PRJEB22553 (rat), and PRJEB23196 (goat).

RNA-seq data processing

RNA-seq data were processed using the high-speed transcript quantification tool Kallisto v0.43.0, as described previously (24), generating gene-level expression estimates as transcripts per million (TPM). Kallisto quantifies expression by building an index of k-mers from a set of reference transcripts and then mapping the reads to these directly (26). The reference transcriptomes for each species, from which Kallisto indices were generated, are given in Supplemental Table I. A two-pass approach to Kallisto was used (24) whereby these transcriptomic indices are iteratively revised and expression requantified. In brief, expression was quantified for an initial analysis (the first pass), the output of which is parsed so as to revise the transcriptome. A second index is then created with a higher proportion of unique k-mers, conferring greater accuracy when (re) quantifying expression. The revised indices include, where possible, de novo assembled transcripts that had not previously been annotated [by taking the set of reads Kallisto could not map during the first pass and assembling them with Trinity version r20140717 (27)] and exclude transcripts not detectably expressed in any library during the initial analysis (detailed in Supplemental Table I). For both the first and second pass index, $k = 31$. The expression of genes involved in arginine metabolism (KEGG pathway ID: map00230; <http://www.genome.jp/kegg/pathway/map/map00330.html>) was then compared across species.

Griess assay

NO production was measured by Griess assay. Nitrite (the product of NO oxidation in culture) was quantified against sodium nitrite standards. Cell culture supernatants from LPS-treated BMDM were added to an equal volume of Griess reagent [1% sulfanilamide, 0.1% *N*-(1-naphthyl) ethylenediamine diHCl, 2.5% phosphoric acid]. The reaction was incubated at 37°C for 30 min then the absorbance measured at 570 nm. As a positive control for NO production, chicken BMDM—prepared as previously described (28)—were stimulated with LPS under the same conditions.

Bovine NOS2 promoter (enhancer) assay

A 150 bp region of the bovine NOS2 promoter covering the Bov-A2 element was synthesized by Eurofins Genomics and cloned into the *Bam*HI/*Sal*I site downstream of the promoter-luc+ transcriptional unit of the pGL3 promoter vector (E1761; Promega). Transient transfections were performed by electroporation of 5×10^6 RAW 264.7 cells with 5 μ g of pGL3-NOS2 construct or empty vector in 0.4 cm electroporation cuvettes at 300 V, 950 μ F using a Bio-Rad Gene Pulser. Transfected cells were cultured at 37°C for 4 h then given fresh media and returned to the incubator overnight. The following day, cells were treated with 100 ng/ml LPS and incubated at 37°C. Control wells containing no LPS were incubated in parallel. After 24 h LPS stimulation, the media were removed, and the cells washed in PBS then lysed in Luciferase assay lysis reagent (E4030; Promega) at -80°C for

<https://doi.org/10.4049/immunohorizons.1700073>

1 h. The cells were collected from the plates by scraping, then the lysates collected in microfuge tubes and vortexed for 10–15 s. The samples were centrifuged at $12,000 \times g$ for 15 s at room temperature then the supernatants collected for luciferase assay. Luciferase reagent was dispensed into an opaque 96-well plate. Then 20 μ l of each sample was added to the wells containing the reagent and the plate vortexed briefly. The plate was analyzed on a Synergy HT Biotek luminometer.

RESULTS

Species differences in NO production

To extend our knowledge of the diversity and evolution of innate immune genes across species, we have adapted methods previously described for the mouse and pig (12) for the production of BMDM from rat, horse, sheep, goat, cattle, and water buffalo. For this study, pig BMDMs were also generated for RNA-seq analysis. In each case, BM cells were grown in recombinant human CSF1 for 7–10 d, after which the cells form a relatively confluent population of macrophages. The cells were then harvested from their culture dishes and counted before reseeding on tissue culture plastic for stimulation with LPS. For each species, we have determined the time course of activation by measuring the inducible expression of *TNF- α* mRNA.

To confirm and extend previous findings, we examined LPS-inducible NO production in a number of species. Fig. 1 shows comparative analysis of water buffalo, cattle, sheep, goat, and horse responses to LPS. In each case, a positive control, chicken BMDM, which we have previously shown produce large amounts of NO in response to LPS (28), was tested side by side. Cattle macrophages made NO in response to LPS treatment at levels similar to chicken BMDM; under similar conditions, water buffalo and goat made lower levels of NO, and sheep macrophages produced no detectable NO. Horse BMDM produced no detectable NO in response to LPS, as previously noted for alveolar macrophages (18). In mice, NO production can also be induced by IFN- γ , and this treatment increases the response to LPS, largely by shifting the LPS dose-response curve rather than increasing the absolute response (29). However, horse macrophages made very low levels of NO even after IFN- γ priming (Supplemental Fig. 1).

RNA-seq analysis of genes involved in arginine metabolism

There are several possible reasons why macrophages might not make detectable NO, even if *NOS2* mRNA is induced. We therefore examined the expression of all relevant genes in each of the species. For comparison across species, we chose the 7 h time point following LPS addition, consistent with a previous comparative analysis of mouse, pig, and human (12). In the current study, we included rat, rather than mouse, as a positive control rodent species, in part also to determine whether the mouse is representative as a rodent species (see *Introduction*). Fig. 2 summarizes the pathways of mammalian arginine metabolism, and Table I shows the expression levels of transcripts encoding enzymes associated with arginine metabolism and the production of the *NOS2*

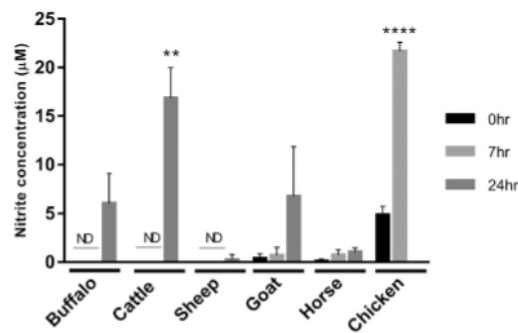


FIGURE 1. LPS-inducible NO production in macrophages.

Supernatants were collected from LPS stimulated (*S. enterica*; 100 ng/ml) BMDM from water buffalo, cattle, sheep, goat, and horse at 0, 7, and 24 h poststimulation and nitrite production measured by Griess assay. Stimulated chicken BMDM 0 and 7 h poststimulation were used as a positive control. Mean nitrite levels are shown with error bars for the SD of the mean for three biological replicates per species, performed in duplicate. Statistically significant differences versus unstimulated cells are indicated (t test; **** $p < 0.0001$, ** $p < 0.01$). ND, not detected.

cofactor, *THB4*. For comparison, we have extracted expression of these genes from the FANTOM5 CAGE tag sequencing dataset on human monocyte-derived macrophage response to LPS; the data are consistent with previously published microarray data (7).

There are a number of features to note. Firstly, all four of the ruminant species induced *NOS2* mRNA in response to LPS, but the maximum levels of stimulated expression were at least 15-fold lower in sheep and goats (TPM \approx 20) compared with water buffalo (TPM >300), and cattle produced even higher levels of mRNA (TPM \approx 900). The induced level of *NOS2* mRNA in sheep [see also BioGPS sheep dataset (www.biogps.org/dataset/BDS_00015/sheep-atlas/)] and goat macrophages was lower than the unstimulated level in rat macrophages (TPM \approx 60). It is unclear why goat macrophages produced detectable NO, where sheep macrophages did not. One explanation may lie in the relatively high expression of genes required for cofactor, *THB4*, production (*PTPS*, *SPR*) in goat macrophages. Horse and pig *NOS2* mRNA was on the limits of detection (TPM <2), although following LPS stimulation, rat *Nos2* mRNA was a further order of magnitude higher than in any of the ruminants (TPM \approx 5000). The second key difference between all of the large animals and rodents is the regulation of genes involved in arginine uptake. In rats, as in mice (19), LPS greatly increased (18-fold) expression of the cationic amino acid transporter, *Slc7a2*, whereas goats were the only large animal species in which *SLC7A2* mRNA was detectable (TPM 6) and regulated to any degree by LPS, with an induced level (TPM \approx 16) still lower than the basal level in the rat (TPM 46). Goat and buffalo also expressed the other cationic arginine transporter, *SLC7A1*, at higher level, inducible in buffalo and constitutive in goat.

<https://doi.org/10.4049/immunohorizons.1700073>

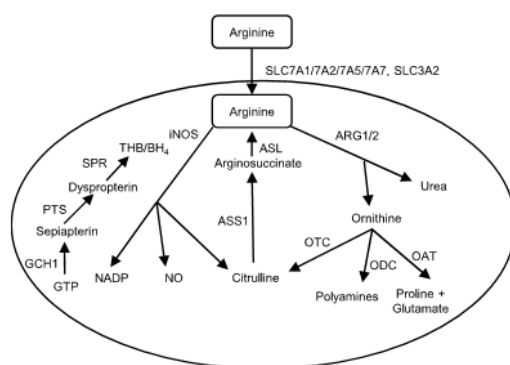


FIGURE 2. Mammalian arginine metabolism pathway in macrophages.

Arginine is transported into mammalian macrophages by amino acid transporters (SLC7A1/7A2/7A5/7A7, SLC3A2), then metabolized by either inducible NO synthase (iNOS) into NO and citrulline, or arginase into ornithine and urea. Citrulline can feed back into arginine synthesis via ASS1 and inducible ASL. Citrulline, polyamines or proline and glutamate can be generated from ornithine via ornithine transcarbamylase (OTC), ornithine decarboxylase (ODC) or ornithine aminotransferase (OAT), respectively. The iNOS cofactor, THB, is generated by GTP via GCH1, PTS, and SPR respectively, and is a rate-limiting step in the production of NO.

The major avenue for arginine uptake in large animal macrophages is likely to be SLC3A2/SLC7A7 (also known as the Y+L or LAT1/CD98 system), which also mediates the uptake of other large neutral amino acids, including tryptophan, and is likely to be involved in inducible tryptophan metabolism. The gene encoding the alternative L chain, SLC7A5, was only expressed at high levels in the goat macrophages (TPM≈115). SLC3A2 and SLC7A7 were both highly expressed in macrophages from all of the large animal species examined, including humans, substantially higher than in rats. In humans at least, SLC7A7 is strongly monocyte-macrophage enriched relative to other cell types and tissues (10); see also data on the BioGPS web portal (www.biogps.org/dataset/GSE1133).

The species studied also differ greatly in their expression of mRNA encoding genes involved in arginine breakdown. *Arg1* has been proposed as a mouse M2 macrophage marker and is strongly inducible by IL-4, but induction was not conserved in human macrophages (21). *Arg1* was induced by LPS in mouse macrophages, but not in human (7). In rat macrophages, *Arg1* was highly expressed and very strongly induced by LPS. In the FANTOM5 dataset (10) neither *ARG1* nor *ARG2* was expressed in human monocytes or macrophages in any activation state. In pigs, as in rats, *ARG1* was highly expressed and strongly induced by LPS, whereas in horse *ARG2* was constitutively expressed at high levels (TPM≈120) but downregulated by LPS stimulation. In each of the ruminant species, *ARG2*, but not *ARG1*, was expressed and

strongly induced by LPS. In rats, and all of the large animals, the ornithine generated by arginase activity is likely metabolized further by ornithine amino transferase and ornithine decarboxylase, which are each constitutively expressed at high levels in macrophages. As discussed by Bogdan (5), arginine might also be derived from either the breakdown of peptides by enzymes such as endoplasmic reticulum-associated aminopeptidase 1, carboxypeptidases M, and D or by resynthesis from citrulline via argininosuccinate synthase 1 (ASS1) and argininosuccinate lyase 1 (ASL). *Ass1*-deficient mice are also deficient in NO production and antimicrobial activity, and this pathway is required to overcome the degradation of arginine by Arg1 (30). This pathway is likely conserved in rats, because *Asl* was constitutive, and *Ass1* was strongly induced by LPS in the rat macrophages. However, in human macrophages, both *ASL* and *ASS1* were on the limits of detection, and *ASS1* was also very low in the other large animals.

In human macrophages, the production of the NOS2 cofactor, THB/BH₄, is apparently constrained by very low expression of the synthetic enzymes PTS and SPR. Indeed, in the FANTOM5 data, *SPR* expression is very low, and *PTS* was barely detectable in monocytes or macrophages under any conditions. Activation of human macrophages by LPS produced a massive induction of *GCH1*, but previous reports indicate the major product is neopterin rather than THB4 (22, 23). Early studies identified serum and urinary neopterin as a marker of immune activation in human and other primates, where this product was undetectable in rodents (31). More recently, neopterin was detected in the serum of LPS-challenged pigs, whereas there was only a marginal and transient increase in serum NO (32).

Gch1 was also strongly induced in rat macrophages by LPS, as previously observed in both BMDM and peritoneal macrophages in mice (7); see also data on www.biogps.org/dataset/GSE10246. In the ruminants and horses, *GCH1* was expressed constitutively, but was further induced (~4-fold) only in cattle. In pigs, *PTS* mRNA was detected at very high levels (TPM≈140). *GCH1* was not annotated in the pig genome (version 10.2) when expression profiles of pig and human macrophages were previously compared (12). Unlike human macrophages, pig macrophages expressed low levels of *GCH1* constitutively but it was not induced by LPS.

Gain and loss of candidate enhancers in the NOS2 promoter

We and others have shown that variation in LPS-inducible gene expression in humans, mice and pigs, including that of *NOS2*, is associated with major differences in promoter architecture including the gain and loss of candidate enhancers (7, 12). The inducible arginine transporter *Slc7a2*, which is essential for NO production in mouse macrophages, provides another example. In the FANTOM5 CAGE data, this gene is highly expressed in liver but undetectable in myeloid cells in any state of activation, whereas in mouse it is expressed at similar levels in liver and activated macrophages. Inducible activity of mouse *Slc7a2* varies between mouse strains, associated with alterations in a distal purine-rich promoter element (33). This element is not conserved in the rat promoter, and indeed the promoter regions of mouse, rat, pig, and human have diverged substantially (Supplemental Fig. 2).

TABLE I. Expression levels of transcripts encoding enzymes associated with arginine metabolism and the production of NO

Gene Name	Description	RNA-Seq							
		Sheep		Goat		Cattle		Buffalo	
		0 h	7 h	0 h	7 h	0 h	7 h	0 h	7 h
ARG1	Arginase 1	0.04	0.05	2.64	2.73	6.05	5.84	0.02	0.01
ARG2	Arginase 2	7.40	56.27	11.82	41.06	48.48	347.99	30.06	153.54
ASL	Argininosuccinate lyase	31.48	14.75	25.40	17.78	38.21	17.99	19.72	6.50
ASS1	Argininosuccinate synthase 1	19.39	10.18	4.38	3.72	10.71	7.65	0.05	0.32
GCH1	GTP cyclohydrolase 1	17.14	32.88	8.31	10.15	22.94	86.98	13.66	10.90
NOS2	NO synthase 2, inducible	0.55	19.09	3.78	19.69	2.14	901.20	3.25	301.37
OAT	Ornithine aminotransferase	362.00	324.62	164.61	167.15	1166.67	854.75	204.40	142.74
ODC1	Ornithine decarboxylase 1	92.12	269.73	340.63	376.01	45.46	18.26	119.02	53.83
PTS	6-pyruvoyltetrahydropterin synthase	17.49	13.66	62.01	62.61	27.53	11.91	36.36	16.32
SLC3A2	Solute carrier family 3, member 2	161.19	167.79	209.91	210.11	98.20	62.87	168.22	146.74
SLC7A1	Solute carrier family 7, member 1	7.91	10.02	38.08	45.94	7.37	6.99	19.95	49.59
SLC7A2	Solute carrier family 7, member 2	0.01	0.04	5.88	15.73	0.04	0.18	0.18	2.03
SLC7A5	Solute carrier family 7, member 5	9.01	21.67	115.47	106.67	5.83	3.46	7.74	7.46
SLC7A7	Solute carrier family 7, member 7	283.90	161.32	109.13	60.78	220.58	120.25	114.72	103.68
SPR	Septipterin reductase	21.00	13.80	78.29	124.30	20.47	4.60	37.28	13.15

Gene Name	Description	RNA-Seq						CAGE	
		Horse		Pig		Rat		Human	
		0 h	7 h	0 h	7 h	0 h	7 h	0 h	7 h
ARG1	Arginase 1	0.10	0.05	70.62	379.11	76.63	1041.60	0.00	0.00
ARG2	Arginase 2	119.23	59.72	13.56	11.91	3.35	1.88	3.10	1.30
ASL	Argininosuccinate lyase	24.06	14.48	13.93	10.35	69.63	50.24	5.80	0.70
ASS1	Argininosuccinate synthase 1	25.85	20.34	0.02	0.04	2.38	250.12	0.00	0.00
GCH1	GTP cyclohydrolase 1	24.77	31.89	9.82	9.67	24.17	189.57	0.70	391.00
NOS2	NO synthase 2, inducible	0.00	0.01	0.66	1.77	59.03	4961.79	0.00	0.00
OAT	Ornithine aminotransferase	103.56	68.81	95.74	83.74	104.93	82.10	83.00	57.00
ODC1	Ornithine decarboxylase 1	98.48	39.73	241.26	195.93	64.55	45.63	5.30	1.30
PTS	6-pyruvoyltetrahydropterin synthase	27.98	16.30	143.49	141.30	11.51	13.01	0.50	0.00
SLC3A2	Solute carrier family 3, member 2	168.35	120.18	238.46	248.84	191.23	289.86	115.00	123.00
SLC7A1	Solute carrier family 7, member 1	13.27	9.72	5.45	4.68	20.02	14.00	0.00	0.00
SLC7A2	Solute carrier family 7, member 2	0.01	0.05	1.00	0.47	46.31	843.81	0.00	0.00
SLC7A5	Solute carrier family 7, member 5	8.97	7.28	13.09	8.81	17.71	14.76	2.70	75.00
SLC7A7	Solute carrier family 7, member 7	57.12	46.60	136.68	198.99	16.97	16.00	71.00	25.00
SPR	Septipterin reductase	10.20	3.55	13.08	8.26	10.08	9.95	21.00	1.80

Expression levels are represented as TPM, and are mean values for each condition from multiple animals. Sheep, $n = 6$; goat, $n = 3$; buffalo, $n = 4$; cattle, $n = 4$; horse, $n = 3$; pig, $n = 3$; rat, $n = 3$; human, $n = 3$. Human data were generated by CAGE-seq, as previously described (10), and all other data were generated by RNA-seq as described.

We were especially interested in the mechanisms distinguishing *NOS2* induction between the four relatively closely related ruminant species. Fig. 3 shows alignment of the proximal promoter regions across species that do, or do not, show induction of *NOS2* mRNA in response to LPS in our experiments or previous studies. In each species there is a TATA box. Despite the relatively low overall conservation, the proximal promoter elements that have been implicated in transcriptional regulation (13, 34), including NF- κ B, Oct1, and C/EBP motifs, are conserved and do not correlate with LPS inducibility. Accordingly, it seems likely that differences among species relate to variation in more distal regulatory elements, such as the enhancer located around -1 kb upstream in the mouse genome.

Fig. 4A shows a pairwise dot-matrix alignment of distal *NOS2* promoters from cattle and human. An arrow indicates the relative location of the mouse enhancer, which was previously shown to be poorly conserved in humans and lacked the enhancer activity detected in the equivalent mouse sequence (34). In this region,

cattle, sheep, and pig genomes are similar to human, with multiple substitutions in the putative mouse LPS responsive element. Regions of relative conservation between the human and bovine *NOS2* 5' flanking region extending up to 25 kb from the transcription start site are interspersed with regions in which there is no detectable alignment. Fig. 4B shows a similar alignment of cattle and sheep, where there is almost perfect conservation with the exception of a number of small insertions. Both the regions of substantial misalignment between the ruminants and other large animals, and the small additional insertions in cattle relative to sheep (and vice versa), are due to the presence of the Bov-A2 SINE retrotransposon, an ancestral element present at up to 200,000 copies in ruminant genomes (35, 36). Fig. 4C shows the alignment of the Bov-A2 element with the cattle *NOS2* promoter region, and Fig. 4D shows the equivalent alignment with the sheep. It is clear that those regions lacking homology with the human promoter are predominantly occupied by partial or complete Bov-A2 elements.

<https://doi.org/10.4049/immunohorizons.1700073>

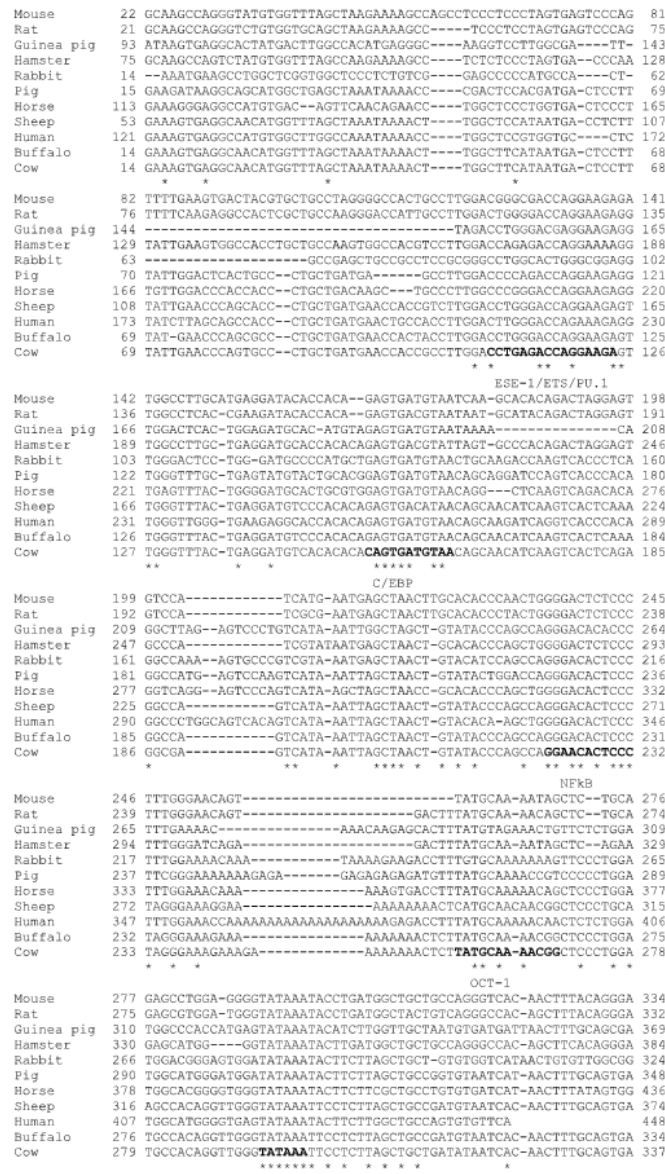


FIGURE 3. Alignment of the NOS2 proximal promoter region across species.
 A 323 bp region of the proximal NOS2 promoter was aligned between 11 species that show LPS-induced NOS2 gene expression or not. Transcription factor binding sites, PU.1, C/EBP, NF-κB, and OCT1 and the TATA box are indicated in bold. Asterisks indicate bases conserved across the species.

<https://doi.org/10.4049/immunohorizons.1700073>

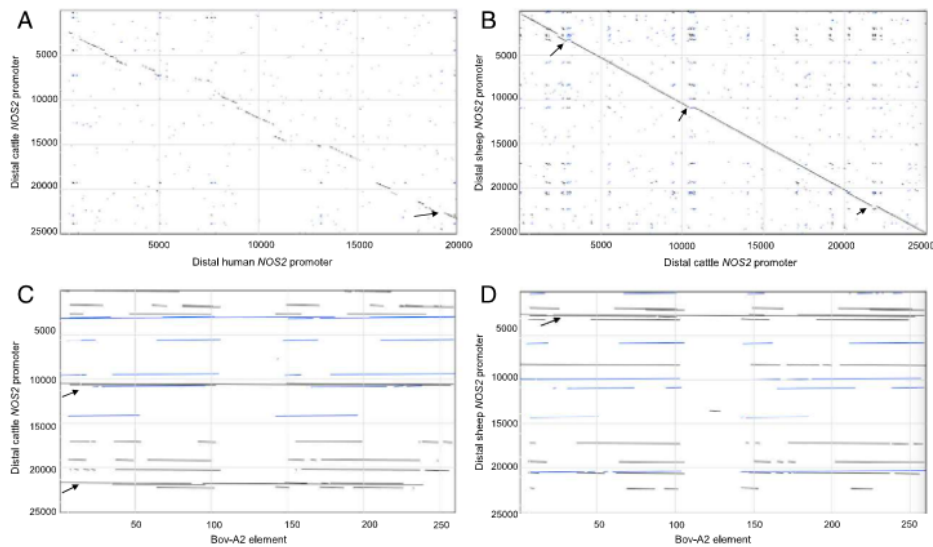


FIGURE 4. Alignment of distal *NOS2* promoters from cattle, human, and sheep, and the Bov-A2 element.

NOS2 promoter sequences were obtained from Ensembl. (A and B) show pairwise dot-matrix alignment of 25 kb sequences upstream of *NOS2* transcription start site from (A) cattle (y-axis) versus human (x-axis), and (B) sheep (y-axis) versus cattle (x-axis). The arrow in (A) indicates the relative location of the mouse *Nos2* enhancer. In (B), small insertions showing misalignment are indicated by arrows. (C and D) show the alignment of the Bov-A2 element with the cattle (C) and sheep (D) 25 kb *NOS2* promoter regions. Arrows indicate regions occupied by partial or complete Bov-A2 elements.

The absence of a Bov-A2 insertion in the proximal *TP53* promoter region has been implicated in regulated mammary involution and the persistence of lactation in bovids compared with other ruminants through functional STAT1 and NF- κ B responsive motifs (37). We have located this proximal insertion in the *NOS2* gene in the bison, water buffalo, and yak genomes, but it was absent in goats. Fig. 5 shows alignments of the *NOS2* Bov-A2 element from four bovid species with the consensus BOV-A2 sequence, and with a distal BOV-A2 sequence extracted from the *TP53* locus. A notable feature is that the direct repeats flanking this insertion are conserved in all bovids, but also in the sheep and goat genomes (data not shown), suggesting that this is a relatively recent insertion whereas the insertion site preexisted in the ancestral ruminant. The aligned sequences in Fig. 5 are also annotated with candidate transcription factor binding sites derived from analysis of the sequence using Jaspar (<http://jaspar.genereg.net>). Damiani et al. (35) have noted the association of BOV-A2 element insertions with regulatory regions of ruminant genomes and have speculated upon their role in transcription regulation. We reasoned that BOV-A2, containing binding sites for so many macrophage-specific (PU.1, CEBP β) and inducible (STAT1, IRF1, NF- κ B) transcription factors, could contribute to the regulated expression of *NOS2* in ruminants, compared with large (nonruminant) animal species, and that the additional BOV-A2 element located more proximally in the bovine genome could explain the increased expression.

The bovine *NOS2* BOV-A2 element is LPS responsive

To confirm the activity of the proximal *NOS2* bovine copy of BOV-A2 as a possible regulatory element, we constructed an enhancer/reporter luciferase construct and transfected the LPS-responsive mouse macrophage cell line, RAW264 (38). This line was previously used to demonstrate the lack of activity of the human *NOS2* promoter and enhancer (34). The results of transient transfection analysis are shown in Fig. 6. Compared to the basal promoter, the presence of the candidate BOV-A2 enhancer element produced both constitutive reporter gene activity and increased expression in the presence of LPS. Plasmid DNA can itself induce NF- κ B-dependent reporter activity via TLR9 (39), and so the basal activity of the *NOS2* Bov-A2 element is most likely partly attributable to activation by this pathway.

DISCUSSION

We have dissected the transcriptional regulation in macrophages of genes associated with arginine metabolism in a range of species. BMDM from sheep, cattle, water buffalo, goat, horse, pig, and rat were cultured under identical conditions, and stimulated with the same stimulus, LPS. Although it has been suggested that macrophages from different species respond differently to cell culture and that arginine metabolism may be different in vivo, it remains the case that there is large divergence between species

<https://doi.org/10.4049/immunohorizons.1700073>

BOV-A2 (C)	1	GCTGCTGCTGCTAAGTCGCTTCAGTCGTCCGACTCTGTGCGACCCCATAGAC	54
TP53 Cow	1	GCTPGCTGCTGCTAAGTCATTTTCAGTCATGTCGGACTCTGTGCAACCCCATGGAC	54
NOS2 Cow	1	CGGATCACTCCATATGCTAAGTCACTTCAGTCGTCCGACTCTGTGACCCCGAGAGAC	60
NOS2 Buffalo	1	CGGATCACTCCATATGCTAAGTCACTTCAGTCGTCCGACTCTGTGACCCCATAGAC	60
NOS2 Bison	1	CGGATCACTCCATATGCTAAGTCACTTCAGTCGTCCGACTCTGTGACCCCGAGAGAC	60
NOS2 Yak	1	CGGATCACTCCATATGCTAAGTCACTTCAGTCGTCCGACTCTGTGACCCCGAGAGAC	60
		* * * * *	
		POU AP1/ATF	NR1H3/RXR
BOV-A2 (C)	55	GGCAGCCCACCAGGCTCCCGCTCCCTGGGATTCTCCAGGCAAGAACAAGTGGAGTGGGTT	114
TP53 Cow	55	GGCAGCCCACCAGGCTCCCGCATCCCTGGGATTCTCCAGGCAAGAACAAGTGGAGTGGGTT	114
NOS2 Cow	61	GGCAGCCCACCAGGCTCCCGCTCCCTGGGATTCTCCAGGCAAGAACAAGTGGAGTGG-TT	119
NOS2 buffalo	61	GGCAGCCCACCAGGCTCCCGCTCCCTGGGATTCTCCAGGCAAGAACAAGTGGAGTGGTT	120
NOS2 Bison	61	GGCAGCCCACCAGGCTCCCGCTCCCTGGGATTCTCCAGGCAAGAACAAGTGGAGTGG-TT	119
NOS2 Yak	61	GGCAGCCCACCAGGCTCCCGCTCCCTGGGATTCTCCAGGCAAGAACAAGTGGAGTGG-TT	119
		* * * * *	
		KLF4/SP1/EGR1	REL/STAT1 STAT1
BOV-A2 (C)	115	GCCATTTCCTTCTCCAATGCATGAAAGTGAAAAGTGAAGTGAAAGTCGCTCAGTCGTGTC	174
TP53 Cow	115	GCCATTTCCTTCTCCAATGCATGAAAGTGAAAAGTGAAGTGAAAGTCGCTCAGTCATGCC	174
NOS2 Cow	120	GCCATTTCCTTCTCCAATGCATGAAAGTGAAAAGTGAAGTGAAAGTGCTCAGTCGTGTC	179
NOS2 Buffalo	121	GCCATTTCCTTCTCCAATGCATGAAAGTGAAAAGTGAAGTGAAAGTGCTCAGTCGTGTT	180
NOS2 Bison	120	GCCATTTCCTTCTCCAATGCATGAAAGTGAAAAGTGAAGTGAAAGTGCTCAGTCGTGTC	179
NOS2 Yak	120	GCCATTTCCTTCTCCAATGCATGAAAGTGAAAAGTGAAGTGAAAGTGCTCAGTCGTGTC	179
		* * * * *	
		STAT1 PU.1/ETS CEBP	IRF1 IRF1 CEBP
BOV-A2 (C)	175	CGACTCTTAGCGACCCCATGGACTGCAGCCTACCAGGCTCCTCCGTCATGGGATTTTCC	234
TP53 Cow	175	CGACTCTTAGCGACCCCATGGACTGCAGCCTGCCAGGATCCTCCATCCATGGGATTTTCC	234
NOS2 Cow	180	CAACGTTTAGCAACCCCATGGACTGCAGCCTCCAGGCTCCTCCGTCATGGGATTTTCC	239
NOS2 Buffalo	181	CAACGTTTAGCGACCCCATGGACTGCAGCCTCCAGGCTCCTCCATCCATGGGATTTTCC	240
NOS2 Bison	180	CAATGTTTAGCGACCCCATGGACTGCAGCCTCCAGGCTCCTCCGTCATGGGATTTTCC	239
NOS2 Yak	180	CAACGTTTAGCGACCCCAT ATGGACTGCAGCCTCCAGGCTCCTCCGTCATGGGATTTTCC	239
		* * * * *	
		STAT	SP1 REL/STAT
BOV-A2 (C)	235	AGGCAAGAGTACTGGAGTGGGGTGCCATTGCCTTCTCC	272
TP53 Cow	235	AGGCAAGAGTACTGGGGTGGGTTGCCATTGCCTTCTCTAA	274
NOS2 Cow	240	AGGCAAGAGTACTGGAGTGGGGTGCCATATCCATAATATCTACTCTTTAAGC	292
NOS2 Buffalo	241	ACGTAAGAGTACTGGAGTGGGGTGCCATATCCATAATATCTACTCTTTAAGC	293
NOS2 Bison	240	AGGCAAGAGTACTGGAGTGGGGTGCCATATCCATAATATCTACTCTTTAAGC	292
NOS2 Yak	240	AGGCAAGAGTACTGGAGTGGGGTGCCATATCCATAATATCTACTCTTTAAGC	292
		* * * * *	
		STAT	

FIGURE 5. The Bov-A2 element is conserved in the NOS2 gene of bovid species.

A ~300 bp region of the cattle TP53 gene and NOS2 gene from cattle, buffalo, bison, and yak were aligned to the consensus BOV-A2 sequence. Candidate transcription factor binding sites derived from analysis with Jaspar are indicated in bold. Asterisks indicate bases conserved across the species.

and NOS2 is only one component of the difference. In a recent review of arginine metabolism in myeloid cells (40), the authors discussed the prevalent uptake of arginine by the Y+ amino acid transport system (SLC7A2), the functional importance of inducible arginase 1 (ARG1) in control of arginine availability, the biological importance of NO production in antimicrobial defense and the fact that in macrophages, the NOS2 product, citrulline, can be recycled to arginine via ASS1 and ASL (30). Our analysis of the response of rat macrophages to LPS demonstrates that each of these responses is shared with mice; Nos2, Arg1, Slc7a2, and Ass1 were each very highly induced after 7 h exposure to LPS and Ass1 was constitutively expressed (Table I). However, of the LPS responses observed in rodents, only the induction of NOS2 and ARG1 was observed to any extent in any nonrodent species.

Jungi et al. (16) reported previously that bovine macrophages grown from BM or blood monocytes, or isolated from alveolar lavage, were able to induce NOS2 mRNA and produce NO in response to LPS. In the same study, goat macrophages produced much less NOS2 mRNA and NO than cattle. We have repeated these studies and extended them to two additional ruminant species, sheep and water buffalo. By contrast to the previous findings, goat macrophages produced detectable NO, despite low expression of NOS2, whereas there was no detectable NO production by sheep macrophages (in which NOS2 was induced to a similar extent) or in horses or pigs, where it was not induced at all. One explanation may be the selective expression of cationic amino acid transporters, SLC7A1 and SLC7A2 in goats relative to the other species (Table I).

https://doi.org/10.4049/immunohorizons.1700073

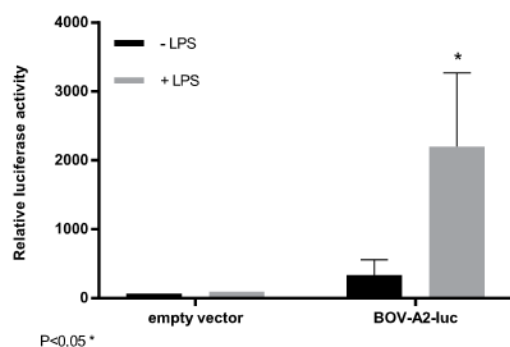


FIGURE 6. The Bov-A2 element is inducible in response to LPS.

RAW 264.7 cells were transfected with a Bov-A2–luciferase enhancer reporter vector or empty vector and stimulated with LPS for 24 h. Relative luciferase activity was measured in control and stimulated cells. The mean relative luciferase activity + SD is shown. This was calculated for replicates and is representative of three independent experiments. Statistically significant difference at 7 h versus 0 h (t test; *p < 0.05).

The comparative analysis we have presented strongly supports the view that the divergent expression of *NOS2* and other genes is a consequence of the evolution of *cis*-acting regulatory elements (7, 12) rather than an idiosyncratic feature of cell culture systems. As shown in Supplemental Fig. 2, the differential regulation of the inducible arginine transporter, *Slc7a2*, in rodent macrophages is associated with the presence of purine-rich binding motifs for the macrophage transcription factor, PU.1, which were shown previously to be functional (31). The unique regulated expression of *ARG2* in ruminant species and horses is also associated with large-scale promoter divergence to the extent that there is little alignment outside –1 kb even between cattle and sheep. There is a BOV-A2 insertion around –3 kb in sheep and goats that is not present in cattle. Multiple insertions of the BOV-A2 retrotransposon produce major differences between the human and pig *NOS2* promoter regions, which are not LPS inducible, and the ruminant *NOS2* promoters, which are. Our data suggest that the recent insertion of a proximal BOV-A2 element in the bovid lineage, shared by cattle, water buffalo, yak, and bison, could contribute to the elevated expression and greater inducibility of *NOS2* in these species. A more global comparative analysis of the RNA-seq datasets may reveal other examples of functional gain and loss of the BOV-A2 element that contribute to species-specific inducible gene expression in ruminant macrophages. The differences in arginine metabolism and production of NO could potentially underlie species-specific susceptibility to pathogens. For example, sheep are considered much more susceptible than cattle to the parasite *Toxoplasma gondii* (41) whereas NO is strongly implicated in both resistance to the parasite, and pathology, in mice based upon analysis of *Nos2* knockouts (42). In overview, our findings extend the evidence that rodents are not always appropriate

models for understanding host defense and pathology in other mammalian species including humans (7, 12).

DISCLOSURES

The authors have no financial conflicts of interest.

ACKNOWLEDGMENTS

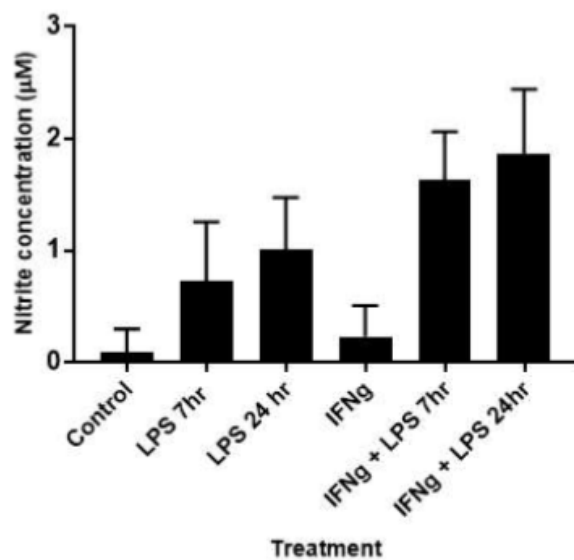
We are grateful for the help of the staff at both Dryden and Langhill Farms, the pathology staff at the Royal (Dick) School of Veterinary Studies, and the Biological Resource Facility at the Roslin Institute. Thanks go to Jenny Geddes and Lucy Freem for the chicken BM cells. Library preparation and sequencing was performed by Edinburgh Genomics, The University of Edinburgh.

REFERENCES

- Nathan, C. F., and J. B. Hibbs, Jr. 1991. Role of nitric oxide synthesis in macrophage antimicrobial activity. *Curr. Opin. Immunol.* 3: 65–70.
- Lyons, C. R., G. J. Orloff, and J. M. Cunningham. 1992. Molecular cloning and functional expression of an inducible nitric oxide synthase from a murine macrophage cell line. *J. Biol. Chem.* 267: 6370–6374.
- Xie, Q. W., H. J. Cho, J. Calaycay, R. A. Mumford, K. M. Swiderek, T. D. Lee, A. Ding, T. Troso, and C. Nathan. 1992. Cloning and characterization of inducible nitric oxide synthase from mouse macrophages. *Science* 256: 225–228.
- MacMicking, J. D., R. J. North, R. LaCourse, J. S. Mudgett, S. K. Shah, and C. F. Nathan. 1997. Identification of nitric oxide synthase as a protective locus against tuberculosis. *Proc. Natl. Acad. Sci. USA* 94: 5243–5248.
- Bogdan, C. 2015. Nitric oxide synthase in innate and adaptive immunity: an update. *Trends Immunol.* 36: 161–178.
- Mattila, J. T., O. O. Ojo, D. Kepka-Lenhart, S. Marino, J. H. Kim, S. Y. Eum, L. E. Via, C. E. Barry III, E. Klein, D. E. Kirschner, et al. 2013. Microenvironments in tuberculous granulomas are delineated by distinct populations of macrophage subsets and expression of nitric oxide synthase and arginase isoforms. *J. Immunol.* 191: 773–784.
- Schroder, K., K. M. Irvine, M. S. Taylor, N. J. Bokil, K. A. Le Cao, K. A. Masterman, L. I. Labzin, C. A. Semple, R. Kapetanovic, L. Fairbairn, et al. 2012. Conservation and divergence in Toll-like receptor 4-regulated gene expression in primary human versus mouse macrophages. *Proc. Natl. Acad. Sci. USA* 109: E944–E953.
- Gross, T. J., K. Kremens, L. S. Powers, B. Brink, T. Knutson, F. E. Domann, R. A. Philibert, M. M. Milhem, and M. M. Monick. 2014. Epigenetic silencing of the human *NOS2* gene: rethinking the role of nitric oxide in human macrophage inflammatory responses. *J. Immunol.* 192: 2326–2338.
- FANTOM consortium. 2014. Transcription and enhancer profiling in human monocyte subsets. *Blood* 123: e90–e99.
- FANTOM Consortium and the RIKEN PMI and CLST (DGT). 2014. A promoter-level mammalian expression atlas. *Nature* 507: 462–470.
- Vitek, M. P., C. Brown, Q. Xu, H. Dawson, N. Mitsuda, and C. A. Colton. 2006. Characterization of NO and cytokine production in immune-activated microglia and peritoneal macrophages derived from a mouse model expressing the human *NOS2* gene on a mouse *NOS2* knockout background. *Antioxid. Redox Signal.* 8: 893–901.
- Kapetanovic, R., L. Fairbairn, D. Beraldi, D. P. Sester, A. L. Archibald, C. K. Tuggle, and D. A. Hume. 2012. Pig bone marrow-derived macrophages resemble human macrophages in their response to bacterial lipopolysaccharide. *J. Immunol.* 188: 3382–3394.

<https://doi.org/10.4049/immunohorizons.1700073>

13. Saldarriaga, O. A., B. L. Travi, G. G. Choudhury, and P. C. Melby. 2012. Identification of hamster inducible nitric oxide synthase (iNOS) promoter sequences that influence basal and inducible iNOS expression. *J. Leukoc. Biol.* 92: 205–218.
14. Rajagopalan-Levasseur, P., D. Lecointe, G. Bertrand, M. Fay, and M. A. Gougerot-Pocidallo. 1996. Differential nitric oxide (NO) production by macrophages from mice and guinea pigs infected with virulent and avirulent *Legionella pneumophila* serogroup 1. *Clin. Exp. Immunol.* 104: 48–53.
15. Dörger, M., N. K. Jesch, G. Rieder, M. R. Hirvonen, K. Savolainen, F. Krombach, and K. Messmer. 1997. Species differences in NO formation by rat and hamster alveolar macrophages in vitro. *Am. J. Respir. Cell Mol. Biol.* 16: 413–420.
16. Jungi, T. W., H. Adler, B. Adler, M. Thöny, M. Krampe, and E. Peterhans. 1996. Inducible nitric oxide synthase of macrophages. Present knowledge and evidence for species-specific regulation. *Vet. Immunol. Immunopathol.* 54: 323–330.
17. Bilham, K., A. C. Boyd, S. G. Preston, C. D. Buesching, C. Newman, D. W. Macdonald, and A. L. Smith. 2017. Badger macrophages fail to produce nitric oxide, a key anti-mycobacterial effector molecule. *Sci. Rep.* 7: 45470.
18. Karagianni, A. E., R. Kapetanovic, B. C. McGorum, D. A. Hume, and S. R. Pirie. 2013. The equine alveolar macrophage: functional and phenotypic comparisons with peritoneal macrophages. *Vet. Immunol. Immunopathol.* 155: 219–228.
19. Kakuda, D. K., M. J. Sweet, C. L. MacLeod, D. A. Hume, and D. Markovich. 1999. CAT2-mediated L-arginine transport and nitric oxide production in activated macrophages. *Biochem. J.* 340: 549–553.
20. Thomas, A. C., and J. T. Mattila. 2014. “Of mice and men”: arginine metabolism in macrophages. *Front. Immunol.* 5: 479.
21. Martínez, F. O., L. Helming, R. Milde, A. Varin, B. N. Melgert, C. Draijer, B. Thomas, M. Fabbri, A. Crawshaw, L. P. Ho, et al. 2013. Genetic programs expressed in resting and IL-4 alternatively activated mouse and human macrophages: similarities and differences. *Blood* 121: e57–e69.
22. Schoedon, G., J. Troppmair, A. Fontana, C. Huber, H. C. Curtius, and A. Niederwieser. 1987. Biosynthesis and metabolism of pterins in peripheral blood mononuclear cells and leukemia lines of man and mouse. *Eur. J. Biochem.* 166: 303–310.
23. Werner, E. R., G. Werner-Felmayer, D. Fuchs, A. Hausen, G. Reibnegger, J. J. Yim, W. Pfeleiderer, and H. Wachter. 1990. Tetrahydrobiopterin biosynthetic activities in human macrophages, fibroblasts, THP-1, and T 24 cells. GTP-cyclohydrolase I is stimulated by interferon-gamma, and 6-pyruvoyl tetrahydropterin synthase and sepiapterin reductase are constitutively present. *J. Biol. Chem.* 265: 3189–3192.
24. Bush, S. J., M. E. B. McCulloch, K. M. Summers, D. A. Hume, and E. L. Clark. 2017. Integration of quantitated expression estimates from polyA-selected and rRNA-depleted RNA-seq libraries. *BMC Bioinformatics* 18: 301.
25. Clark, E. L., S. J. Bush, M. E. B. McCulloch, I. L. Farquhar, R. Young, L. Lefevre, C. Pridans, H. G. Tsang, C. Wu, C. Afrasiabi, et al. 2017. A high resolution atlas of gene expression in the domestic sheep (*Ovis aries*). *PLoS Genet.* 13: e1006997.
26. Bray, N. L., H. Pimentel, P. Melsted, and L. Pachter. 2016. Near-optimal probabilistic RNA-seq quantification. *Nat. Biotechnol.* 34: 525–527.
27. Grabherr, M. G., B. J. Haas, M. Yassour, J. Z. Levin, D. A. Thompson, I. Amit, X. Adiconis, L. Fan, R. Raychowdhury, Q. Zeng, et al. 2011. Full-length transcriptome assembly from RNA-Seq data without a reference genome. *Nat. Biotechnol.* 29: 644–652.
28. Wu, Z., T. Hu, L. Rothwell, L. Vervelde, P. Kaiser, K. Boulton, M. J. Nolan, F. M. Tomley, D. P. Blake, and D. A. Hume. 2016. Analysis of the function of IL-10 in chickens using specific neutralising antibodies and a sensitive capture ELISA. *Dev. Comp. Immunol.* 63: 206–212.
29. Schroder, K., M. J. Sweet, and D. A. Hume. 2006. Signal integration between IFN γ and TLR signalling pathways in macrophages. *Immunobiology* 211: 511–524.
30. Qualls, J. E., C. Subramanian, W. Rafi, A. M. Smith, L. Balouziyan, A. A. DeFreitas, K. A. Shirey, B. Reutterer, E. Kernbauer, S. Stockinger, et al. 2012. Sustained generation of nitric oxide and control of mycobacterial infection requires argininosuccinate synthase 1. *Cell Host Microbe* 12: 313–323.
31. Duch, D. S., S. W. Bowers, J. H. Woolf, and C. A. Nichol. 1984. Biopterin cofactor biosynthesis: GTP cyclohydrolase, neopterin and biopterin in tissues and body fluids of mammalian species. *Life Sci.* 35: 1895–1901.
32. Myers, M. J., D. E. Farrell, D. C. Palmer, and L. O. Post. 2003. Inflammatory mediator production in swine following endotoxin challenge with or without co-administration of dexamethasone. *Int. Immunopharmacol.* 3: 571–579.
33. Sans-Fons, M. G., A. Yeramian, S. Pereira-Lopes, L. F. Santamaria-Babi, M. Modolell, J. Lloberas, and A. Celada. 2013. Arginine transport is impaired in C57Bl/6 mouse macrophages as a result of a deletion in the promoter of Slc7a2 (CAT2), and susceptibility to *Leishmania* infection is reduced. *J. Infect. Dis.* 207: 1684–1693.
34. Zhang, X., V. E. Laubach, E. W. Alley, K. A. Edwards, P. A. Sherman, S. W. Russell, and W. J. Murphy. 1996. Transcriptional basis for hyporesponsiveness of the human inducible nitric oxide synthase gene to lipopolysaccharide/interferon-gamma. *J. Leukoc. Biol.* 59: 575–585.
35. Damiani, G., S. Florio, S. Panelli, E. Capelli, and M. Cuccia. 2008. The Bov-A2 retroelement played a crucial role in the evolution of ruminants. *Riv. Biol.* 101: 375–404.
36. Onami, J., M. Nikaïdo, H. Mannen, and N. Okada. 2007. Genomic expansion of the Bov-A2 retroposon relating to phylogeny and breed management. *Mamm. Genome* 18: 187–196.
37. Dekel, Y., Y. Machluf, S. Ben-Dor, O. Yifa, A. Stoler, I. Ben-Shlomo, and D. Bercovich. 2015. Dispersal of an ancient retroposon in the TP53 promoter of Bovidae: phylogeny, novel mechanisms, and potential implications for cow milk persistency. *BMC Genomics* 16: 53.
38. Aung, H. T., K. Schroder, S. R. Himes, K. Brion, W. van Zuylen, A. Trieu, H. Suzuki, Y. Hayashizaki, D. A. Hume, M. J. Sweet, and T. Ravasi. 2006. LPS regulates proinflammatory gene expression in macrophages by altering histone deacetylase expression. *FASEB J.* 20: 1315–1327.
39. Stacey, K. J., G. R. Young, F. Clark, D. P. Sester, T. L. Roberts, S. Naik, M. J. Sweet, and D. A. Hume. 2003. The molecular basis for the lack of immunostimulatory activity of vertebrate DNA. *J. Immunol.* 170: 3614–3620.
40. Rodriguez, P. C., A. C. Ochoa, and A. A. Al-Khami. 2017. Arginine metabolism in myeloid cells shapes innate and adaptive immunity. *Front. Immunol.* 8: 93.
41. Esteban-Redondo, I., S. W. Maley, K. Thomson, S. Nicoll, S. Wright, D. Buxton, and E. A. Innes. 1999. Detection of *T. gondii* in tissues of sheep and cattle following oral infection. *Vet. Parasitol.* 86: 155–171.
42. Khan, I. A., J. D. Schwartzman, T. Matsuura, and L. H. Kasper. 1997. A dichotomous role for nitric oxide during acute *Toxoplasma gondii* infection in mice. *Proc. Natl. Acad. Sci. USA* 94: 13955–13960.



Supplementary Figure 1. IFN γ does not significantly induce NO production in horse BMDM. Horse BMDM were stimulated with LPS at 0, 7, and 24 hr with or without IFN γ treatment. Nitrite concentration was measured by Griess assay. T-test was performed between LPS and LPS + IFN γ treatment at each timepoint, however differences were not statistically significant. Error bars represent the SD of the mean of triplicates.

```

Human SLC7A2  GA---AAATTAACAGGCTTTCACATTGTGACTT-AATCTTATCAGAGACTCCTAAAGTAAACAATAGCCGAGTAGGAGAA
Rat Slc7a2    TAGAAAAATAAA--GAGTTTCACATTGTGACTTTAATCTTATCAGAGACTCCTAAAGCAAGCAATAGCACAGAACGAGAA
Mouse Slc7a2  TA---AAATCAA--GAGTTTCACATTGTGACTTTAATCTTATCAGAGACTCTAAAGCAA---ATAGCACAGAAATGAAAA
Pig SLC7A2    TA---AAATTAACAGAGTTTCATATTGTGCTTTTAACTCTTATCAGAGACTCCTAAAGTAAACAATAGCCGAGTAGGAGAA
*   *   *   *   *   *   *   *   *   *   *   *   *   *   *   *   *   *   *   *   *   *   *   *

Human SLC7A2  ACCCTGATTGTGTAACCTTCTGCTCTTGCCTGCCCTGGAAATA----ATGTCATTTCTTA--TAAACCCACCCCAACAAT
Rat Slc7a2    AGCTCGATTGTGTAACCTTCTGTTTTGTCTGGCTAGGAAATACCAAGTATCCTTTTCTT-AAAAACCCACCTCCAAATAAC
Mouse Slc7a2  ACCTCGATTGTGTAACCTTCTGTTTTGTCTGGCTATGAAATACCAAGTATCCTGTTTCTTTAAAAACCCACTCCAAATAAC
Pig SLC7A2    AACTTGGTTGTGTAACCTCTTG-----GAAATAGCAAATGTGCTTCTT--ATAGCTCGCCTTAAGTCAT
*   *   *   *   *   *   *   *   *   *   *   *   *   *   *   *   *   *   *   *   *   *   *

Human SLC7A2  CGTGACTACGTATTCATACCACTGGAGTCTTCCAAAAATAGCAACTGCACATTA-----TTTATCAA
Rat Slc7a2    CGTGACTGCCCTGCCCTTATTCACAAGTCT----GAAGTCTCGAGTTTGTCTTCACTAT-----GATTTCAATAC
Mouse Slc7a2  CATGACTATG-ACCTGCCCTATTCACGAGTCT----GGAATCTTCAAGTTTGT-----ATTTCAATAC
Pig SLC7A2    CAGGTCACCTGTTCACTTCACTGGGACTTTCCAA-ATAGCAACTAAATATGCAATAAACGGTTTACAGGTTTATTTG
*   *   *   *   *   *   *   *   *   *   *   *   *   *   *   *   *   *   *   *   *   *   *

Human SLC7A2  CGTTTAGTTTGCAATTT-GACAAAGCACATCCACCTGGGCTTCCATTTATCATGCTATTTATATATTTATTTATTTT
Rat Slc7a2    AGAAGTGATACTTTT-GACAAAGCACATCTATCTAGGCTTCT-----AGTTTATTAATACATATACTACTATTTT
Mouse Slc7a2  AGAACGTGATACTTTTAAACAAAGCTCATCTATCTGGGCTTCT-----AGTTTATTAATACATATACTACTATTTT
Pig SLC7A2    TGAAG-TAATACTATTTGACAAAGCACTCCCATCTGGGTTCTTTTATCAGAGGTCGTTGTTATTTTACTATTTATTTT
*   *   *   *   *   *   *   *   *   *   *   *   *   *   *   *   *   *   *   *   *   *   *

Human SLC7A2  CTTATTTCCAAAATCT--TTGTAGAATGAAAGTAAACGGGGGAC-----CAAACCCCACTT
Rat Slc7a2    TATGTTCCCAATTTCTCAATGAGAGAGT-----GAGGGAAAGAGGGAGGGAGAGGAAAGAAAGAAATCCTGCTT
Mouse Slc7a2  TATGTTCCCAATTTCTCAATGAGAGAGGGAGAGAAAGAGGGAGGGAGGGAGAGGGAAAGAAAGAAATCCTGCTT
Pig SLC7A2    CTTATTTACAAAATCC--TCGCAGACTAAAACCTAAATCAAGTCAG-----GGACAAAATCCCACT
*   *   *   *   *   *   *   *   *   *   *   *   *   *   *   *   *   *   *   *   *   *   *

Human SLC7A2  A---GAACTCTGCTTAGAAGATTGCGAAATGCCCTTG-----AGGTTTGGTCTCCAGGAGAGCAGCAA
Rat Slc7a2    AGAAGAAACCT-CAGAAATGCCCTGCCCCACCCACACACACATTGAGATTGGTTCTGCCAAAGAGA----GC
Mouse Slc7a2  AGAAGAAACCT-CAGAAATGCCCTGCCCCACCCACCCCT-----AGATTGGTCTTCCAGGAAAGGGGGC
Pig SLC7A2    GAAGGAACTCTGCTTAGAAGCTCGGAGATGGCCCTG-----AGTTTGGGTCCT-CCATGGAAGGCAAGA
*   *   *   *   *   *   *   *   *   *   *   *   *   *   *   *   *   *   *   *   *   *   *

Human SLC7A2  GTTATCTCGCGCGCAG----CCTCTCTCCCGGCCCGCGCCACCG-----GCCTAGCCCGGGG
Rat Slc7a2    GTTTCCCTCTGCCAAG----CCCTCGCTCTCGGACCCACGCCACCC-----ACCTACCCACCAGC---GAG
Mouse Slc7a2  ATTTCCCTCTGCCAAA----CCCTCGCTCTCGGACCCACGCCACCC-----ACC-----CCAGC---GGG
Pig SLC7A2    ATTCACCTCTCGCTGGGTGTGCCCTCTCCCGCCGACCTGCCCCCACTGCTCTCCGGAGCCACCAGCCCGCCAGG
*   *   *   *   *   *   *   *   *   *   *   *   *   *   *   *   *   *   *   *   *   *   *

Human SLC7A2  CTAGCGCCCGC-CCACGTGTGCTCGGCTCCAGGCA--AACCCG-----CTGAGCAGCGGCCACACCCGCCACC
Rat Slc7a2    CAAGCTTGTA--CCACGTGTGCTACACCTGGCCCTGACCCTA-----CAGAGCGCGGAG-CTAGACACCCGCTTCC
Mouse Slc7a2  CAAGCGTGAATCCACGTGCGCGCGGCCCTGATCCTGACCTGACCTTTTCAGAAGCTTGAG-ITAGACACCCGCTTCC
Pig SLC7A2    CAAGCGCACGC-CCACGTGTGCCACGCTCGGGAGGGAGACTGAAC---TAGCGGCTTGCAGCCGGACCGCCGCTTACC
*   *   *   *   *   *   *   *   *   *   *   *   *   *   *   *   *   *   *   *   *   *   *

Human SLC7A2  CCGGGATTGGTCAGCGCGCCG--GGGCCCGCGGGAGGCGGGCTC-GGGGTGCGCTTCCGGGAGCGGAGGAGGCGG
Rat Slc7a2    T-GGAATCT---CAGCGTGCTG-----GAGGGAGCAGCGCTCCAGGAGGGGTTCGAGGCCGAGGAGGGGGCGG
Mouse Slc7a2  T-GGAGTCT---CTGCGCGCCCGCCCGGAGCCGTGACAAAACGCTCCAGGCGAGGGTTCGCGAGCAGGAGGGGGCGG
Pig SLC7A2    C-CAGGATTGGCCGCGCGGTGG-----GGCGGGAGGCGGGCTCGGGTGGGGGGTCTGAGAGCGCGGAGAGAGAA
*   *   *   *   *   *   *   *   *   *   *   *   *   *   *   *   *   *   *   *   *   *   *

Human SLC7A2  TGCCGCC-----GGCCCGC-GCCCGCC-----CCGCCCGG-GTGGCTACACAGAGGG----
Rat Slc7a2    AACGGCCCTGCCCTCGAGGCCCGCCCTCGGGCCCGCC--TFGCCCCGCCCTCCGCTTCTACTCAGAGGGTTGC
Mouse Slc7a2  GACGGCC-----CCGCCCTCGCTGCCCGCCCACTCCGCCCGCCCTCCGCTTCTACTCAGAGGG----
Pig SLC7A2    GGGGGCG-----GTTCCACCGGGCAGCCCGCC-----CCGGCGGGCTACACAGCT-----
*   *   *   *   *   *   *   *   *   *   *   *   *   *   *   *   *   *   *   *   *   *   *

Human SLC7A2  ---GCGCCACGTGCCAGCCC
Rat Slc7a2    CCACGTGCCACGTGCCAGCCC
Mouse Slc7a2  ---GTGCCACGTGCCAGCCC
Pig SLC7A2    ---GCGCCACGTGCCAGTCC
*   *   *   *   *   *   *   *   *   *   *   *   *   *   *   *   *   *   *   *   *   *   *

```

Supplementary Figure 2. Alignment of proximal promoters of *SLC7A2* in multiple species. Promoter sequences were downloaded from ENSEMBL. The last base corresponds to the peak of transcription initiation for the gene in mouse and human based upon the data from the FANTOM Consortium (Ref 10) on the Zenbu browser (<http://fantom.gsc.riken.jp/zenbu/>). Red highlight indicates the purine-rich element highlighted in Ref 31, which is not conserved in rat. However, note that both species have at least two candidate PU.1 sites containing the GGAA core (underlined).

9.3 Macrophage colony-stimulating factor (CSF1) controls monocyte production and maturation and the steady-state size of the liver in pigs

Am J Physiol Gastrointest Liver Physiol 311: G533–G547, 2016.
First published July 21, 2016; doi:10.1152/ajpgi.00116.2016.

Macrophage colony-stimulating factor (CSF1) controls monocyte production and maturation and the steady-state size of the liver in pigs

Kristin A. Sauter,^{1*} Lindsey A. Waddell,^{1*} Zofia M. Lisowski,¹ Rachel Young,¹ Lucas Lefevre,¹ Gemma M. Davis,¹ Sara M. Clohisey,¹ Mary McCulloch,¹ Elizabeth Magowan,² Neil A. Mabbott,¹ Kim M. Summers,¹ and David A. Hume¹

¹The Roslin Institute and Royal (Dick) School of Veterinary Studies, University of Edinburgh, Easter Bush, Scotland, United Kingdom; and ²Agri-Food and Biosciences Institute, Large Park, Hillsborough, Northern Ireland, United Kingdom

Submitted 21 March 2016; accepted in final form 17 July 2016

Sauter KA, Waddell LA, Lisowski ZM, Young R, Lefevre L, Davis GM, Clohisey SM, McCulloch M, Magowan E, Mabbott NA, Summers KM, Hume DA. Macrophage colony-stimulating factor (CSF1) controls monocyte production and maturation and the steady-state size of the liver in pigs. *Am J Physiol Gastrointest Liver Physiol* 311: G533–G547, 2016. First published July 21, 2016; doi:10.1152/ajpgi.00116.2016.—Macrophage colony-stimulating factor (CSF1) is an essential growth and differentiation factor for cells of the macrophage lineage. To explore the role of CSF1 in steady-state control of monocyte production and differentiation and tissue repair, we previously developed a bioactive protein with a longer half-life in circulation by fusing pig CSF1 with the Fc region of pig IgG1a. CSF1-Fc administration to pigs expanded progenitor pools in the marrow and selectively increased monocyte numbers and their expression of the maturation marker CD163. There was a rapid increase in the size of the liver, and extensive proliferation of hepatocytes associated with increased macrophage infiltration. Despite the large influx of macrophages, there was no evidence of liver injury and no increase in circulating liver enzymes. Microarray expression profiling of livers identified increased expression of macrophage markers, i.e., cytokines such as TNF, IL1, and IL6 known to influence hepatocyte proliferation, alongside cell cycle genes. The analysis also revealed selective enrichment of genes associated with portal, as opposed to centrilobular regions, as seen in hepatic regeneration. Combined with earlier data from the mouse, this study supports the existence of a CSF1-dependent feedback loop, linking macrophages of the liver with bone marrow and blood monocytes, to mediate homeostatic control of the size of the liver. The results also provide evidence of safety and efficacy for possible clinical applications of CSF1-Fc.

hepatosplenomegaly; CD163; macrophages; hepatostat; M-CSF

NEW & NOTEWORTHY

This study is based on extensive studies in the mouse of the role of CSF1 in monocyte-macrophage production and differentiation and the function of macrophages in the control of hepatocyte proliferation. We use a novel form of CSF1, an Fc fusion protein, to demonstrate that the findings in mice can be extended to large animals. We discuss the possible role for CSF1 in homeostatic control of the size of the liver.

MACROPHAGE COLONY-STIMULATING FACTOR (CSF1) is an essential growth and differentiation factor for cells of the macrophage lineage (23). Subsequent to the original isolation of human CSF1 cDNA in the 1980s and demonstration that injection of the recombinant CSF1 protein can expand macrophage popu-

lations in mice (24), there were a number of clinical trials of applications in cancer and other indications (23). The interest in CSF1 as a therapeutic agent has been reinvigorated by evidence of the requirement for macrophages in tissue regeneration in multiple organs (7) and the finding that macrophages generated in response to CSF1 have trophic roles (9, 43). CSF1 treatment has been shown to promote regeneration and repair in injury models in the kidney (1), brain (5, 37), and bone (6). The pleiotropic impacts of CSF1 mutations in mice (12) suggest that repair in most tissues is reliant on macrophages that depend on this growth factor.

Applications of CSF1 therapy were constrained by the very short half-life of the 150-amino acid active form of CSF1. We developed a bioactive protein with a longer half-life in the circulation. We fused pig CSF1, which is equally active in all mammalian species tested (20), with the Fc region of pig IgG1a (CSF1-Fc) (21). The expected increase in half-life was confirmed, and CSF1-Fc administration to mice produced substantial increases in circulating monocyte and tissue macrophage numbers, at much lower doses than the native protein. An unexpected effect of the treatment was a substantial increase in the size of the liver, associated with extensive hepatocyte proliferation (21). This observation was consistent with previous data implicating CSF1-dependent macrophages in hepatic regeneration. Acute liver failure in human patients, for example due to paracetamol toxicity, is associated with the loss of clearance functions that protect the body against the contents of the portal blood. Circulating CSF1 levels in human patients upon admission to hospital with paracetamol poisoning were found to be predictive of subsequent prognosis (46). Administration of CSF1-Fc in mouse models produced both accelerated regeneration of the liver and, perhaps more importantly, very rapid restoration of clearance functions (21, 44, 46).

Pigs have been used increasingly as models of human disease (17). The gene expression profiles of stimulated mouse and human macrophages differ greatly, and those of pig macrophages are much more human-like (29). Aside from the possible applications as human disease models, pigs are a major livestock species. Early weaning in pigs, when the mucosal barrier and innate immune systems are immature, is associated with susceptibility to a very wide range of mucosal and systemic bacterial and viral infections that produce significant losses (3). The results obtained in mice cannot necessarily be extrapolated to large animals, including humans, in which the profiles of macrophage activation by both CSF1 and microbial stimuli are very different (29). Our results confirm that, as in the mouse, CSF1-Fc can drive hepatocyte proliferation and modulate the size of the liver in a large animal model. The

* K. A. Sauter and L. A. Waddell contributed equally to this work.

Address for reprint requests and other correspondence: D. A. Hume, The Roslin Institute, Easter Bush EH25 9RG, Scotland, United Kingdom (e-mail: david.hume@roslin.ed.ac.uk).

data support applications of CSF1-Fc in liver regeneration and provide further evidence for the role of CSF1 in monocyte/macrophage maturation. In combination with earlier data, they reinforce the conclusion that circulating CSF1 is a central contributor to the homeostatic control of the size of the liver.

MATERIALS AND METHODS

Animals. Approval was obtained from Protocols and Ethics Committees of Roslin Institute or Agri-Food and Biosciences Institute (AFBI) for the trials. The experiments were carried out under the authority of a UK Home Office Project License, under the regulations of Animals (scientific procedures) Act 1986. CSF1-Fc was made as previously described (21) and provided by Zoetis.

Large White pigs ~8.5 wk of age from one litter were used. Four days prior to the first injection each pig was weighed and had blood collected into an EDTA tube. Pigs were injected subcutaneously once a day for a total of 3 days with the appropriate volume of CSF1-Fc (0.75 mg/kg; $n = 6$) or PBS vehicle ($n = 5$). PBS injection was used to control for the possible impact of stress and restraint associated with treatment. In experiments on weaners, Large White \times Landrace pigs ~4 wk of age from three litters were used. Six days prior to the first injection each pig was weighed and an estimated weight was extrapolated for each for the first injection day. Pigs were injected intramuscularly once a day for 2 days with the appropriate volume of CSF1-Fc (0.75 mg/kg; $n = 12$) or PBS ($n = 12$). On the second injection day the pigs were weaned. All pigs were sedated with ketamine and azaperone before being euthanized by captive bolt. Neither subcutaneous nor intramuscular injection produced any side effects.

Isolation of PBMC and BMC. Blood was collected into blood collection bags containing acid citrate dextrose (ACD) (Sarstedt) or into beakers containing ACD (Sigma). The buffy coat was layered onto Lymphoprep (Axis-Shield) and centrifuged for 25 min at 1,200 g with no brake. Peripheral blood mononuclear cells (PBMC) were retrieved and red cells were removed with cell lysis buffer (BioLegend). Pig bone marrow cells (BMC) were obtained by flushing the bone marrow from ribs with RPMI/5 mM EDTA followed by removal of red cells with cell lysis buffer. All isolated cells were suspended in PBS prior to counting and cryopreservation.

Flow cytometry analysis. Cells were washed, pelleted, resuspended in blocking buffer (PBS/2% heat inactivated FCS), transferred to a 96-well plate (V-bottom), and incubated on ice for 15–20 min. The plate was centrifuged for 4 min at 400 g followed by removal of supernatant. Cells were resuspended in 100 μ l of PBS containing the appropriate antibody or isotype control (Table 1). Samples were

incubated at 4°C in the dark for 30 min before being washed two times with 200 μ l PBS. Cells were resuspended in 600 μ l PBS with 0.1% SYTOX blue (Invitrogen) immediately prior to analysis using a BD Fortessa LSR flow cytometer (Becton Dickinson). Analysis was performed using FlowJo software (FlowJo).

Complete blood count analysis. An aliquot of blood from ACD blood collection bags was analyzed for complete blood cell counts. Total white blood cell (WBC) was measured on the Siemens Advia 2120 analyzer. WBC differential counts were performed by making a blood smear counterstained with Giemsa stain prior to cells of each cell type being counted. The absolute value for each WBC type was determined by using the total WBC and % leukocytes. Manual platelets counts were carried out using a hemocytometer slide (by the R(D)SVS Clinical Pathology Laboratory, University of Edinburgh).

Plasma analysis. Plasma was analyzed by R(D)SVS Clinical Pathology Laboratory for cortisol (performed on Siemens Immulite analyzer) as well as a large animal liver damage profile (performed on the IL650 analyzer from Instrumentation Laboratories).

Tissue processing. Tissues were dissected, weighed (liver, spleen, and kidney), and placed in 10% neutral buffered formalin or RNAlater (Ambion). For histology, tissues were processed overnight using an Excelsior tissue processor (Thermo Fisher Scientific). Sections were embedded in paraffin wax prior to 4- μ m sections cut and mounted onto slides (Superfrost Plus, Thermo Fisher Scientific). Slides were dried overnight at 37°C before 60°C for 25 min. Sections were stained with H&E or immunohistochemistry was performed by R(D)SVS pathology department.

Immunohistochemistry for CD163. Antigen retrieval was performed with proteinase K (Dako S302030) for 10 min. Nonspecific protein binding was blocked using 2.5% goat serum (Vector Laboratories) for 20 min. Endogenous peroxidase activity was blocked using Dako REAL peroxidase blocker (Dako S202386) for 10 min. Sections were incubated for 60 min using mouse anti-pig CD163 (Serotec MCA2311GA) diluted 1/30. Visualization using secondary reagent Dako Envision mouse HRP (Dako K4007) for 40 min followed by DAB (Newmarket Scientific Monosan Dab substrate kit cat. no. MON-APP177) for 10 min and DAB enhancer for 3 min (Newmarket Scientific DAB concentrate cat. no. CO7-25) was performed by the R(D)SVS pathology department. The staining was analyzed using Image J (Fiji).

Immunohistochemistry for Ki67 and PCNA. Antigen retrieval was performed by boiling in 10 mM sodium citrate buffer. Nonspecific protein binding was blocked using 2.5% goat serum (Vector Laboratories) for 20 min. Endogenous peroxidase activity was blocked using Dako REAL peroxidase blocker (Dako S202386) for 10 min. Sections were incubated for 60 min using rabbit anti-human Ki67 (AbCam AB15580) diluted 1/10,000. Visualization was performed with secondary reagent ImmPRESS HRP anti-rabbit IgG (Peroxidase Polymer; VectorMP-7401) for 30 min followed by DAB (Newmarket Scientific Monosan Dab substrate kit cat. no. MON-APP177) for 10 min and DAB enhancer for 3 min (Newmarket Scientific DAB concentrate cat. no. CO7-25).

Statistical analysis. Data were analyzed by *t*-tests. Results are presented as treatment group means \pm SE. All analyses were performed using GraphPad Prism 5.0 (GraphPad Software). A *P* value < 0.05 was considered statistically significant.

Microarray. Total RNA was prepared from liver samples using TRIzol, prepared for hybridization using the Ambion WT Expression Kit (Life Technologies), following the manufacturer's instructions, except for the input amount of RNA (500 ng input instead of 100 ng) and hybridized in a random order to the Affymetrix Porcine Gene 1.1 ST array (performed by Edinburgh Genomics, University of Edinburgh). Statistical analysis of the array data utilized Partek Genomic Suite (Partek). For network analysis, the normalized array data were uploaded to the software Biayout *Express*^{3D} (<http://www.biayout.org/>) as described previously (18, 30). The data from the microarray are available at Gene Expression Omnibus NCBI (<http://www.ncbi.nlm.nih.gov/geo/>) accession code GSE78837.

Table 1. Antibodies used in flow cytometry

Antigen	Conjugate	Isotype	Supplier	Dilution	Isotype Control
CD16	RPE	IgG1	AbD Serotec, MCA1971PE	1:200	AbD Serotec, MCA928PE
CD14	FITC	IgG2b	AbD Serotec, MCA1218F	1:50	AbD Serotec, MCA691F
CD163	RPE	IgG1	AbD Serotec, MCA2311PE	1:100	AbD Serotec, MCA928PE
CD172a	RPE	IgG1	Southern Biotech, 4525-09	1:400	AbD Serotec, MCA928PE
CD169	FITC	IgG1	AbD Serotec, MCA2316F	1:100	AbD Serotec, MCA928F
CD117	AF488	IgG1	AbD Serotec, MCA2598A48	1:10	Biologend, 400109
CD3	FITC	IgG1	AbD Serotec, MCA5951F	1:100	AbD Serotec, MCA928F
Antigen	Conjugate	Isotype	Supplier	Concentration	Secondary Antibody
CSF1R	Purified	IgG2a	Produced in-house	5 μ g/ml	Biologend, 405308, 1:400 dilution

Summary information for all monoclonal antibodies used for flow cytometry staining, including dilution, manufacturer, and relevant isotype control.

RESULTS

CSF1-Fc expands macrophage populations in blood and organs. We first examined 8-wk-old pigs of both sexes from the same litter, with control and treated groups weight matched in pairs. Based on mouse data (21) we used a dose of 0.75 mg/kg for three daily treatments followed by cull 24 h after final injection. In previous studies, we have compared CSF1-Fc with the native, non-Fc conjugate, form of CSF1 as a control protein. Native CSF1 has a much shorter half-life and at the same dose had no effect on monocyte-macrophage numbers (21). We have not compared CSF1-Fc directly with an irrelevant fusion protein, or with an isotype control for the Fc component. However, an equivalent dose of IgG1 (10–20 mg depending on the size of the pig) would have no impact on the plasma IgG concentration (15–30 mg/ml). CSF1-Fc treatment of macrophages *in vitro* did not induce proinflammatory cytokines (21) and, in keeping with the lack of intrinsic proinflammatory activity, there was no evidence of any reaction at the sites of injection in any treated animals. The most obvious effect of CSF1-Fc administration was hepatosplenomegaly. CSF1-Fc doubled the spleen/body weight ratio and increased the liver/body weight ratio by 40% after only 4 days (Fig. 1A). The total WBC count was significantly increased, mainly due to lymphocytosis in addition to the expected monocytosis (Fig. 1B).

CSF1-Fc accelerates the maturation of macrophage populations in peripheral blood monocytes. CSF1 has been implicated in the maturation of blood monocytes in both mice and humans, driving the formation of the nonclassical (CD14^{low}, CD16^{high}) subset in humans (Ly6C^{low} in mice) (31, 33). Pig blood monocytes can also be separated into subsets based on expression of surface markers, although the distinctions are not as clear as in other species (16). Expression of various markers by peripheral blood monocytes was assessed by flow cytometry staining (Fig. 2). In addition to the increase in total WBC seen in Fig. 1, the proportion of monocytes, detected by CD172a (SIRPA) was increased around twofold (Fig. 2B). The proportion of cells expressing CD16 was also increased (Fig. 2A). No increase was seen in the percentage of CD3⁺ lymphocytes (Fig. 2C) The best-characterized monocyte maturation marker in pigs is the haptoglobin receptor, CD163 (16), which has also been implicated as a receptor for the major pig viral pathogen, porcine reproductive and respiratory syndrome (PRRSV) (14), and which varies inversely with CD14 expression. Double staining with the two markers indicated that CSF1-Fc shifted the profiles of both markers, favoring expansion of the CD163⁺ cells (Fig. 2D). The results are consistent with an impact of CSF1-Fc to promote both monocyte production/release and maturation.

Impact of CSF1-Fc treatment on the bone marrow. We next investigated whether the ability of CSF1-Fc to promote monocytosis was associated with expansion of progenitor pools in the marrow (Fig. 3). Figure 3, A and B, demonstrates a substantial increase in large CD14⁺ monocytes, and even greater increase in CD163⁺ cells in the marrow of treated animals, consistent with the pattern seen in blood. Aside from monocyte progenitors, a key population of macrophages in bone marrow forms the center of hemopoietic islands. In mice, these cells express sialoadhesin (CD169, which provides a receptor for immature erythrocytes) and are critical for suc-

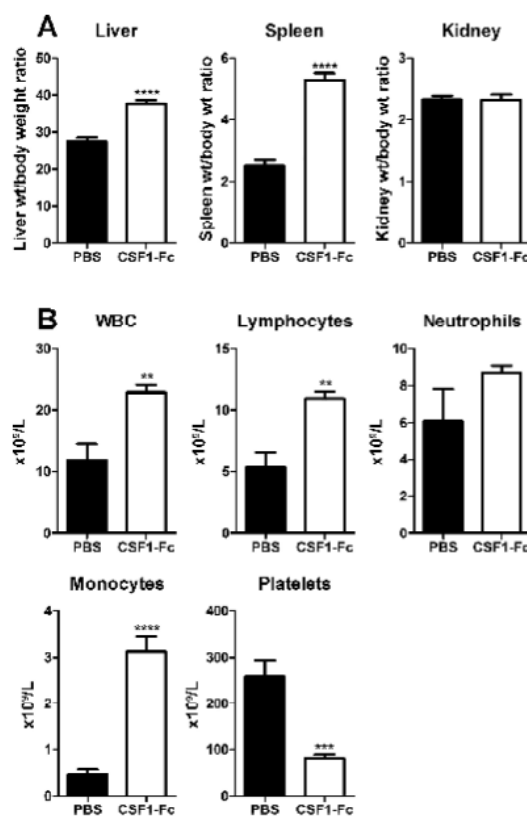


Fig. 1. Effect of CSF1-Fc on organ weights and white blood cell (WBC) counts. Pigs (8-wk-old males and females) were injected with PBS or 0.75 mg/kg CSF1-Fc for 3 days prior to euthanasia on day 4. Blood was collected into EDTA tubes postmortem and complete blood count assessment was performed. Graphs show means \pm SE. ** P < 0.01, *** P < 0.001, **** P < 0.0001 by *t*-test; n = 5–6 pigs per treatment. A: liver weight/body weight ratio, spleen weight/body weight ratio, and kidney weight/body weight ratio. B: total WBC count, lymphocyte number, neutrophil number, monocyte number, and platelet number.

cessful engraftment in bone marrow transplantation (10). As shown in Fig. 3C, the CSF1-Fc treatment produced a substantial increase in the CD169⁺ population in pigs. The CSF1-Fc treatment did not expand the small percentage of cells that express CD117 (KIT), a marker of the stem cell population (Fig. 3D), suggesting that CSF1-Fc acts primarily to promote proliferation/expansion of committed progenitors. In bone marrow of pig, neither CD172a nor CD16 provides a useful marker of monocyte lineage cells, being detected on the large majority of the cells (Fig. 4, A and B) and only marginally increased by CSF1-Fc. We also examined the expression of the CSF1R (CD115) using either a recently described monoclonal antibody (39) or labeled CSF1-Fc. There was some evidence of expansion of the positive cell populations in each case, but the levels of labeling were very low (Fig. 4, C and D). We suggest that the receptor may be downregulated by CSF1-Fc.

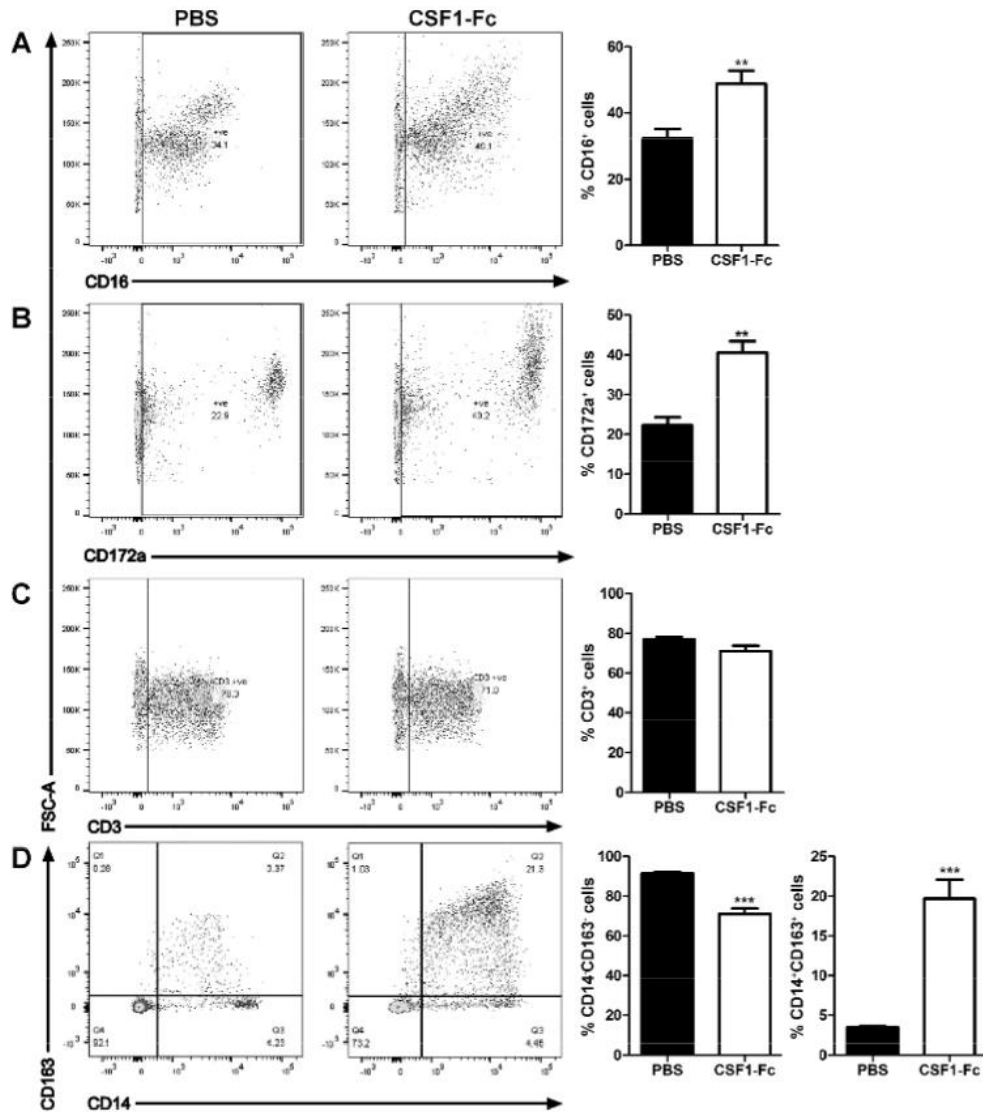


Fig. 2. Effect of CSF1-Fc on PBMCs. Pigs (8-wk-old males and females) were injected with PBS or 0.75 mg/kg CSF1-Fc for 3 days prior to euthanasia on *day 4*. Blood was collected as described in MATERIALS AND METHODS. PBMCs were analyzed via flow cytometry for expression of CD16 (A), CD172a (B), CD3 gated on the lymphocyte population exclusively (C), or CD163/CD14 (D) with exclusion of dead cells using SYTOX blue. Representative flow cytometry plots are shown. Graphs show means \pm SE. ** $P < 0.01$, *** $P < 0.001$ by *t*-test; $n = 4-5$ pigs per treatment.

Origin of the increase in liver and spleen weight. CSF1-Fc treatment caused a substantial increase in macrophage numbers in both organs, detectable by immunolocalization of CD163. In immunostained sections of liver CSF1-Fc treatment increased CD163⁺ area (quantified with ImageJ) from an average of less than 0.5% to an average of over 9% (Fig. 5A). In spleen CSF1-Fc treatment had an even greater effect, causing an

increase of CD163⁺ area from an average from $\sim 1\%$ to 16% (Fig. 5B). As in mice (21), in the spleen the majority of the increase in size could be attributed to increased red pulp macrophages and also to expansion of the marginal zones.

By contrast, the increase in the area apparently occupied by macrophages is not sufficient to explain the substantial increase in the size of the liver. Sections of liver were stained for the

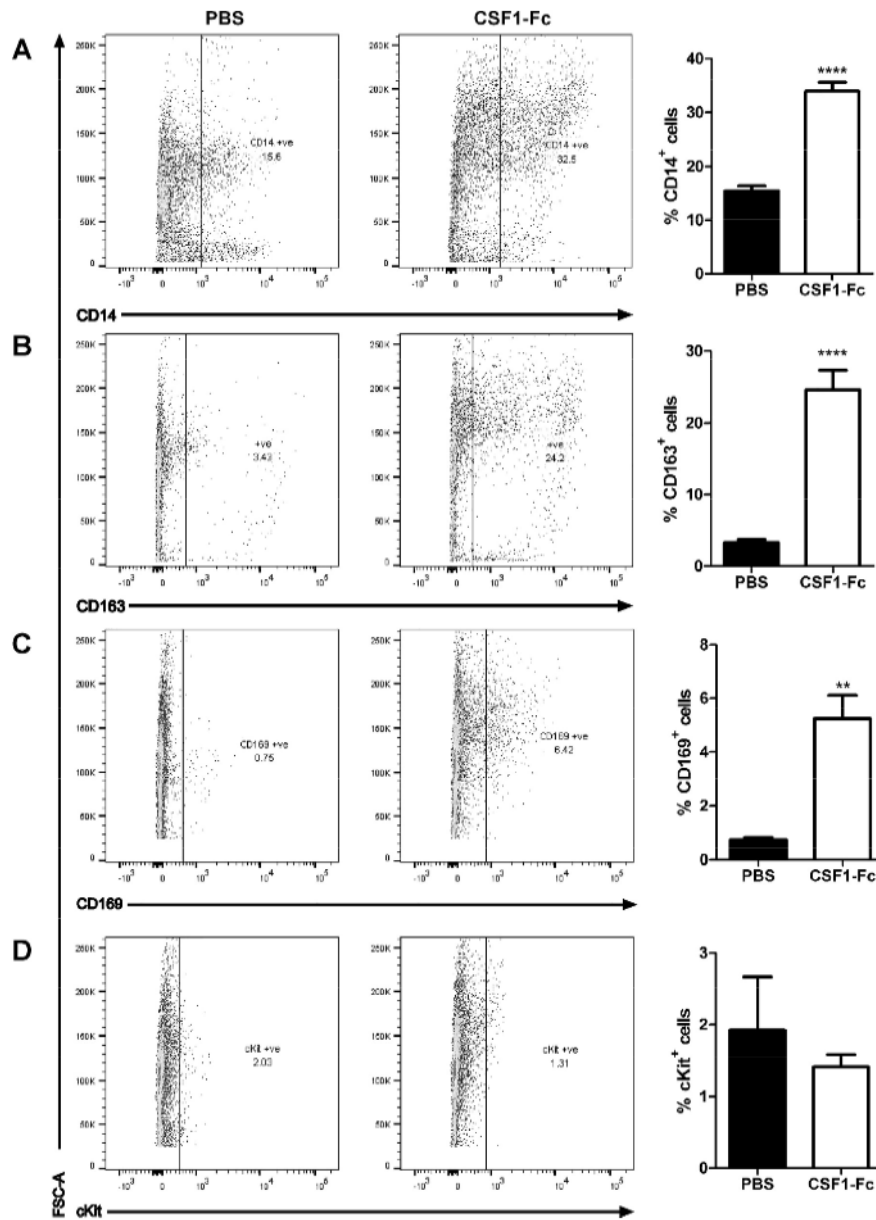


Fig. 3. Effect of CSF1-Fc on bone marrow (BM) cells. Pigs (8-wk-old males and females) were injected with PBS or 0.75 mg/kg CSF1-Fc for 3 days prior to euthanasia on day 4. BM from ribs was collected as described in MATERIALS AND METHODS. BM cells were analyzed via flow cytometry for expression of CD14 (A), CD163 (B), CD169 (C), or cKit (D) with exclusion of dead cells using SYTOX blue. Representative flow cytometry plots are shown. Graphs show means \pm SE. ** $p < 0.01$, **** $p < 0.0001$ by t -test; $n = 4$ –5 pigs per treatment.

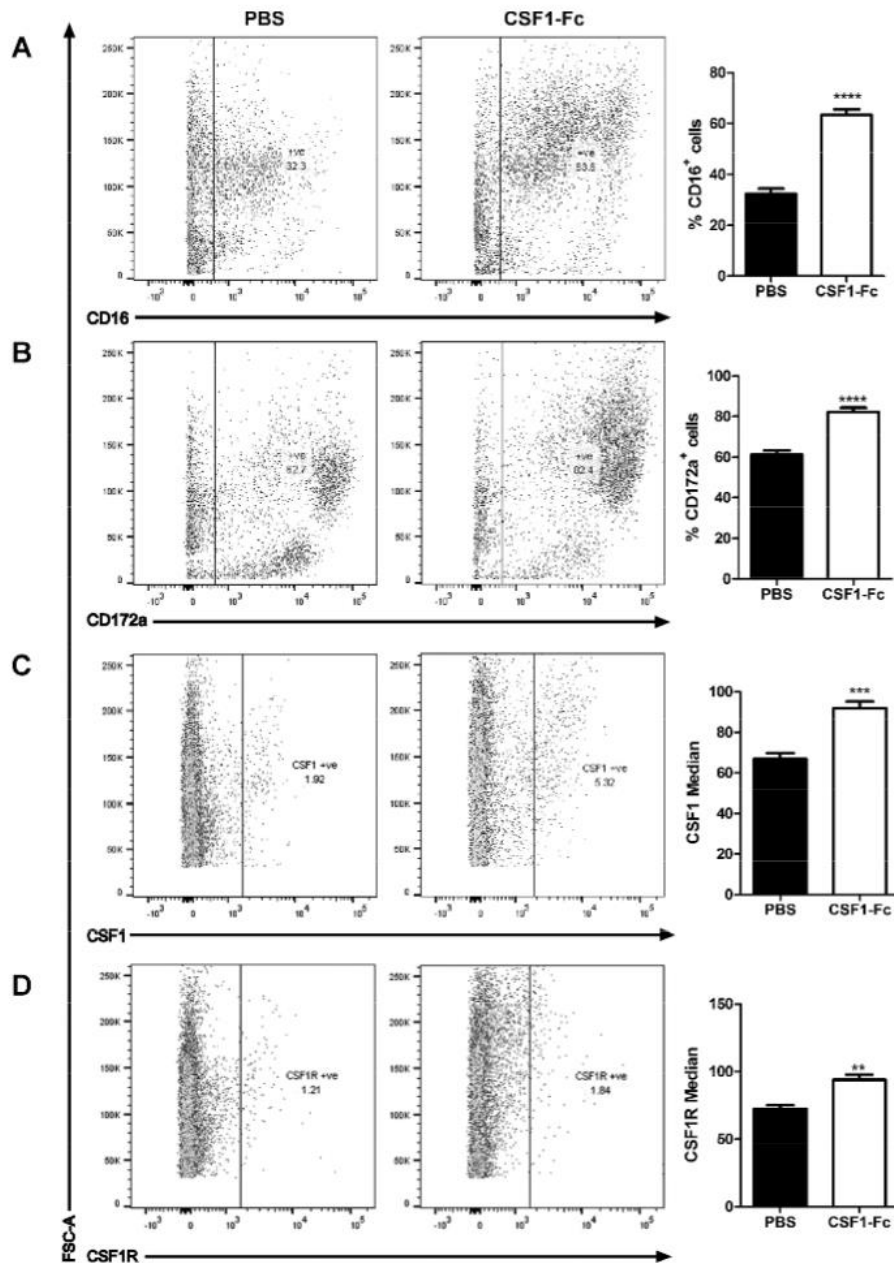


Fig. 4. Further effect of CSF1-Fc on BM cells. Pigs (8-wk-old males and females) were injected with PBS or 0.75 mg/kg CSF1-Fc for 3 days prior to euthanasia on *day 4*. BM from ribs was collected as described in MATERIALS AND METHODS. BM cells were analyzed via flow cytometry for expression of CD16 (A), CD172a (B), CSF1 (C), or CSF1R (D) with exclusion of dead cells using SYTOX blue. Representative flow cytometry plots are shown. Graphs show the mean percentage positive cells \pm SE, or the median fluorescent intensity. ** $P < 0.01$, *** $P < 0.001$, **** $P < 0.0001$ by *t*-test; $n = 4$ –5 pigs per treatment.

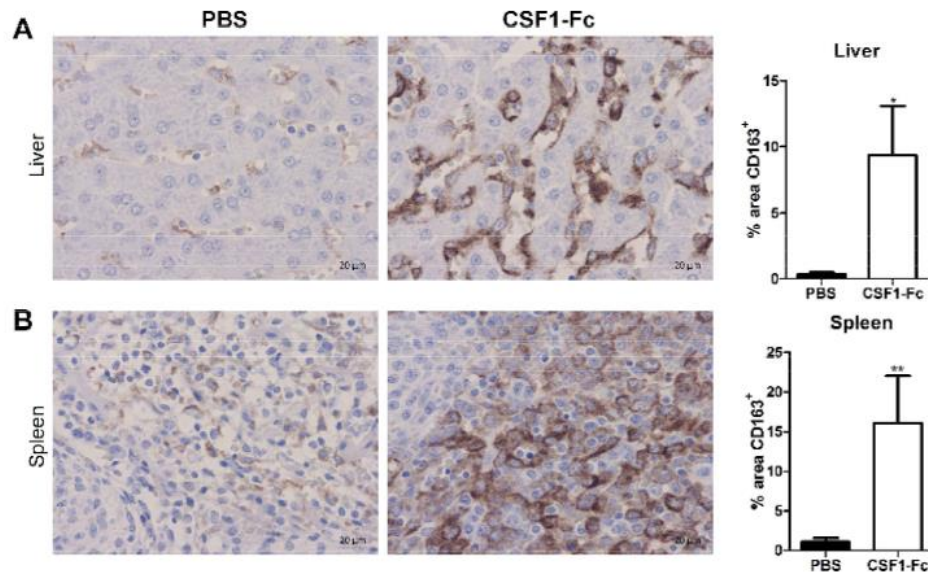


Fig. 5. Effect of CSF1-Fc on tissue macrophages. Pigs (8-wk-old males and females) were injected with PBS or 0.75 mg/kg CSF1-Fc for 3 days prior to euthanasia on day 4. Formalin fixed liver (A) and spleen (B) tissue was prepared and stained for CD163. Representative images are shown. Scale bar = 20 μ M. Using ImageJ software the total CD163⁺ area was calculated from 2 representative images per pig per organ. Graphs show means \pm SE. * P < 0.05, ** P < 0.01 by t -test; n = 4–5 pigs per treatment.

proliferative cell marker Ki67. Figure 6 shows images of the liver from two control and two CSF1-Fc-treated pigs. The pigs are relatively young, and still growing, and accordingly there is significant ongoing proliferation evident from Ki67 staining. The vast majority of Ki67⁺ nuclei in both control and CSF1-Fc-treated pig livers were large and round, consistent with identity as hepatocytes. Macrophage nuclei are more difficult to visualize in histological sections, because the cells and nuclei are much smaller and ramified in the sinusoids. Very occasional smaller Ki67⁺ nuclei visible in the sinusoids suggested that some infiltrating monocyte-macrophages were also proliferative, as shown directly in the mouse system (46). The images in Fig. 6 also show an obvious increase in cellularity in response to CSF1-Fc. We counted the total nuclei and the proportion stained with anti-Ki67 in representative large fields from each animal. As shown in Fig. 6, CSF1-Fc treatment almost doubled the total number of nuclei in each field and produced a threefold increase in the percentage of those nuclei stained with anti-Ki67. Essentially the same findings were made with staining for proliferating cell nuclear antigen (PCNA) (not shown). The sections in Fig. 6 show no evidence of pathology in the liver; notably, there are no pyknotic nuclei and granulocytes are absent. Granulocyte infiltration is the hallmark of tissue injury, including injury to the liver (27).

Changes in the liver might occur secondary to alterations in the gut. CSF1 has been attributed indirect functions in control of proliferation and differentiation of gastrointestinal epithelium (26, 45). Treatment with CSF1-Fc in pigs produced a small but significant increase in the mean villus length of the mid jejunum but had no detectable effect in the ileum, cecal

base, or ascending colon (Fig. 7). There was also no significant change in goblet cell number.

Effect of CSF1-Fc on liver function. A panel of biochemical tests to measure serum enzymes, bile acid, bilirubin, and protein concentrations was performed to assess hepatic function. The only change was a small increase in bile acids and bilirubin in serum from CSF1-Fc-treated pigs (Fig. 8), only marginally outside the normal range (50). Since standard enzymic indicators of liver injury (alkaline phosphatase, alanine aminotransferase, γ -glutamyl transpeptidase) were unchanged, the increase in bile acids probably reflects the increased size of the liver. To examine the impact of CSF1-Fc on liver function in more detail, we profiled the transcriptome. The expression results were filtered to remove genes detected below an arbitrary relative intensity threshold and also genes that did not differ by more than 1.5-fold between the highest and lowest value in the nine samples. The second criterion removed around 30% of probes on the microarray, including many hepatocyte-specific gene products. Figure 9C shows that the relative abundance of representative examples of these known hepatocyte gene products, albumin (*ALB*), *CD14*, *FETUIN*, and transferrin (*TF*), within the total liver RNA pool was unchanged in response to CSF1-Fc. In other words, the infiltration of the liver by macrophages was insufficient to dilute the contribution of hepatocyte mRNA to the total mRNA pool. That finding is consistent with the histological observation above, that even in the CSF1-Fc-stimulated state the infiltrating macrophages appear to make up no more than 10% of the total area of the liver. Hence, the 40% increase in total liver weight can be attributed primarily to an increase in

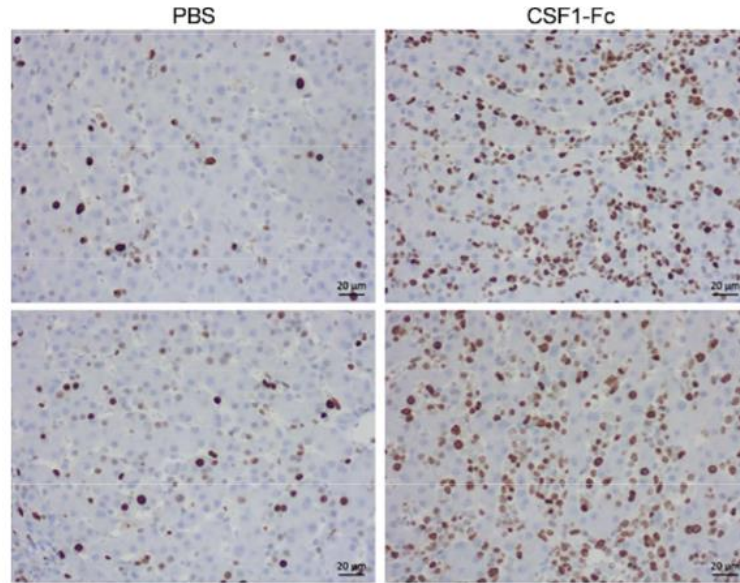
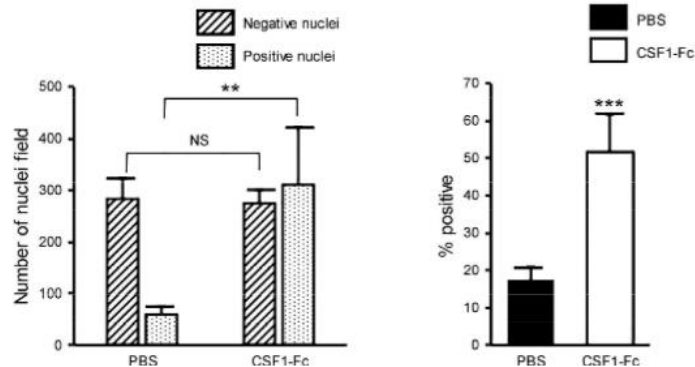


Fig. 6. Effect of CSF1-Fc on liver proliferation. Pigs (8-wk-old males and females) were injected with PBS or 0.75 mg/kg CSF1-Fc for 3 days prior to euthanasia on day 4. Formalin fixed liver tissue was prepared and stained for Ki67 as described in MATERIALS AND METHODS. Top: representative fields from 2 separate control (PBS, left) or CSF1-Fc-treated (right) pigs. Individual Ki67⁺ and Ki67⁻ nuclei in representative fields from each animal were counted as shown at bottom. ** $P < 0.01$, *** $P < 0.001$; NS, not significant.



hepatocytes, consistent with the extensive proliferation and increased cellularity shown in Fig. 6.

We clustered the included probe sets based on expression pattern and displayed them using Bioclayout *Express*^{3D}. The advantage of using the clustering approach is that genes that might appear regulated, but in only a subset of animals, appeared in separate smaller clusters. These may reflect the interanimal variation in macrophage-inducible gene expression that we documented previously in a study of pig breeds (30). The gene lists of specific clusters are provided in Supplemental Table S1. (Supplemental Material for this article is available online at the Journal website.) Functional annotations of the two large clusters were tested using DAVID (Supplemental Table S2). *Cluster 1*, the set of genes elevated in all CSF1-Fc-treated pigs, was clearly enriched for genes involved in the cell cycle and innate immunity, whereas *cluster 2*, the set that was

reduced in the CSF1-Fc-treated pigs, was enriched in genes involved in metabolism. Importantly, there is no evidence among the induced genes of expression of apoptosis-associated genes, no induction of acute phase genes, and no appearance of classical granulocyte marker genes such as S100A8/S100A9 or MPO. Figure 9 shows the expression profiles of a number of genes that highlight the biological processes involved. *Cluster 1* (Fig. 9A) includes many genes that were shown previously (18) to be restricted to macrophages, such as the transcription factor *SPI1*; surface markers *SIRPA*, *EMR1*, and *ITGAM*; known CSF1-inducible genes *PLAU*, *MMP9*, *CHI3L1*, and *CIQ*; endocytic receptors *MARCO*, *MSR1*, and *FCGR1A*; and pattern recognition receptors *TLR1*, 2, 4, 6, 7, 8, and 9. On average, the relative contribution of *cluster 1*, macrophage-specific genes, to the liver total RNA increased by three- to fivefold in response to CSF1-Fc, again consistent with the

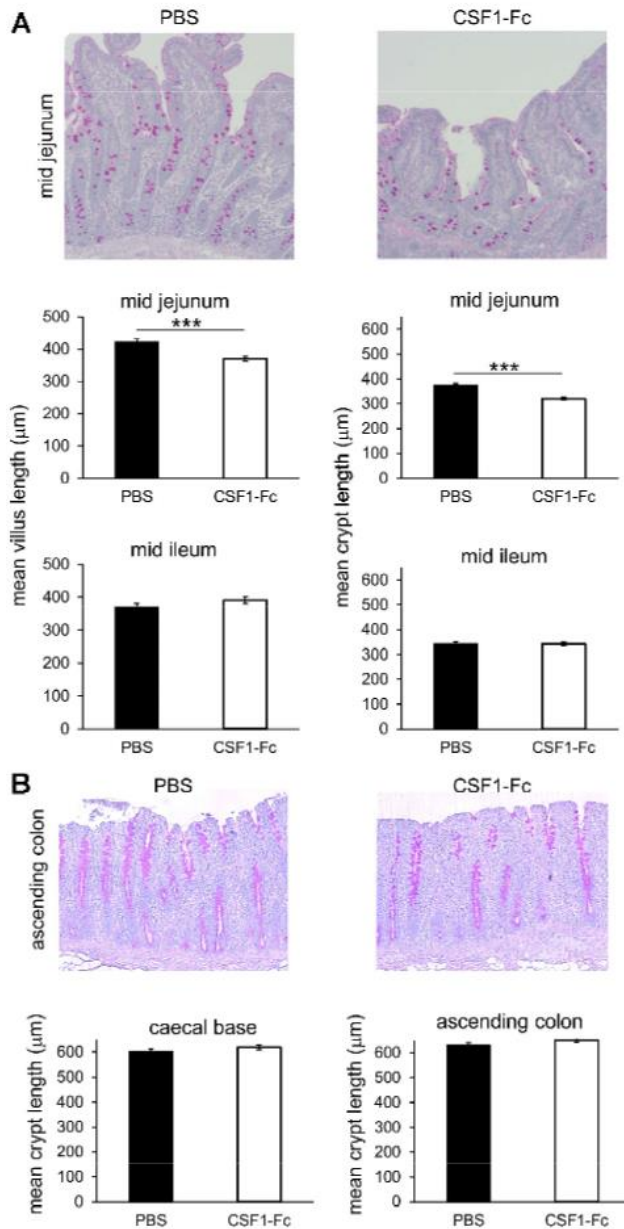


Fig. 7. Effect of CSF1-Fc on the gut. Pigs (8-wk-old males and females) were injected with PBS or 0.75 mg/kg CSF1-Fc for 3 days prior to euthanasia on *day 4*. Formalin fixed sections of gut tissue were prepared and stained for periodic acid-Schiff to show the goblet cells. Representative images are shown. Graphs show means \pm SE. *** $P < 0.001$ by *t*-test; $n = 4$ –5 pigs per treatment. *A*: small intestine: mid jejunum and mid ileum. Mean villus length (μm) was measured from 112–120 villi per tissue per group. Mean crypt length (μm) was measured from 100 crypts per tissue per group. *B*: large intestine: ascending colon and caecal base. Mean crypt length (μm) was measured from 50–80 crypts per tissue per group.

histological evidence of increased macrophage content shown in Fig. 5. In mice, the recruited monocytes express the chemokine receptor CCR2 and apparently respond to CCL2 (49). By contrast, *CCR1* was enriched in the liver mRNA of treated pigs, alongside three of its known ligands, *CCL8*, *CCL14*, and

CCL3L1. As previously observed in mice (46), monocytes recruited to the treated livers apparently responded to proinflammatory signals, since *cluster 1* contained numerous known LPS-inducible genes (29) such as inflammatory cytokines *TNF*, *IL1A*, and *IL1B*; interferon targets *IDO1*; multiple type 1

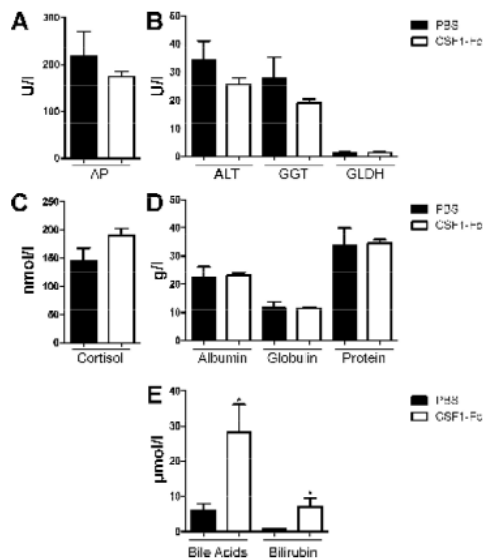


Fig. 8. Effect of CSF1-Fc on circulating markers of liver damage. Pigs (8-wk-old males and females) were injected with PBS or 0.75 mg/kg CSF1-Fc for 3 days prior to euthanasia on day 4. Plasma was produced from whole blood collected in an ACD blood collection bag. Graphs show means \pm SE. * $P < 0.05$ by *t*-test; $n = 5$ –6 pigs per treatment. A: alkaline phosphatase (AP). B: alanine aminotransferase (ALT), γ -glutamyl transpeptidase (GGT), and glutamate dehydrogenase (GLDH). C: cortisol. D: albumin, globulin, and total protein. E: bile acids, and bilirubin.

interferon targets *IRF1*, *IRF5*, *IFITM2*, and *IFIT3*; TGFB1; and costimulators of T cell activation *CD40*, *CD80*, and *CD86*. Cluster 1 also contains numerous cell cycle-associated genes, including *PCNA*; the key transcription factors *FOXM1*, *E2F4*, *E2F7*, and *E2F8*; and several cyclin genes *CCNA2*, *CCNA3*, *CCNB2*, *CCNB3*, *CCND2*, and *CCND3*. The increased expression of enzymes of glycolysis *HK1*, *HK2*, *HK3*, *PFKP*, *PGK1*, *PGD*, *PKM*, *GPI*, *GAPDH*, and *LDHA* also reflects the requirement for aerobic glycolysis in proliferating cells (25).

Cluster 2 (Fig. 9B), the set of genes reduced in the CSF1-Fc-treated pigs, most likely reflects the functional zonation of the liver between periportal and perivenous regions of liver lobules (8, 19, 48) and the selective proliferation of cells derived from portal progenitors that has been observed in regenerating liver (15, 34, 36). It includes genes involved in xenobiotic metabolism and detoxification, notably P450 family (e.g., *CYP1A1*, *CYP2E1*), glutathione *S*-transferases (e.g., *GSTAA2*) and aldo-ketoreductases (e.g., *AKR1C1*), and the gluconeogenic enzyme *PCK2*, that are known to be enriched in perivenous locations. The cluster contains the gene for the regulator of hepatocyte stem cells, *SOX9* (2), indicating that these cells are not expanded in the CSF1-Fc-treated livers. Unexpected members of this cluster are genes for the growth hormone receptor (*GHR*) and the target, *IGF1*, and both estrogen (ESR1) and androgen (AR) receptors. Also unexpected is the inclusion of the receptor for hepatocyte growth factor, *MET*, which is implicated in regeneration (36), but this might reflect autoregulation in response to its ligand (52).

CSF1-Fc treatment in weaning pigs. Although models of acute liver failure in pigs have been described (32, 41), and may be one path to clinical development of CSF1-Fc as a treatment, it is challenging to perform sufficient replicates to test a clinical intervention. We therefore considered an alternative in production pigs. Commercial pigs are normally weaned at 4 wk, when the gut is immature. Diarrhea and disseminated infections with organisms such as *Escherichia coli* and *Streptococcus suis* are relatively common (38). In this respect, the pig has been studied as a model of early-life stress (42). The biology of early weaning in pigs may also be relevant to intestinal failure-associated liver disease in neonates and children (40).

Weaner pigs were treated with a higher dose of 1.0 mg/kg CSF1-Fc for two daily injections, immediately prior to weaning and on the day of weaning followed by euthanasia 24 h following the final injection. At this early time point, there was already a significant increase in the spleen/body weight ratio and a trend toward increased liver/body weight ratio (Fig. 10A). The number of CD163⁺ cells was more than tripled in the bone marrow, from ~10% to over 30% (Fig. 10B), and increased numbers of CD163⁺ macrophages were confirmed by immunostaining in liver and spleen (Fig. 10C). At this time point, there was not a significant monocytosis, indicating that both marrow expansion and tissue macrophage proliferation precede monocyte expansion and are likely direct effects of CSF1-Fc.

We repeated the treatment in a larger cohort of weaned pigs. This study was conducted in a high health status research unit, which reflected commercial practice. We explicitly removed zinc from the feed, which is usually added to reduce weaning-associated infections. Given the production of inflammatory cytokines and reduction in IGF-1 in the liver of treated pigs, we measured weight gain daily in all animals. CSF1-Fc (0.75 mg/kg) was administered to pigs for two daily intramuscular injections on the day before and the day of weaning, and pigs were killed 5 days after the second injection. Although some pigs showed evidence of mild postweaning diarrhea, all the animals in both groups continued to gain weight rapidly (Fig. 11A). The treated pigs, like the treated mice left for longer after the final injection, demonstrated hepatosplenomegaly (Fig. 11B), and the increased numbers of CD163⁺ macrophages in the liver remained evident after 5 days (Fig. 11C).

DISCUSSION

In this study we have extended previous studies in mice (21) to examine the impact of a sustained increase in CSF1 activity on monocyte-macrophage homeostasis. All of the impacts we have observed are consistent with the known biological activity of CSF1. In mice, the same impacts on monocyte-macrophage numbers and maturation can be generated by injection of very much higher doses of native CSF1 (21) or injection of a much larger native form of human CSF1 (24). The doses of native CSF1 required are prohibitive in a large animal. Although we cannot entirely eliminate other functional contributions of the Fc component, the increase in circulating half-life is the most obvious explanation for the increased efficacy compared with native CSF1.

The nature of the so-called hepatostat, which determines that the liver returns to a size that is strictly proportional to body

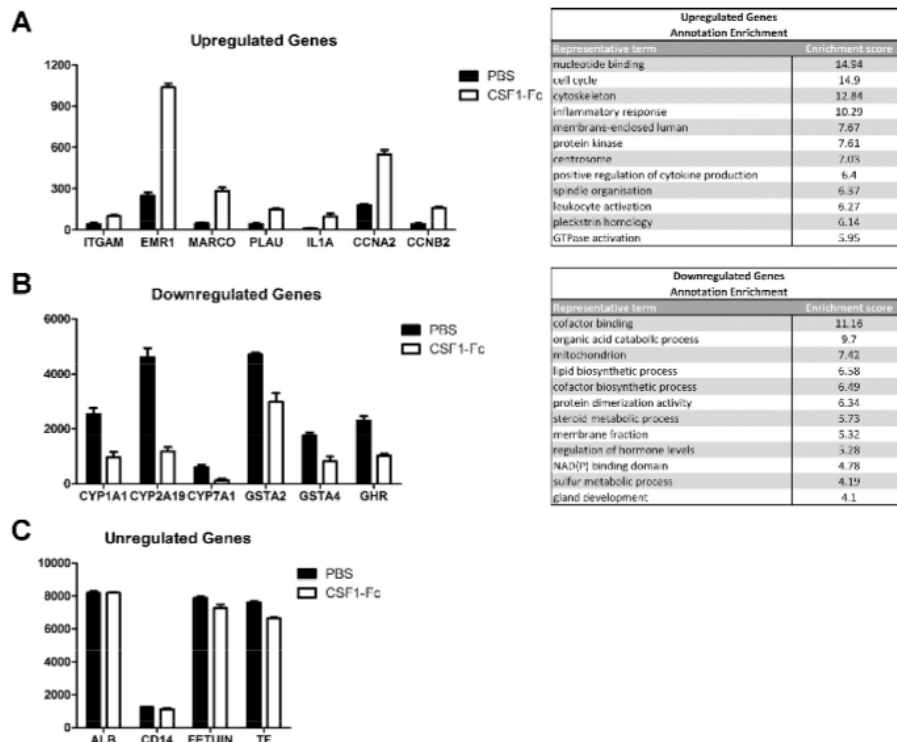
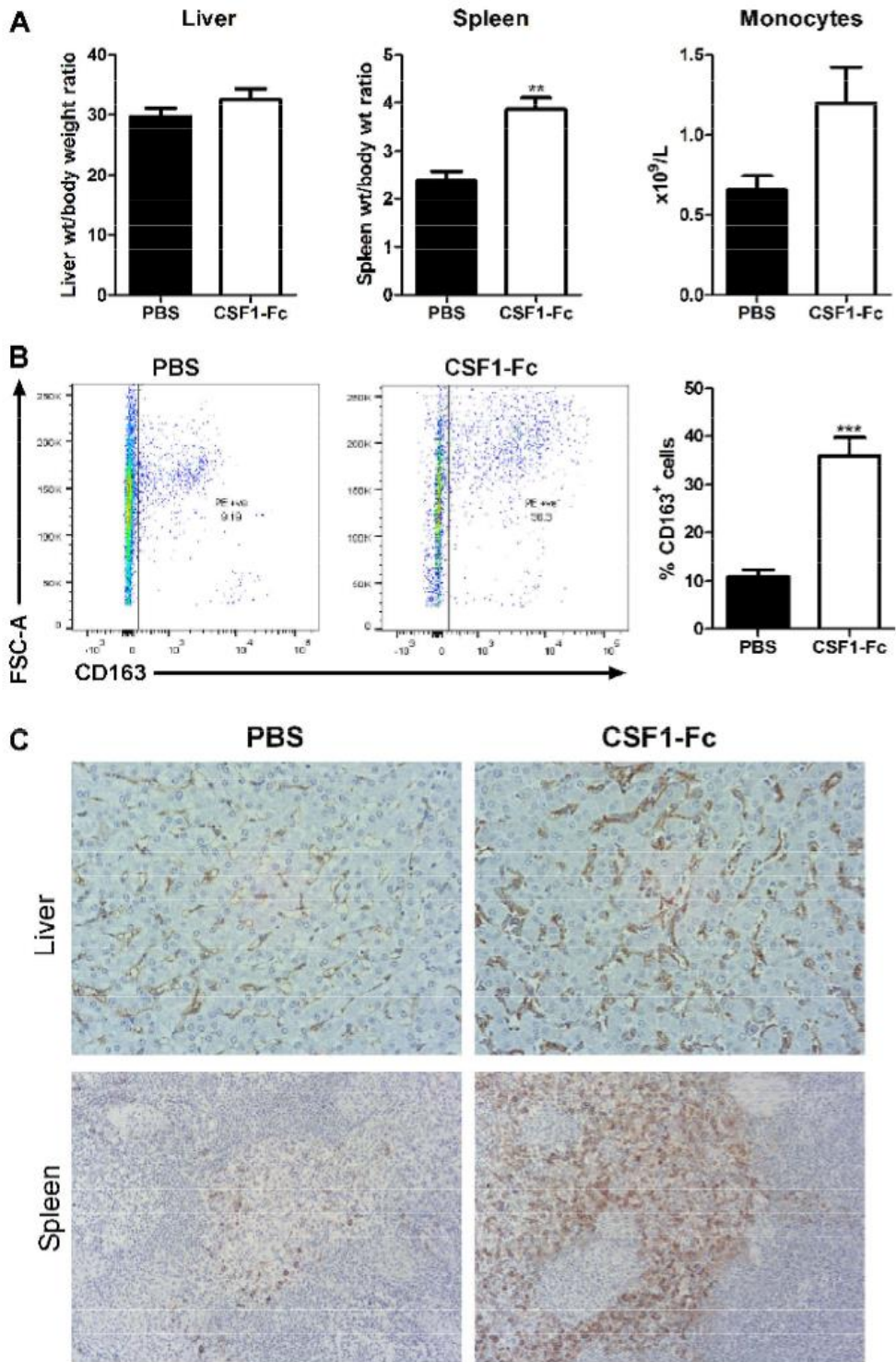


Fig. 9. Effect of CSF1-Fc on gene expression in the liver. Pigs (8-wk-old males and females) were injected with PBS or 0.75 mg/kg CSF1-Fc for 3 days prior to euthanasia on *day 4*. Liver tissue was collected in RNAlater and RNA was prepared and submitted for microarray analysis. *A*: expression profiles of a number of genes from *cluster 1*: upregulated genes in CSF1-Fc-treated pigs and a table of the top 12 enrichment clusters with representative terms. *B*: expression profiles of a number of genes from *cluster 2*: downregulated genes in CSF1-Fc-treated pigs and a table of the top 12 enrichment clusters with representative terms. *C*: expression profiles of a number of genes that were unregulated.

size, has continued to be something of a mystery (34, 35). Although there are many candidates, including growth factors and inhibitors, extracellular matrix proteins and metabolites, and circulating hormones that can regulate hepatic regeneration, it is unclear how any of them functions as a sensor. In a previous study, we made the striking observation that CSF1 treatment of mice (using an Fc conjugate with an increased circulating half-life) was able to increase the size of the liver as well as the number of Kupffer cells. This ability is quite unique. In the present study, we have extended the finding to the domestic pig, an animal that is considerably more human-like in size and vascular biology. The data in Fig. 6 show that a major impact of CSF1-Fc treatment in pigs is to increase the number of hepatocytes through extensive proliferation, so that the total cellularity of the liver is increased even more than the increase in total liver weight. Hepatocyte proliferation, as opposed to hypertrophy, is also a feature of liver regeneration in response to partial hepatectomy (34–36). We have made the reciprocal observation in mice; namely, that prolonged depletion of Kupffer cells with anti-CSF1R treatment leads to a reduction in the size of the liver (45). Others have shown that liver regeneration is greatly impaired in CSF1-deficient or

anti-CSF1R-treated mice (46) and in mice depleted of blood monocytes (15) and have promoted liver repair by infusing CSF1-stimulated macrophages into the portal vein (47). The impact of CSF1-Fc on hepatic growth in mice was dependent on monocyte recruitment, as evident from the impact of knockout of CCR2 (46). The role of monocyte-macrophage products, including the inflammatory cytokines TNF, IL1, and IL6, in hepatocyte proliferation has been well recognized (22, 46). CSF1-Fc action in mice was partly dependent on IL6 (46), which was also induced in all of the CSF1-Fc-treated pigs. The effect of CSF1-Fc treatment demonstrates that CSF1-dependent monocyte recruitment is both necessary and sufficient to drive hepatic proliferation and can drive it beyond the homeostatic limits even in a large animal.

The effect of CSF1 treatment supports other evidence of the existence of a homeostatic feedback loop. Macrophages, notably those of the liver (4) and blood monocytes (51), together regulate the level of circulating CSF1 via receptor-mediated endocytosis. This mechanism is evident from the massive increase in circulating CSF1 seen in animals treated with anti-CSF1R (33), and the importance of the liver is evident in patients following partial resection (46). The CSF1-Fc



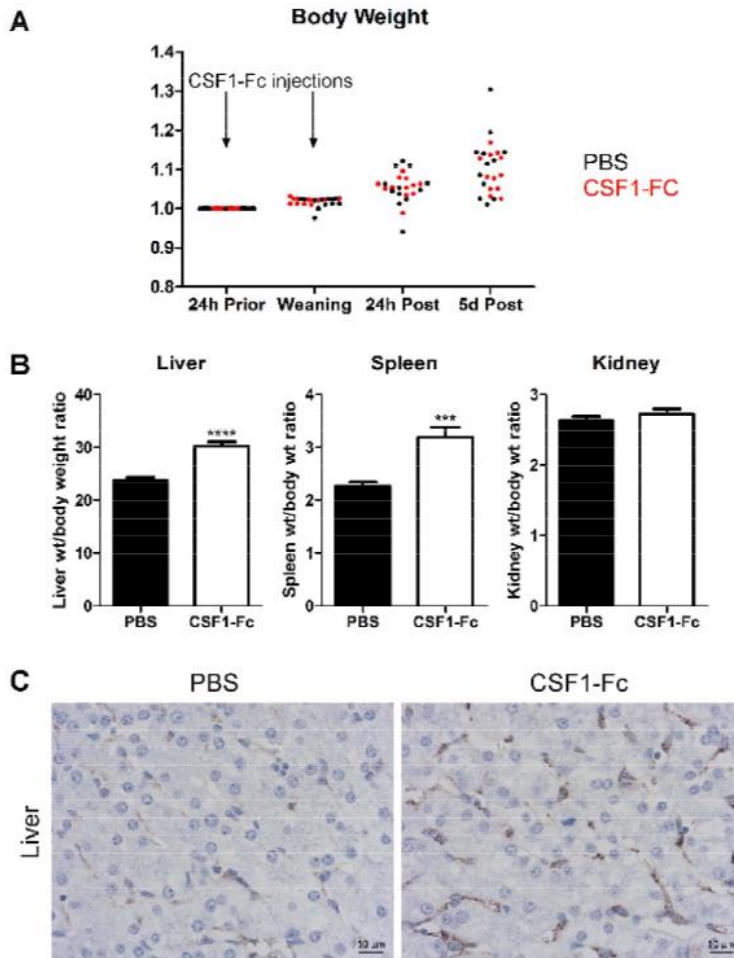


Fig. 11. Long-lasting effect of CSF1-Fc in weaning pigs. Pigs (4-wk-old males and females) were injected with PBS or 0.75 mg/kg CSF1-Fc for 2 days prior to euthanasia 5 days after the final injection; $n = 12$ pigs per treatment. *A*: body weight was recorded at each of the time points shown and total body weight change over the duration of the experiment was graphed for PBS treated pigs (black) and CSF1-Fc-treated pigs (red). *B*: bar graphs show means \pm SE. **** $P < 0.001$, *** $P < 0.0001$ by *t*-test. Graphs show liver weight/body weight ratio, spleen weight/body weight ratio, and kidney weight/body weight ratio. *C*: formalin-fixed liver tissue was prepared and stained for CD163. Representative images are shown. Scale bar = 10 μ m.

treatment reveals that elevated CSF1 can provoke expansion of the committed monocyte pool in the marrow (Fig. 3), maturation of the monocytes toward a resident phenotype (Fig. 2), and infiltration of the liver (Fig. 5). Hence, the physiological hepatostat (34–36) may actually be a “macrostast.” Of course, the increased macrophage numbers in the liver elicited by CSF1 produce secondary impacts, not only removing potential toxins from the portal blood, but altering the balance of metabolism in the liver between portal and

venous-associated functions. Interestingly, resident Kupffer cells are selectively located toward the portal vein in mouse liver lobules (13), which might also serve to localize macrophage-derived hepatocyte proliferative signals.

The expression profiling of the livers of the CSF1-Fc-treated pigs (Fig. 9) closely parallels results obtained previously in the mouse system (21). The newly recruited monocytes clearly respond to TLR-mediated and other signals to express the large majority of transcripts seen when CSF1-stimulated bone mar-

Fig. 10. Effect of a short course of CSF1-Fc in weaning pigs. Pigs (4-wk-old males and females) were injected with PBS or 1 mg/kg CSF1-Fc for 2 days prior to euthanasia on *day 3*. Graphs show means \pm SE. * $P < 0.05$, ** $P < 0.01$, *** $P < 0.001$ by *t*-test; $n = 5$ pigs per treatment. *A*: blood was collected into EDTA tubes postmortem and complete blood count assessment was performed. Graphs show liver weight/body weight ratio, spleen weight/body weight ratio, and monocyte number. *B*: BM from ribs was collected as described in MATERIALS AND METHODS. BM cells were analyzed via flow cytometry for expression of CD163 with exclusion of dead cells using SYTOX blue. Representative flow cytometry plots are shown. *C*: formalin-fixed liver and spleen tissue was prepared and stained for CD163. Representative images are shown.

row-derived macrophages respond to LPS (29). However, classical neutrophil chemoattractants such as IL8 were not detected; we found no evidence of neutrophil infiltration, no induction of classical acute phase response or apoptosis genes, and no evidence of damage to liver cells. Furthermore, the pigs showed no adverse impacts, and in weaners the treatment did not impair their rapid growth (Fig. 11). This is consistent with earlier data, in which recombinant CSF1 has previously been administered in Phase 1 clinical trials by continuous infusion to humans and was well-tolerated (11, 28), and indicates that the Fc fusion protein does not produce any additional toxicity. The lack of severe consequences may be attributed in part to induction of the anti-inflammatory cytokines IL10 and TGFB1 in the liver of the treated animals. Whatever the mechanism, the outcome suggests that CSF1-Fc specifically promotes a proregenerative cellular response in liver, as it does in other organs (23).

In the final set of experiments (Fig. 11), we progressed toward the clinical application of CSF1-Fc in a pig model. The model may also reflect a practical application in pig production to bolster the innate immune system at weaning. We showed that only two doses, administered intramuscularly, were sufficient to produce a sustained increase in monocyte count, liver size, and liver macrophage numbers and produced no adverse local reaction. We propose that CSF1-Fc could provide protection against disseminated infections arising from the immature gut of early-weaned animals. Similarly, clearance functions of the macrophages of the liver are crucial to prevent sepsis in acute liver failure in humans, and CSF1-Fc rapidly promoted clearance functions in mouse disease models (46). The fact that administration of CSF1-Fc to pigs increased the size of the liver and the liver macrophage population (i.e., the clearance capacity, noting also the increased expression of clearance receptors in the array profiles) has an obvious relevance to human acute liver failure. Accordingly, we suggest that the fundamental understanding of the central role of CSF1 in liver homeostasis can potentially translate into both human clinical and veterinary applications.

ACKNOWLEDGMENTS

We thank the staff at the Biological Resource Facility and Dryden Farm (at the Roslin Institute) and staff at the AFBI-NI for their assistance in planning and executing the animal studies. We thank colleagues at Zoetis for providing the CSF1-Fc, specifically the authors listed in our previous publication (21). We also show our gratitude to Iveta Gazova, Anna Raper, and Jun Hu for helping to process samples and deliver them to their appropriate locations.

Present address for G. M. Davis: The University of Manchester, Oxford Road, Manchester M13 9PL, United Kingdom.

GRANTS

This work was funded by Department of Agriculture and Rural Development Evidence and Innovation Fund, project 13/1/04 (E. Magawan). This work was supported by project (BB/J014672/1 and BB/M024288/1) from the Biotechnology and Biological Sciences Research Council (N. A. Mabbott).

The Roslin Institute is supported by Institute Strategic Programme Grant funding and National Capability funding from the Biotechnology and Biological Sciences Research Council (BB/J004235/1, BB/J004316/1, BB/J004227/1, BB/J004332/1, BB/J004243/1).

DISCLOSURES

D. A. Hume has a patent on CSF1-Fc in liver.

AUTHOR CONTRIBUTIONS

K.A.S., L.A.W., and D.A.H. conception and design of research; K.A.S., L.A.W., Z.M.L., R.Y., L.L., G.M.D., S.M.C., M.M., and E.M. performed

experiments; K.A.S., L.A.W., N.A.M., K.M.S., and D.A.H. analyzed data; K.A.S., L.A.W., N.A.M., K.M.S., and D.A.H. interpreted results of experiments; K.A.S., L.A.W., N.A.M., and K.M.S. prepared figures; K.A.S., L.A.W., and D.A.H. drafted manuscript; K.A.S., L.A.W., N.A.M., K.M.S., and D.A.H. edited and revised manuscript; K.A.S., L.A.W., Z.M.L., R.Y., L.L., G.M.D., S.M.C., M.M., E.M., N.A.M., K.M.S., and D.A.H. approved final version of manuscript.

REFERENCES

1. Alikhan MA, Jones CV, Williams TM, Beckhouse AG, Fletcher AL, Kett MM, Sakkal S, Samuel CS, Ramsay RG, Deane JA, Wells CA, Little MH, Hume DA, Ricardo SD. Colony-stimulating factor-1 promotes kidney growth and repair via alteration of macrophage responses. *Am J Pathol* 179: 1243–1256, 2011.
2. Alison MR, Lin WR. Hepatocyte turnover and regeneration: virtually a virtuoso performance. *Hepatology* 53: 1393–1396, 2011.
3. Bailey M, Haverson K, Inman C, Harris C, Jones P, Corfield G, Miller B, Stokes C. The development of the mucosal immune system pre- and post-weaning: balancing regulatory and effector function. *Proc Nutr Soc* 64: 451–457, 2005.
4. Bartocci A, Mastrogiannis DS, Migliorati G, Stockert RJ, Wolkoff AW, Stanley ER. Macrophages specifically regulate the concentration of their own growth factor in the circulation. *Proc Natl Acad Sci USA* 84: 6179–6183, 1987.
5. Boissonneault V, Filali M, Lessard M, Relton J, Wong G, Rivest S. Powerful beneficial effects of macrophage colony-stimulating factor on beta-amyloid deposition and cognitive impairment in Alzheimer's disease. *Brain* 132: 1078–1092, 2009.
6. Cenci S, Weitzmann MN, Gentile MA, Aisa MC, Pacifici R. M-CSF neutralization and egr-1 deficiency prevent ovariectomy-induced bone loss. *J Clin Invest* 105: 1279–1287, 2000.
7. Chazaud B. Macrophages: supportive cells for tissue repair and regeneration. *Immunobiology* 219: 172–178, 2014.
8. Chen BP, Kuziel WA, Lane TE. Lack of CCR2 results in increased mortality and impaired leukocyte activation and trafficking following infection of the central nervous system with a neurotropic coronavirus. *J Immunol* 167: 4585–4592, 2001.
9. Chitu V, Stanley ER. Colony-stimulating factor-1 in immunity and inflammation. *Curr Opin Immunol* 18: 39–48, 2006.
10. Chow A, Huggins M, Ahmed J, Hashimoto D, Lucas D, Kunisaki Y, Pinho S, Leboeuf M, Noizat C, van Rooijen N, Tanaka M, Zhao Z.J, Bergman A, Merad M, Frenette PS. CD169(+) macrophages provide a niche promoting erythropoiesis under homeostasis and stress. *Nat Med* 19: 429–436, 2013.
11. Cole DJ, Sanda MG, Yang JC, Schwartztruber DJ, Weber J, Ettinghausen SE, Pockaj BA, Kim HI, Levin RD, Pogrebniak HW, Balkissoon J, Fenton RM, DeBarge LR, Kaye J, Rosenberg SA, Parkinson DR. Phase I trial of recombinant human macrophage colony-stimulating factor administered by continuous intravenous infusion in patients with metastatic cancer. *J Natl Cancer Inst* 86: 39–45, 1994.
12. Dai XM, Ryan GR, Hapel AJ, Dominguez MG, Russell RG, Kapp S, Sylvestre V, Stanley ER. Targeted disruption of the mouse colony-stimulating factor 1 receptor gene results in osteopetrosis, mononuclear phagocyte deficiency, increased primitive progenitor cell frequencies, and reproductive defects. *Blood* 99: 111–120, 2002.
13. Dixon JE, Allan JE, Doherty PC, Hume DA. Immunohistochemical analysis of the involvement of F4/80 and Ia-positive macrophages in mouse liver infected with lymphocytic choriomeningitis virus. *J Leukoc Biol* 40: 617–628, 1986.
14. Duan X, Nauwynck HJ, Pensaert MB. Effects of origin and state of differentiation and activation of monocytes/macrophages on their susceptibility to porcine reproductive and respiratory syndrome virus (PRRSV). *Arch Virol* 142: 2483–2497, 1997.
15. Elsegood CL, Chan CW, Degli-Esposti MA, Wikstrom ME, Domenichini A, Lazarus K, van Rooijen N, Ganss R, Olynyk JK, Yeoh GC. Kupffer cell-monocyte communication is essential for initiating murine liver progenitor cell-mediated liver regeneration. *Hepatology* 62: 1272–1284, 2015.
16. Fairbairn L, Kapetanovic R, Beraldi D, Sester DP, Tuggle CK, Archibald AL, Hume DA. Comparative analysis of monocyte subsets in the pig. *J Immunol* 190: 6389–6396, 2013.
17. Fairbairn L, Kapetanovic R, Sester DP, Hume DA. The mononuclear phagocyte system of the pig as a model for understanding human innate immunity and disease. *J Leukoc Biol* 89: 855–871, 2011.

18. Freeman TC, Ivens A, Baillie JK, Beraldi D, Barnett MW, Dorward D, Downing A, Fairbairn L, Kapetanovic R, Raza S, Tomoiu A, Alberio R, Wu C, Su AI, Summers KM, Tuggle CK, Archibald AL, Hume DA. A gene expression atlas of the domestic pig. *BMC Biol* 10: 90, 2012.
19. Gougelet A, Torre C, Vebber P, Sartor C, Bachelot L, Denechaud PD, Godard C, Moldes M, Burnol AF, Dubuquoy C, Terris B, Guillonneau F, Ye T, Schwarz M, Braeuning A, Perret C, Colnot S. T-cell factor 4 and beta-catenin chromatin occupancies pattern zonal liver metabolism in mice. *Hepatology* 59: 2344–2357, 2014.
20. Gow DJ, Garceau V, Kapetanovic R, Sester DP, Fici GJ, Shelly JA, Wilson TL, Hume DA. Cloning and expression of porcine Colony Stimulating Factor-1 (CSF-1) and Colony Stimulating Factor-1 Receptor (CSF-1R) and analysis of the species specificity of stimulation by CSF-1 and Interleukin 34. *Cytokine* 60: 793–805, 2012.
21. Gow DJ, Sauter KA, Pridans C, Moffat L, Sehgal A, Stutchfield BM, Raza S, Beard PM, Tsai YT, Bainbridge G, Boner PL, Fici G, Garcia-Tapia D, Martin RA, Oliphant T, Shelly JA, Tiwari R, Wilson TL, Smith LB, Mabbott NA, Hume DA. Characterisation of a novel Fc conjugate of macrophage colony-stimulating factor. *Mol Ther* 22: 1580–1592, 2014.
22. Heymann F, Tacke F. Immunology in the liver — from homeostasis to disease. *Nat Rev Gastroenterol Hepatol* 13: 88–110, 2016.
23. Hume DA, MacDonald KP. Therapeutic applications of macrophage colony-stimulating factor-1 (CSF-1) and antagonists of CSF-1 receptor (CSF-1R) signaling. *Blood* 119: 1810–1820, 2012.
24. Hume DA, Pavli P, Donahue RE, Fidler IJ. The effect of human recombinant macrophage colony-stimulating factor (CSF-1) on the murine mononuclear phagocyte system in vivo. *J Immunol* 141: 3405–3409, 1988.
25. Hume DA, Weidemann MJ. Role and regulation of glucose metabolism in proliferating cells. *J Natl Cancer Inst* 62: 3–8, 1979.
26. Huynh D, Akcora D, Malaterre J, Chan CK, Dai XM, Bertonecello I, Stanley ER, Ramsay RG. CSF-1 receptor-dependent colon development, homeostasis and inflammatory stress response. *PLoS One* 8: e56951, 2013.
27. Jaeschke H. Mechanisms of Liver Injury. II. Mechanisms of neutrophil-induced liver cell injury during hepatic ischemia-reperfusion and other acute inflammatory conditions. *Am J Physiol Gastrointest Liver Physiol* 290: G1083–G1088, 2006.
28. Jakubowski AA, Bajorin DF, Templeton MA, Chapman PB, Cody BV, Thaler H, Tao Y, Filippa DA, Williams L, Sherman ML, Garnick MB, Houghton AN. Phase I study of continuous-infusion recombinant macrophage colony-stimulating factor in patients with metastatic melanoma. *Clin Cancer Res* 2: 295–302, 1996.
29. Kapetanovic R, Fairbairn L, Beraldi D, Sester DP, Archibald AL, Tuggle CK, Hume DA. Pig bone marrow-derived macrophages resemble human macrophages in their response to bacterial lipopolysaccharide. *J Immunol* 188: 3382–3394, 2012.
30. Kapetanovic R, Fairbairn L, Downing A, Beraldi D, Sester DP, Freeman TC, Tuggle CK, Archibald AL, Hume DA. The impact of breed and tissue compartment on the response of pig macrophages to lipopolysaccharide. *BMC Genomics* 14: 581, 2013.
31. Korkosz M, Bukowska-Strakova K, Sadis S, Grodzicki T, Siedlar M. Monoclonal antibodies against macrophage colony-stimulating factor diminish the number of circulating intermediate and nonclassical (CD14(++)CD16(+))CD14(+)CD16(++) monocytes in rheumatoid arthritis patient. *Blood* 119: 5329–5330, 2012.
32. Lee KC, Palacios Jimenez C, Alibhai H, Chang YM, Leckie PJ, Baker LA, Stanzani G, Priestsmall SL, Mookerjee RP, Jalan R, Davies NA. A reproducible, clinically relevant, intensively managed, pig model of acute liver failure for testing of therapies aimed to prolong survival. *Liver Int* 33: 544–551, 2013.
33. MacDonald KP, Palmer JS, Cronau S, Seppanen E, Olver S, Raffelt NC, Kuns R, Pettit AR, Clouston A, Wainwright B, Branstetter D, Smith J, Paxton RJ, Cerretti DP, Bonham L, Hill GR, Hume DA. An antibody against the colony-stimulating factor 1 receptor depletes the resident subset of monocytes and tissue- and tumor-associated macrophages but does not inhibit inflammation. *Blood* 116: 3955–3963, 2010.
34. Michalopoulos GK. Advances in liver regeneration. *Expert Rev Gastroenterol Hepatol* 8: 897–907, 2014.
35. Michalopoulos GK. Liver regeneration after partial hepatectomy: critical analysis of mechanistic dilemmas. *Am J Pathol* 176: 2–13, 2010.
36. Michalopoulos GK. Principles of liver regeneration and growth homeostasis. *Compr Physiol* 3: 485–513, 2013.
37. Mitrasinovic OM, Vincent VA, Simsek D, Murphy GM Jr. Macrophage colony stimulating factor promotes phagocytosis by murine microglia. *Neurosci Lett* 344: 185–188, 2003.
38. Moeser AJ, Klook CV, Ryan KA, Wooten JG, Little D, Cook VL, Blakslager AT. Stress signaling pathways activated by weaning mediate intestinal dysfunction in the pig. *Am J Physiol Gastrointest Liver Physiol* 292: G173–G181, 2007.
39. Moffat L, Rothwell L, Garcia-Morales C, Sauter KA, Kapetanovic R, Gow DJ, Hume DA. Development and characterisation of monoclonal antibodies reactive with porcine CSF1R (CD115). *Dev Comp Immunol* 47: 123–128, 2014.
40. Nehra D, Fallon EM, Puder M. The prevention and treatment of intestinal failure-associated liver disease in neonates and children. *Surg Clin North Am* 91: 543–563, 2011.
41. Newsome PN, Henderson NC, Nelson LJ, Dabos C, Filippi C, Bellamy C, Howie F, Clutton RE, King T, Lee A, Hayes PC, Plevris JN. Development of an invasively monitored porcine model of acetaminophen-induced acute liver failure. *BMC Gastroenterol* 10: 34, 2010.
42. Pohl CS, Medland JE, Moeser AJ. Early-life stress origins of gastrointestinal disease: animal models, intestinal pathophysiology, and translational implications. *Am J Physiol Gastrointest Liver Physiol* 309: G927–G941, 2015.
43. Pollard JW. Trophic macrophages in development and disease. *Nat Rev Immunol* 9: 259–270, 2009.
44. Sauter KA, Pridans C, Sehgal A, Bain CC, Scott C, Moffat L, Rojo R, Stutchfield BM, Davies CL, Donaldson DS, Renault K, McColl BW, Mowat AM, Serrels A, Frame MC, Mabbott NA, Hume DA. The MacBlue binary transgene (csf1r-gal4VP16/UAS-ECFP) provides a novel marker for visualisation of subsets of monocytes, macrophages and dendritic cells and responsiveness to CSF1 administration. *PLoS One* 9: e105429, 2014.
45. Sauter KA, Pridans C, Sehgal A, Tsai YT, Bradford BM, Raza S, Moffat L, Gow DJ, Beard PM, Mabbott NA, Smith LB, Hume DA. Pleiotropic effects of extended blockade of CSF1R signaling in adult mice. *J Leukoc Biol* 96: 265–274, 2014.
46. Stutchfield BM, Antoine DJ, Mackinnon AC, Gow DJ, Bain CC, Hawley CA, Hughes M, Francis B, Wojtacha D, Man TY, Dear JW, Devey LR, Mowat AM, Pollard JW, Park BK, Jenkins SJ, Simpson KJ, Hume DA, Wigmore SJ, Forbes SJ. CSF1 restores innate immunity after liver injury in mice and serum levels indicate outcomes of patients with acute liver failure. *Gastroenterology* 149: 1896–1909.e14, 2015.
47. Thomas JA, Pope C, Wojtacha D, Robson AJ, Gordon-Walker TT, Hartland S, Ramachandran P, Van Deemter M, Hume DA, Iredale JP, Forbes SJ. Macrophage therapy for murine liver fibrosis recruits host effector cells improving fibrosis, regeneration, and function. *Hepatology* 53: 2003–2015, 2011.
48. Torre C, Perret C, Colnot S. Molecular determinants of liver zonation. *Prog Mol Biol Transl Sci* 97: 127–150, 2010.
49. Tsou CL, Peters W, Si Y, Slaymaker S, Aslanian AM, Weisberg SP, Mack M, Charo IF. Critical roles for CCR2 and MCP-3 in monocyte mobilization from bone marrow and recruitment to inflammatory sites. *J Clin Invest* 117: 902–909, 2007.
50. Visser JJ, Bom-van Noorloos AA, Meijer S, Hoitsma HF. Serum total bile acids monitoring after experimental orthotopic liver transplantation. *J Surg Res* 36: 147–153, 1984.
51. Yona S, Kim KW, Wolf Y, Mildner A, Varol D, Breker M, Strauss-Ayali D, Viukov S, Guillemins M, Misharin A, Hume DA, Perlman H, Malissen B, Zelzer E, Jung S. Fate mapping reveals origins and dynamics of monocytes and tissue macrophages under homeostasis. *Immunity* 38: 79–91, 2013.
52. Zhang J, Babic A. Regulation of the MET oncogene: molecular mechanisms. *Carcinogenesis* 2016.

9.4 Activation of macrophages in the mucosa and muscularis of jejunum in horses undergoing abdominal surgery for strangulating small intestinal obstructions



Z. Lisowski^{1,2}, T. Mair³, L. Lefevre^{1,4}, D. Hume^{1,5},
N. Hudson^{1,2}, S. Pirie^{1,2}


¹ The Roslin Institute, The University of Edinburgh, UK
² Royal (Dick) School of Veterinary Studies, University of Edinburgh, UK
³ Bell Equine Veterinary Clinic, Maidstone, UK
⁴ UK Dementia Research Institute, University of Edinburgh, UK
⁵ Mater Research, Brisbane, Australia

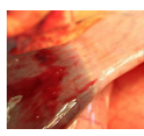
Zofia.lisowski@ed.ac.uk

Activation of macrophages in the mucosa and muscularis of jejunum in horses undergoing abdominal surgery for strangulating small intestinal obstructions

INTRODUCTION

MATERIALS AND METHODS

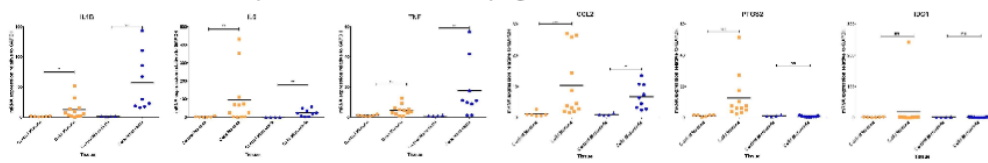
- 
 - Postoperative ileus (POI) is the functional inhibition of propulsive intestinal motility following abdominal surgery
 - Rodent and human-based studies have demonstrated manipulation-induced activation of intestinal muscularis macrophages (MM) in the pathophysiology
 - LPS translocation from the gut lumen is also an activator of MMs
 - Few equine studies have focussed on the pathogenesis of POI in the horse


 - Intestinal tissue was collected from horses undergoing colic surgery (n=12) for a small intestinal strangulation
 - Samples were collected from the healthy margins of resected intestine
 - Tissue from control cases was obtained from intestine of horses with no gastrointestinal disease
 - RNA was extracted from the resection margins and the tissue analysed for genes associated with macrophage activation

The aim of this study was to evaluate gene expression in intestine from horses undergoing abdominal surgery for colic to determine whether there was evidence of intestinal macrophage activation.

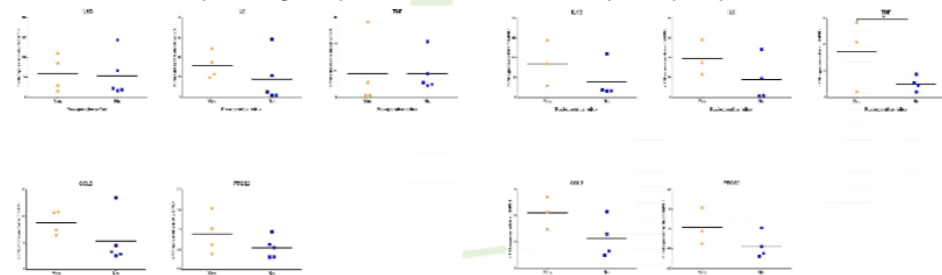
RESULTS

Gene expression associated with macrophage activation is increased in colic cases



- Relative expression of IL-6, IL-1 β and TNF- α was significantly greater ($p < 0.05$) in both mucosa and muscularis of colic cases compared to controls.
- These genes are associated with the activation of macrophages (see poster PO1.15).
- These genes all affect intestinal motility by suppressing normal smooth muscle function.
- Relative expression of CCL2 was significantly increased ($p < 0.05$) in the mucosa and muscularis of colic cases. CCL2 promotes recruitment of other immune cells (monocytes and leukocytes) to the region. These incoming cells can also impair intestinal motility by releasing nitric oxide (neutrophils) and prostaglandins (monocytes) which inhibit smooth muscle contractions.
- PTGS2 was only significantly increased in the mucosa of colic cases. This may be due to cells in the mucosa being activated sooner than those in the muscularis
- There was no significant increase in IDO1 observed in the mucosa and muscularis of colic cases compared to controls. The reason is unclear, but may suggest macrophages are activated by different pathways, or that not enough time had passed at the time of tissue collection for changes to be observed.

Comparison of gene expression in horses with and without pre- and post-operative reflux



No differences in gene expression were observed in horses that had pre-operative reflux

Graph details: Scatter plots showing mRNA expression of target genes relative to GAPDH. Results calculated using 2^{-CT} method. Mean value represented by black line. Significance of relative mRNA expression between control and surgical samples were performed with a Mann-Whitney U test. * $p < 0.05$, ** $p < 0.01$, *** $p < 0.001$

With the exception of TNF ($p < 0.05$), no significant differences in gene expression were observed in horses that had post-operative reflux. Horses that had post-operative reflux generally had a higher mean of expression than those that didn't and larger numbers are required to draw any conclusions.

CONCLUSIONS

These preliminary data support the hypothesis that intestinal surgery results in the activation of the intestinal macrophage population. Further work is required to elucidate whether the risk of developing POI is related to the magnitude of macrophage activation during surgery.





THE UNIVERSITY of EDINBURGH

This work was funded by
the Horserace Betting Levy Board



9.5 Generation and characterisation of equine bone marrow-derived macrophages



Z.M. Lisowski^{1,2}, K. Sauter^{1,2}, C. Pridans³, R. Young^{1,2}, L. Lefevre⁴, L. Waddell^{1,2}, A. Raper^{1,2}, D. Hume⁵, S. Pirie^{1,2}, N. Hudson^{1,2}

¹The Roslin Institute, The University of Edinburgh, UK
²Royal (Dick) School of Veterinary Studies, University of Edinburgh, UK
³Centre for Inflammation Research, The University of Edinburgh, UK
⁴UK Dementia Research Institute, University of Edinburgh, UK
⁵Walter Research, Brisbane, Australia

Zofia.lisowski@ed.ac.uk

Generation and characterisation of equine bone marrow-derived macrophages

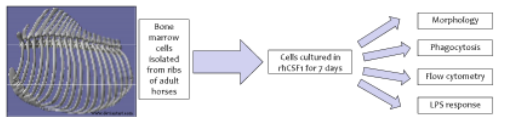
INTRODUCTION

- Bone marrow derived macrophages (BMDMs) are primary macrophage cells which are derived from bone marrow cells *in vitro* in the presence of colony-stimulating factor 1 (CSF1)
- Macrophages play a role in a number of important equine diseases e.g. equine infectious anaemia virus
- BMDMs can be used as an *in vitro* model for tissue resident macrophages of the innate immune system

STUDY AIMS

- To generate macrophages from bone marrow cells of adult horses
- To characterise equine bone marrow derived macrophages (eqBMDMs)

MATERIALS AND METHODS



RESULTS

Optimising culture conditions of equine bone marrow derived macrophages

An MTT assay was performed to identify optimal culture conditions for eqBMDMs. Cells cultured in horse serum in the presence of CSF-1 differentiated into macrophages, whereas cell populations without CSF-1 did not differentiate and remained small, circular and not adherent (Fig 1).

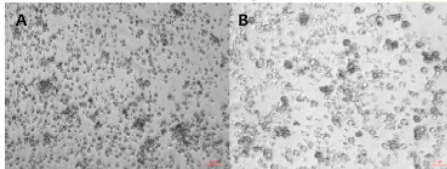


Figure 1. Morphology of cells at Day 7 in culture without recombinant human CSF-1 (rhCSF1) (A) and with rhCSF1 (B). EqBMDMs (n=3) were cultured in 20% horse serum (HS) at 2.5 x 10⁶ cells/ml for up to 14 days with or without rhCSF-1.

Morphology

Cells were examined using either light microscopy (Fig. 2) or using a confocal microscope (Fig 3). Cells had the expected morphology of macrophages; they were stellate and had an increased granularity and were adherent to bacteriological plastic.

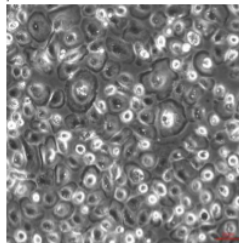


Figure 2. Cells at Day 7

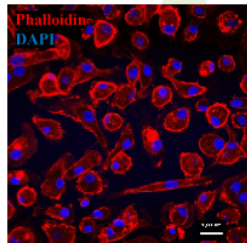


Figure 3. Cells at Day 10

Differentiated cells were functional phagocytes

Isolated cells were cultured for seven days in rhCSF-1 and phagocytic activity was evaluated using 2 methods: (a) Zymosan A *Saccharomyces cerevisiae* BioParticle assay followed by cell fixation, staining with DAPI and phalloidin and confocal microscopy; (b) pHrodo Red *Escherichia coli* BioParticle assay followed by flow cytometric analysis.

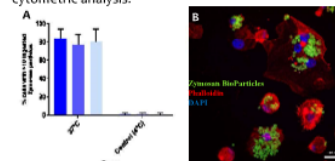


Figure 4. Zymosan phagocytosis assay. Cells from 6 horses were cultured on bacteriological plastic for 10 days in rhCSF-1. On Day 10 media was replaced with media containing Zymosan particles and cells were incubated with the Zymosan particles for 1 hour at 37°C. Control cells had Zymosan particles added but were kept at 4°C. More than 20% of cells had phagocytosed Zymosan bio-particles (A). (B) is a confocal image of macrophages with phagocytosed Zymosan particles. Bar = 20µm

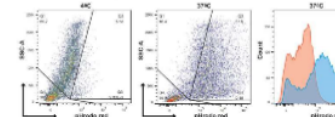


Figure 5. pHrodo BioParticle phagocytosis assay. Cells from 6 horses were cultured with rhCSF-1 on bacteriological plastic for 7 days. On day 10 adhered cells were gently removed and cells combined before adding pHrodo Red *Escherichia coli* BioParticle for 1 hour at 37°C before being analysed by flow cytometry. Control cells were kept at 4°C for 1hr.

Differentiated cells expressed CD14

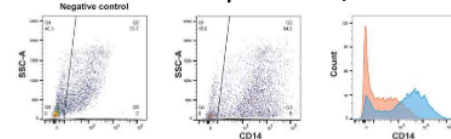


Figure 6. Flow cytometry of equine alveolar macrophages and eqBMDMs. EqBMDMs were cultured for 7-10 days in rhCSF-1 (n=6). When confluent, adhered cells were stained for flow cytometry. Size (forward light scatter (FSC)) and granularity (side scatter (SSC)) were used for cell discrimination (data not shown).

LPS induced TNFα and IDO but not NOS2 expression in eqBMDMs

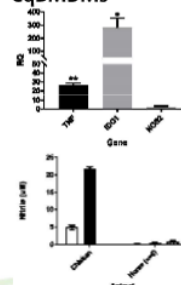


Figure 7. Relative quantification (RQ) of TNF-α, IDO and NOS2 in eqBMDMs after being in culture with LPS for 7hrs. Cryopreserved eqBMDMs from 3 horses were cultured until confluent and adherent (Day 10). Cells were plated at 2 x 10⁶ cells/well and left to rest overnight, in optimal conditions described earlier. The media was replaced and LPS (100ng/ml) added for 7 hours. Control samples had culture media changed only. RNA was extracted and RQ relative to the housekeeping gene GAPDH for TNF-α, IDO and NOS2 was measured by qPCR. Grapish show median ± 95 CI. Significance was determined using a paired t-test. *p<0.05, **p<0.005.

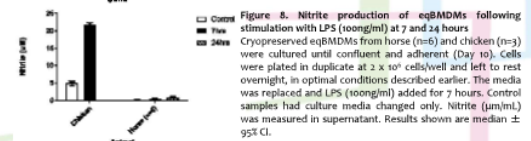


Figure 8. Nitrite production of eqBMDMs following stimulation with LPS (100ng/ml) at 7 and 24 hours. Cryopreserved eqBMDMs from horse (n=6) and chicken (n=3) were cultured until confluent and adherent (Day 10). Cells were plated in duplicate at 2 x 10⁶ cells/well and left to rest overnight, in optimal conditions described earlier. The media was replaced and LPS (100ng/ml) added for 7 hours. Control samples had culture media changed only. Nitrite (µM/ml) was measured in supernatant. Results shown are median ± 95% CI.

CONCLUSIONS

- A protocol was developed for the generation of eqBMDMs by cultivation of bone marrow in rhCSF1.
- Morphological features, the ability to phagocytose particles and the ability to produce cytokines in response to LPS confirmed the cells were macrophages.
- Species specific differences, such as nitric oxide production, highlights the potential pitfalls of using rodent derived data to study equine disease. Unlike mice, but similar to human macrophages, eqBMDMs do not produce nitric oxide in response to LPS
- The method described allows generation of a homogenous population of eqBMDMs to further study their role in the equine innate immune system





This work was funded by
 the Horserace Betting Levy
 Board



9.6 Transcriptomic response of equine bone marrow-derived macrophages cultured in macrophage colony-stimulating factor (CSF-1) to lipopolysaccharide (LPS)



Z. Lisowski^{1,2}, S. Bush^{1,3}, S. Pirie^{1,2},
N. Hudson^{1,2}, D. Hume^{1,4}

¹ The Roslin Institute, The University of Edinburgh, UK
² Royal (Dick) School of Veterinary Studies, University of Edinburgh, UK
³ Nuffield Department of Clinical Medicine, University of Oxford, UK
⁴ Mater Research, Brisbane, Australia
Zofia.lisowski@ed.ac.uk

Transcriptomic response of equine bone marrow-derived macrophages cultured in macrophage colony-stimulating factor (CSF-1) to lipopolysaccharide (LPS)

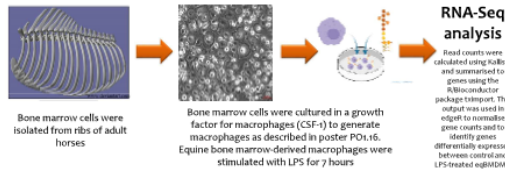
INTRODUCTION

MATERIALS AND METHODS

• Endotoxaemia, the accumulation of endotoxin in the bloodstream, is a leading cause of death in horses

• The binding of lipopolysaccharide (LPS), a Gram-negative bacterial marker, to the CD14/MD2/TLR4 complex on macrophages results in the release of cytokines, including TNF, IL-1 and IL-6

• Whilst the macrophage response to LPS is similar across species, species-specificity exists with respect to the sensitivity to LPS; horses and humans are particularly sensitive in comparison to rodents.

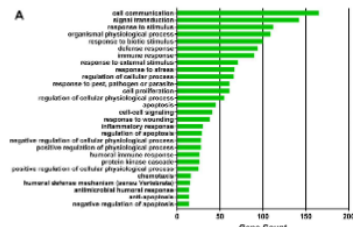


Using RNA-Seq data from LPS-stimulated equine bone marrow-derived macrophages (eqBMDMs), we analysed the transcriptomic response of eqBMDMs to LPS

RESULTS

The top 100 differentially expressed genes included genes associated with the initiation and maintenance of inflammation

The top 100 upregulated genes included IL-1B, IL-6, TNF-α, and CXCL8. GO term analyses using GATHER showed genes associated with cell communication and signal transduction (e.g. SOCS1, SOCS3, MAP2K6, STAT1, STAT2, STAT3 and STAT4), response to stimulus (e.g. CXCL2, CXCL3, CXCL6, IL10, IL12B and TNF-α) and immune response as the main groups of genes upregulated, consistent with LPS stimulation of macrophages.



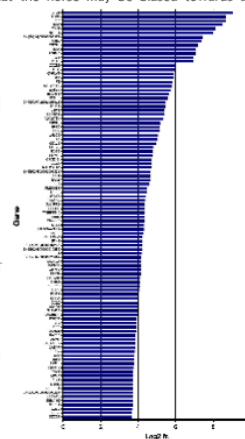
Main functional groups of induced genes of eqBMDMs stimulated with LPS
Histograms show main GO terms induced by LPS in eqBMDMs. Data was analysed using the GO term analysis tool in GATHER. All genes with Log2 fc of >1.5 or <-1.5 with p<0.02 were included. Results are for all GO terms with p<0.05 and Bayes Factor >6 (Chang and Nevins 2006).

Cytokine and chemokine signalling in response to LPS is consistent with the induction of a strong neutrophilic response

- Chemokines are secreted by cells at the site of inflammation to recruit leukocytes to the site of inflammation.
- The expression of genes encoding cytokines and chemokines associated with LPS stimulation of macrophages were all significantly upregulated (p<0.02) and contained within the list of top 100 DE genes in eqBMDMs. These included the inflammatory cytokines TNF-α, IL12B, IL6, IL1B and IL10 and chemokines CXCL2, CXCL3, CXCL8, CCL3, CCL4, CCL5 and CCL22.
- In eqBMDMs, CXCL6 is one of the most upregulated genes.
- CXCL6, also known as granulocyte chemoattractant protein 2 (GCP-2), signals the recruitment of neutrophils, via their surface expression of CXCR1 and CXCR2 receptors (Wuyts et al. 1997).
- Other chemokines mediating the recruitment of neutrophils in mice include CXCL1, LFA-1, CD11b/Mac-1, ICAM-1, VCAM-1, ICAM-2, PECAM-1 and CXCL2 (Reichel et al. 2012). In eqBMDMs, CXCL2, ICAM-1, VCAM-1, PECAM-1 and CCL3 were upregulated suggesting that the horse may be biased towards a strong neutrophilic response (Table 1).

Gene	TPM 0 hours	TPM 7 hours
CXCL6	9.063	978.278
CXCL2	51.594	164.963
ICAM-1	67.395	399.324
ICAM-2	35.219	21.477
VCAM-1	17.361	193.913
PECAM-1	0.295	0.528
CCL3	1394.299	7608.37
LFA-1	7.166	7.314

Table 1. TPM values of genes involved in the neutrophilic response



Top 100 genes in eqBMDMs induced by LPS
RNA-Seq data of genes induced by LPS in eqBMDMs as identified by Log2 fc and p<0.02. Genes with Ensembl IDs are genes not annotated to the horse genome and with no orthologues.

Genes associated with LPS-induced feedback are reduced/absent in the horse

- An important feature of the macrophage response to LPS is the mechanisms by which induced transcripts and proteins are 'switched off' e.g. IL-10
- Genes that in mice either reduce or increase responsiveness to LPS were analysed in the list of DE expressed genes upregulated and downregulated in eqBMDMs in response to LPS
- Amongst genes that suppress the LPS response only 5 (BIRC3, IER3, IL27, ADORA7A and EB13) are present in the top 100 genes DE in eqBMDMs. Twenty-two were present out of all the genes (n=808) significantly upregulated in eqBMDMs. Two genes were downregulated.
- Conversely, 13 genes that increase sensitivity to the LPS response were in the most DE genes, with 3 (STAT4, FPR1 and PDE4B) being in the top 100 genes

CONCLUSIONS

Our data shows species-specific variation in innate immune biology. In particular, CXCL6 upregulation signals the recruitment of neutrophils, suggesting the horse may be biased towards a strong neutrophilic response. The low numbers of specific LPS-induced regulators in eqBMDMs could contribute to the LPS hypersensitivity of the horse.





This work was funded by
the Horseracing Betting Levy
Board



9.7 Distribution of Macrophages in the Gastrointestinal Tract of Horses



12

DEPLETION OF PULMONARY INTRAVASCULAR MACROPHAGES RESCUES INFLAMMATION-INDUCED DELAYED NEUTROPHIL APOPTOSIS IN HORSES

¹Anderson S.L., ²Duke-Novakovski T., ²Robinson A.R.,

²Townsend H.G. and ³Singh B.

¹Lincoln Memorial University, College of Veterinary Medicine, 6965 Cumberland Gap Pkwy, Harrogate, TN 37752, USA;

²University of Saskatchewan, Western College of Veterinary Medicine, 52 Campus Drive, Saskatoon, SK S7N5B4, Canada;

³University of Calgary, College of Veterinary Medicine, Calgary, AB T2N4Z6, Canada.

Email: stacy.anderson@lmunet.edu.

Background: Dysregulation of neutrophil apoptosis may contribute to the development of an excessive systemic inflammatory response in horses.

Objective: The objective of this study was to determine the effect of depleting pulmonary intravascular macrophages (PIMs) on the development of systemic inflammation and circulating neutrophil lifespan, using an experimental model of intestinal ischemia and reperfusion injury in horses.

Methods: Neutrophils were isolated before and after surgery from horses that were randomized to 3 treatment groups: sham celiotomy (CEL), intestinal ischemia and reperfusion (IR), intestinal ischemia and reperfusion with gadolinium chloride treatment to deplete pulmonary intravascular macrophages (IRGC). Neutrophil apoptosis was assessed with Annexin V and propidium iodide staining quantified with flow cytometry and caspase-3, -8, and -9 activities in neutrophil lysates.

Results: All horses experienced a systemic inflammatory response following surgery. Ex vivo neutrophil apoptosis was significantly delayed in neutrophils isolated post-operatively, except in IRGC horses. Caspase-3, -8, and -9 activities were significantly reduced in neutrophils isolated post-operatively from IR horses, but not IRGC horses.

Conclusions: Following surgery, ex vivo equine neutrophil apoptosis is delayed via down-regulation of caspase activity, but is rescued by depleting PIMs, implicating these cells as potential regulators of circulating neutrophil apoptosis.

Ethical animal research: Ethical approval was obtained from the University of Saskatchewan Committee on Animal Care and Supply and the University of Saskatchewan Animal Research Ethics Board. **Source of funding:** None. **Competing interests:** None.

13

DISTRIBUTION OF MACROPHAGES IN THE GASTROINTESTINAL TRACT OF HORSES

¹Lisowski Z.M., ²Mair T.S., ¹Sauter K.A., ¹Waddell L.A., ¹Pirie R.S.,

¹Hudson N.P.H. and ¹Hume D.A.

¹The Roslin Institute and Royal (Dick) School of Veterinary Studies, University of Edinburgh, Easter Bush, Midlothian EH25 9RG, UK; ²Bell Equine Veterinary Clinic, Mereworth, Maidstone, Kent ME18 5GS, UK.

Email: tim.mair@blinternet.com.

Background: Resident tissue macrophages, such as those found in the gastrointestinal tract (GIT), are specialised cells with tissue-specific roles. Rodent and human data shows that, during abdominal surgery, activation of macrophages resident in the muscularis plays a key role in the pathogenesis of postoperative ileus, which affects up to 50% of horses undergoing abdominal

surgery. Studies of resident macrophages in the horse GIT are lacking.

Objectives: This study aimed to immunohistochemically identify and plot the distribution of resident macrophages in the equine GIT.

Methods: 11 adult horses (median age: 15 yrs, range: 6–26 yrs) were subjected to elective euthanasia for reasons unrelated to the GIT. Sections of intestinal tissue were collected from 14 anatomically-defined sites from the stomach to the small colon. Tissues were fixed in formalin prior to staining with an antibody against CD163 for macrophage identification. Cell numbers were quantified at each anatomical point. Location and distribution within the tissue were also analysed.

Results: CD163+ve cells were present in all tissue layers; mucosa, submucosa, muscularis externa and serosa. The highest and lowest number of CD163+ve cells were detected in the submucosa and mucosa, respectively. CD163+ve cells were regularly distributed within the muscularis externa, with accumulations adjacent to the myenteric plexus.

Conclusions: Macrophages are distributed throughout the length of the normal equine GIT. This study forms a basis for further work on immune populations in the GIT in normal and diseased tissue. Their close proximity to the myenteric plexus, and therefore to GI motility effector cells, warrants further study.

Ethical animal research: Ethical approval obtained from The University of Edinburgh School of Veterinary Medicine Ethical Review Committee and owner consent obtained. **Source of funding:** ZML is funded by the Horserace Betting Levy Board. **Competing interests:** No conflicts of interest.

Poster Presentations

14

THE DEVELOPMENT OF AUGMENTED REALITY SMARTPHONE APPS FOR IMPROVING OWNER EDUCATION AND UNDERSTANDING OF COLIC IN HORSES

Burford J.H. and Wild I.V.

School of Veterinary Medicine and Surgery, University of Nottingham, Sutton Bonington, Nottinghamshire LE12 5RD.

Email: john.burford@nottingham.ac.uk.

Background: With over three-quarters of adults in the UK now owning smartphones, there is a huge opportunity to innovate and use these as tools for client education and engagement. Augmented reality allows users to enhance their real world with digital media.

Objectives: To determine the practicality of using the camera device on smartphones to produce a graphic overlay displaying anatomic features over a real-time image of a live horse.

Methods: Programming was performed using the Wikitude SDK using two programming environments, Xcode and Android Developer. This allowed code to be written in two popular smartphone operating systems, Apple iOS and Google Android respectively. Digital images of seven horses were used to create digital targets for the software. Bespoke anatomic drawings were digitised to be used as overlays. Testing was performed on the target cohort and a further five horses and ponies. Only horses of solid colour were used as targets and controls.

Results: Coding was created for both operating systems which was able to successfully and reliably superimpose the digital image of horse anatomy over the screen image when the camera was pointed at a horse. This could be performed without the use of fiducial markers.

9.8 Isolation and characterisation of the equine bone marrow derived macrophage.



Isolation and characterisation of the equine bone marrow derived macrophage

Z.M. Lisowski, C. Pridans, L.A. Waddell, R. Young, K.A. Sauter, L. Lefevre, A. Raper, E.L. Clark, N.P.H. Hudson, S.R. Pirie, D.A. Hume
Roslin Institute and Royal (Dick) School of Veterinary Studies, University of Edinburgh, UK

INTRODUCTION

- Bone marrow derived macrophages (BMDMs) are primary macrophage cells which are derived from bone marrow cells *in vitro* in the presence of colony-stimulating factor 1 (CSF1)
- Macrophages play a role in a number of important equine diseases e.g. equine infectious anaemia virus
- BMDMs can be used as an *in vitro* model for tissue resident macrophages of the innate immune system

STUDY AIMS

- To generate macrophages from bone marrow cells of adult horses
- To characterise equine bone marrow derived macrophages (eqBMDMs)

MATERIALS AND METHODS



RESULTS

Optimising culture conditions of equine bone marrow derived macrophages

An MTT assay was performed to identify optimal culture conditions for eqBMDMs. Isolated cells were cultured in complete medium with and without recombinant human CSF1 (rhCSF1) and either in 20% fetal calf serum (FCS) or 20% horse serum (HS). Cells were analysed on days 7, 10 and 14. Cells were cultured on non-TC sterilin dishes.

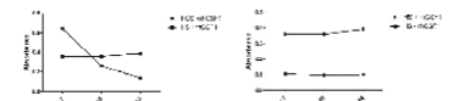


Figure 1. Comparison of metabolic activity of cells in 20% horse serum and 20% fetal calf serum, and cells in 20% horse serum with or without rhCSF1. Cells in horse serum and in the presence of rhCSF1 showed greatest activity. However, cells with rhCSF1 in fetal calf serum became less viable from day 7 onwards. Cells in horse serum with no rhCSF1 showed minimal activity. Absorbance read at 570nm.

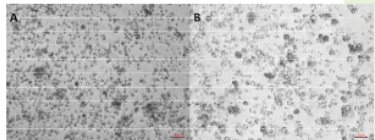


Figure 2. Morphology of cells at Day 7 in culture without rhCSF1 (A) and with rhCSF1 (B). Cells in culture without rhCSF1 were smaller and showed less proliferation and viability compared to cells in culture with rhCSF1.

Morphology

Cells were examined using either light microscopy (Fig. 3) or were fixed onto microscope slides, stained with DAPI and Phalloidin and examined using a confocal microscope (Fig 4). Cell populations showed the expected stellate, adherent morphology of macrophages.

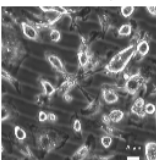


Figure 3. Cells at Day 7

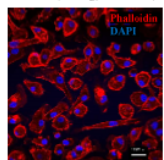


Figure 4. Cells at Day 10

Phagocytosis assay

Isolated cells were cultured for seven days in rhCSF1 and phagocytic activity was evaluated using 2 methods: (a) Zymosan A *Saccharomyces cerevisiae* BioParticle assay followed by cell fixation, staining with DAPI and phalloidin and confocal microscopy; (b) pHrodo Red *Escherichia coli* BioParticle assay followed by flow cytometric analysis.

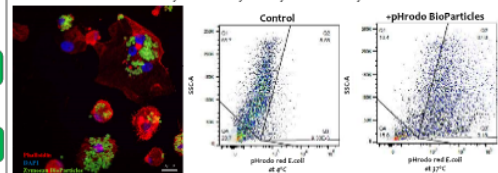


Figure 5. Differentiated eqBMDMs phagocytosing Zymosan A Bio Particles viewed by confocal microscopy. Figure 6. Analysis of eqBMDMs by flow cytometry to show phagocytic uptake of pHrodo Red BioParticles. See Fig. 7 for gating strategy. Differentiated eqBMDMs phagocytosed Zymosan A *S. cerevisiae* BioParticles and pHrodo Red *E. coli* BioParticles showing that these cells are functional macrophages.

Analysis of cells by flow cytometry

On day 7, non adherent cells and adhered cells were stained for flow cytometry. Size (forward light scatter (FSC)) and granularity (side scatter (SSC)) were used for cell discrimination (Fig. 7). CD14 and CD163 were used as macrophage markers (Fig. 8).

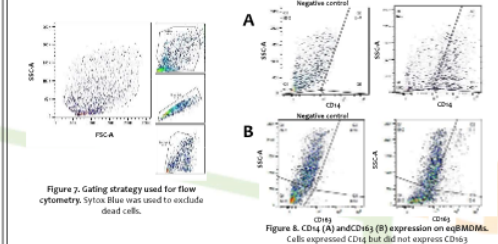


Figure 7. Gating strategy used for flow cytometry. Sytox Blue was used to exclude dead cells. Figure 8. CD14 (A) and CD163 (B) expression on eqBMDMs. Cells expressed CD14 but did not express CD163.

Response of eqBMDMs to LPS

eqBMDMs were stimulated with 100ng/ml LPS on day 7 for 7 hours. Gene expression was measured with RT-qPCR and Griess assay was performed to measure nitrite.

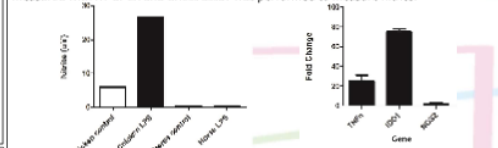


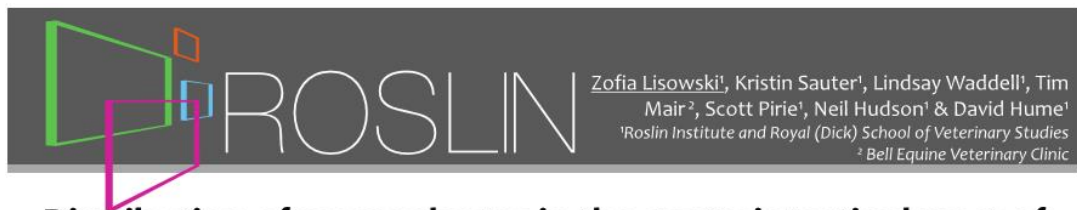
Figure 9. Nitrite production measured in supernatant of stimulated cells. Nitrite was induced in chicken but not in horse BMDMs. Figure 10. Expression of TNF α , iNOS1 and NOS2 in eqBMDMs after stimulation with LPS. Results are expressed as fold change against the value for GAPDH.

CONCLUSIONS

- A protocol was developed for the generation of eqBMDMs
- eqBMDMs were functional as they could phagocytose BioParticles
- Cells expressed CD14, although a subset did not, which indicates a subpopulation. In the absence of markers for the horse we have not yet been able to define this subset further
- CD163 was not expressed due to CD163 being a marker of tissue macrophages
- eqBMDMs did not metabolise arginine to produce nitric oxide (unlike mouse and chicken), but metabolised tryptophan through the induction of indoleamine dioxygenase, similar to pig and human BMDMs
- eqBMDM can be used for further study of the equine innate immune system



9.9 Distribution of macrophages in the gastrointestinal tract of normal horses



Distribution of macrophages in the gastrointestinal tract of normal horses

RESIDENT INTESTINAL MACROPHAGES

- Largest compartment of mononuclear phagocytes in the body in two phenotypically distinct groups:
 1. Mucosal
 - Eliminate invading pathogens
 - Maintain epithelial barrier integrity
 - Luminal content sampling
 2. Muscularis
 - Less is known about their role
 - Recent data suggests they have a role in the regulation of gastrointestinal motility in mice¹
- Despite being implicated in several diseases very little is known about the normal macrophage population in the gastrointestinal tract of the horse

AIM

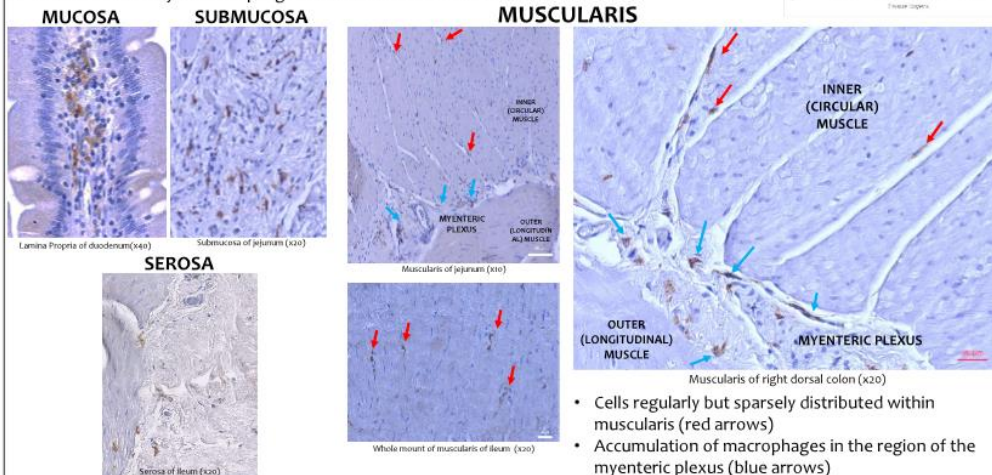
- To immunohistochemically identify and plot the distribution of resident intestinal macrophages in the normal equine gastrointestinal tract, targeting CD163 for macrophage identification

METHODS

- Intestinal tissue collected from 14 anatomically defined locations from the stomach to the small colon from 10 adult horses with no history of recent gastrointestinal disease
- Tissue stained with CD163 to identify macrophages
- Cells quantified using ImageJ analysis software

RESULTS

- Macrophages cells were present throughout the length of the gastrointestinal tract
- Macrophages are present in all intestinal tissue layers; mucosa, submucosa, muscularis externa and serosa.
- The highest density of macrophages was detected in the mucosa and submucosa
- The lowest density of macrophages was detected in the muscularis



- Cells regularly but sparsely distributed within muscularis (red arrows)
- Accumulation of macrophages in the region of the myenteric plexus (blue arrows)

CONCLUSIONS AND FURTHER WORK

Macrophages are present in all layers of the intestine and throughout the equine gastrointestinal tract and are a constant and regularly distributed population. The increase in numbers near the myenteric plexus region has also been reported in other species. This suggests macrophages potentially interact with the motility effector cells of the intestine, such as the enteric neurons, interstitial cells of Cajal and enteric glial cells and warrants further investigation especially in conditions affecting gastrointestinal motility.

9.10 Targeting the macrophage in equine post-operative ileus



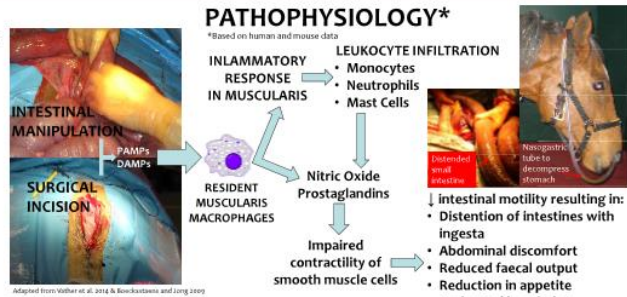
The role of the macrophage in equine post operative ileus



- Colic (abdominal pain) is common in the horse and is a high health and financial concern for owners
- 10% of cases are unresponsive to medical treatment and require abdominal surgery
- Post operative ileus (POI) is the functional inhibition of propulsive intestinal motility following abdominal surgery
- POI develops as a result of complex interactions between immune cells and the enteric nervous system
- Up to 60% of horses undergoing abdominal surgery will develop POI, with a reported mortality rate of up to 86%¹

RESIDENT INTESTINAL MACROPHAGES

- Largest compartment of mononuclear phagocytes in the body² in 2 phenotypically distinct groups
 1. Mucosal
 - Eliminate invading bacteria
 - Maintain epithelial barrier integrity
 - Luminal content sampling
 2. Muscularis
 - Less is known about their role
 - Regulate gastrointestinal motility³
- POI prevention by inhibition of muscularis macrophages has supported their role in the development of POI⁴



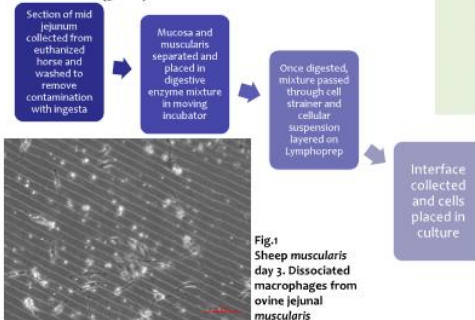
PROJECT AIMS

Determine the location and distribution of inflammatory cells in normal horse intestine	Assess spatial relationships, if any, between inflammatory cells and enteric motility effector cells	Develop a protocol for isolation of macrophages from equine muscularis and mucosa	Mouse model of POI and the use of MacGreen and MacBlue mice for imaging intestinal macrophages	Microarray – comparison of normal intestine with diseased intestine
---	--	---	--	---

PRELIMINARY WORK

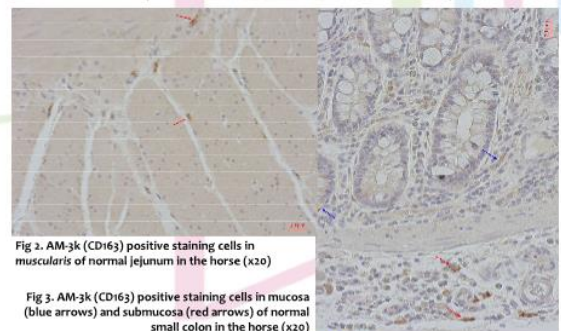
Isolation of macrophages from jejunum

- Section of mid jejunum removed and mucosa and muscularis separated and digested separately
- Initial work done on sheep intestine due to availability of tissue (3R's)



Immunohistochemistry

- Tissue collection from multiple anatomical points, from stomach to small colon, of normal horses
- Immunohistochemistry protocols for inflammatory cells (macrophages, mast cell and neutrophils) and enteric motility effector cells (interstitial cells of Cajal and neurons)



BBSRC bioscience for the future	EBRC East of Scotland Research Consortium	THE UNIVERSITY OF EDINBURGH	IBLB	References 1. Mair and Smith 2005 2. Lee et al. 1985 3. Muller et al. 2014 4. Welner et al. 2004
---------------------------------	---	-----------------------------	------	--

9.11 Appendix 8: Table of $2^{-\Delta\Delta C_t}$ values used in analysis of colic cases

Tissue Description	Animal ID	ddCt IL1B	ddCt IL6	ddCt PTGS2	ddCt TNF	ddCt CCL2	ddCt IDO1
Mucosa	Control 1	1.12	0.17	0.19	0.59	0.58	0.90
Mucosa	Control 2	0.44	0.46	0.69	1.22	0.66	0.32
Mucosa	Control 3	0.90	0.97	1.59	1.11	0.94	2.21
Mucosa	Control 4	1.72	2.49	1.59	2.01	1.02	2.72
Mucosa	Control 5	2.01	8.39	1.74	0.94	2.75	0.45
Mucosa	Control 6	0.65	0.63	1.71	0.65	0.98	1.27
<i>Mucosa distal</i>	<i>Case B</i>	3.37	3.46	14.13	0.86	5.26	2.31
<i>Mucosa distal</i>	<i>Case C</i>	3.67	468.03	115.97	2.13	97.43	3.01
<i>Mucosa distal</i>	<i>Case D</i>	13.66	67.59	6.30	6.28	4.65	0.68
<i>Mucosa distal</i>	<i>Case E</i>	5.82	7.66	7.18	6.63	3.87	2.73
<i>Mucosa distal</i>	<i>Case F</i>	9.82	73.46	6.25	2.87	8.74	2.89
<i>Mucosa distal</i>	<i>Case A</i>	52.12	352.74	17.41	3.02	25.91	0.11
<i>Mucosa distal</i>	<i>Case H</i>	8.40	23.19	6.53	2.33	7.09	0.20
<i>Mucosa distal</i>	<i>Case L</i>	6.92	25.29	7.64	12.59	3.27	1.09
<i>Mucosa proximal</i>	<i>Case B</i>	2.29	2.85	10.30	0.91	2.91	3.03
<i>Mucosa proximal</i>	<i>Case C</i>	3.15	111.47	51.64	2.21	26.50	242.48
<i>Mucosa proximal</i>	<i>Case E</i>	1.71	1.11	4.05	3.58	1.69	0.55
<i>Mucosa proximal</i>	<i>Case G</i>	6.01	23.53	5.01	5.12	3.90	0.01
<i>Mucosa proximal</i>	<i>Case H</i>	15.59	70.50	7.59	4.43	14.35	1.20
<i>Mucosa proximal</i>	<i>Case I</i>	0.29	3.08	3.29	0.91	2.14	1.82
<i>Mucosa proximal</i>	<i>Case J</i>	31.83	432.27	27.29	9.32	27.04	1.38
<i>Mucosa proximal</i>	<i>Case L</i>	1.47	2.13	2.39	4.92	2.06	0.32
Muscularis	Control 1	1.11	1.42	1.67	1.00	0.79	0.84
Muscularis	Control 2	0.56	0.74	1.13	1.37	0.77	1.58
Muscularis	Control 3	1.37	1.18	0.60	0.73	1.07	0.64
Muscularis	Control 4	1.17	0.81	0.89	1.00	1.54	1.18
<i>Muscularis distal</i>	<i>Case A</i>	18.68	1.97	0.31	8.83	2.51	1.70
<i>Muscularis distal</i>	<i>Case B</i>	15.66	48.67	1.03	1.27	10.85	0.93
<i>Muscularis distal</i>	<i>Case F</i>	110.25	19.45	0.39	11.11	6.47	0.14
<i>Muscularis distal</i>	<i>Case I</i>	17.39	2.41	0.55	17.48	3.31	0.18
<i>Muscularis distal</i>	<i>Case J</i>	85.42	23.17	0.63	56.75	7.41	0.13
<i>Muscularis proximal</i>	<i>Case C</i>	22.73	5.20	0.30	10.96	2.84	1.90
<i>Muscularis proximal</i>	<i>Case K</i>	29.49	35.11	1.54	1.36	10.68	0.06
<i>Muscularis proximal</i>	<i>Case D</i>	143.76	58.21	0.95	41.82	13.53	2.25
<i>Muscularis proximal</i>	<i>Case H</i>	67.02	21.67	0.64	9.77	4.51	0.64

Figure 9-1 $2^{-\Delta\Delta C_t}$ values of target genes from colic and control cases

Tissue Description	Animal ID	ddCt IL1B	ddCt IL6	ddCt PTGS2	ddCt TNF	ddCt CCL2	ddCt IDO1
Mucosa	Control 1	1.12	0.17	0.19	0.59	0.58	0.90
Mucosa	Control 2	0.44	0.46	0.69	1.22	0.66	0.32
Mucosa	Control 3	0.90	0.97	1.59	1.11	0.94	2.21
Mucosa	Control 4	1.72	2.49	1.59	2.01	1.02	2.72
Mucosa	Control 5	2.01	8.39	1.74	0.94	2.75	0.45
Mucosa	Control 6	0.65	0.63	1.71	0.65	0.98	1.27
<i>Mucosa distal</i>	<i>Case A</i>	52.12	352.74	17.41	3.02	25.91	0.11
Mucosa proximal	Case B	2.29	2.85	10.30	0.91	2.91	3.03
Mucosa proximal	Case C	3.15	111.47	51.64	2.21	26.50	242.48
<i>Mucosa distal</i>	<i>Case D</i>	13.66	67.59	6.30	6.28	4.65	0.68
Mucosa proximal	Case E	1.71	1.11	4.05	3.58	1.69	0.55
<i>Mucosa distal</i>	<i>Case F</i>	9.82	73.46	6.25	2.87	8.74	2.89
Mucosa proximal	Case G	6.01	23.53	5.01	5.12	3.90	0.01
Mucosa proximal	Case H	15.59	70.50	7.59	4.43	14.35	1.20
Mucosa proximal	Case I	0.29	3.08	3.29	0.91	2.14	1.82
Mucosa proximal	Case J	31.83	432.27	27.29	9.32	27.04	1.38
<i>Mucosa distal</i>	<i>Case K</i>	6.92	25.29	7.64	12.59	3.27	1.09
Mucosa proximal	Case L	1.47	2.13	2.39	4.92	2.06	0.32
Muscularis	Control 1	1.11	1.42	1.67	1.00	0.79	0.84
Muscularis	Control 2	0.56	0.74	1.13	1.37	0.77	1.58
Muscularis	Control 3	1.37	1.18	0.60	0.73	1.07	0.64
Muscularis	Control 4	1.17	0.81	0.89	1.00	1.54	1.18
<i>Muscularis distal</i>	<i>Case A</i>	18.68	1.97	0.31	8.83	2.51	1.70
<i>Muscularis distal</i>	<i>Case B</i>	15.66	48.67	1.03	1.27	10.85	0.93
Muscularis proximal	Case C	22.73	5.20	0.30	10.96	2.84	1.90
Muscularis proximal	Case D	143.76	58.21	0.95	41.82	13.53	2.25
<i>Muscularis distal</i>	<i>Case F</i>	110.25	19.45	0.39	11.11	6.47	0.14
Muscularis proximal	Case H	67.02	21.67	0.64	9.77	4.51	0.64
<i>Muscularis distal</i>	<i>Case I</i>	17.39	2.41	0.55	17.48	3.31	0.18
<i>Muscularis distal</i>	<i>Case J</i>	85.42	23.17	0.63	56.75	7.41	0.13
Muscularis proximal	Case K	29.49	35.11	1.54	1.36	10.68	0.06

Figure 9-2 $2^{-\Delta\text{-ddCt}}$ values of target genes in colic cases and non-colic control horses